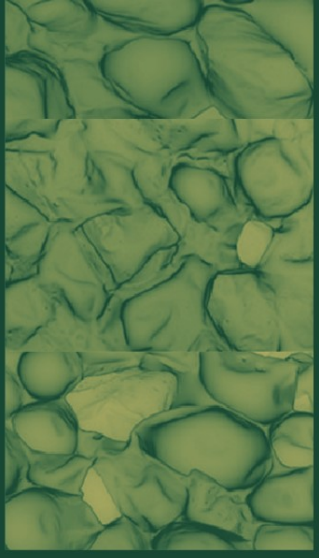

FOOD ENGINEERING SERIES

Gustavo F. Gutiérrez-López
Gustavo V. Barbosa-Cánovas
Jorge Welti-Chanes
Efrén Parada-Arias
Editors

Food Engineering

Integrated Approaches

Springer

Food Engineering: Integrated Approaches

FOOD ENGINEERING SERIES

Series Editor

Gustavo V. Barbosa-Cánovas, Washington State University

Advisory Board

Titles

José M. Aguilera and Peter J. Lillford, *Food Materials Science* (2008)
José M. Aguilera and David W. Stanley, *Microstructural Principles of Food Processing and Engineering*, Second Edition (1999)
Stella M. Alzamora, María S. Tapia, and Aurelio López-Malo, *Minimally Processed Fruits and Vegetables: Fundamental Aspects and Applications* (2000)
Gustavo V. Barbosa-Cánovas, Enrique Ortega-Rivas, Pablo Juliano, and Hong Yan, *Food Powders: Physical Properties, Processing, and Functionality* (2005)
Gustavo F. Gutiérrez-López, Gustavo V. Barbosa-Cánovas, Jorge Welti-Chanes, Efrén Parada-Arias, *Food Engineering: Integrated Approaches* (2008)
Richard W. Hartel, *Crystallization in Foods* (2001)
Rosana G. Moreira, M. Elena Castell-Perez, and Maria A. Barrufet, *Deep-Fat Frying: Fundamentals and Applications* (1999)
Marc E.G. Hendrickx and Dietrich Knorr, *Ultra High Pressure Treatments of Food* (2002)
S. Donald Holdsworth and Ricardo Simpson, *Thermal Processing of Packaged Foods, Second Edition* (2008)
Lothar Leistner and Grahame Gould, *Hurdle Technologies: Combination Treatments for Food Stability, Safety, and Quality* (2002)
Michael J. Lewis and Neil J. Heppell, *Continuous Thermal Processing of Foods: Pasteurization and UHT Sterilization* (2000)
Jorge E. Lozano, *Fruit Manufacturing* (2006)
Rosana G. Moreira, *Automatic Control for Food Processing Systems* (2001)
M. Anandha Rao, *Rheology of Fluid and Semisolid Foods: Principles and Applications, Second Edition* (2007)
Javier Raso Pueyo and Volker Heinz, *Pulsed Electric Field Technology for the Food Industry: Fundamentals and Applications* (2006)
George D. Saravacos and Athanasios E. Kostaropoulos, *Handbook of Food Processing Equipment* (2002)
Stavros Yanniotis, *Solving Problems in Food Engineering* (2008)

Food Engineering: Integrated Approaches

Edited by

Gustavo F. Gutiérrez-López
Instituto Politécnico Nacional
México, DF, México

Gustavo V. Barbosa-Cánovas
Washington State University
Pullman, WA, USA

Jorge Welti-Chanes
Universidad de las Américas-Puebla
Cholula, Puebla, México

and

Efrén Parada-Arias
Instituto Politécnico Nacional
México, DF, México

Springer

Gustavo F. Gutiérrez-López
Escuela Nacional de Ciencias Biológicas
Instituto Politécnico Nacional
Carpio y Plan de Ayala s/n
Col. San Tómas
Código Postal 11340, México, D.F.
Email: gustavog@prodigy.net.mx

Gustavo V. Barbosa-Cánovas
Biological System Engineering Dept.
Washington State University
Pullman, WA 99164-6120, USA
Email: barbosa@wsu.edu

Jorge Welti-Chanes
Departamento de Ingeniería Química y Alimentos
Universidad de las Américas-Puebla
Santa Catarina Mártir 72820
Cholula, Puebla, México
Email: jorges.welti@udlap.mx

Efrén Parada-Arias
Escuela Nacional de Ciencias Biológicas
Instituto Politécnico Nacional
Carpio y Plan de Ayala s/n
Col. San Tómas
Código Postal 11340, México, D.F.
Email: eparada@ipn.mx

Series Editors:

Gustavo V. Barbosa-Cánovas
Washington State University
Department of Biological Systems Engineering
Pullman, Washington 99164-6120, USA

ISBN: 978-0-387-75429-1 e-ISBN: 978-0-387-75430-7

Library of Congress Control Number: 2007938046

Printed on acid-free paper

9 8 7 6 5 4 3 2 1

springer.com

To our families

Preface

Food engineering has developed to a level at which integrated approaches to the various situations involved in the discipline have become the essential ingredients of successful process and product development. For this reason, it is relevant to identify recent and ongoing efforts toward the use and inclusion of tools and disciplines within the food engineering field.

Food Engineering: Integrated Approaches presents an up-to-date review of important food engineering concepts, issues and recent advances in the field. Distinguished food engineers and food scientists from key institutions worldwide have contributed chapters that provide a deep analysis of their particular subjects. At the same time, each topic is framed within the context of a broader more integrated approach, demonstrating its relationship and interconnectedness to other areas. The premise of this work, therefore, is to offer both a comprehensive understanding of food engineering as a whole and a thorough knowledge of individual subjects. This approach appropriately conveys the basic fundamentals, state-of-the-art technology, and applications of the involved disciplines, and further encourages scientific collaboration among researchers.

This book is mainly directed to academics, and to undergraduate and postgraduate students in food engineering, food science and food technology. Scholars will find a selection of innovative topics ranging from bubbles in food and transport phenomena in food systems to practical food processing applications at the industrial level. Professionals working in food research centers and food industries may also find this book useful.

This book was produced through an Iberoamerican effort to integrate food engineering in a comprehensive way. This work has been made possible by the catalyzing activity of the Iberoamerican Program of Science and Technology for Development (CYTED), which has provided an appropriate forum for the launching of food engineering networks and projects from which the Iberoamerican

Congresses on Food Engineering series were conceived. The general subjects covered were discussed in the fifth version of this series, and carefully updated and revised for their inclusion in this book.

The first chapter describes the activity of CYTED program in the Agri-Food area. The next 12 chapters review novel applications of engineering principles, transport phenomena and new scopes for analyzing food processing, and constitute a platform for the next two chapters. These chapters provide a framework for the integrated approach to food engineering and a view of the profound scope of food product design. This framework constitutes the basis for the following 17 chapters, in which specific examples of an integrated approach to food engineering are presented, with the aim of covering as broadly and deeply as possible the different subjects discussed. Finally, two chapters on food engineering education programs are presented, with the purpose of disseminating alternatives for internationalizing students and supervisors' activities in food studies.

It is very likely that many of the procedures and techniques described are being or will be used in the food industry. It is hoped that this volume will constitute a worthy addition to the existing literature on food engineering and that readers will find in it balanced, systematic and harmonized information.

G. F. Gutiérrez-López
G. V. Barbosa-Cánovas
J. Welti-Chanes
E. Parada-Arias

Acknowledgements

The editors wish to express their gratitude to the following institutions and individuals who contributed to making this book possible:

The National Polytechnic Institute (IPN), Mexico City, Mexico; the National School of Biological Sciences (ENCB-IPN), Mexico City, Mexico; the Center for Non-thermal Processing of Food, Washington State University, Pullman, USA; the Universidad de las Américas, Puebla, Mexico; and the Ibero-American Program for Science and Technology for Development (CYTED).

Thanks to Jeanne C. Bagby, Intensive American Language Center, Washington State University, Pullman, USA, for her professionalism and dedication throughout the entire editing process; to Dr. Enrique Villa Rivera, Director General, IPN, Mexico, for his constant support and encouragement to make CIBIA V a reality, as well as this book; to the CIBIA V Organizing Committee team: Liliana Alamilla, Jorge Chanona, Carlos Ordorica and María Elena Sosa for their efficient and intensive work and support towards the preparation of this book.

Finally, we wish to thank our fellow colleagues: Lidia Dorantes, Gloria Dávila, Ma. Eugenia Jaramillo, Rosalva Mora, Cristian Jiménez, Georgina Calderón, Humberto Hernández and Reynold Farrera for their valuable comments and suggestions throughout the preparation of the book; and Vicky Aguilar, Raúl Elías, Darío Iker Téllez and Maribel Cornejo from ENCB-IPN for their decisive participation in helping the editors prepare the final version of this book by revising references, formatting the manuscript, and incorporating in the text all the editorial comments.

Contents

Editors

Gustavo F. Gutiérrez-López received his Bachelor of Science in Biochemical Engineering and Master of Science in Food Science and Technology from the National Polytechnic Institute of Mexico, and his Master of Science in Food Process Engineering and Ph.D. in Food Engineering from the University of Reading, U.K. He is currently professor of Food Engineering and chair of the Ph.D. program in Food Science and Technology at the National School of Biological Sciences of the National Polytechnic Institute of Mexico.

Gustavo V. Barbosa-Cánovas received his Bachelor of Science in Mechanical Engineering from the University of Uruguay and his Master of Science and Ph.D. in Food Engineering from the University of Massachusetts at Amherst. He is currently Professor of Food Engineering at Washington State University and Director of the Center for Nonthermal Processing of Food.

Jorge Welti-Chanes received his bachelor of science in Biochemical Engineering and Master of Science in Food Engineering from the Technology and Superior Studies Institute of Monterrey, Mexico and Ph.D. in Food Science from the University of Valencia, Spain. He is currently professor of Food Engineering at the University of the Americas, Puebla, Mexico and distinguished Visiting Professor at Texas Christian University and at the Autonomous University of Chihuahua, Mexico.

Efrén Parada-Arias received his Bachelor of Science in Biochemical Engineering and Master of Science in Food Science and Technology from the National Polytechnic Institute of Mexico, and his Ph. D. in Food Technology from the Polytechnic University of Valencia, Spain. He has been professor of Food Science and Food Engineering at the National School of Biological Sciences of the National Polytechnic Institute of Mexico and is currently the Secretary General of this Institute.

Contributors

N.C. Acevedo
Departamento de Industrias y de Química Orgánica, Universidad de Buenos Aires, Buenos Aires, Argentina

J.M. Aguilera
Departamento de Ingeniería Química y Bioprocesos, Pontificia Universidad Católica, Santiago, Chile

L. Alamilla-Beltrán
Departamento de Ingeniería Bioquímica, ENCB-Instituto Politécnico Nacional, México DF, México

E. Alvarez-Parrilla
Departamento de Ciencias Básicas, Universidad Autónoma de Ciudad Juárez, Chihuahua, México

J. de D. Alvarado
Facultad de Ciencia e Ingeniería de Alimentos de Ambato, Universidad Técnica de Ambato, Ambato, Ecuador

S.M. Alzamora
Departamento de Industrias, Universidad de Buenos Aires, Buenos Aires, Argentina

A. Andrés
Instituto de Ingeniería de Alimentos para el Desarrollo, Universidad Politécnica de Valencia, Valencia, España

M.C. Añón
Centro de Investigación y Desarrollo en Criotecnología de Alimentos, Universidad Nacional de La Plata - CONICET, La Plata Argentina

J. Araujo
Departamento de Ingeniería Bioquímica, ENCB-Instituto Politécnico Nacional, México DF, México

J.F. Ayala-Zavala
Centro de Investigación en Alimentación y Desarrollo, Hermosillo, México

G.V. Barbosa-Cánovas
Center for Nonthermal Processing of Food, Washington State University, Pullman, USA

A.del P. Beléia
Departamento de Ciência e Tecnologia de Alimentos, Universidade Estadual de Londrina, Londrina PR, Brazil

L.A. Bello-Pérez
Departamento de Desarrollo Tecnológico, CEPROBI-Instituto Politécnico Nacional, Yautepec, México

D. Bermúdez
Center for Nonthermal Processing of Food, Washington State University, Pullman, USA

N. Bertola
Centro de Investigación y Desarrollo en Criotecnología de Alimentos, Universidad Nacional de La Plata - CONICET, La Plata, Argentina

N. Betoret
Instituto de Ingeniería de Alimentos para el Desarrollo, Universidad Politécnica de Valencia, España

V. Bifani
Departamento de Ingeniería Química, Universidad de La Frontera, Temuco, Chile

M. del P. Buera
Departamento de Industrias y de Química Orgánica, Universidad de Buenos Aires, Buenos Aires, Argentina

G. Calderón Domínguez
Departamento de Ingeniería Bioquímica, ENCB-Instituto Politécnico Nacional, México DF, México

C. Campos
Departamento de Industrias, Universidad de Buenos Aires, Buenos Aires, Argentina

A. Carmona
Departamento de Ingeniería Bioquímica, ENCB-Instituto Politécnico Nacional, México DF, México

R. Carvalho
Departamento de Engenharia de Alimentos, Universidade de São Paulo, Pirassununga SP, Brazil

J. Chanona-Pérez
Departamento de Ingeniería Bioquímica, ENCB-Instituto Politécnico Nacional, México DF, México

F. Coll Cárdenas
Centro de Investigación y Desarrollo en Criotecnología de Alimentos, Universidad Nacional de La Plata - CONICET, La Plata, Argentina

M.G. Corradini
Department of Food Science, University of Massachusetts, Amherst, USA

R. Cruz-Valenzuela
Centro de Investigación en Alimentación y Desarrollo, Hermosillo, México

L.A. de la Rosa
Departamento de Ciencias Básicas, Universidad Autónoma de Ciudad Juárez, Ciudad Juárez, México

J.J. de Pablo
Department of Chemical and Biological Engineering, University of Wisconsin, Madison, USA

R. Deliza
Laboratório de Análise Sensorial e Instrumental, EMBRAPA Agroindústria de Alimentos, Rio de Janeiro, Brazil

G. Denavi
Centro de Investigación y Desarrollo Criotecnológico de Alimentos, Universidad Nacional de La Plata, La Plata, Argentina

R.M. Desentis-Mendoza
Departamento de Ingeniería Bioquímica, ENCB-Instituto Politécnico Nacional, México DF, México

L. Dorantes
Departamento de Ingeniería Bioquímica, ENCB-Instituto Politécnico Nacional, México DF, México

E. Dumoulin
Dept. Génie Industriel Alimentaire et Laboratoire Associé INRA, ENSIA, Massy, France

L. Famá
Departamento de Física, Universidad de Buenos Aires, Buenos Aires, Argentina

C. Ferrero
Departamento de Ingeniería Química Centro de Investigación y Desarrollo en Criotecnología de Alimentos, Universidad Nacional de La Plata - CONICET, La Plata, Argentina

I. Figueroa
Departamento de Procesos Químicos, Universidad Técnica Federico Santa María, Valparaíso, Chile

M.V. Filippi
PLAPIQUI-Universidad Nacional del Sur, Bahía Blanca, Argentina

P. Fito
Instituto de Ingeniería de Alimentos para el Desarrollo, Universidad Politécnica de Valencia, Valencia, España

P.J. Fito
Instituto de Ingeniería de Alimentos para el Desarrollo, Universidad Politécnica de Valencia, Valencia, España

S. Flores
Departamento de Industrias, Universidad de Buenos Aires, Buenos Aires, Argentina

M. García
Centro de Investigación y Desarrollo Criotecnológico de Alimentos, Universidad Nacional de La Plata - CONICET, La Plata, Argentina

M. García-Garibay
Departamento de Biotecnología, Unidad Iztapalapa-Universidad Autónoma Metropolitana, México DF, México

D.B. Genovese
PLAPIQUI-Universidad Nacional del Sur, Bahía Blanca, Argentina

L. Gerschenson
Departamento de Industrias, Universidad de Buenos Aires, Buenos Aires, Argentina

L. Giannuzzi
Centro de Investigación y Desarrollo en Criotecnología de Alimentos, Universidad Nacional de La Plata - CONICET, La Plata, Argentina

C. Gómez-Guillén
Instituto del Frío, Consejo Superior de Investigaciones Científicas, Madrid, España

G.A. González-Aguilar
Centro de Investigación en Alimentación y Desarrollo, Hermosillo, México

M.V.E. Grossmann
Departamento de Ciência e Tecnologia de Alimentos, Universidade Estadual de Londrina Londrina PR, Brazil

C. Gumeta Chávez
Departamento de Ingeniería Bioquímica, ENCB-Instituto Politécnico Nacional México DF, México

N. Gutiérrez
Departamento de Industrias, Universidad de Buenos Aires, Buenos Aires, Argentina

G.F. Gutiérrez-López
Departamento de Ingeniería Bioquímica, ENCB-Instituto Politécnico Nacional, México DF, México

H. Hernández-Sánchez
Departamento de Ingeniería Bioquímica, ENCB-Instituto Politécnico Nacional, México DF, México

K. Hofsetz
Departamento de Engenharia de Alimentos, FEA-Universidade Estadual de Campinas, Campinas SP, Brazil

M.D. Hubinger
Departamento de Engenharia de Alimentos, FEA-Universidade Estadual de Campinas, Campinas SP, Brazil

M. Ihl
Departamento de Ingeniería Química, Universidad de La Frontera, Temuco, Chile

M.E. Jaramillo-Flores
Departamento de Ingeniería Bioquímica, ENCB-Instituto Politécnico Nacional México DF, México

A.R. Jiménez Aparicio
Departamento de Biotecnología, CEPROBI-Instituto Politécnico Nacional, Morelos, México

J. Jiménez-Guzmán
Departamento de Biotecnología, Unidad Iztapalapa-Universidad Autónoma Metropolitana, México

P. Juliano
Center for Nonthermal Processing of Food, Washington State University, Pullman, USA

R.G. Junqueira
Departmento de Alimentos, Faculdade de Farmácia, UFMG, Belo Horizonte, Brazil

L.H.E.S. Laboissiere
Departmento de Alimentos, Faculdade de Farmácia, UFMG, Belo Horizonte, Brazil

J.B. Laurindo
Departamento de Engenharia Química e Engenharia de Alimentos, Universidade Federal de Santa Catarina, Florianópolis SC, Brazil

M. Le Maguer
Department of Food Science, University of Guelph, Canada

C.C. Lopes
Departamento de Engenharia de Alimentos, FEA-Universidade Estadual de Campinas, Campinas SP, Brazil

J.E. Lozano
PLAPIQUI-Universidad Nacional del Sur, Bahía Blanca, Argentina

S. Mali
Departamento de Ciência e Tecnologia de Alimentos, Universidade Estadual de Londrina, Londrina PR, Brazil

A.M. de B. Marcellini
Departmento de Enegenharia de Alimentos en Nutrição, FEA-Universidade Estadual de Campinas, Campinas SP, Brazil

V.Y. Martínez
Departamento de Industrias, Universidad de Buenos Aires, Buenos Aires, Argentina

M.N. Martino
Centro de Investigación y Desarrollo Criotecnológico de Alimentos, Universidad Nacional de La Plata - CONICET, La Plata, Argentina

A. Mauri
Centro de Investigación y Desarrollo Criotecnológico de Alimentos, Universidad Nacional de La Plata, La Plata, Argentina

L. Mayor
Departamento de Engenharia Química, Univerisidade de Porto, Porto, Portugal

F.M. Mazzobre
Departamento de Industrias, Universidad de Buenos Aires, Buenos Aires, Argentina

F. Menegalli
Departamento de Engenharia de Alimentos, Universidade Estadual de Campinas, Campinas SP, Brazil

J.A. Mendoza Pérez
Secretaría de Marina, Armada de México, México DF, México

S. Molina Ortíz
Centro de Investigación y Desarrollo Criotecnológico de Alimentos, Universidad Nacional de La Plata, La Plata, Argentina

P. Montero
Instituto Del Frío, Consejo Superior de Investigaciones Científicas, Madrid, España

H. Mújica-Paz
Escuela de Ciencias Químicas, Universidad Autónoma de Chihuahua, Chihuahua, México

A.B. Nieto
Departamento de Industrias, Universidad de Buenos Aires, Buenas Aires, Argentina

K. Niranjan
School of Food Biosciences, The University of Reading, United Kingdom

M.D. Normand
Department of Food Science, Amherst, University of Massachusetts, USA

S. Ohtake
Department of Chemical and Biological Engineering, University of Wisconsin, Madison, USA

C. Ordorica-Vargas
Departamento de Ingeniería Bioquímica, ENCB-Instituto Politécnico Nacional, México DF, México

E. Parada-Arias
Departamento de Ingeniería Bioquímica, ENCB-Instituto Politécnico Nacional, México DF, México

M. Peleg
Department of Food Science, University of Massachusetts, Amherst, USA

E. Pérez
Departamento de Ingeniería Química y Alimentos, Universidad de las Américas, Puebla, México

F. Pérez
Departamento de Ingeniería Química y Alimentos, Universidad de las Américas, Puebla, México

A.M.R. Pilosof
Departamento de Industrias, Universidad de Buenos Aires, Buenos Aires, Argentina

A. Pinotti
Centro de Investigación y Desarrollo Criotecnológico de Alimentos, Universidad Nacional de La Plata - CONICET La Plata, Argentina

R. Quevedo
Departamento de Ciencias y Tecnología de Alimentos, Universidad de Los Lagos, Osorno, Chile

C. Ramírez
Departamento de Ingeniería Química, Universidad de La Frontera, Temuco, Chile

M. Ramírez-Gilly
Departamento de Alimentos y Biotecnología, Universidad Autónoma de México, México DF, México

M. Ramos
Instituto de Fermentacones Industriales-CSIC, Madrid, España

I. Recio
Instituto de Fermentacones Industriales-CSIC, Madrid, España

A.M. Rojas
Departamento de Industrias,
Universidad de Buenos Aires,
Buenos Aires, Argentina

C.A. Romero-Bastida
Departamento de Desarrollo
Tecnológico, CEPROBI-Instituto
Politécnico Nacional, Yuatepec,
México

A. Rosenthal
Departmento de Enegenharia e
Tecnologia Alimentos, EMBRAPA
Agroindústria de Alimentos,
Rio de Janeiro, Brazil

S. Ruiz-Cruz
Centro de Investigación en
Alimentación y Desarrollo
Hermosillo, México

D. Salvatori
Departamento de Química,
Universidad Nacional del Comahue,
Buenos Aires, Neuquén,
Argentina

B.E. Sánchez-Basurto
Departamento de Alimentos y
Biotecnología, Universidad Nacional
Autónoma de México,
México DF, México

P.R. Santagapita
Departamento de Industrias,
Universidad de Buenos Aires,
Buenos Aires, Argentina

C. Schebor
Departamento de Industrias y de
Química Orgánica, Universidad
de Buenos Aires, Buenos Aires,
Argentina

L.A. Segura
Departamento de Ingeniería de
Alimentos, Universidad del Bío-Bío
Chillán, Chile

A.M. Sereno
Departamento de Engenharia
Química, Univerisidade de Porto,
Porto, Portugal

A. Silva
Departamento de Ingeniería
Química, Universidad de La
Frontera, Temuco, Chile

C.L.M. Silva
Escola Superior de Biotecnologia,
Universidade Catolica de Porto,
Porto, Portugal

S.F.J. Silva
School of Food Biosciences,
The University of Reading,
United Kingdom

R. Simpson
Departamento de Procesos Químicos,
Universidad Técnica Federico Santa
María, Valparaíso, Chile

P.R. Singh
Department of Biological and
Agricultural Engineering,
University of California, Davis, USA

S.K. Singh
Department of Biological and
Agricultural Engineering
University of California, Davis, USA

P. Sobral
Departamento de Engenharia de
Alimentos, Universidade de São
Paulo, Pirassununga SP, Brazil

J.L. Solleiro
Centro de Ciencias Aplicadas y Desarrollo Tecnológico, Universidad Autónoma de México, México DF, México

A. Tecante
Departamento de Alimentos y Biotecnología, Universidad Autónoma de México, México DF, México

A. Teixeira
Department of Agricultural Engineering, University of Florida Gainesville, USA

A. Valdez-Fragoso
Escuela de Ciencias Químicas, Universidad Autónoma de Chihuahua, México

F. Vergara-Balderas
Departamento de Ingeniería Química y Alimentos, Universidad de las Américas, Puebla, México

P.E. Viollaz
Departamento de Industrias, Universidad de Buenos Aires, Buenos Aires, Argentina

J. Welti-Chanes
Departamento de Ingeniería Química y Alimentos, Universidad de las Américas, Puebla, México

F. Yamashita
Departamento de Ciência e Tecnologia de Alimentos, Universidade Estadual de Londrina, Londrina PR, Brazil

P.B. Zamudio-Flores
Departamento de Desarrollo Tecnológico, CEPROBI-Instituto Politécnico Nacional, Yautepec, México

N.E. Zaritzky
Centro de Investigación y Desarrollo en Criotecnología de Alimentos, Universidad Nacional de La Plata - CONICET y Facultad de Ingeniería, La Plata Argentina

1
Scientific and Technological Cooperation in the Agri-Food Sector: The Case of the CYTED Program

J.L. Solleiro and G.F. Gutiérrez-López

1.1. Introduction

The Latin American Program of Science and Technology for Development (Spanish acronym: CYTED) was created in 1984 by an interinstitutional agreement signed by 19 countries in Latin America, Spain and Portugal.

CYTED is an international program that promotes scientific and technological cooperation with the objective of contributing to the harmonic development of the Latin American region by promoting cooperation among research groups from universities, research centers and innovative companies in Iberoamerican countries, in order to attain transferable scientific and technological results from productive systems and social policies.

The CYTED program is organized according to a decentralized model, and its structure has a dual framework: institutional and functional. The institutional frame comprises the bodies responsible for the scientific and technological policies of the 21 participant countries, called the *Signatory Bodies of the Program*. Each body is responsible for the management of the program at national levels, and the manage-ment and coordination of the activities is directed by the General Secretariat of the program.

By 2005, CYTED had generated 76 thematic networks, 95 research projects and 166 innovation projects, with the participation of more than 10,000 Latin American scientists and technologists (Fig. 1.1), as well as promoting integrated approaches to food science and technology related activities.

The CYTED program develops its internationally cooperative activities by means of the following instruments, referred to as "actions":

- Thematic networks
- Research projects
- Individual members' research projects
- IBEROEKA innovation projects

The first three are developed and managed within the frame of Thematic Areas and the fourth trough the Network of Managing Bodies: IBEROEKA.

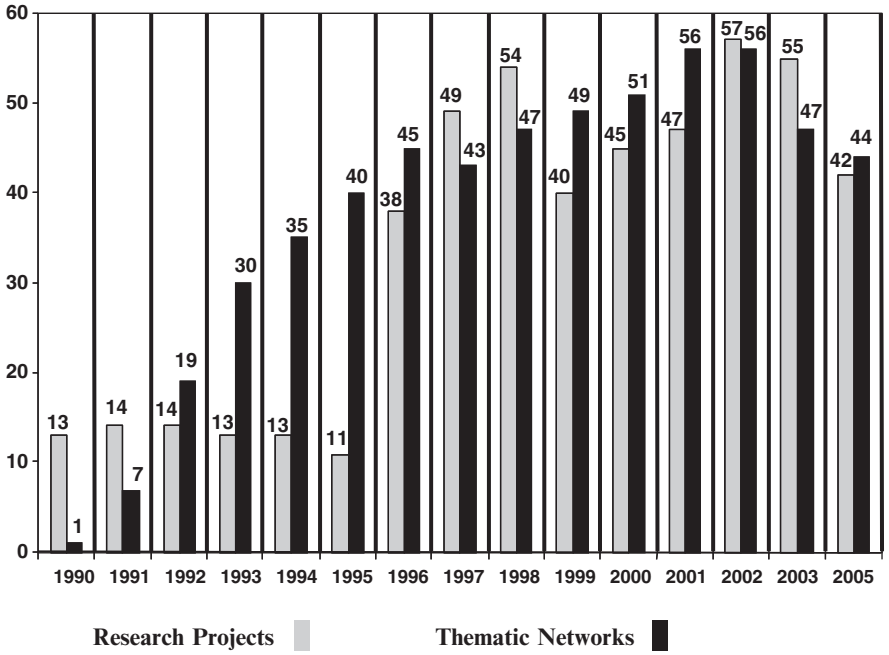

FIG. 1.1. Evolution of CYTED actions 1990–2005

The objectives of the above actions are:

- Thematic networks: to facilitate the scientific relations and the transference of knowledge among the research units of different countries
- Coordination of research projects: make it possible to obtain scientific and technological results that can improve the scientific and technological capacities of institutions and companies of the region
- Group research projects: to impel the development of the Latin American region through the generation of new products and innovative processes or services in the region
- IBEROEKA projects: to foment the cooperation of enterprises in Latin American and European markets to improve the competitiveness and position of the companies in the region.

1.1.1. Thematic Areas of CYTED

In 2005, the old structure of CYTED, which was based on subject-based subprograms, was replaced by a new scheme of thematic areas:

- Agri-food
- Health
- Promotion of industrial development
- Sustainable development
- Technologies of information and communication
- Science and society

Within the frame of the above areas, high-priority thematic lines are being financed. Proposals are generated by researchers in Latin American countries on the basis of an open call.

1.1.2. Agriculture and Food (Agri-food) Area

The CYTED Program has recognized that the agriculture and food sector must contribute scientifically and technologically to integrated productive systems in order to optimize the use of resources and to assure long-term sustainable agriculture. To achieve the last objective, biologically and chemically productive based methods are carefully chosen and evaluated, giving consideration to the protection of the environment. These integrated systems of production must provide good agronomic yields, optimal qualities of products and low levels of residues. From the commercialization point of view, production has to supply goods with added value to attract the preference of a wide sector of the population, especially of consumers aware of the importance of healthy and non-contaminating foods.

1.1.3. Agri-Food Mission

In 2005, CYTED approved the mission of this area, which is "to promote and fortify the excellence of research in production, treatment and food storage, to contribute to alleviation of security problems such as availability, distribution and safety of products, as well as to increase their added value. Also, it will seek the effective transference of research results to the population and companies, in this way supporting the sustainability of production and the improvement of the quality of life of the people of the region." The following vision to the year 2010 has been proposed.

1.1.4. Area Vision to Year 2010

The area vision to the year 2010 is stated as follows: "To be effective for development and adaptation of new technologies, as well as to improve traditional techniques in order to raise the competitive level of the agri-food sector and to increase the quality of life in Iberoamerican countries, by means of scientific and technological cooperation" within the area. To define this vision, a proposal of lines for future work has been elaborated, reflecting the intention to promote the application of technologies in the different agri-food processes (see Table 1.1)

Table 1.1. Agri-food areas: Lines of research for future work

Research lines for the future
• Modern methods of genetic improvement and animal reproduction
• Modern methods of improvement of plant reproduction
• Generation of diagnostic methods for diseases of plants and animals
• Advanced methods of food storage: Inclusion of irradiation and modern packing techniques
• Production in barren and semi-arid zones
• Functional foods
• Viable technologies for reproduction, larvae culture, nutrition, improvement of cultivation processes and pathology control in aquaculture
• Fishing biotechnology
• Food safety and traceability
• Improvement of food processing and clean technologies

1.2. CYTED Priorities in the Transition Period 2005–2006

During 2005, the transition of the old model based on subprograms to the new structure of the thematic areas was made; an open call for the financial support of proposals was launched. Given budgetary limitations, it was necessary to define high priority lines by taking into account the following points:

- The high degree of heterogeneity of scientific, technological and productive levels existing in the Iberoamerican region
- The enormous diversity of interests and potentialities between countries comprising this community
- The recommendations of groups working within the frame of CYTED in the structure of the subprograms

Criteria for decision making in relation to new financed activities:

- Scientific and technological strengths of the groups
- Regional pertinence
- Attractiveness to market
- Projection to the future
- Technical, economical and social scientific relevance
- Viability of the application of the products of the proposal (technical, economical and institutional), implicating the existence of users interested in the results
- Social impact of the cooperation in terms of contributions to solving the problems of the Latin American population

CYTED supported projects in 2005:

- Scientific and technological bases for functional food production from green banana
- Baking products for specific needs
- Development of technologies for integral handling of apple tree diseases

- Latin American network of innovation indicators and impact of science and technology in the agri-food sector

Considering the 2005 experience, it is possible to conclude that it is necessary to reinforce the evaluation process by means of peer-based evaluating processes.

Also, it was concluded that it is necessary to face the lack of experience of individual researchers and to identify partners for structuring successful financed action. It is therefore essential to improve the ways in which the formulation of proposals is carried out and to consider participants from different countries. To accomplish this task, a wide network of contacts should be formed, with the aim of increasing the proportion of researchers from countries with small scientific and technological communities.

1.3. Priorities for 2006

The year 2006 was the first year in which the new structure of CYTED was used as the framework for operation. The defined high-priority lines depicted in Table 1.2 represent the first step toward the above-mentioned vision of the CYTED program. Description of these lines is also provided in Table 1.3.

TABLE 1.2. Summary of the open lines (2006)

Research Lines	Potential Actions
• Aquaculture Viable technological alternatives to take advantage of the productive potential of the region	Thematic network or research projects
• Animal protein production New technologies for sustainable animal production that will contribute to satisfying regional needs for animal protein	Thematic network or research projects
• Processing and quality assurance of foods Technologies and procedures to improve food safety, traceability and efficiency of processing, as well as to develop new processes and products	Thematic network or coordination action on research projects
• Vegetal production systems with integrated plague handling Effective solutions to combat plagues and diseases of different cultivars, in conjunction with reduction of negative impacts on the environment	Thematic network or research projects
• Production systems for infertile semi-arid areas and soil-climatic conditions of limited productive resources Viable and sustainable productive systems that allow profitable production technologies in infertile and semi-arid zones	Associated research project

TABLE 1.3. Description of research lines 1, 2, 3, 4

Research Line 1	Aquaculture
General Objective	To develop viable technological alternatives to take advantage of the productive potential of aquaculture resources in the region
Specific Objectives	Development and application of knowledge in the following areas: • Reproduction • Yeast culture • Nutrition Improvement of agricultural production processes and pathological control: • prophylaxis, treatments and vaccines
Action	Thematic network or research projects
Research Line 2	**Animal Protein Production**
General Objective	To generate new technologies of sustainable animal production that will contribute to satisfying the needs for protein of animal origin
Specific Objectives	To develop and apply knowledge-related activities to the following areas: • Feeding systems • Handling • Genetic reproduction improvement • Animal health
Action	Thematic network or research projects
Research Line 3	**Food Processing and Quality**
General Objective	To generate technologies and procedures to improve food safety, traceability and efficiency of processing, as well as to develop new processes and products
Specific Objectives	To improve systems, processes and products to assure quality, food safety and traceability to fulfill national and international standards
Action	Thematic network or research projects
Research Line 4	**Vegetal Production Systems with Integrated Handling of Plagues**
General Objective	To generate effective solutions for the control of plagues and diseases in conjunction with reduction of negative impacts on the environment
Specific Objectives	To develop and apply knowledge to develop different strategies for integrated handling of plagues such as: • Biological controls • New agronomics practices • Genetically modified seeds • Rational use of plague control agents
Action	Thematic network or research projects

(continued)

TABLE 1.3. (continued)

Research Line 5	Production Systems for Infertile, Semi-arid Zones and Soil-climatic Conditions of Limited Productive Resources
General Objective	To develop viable and sustainable productive systems that allow profitable production of foods in infertile and semi-arid zones
Specific Objectives	To develop new technologies and integral solutions for production under drought conditions
Action	Research project

As a complement to the actions mentioned in Table 1.2, training activities are also being carried out based on courses in which the possibilities of collaboration within other bodies, particularly the Spanish Agency of Cooperation with Iberoamerican Countries, are described.

1.4. Conclusions and Perspective

CYTED can generate new areas for scientific and technological cooperation in the Latin American region. This action will depend on the way in which the scientific community defines multilateral cooperation activities. Food production and distribution activities are subject to a process of transformation due to advances in biological sciences and new and emerging technologies, as well as innovations in logistics. New consumer demands are appearing, given the changing needs of the population and commercial pressures imposed by international regulating agencies.

Latin American countries cannot simply observe innovative tendencies; they must be reactive to modernity, and for this reason, the systematic and joint participation of researchers, producers and international agencies must be induced. The CYTED program can act as a catalyst for innovation in the agri-food sector, thanks to the formation of a valuable network of scientists and technologists. This network must be extended and renewed continuously, as this ongoing process constitutes the basis for the formulation of networks and projects. Nowadays, any specialist of the region can initiate and submit a proposal for a financed action in CYTED. Although the program has a highly ranked benefit-to-cost ratio, it also has a tendency toward growth and not to mature; therefore, it will only be possible to meet the challenges faced by the agri-food area by increasing cooperative actions and interchange of experiences among individuals. As CYTED becomes more visible, it will attract more attention from governments and politicians. It is also necessary to go beyond academic circles by entering into industrial scenarios. The level of participation of the various components of scientific

cooperation, innovation and transfer of technology must be increased; institutions of higher education and research, farmers, agricultural commodities producers, food companies, public institutions, non-government organizations and international agencies for agricultural development must all become more involved.

Finally, to reinforce the financial strategy, it is important that CYTED extend its network of strategic alliances. The relationship of CYTED with regional science and technology organizations has produced very good results. The key to consolidate this strategy is to increase the resources directed to CYTED action and to gradually turn CYTED into a constructor of networks that will contribute to an integrated approach to food science and technology related activities.

2
Food Sterilization by Combining High Pressure and Thermal Energy

G.V. Barbosa-Cánovas and P. Juliano

2.1. High Pressure Processing: An Industrial Reality

High pressure processing (HPP) is an industrially tested technology that offers a more natural, environmentally friendly alternative for pasteurization or shelf life extension of a wide range of food products (Welti-Chanes et al., 2005). Commercial high pressure, low temperature methods achieve inactivation of vegetative microorganisms by subjecting vacuum-sealed food in flexible packaging to treatment at hydrostatic pressures of 600 MPa (or less) and initial temperatures lower than 40°C for one to fifteen min depending upon the product application. The use of lower temperatures has allowed better retention of sensory attributes characteristic of "fresh" or "just prepared," as well as food nutritional components (Cano and de Ancos, 2005). As a result, HPP has become a post packaging technology convenient for foods whose quality would otherwise be altered by heat pasteurization.

Among many advantages, HPP can add significant value to low-cost or heat-sensitive raw materials and other prepared foods. Furthermore, similar quality levels can be reached when processing large volumes or larger samples. Different from heat penetration, hydrostatic pressurization allows "instant" pressure transmission in fluids and semisolids within the pressure vessel, thereby achieving reduced product damage from lower temperatures. Moreover, HPP can add significant shelf life to an existing refrigerated product (Hjelmqwist, 2005). In fact, it has the potential to deliver chemical- or additive-free products with minimum impact on shelf life.

Like any other food preservation processes, HPP is product specific, making shelf life extension dependent on food composition, the presence of enzymes, and on the actual bacterial species/strains present in a given food factory. Another use of HPP is in texture modification of foods with high protein content.

Tenderized meats and modified dairy or egg-based ingredients of varied functionality are some examples of the benefits observed in texture modification (Montero and Gómez-Guillén, 2005; Guamis et al., 2005).

The US Food and Drug Administration (FDA) and Department of Agriculture (USDA) have approved HPP as a post package pasteurization technology for

manufacture of shelf-stable high-acid foods and pasteurized low-acid food products, and developed guidelines and regulations for those products (21CFR114 and 21CFR113). Furthermore, the European Commission on food regulations has adapted existing legislation on novel foods to products processed by HPP (EC258/97; European Commission, 2002; Barbosa-Cánovas et al., 2005a).

The term "pasteurization," originally specifying the destruction of non-spore-forming foodborne pathogens by heat, has been extended to HPP and other validated pathogen-lethality technologies. Members of the National Advisory Committee on Microbiological Criteria for Foods (NACMCF, an advisory group chartered by the USDA's Food Safety and Inspection Service, the FDA, the Centers for Disease Control and Prevention, the National Marine Fisheries Service, and the Department of Defense Veterinary Service Activity) have jointly established this revised definition of pasteurization, providing specific considerations for a number of thermal (cooking, microwave processing, ohmic/inductive heating, steam and hot water treatments) and nonthermal (HPP, UV radiation, pulsed electric fields, etc.) preservation processes (NACMCF, 2004; 2005).

Moreover, the FDA and USDA have promoted the implementation of Good Manufacturing Practices (GMP) as well as procedures for Hazard Analysis and Critical Control Point (HACCP) in HPP production facilities for refrigerated or pasteurized foods to ensure product safety. A food safety management standard that can be implemented when designing an HPP factory has also been developed by the International Standardization Organization (ISO) (Tapia, et al. 2005; Surak, 2006).

High pressure processing provides new opportunities for the food industry to develop new products for consumers. About 80 full scale HPP units in the world are run by 55 companies worldwide (Leadley, 2005; Hendricks, 2005). Most applications in Europe are in Italy, Spain, and Portugal, whereas others are spread around the United States, Mexico, and Japan. A number of companies are forming consortia to develop new products and new applications using high pressure technologies, such as low-acid food sterilization (de Heij et al., 2005). Among these companies are Kraft, Hormel, Unilever, Basic American Foods, Stork Food and Dairy Systems, Washington Farms, ConAgra, and Avomex.

HPP has demonstrated strong potential for the delivery of a wide range of high quality chilled products with extended shelf life. Among these, rare and cooked meats, fruits, vegetables, fresh herbs, and a variety of products prepared with these ingredients can be mentioned. Some of the products already commercialized in the worldwide market (Table 2.1) are fresh-like foods (e.g., new varieties of avocado products and juices) and ready-to-eat (or heat and serve) meat/meals. The food industry has shown interest in using HPP technology for the development of modified dairy-based items (desserts, puddings), sauces and savory foods, whole muscle meats (partially precooked), and for the improvement of shucking efficiency and seafood safety.

HPP technology, as commercially defined today, is unable to produce low-acid shelf stable products, since bacterial spore inactivation requires high pressures of at least 800–1700 MPa at room temperature, far in excess of what is commercially

TABLE 2.1. High pressure commercial chilled products (adapted from NC Hyperbaric, 2004)

Product types	Countries*	Shelf life achieved (4°C to room temperature)
Juices and beverages	Japan, France, Mexico, USA, Lebanon, UK, Portugal, Italy, Ireland, Czech Republic	21 d. to 12 mo.
Vegetable products	Japan, USA, Italy, Canada	1 to 6 mo.
Meat products	Japan, Spain, USA, Italy	21 d. to 2 mo. (cooked products)
Seafood products	Japan, USA, Australia, Canada, Spain	10 d. to 2 mo.

*Countries are listed in order of product appearance in the market

feasible (Farkas and Hoover, 2000; Leadley, 2005). Even foods with pH lower than 4.5 require refrigerated storage and other preservation hurdles to prevent enzymatic degradation reactions and to inhibit spore germination. It was not until the early 1970s when studies on *Clostridium* species demonstrated the need to combine pressure and heat to achieve spore inactivation (Sale et al., 1970; Heinz and Knorr, 2001). Furthermore, inactivation data on *C. botulinum* spores date from the late 1990s (Rovere et al., 1998; Reddy et al., 1999; Heinz and Knorr, 2001), where pressures in the range of 690 to 900 MPa were combined with initial temperatures between 50 and 70°C. The following section will provide an in depth description of the potential application of high pressure combined with heat in commercial sterilization.

2.2. High Pressure Thermal Sterilization

High pressure high temperature (HPHT) processing, or pressure-assisted thermal processing (PATP), involves the use of moderate initial chamber temperatures between 60°C and 90°C in which, through internal compression heating at pressures of 600 MPa or greater, in-process temperatures can reach 90°C to 130°C. The process has been proposed as a high-temperature short-time process, where both pressure and compression heat contribute to the process's lethality (Leadley, 2005). In this case, compression heat developed through pressurization allows instantaneous and volumetric temperature increase, which, in combination with high pressure, accelerates spore inactivation in low-acid media. Several recently developed patents show a number of approaches for the attainment of commercial food sterility in selected low-acid foods (Meyer et al., 2000; Wilson and Baker, 2000; van Schepdael et al., 2002; März, 2002, 2003; Wilson and Baker, 2003; Cooper et al., 2004). Some of these microbial spore inactivation approaches proposed combining (de Heij et al., 2003; Leadley, 2005): (a) two low pressure pulses at 200–400 MPa (the first one for spore germination and the second for germinated cell inactivation); (b) a low pressure pulse at 200 to 400 MPa for spore germination followed by a thermal treatment at 70°C for 30 min for vegetative cell inactivation; (c) package preheating above 75°C and pressurization at 620 to 900 MPa for 1 to

20 min; and (d) package preheating above 70°C and applying two or more pulses at 400 to 900 MPa for 1 to 20 min.

Three of the above-mentioned approaches have proven inconvenient from either a microbiological or an economical perspective. When applying low pressures between 200 and 400 MPa, combined with moderate temperature [cases (a) and (b)], residual dormant spores have been detected after treatment (van Opstal et al., 2004; Leadley, 2005), making this option unlikely for a commercial process. Moreover, a high pressure multiple pulse approach [case (d)] is not recommended, as additional cycles decrease equipment lifetime and increase maintenance costs (de Heij et al., 2003). Hence, application of a single pulse above 600 MPa for 5 min or less [case (c)], combined with initial temperatures above 60°C, would be more cost-effective and a safer approach for industrial purposes (de Heij et al., 2005). As will be explained later, success of this processing approach depends on the efficient use of compression heat in achieving nearly adiabatic conditions.

2.2.1. Advantages of HPHT Processing

Recent publications claim that the main advantage of HPHT treatment is its shorter processing time compared to conventional thermal processing in eliminating spore-forming microorganisms (Fig. 2.1; Matser et al., 2004).

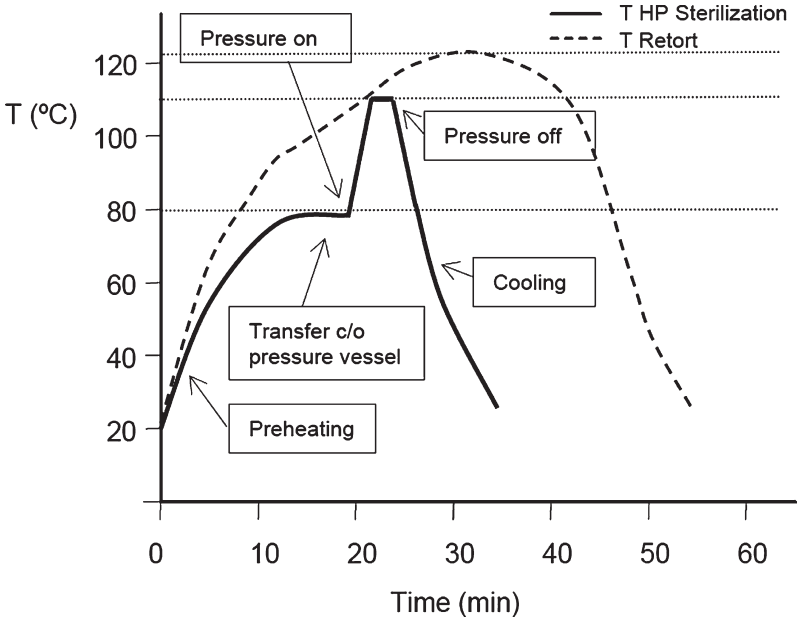

FIG. 2.1. Typical product temperature profiles in a retort and HPHT process. Processing steps during pressurization

This shorter process time and ultimate pressurization temperatures lower than 121°C have resulted in higher quality and nutrient retention in selected products. For example, better retention of flavor components in fresh basil, firmness in green beans, and color in carrots, spinach and tomato puree have been found after HPHT processing (Krebbers et al., 2002; Krebbers et al., 2003). Nutrients such as vitamins C and A have also shown higher retention after HPHT processing in comparison to retort methods (Matser et al., 2004).

One more benefit of HPHT processing is its use to process non-pumpable foodstuffs like soups containing solid ingredients such as noodles, barley, and/or cut-up vegetables and meat (de Heij et al., 2005).

As mentioned earlier, high pressure low temperature processing provides direct product scale-up and higher efficiency for larger volumes of food, compared to thermal processing, due to "instant" hydrostatic pressure transmission. Similarly, HPHT processing is suitable for larger sizes, as compression heating to high temperatures is instantly achieved throughout the entire package volume. Nevertheless, the preheating step, or the period of time necessary to reach initial product temperature before pressurization, needs to be considered when evaluating overall processing time. A long preheating time, especially in a large container, may lower product quality retention at the end of the HPHT process.

Although the HPHT process can be seen as advantageous due to its shorter time, lower processing temperatures cannot yet be assured for *C. botulinum* inactivation until optimal temperature/pressure/time combinations are identified. Section 2.5 will highlight some of the latest findings in terms of HPHT processing conditions required for *C. botulinum* and surrogate inactivation.

2.2.2. Potential HPHT Processed Foods

Production of shelf stable foods intended for outdoor, military, or humanitarian use has shown a tremendous increase since the late 1970s, when the concept of Meals Ready-to-Eat (MRE) packed in flexible plastic retort pouches was introduced (Mermelstein, 2001; Hirsch et al., 2005). However, the quality and nutrition challenges encountered in the development of certain foods have led to considering alternative manufacturing processes. There are a number of foods that cannot be turned into shelf-stable products by means of retort processing due to the non-acceptable or low quality values obtained after long exposure to high heat. Nonetheless, some of these foods show potential for commercial sterilization using HPHT treatment.

Products stabilized using HPHT processing can be categorized as long-life, chill- stable, and shelf-stable. The chill-stable category includes meat snacks, vegetables, and ready-to-eat meals, or heat and serve meats, among many products (Franceschini et al., 2005).

Potential HPHT shelf-stable products may include egg-based breakfast items, meat joints, pot roasts/stews, high quality soups, ready-to-drink teas/coffees, dairy desserts/smoothies, cheese/cream sauces, low-acid pasta sauces, high quality fruits/vegetables, and liquid flavors/herbs (Stewart, 2005).

The quality, acceptability, and nutritional value of these products will not only depend on the developed formulation, but also on the design of the process, i.e., the preheating equipment, the high pressure system, and the packaging material chosen.

2.3. Developing a High-Pressure High-Temperature System

A high-pressure system designed for commercial sterilization purposes must at least be able to withstand high pressures within the range of 600–800 MPa, chamber temperatures up to 98°C, and retain product temperatures created during compression up to 130°C. This can mainly be accomplished by building a pressure chamber of appropriate thickness, adapting an insulated polymeric liner with a sample carrier, and a pumping system that rapidly injects preheated compression fluid. Sections below will describe in more detail requirements for existing pressure systems working at HPHT conditions.

2.3.1. Available Equipment and System Requirements for HPHT Conditions

A typical batch high-pressure machine system is made of a thick wire-wound cylindrical steel vessel with two end closures, a low-pressure pump, an intensifier that uses liquid from the low-pressure pump to generate high-pressure process fluid for system compression, and necessary system controls and instrumentation (Farkas and Hoover, 2000). For HPHT processing (or pressures over 400 MPa), pressure vessels can be built with two or more concentric cylinders of high tensile strength steel. The outer cylinders compress the inner cylinders such that the wall of the pressure chamber is always under some residual compression at the design operating pressure. In some designs, cylinders and frame are prestressed by winding layer upon layer of wire under tension. The tension in the wire compresses the vessel cylinder so that the diameter is reduced (Hjelmqwist, 2005). This special arrangement allows an equipment lifetime of over 100,000 cycles at pressures of at least 680 MPa. The preferred practice is to design high-pressure chambers with stainless steel food-contacting parts so that filtered (potable) water can be used as the isostatic compression fluid (Farkas and Hoover, 2000).

During pressurization at high temperature conditions, a temperature increase is produced in both the compression fluid and food (Ting et al., 2002). However, since compression heating in the system steel vessel is almost zero (Ting et al., 2002; de Heij et al., 2003), there is heat loss toward the chamber wall. In theory, heat generated by compression is dissipated by a combination of conduction and convection within the pressurizing fluid in the chamber and transfer of heat across the chamber wall into the surroundings (Carroll et al., 2003). Heat dissipation may cause cooling down of the sample during both come up and holding time, which may thereby decrease spore inactivation effectiveness (de Heij et al., 2002; Ardia et al., 2004). Thus, it is important to avoid heat loss through the chamber system.

A number of high-pressure systems specified for high pressure (600–1000 MPa) and high temperature (130°C) have been developed. There are several designs for vessel volumes ranging from micro/laboratory scale (0.02-2 L) to pilot scale (10–35 L). However, not all systems fulfill equal requirements in terms of pumping speed, compression-heat retention, and type of compression fluid used (Balasubramaniam et al., 2004). In most cases, vessels are heated to initial temperature by means of an internal heater (jacket or coils), which also controls the temperature. However, this is not enough to retain compression heat generated during pressurization.

Modern systems are required to use several features for heat loss prevention by mainly: (a) adapting a dense polymeric insulating liner with a free moving piston at the bottom or valve to allow adequate pressure transmission; (b) preheating the inflowing pressurization fluid and pipes; and (c) preheating the vessel at a temperature higher than the initial fluid/sample temperature. Successful installation of these features can make the system close to adiabatic and, in this way, maximize preservation efficacy at chosen HPHT conditions.

High pressure vessels insulated from the interior by means of a cylindrical liner can prevent heat losses through the steel structure. In this case, a material with low thermal conductivity (less than 1 W/m/K) is required as part of the vessel design (de Heij et al., 2003). This product container (5 mm or more in wall thickness) can be made of polymeric materials such as dense polypropylene, polyoxymethylene, polyetheretherketone, or ultra-high-molecular-weight polyethylene to provide intended heat retention (de Heij et al., 2003). Compression heating rates of these materials have not yet been determined; however, empirical testing has proven their benefit for heat loss prevention. Fig. 2.2 shows the

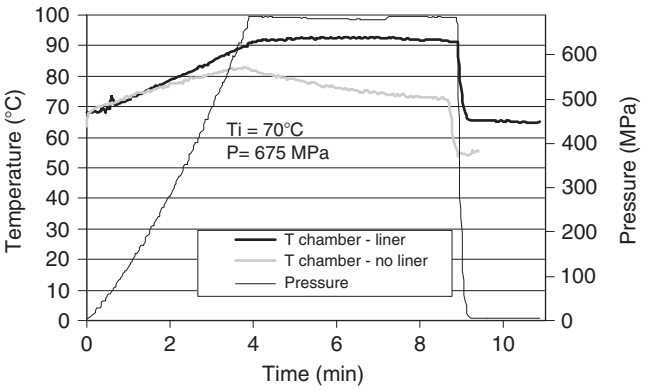

FIG. 2.2. Temperature profiles of pressurized water at 70°C initial temperature and 680 MPa when: a) compressed water is in pressure vessel; b) compressed water is in preheated polypropylene liner. Data was extracted from a cylindrical liner (internal diameter 75 mm, external diameter 100 mm, height 21.5 mm) made with a movable lid inserted into a 1.7 L high pressure chamber (Engineered Pressure Systems, Inc., model #914-100, Haverhill, MA)

temperature profile of water in a white polypropylene liner (25 mm wall thickness) during pressurization in a 1.7 L vessel.

Some laboratory scale systems require using compression fluid mixtures such as food-approved oil or water containing FDA- and USDA-approved lubricants, and anti-corrosion agents. Water solutions of castor oil, silicone oil, and sodium benzoate are sometimes used as pressure-transmitting fluids (Ting et al., 2002). For HPHT processing of foods, typical fluids used in pressure vessels include water with glycerol, edible oils, and water/edible oil emulsions (Meyer et al., 2000). High compression heating of oil-added compression fluids can be of aid for additional compression heating retention. However, for commercial purposes, the use of potable water is the most recommended compression medium.

Pressure vessel size also plays an important role in the compression heating retention (Ting et al., 2002), since larger size non-insulated vessels have been shown to retain more heat during holding time (Hartmann and Delgado, 2003). At least three 35 L pilot sterilization units have been built in the world, each designed by Avure Technologies (USA, The Netherlands, Italy, and Australia), and no machine has yet been designed for industrial use. The latest 35 L vessel design receives compression water from the intensifier after being passed through an ultra-high pressure heater to reach initial target temperature. Another heat retention aid is the addition of preheated water from a fill tank once the product carrier, which is inserted into a cylindrical polymeric liner, is placed inside the vessel to avoid residual air after chamber closure. A series of automatic controls recirculate water prior to starting pressurization to assure that initial target temperature is reached in both the compression fluid and samples.

Ideally, a proper HPHT system requires thermocouples that provide reliable in-package temperature readings during the pressurization process. For this purpose, unpublished research has been performed by high pressure equipment manufacturers, who have screened thermocouples for types K (chromel/alumel), J (iron/constantan), and T (copper/constantan) in terms of accuracy, precision, and signal response, when exposed to HPHT conditions. Furthermore, systems that hermetically fix thermocouples inside the pouches are being tested. There are also pH measurement devices being developed to work under HPHT conditions.

The stage after pressure release is also an important part of the process. Assuming that spore inactivation depends on preheating and pressurization steps, it is important to optimize the cooling phase in order to prevent overheating and to maximize quality retention. In this case, samples can immediately be removed and transported into a turbulent low temperature water bath at the end of the pressure cycle.

2.3.2. HPHT Processing and Critical Steps

A single pulse HPHT process involves six main process time intervals: (i) sample vacuum packaging and product loading, (ii) preheating to target temperature, (iii) product equilibration to initial temperature, (iv) product temperature increase to pressurization temperature by means of compression heating, (v) product temperature

decrease during decompression, and (vi) product cooling to ambient temperature. Each of these steps (illustrated in Fig. 2.3) marks the temperature evolution of the process. However, reaching the preheating target temperature inside the food, maintaining it up to the pressure pump starts, achieving constant target pressure, and retaining heat inside the product during pressure come up and holding time are all critical to achieving consistent product sterility.

When looking at the overall process flow chart (Fig. 2.3), two main control points can be distinguished as critical to safety: preheating and pressurization. As observed before, target pressurization temperature in all pouches inside the chamber or liner, as well as in all parts of the food, depends on the target preheating temperature before pressure is initiated. As a result, process variables must be controlled in different sections of the preheating/pressure system to assure that conditions required for spore inactivation are met.

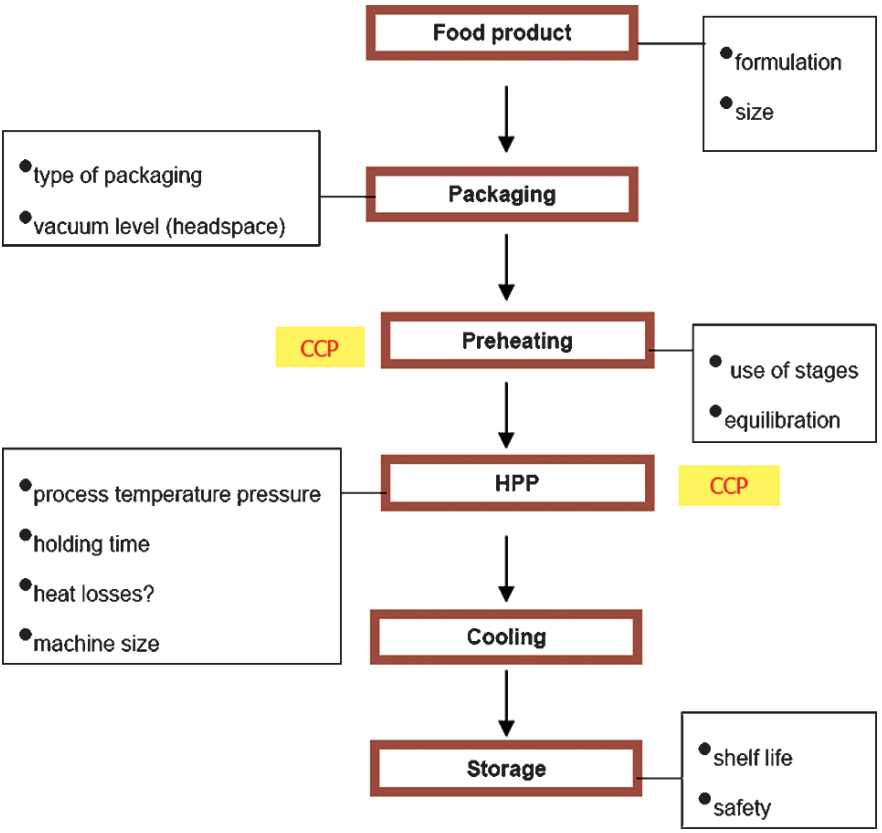

FIG. 2.3. Flow chart of HPHT process showing critical control points (CCP) for food safety as well as other process variables

2.3.2.1. Critical Factors

During an HPHT process, the amount of heat received is determined by three main conditions: target preheating/equilibration temperature, selected pressure, and pressure/temperature holding time. Furthermore, there are other inherent factors such as the presence of lower temperature sites in the vessel, pressure come up rate, pressure holding, decompression rate, and food/package properties. All need to be accounted for when evaluating sterilization performance.

2.3.2.1a. Temperature Distribution. In terms of temperature distribution within a non-insulated system, "cold spots" are located close to the vessel wall. This may cause the product fraction located near the wall to cool down and not match the final temperature obtained at the center of the vessel (de Heij et al., 2002; Ting et al., 2002; Otero and Sanz, 2003; Ardia et al., 2004).

Another factor influencing vessel temperature distribution is the (preheated) liquid entering the vessel (2-30 mL, depending on vessel dimensions), which can cool down the transmission fluid located inside the vessel.

Three-dimensional numerical simulations have illustrated temperature gradients created by incoming fluid at the entrance of the vessel (Hartmann and Delgado, 2002).

In order to decrease cooling caused by the inflowing pressurizing fluid, the system can be modified according to the following (de Heij et al., 2003; Balasubramaniam et al., 2004): (a) An internal pressure intensifier can be incorporated to decrease the amount of liquid entering the machine; (b) the pressurizing fluid, the high-pressure pipes, and the external intensifier system in the high-pressure pump can be preheated to a higher initial temperature; and (c) insulation with a special liner can be added to prevent contact between packages and entering fluid. These solutions can be executed according to (i) the pressure vessel dimensions, (ii) the initial temperature specified for the preheating system, (iii) the compression fluid used by the specific machine, and (iv) the intensifier system, including the incoming fluid. If all processing aids are simultaneously applied, temperature loss during come up and holding times can reach a minimum. However, up until now there has been no existing equipment that can guarantee a heat retention efficiency of 100%.

The difference between the temperature of the fluid/package system before and after high-pressure processing can indicate the extent of heat loss during processing (Ting et al., 2002). Thus, based on what was discussed above, the following parameters can be used to account for the overall process performance concerning product safety:

- Target preheating/equilibration temperature
- Target temperature at maximum (constant) pressure
- Temperature at the end of holding/pressurization time
- Temperature at the end of pressure release

Rates of preheating, compression (pressure come-up time), and cooling can be associated with the process performance in terms of processing time, or time of exposure of the food package to high heat.

2.3.2.1b. Pressure come-up time. The pressure rise period has proven important concerning spore inactivation, since bacterial spores can be inactivated at zero holding time when combined with temperature (Koutchma et al., 2005). In this case, come-up time, or compression rate, is determined by setting the power of the low-pressure pump (driving the intensifier) and the target process pressure (Farkas and Hoover, 2000; Balasubramaniam et al., 2004). For a specific process, variability in the compression rate must be determined and tolerance should be specified for the inactivation process. Moreover, effects on compression rate variation in spore inactivation are still unknown, and its determination could help establish a compression rate tolerance.

2.3.2.1c. Constant Pressure. Maintaining a constant pressure during pressurization is also essential for compression heat retention. In modern high-pressure systems, pressure intensifiers and automatic pressure control maintains pressure constant during the holding time. High-pressure equipment allows controlling pressure within ± 0.5% (e.g., ± 3.4 MPa at 680 MPa) and recording it to the same level of accuracy (Farkas and Hoover, 2000).

2.3.2.1d. Decompression Rate. It is unclear whether the decompression rate is critical for spore inactivation. However, from a process efficiency perspective, it would be desirable to achieve ambient pressure recovery in the shortest possible time. Control of decompression rate should be recommended based on the results of the effect of pressure-release rate on spore inactivation, which is still unknown. Single stroke intensifiers may be used to control the decompression rate of a system (Farkas and Hoover, 2000).

2.3.2.1e. Food Package-related Factors. Factors that are food-related include the package dimensions and weight, food molecular properties (pH, composition, water activity), and thermophysical/structural properties (volume, shape, density/porosity, compressibility, specific heat, thermal expansion coefficient). Variation of these properties may affect temperature uniformity in the treated food. Uniform initial target temperature of the food sample is desirable to achieve a uniform temperature increase in a homogenous system during compression (Farkas and Hoover, 2000; Meyer et al., 2000). Non-homogeneities in terms of composition, presence of food pieces, or uneven preheating (e.g., from microwaves) may affect the temperature distribution during pressurization. Hence, it is important to analyze and quantify the effect of each factor on the overall process performance and to evaluate the most critical ones.

2.3.3. Compression Heating in HPHT Processing

In general, compression/decompression temperature and pressure curves are nearly linear and, therefore, compression rate can be assumed constant for a given time interval. Once target temperature is fixed, a constant compression rate should provide a constant compression heating. However, as indicated by the

compression heating equation (Eq. 2.1), this will depend on how the volumetric expansion coefficient α_p (1/K), the density ρ (kg/m^3), and the isobaric heat capacity C_p (J/kg.K) of both the food and liquid will change during pressurization time (Carrol et al., 2003).

$$\frac{dT}{dP} = \frac{T\alpha_p}{\rho C_p} \tag{2.1}$$

where T is the temperature (K) of the food or compression fluid.

Both the temperature of the product and compression fluid may rise 20–40°C during high-pressure treatment, whereas, as stated before, the steel pressure vessel is not subjected to significant compression heating (de Heij et al., 2002; Ting et al., 2002). As shown in Fig. 2.4, several food components provide variable compression heating rates. Therefore, temperature increase may vary in foods with relatively complex composition. In fact, the compression heating rates of fats and oils can be up to three times higher than in water (Ting et al., 2002; Rasanayagam et al., 2003).

Not much data has been reported on the compression heating rate for food products at HPHT conditions. Balasubramaniam et al. (2004) reported compression heating of water at 4.0, 4.6, and 5.3°C/100 MPa and initial temperatures of 60, 75, and 90°C, respectively. However, Rasanayagam et al. (2003) observed little or no increase in compression heating in oils and fats due to higher initial temperature.

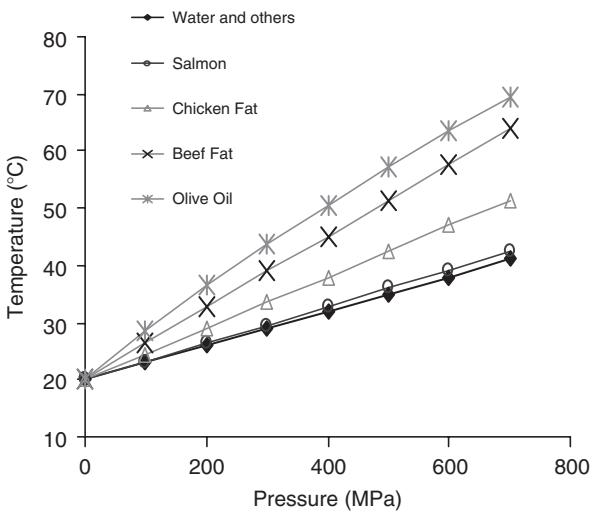

FIG. 2.4. Temperature elevation from room temperature due to pressurization up to 700 MPa (modified from Barbosa-Cánovas and Rodríguez, 2005)

Equation (2.1) has been applied using small pressure intervals of ΔP (around 10 MPa) to predict compression heating of water in the range of 0.1 up to 350 MPa and initial temperatures of 22 and 62°C (Otero et al., 2000). The authors reported the decompression cooling rate (rather than compression heating) after holding time, and good agreement was found with experimental data when using values for ρ, α, and C_p taken from the literature (Ter Minassian et al., 1981). Moreover, Ardia et al. (2004) predicted temperature rise in water, sugar solutions, and orange juice by comparing data from the National Institute of Standards and Technology (NIST) (Harvey et al., 1996) and experimental measurements done in a high pressure machine. They found no significant deviations between NIST and experimental results for water obtained from the Multivessel Model U111 (Unipress, Warsaw, PL) for distilled water, even at sterilization conditions (initial liquid temperature of 80°C at 600 MPa).

For predictions in sugar solutions and orange juice, Eq. (2.1) was rewritten using α for water and implementing NIST formulations for the regressive calculation of each property (Eq. 2).

$$\Delta T = \int_{P_0}^{P_1} \frac{\alpha}{\rho_{mixture} . C_{pmixture}} \cdot T \cdot dP \tag{2.2}$$

For sugar solutions, mixing rules (Eqs. 2.3 and 2.4) were used to express density and the specific heat of a pure solid/water mixture, $\rho_{mixture}$ and $C_{p\ mixture}$, as a function of temperature:

$$\rho_{mixture} = \left[\frac{[W]}{\rho_{water}} + \frac{[S]}{\rho_{solid}} \right]^{-1} = \left[\frac{[W]}{\rho_{water}} + \frac{[S]}{\left[\frac{1587.9}{1 + 0.000107(T-15)} \right]} \right]^{-1} \tag{2.3}$$

$$C_{p\ mixture} = [W] \cdot C_{p\ water} + [S] \cdot C_{p\ solid} = [W] \cdot C_{p\ water} + [S] \cdot \xi \cdot (1622 + 7.125 \cdot T) \tag{2.4}$$

where [W] and [S] are the relative amounts of water and solid (in mass or volume percentage, respectively). Since mixing rules equations are applicable at ambient pressure, an empirical correction factor was used to correctly fit the experimental results for $C_{p\ mixture}$:

$$\xi = \frac{C_{p\ water}(T, 0.1\ MPa)}{C_{p\ water}(T, p)^{0.75}} \tag{2.5}$$

where the numerator is represented by C_p of water calculated at atmospheric pressure and the denominator denotes C_p of water at higher pressure conditions.

Ardia et al. (2004) found no significant deviations for sugar solutions in the range of 0.1 to 600 MPa, while good continuity was found when extrapolating between 600 and 1400 MPa. When simulating the heat of compression in orange juice with a 9% solid content, no evident deviations from measured temperature were detected. Thus, the model produced satisfactory and reproducible compression temperature rise even at sterilization conditions. This means that the α, ρ, and C_p values of pure water determined from the NIST database were also accurate for predicting the increase in temperature, even at sterilization conditions (Eq. 2.2).

2.3.4. Packaging for HPHT Processing

Packaging materials selected for shelf-stable products must meet a number of requirements in terms of seal strength, overall integrity, and barrier properties to oxygen and water vapor. However, little is known about the effect of HPHT conditions on polymeric laminates. Recent studies have found that aluminum foil laminated retort pouches designed to withstand a temperature of 121°C may delaminate and blister after a thermal pressure process, particularly at chamber temperatures >90°C and >200 MPa (Schauwecker et al., 2002; Caner et al., 2004).

Delamination during pressurization has been mainly observed in areas in contact with trapped air (undergoing higher compression heating) and in folded parts (suffering higher localized stress at hydrostatic compression). Some researchers claim that HPHT conditions decompose portions of the adhesive layer, causing other layers (e.g., polyethylene and foil laminate in retort pouches) to separate. Research on several laminates to identify packaging materials suitable for HPHT conditions is ongoing. Special attention is being given to the effect of HPHT treatment on packaging components and the contribution of air retained in packages (or headspace) to delamination.

Another aspect to consider about a packaging material is its behavior as a barrier to heat and pressure transfer. During preheating and cooling steps, the container material constitutes an intermediate barrier in the transfer of heat from the heating medium into the product and from the product to the cooling medium. The thickness of the material, as well as its thermal diffusivity, can affect the rate of heat conduction to (or from) the product during preheating (or cooling). During the pressurization stage, packaging material such as polypropylene has been shown to act as an insulating barrier, preventing heat loss from the product (Hartmann and Delgado, 2003). Other than the laminate composition and thickness, the headspace left inside the package as well as internal stresses from the vacuum created are additional factors to consider in the transfer of pressure and heat.

2.4. Preheating Step: Design and Quality Optimization

Correct performance of the preheating step is critical to ensure that the temperature of the food product matches the target initial temperature. As already mentioned, a uniform initial target temperature throughout the food sample is desirable to

achieve a uniform temperature increase in a homogenous system during compression (Farkas and Hoover, 2000; Meyer et al., 2000). If "cold spots" are present within the food, some areas in the product will not reach the target process temperature during pressurization, thereby posing a safety risk in those areas with lower temperature (Meyer et al., 2000). However, an extended preheating time can also affect the quality characteristics of the food product, so in order to maximize quality retention, it is desirable to minimize the duration of preheating needed to reach the target initial temperature (Barbosa-Cánovas et al., 2005b; Juliano et al., 2006b).

2.4.1. Preheating Design for Optimal Quality Retention

Several alternatives have been proposed to save preheating time, for example, the use of still water baths set at temperatures higher than the target temperature, and other heat transfer aids such as steam, steam injection in water, water circulation pump systems, or dielectric heating (Hoogland et al., 2001; Juliano et al., 2006b). However, care must be taken when adopting faster preheating methods, as they can affect initial temperature distribution within the food package. Since faster preheating methods provide less uniformity, they require a longer time for equilibration to achieve temperature homogeneity.

In practice, carrier operation time can be reduced by using a two-stage preheating approach, i.e., by having samples preheated at a lower temperature in a separate vessel. In this case, the sample should undergo two equilibration steps: (1) equilibrating in a still water bath at a lower temperature (e.g., 60°C) and (2) placing samples in a carrier, preheating up to target temperature, and equilibrating at target temperature. An alternative approach in step 2 is to preheat the food to a temperature greater than the target temperature. This will shorten equilibration time and assure that all parts of the food reach the initial temperature (Barbosa-Cánovas et al., 2005b). In both cases, two-stage preheating could result in improved productivity, especially in larger packages. Choosing this approach will depend on product composition and its sensitivity to long-time exposure to moderate temperatures. As will be discussed further, the dimensions and thermal properties of the test sample and vessel determine equilibrium time (step 2) inside the chamber (Balasubramaniam et al., 2004).

2.4.2. Factors Affecting Preheating

Factors related to package geometry, product characteristics, and heating system can affect preheat time (NFPA 1985) and are organized in Table 2.2 for each element in the preheating system.

In thermal processing, pouches usually have a slab geometry design to achieve a more rapid heat penetration due its thin profile and high surface-area-to-volume ratio (NFPA 1985). Therefore, container thickness can be considered the main factor affecting heating rate. If containers are placed in hot water, the water vapor released and residual gas retained inside may expand the container, altering its

TABLE. 2.2. Factors affecting heat transfer during preheating of packaged foods

Process variable	System element	Process factors	Parameters
Fluid temperature	Preheating system	• Type of system • Ratio of fluid mass:product mass (number of packages) • Racking system (separation between container, circulation between layers, package restraint to specified thickness) • Heat transfer aids (steam, steam/vapor, microwaves, radiofrequencies, circulation pumps)	• Heat transfer coefficient • Heating rate
Target preheating temperature	Container geometry	• Packaging material (composition, thickness) • Package thickness • Fill weight • Sample confining system (racks, trays, cassettes) • Container headspace (amount of air in the package) • Container shape • Distribution of food particulates	• Package thermal diffusivity* • Time to reach target temperature • Temperature equilibration time
	Product characteristics	• Composition of ingredients • Particulate size • Soluble solids • Physical state (fresh/cooked, liquid, semisolid, frozen) • Food structure (homogeneity) • Occluded gases • Viscosity	• Product thermal diffusivity*

*Thermal diffusivity γ is known as the ratio of the heat conducted to the heat stored and is calculated using the following expression: $\gamma = k/(\rho\ C_p)$, where k is the thermal conductivity, ρ is the specific density, and C_p is the specific heat

thickness. In retort processing, thickness is controlled with overpressure, which also ensures seal integrity. In an HPHT process, internal product temperatures can be as high as 90°C in preheating systems, in which case, package thickness can be controlled by other physical means. For example, polymeric racks, grid trays, and cassettes can be specially designed to hold the container in place, avoiding sample mobility and maintaining pouch thickness.

In laboratory scale HPHT processes, samples are generally preheated in selected baths in a carrier and immediately transferred inside the liner for product equilibration. This liner can later be located inside the high pressure machine for

subsequent pressurization. Another option, currently used in pilot scale vessels, is to directly perform preheating inside the liner, while having samples stacked in the carrier. Liners should include steam/air injection and circulation pumps for stirring of the heating media. If higher preheating fluid temperature is used, the liner system needs a means of decreasing fluid temperature at the end of preheating near to the target product temperature (e.g., from 100 to 80°C). Temperature decrease of the preheating fluid inside the liner will avoid temperature overshooting during product equilibration and pressurization steps while the liner is located inside the pressure chamber. One alternative would be to partially remove the heating fluid and mix it with water preheated at initial pressurization temperature. In this case, highly controlled automatic devices that regulate the inflow/outflow of fluid until the system reaches initial target pressurization temperature need to be designed.

In order to ensure proper temperature exposure to all packages in the system, the racking system should be designed in a way that water circulation is parallel to the container length or width. Furthermore, the separation between each container layer should be calculated to permit water/steam/air mixture circulation and assure temperature uniformity. Given the importance of this critical step, a reference temperature device, similar to the mercury-in-glass thermometer used in retorts, should be added to the system.

Other factors related to the container geometry, e.g., fill weight, container size, and product characteristics (Table 2.2), need to be identified when adapting a preheating system to a particular product and processing. Container geometry is defined by the package shape and distribution of the food and its particulates, which can affect preheating rate. As previously mentioned, heating rate is also a function of the food's physical and chemical properties, and variation of these properties mainly depends on product formulation. If the product is a semisolid, minor variations in formulation might not significantly change the rate of heat penetration. Moreover, heat transfer rate can be associated with the thermal diffusivities of the package and food components of the semisolid (Palazoglu, 2006). On the other hand, foods containing sufficient free liquid to promote convection may change heat transfer drastically according to their composition (e.g., due to added starch or other thickening agents), thereby changing heat penetration rate.

2.4.3. Heat Penetration Evaluation

Evaluation of heat penetration during preheating is important for comparative purposes, particularly when characterizing a system modified for faster temperature rise, during scale-up studies using multiple pouch stacks, or when testing larger size products. Primarily, an adequate temperature login system must be installed to provide reliable temperature profiles used to determine preheating efficiency. Plastic stuffing boxes can help fixing the thermocouples at the center of the pouch (or at the slowest heating position) for accurate determination of heat penetration profiles. Other thermocouple positioning devices shown in guidelines from the US National Food Processors Association can also be adapted (NFPA, 1985).

Heat penetration can be evaluated by using the heating rate index f_h and heating lag factor j_h (Holdsworth, 1997). The heating rate index f_h and heating lag factor j_h can be determined by using Eqs. (2.6) and (2.7) (Holdsworth, 1997):

$$\log u = \log\left(\frac{T_R - T}{T_R - T_0}\right) = -\frac{t}{f_h} + \log j \tag{2.6}$$

where u is the reduced temperature, T is the temperature at the geometric center of the package, T_0 is the initial product temperature, T_R is the reference temperature of the heating medium, and j is the extrapolated lag factor. The corrected heating lag factor j_h can be determined from the 58% come-up time (t_{58}), which corresponds to an additional 42% of come-up time needed to reach the target temperature.

$$j_h = 10^{-\frac{t_{58}}{f_h} + \log j} \tag{2.7}$$

The lag factor j_h is related to the lag time needed to reach uniform heating rate values. The accuracy of heat penetration determination depends, among other factors, on the headspace inside the pouch, as well as the internal vapor pressure created due to increased temperature, which can influence the j_h value due to convective currents in contact with the product surface. Accuracy of temperature readings may also be affected by the type of thermocouples used, thermocouple entry system into the package, and use of connectors and extension wires (NFPA, 1985).

When comparing different preheating methods, the heat transfer coefficient can provide additional information on preheating efficiency. It can be calculated either by empirical correlations between dimensionless numbers (e.g., Nussell and Reynolds number) or by fitting simplified Fourier balances to experimental temperature histories. The instant heat transfer coefficient h can be determined by solving the following overall heat balance equation (Varga and Oliveira, 2000):

$$\rho C_p V \frac{dT^t_{ave}}{dt} = h_1 A\left(T^t_\infty - T^t_{surf}\right) \tag{2.8}$$

where T_∞, T_{surf}, and T_{ave} are the heating medium and product surface and volume average temperatures, respectively. Since this expression defines an instant value, the superscript and subscript t indicate that these variables are a function of time.

Varga and Oliveira (2000) showed that more reliable results can be obtained from the derivatives of average heat transfer coefficient $\bar{h}_t$, instead of calculating h_t values for short time steps in the preheating process.

The average external heat transfer coefficient $\bar{h}_t$ between zero and time t was defined as:

$$\overline{h_t} = \frac{\int_0^t h_t dt}{t - t_0} \tag{2.9}$$

where t_0 is the initial time for the preheating stage (depending on whether a one- or two-stage preheating is considered). Varga and Oliveira (2000) offered two solutions to determine the average external heat transfer coefficient from t_0 to several values of t considered: (a) integrating the heat balance (Eq. 2.8) or (b) using the residual sum of the square method to minimize the difference between experimental and model temperatures. A detailed description of this methodology escapes the scope of this manuscript and can be found in the mentioned reference.

2.5. Microbial Engineering and Regulatory Implications

Bacterial spore inactivation depends on pressure applied and initial temperature of the food and vessel. Most thermal baro-resistant spores are inactivated at pressures 600 MPa or greater, in combination with initial temperature above 60°C. However, relatively low pressures (below 200 MPa) can trigger spore germination (Patterson, 2005; Leadley, 2005). Furthermore, studies on target microorganisms for inactivation and related safety assurance of canned food products, such as for *Clostridium botulinum,* have shown large variation in the pressure resistance of different spore strains (Margosch et al., 2004; Margosch, 2005; Gola and Rovere et al., 2005).

2.5.1. Inactivation of C. botulinum Strains by HPHT Processing

Until now, the resistance to pressure and temperature has been studied with at least five *C. botulinum* strains in varied conditions and media (Reddy et al., 1999; Reddy et al., 2003; Margosch et al., 2004; Gola and Rovere, 2005). *C. botulinum* spores type E in pH 7 buffer, for example, have been reduced 4.5 logs at 50°C/758 MPa/5 min and 5 logs at 40°C/827 MPa/10 min (Reddy et al., 1999). Furthermore, *C. botulinum* type A was reduced by more than 3 log units in pH 7 buffer and crab meat following treatment at 75°C/827 MPa/20 min (Reddy et al., 2003). Other studies on several *C. botulinum* strains (types A, B, F proteolytic, B non-proteolytic) in mashed carrots were carried out by Margosch et al. (2004) and Margosch (2005). They found that treatment at 80°C/600 MPa/1 s reduced strains by more than 5.5 log cycles to none at all. In particular, non-proteolytic *C. botulinum* type B was the least resistant strain and was reduced by more than 5.5 log cycles after 80°C/600 MPa/1 s. In comparison, proteolytic *C. botulinum* type A had more than 5 log reductions after 80°C/600 MPa/12 min treatment, and proteolytic *C. botulinum* type B spores were inactivated by less than three orders of magnitude at 80°C/600 MPa/60 min.

Since spore resistance also proved to be product dependent, more research is needed to find the optimum inactivation pressure/temperature/time conditions for *C. botulinum* strains in particular products, as the type of medium may influence spore germination rates (Margosch, 2005). Moreover, understanding how HPHT conditions affect bacterial neurotoxins produced is worth of consideration (Margosch et al., 2005).

2.5.2. *Inactivation of Microbial Spore Surrogates by HPHT Processing*

Regarding other spore-forming microorganisms, microbial studies have proven that an initial chamber/product temperature of 75-85°C and pressure 600-827 MPa can effectively inactivate target heat resistant spore-forming bacteria commonly used as indicators of food safety and shelf stability (Heinz and Knorr, 2001). In particular, *Bacillus stearothermophilus* spores were reduced 5 log cycles in phosphate buffer and beef broth at 70°C/700 MPa/3 min (Gola et al., 1996; Rovere et al., 1998), and at least 4.5 log cycles in meat balls in tomato puree at 90°C/700 MPa/30 s (Krebbers et al., 2003). Furthermore, *B. stearothermophilus* spores were inactivated in egg patties at 700 MPa and 105°C (Rajan et al., 2006a; Rajan et al., 2006b; Koutchma et al., 2005). Koutchma et al. (2005) also showed that 700 MPa/105°C/4 min was sufficient to destroy 6 logs of *B. stearothermophilus* in spore strips in egg patties, whereas 6 logs of *C. sporogenes* PA 3679 at 700 MPa/110°C/5 min were destroyed in the same media.

Other spore genii such as *Bacillus licheniformis* spores suspended in pH 7.0 buffer were also inactivated at 60°C/600 MPa/20 min (Taki et al., 1991), and reduced 6 logs in pH 7 buffer and beef broth at 70°C/700 MPa/5 min (Gola et al., 1996; Rovere et al., 1998). *Bacillus cereus* spores were also reduced 8 logs in pH 7 buffer at 60°C/690 MPa/1 min with previous sporulation at 37°C (Raso et al., 1998), and 5 logs in beef broth at 70°C/700 MPa/5 min (Rovere et al., 1998). Similarly, *Bacillus subtillis* spores were inactivated at 827 MPa and a process temperature ranging from 102 to 107°C, yielding up to a 6 log reduction (Balasubramaniam and Balasubramaniam, 2003).

Moreover, *B. amyloliquefaciens* was higher in HPHT resistance than *C. botulinum* strains (Margosch, 2005), becoming a potential surrogate for future research in HPHT sterilization (Margosch et al., 2004). Ahn et al. (2005) obtained up to 7–8 log reductions with *B. amyloliquefaciens* after treatment at 700 MPa and 121°C for less than 1 min.

It is worth mentioning that data reported by several authors on spore inactivation were not obtained at the same conditions due to heat loss experienced in the chamber using machines of different sizes, the compression fluids, and heat retention configurations (de Heij et al., 2002; Balasubramaniam and Balasubramaniam, 2003; Ardia et al., 2004; Balasubramaniam et al., 2004). Thus, in many cases, data may not be comparable. Previous research has proven by means of numerical simulation the difference in inactivation reduction of *Alicyclobacillus acidoterrestris* spores at 50°C/800MPa (Ardia et al., 2004) and *B. stearothermophilus* (de Heij et al., 2002) at 700 MPa/121°C/2-90s pulses between the center and inner side-wall of pressure vessel. Particularly, Ardia et al. (2004) predicted that a difference of 3–4°C between these two crucial points would result in a difference of approximately 6 log reductions between the center and inner side-wall of a polyethylene container located inside the pressure vessel. De Heij et al. (2002) predicted a 15°C difference between the center and vessel side-wall, giving a rough difference of 5 log cycles.

2.5.3. *Regulatory Perspective*

During the last five years, high pressure sterilization initiatives have been started by two consortia, one in the US and one in Europe, offering a new technology that will rival or complement conventional canning. Although 21CFR113 was not intended for pressure-processed low-acid vegetables and seafood, it is likely to be applicable since heat is included during compression (Sizer et al., 2002). Other parts in the US Code of Federal Regulations (9CFR318.300 and 9CFR381.300) applicable to the sterilization of food products containing 3 percent or more raw (2 percent cooked) meat or poultry could also be used for this technology.

A standard scenario for commercial sterilization using high pressure processing can be defined as the combination of 700 MPa and a final process temperature of 121°C (initial temperature 90°C) with a holding time of 3 min. In this case, an F_0 value of approximately 3 min (corresponding to a 12D reduction of *C. botulinum* spores) is obtained by only accounting for the thermal component and neglecting the pressure effect on microbial inactivation (Sizer et al., 2002). This standard scenario would allow filing HPHT treatment as a thermal process according to 21CFR113 as a first approach, avoiding the use of large volumes of microbial inactivation data and special kinetic models to account for the combined effect of temperature and pressure.

On the other hand, various researchers are gathering safety data on microbial inactivation, as well as process data, to model the kinetics of *C. botulinum* inactivation that will allow identifying process performance criteria for process validation and process filing with regulatory agencies such as the FDA.

2.5.3.1. FSO Concept in High-Pressure Sterilization

The concept of Food Safety Objective (FSO) has been introduced by the Codex Committee on Food Hygiene (Codex, 2004) as the "maximum frequency or concentration of a hazard in a food at the time of consumption that provides or contributes to the appropriate level of protection (ALOP)" (NACMFS, 2005). This concept is also emerging as a regulatory parameter for evaluating the efficacy of novel technologies to inactivate target pathogenic microorganisms. An inactivation performance criterion can be expressed as follows (NACMFS, 2005):

$$H_0 - \sum R + \sum I \leq \text{FSO (or PO)} \tag{2.10}$$

where FSO is the food safety objective, PO is the performance objective, H_0 is the initial level of the hazard, Σ R is the total (cumulative) reduction of hazard on a $\log_{10}$ scale, and Σ I is the total (cumulative) increase of hazard on a $\log_{10}$ scale.

Alternatively, the Performance Objective (PO), or "the maximum frequency and/or concentration of a hazard in a food at a specified step in the food chain prior to consumption that provides or contributes to an FSO or ALOP, as applicable" (Codex, 2004), can be used in Eq. (2.10) to establish process performance. In the context of risk analysis, an FSO would be based on a public health goal that provides an ALOP or "reasonable certainty of no harm." Since the most resistant

microorganism of public health significance in HPHT sterilization of low-acid foods is *C. botulinum*, an FSO could be defined as the achievement of a <100 cfu *C. botulinum*/g in a food at the point of consumption.

2.5.4. *Process Performance Criteria Accounting for Temperature History and Inactivation Kinetics*

As mentioned before, the 21CFR113 primarily stipulates minimum temperature requirements for commercially sterilizing low acid foods. However, inactivation of *C. botulinum* has not been validated for thermally pressurized foods, not only due to the lack of inactivation data for several strains, but also because the microbial performance or process outcome criterion has not yet been established for comparison purposes (Koutchma et al., 2005). This process performance criterion should include inactivation kinetic parameters of *C. botulinum*, along with other parameters that account for the pressure and temperature profile during the established HPHT sterilization process.

The following paragraphs will describe approaches to determining parameters that simultaneously account for uniformity and the sterility of an HPHT process and that can therefore be applied in process validation.

2.5.4.1. Conventional Thermal Processing Approach

Koutchma et al. (2005) showed that the HPHT process may be validated by applying concepts such as decimal reduction time (D_T, D_P) and temperature sensitivity (Z_T, Z_P), traditionally used in conventional thermal processing of low-acid foods. The authors based their research on evidence reported on the linearity of microbial inactivation curves (semilog scale) of classical surrogates, namely *B. stearothermophilus* and *C. sporogenes* PA 3679, at a pressure range of 600–800 MPa and process temperature range of 91–108°C. They found that thermal sensitivity of PA 3679 spores (Z_P values) did not vary with pressure, nor did pressure sensitivity (Z_T values) vary with temperature at these ranges. They were able to calculate F_0 values for the HPHT sterilization process by adapting a concept established by Pflug (1987) to calculate the process lethality, which included the initial microbial load. Nevertheless, research is ongoing since Z values of *C. botulinum* spores at a reference sterilization temperature 121°C are necessary for quantifying the additional contribution of pressure in an HPHT process in terms of lethality and overall thermal death time. In order to separate the pressure effect, care must be taken when comparing an HPHT process with a conventional thermal process, since processing factors (i.e., package geometry, food media, temperature measurement, etc.) should be reproducible at only-thermal and thermal pressurization conditions. Furthermore, F_0 values accounting for the thermal components should coincide in both processes. Due to the asymmetric reduced temperature semilog scale profile obtained in an HPHT process, the General Method (Holdsworth, 1997) could most accurately determine F_0 values from temperature profiles in commercial software packages.

2.5.4.2. Weibullian Approach

Peleg et al. (2005) identified a theory to redefine the concept of "thermal death time" for non-isothermal heat treatments like HPHT processing that was an alternative to the F_0 value concept, by describing *C. botulinum* inactivation kinetics using a power law or "Weibullian" model with temperature dependent parameters:

$$\log\left[\frac{N(t)}{N_0}\right] = -b(T)t^{n(T)} \tag{2.11}$$

where N_0 is the initial number of microorganisms and $N(t)$ is the number of surviving microorganisms at time t. The parameters $b(T)$ and $n(T)$ are a function of the applied temperature. A similar model can be used to describe the HPHT process using model parameters, b and n, as functions of both pressure and temperature (Campanella and Peleg, 2001). Thus, the combined effect of pressure and temperature of the process can be accounted for in this expression:

$$\log\left[\frac{N(t)}{N_0}\right] = -b(P,T)t^{n(P,T)} \tag{2.12}$$

The relationship between parameters b and n with pressure and temperature can be determined from experimental survival curves obtained at combined pressures and temperatures. In order to know the effects of pressure and temperature on parameters b and n, the temperature [i.e., T(t)] and pressure [i.e., P(t)] histories must be known. Thus, an analytical heat transfer model to express T(t) and P(t) needs to be incorporated into Eq. (2.12). Once parameters $b(t)$ and $n(t)$ are known, inactivation of microorganisms at selected pressure and temperature can be predicted. Peleg et al. (2003) and Peleg et al. (2005) proposed a methodology to estimate survival parameters b and n for conditions of variable pressure and temperature. However, as said before, no sufficient *C. botulinum* data exists that validates the model. Once data is collected for a tolerable number of *C. botulinum* strains, these parameters could eventually be used to validate an established HPHT sterilization process.

The advantage of this approach is that parameters will depend on the actual thermal pressurization history; therefore, more accurate conditions to reach sterilization can be defined to establish a given HPHT process. This approach allows process optimization to minimize over processing, and increases the chances of yielding higher quality foods with increased nutritional content (Peleg et al., 2005).

2.5.4.3. Alternative Performance Criteria

Design of thermal process operations requires the use of heat transfer models to determine process parameters that account for temperature in terms of its distribution within the food or equipment during treatment (Nicolaï et al., 2001).

This concept can be extended to build models that not only account for temperature distribution, but also for microbial survivor distribution. Numerical heat transfer models that incorporate inactivation constants as a function of pressure and temperature have been proposed to account for the extent of combined temperature and pressure inside the pressure vessel (Denys et al., 2000; Hartmann and Delgado, 2003).

For instance, the temporal and spatial distribution of activity of *Bacillus subtillis* α-amylase and cfu-concentration of *E. coli* (Hartmann et al., 2003) was described with the first order inactivation kinetics equation in terms of continuum mechanics and scalar transport (Ludikhuyze et al., 1997):

$$\frac{\partial A}{\partial t} + u\frac{\partial A}{\partial x} + v\frac{\partial A}{\partial y} + w\frac{\partial A}{\partial z} = -K(P,T)A \tag{2.13}$$

where A is the relative activity (actual activity related to the initial activity, varying between 100% with values close to zero), $K(P,T)$ is the inactivation rate constant, and u, w, and v are the components of the fluid velocity vector in the x-, y-, and, z-directions, respectively. Velocity vectors were taken from thermal and fluid dynamic conservation equations of mass, momentum and energy (Hartmann and Delgado, 2003). Eq. (2.13) represents the coupling between the activity A and the flow field (i.e., the velocity of the vessel fluid and fluid inside packages) and the coupling of A and the temperature distribution. In this way, the pressure-temperature-time profiles, calculated through the model, were integrated through a numerical scheme, and the activity retention could be evaluated at any point in time and vessel space.

This model allowed obtaining inactivation distribution per package located at specified volumetric regions in the vessel. For this purpose, a volume-weighted averaging can be carried out for each package, and arithmetic averaging of all packages can provide an idea of global inactivation effectiveness (Hartmann and Delgado, 2003). Furthermore, a process uniformity parameter, Λ, has been defined in terms of the average relative activity retention, i.e.,

$$\Lambda = \frac{A_{ave\_\min}}{A_{ave\_\max}} \tag{2.14}$$

where A_{ave_min} is the minimum average activity retention and A_{ave_max} is the maximum average activity retention (Hartmann and Delgado, 2003). A similar inactivation distribution analysis can be performed by means of thermal and fluid dynamic models that include inactivation kinetic equations for pressure/temperature resistant spore-forming bacteria such as *C. botulinum*. In this case, microorganisms should be assumed as a transport quantity varying over space and time (Hartmann et al., 2003). This would allow calculations of temperature uniformity during HPHT sterilization processes, of special use in scale-up studies. A few works have already integrated thermodynamic, heat transfer, and spore inactivation kinetic models to predict the effect of temperature evolution at

selected points in the pressure vessel on spore inactivation (de Heij et al., 2002; Ardia et al., 2004). A mathematical model integrating thermodynamics and inactivation kinetics of *Bacillus stearothermophilus* was built to predict temperature distribution in the high-pressure vessel (de Heij et al., 2002). In this case, an axi-symmetric one-dimensional finite element model based on heat conduction was developed, which predicted temperature at the vessel wall and at the center. A first order kinetic constant k was found from spore inactivation data and fit into a modified Arrehnius-Eyring equation (Eq. 2.15), expressed as follows as a function of pressure and temperature:

$$k = k_{ref} e^{\frac{E_a}{R}\left(\frac{1}{T_{ref}} - \frac{1}{T}\right)} - V_a\left(P - P_{ref}\right) \tag{2.15}$$

where volume V_a is the activation volume, E_a is the activation energy, and R is the universal gas constant (8.314 J/mol/K). Although this contribution does not clearly specify results in terms of microbial reduction, as already mentioned, the model could predict temperature profiles at selected vessel points and illustrate the lower log cycle reduction achieved near the vessel walls after a two-cycle 700 MPa/121°C/90s process.

Similarly, Ardia et al. (2004) modeled compression heating using a finite element method, also based on heat conduction in radial coordinates. The model, based on Eq. (2.1), included dT/dP as a time dependent heat source during the compression or de-compression phase. The numerical routine implemented NIST formulations (Harvey et al., 1996) for regressive calculation of the thermal expansion coefficient α, density ρ, and specific heat C_p. To account for temperature increase due to compression, a microbial inactivation model was included into the finite difference scheme, yielding the degree of inactivation (log cycle reductions) for any radial position. In this case, the time dependent inactivation was mathematically expressed assuming n^{th} order inactivation kinetics:

$$\frac{dN}{dt} = -k \cdot N^n \tag{2.16}$$

The inactivation rate constant was then expressed as a function of pressure and temperature using the Arrhenius-Eyring equation:

$$In(k) = \frac{1}{RT}\left(E_a - \Delta V^* P\right) \tag{2.17}$$

where the activation volume ΔV^* is the characteristic parameter for the pressure dependence of the rate constant. This modeling approach predicted the inactivation of *Alicyclobacillus acidoterrestris* spores at 50°C/ 800 MPa in geometrically defined locations, finding (as mentioned before) a difference of 6 log cycles inactivation at the center of the pressure chamber and closer to the chamber walls (due to a 3–4°C difference at the end of pressurization).

2.5.5. Synergistic Approach

A number of foods composed of heat-labile components, relevant in terms of product quality and nutrition, can be affected by HPHT conditions necessary for sterilization (Matser et al., 2004; van Loey et al., 1998). In this case, additional synergies can be tried by using food additives and preservatives, such as bacteriocins (inactivation by membrane pore formation), surfactants like sucrose esters (affecting both proteins and biomembrane structure and function), acidulants (providing specificity in antimicrobial inactivation), humectants, chelating agents, and others.

Kalchayanand et al. (2003) showed that, at moderate pressure, bacterial spores can be induced to germinate and outgrow, at which stage they can be killed by bacteriocin-based biopreservatives. In this study, inactivation of *Clostridium laramie* spores or a mixture of 4 clostridial spores (*C. sporogenes*, *C. perfringens*, *C. tertium*, and *C. laramie*) in roast beef with added preservative mixtures (pediocin, nisin, lysozyme, Na-EDTA, and BPy) were subjected to treatment at 60°C/345 MPa/5 min. It was found that a combination of HP with bacteriocins extended the shelf life of inoculated roast beef up to 7 days at 25°C and up to 84 days at 4°C. Stewart et al. (2000) showed that *B. subtilis* and *C. sporogenes* ATCC 7958 were especially sensitive to nisin addition. A marked synergistic decrease in spore count was detected with pressurization at 250–300 MPa combined with 45°C and pH less than or equal to 6.0 in the presence of sucrose laureate fatty esther.

Moreover, Shearer et al. (2000) investigated the addition of sucrose laurate and combined treatment at 45°C/392 MPa/10–15 min, finding 3–5.5 log reductions for *B. subtilis* in milk, *B. cereus* in beef, *B. coagulans* in tomato juice (pH 4.5), *Alicyclobacillus* sp. in tomato juice (pH 4.5), and *Alicyclobacillus* sp. in apple juice. In this study, sucrose laurate appeared to be inhibitory rather than lethal to spores. However, its application to food as an extra hurdle may allow the use of lower temperatures in combination with pressure.

2.6. Quality of Selected HPHT Processed Foods

Even though extensive research has been done on bacterial spore inactivation, quality validation studies of low-acid foods after HPHT treatment have rarely been performed. Furthermore, little consumer data on HPHT processed products have been reported, and few comparisons exist in the literature with retort processing on consumer acceptability. Information on appearance, texture, and flavor/aroma mostly exists in terms of analytical evaluations of HPHT treated products such as broccoli juice, green beans, tomato puree, and meat sauce (van Loey et al., 1998; Rovere et al., 2000; Krebbers et al., 2003; Matser et al., 2004). Indeed, a number of high pressure, high temperature (HPHT) treated low-acid foods such as meat, milk, and vegetable products showed more desirable texture, color, and flavor/aroma retention in comparison to retorted products and, in some cases, to

frozen products (Hoogland et al., 2001; Krebbers et al., 2002; Krebbers et al., 2003; Matser et al., 2004).

Color, it has been shown, can be retained in selected vegetables (Matser et al., 2004). For instance, spinach has been found to retain higher color intensity than conventionally sterilized spinach after two pulses at 90°C/700 MPa/30s. Furthermore, tomato puree treated at 90°C/700 MPa/30s also retained color, whereas color degradation was greater after conventional retort treatment. This data was supported by a sensory panel that found higher color acceptability in tomato puree treated at HPHT conditions, in comparison to retorted samples. Lycopene content was maintained in this case, while a lower content was found after retort treatment (Krebbers et al., 2003). Moreover, Juliano et al. (2006a, b) indicated that HPHT treatment at 70°C/700 MPa/5 min can maintain color and appearance of selected scrambled egg patty formulations (as evaluated by a trained panel).

Regarding texture, firmness of HPTS-treated green beans after 75°C/1000 MPa/80s was much higher than those conventionally retorted, dried, or frozen (Krebbers et al., 2002). HP treated tomato puree (90°C/700 MPa/30s/121°C) displayed lower serum separation and higher viscosity than the retorted product. Previous studies have also identified that utilization of lower pressurization temperatures can significantly improve the texture and water retention of scrambled egg patties (Juliano et al., 2006b). In fact, previous studies on high pressure formation of gels from whole liquid eggs, egg white, egg yolk, and egg yolk/white (Ma et al., 2001; Ahmed et al., 2003; Lee et al., 1999) have shown that pressures greater than 600 MPa not only increase apparent viscosity, but also provide instantaneous gelation of egg yolk and egg white.

Flavor components in fresh basil were best retained after HPHT processing (two pulses of 85°C/700 MPa) in comparison to freezing, conventional retorting, and drying. Egg flavor retention has also been reported in high pressure high temperature treated egg patties at 700 MPa/105°C/5 min (Juliano et al., 2006b).

2.6.1. Shelf-Stable Egg-Based Products Processed by HPHT: A Case Study

Manufacturing of acceptable shelf-stable egg products using conventional thermal processing remains a challenge, as retort processing yields undesirable flavors, greenish-gray discoloration, and detrimental changes in texture and syneresis (Baliga, et al., 1969; Wesley et al., 1982; Luechapattanaporn et al., 2005). In fact, the US Army recently stopped the production of retorted scrambled eggs in plastic institutional trays due to the dissatisfaction found by military consumers with respect to the quality of this benchmark product (Dunne, 2005).

At present, Washington State University (WSU), in conjunction with The Ohio State University (OSU) and the National Center for Food Safety and Technology (NCFST) has been directing a short-term Combat Rations Network (CORANET, US Defense Logistics Agency) project for the development of shelf-stable egg products using HPHT processing. The project, run under the guidance of the US

Natick Soldier Systems Center, has been part of a series of efforts carried out to identify processing alternatives for the manufacture of acceptable shelf-stable egg-based products. Alternatives include the use of high-temperature short-time retort processing, radiofrequency heating, freeze-drying, and refractance windows drying. The HPHT processing project had the active collaboration of experts from industry in various fields, including the high pressure equipment design team from Avure Technologies, the egg product development team from Michael Foods Egg Products Company, the high pressure processing packaging development team from ALCAN, and military ration developers from Wornick, Ameriqual, and Sopakco.

Among existing precooked egg products, scrambled egg patties were identified as an adequate product for high-pressure processing, especially during HPHT processing, due to their semisolid homogeneous structure (Juliano et al., 2006b). During the first phase of this project, several efforts have been directed in terms of formulation development, microbial challenge studies, identification of adequate processing conditions, as well as packaging studies.

The team focused on identifying the effects of HPHT conditions on commercial and modified egg patty formulations. Two processing strategies were initially proposed for egg-based product commercial sterilization and *C. botulinum* inactivation: (a) standard thermal sterilization treatment at process temperature 121°C accelerated by the application of 700 MPa with holding time at 3 min, and (b) thermal HPHT treatment using lower temperature than in (a) with increased holding time. Option (a) was considered with the purpose of facilitating FDA approval as a thermal process. In both cases, microbial challenge studies have helped in the selection of processing conditions. Furthermore, inactivation kinetics studies, incubation tests, packaging identification, and compression heating studies gave a deeper understanding of the process. Results of these endeavors, after iterative steps, are highlighted in the following sections.

2.6.1.1. Egg Patty Formulation Identification for HPHT Conditions

Michael Foods has played a key role in the development and production of 6 egg patty formulations that were supplied to WSU, NCFST and OSU for testing. Trained and consumer sensory panels at WSU, along with additional physical tests (texture profile analysis, quantification of syneresis, and instrumental color measurements) have helped identify a formulation suitable in flavor, aroma, and appearance.

A six-member descriptive panel trained at WSU analyzed a basic formulation (whole eggs, water, soybean oil, modified food starch, whey solids, salt, nonfat dried milk, and citric acid) and other formulations with added water, cheddar cheese particles, xanthan gum, EDTA and flavors. Formulations with added xanthan gum, EDTA and flavors, treated at 700 MPa/105°C/5 min, showed higher tones of butter flavor as well as lower tones of rancid, unclean and retort flavor than the basic formula after pressure (Juliano et al., 2006b).

Texture was initially identified as one of the most challenging problems in the quality of the egg products after pressurization at process temperatures greater

than 100°C (Juliano et al., 2006b). It was found that the addition of xanthan gum and water significantly decreased the hardness of high pressure treated patties by 30–55% after 700 MPa/105°C/5 min (Juliano et al., 2006a). Furthermore, addition of xanthan gum reduced the water loss (or syneresis) after pressure.

Results of a 40-member consumer panel verified previous studies on the effects of process temperature on product quality after HPHT processing. It was found that decreasing the high pressure process temperature from 121 to 105°C at 700 MPa improved the overall acceptability of HPHT treated formulations with added xanthan gum. A formulation containing 20% Cheddar cheese and treated at 105–110°C and 700 MPa obtained ratings similar to the untreated egg patty controls (Juliano et al., 2007).

Testing in a DUST 35 L machine (QUINTUS Food Autoclave Type 35L-600, Avure Technologies, Kent, WA) showed that texture can be improved by using lower vacuum packaging conditions, whereas texture of the patty was not affected when processed in smaller 1.5 L chambers (Quintus Food Processor-6, Flow Autoclave systems, Columbus, OH) and 1.7 L chambers (Engineered Pressure Systems, Inc., model #914-100, Haverhill, MA). Furthermore, the three centers (WSU, NCFST and OSU) studied the effect of HPHT processing on the pH of the basic egg formulation and formulation with added xanthan gum, detecting no significant changes after processing.

2.6.1.2. Preheating Studies

By working with different preheating systems, trials were conducted to reduce preheating times and to minimize decreased quality and excessive use of heat due to long preheating periods (Juliano et al., 2006b). Comparisons were made between preheating with an electrical heater, a water kettle with steam jacket, a water kettle with steam injection, or microwaves, showing that microwaves and steam injection elevated patty temperatures up to 75°C most quickly.

Considering that microwave heating showed significant temperature gradients within the patties (proven by means of infrared imaging), direct steam injection was shown to be advantageous in reducing preheating time. One other effect found was that the type of packaging material influenced preheating times. Aluminum foil-based laminates provided better penetration rates than non-foil ones.

2.6.1.3. Compression Heating of Egg-Based Products

Determination of compression heating properties of egg mixtures gave no significant differences with water. The compression heating factor of egg patties ranged from 3.3°C/100 MPa to 4.8°C/100 MPa at the initial process temperatures of 25°C and 80°C, respectively. Therefore, no temperature gradients between the compression fluid and the egg patties are expected due to different compression heating.

2.6.1.4. Microbial Challenge Studies

Microbial inactivation studies were carried out by NCFST and OSU. Inactivation of *B. stearothermophilus* was studied after different stages in the process: (a) baking of the egg mix to form patties, (b) after preheating and (c) after HPHT

processing. *B. stearothermophilus* spore inoculated into the egg mix showed a one log cycle reduction after baking. After treatment at 700 MPa/105°C, inactivation of *B. stearothermophilus* (ATCC 7953) spores in egg patties was accelerated (Rajan et al., 2006b). The resistance of *B. stearothermophilus*, given by its D-values, also proved to be much lower when using pressure. Inactivation of *B. stearothermophilus* in spore strips located between two egg patties can be reduced by at least 6 log cycles at 688 MPa/ 105°C/5 minutes (Koutchma et al., 2005). However, *Clostridium sporogenes* (PA 3679) bioindicator spores were more resistant than *Bacillus stearothermophilus* and needed a process temperature of at least 110°C.

2.6.1.5. Identification of Packaging Materials for HPHT Processing

Throughout the first phase, project partners worked with different packaging companies to identify suitable individual flexible pouches (clear and foil laminates). Selected plastic and foil-laminated pouches from Kapak, Pyramid, ALCAN, and Smurfit-Stone manufacturers were screened for their ability to withstand HPHT and retort treatments. Overall packaging integrity, oxygen permeability (determined from a Mocon-Oxtran unit), and seal strength (determined from tensile tests using an Instron texture analyzer) were evaluated before and after treatments at NCFST facilities. In addition, pouches were tested for delamination, flex damage, or other treatment-related anomalies.

It was proven that foil laminates from Pyramid and Smurfit-stone (48 ga. polyethylene/ adhesive/ 0.0005" aluminum foil/adhesive/ 4 mL polyolefin) retained their barriers during steam injection preheating and HPHT treatment. However, a statistically significant loss of barrier was found in clear plastic pouches from Pyramid without aluminum foil. Seal strength of all packaging materials was not significantly affected by HPHT and HP low temperature treatments, while retort at 121°C decreased seal strength. Furthermore, WSU, in partnership with ALCAN Packaging, identified a pouch made of coextruded laminates that provided almost no blistering and low oxygen permeability after pressure under a worst-case scenario condition (700 MPa/121°C/3 min). ALCAN packaging material composition was a 60 ga. biaxial nylon/adhesive/5.0 mL ethylene vinyl alcohol (EVOH) coextruded sealant.

2.6.1.6. Incubation Tests – Shelf Stability Studies

Egg patties (basic formulation) were treated in WSU's 1.7 L machine at pressures between 200 and 700 MPa, with holding time of 5 min and initial temperature of 90°C for storage testing. Treated and untreated packages were stored at room temperature and 37°C for one year. Results indicated that at pressures above 400 MPa, no pouches showed production of gas or decomposition. HPHT treated patties stored at room temperature for one year maintained initial color, hardness and aroma. Moreover, other non-inoculated formulations tested in the NCFST/ Avure 35 L pilot machine also remained stable (no gas formation) for six months when stored at 37°C after 700 MPa/105°C treatment.

Another set of samples were inoculated with *B. stearothermophilus* spores (7.5×10^6 spore/g) at OSU laboratories and treated at 700 MPa/105°C/5 min. The product remained stable after at least two months storage at 37°C.

2.7. Final Remarks

The concept of combining high hydrostatic pressure and heat to commercially sterilize low-acid foods emerged in the early 1970s and is scaling up from the laboratory bench to the pilot plant. At least four pilot 35 L high pressure vessels located around the world are being used today as part of various industrial/government consortia projects to identify the benefits of HPHT processing for several products.

Patents have been published proposing different approaches, among which the application of a single pressure pulse of 600 MPa or greater, combined with temperature between 90 and 130°C, seems most appropriate from a food safety and economic point of view. This approach defines a high temperature short time sterilization process, which has been proven to provide improved flavor, texture, color and nutrient retention in selected food components, in comparison to retort. At this stage of development, HPHT technology can be claimed advantageous for its shorter processing time. However, lower processing temperatures than 121°C cannot yet assure sterilization. For this purpose, additional microbial inactivation data on many *C. botulinum* strains as well as surrogate spore-forming microorganisms of higher resistance (to be identified) are greatly needed. Hence, based on the current knowledge, regulatory approval can only be obtained by filing this technology as a thermal process, following the guidelines established in the 9CFR318.300, 9CFR381.300, and 21CFR113.

Once *C. botulinum* inactivation data on several strains is gathered (together with process data) kinetic models can be developed for HPHT conditions. In fact, microbial kinetic models in combination with heat transfer models could be used to express overall process performance in terms of energy use. Overall parameters obtained for these models would completely account for (or be directly related to) individual performance parameters such as preheating rate, pressure come-up time, target preheating/equilibration temperature, target temperature at maximum pressure, temperature at the end of holding/ pressurization time, and temperature at the end of pressure release.

Synergistic approaches through the addition of natural antimicrobial preservatives such as bacteriocins can help reduce the HPHT conditions needed to reach sterilization, providing opportunities for the development of products with more heat labile components. The FSO concept can help establish optimal conditions and ingredient addition for sterilization from a regulatory standpoint.

Attainment of optimal sterilization conditions is also related to the efficient use of compression heat developed during pressurization. Equipment modification with heat retention aids such as an insulating polymeric liner at chamber walls, preheated pressurization fluids, and an internal pressure intensifier to decrease

the amount of inflowing pressurization fluid, can yield more uniform temperature distribution across the chamber vo-lume. If a nearly adiabatic state is achieved inside the liner, pressure holding times may be decreased, as temperature will be uniform, even near the steel chamber walls.

The preheating step has been identified as a critical control point in the overall process since it determines the achievement of the target pressurization temperature in all food packages. A number of factors intervening in the preheating step have been listed, among which the preheating method used and package geometry seem the most relevant. Furthermore, the equilibration step after preheating is important to assure temperature homogeneity inside the food packages before pressure come-up time. From a quality perspective, minimization of preheating times, by selecting faster preheating methods, could help improve food attributes at the end of the HPHT process. A two-stage preheating approach has been proposed to save carrier operating time.

HPHT technology has the potential to manufacture shelf-stable egg, vegetable, meat and dairy products, but more information is needed in terms of the sensory quality of HPHT products and consumer preferences. Further studies on the effect of HPHT conditions on separate food components and developed formulations will allow identification of specific study cases. Once products are identified, characterization in terms of shelf life can be carried out. In this case, shelf stability of developed HPHT processed foods will not only depend on the treatment applied, but also on the barrier provided by the selected packaging material. Efforts are ongoing to identify packaging materials that meet the requirements for overall integrity, specific seal strength and gas permeability after HPHT treatment.

In conclusion, defining the conditions *of C. botulinum* inactivation is fundamental to establishing further product development studies on novel HPHT treated foods to satisfy the shelf-stable ready-to-eat markets. In addition, validation of process performance criteria related to *C. botulinum* inactivation, and pressure and temperature history will not only allow process filing with regulatory agencies, but will help establish a business case for transforming HPHT processing into an industrial reality.

References

9CFR318.300, 2002, Animals and Animal Products. Entry into Official Establishments; Reinspection and Preparation of Products. Canning and Canned Products, in: *Food Safety and Inspection Service, US Department of Agriculture. Code of Federal Regulations (CFR),* Federal Register, US Government Printing Office, Washington, DC, Title 9, Chapter III, Part 318, Subpart G.

9CFR381.300, 2003, Animals and Animal Products. Poultry Products Inspection Regulations. Canning and Canned Products, in: *Food Safety and Inspection Service, US Department of Agriculture. Code of Federal Regulations (CFR),* Federal Register, US Government Printing Office, Washington, DC. Title 9, Chapter III, Part 381, Subpart X.

21CFR113, 2005, Food and Drugs. Food for Human Consumption, Thermally Processed Low-Acid Foods Packaged in Hermetically Sealed Containers, in: *US Food and Drug Administration, Department of Health and Human Services, Code of Federal*

Regulations (CFR), Federal Register, US Government Printing Office, Washington, DC, Title 21, Chapter I, Subchapter B, Part 113.

21CFR114, 2005, Food and Drugs. Food for Human Consumption. Acidified Foods, in: *US Food and Drug Administration, Department of Health and Human Services. Code of Federal Regulations (CFR)*, Federal Register, US Government Printing Office, Washington, DC, Title 21, Chapter I, Subchapter B, Part 114.

Ahmed, J., Ramaswamy, H.S., Alli, I., and Ngadi M., 2003, Effect of High Pressure on Rheological Characteristics of Liquid Egg, *Lebensm.- Wiss. U.-Technol*. **36**(5):517–524.

Ahn J., Balasubramaniam, V.M., and Yousef A.E., 2005, Effect of Pressure-Assisted Thermal Processing on the Inactivation of Selected *Clostridium* and *Bacillus* Surrogate Spores [Abstract]. *Nonthermal Processing Workshop*, September 15-16, Philadelphia, PA, USDA Eastern Regional Research Center, USDA ARS Eastern Regional Research Center, Wyndmoor, PA, Abstract no.# p. 24.

Ardia, A., Knorr, D., and Heinz V., 2004, Adiabatic Heat Modeling for Pressure Build-Up During High-Pressure Treatment in Liquid-Food Processing, *Food Bioprod. Process*. **82**(C1):89–95.

Balasubramaniam, S., and Balasubramaniam V.M., 2003, Compression Heating Influence of Pressure Transmitting Fluids on Bacteria Inactivation During High Pressure Processing, *Food Res. Int*. **36**(7):661–668.

Balasubramaniam, V.M., Ting, E.Y., Stewart, C.M., and Robbins J. A., 2004, Recommended Laboratory Practices For Conducting High-Pressure Microbial Inactivation Experiments, *Innov. Food Sci. Emerg. Technol*. **5**(3):299–306.

Baliga, B.R., Rao, A.S., and Lahiry N.L., 1969, Prevention of Browning in Hard Boiled Eggs During Canning. *J. Food Sci. Technol*. **6**(3):200–204.

Barbosa-Cánovas, G.V., Juliano, P., and Keener L., 2005a, Legislative Issues with Respect to Processed Food, in: *Global Harmonization of Legislation of Food Products and Processes*, Institute of Food Technologists Conference. New Orleans, July 2005, pp. 27–3.

Barbosa-Cánovas, G.V., Juliano, P., Koutchma, T., Balasubramaniam, V.M., Mathews, J.W., and Dunne C.P. 2005b, High Pressure Thermal Sterilization of Precooked Egg Patties: Factors Affecting Preheating Efficiency, in: *High Pressure Processing*, American Institute of Chemical Engineers Annual Meeting, Cincinnati, p. 572c.

Barbosa-Cánovas, G.V., and Rodríguez J.J., 2005, Thermodynamic Aspects of High Hydrostatic Pressure, in: *Novel Food Processing Technologies*, G.V. Barbosa-Cánovas, M.S. Tapia and M.P. Cano (eds.), CRC Press, New York, pp. 183–206.

Campanella, O.H., and Peleg M., 2001, Theoretical Comparison of a New and the Traditional Method to Calculate *Clostridium Botulinum* Survival During Thermal Inactivation, *J. Sci. Food Agr*. **81**:1069–1076.

Caner, C., Hernandez, R.J., Pascall, M., Balasubramaniam, V.M., and Harte B.R., 2004, The Effect of High-Pressure Food Processing on the Sorption Behavior of Selected Packaging Materials, *Packaging Technol. Sci*. **17**(3):139–153.

Cano, M.P., and De Ancos B., 2005, Advances in Use of High Pressure Processing and Preservation of Plant Foods, in: *Novel Food Processing Technologies*, G.V. Barbosa-Cánovas, M.S. Tapia and M.P. Cano (eds.), CRC Press, New York, pp. 283–310.

Carroll, T., Chen, P., and Fletcher A., 2003, A Method to Characterize Heat Transfer During High-Pressure Processing, *J. Food Eng*. **60**:131–135.

Codex, 2004, *Procedural Manual of the Codex Alimentarius Commission*, 14 Ed., Codex Alimentarius Commission. Rome.

Cooper, K.L., Call, M.K., and Meyer R.S. (Inventors), 2004, Ultra-High Pressure Vegetable Sterilization Method and Product, patent: U.S. 20040191382.

De Heij, W.B.C., van den Berg, R.W., van Schepdael, L., Hoogland, H., and Bijmolt H., 2005, Sterilization–only better, *New Food* **8**(2):56,58–61.

De Heij, W., van Schepdael, L., van den Berg, R., and Bartels P., 2002, Increasing Preservation Efficiency and Product Quality Through Control of Temperature Profiles in High Pressure Applications, *High Pressure Res*. **22**(3–4):653–657.

De Heij, W.B.C., van Schepdael, L.J.M.M., Moezelaar, R., Hoogland, H., Matser, A.M., and van den Berg R.W. 2003. High-Pressure Sterilization: Maximizing the Benefits of Adiabatic Heating. *Food Technol*. **57**(3):37–42.

Denys, S., van Loey, A.M., and Hendrickx M.E. 2000. A Modeling Approach for Evaluating Process Uniformity During Batch High Hydrostatic Pressure Processing: Combination of a Numerical Heat Transfer Model and Enzyme Inactivation Kinetics, *Innov. Food Sci. Emerg. Technol*. **1**(1):5–19.

Dunne, C.P., 2005, *Personal Communication*, U.S. Army Natick Soldier Center, Department of Defense, August 5.

EC258/97, 1997, Novel Foods and Novel Food Ingredients, Regulation (EC) No 258/97 of the European Parliament and of the Council of 27 January 1997, Official Journal L 043, 14/02/1997, pp. 0001–0006.

European Commission, 2002, Implementation of Regulation (EC) No 258/97 of the European Parliament and of the Council of 27 January 1997 Concerning Novel Foods and Novel Food Ingredients, Directorate General Health and Consumer Protection (SANCO D4), European Commission. (March 10, 2006); http://europa.eu.int/comm/food/food/biotechnology/novelfood/initiatives_en.htm.

Farkas, D.F., and Hoover D.G., 2000, High Pressure Processing, in: *Kinetics of Microbial Inactivation for Alternative Food Processing Technologies*, *J. Food Sci*. Supplement, pp. 47–64.

Franceschini, B., Gola, S., Rovere, P.P., and Frustoli M., 2005, Application of High Hydrostatic Pressure to Increase the Safety and the Shelf-Life of Ready-To-Eat (RTE) Traditional Meals, *Ind. Conserve*. **80**(4):391–409.

Gola, S., Foman, C., Carpi, G., Maggi, A., Cassara, A., and Rovere P., 1996, Inactivation of Bacterial Spores in Phosphate Buffer and in Vegetable Cream Treated with High Pressure, in: *High Press Biosci. Biotechnol*, R. Hayashi and C. Balny (eds.), Elsevier Science B.V., Amsterdam, pp. 253–259.

Gola, S., and Rovere, P.P., 2005, Resistance to High Hydrostatic Pressure of Some Strains of *Clostridium Botulinum* in Phosphate Buffer, *Ind. Conserve*. **80**(2):149–157.

Guamis, B., Pla, R., Trujillo, A.J., Capellas, M., Gervilla, R., Saldo, J., and Yuste J., 2005, High Pressure Processing of Milk and Dairy and Egg Products, in: *Novel Food Processing Technologies*, G.V. Barbosa-Cánovas, M.S. Tapia and M.P. Cano (eds.), CRC Press, New York, pp. 343–360.

Hartmann, C., and Delgado, A., 2002, Numerical Simulation of Convective and Diffusive Transport Effects on a High-Pressure Induced Inactivation Process, *Biotechnol. Bioeng*. **79**:94–104.

Hartmann, C., and Delgado, A., 2003, The Influence of Transport Phenomena During High-Pressure Processing of Packed Food on The Uniformity of Enzyme Inactivation, *Biotechnol. Bioeng*. **82**(6):725–735.

Hartmann, C., Delgado, A., and Szymczyk J., 2003, Convective and Diffusive Transport Effects in a High Pressure Induced Inactivation Process of Packed Food, *J. Food Eng*. **59**(1):33–44.

Harvey, A.H., Peskin, A.P., and Sanford A.K., 1996, NIST/ASTME – IAPSW Standard Reference Database 10, version 2.2.

Heinz, V., and Knorr D., 2001, Effect Of High Pressure On Spores, in: *Ultra High Pressure Treatment of Foods*, M.E.C. Hendrickx and D. Knorr (eds.), Kluwer Academic/Plenum Publishers, New York, pp. 77–116.

Hendricks, M., 2005, Pathways to Commercialization: From Academia to the Marketplace Academic Incubators and Innovation (European Model), in: *Commercializing Nonthermal Technologies*, Institute of Food Technologists Continuing Technical Education Committee. New Orleans, pp. 15–16.

Hirsch, E.S., Kramer, F.M., and Meiselman H.L., 2005, Effects of Food Attributes and Feeding Environment on Acceptance, Consumption and Body Weight: Lessons Learned in a Twenty-Year Program of Military Ration Research. US Army Research (Part 2). *Appetite* **44**(1):33–45.

Hjelmqwist, J., 2005, Commercial High Pressure Equipment, in: *Novel Food Processing Technologies*, G.V. Barbosa-Cánovas, M.S. Tapia and M P. Cano (eds.), CRC Press, New York, pp. 361–374.

Holdsworth, S. D., 1997, *Thermal Processing of Packaged Foods*, Blackie Academic & Professional, New York, pp.112–120.

Hoogland, H., de Heij, W., and van Schepdael L., 2001, High Pressure Sterilization: Novel Technology, New Products, New Opportunities, *New Food*, **4**(1):21–26.

Juliano, P., Clark, S., Koutchma, T., Ouattara, M., Mathews, J.W., Dunne, C.P., and Barbosa-Cánovas G. V., 2007, Consumer And Trained Panel Evaluation Of High Pressure Thermally Treated Scrambled Egg Patties, *J. Food Qual*. **30**(1):57–80.

Juliano, P., Li, B., Clark, S., Mathews, J.W., Dunne, P.C., and Barbosa-Cánovas G.V., 2006a, Quality and Sensory Analysis of Precooked Egg Products After High Pressure Processing Combined with Low and High Temperatures, *J. Food Qual*. **29**(5):505–530.

Juliano, P., Toldrà, M., Koutchma, T., Balasubramaniam, V.M., Clark, S., Mathews, J.W., Dunne, C.P., Sadler, G., and Barbosa-Cánovas G.V., 2006b, Texture and Water Retention Improvement in High Pressure Thermally Sterilized Scrambled Egg Patties. *J. Food Sci*. **71**(2):E52–61.

Kalchayanand, N., Dunne, C.P., Sikes, A., and Ray, B., 2003, Inactivation of Bacterial Spores by Combined Action of Hydrostatic Pressure and Bacteriocins in Roast Beef, *J. Food Saf*. **23**(4):219–231.

Koutchma, T., Guo, B., Patazca, E., and Parisi B., 2005, High Pressure–High Temperature Inactivation of *Clostridium Sporogenes* Spores: From Kinetics To Process Verification, *J. Food Process. Eng*. **28**(6):610–629.

Krebbers, B., Matser, A.M., Hoogerwerf, S.W., Moezelaar, R., Tomassen, M.M.M., and van den Berg R.W., 2003, Combined High-Pressure and Thermal Treatments for Processing of Tomato Puree: Evaluation of Microbial Inactivation and Quality Parameters, *Innov Food Sci Emerg Technol*. **4**(4):377–85.

Krebbers, B., Matser, A.M., Koets, M., and van den Berg R.W., 2002, Quality and Storage-Stability of High-Pressure Preserved Green Beans, *J Food Eng*. **54**(1):27-33.

Leadley, C., 2005, High Pressure Sterilisation: A Review. *Campden & Chorleywood Food Research Association* **47**:1–42.

Lee, D.U., Heinz, V., and Knorr D., 1999, Evaluation of Processing Criteria for the High Pressure Treatment of Liquid Whole Egg: Rheological Study, *Lebensm.- Wiss. U.-Technol*. **32**(5):299–304.

Ludikhuyze, L., van den Broeck, I., Weemaes, C.A., and Hendrickx M.E., 1997, Kinetic Parameters For Temperature-Pressure Inactivation Of Bacillus Subtilis α-Amylase Under Dynamic Conditions, *Biotechnol. Prog*. **13**:617–623.

Luechapattanaporn, K., Wang, Y., Wang, J., Tang, J., Hallberg, L.M., and Dunne C.P., 2005, Sterilization of Scrambled Eggs in Military Polymeric Trays by Radio Frequency Energy, *J. Food Sci*. **70**(4):288–294.

Ma, L., Chang, F.J., Barbosa-Cánovas, G.V., and Swanson B.G., 2001, Comparison Study of Pulsed Electric Fields, High Hydrostatic Pressure, and Thermal Processing on the Electrophoretic Patterns of Liquid Whole Egg, in: *Pulsed Electric Fields in Food Processing: Fundamental Aspects and Applications*, *G*.V. Barbosa-Cánovas and H. Zhang (eds.), Technomic Publishing Co., Lancaster, pp. 225–240.

Margosch, D., 2005, *Behavior of Bacterial Endospores and Toxins as Safety Determinants in Low Acid Pressurized Food*, Doctoral Dissertation, Technischen Universität Berlin.

Margosch, D., Ehrmann, M.A., Gaenzle, M.G., and Vogel R.F., 2004, Comparison of Pressure and Heat Resistance of *Clostridium Botulinum* and Other Endospores in Mashed Carrots, *J. Food Prot*. **67**(11):2530–2537.

Margosch, D., Moravek, M., Gaenzle, M.C., Maertlbauer, E., Vogel, R F., and Ehrmann M.A., 2005, Effect of High Pressure and Heat on Bacterial Toxins, *Food Technol. Biotechnol*. **43**(3):211–217.

März, A., 2002, Method for Inactivating Microorganisms Using High Pressure Processing. Patent number: EP 1 201 252 A1.

März, A., 2003, Method for Inactivating Microorganisms Using High Pressure Processing. Patent number: US 6635223.

Matser, A.M., Krebbers, B., van den Berg, R.W., and Bartels P.V., 2004, Advantages of High Pressure Sterilization on Quality of Food Products, *Trends Food Sci Technol*. **15**(2):79–85.

Mermelstein, N.H., 2001, Military and Humanitarian Rations, *Food Technol*. **55**(11):73–75.

Meyer, R.S., Cooper, K.L., Knorr, D., and Lelieveld H.L.M., 2000, High-Pressure Sterilization of Foods. *Food Technol*. **54**(11):67–68, 70–72.

Montero, P. and Gómez-Guillén M.C., 2005, High Pressure Applications on Myosystems, in: *Novel Food Processing Technologies*, G.V. Barbosa-Cánovas, M.S. Tapia and M.P. Cano (eds.), CRC Press, New York, pp. 311–342.

NACMCF (National Advisory Committee on Microbiological Criteria for Foods), 2004, Requisite Scientific Parameters for Establishing the Equivalence Oof Alternative Methods of Pasteurization. (Washington; March 10, 2006) http://www.fsis.usda.gov/About_FSIS/NACMCF/index.asp.

NACMCF. 2005. Consideration for Establishing Safety-Based Consume-By Date Labels for Refrigerated Ready-To-Eat Foods, *J. Food Prot*. **68**(8):1761-1775.

NC Hyperbaric, 2004, *High Pressure Processing. Technology That Makes Sense*. [Commercial booklet], Burgos.

NFPA. 1985. *Guidelines for Thermal Process Development for Foods Packaged in Flexible Containers*. National Food Processors Association (NFPA), New York.

Nicolaï, M.B., Scheerlinck, N., Verboven, P., and Baerdemaeker J.D. 2001. Stochastic Finite-Element Analysis of Thermal Food Processes, in: *Food Processing Operations Modeling. Design and Analysis, J*. Irudayaraj (ed.), Marcel Dekker, New York, pp. 265–304.

Otero, L., Molina-Garcia, A.D., and Sanz P.D., 2000, Thermal Effect in Foods During Quasi-Adiabatic Pressure Treatments, *Innov. Food Sci. Emerg. Technol*. **1**:119-126.

Otero, L., and Sanz P.D., 2003, Modeling Heat Transfer in High Pressure Food Processing: A Review. *Innov. Food Sci. Emerg. Technol*. **4**(2):121–134.

Patterson, M.F., 2005, A Review: Microbiology of Pressure-Treated Foods, *J. Applied Microbiol*. **98**:1400–1409.

Palazoglu, K., 2006, Influence of Convective Heat Transfer Coefficient on the Heating Rate of Materials with Different Thermal Diffusivities, *J. Food Eng*. **73**(3):290–296.

Peleg, M., Normand, M.D., and Campanella O.H., 2003, Estimating Microbial Inactivation Parameters from Survival Curves Obtained Under Varying Conditions–The Linear Case, *Bull. Math. Biol*. **65**:219–234.

Peleg, M., Normand, M.D., and Corradini M.G., 2005, Generating Microbial Survival Curves During Thermal Processing in Real Time, *J. Appl. Microbiol*. **98**:406–417.

Pflug, I.J., 1987, Using the Straight-Line Semi Logarithmic Microbial Destruction Model As an Engineering Design Model for Determining the F-Value for Heat Processes, *J. Food Prot*. **50**(4):342–246.

Rajan, S., Ahn, J., Balasubramaniam, V.M., and Yousef A. E., 2006a, Combined Pressure-Thermal Inactivation Kinetics of *Bacillus Amyloliquefaciens* Spores in Mashed Egg Patty Mince, *J. Food Prot*. (In press.)

Rajan, S., Pandrangi, S., Balasubramaniam, V.M., and Yousef A.E., 2006b, Inactivation of *Bacillus stearothermophilus* spores in egg patties by pressure assisted thermal processing, *LWT-Food Sci. Technol*. (In press.)

Rasanayagam, V., Balasubramaniam, V.M., Ting, E., Sizer, C.E., Bush, C., and Anderson C., 2003, Compression Heating of Selected Fatty Food Materials During High-Pressure Processing, *J. Food Sci*. **68**(1):254–259.

Raso, J., Barbosa-Cánovas, G.V., and Swanson B.G. 1998. Sporulation Temperature Affects Initiation of Germination and Inactivation by High Hydrostatic Pressure of *Bacillus Cereus. J. Appl. Microbiol*. **85**:17–24.

Reddy, N.R., Solomon, H.M., Fingerhut, G.A., Rhodehamel, E.J., Balasubramaniam, V.M., and Palaniappan S., 1999, Inactivation Of *Clostridium Botulinum* Type E Spores By High Pressure Processing, *J. Food. Saf*. **19**:277–288.

Reddy, N.R., Solomon, H.M., Tetzloff, R.C., and Rhodehamel E.J., 2003, Inactivation of *Clostridium Botulinum* Type A Spores by High Pressure Processing at Elevated Temperatures, *J. Food Prot*. **66**(8):1402–1407.

Rovere, P., Gola, S., Maggi, A., Scaramuzza, N., and Miglioli L., 1998, Studies on Bacterial Spores by Combined Pressure-Heat Treatments: Possibility to Sterilize Low-Acid Foods, in: *High Pressure Food Science, Bioscience and Chemistry*, N.S. Isaacs (ed.), The Royal Society of Chemistry, Cambridge, pp. 354–63.

Rovere, P., Squarcina, N., Gola, S., Sandei, L., Iametti, S., and Carpi G., 2000, Effect of Thermal Treatment Under High Pressure on the Quality of a Meat Sauce, *High Pressure Res*. **19**:99–107.

Sale, A.J.H., Gould, G.W., and Hamilton W.A., 1970, Inactivation of Bacterial Spores by High Hydrostatic Pressure, *J. Gen. Microbiol*. **60**:323–334.

Schauwecker, A., Balasubramaniam, V.M., Sadler, G., Pascall, M.A., and Adhikari C., 2002, Influence of High-Pressure Processing on Selected Polymeric Materials and on the Migration of a Pressure-Transmitting Fluid, *Packaging Technol. Sci*. **15**:255–262.

Shearer, A.E.H., Dunne, C.P., Sikes, A., and Hoover D.G., 2000, Bacterial Spore Inhibition and Inactivation in Foods by Pressure, Chemical Preservatives, and Mild Heat, *J. Food Prot*. **63**(11):1503–1510.

Sizer, C.E., Balasubramaniam, V.M., and Ting E., 2002, Validating High-Pressure Processes for Low-Acid Foods, *Food Technol*. **56**(2):36-57.

Stewart, C.M. 2005. HPP Safety and Quality Data, in: *Commercializing Nonthermal Technologies*, Institute of Food Technologists Continuing Technical Education Committee, New Orleans, pp. 15–16.

Stewart, C.M., Dunne, C.P., Sikes, A., and Hoover D.G., 2000, Sensitivity of Spores of *Bacillus Subtilis* and *Clostridium Sporogenes* PA 3679 to Combinations of High Hydrostatic Pressure and Other Processing Parameters, *Innov. Food Sci. Emerg. Technol*. **1**(1):49–56.

Surak, J.G., 2006, Global Harmonization: Foods Safety Management Standards, *Int. Rev. Food Sci. Technol*. Winter 2005/2006: 34–36.

Taki, Y., Awano, T., Toba, S., and Mitsuura N. 1991. Sterilization of *Bacillus Sp*. Spores by Hydrostatic Pressure, in: *High Pressure Science for Food*, R. Hayashi (ed.), Sanei Pub. Co., Kyoto, pp. 217–24.

Tapia, M.S., Arispe, I., and Martínez A., 2005, Safety and Quality in the Food Industry, in: *Novel Food Processing Technologies*, G.V. Barbosa-Cánovas, M.S. Tapia and M.P. Cano (eds.), CRC Press, New York, pp. 669–680.

Ter Minassian, L., Pruzan, P. and Soulard A., 1981, Thermodynamic Properties of Water Under Pressure up to 5 Kbar and Between 28 and 120°C. Estimations in the Supercooled Region Down to -40°C, *J. Chem. Phys*. **75**:3064–3072.

Ting, E., Balasubramaniam, V.M., and Raghubeer E., 2002, Determining Thermal Effects In High-Pressure Processing. *Food Technol*. **56**(2):31–35.

Van Loey, A., Ooms, V., Weemaes, C., van den Broeck, I., Ludikhuyze, L., Indrawati, Denys, S., and Hendrickx M., 1998, Thermal and Pressure-Temperature Degradation of Chlorophyll in Broccoli (*Brassica Oleraces L. Italica*) Juice: A Kinetic Study. *J. Agr. Food Chem*. **46**:5289–5294.

Van Opstal, I., Bagamboula, C.F., Vanmuysen, S.C.M., Wuytack, E.Y., and Michiels C.W., 2004, Inactivation of *Bacillus Cereus* Spores in Milk by High Pressure and Heat Treatments, *Int. J. Food Microbiol*. **92**:227–234.

Van Schepdael, L.J.M.M., de Heij, W.B.C., and Hoogland H., 2002, Method for high pressure preservation, patent: PCT WO 02/45528 A1.

Varga, S., and Oliveira, J.C., 2000, Determination of the Heat Transfer Coefficient Between Bulk Medium and Packed Containers in a Batch Retort, *J. Food Eng*. **44**(4):191–198.

Welti-Chanes, J., López-Malo, A., Palou, E., Bermúdez, D., Guerrero-Beltrán, J.A., and Barbosa-Cánovas G. V. 2005. Fundamentals and Applications of High Pressure Processing of Foods, in: *Novel Food Processing Technologies*, G.V. Barbosa-Cánovas, M.S. Tapia, M.P. Cano, (eds.), CRC Press, New York, pp. 157–182.

Wesley, R.D., Rousselle, J.R., Schwan, D.R., and Stadelman W.J., 1982, Improvement in Quality of Scrambled Egg Products Served from Steam Table Display, *Poultry Sci*. **61**(3):457–462.

Wilson, M.J., and Baker R., 2000, High Temperature/Ultra-High Pressure Sterilization of Foods, Patent: US 6,086,936.

Wilson, M.J., and Baker R., 2003, High Temperature/Ultra-High Pressure Sterilization of Low Acid Foods, Patent: EU 1 295 537 A2.

3
Nonlinear Kinetics: Principles and Potential Food Applications

M.G. Corradini, M.D. Normand, and M. Peleg

3.1. Introduction

Traditionally, the progress of many processes affecting the safety and quality of foods, notably microbial inactivation and the thermal degradation of vitamins has been described in terms of first order kinetics. According to this concept, the "survival ratio" y(t), be it the fraction of survival cells or spores, i.e., N(t)/N_0, where N(t) and N_0 are the momentary (instantaneous) and initial numbers, or C(t)/C_0, where C(t) and C_0 are the momentary and initial vitamin's concentration, is given by:

$$\frac{dy(t)}{dt} = -k(T)y(t) \tag{3.1}$$

which upon integration yields:

$$y(t) = \exp[-k(T)t] \tag{3.2}$$

$$\log y(t) = -k(T)t \tag{3.3}$$

where k(T) is a temperature dependent rate constant. A similar model can be written for exponential growth, in which case the negative sign is dropped. However, exponential growth, either of a microbial population or of any chemical compound concentration cannot continue indefinitely for obvious reasons. Hence, growth, especially of microorganisms in a closed habitat, must be described by alternative models. These can be classified as:

(a) models derived from the classic continuous *logistic equation* (Verhulst's model):

$$\frac{dy(t)}{dt} = r(T)y(t)\left[1 - \frac{y(t)}{y_{asympt}(T)}\right] \tag{3.4}$$

where y(t) is the linear or logarithmic growth ratio, i.e., [N(t)-N_0]/N_0 or log[N(t)/N_0], respectively, r(T) is the characteristic temperature dependent rate constant

and y_{asympt}(T) (commonly and erroneously dubbed "max") is the asymptotic growth ratio, representing the habitat's carrying capacity. Examples of these are the Baranyi-Roberts model (Baranyi and Roberts, 1994) and Fujikawa et al. (2004). In the former, r(T) is replaced by a function intended to account for the physiological state of the population at the time of its introduction to the new medium. In the latter, a power term is added to the original logistic model to improve its fit to experimental sigmoid growth curves.

(b) Descriptive algebraic models, the most familiar of which is the Gompertz model (McKellar and Lu, 2004):

$$\log[y(t)] = A(T) + C(T)\exp\{-\exp\{-B(T)[t-\mu(T)]\}\} \tag{3.5}$$

where μ(T) is the inflection point location and A(T), B(T) and C(T) are coefficients, all temperature dependent adjusted regression parameters.

The temperature dependence of both the growth and inactivation/degradation rate constants has been traditionally assumed to obey the Arrhenius equation (Purich and Allison, 2000):

$$k(T) = k(T_{ref}) \cdot \exp\left[\frac{E_A}{R}\left(\frac{1}{T} - \frac{1}{T_{ref}}\right)\right] \tag{3.6}$$

where $k(T_{ref})$ is the rate constant at a reference temperature T_{ref}, E_A the "energy of activation" and R the universal gas constant. In microbial and enzyme inactivation, and sometimes even in vitamin degradation (Labuza, n.d.; Purich and Allison, 2000), the temperature dependence of the reciprocal of k(T), known as the "D value", has been assumed to obey the relationship:

$$\log_{10}\left(\frac{D(T)}{D(T_{ref})}\right) = \frac{T - T_{ref}}{z} \tag{3.7}$$

where z is the temperature span at which the "D value" increases or decreases by a factor of ten. Although Eqs. (3.6) and (3.7) are mutually exclusive models, their parameters are frequently displayed in textbooks and websites side by side without comment. Despite their wide use in microbiology and food physical chemistry and biochemistry, the two models can have serious drawbacks. For example:

(a) For either to be correct, all the isothermal inactivation, degradation or growth curves need to be log linear, i.e., the process has to follow the first order kinetics model. Unfortunately, there is growing evidence that in many systems, this condition is not satisfied (e.g., Peleg and Cole, 1998; van Boekel, 2002; Corradini and Peleg, 2004). This should not come as a surprise. The first order kinetics model is the hallmark of radioactive decay or simple chemical reactions, where the probability of a disintegration event or interaction does not change with time, because the atoms or reactants remain unchanged throughout the process duration. This need

not be the case in biological systems and complex biochemical reactions, where both the "reactants" and chemical environment are continuously changing (Peleg et al., 2004.)

(b) The Arrhenius equation was developed for simple chemical reactions having a single energy of activation. There is no reason to assume that biological and complex biochemical processes having several interactive pathways must be universally coordinated in such a way that they will always produce a single energy of activation as if they were one single reaction between two gases under low pressure, for which the model was originally derived (Barrow, 1996). The same can be said about the log linear model that has produced the z value. Its universality, if it had existed, would also require a coordinated kinetics that would be very difficult to explain in mechanistic terms. But let us assume that the two models (Eqs. 3.6 and 3.7) were only used as an approximation with no mechanistic significance assigned to their coefficients. Even then they would be a poor choice for several reasons:

1. The rate constant k(T) or its reciprocal D(T) are both derived from data after their logarithmic transformation. Therefore, in the pertinent temperature rate, they rarely change by several orders of magnitude that would justify a second logarithmic transformation. In the Arrhenius model, the rationale of compressing the temperature scale is also highly questionable. For example, for most biochemical reactions, the range between 5 and 40°C is quite significant and so is the range of 90 to 120°C in sporal inactivation. Yet they are compressed to the modest 0.0036 – 0.0032 and 0.00275 – 0.0025 K^{-1} intervals after the transformation required by the Arrhenius model (Peleg, 2006).
2. Both models entail that the logarithmic rate in the same chemical environment is solely a function of temperature but not of time, i.e., k(T) or D(T) are totally independent of the temperature history of the food (Peleg et al., 2004). To demonstrate this point, consider the following hypothetical scenario: A food containing a heat sensitive vitamin, let's say, or inoculated with a bacterium and stored at a fairly low but nondestructive temperature is divided into two halves I and II. The first, I, is heated quickly to a highly destructive or lethal temperature, kept at this temperature for awhile and then cooled to a somewhat lower, but still destructive or lethal temperature, as shown in Fig. 3.1. The second, II, is kept at the original temperature and then quickly heated to the same temperature to which the first half has been cooled. From this point on, both halves are kept at the same destructive lethal temperature, as also shown schematically in the figure. Now, according to the traditional first order kinetics, combined with the Arrhenius or log linear model, the vitamin's concentration or the size of the bacterium's population in the two halves of the food would be very different – no problem here. But since these two halves have reached the same temperature, the vitamin's logarithmic decay rate or the bacterium's logarithmic mortality rate must be exactly the same! This is very unlikely, and for this reason alone, the whole approach to modeling food kinetics has to be re-examined and revised (Peleg, 2006).

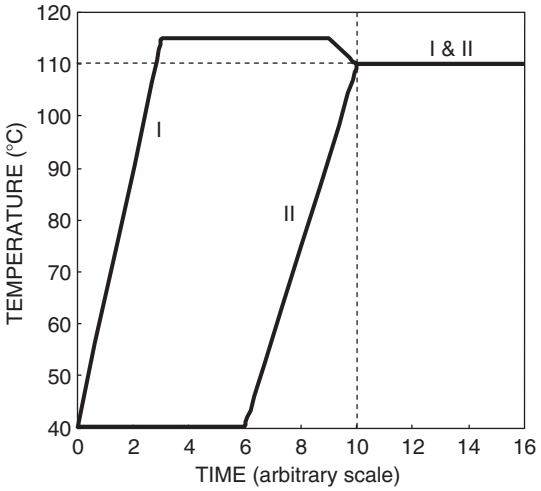

FIG. 3.1. A food containing a heat sensitive vitamin or inoculated with a bacterium and stored at a fairly low but nondestructive temperature is divided into two halves, I and II. The first, I, is heated quickly to a highly destructive or lethal temperature. If the traditional temperature dependence models were correct, the logarithmic decay rate of the two halves must be the same, kept at this temperature for awhile and then *cooled* to a somewhat lower, but still destructive or lethal temperature. The second, II, is kept at the original temperature and then quickly *heated* to the same temperature to which the first half has been cooled. From this point on, both halves are kept at the same destructive lethal temperature

3. Suppose that there were food systems whose kinetics indeed followed the first order kinetics and a meaningful k(T) or D(T) could represent it. In this case, linearization of the plot depicting the rate constant or reciprocal's temperature dependence on semi logarithmic coordinates would carry the risk of amplifying experimental errors. Or alternatively, even a slight but true deviation from the assumed linearity might result in an exponential error, as shown in Fig. 3.2.

These shortcomings or potential shortcomings of the traditional models can be all eliminated, but this requires their reformulation as nonlinear rate models. Fortunately, as will be demonstrated below, the tools to handle such models are readily available, and they can be used in many situations that are encountered in food processing, handling and storage.

3.2. Nonlinear Kinetics

The starting point is that we do not have to assume *a priori*, let alone know in advance, what the system's kinetics is. This applies to processes involving inactivation and degradation or growth and accumulation. All we rely on are sets of isothermal experimental data of loss or growth. At least certain kinds of

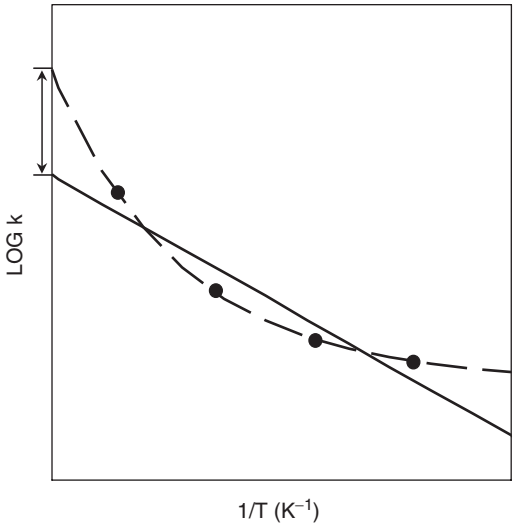

FIG. 3.2. A slight-but-true deviation from the assumed linearity might result in an exponential error

inactivation parameters can also be extracted from non-isothermal survival or degradation curves—see below—but this requires dense and highly reproducible experimental data (Peleg and Normand, 2004; Peleg et al., 2004). For simplicity, we'll show two kinds of processes, a Weibullian–power law inactivation or degradation and logistic growth or accumulation. It will become evident that the methodology can be applied to other decay or growth patterns as has been demonstrated elsewhere (Peleg et al., 2003; Corradini and Peleg, 2005). We'll concentrate on the mathematical procedure rather than on the models' mechanistic interpretation and the considerations that had led to their development. These are amply discussed in the publications already cited.

3.2.1. Power Law (Weibullian) Log-Logistic Decay

Consider an isothermal survival curve of the kind shown in Fig. 3.3., i.e., having upward or downward concavity. It is obvious that the local slope (momentary rate) is time dependent. Such curves, more often than not can be fitted by the power law model with a constant power:

$$\log_{10} y(t) = -b(T)t^n \tag{3.8}$$

where b(T) is a rate constant and n a constant. Upper concavity is expressed by $n<1$, downward concavity by $n>1$ and linearity ("first order kinetics") by $n=1$ (Fig. 3.4). Thus, the log linear model is just a special case of Eq. (3.8). Consequently, all that follow would apply to the conventional models, but not vice versa. Also, the

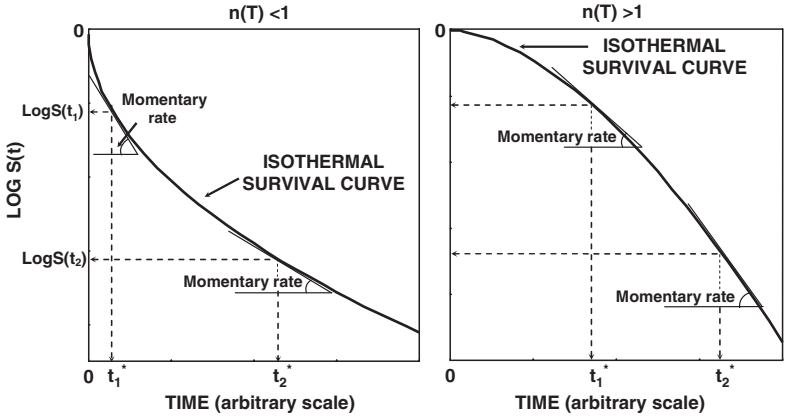

FIG. 3.3. Isothermal survival curve having upward (left) or downward concavity (right)

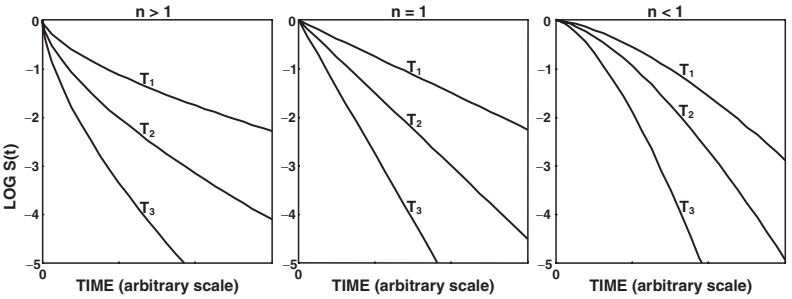

FIG. 3.4. A series of isothermal survival or decay curves

constancy of n is not a prerequisite and the methodology can easily be extended to a temperature dependent n(T) – see Mattick et al. (2001) for example.

A series of isothermal survival or decay curves would most probably look like what is shown schematically in Fig. 3.4. The temperature dependence of b(T) can be described by several alternative models (Corradini et al., 2005), as demonstrated in Fig. 3.5. For microbial and enzyme inactivation, our preference is the log logistic model:

$$b(T) = \log_e \{1 + \exp[k(T - T_c)]\} \tag{3.9}$$

where T_c marks the temperature at which destruction starts to accelerate and k the slope of b(T)'s climb at temperature well above T_c.

The advantage of this model is that it properly accounts for the qualitative difference between the effects of low and high temperatures on the survival of microbes and enzymes.

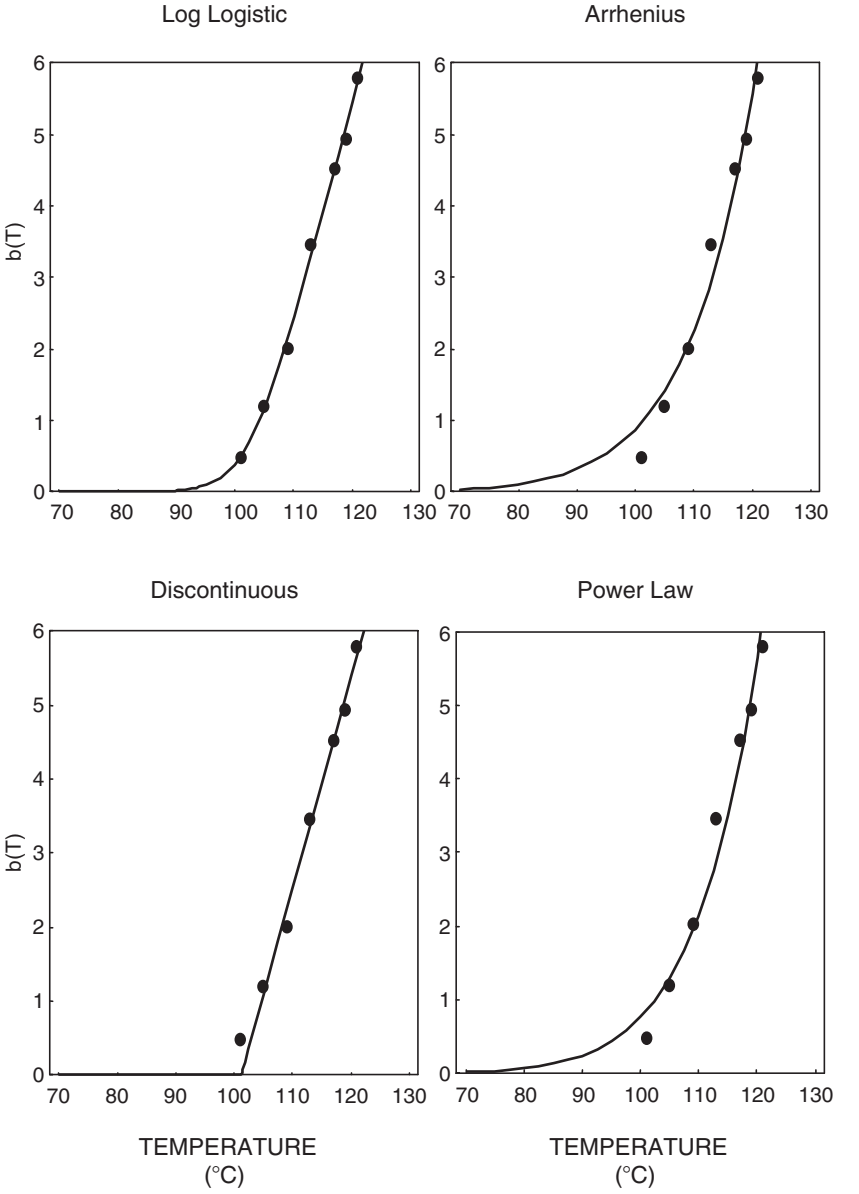

FIG. 3.5. The temperature dependence of the b(T) of *C. botulinum* spores described by four alternative models. Notice that the difference in fit are primarily expressed around the inactivation's onset. The original data is from Anderson et al. (1996)

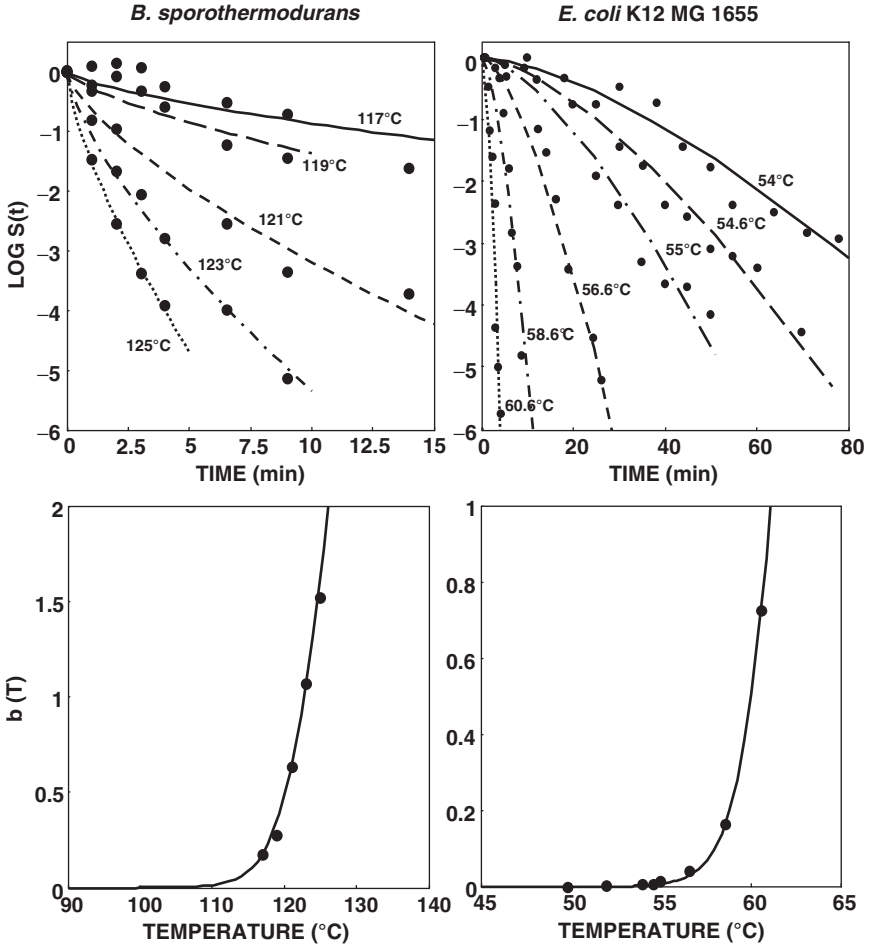

FIG. 3.6. The fit of Eqs. (3.8) and (3.9) to experimental survival data published by Periago et al. (2004) and Valdramidis et al. (2004) – left and right respectively

The fit of Eqs. (3.8) and (3.9) to published decay curves of different kinds is demonstrated in Fig. 3.6.

According to this model, a *non-isothermal* decay curve y(t) vs. t can be constructed by assuming that its local (momentary) slope is the slope of the isothermal curve the at momentary temperature at a time t^* that corresponds to the momentary value of y(t), shown in Fig. 3.3.

Written mathematically, the momentary isothermal slope of the curve is as follows:

$$\left|\frac{dy(t)}{dt}\right|_{T=const.} = -b(T)t^{n-1} \tag{3.10}$$

and

$$t^* = \left[-\frac{\log_{10} y(t)}{b(T)} \right]^{\frac{1}{n}} \tag{3.11}$$

which yields the differential rate equation:

$$\frac{dy(t)}{dt} = b\left[T(t)\right] \cdot n \left\{ -\frac{\log_{10} y(t)}{b[T(t)]} \right\}^{\frac{n-1}{n}} \tag{3.12}$$

or when b(T) can be described by the log logistic model (Eq. 3.9)

$$\frac{dy(t)}{dl} = \log_e \left\{ 1 + \exp\left\{ k\left[T(t) - T_c \right] \right\} \right\} n \left\{ \frac{-\log_{10} y(t)}{\log_e \left\{ 1 + \exp\left\{ k\left[T(t) - T_c \right] \right\} \right\}} \right\}^{\frac{n-1}{n}} \tag{3.13}$$

This rate model, despite its cumbersome appearance can be easily solved by modern mathematical software and even with general purpose software like MS Excel® (Peleg et al., 2005).

The predictive ability of the model is demonstrated in Fig. 3.7. Notice that alternative models can also be used. As long as the alternative models have good fit to the experimental isothermal data, the chosen model's format is unimportant, provided that it is only used to predict decay/survival curves under conditions covered by the isothermal experimental data and not for extrapolation.

3.2.2. Time Equivalent

Thermobacteriologists and food engineers are accustomed to the concept of an "F_0 value" which is supposed to be a measure of the equivalency of a non isothermal heat process to one performed at a constant reference temperature. Traditionally, this temperature has been 121.1°C (250°F) for heat sterilization of low acid foods. The problem with the "F_0 value" as a degree of inactivation measure is that it has a meaning *if and only if* the organism's or spore's isothermal survival curves are *all* log linear and the temperature dependence of the "D values" is log linear too. In any other case, including that where the survival curves are log linear but the temperature dependence of the rate constant k is governed by the Arrhenius equation, the use of the concept will result in considerable discrepancies between the calculated and actual survival ratios (see Datta, 1993 and Peleg, 2003). The problem can be avoided if the "F_0 value" is replaced by the actual equivalent time at a reference temperature, which can be either calculated or determined graphically for any inactivation model. In this way, the requirement of log linearity is totally eliminated, and as long as the non isothermal process does not produce growth and the process is too short for biological adaptation, there are no restrictions on either the primary or secondary models that describe the organism's inactivation. The construction of the "equivalent time at reference temperature" is shown

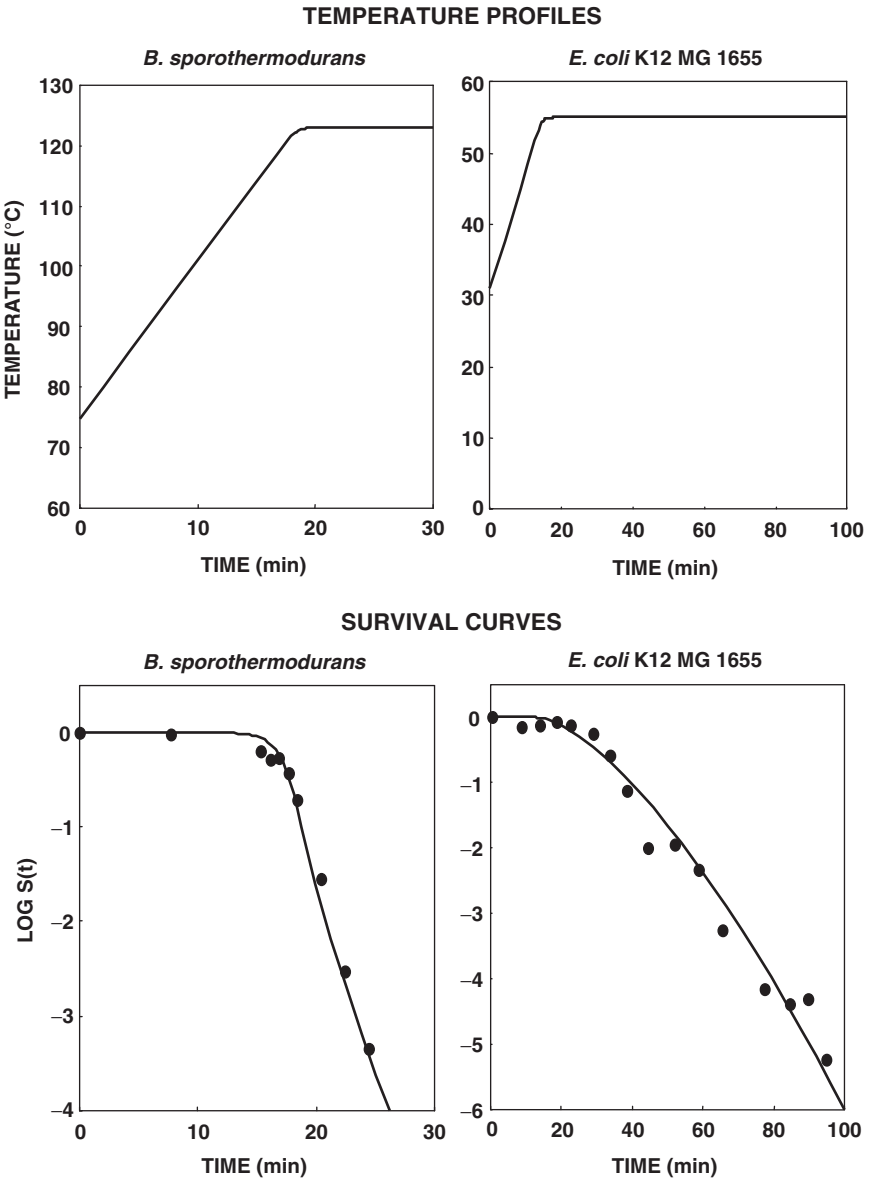

FIG. 3.7. Demonstration of the predictive ability of the non isothermal survival model (Eq. 3.13) to survival data published by Periago et al. (2004) and Valdramidis et al. (2004). Circles – experimental survival ratios, solid lines – the survival curve calculated from isothermal data

schematically in Fig. 3.8 (Corradini et al., 2005). For the simplified Weibullian model (Eq. 3.8) with a constant exponent n, it can be calculated from:

$$T_{equivalent@Tref}(t) = \left[\frac{-\log_{10} S(t)}{b(T_{ref})}\right]^{\frac{1}{n}} \tag{3.14}$$

and plotted together with survival ratio as a measure of a thermal process progress.

3.2.3. *Logistic Growth or Accumulation*

Consider that a sigmoid isothermal growth can be described by the empirical model:

$$y(t) = \frac{a(T)}{1+\exp\left\{k(T)\left[t_c(T)-t\right]\right\}} - \frac{a(T)}{1+\exp\left[k(T)\,t_c(T)\right]} \tag{3.15}$$

where y(t) is the linear or logarithmic growth/accumulation *ratio*, a(T) is the approximate temperature dependent asymptotic level of y(t), $t_c(T)$ the temperature dependent time that marks the region where exponential growth occurs and k(T) a temperature dependent marker of the curve's steepness at this region. The rationale of adding the usually small second term to the right side of the equation is to assure that at t = 0, y(t) = 0 (Corradini and Peleg, 2005). Thus, the actual asymptotic ratio is $a(T)(1-1/\{1+\exp[k(T)t_c(T)]\})$.

A schematic view of an isothermal logistic growth curve is shown in Fig. 3.9. As before, the slope of the curve, or the momentary isothermal growth rate, is a function of time. [It is curious that this notion, taken for granted in microbial growth modeling, is sometimes fiercely opposed when applied to microbial

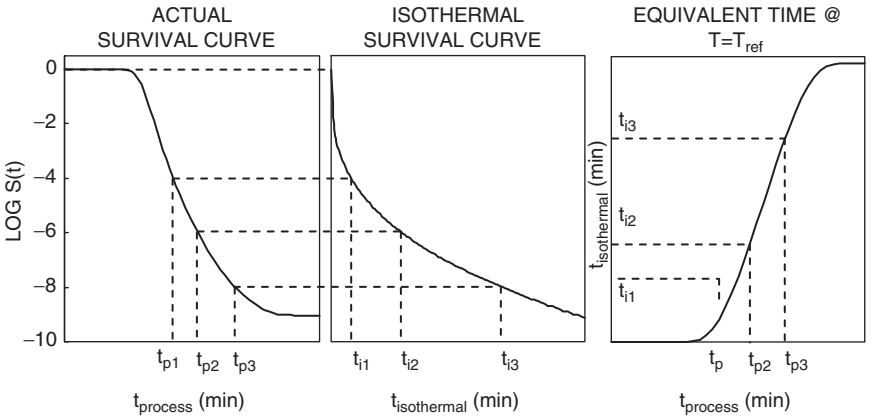

FIG. 3.8. Schematic view of the construction of the "equivalent time at a reference temperature"

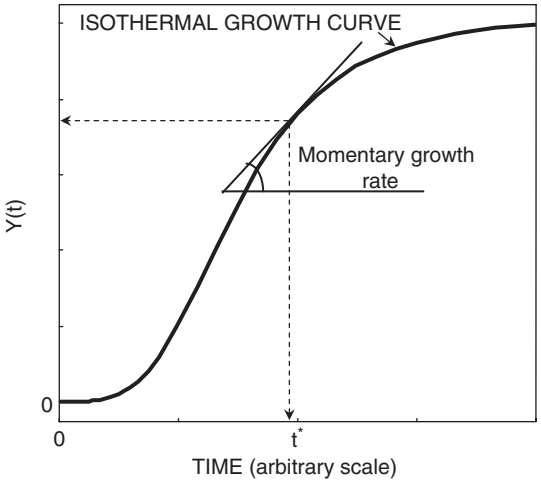

FIG. 3.9. Schematic view of a normalized isothermal logistic curve

inactivation and degradation kinetics]. The temperature dependence of the growth parameters a(T), k(T) and t_c(T) can be described by an *ad hoc* empirical model. An example is shown in Fig. 3.10.

As in inactivation, the assumption, which again can be verified by testing the model's predictions against experimental observations, is that the momentary non-isothermal growth rate is the momentary isothermal growth rate a time that corresponds to the momentary growth ratio. Thus, the non-isothermal growth or accumulation curve can be constructed in a similar manner, as shown schematically in Fig. 3.11. The predictive ability of the model is demonstrated in Fig. 3.12. Again, alternative models can also be constructed, and as long as they are not used for extrapolation, the choice of the particular model will hardly affect the predictions' quality (Corradini and Peleg, 2005).

All the above demonstrates that if an organism's survival or growth parameters are known, one can translate a time-temperature relationship into a corresponding inactivation or growth curve—see below. Or alternatively, if the decay or accumulation parameters of a nutrient or pigment are known, then one can convert the time temperature data into a corresponding quality loss curve.

3.3. Potential Food Applications

Programs written in MS Excel® to perform the calculation of microorganisms' response to changing temperature, be it inactivation or growth, are now posted on the web. See www-unix.oit.umass.edu/~aew2000/CBotSurvival.html and www.unix.oit.umass.edu/~aew 2000/MicrobeGrowthModelA.html. [A similar program to describe the response of microorganisms to the presence of a volatile/unstable disinfectant is also included.] Each program is presented in two formats: In the first,

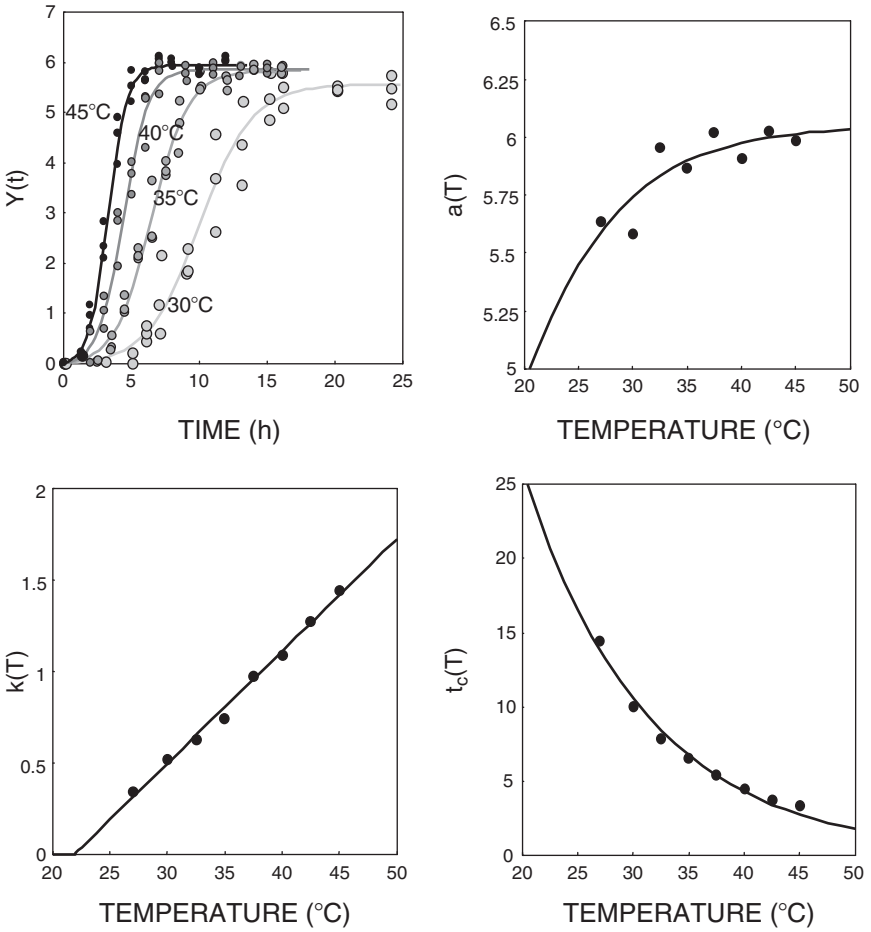

FIG. 3.10. The fit of the isothermal growth of *C. perfringens* and the temperature dependence of the growth parameters a(T), k(T) and t_c(T). The original data are from Amezquita et al. (2005)

the temperature (or concentration) is generated through a mathematical formula whose parameters can be chosen or adjusted by the user. The user can also choose or adjust the organisms' inactivation or growth parameters, known or assumed. In the second, the user can paste his or her own time-temperature (or concentration) data and modify or edit them at will. The programs work in real time and, in principle at least, the source of the time-temperature data can be the output of a digital thermometer or thermometers placed in the point or points of interest, or an industrial sensor/controller. This means that with the right parameters of the organism or spore in question, one can translate time-temperature data, continuously, into theoretical degree of inactivation, in terms of a momentary theoretical survival

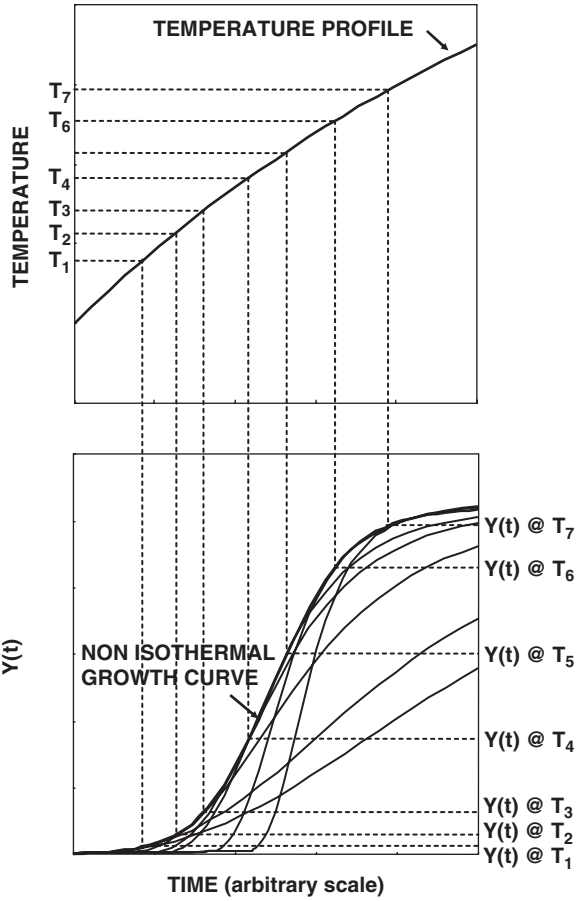

FIG. 3.11. The momentary non isothermal growth rate is the momentary isothermal growth rate at a time that corresponds to the momentary growth ratio. Thus, the non isothermal growth or accumulation curve can be constructed in a similar manner to that of a survival curve

ratio and/or equivalent time at a reference temperature (instead of the "F_0 value," which is limited to very few organisms, if any). A theoretical growth ratio can also be calculated in a similar manner, as will be demonstrated below.

3.3.1. Monitoring Industrial Heat Sterilization Processes

The programs' output for an ineffective heating cycle is shown in Fig. 3.13. The insufficient process can be "corrected" by elevating the temperature and/or extending the heating stage, as shown in Fig. 3.14, both very easy to arrange by adjusting the heat profile parameters. Such simulations can be used to study how changes in the process conditions will affect its theoretical lethality.

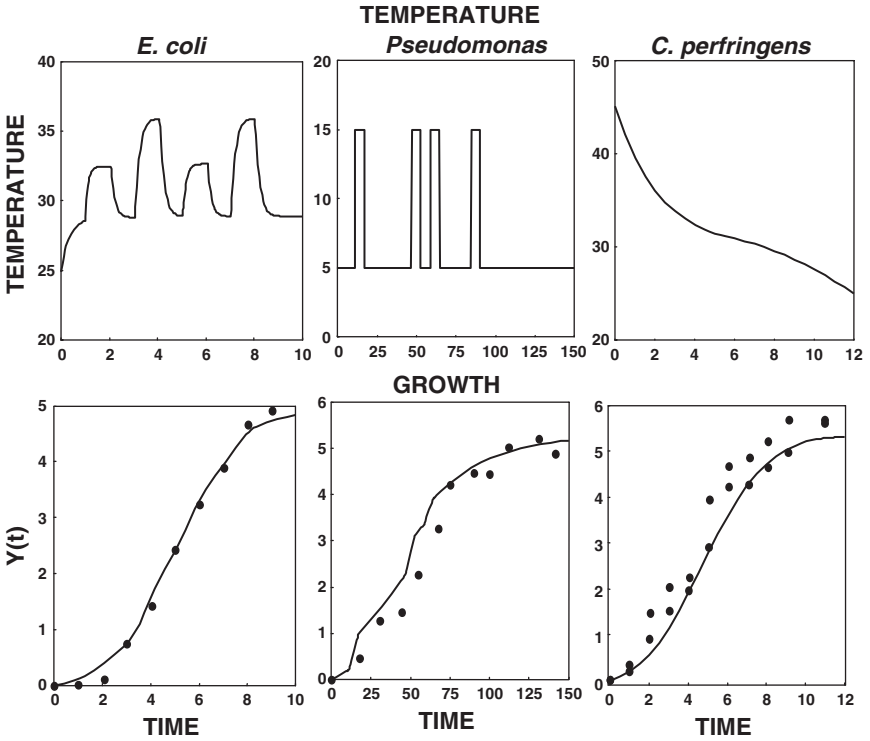

FIG. 3.12. Demonstration of the predictive ability of the non isothermal growth model based on Eq. (3.15) as the primary model. The solid circles are the experimental growth ratios and the solid lines – the growth curves calculated from isothermal data. The original data are from Fujikawa et al. (2004), Koutsoumanis et al. (2001) and Amezquita et al. (2005), respectively

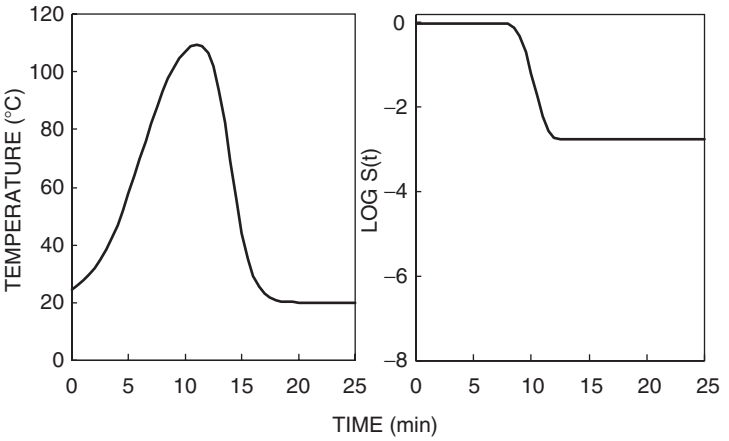

FIG. 3.13. Programs' output for an ineffective heating cycle

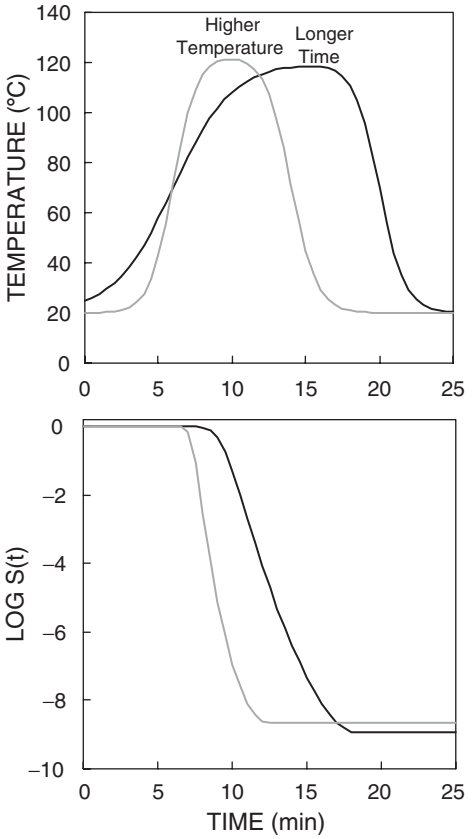

FIG. 3.14. The insufficient process can be "corrected" by elevating the temperature and/or extending the heating stage

Another hypothetical scenario is the case of steam interruption shown in Fig. 3.15 (left). Again the temperature drop can be remedied by increasing the target temperature and/or prolonging the heating stage as also shown in the figure (right). At least in principle, such corrections can be made in real time by an operator or through programming an automatic controller. The quality implications of the "remedy" can be assessed by running the new profiles with the degradation parameters of a key vitamin or pigment.

3.3.2. Following and Predicting Changes During Storage and Transportation

The program can be used to simulate or estimate, in real, time microbial growth in a stored or transported food when its temperature fluctuates. An example of simulated growth of *Pseudomonas* in refrigerated fish subjected to oscillating temperatures is shown in Fig. 3.16. Such simulations can be used to either determine

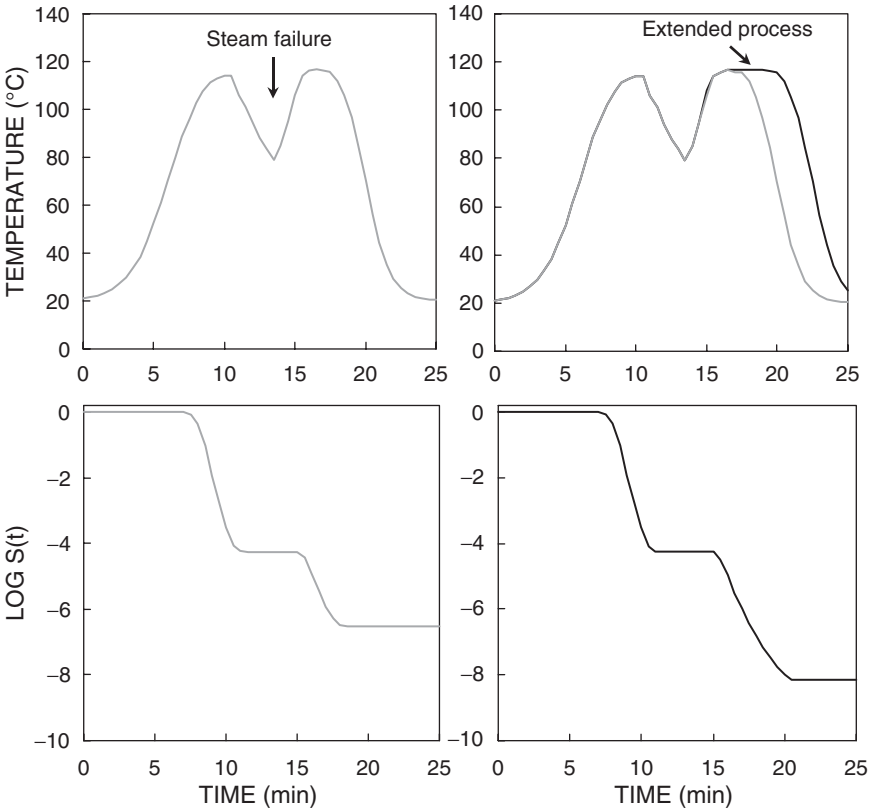

FIG. 3.15. A hypothetical scenario case of steam interruption (left) and how it can be corrected by prolonging the heating stage (right)

the product's shelf life under existing conditions or to identify conditions that will result in extended shelf life. Similar analysis can be performed on a product that contains a dissipating chemical agent, such as in an active package, after all the agent has been released. An example of such a hypothetical scenario is shown in Fig. 3.17. [It is not meant to account for any specific organism and bacteria, only to demonstrate that the methodology to do such calculation already exists].

3.4. Future Applications

3.4.1. Risk Assessment

The programs available as freeware (see 3.3) have a variety of potential uses. They can be expanded to simulate not only a single inactivation or growth curve, but several simultaneously, and in response to randomly varying conditions within a specified range.

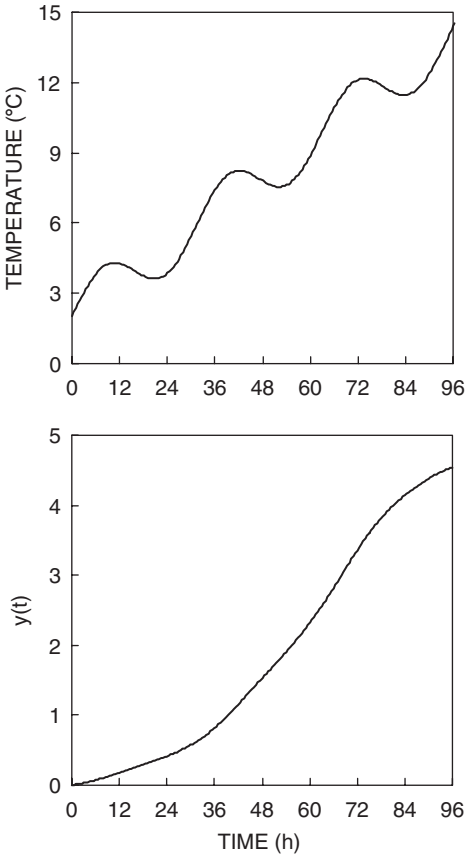

FIG. 3.16. Example of simulated growth of *Pseudomonas* in refrigerated fish subjected to oscillating temperatures

Examples are shown in Figs. 3.18 and 3.19. If one can have a solid estimate of the temperature range and the inactivation or growth parameters of the organism in question, then one can have a quantitative assessment of the number of units or packages that will have an insufficient treatment or an undesirable level of growth after a specified time.

The curves shown in the two figures were all created with Mathematica® (Wolfram Research, Champaign, IL USA.) and are not yet available as freeware on the web.

3.4.2. Estimation of the Number of Residual Living Cells or Viable Spores in a Given Volume

Heat transfer theories are well developed, and so is their implementation in thermal processing of food. It is therefore possible to use heat conductivity models to

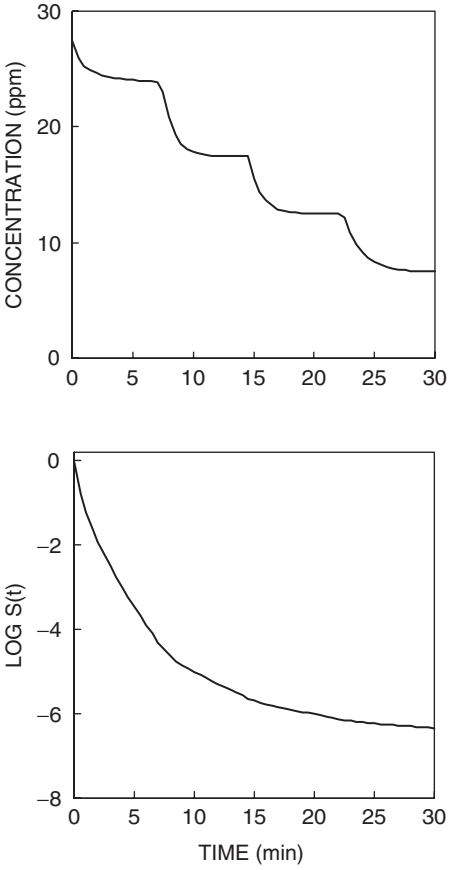

FIG. 3.17. A hypothetical scenario of a dissipating antimicrobial agent (top) and corresponding survival curve of the targeted organism (bottom)

calculate the thermal history of any and all the points in a given body, not only in the coldest, hottest or any other specific location. Thus, heat transfer and mortality or growth kinetics models can be combined, in order, to estimate the number of cells or spores in a given volume at any time.

Recent examples can be found in the work of Amézquita et al. (2005), except that they used a traditional inactivation model and Halder et al. (2007) who used both the traditional and the Weibullian models for comparison. Since microbial inactivation and other changes that a food undergoes during a heat process do not have the same rate, one can conceive situations where the distribution of surviving cells or spores, if any, will be very different from those of the residual vitamins, lost pigments and other quality attributes.

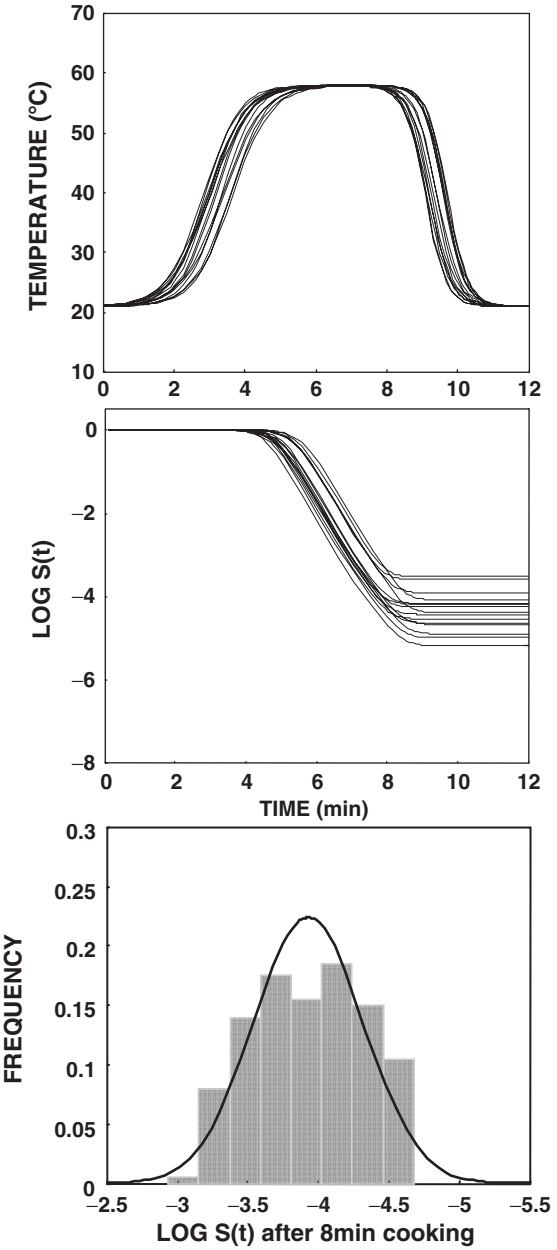

FIG. 3.18. Simulated randomly varied temperature profiles (top), corresponding survival curves (middle) and the distribution of the survival ratios after 8 minutes (bottom)

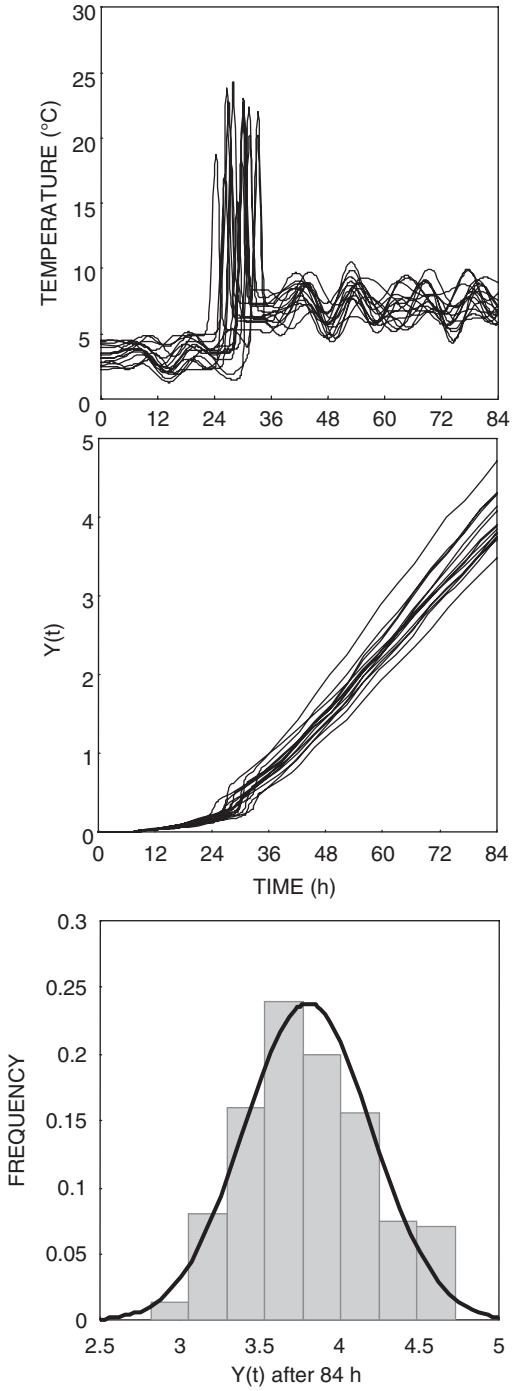

FIG. 3.19. Realistic temperature histories of a refrigerated food from the retailer to consumption (top), corresponding growth curve (middle) and the distribution of the growth ratios after 84 hours

The development of combined programs to estimate the changes in several properties simultaneously would enable determination of the overall nutritional and organoleptic quality of processed foods, not only their safety.

Moreover, in principle at least, the method can be used to evaluate the consequences of scenarios where inactivation is followed by growth or vice versa (Corradini and Peleg, 2006). An example of the former is resumed growth after incomplete inactivation (e.g., Amézquita et al., 2005) or inactivation after a growth stage, as in certain slow cooking processes.

A schematic view of these two kinds of situations is shown in Figs. 3.20 and 3.21. Although the application of such methods is well in the future, the

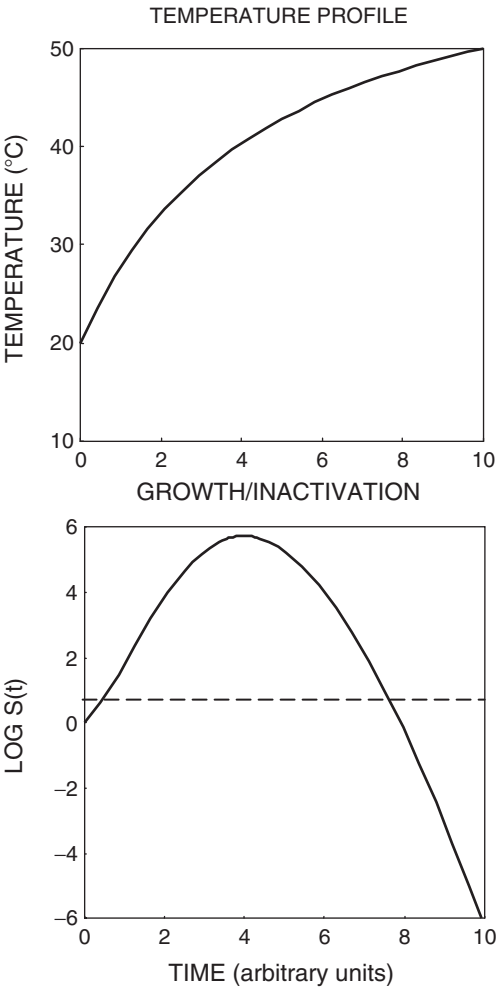

FIG. 3.20. Schematic view of the onset of heat inactivation after a period of growth at moderate temperatures

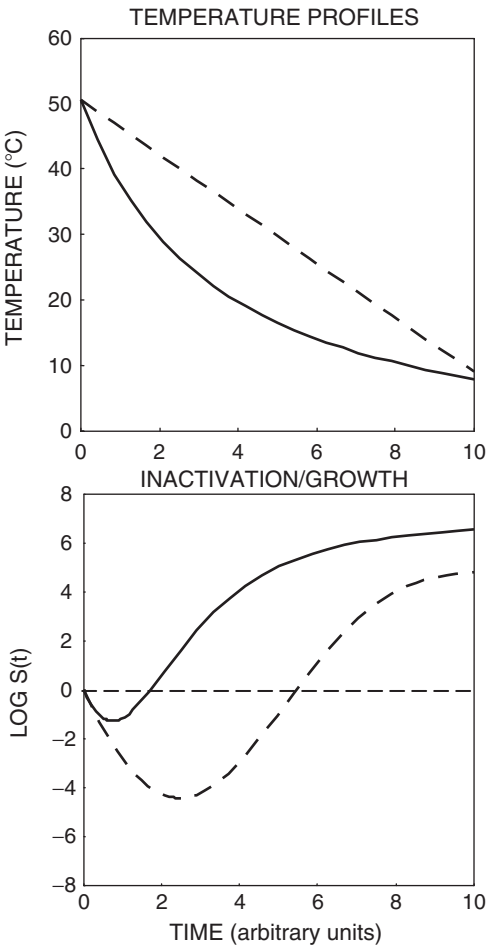

FIG. 3.21. Schematic view of the onset of growth during the cooling of an incompletely pasteurized food

mathematical tools to formulate and solve the models' equations are already available and so is the software to perform the calculation.

Acknowledgement This chapter is based on a paper with the same title presented at the 5th Ibero American Congress of Food Engineering (CIBIA V). The third author (MP) expresses his sincere thanks to Dr. Gustavo Fidel Gutierrez, Dr. Jorge Welti-Chanes and the organizers of the congress for the invitation to present this work in the congress, and for their warm and generous hospitality.

References

Amézquita A., Weller, C.L., Wang, L., Thippareddi, H., and Burson D.E, 2005, Development of an Integrated Model for Heat Transfer and Dynamic Growth of *Clostridium Perfringens* During the Cooling of Cooked Boneless Ham, *Int. J. Food Microbiol*. **101**:123–144.

Anderson, W.A., McClure, P.J., Baird-Parker, A.C., and Cole, M.B., 1996, The Application of a Log-logistic Model to Describe the Thermal Inactivation of *Clostridium botulinum* 213B at Temperatures below 121.1 °C, *J. Appl. Bacteriol*. **80**:283–290.

Baranyi, J., and Roberts T.A. 1994, A Dynamic Approach to Predicting Bacterial Growth in Food. *Int., J. Food Microbiol,* **23**:277–294

Barrow G.M. 1996, *Phys. Chem*., McGraw Hill, New York.

Corradini, M.G., and Peleg M., 2004, A Model of Non-Isothermal Degradation of Nutrients, Pigments and Enzymes, *J. Sci. Food Agric.,* **84**:217–226.

Corradini, M.G., and Peleg M., 2005, Estimating Non-Isothermal Bacterial Growth in Foods from Isothermal Experimental Data. *J. Appl. Microbiol*. **99**:187–200.

Corradini, M.G., and Peleg M., 2006, On Modeling and Simulating Transitions Between Microbial Growth and Inactivation or Vice Versa, *Int. J. Food Microbiol*. (In preparation).

Corradini, M.G., Normand, M.D., and Peleg M., 2005, Calculating the Efficacy of Heat Sterilization Processes. *J. Food Eng*. **67**:59–69.

Corradini, M.G., Normand, M.D., and Peleg M. 2006. On Expressing the Equivalence of Non Isothermal And Isothermal Heat Sterilization Processes, *J. Sci. Food Agric*. (In preparation).

Datta A.K., 1993, Error Estimates For Approximate Kinetic Parameters Used In Food Literature, *J. Food Eng*. **18**:181–199.

Fujikawa, H., Kai, A., and Morozumi S., 2004, A New Logistic Model for *Escherichia Coli* Growth at Constant and Dynamic Temperatures, *Food Microbiol*. **21**:501–509.

Halder, A., Datta, A.K., and Geedipalli, S.S.R., 2007, Uncertainty in Thermal Process Calculations due to Variability in First Order and Weibull Kinetic Parameters, *J. Food Sci.* **72**:E155–167.

Koutsoumanis, K., 2001, Predictive modeling of the shelf life of fish under non-isothermal conditions, *Applied and Environmental Microbiology* **67**:1821–1829.

Labuza T.P. (n.d.). FScN 8334, Reaction Kinetics of Food Deterioration. http://courses.che.umn.edu/ 00fscn8334-1f/FScN8334Reading.html

Mattick, K.L., Legan, J.D., Humphrey, T.J., and Peleg M., 2001, Calculating *Salmonella* Inactivation in Non-Isothermal Heat Treatments from Isothermal Non Linear Survival Curves, *J. Food Prot.,* **64**:606–613.

McKellar, R., and Lu X. (eds.), 2004, Modeling Microbial Responses on Foods, CRC Press, Boca Raton.

Peleg M. 2003. Microbial Survival Curves: Interpretation, Mathematical Modeling and Utilization. *Comments Theor. Biol*. **8**: 357–387.

Peleg M., 2006, *Advanced Quantitative Microbiology for Foods and Biosystems: Modeling and Predicting Ggrowth and Inactivation*, CRC Press, Boca Raton (In preparation).

Peleg, M., and Cole M.B., 1998, Reinterpretation of Microbial Survival Curves. *Crit. Rev. Food Sci. Nutr*. **38**:353–380.

Peleg, M., Corradini, M.G., and Normand M.D., 2004, Kinetic Models of Complex Biochemical Reactions and Biological Processes, *Chem. Ing. Tech*. **76**:413–423.

Peleg, M., and Normand, M.D., 2004, Calculating Microbial Survival Parameters and Predicting Survival Curves from Non-Isothermal Inactivation Data, *Crit. Rev. Food Sci. Nutr*. **44**:409–418.

Peleg M., Normand, M.D., and Campanella O.H., 2003, Estimating Microbial Inactivation Parameters from Survival Curves Obtained Under Varying Conditions: The Linear Case, *Bull. Math. Biol*. **65**:219–234.

Peleg, M., Normand, M.D., and Corradini M.G., 2005. Generating Microbial Survival Curves During Thermal Processing in Real Time, *J. Appl. Microbiol*. **98**:406–417.

Periago, P.M., van Zuijlen, A., Fernandez, P.S., Klapwijk, P.M., ter Steeg, P.F., Corradini, M.G., and Peleg, M., 2004, Estimation of the Non-Isothermal Inactivation Patterns of *Bacillus sporothermodurans* IC4 Spores in Soups from their Isothermal Survival Data, *Int. J. Food Microbiol.* **95**:205–218.

Purich, D., and Allison R.D., 2000, *Handbook of Biochemical Kinetics*. Academic Press, San Diego.

Valdramidis, V.P., Geeraerd, A.H., Bernaerts, K., and van Impe, J.F., 2004, Dynamic versus Static Thermal Inactivation: the Necessity of Validation Some Modeling and Microbial Hypotheses, paper 434. In Proceedings of the 9th International Conference of Engineering and Food (ICEF 9), Montpellier, France. Societé de Chimie Industrielle, Paris, France. (CD-ROM.)

van Boekel M.A.J.S., 2002, On the Use of the Weibull Model to Describe Thermal Inactivation of Microbial Vegetative Cells, *Int. J. Food Microbiol*. **74**:139–159.

4
Consequences of Matrix Structural Changes on Functional Stability of Enzymes as Affected by Electrolytes

M.F. Mazzobre, P.R. Santagapita, N. Gutiérrez, and M. del P. Buera

4.1. Introduction

The conservation of labile biomolecules in fields such us biology, pharmaceuticals, and food science is generally performed in dehydrated or frozen media. An equilibrium state does not exist in these systems, but they can reach several states of metastability. The conservation of desirable properties in foods and ingredients is then governed by conditions of metastability, often based on the maintenance of amorphous metastable properties of the systems (Suzuki et al., 1997; Sun and Leopold, 1997; Mazzobre and Buera, 1999). While biomolecules are not under a thermodynamically stable condition, they are kinetically stabilized. The action of cryo- and dehydro-protectants can be ascribed to both kinetic and specific effects. At the kinetic level, the protectants promote the formation of amorphous, glassy systems and influence the kinetics of reactions responsible for deterioration during storage. At the specific level, they are believed to interact with biological structures and to stabilize them during freezing or drying, although by different mechanisms (Carpenter et al., 1986). During freezing of aqueous solutions or biological material, ice formation leads to a freeze-concentrated unfrozen phase with properties (such as pH, ionic strength, and viscosity) significantly different from those of the original system (Pikal, 1999).

The representation of the conditions of the system in a temperature-composition state diagram is a very useful tool to analyze the stability of simple systems. In these supplemented diagrams, the curves corresponding to equilibrium conditions and the glass transition temperature (T_g) of the system are plotted as a function of water content. The T_g curve, corresponding to non-equilibrium conditions, allows establishment of some notion of the time in which a certain event will take place or what changes will be kinetically delayed/inhibited under certain conditions. Viscosity plays an important role in restricting the freedom of reordering of polymers and sugars, inhibiting its recrystallization (Parker and Ring, 1995; Chinachotti, 1997). In agreement with the relations obtained for synthetic polymers, and applicable to biopolymers, the viscosity of the systems is determined by the difference between the temperature of the system and its glass transition temperature (Levine and

Slade, 1988; Slade and Levine, 1993; Arvanitoyannis and Blanshard, 1994). Some of our previous work has demonstrated that the thermal transitions and phase changes affect the kinetics of chemical reactions or protein stability (Parker and Ring, 1995; Mazzobre et al., 1999; Burin et al., 2004; Buera et al., 2005; Acevedo et al., 2006). Nevertheless, the recrystallization of water or solutes in the systems may be kinetically modified by selecting adequate excipients (Roos and Karel, 1991a; Gabarra and Hartel, 1998).

Evidence exists on the modification of the thermophysical properties of concentrated aqueous trehalose solutions by the presence of various chlorides or sodium tetraborate (Miller et al., 1997; Longinotti et al., 2001). Several physical methods have also provided evidence for the existence of sugar-metal complexes in solution, and many complexes of sugars and sugar derivatives with inorganic salts have been isolated in solid and often in crystalline form (Angyal, 1973; Morel-Desrosier et al., 1991). The objective of the present work was to explore the effect of salts on the physical properties of freeze-dried or dehydrated sugar systems and their relationship to enzyme stabilization. These relationships were analyzed on the basis of state diagrams, considering structural changes and intermolecular interactions.

4.2. Materials and Methods

Honey (of multifloral origin, from Chaco, Argentina), soy extract (obtained from soybeans by a modification of the Natelson method (Natelson et al., 1951)), malt extract (obtained from Cervecería Quilmes (2000), Argentina) and β-galactosidase (EC 3.2.1.23) from *Aspergillus oryzae* (Sigma Chemical Co., St. Louis, MO) were employed as enzyme sources. Adequate dilutions of honey were employed to measure amylase activity; soy extract was used as source of the enzymes amylase, urease and aspartate amino transferase (ASP/GOT), and malt extract was used as the source of amylase and urease.

4.2.1. Preparation of the Model Systems

For the cryo-concentrated systems, solutions containing the corresponding enzyme extract in the presence of 20% (w/v) of trehalose or sugar-salt mixtures (NaCl, $CaCl_2$, NaCl, KCl, $MgCl_2.6H_2O$, $Na_3C_6H_5O_7.2H_2O$ (NaCit), $Mg(C_2H_3O_2)_2$ ($MgAc_2$) or $KC_2H_3O_2$ (KAc), all Merck, Darmstadt, Germany, p.a. grade) in a 5:1 molar ratio were prepared and stored at −26° C up to 60 days.

Amorphous dehydrated systems were obtained by freeze-drying solutions containing the selected enzyme extract in the presence of 20% (w/v) of trehalose (T) (Hayashibara Co, Ltd., Shimoishii, Okayama, Japan/ Cargill Inc., Minneapolis, MN) or sugar-salt mixtures (the same salts and proportions used for cryo-concentrated systems). Aliquots of 1 mL of each model solution were placed in 3 mL vials,

frozen for 24 h at −26°C and immersed in liquid air (temperature −200°C) before freeze-drying in a Heto Holten A/S, cooling trap model CT 110 freeze-dryer (Heto Lab equipment, Denmark) which operated at a condenser plate temperature of −110°C and at a chamber pressure of $4*10^{-4}$ mbar. In order to obtain samples with mass fraction of water (W) from 0.05 to 0.15, the freeze-dried samples were transferred into vacuum desiccators and exposed over saturated salt solutions from 11 to 43 % relative vapor pressure at 25°C.

4.2.3. Storage Conditions

The solutions for the cryo-concentration studies were stored at −26°C for up to 60 days. After setting the dehydrated systems to the desired moisture content, the vials were hermetically sealed, and the stability of the enzyme preparations was tested by stressing at 55°C. At suitable intervals, two samples were removed from the freezer or oven, respectively, maintained for 15 min at 25°C, and the remaining activity was determined as described below; average values of two measurements were reported.

4.2.4. Enzyme Activity

After storage, enzyme activity was measured by incubating the samples in excess of the corresponding substrate in order to obtain the maximum catalytic activity. I_2 in HCl 0.02M was employed to determine the degree of starch (500 mg/L) hydrolysis as a measure of α-amylase activity (Tietz, 1999) (all reactants were provided by Wienerlab, Rosario, Argentina). To determine urease activity, urea was used as a substrate and (in the presence of 2-oxoglutarate, NADH and glutarate dehydrogenase at pH 7), NADH consumption was measured by absorbance at 340 nm (all reactantants provided by Wienerlab, Rosario, Argentina), as described by Faulkner and King (1970). For the aspartate amino transferase activity, aspartate was used as a substrate, which reacted with 2-oxoglutarate, and, in the presence of malate dehydrogenase and lactate dehydrogenase at pH 7.8, L-malate was formed and NADH consumption was measured, as described by Amador and Wacker (1962). β-galactosidase activity was spectrofotometrically measured at 420 nm through the amount of o-nitrophenol produced in the presence of the substrate o-nitrophenyl-β-D-galactopyranoside (ONPG) at pH 4.5, as previously reported (Park et al., 1979).

For each enzyme containing system, two independent runs were performed, in which two samples were taken at a selected time for each run, and two replicates of each sample were analyzed, reporting the average of eight measurements for each storage time. The relative error (at 95% confidence interval) was 5%, calculated from eight measurements of the same sample. The enzyme activity determined after a given treatment (A) was related to the activity measured in the initial conditions (A_0), and the remaining activity (R.A.) was expressed as: R.A. = 100 A/A_0.

4.2.5. *Thermophysical Properties*

A differential scanning calorimeter (DSC) system (Mettler-Toledo equipment model 822, Mettler Toledo AG, Switzerland) and STARe Thermal Analysis System version 3.1 software (Mettler Toledo AG) were used for all measurements. The instrument was calibrated with indium and zinc.

The dynamic method was used to determine glass transition temperature (T_g), crystallization temperatures of sugar (T_c) or water (T_{wc}), heats of sugar crystallization (ΔH_c) or melting (ΔH_m) and heats of water crystallization (ΔH_{wc}) or melting (ΔH_{wm}) in the model systems. Each sample was heated at a rate of 10°K/min. Glass transition temperatures were recorded as the onset of discontinuity in the curves of heat-flow versus temperature. A statistical analysis with several replicates indicated that for the thermophysical properties determined in the sugar systems, a minimum of two replicates should be made to obtain values in the 95% confidence interval. Analysis in duplicate involved 40μL hermetically sealed aluminium pans (Mettler) containing samples (10–15 mg). An empty pan was used as a reference.

4.2.6. *Degree of Sugar or Water Crystallization*

The area of endothermal peaks obtained in the DSC scans for dehydrated samples was used to estimate the degree of trehalose dehydrate crystallization by comparing it to the calorimetric enthalphy of the melt of pure trehalose dihydrate, which was 139 J/g measured under the same conditions.

In the frozen samples, the amount of ice formed after storage under isothermal conditions at −26°C was calculated by comparing the endothermal peaks obtained in the DSC scans to the calorimetric enthalphy of melting for pure water (330 J/g), and the amount of ice formed during the dynamic heating was calculated from the area of the exothermic peak in relation to pure water enthalphy.

4.3. Results

Figure 4.1 shows the temperature/composition regions of a phase/state diagram for trehalose-water systems, on which the dehydrated and frozen samples were studied. This kind of diagram can help to predict whether the systems are under thermodynamic or kinetic control for given composition–temperature conditions, provided that the thermal history of the samples is known.

Starting from an amorphous-vitreous state where the system is considered to be "stable," it may be driven to the supercooled state, both by increasing temperature (points segments 2–3 and 4–5 in Fig. 4.1) and/or by increasing the water content (segment 4–6 in Fig. 4.1). In the supercooled states, recrystallization of sugars or water can occur, leading to loss of the protective effect of the amorphous matrices and consequent deterioration of biomolecules and biological structures (Suzuki et al., 1997; Sun and Leopold, 1997; Mazzobre and Buera, 1999).

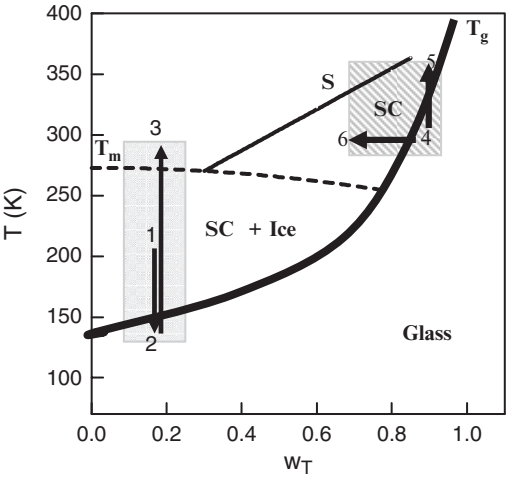

FIG. 4.1. Phase/state diagram for trehalose-water showing the regions where the effects of salts were investigated: Crystallization of sugar and sugar-salt; crystallization of water in sugar or sugar-salt solutions. Solubility and T_g curves are plotted as a function of mass fraction of trehalose (W_T). S, solubility curve; T_m, liquidus curve; T_g, glass transition curve; SC, supercooled

The point at which the equilibrium liquids curve intercepts the non-equilibrium T_g curve defines the point (T_g'; w_g') that represents the particular temperature/solute concentration at which water crystallization is kinetically inhibited. w_g' represents the lowest mass fraction of water associated with the amorphous matrix that can be obtained by solute concentration due to ice crystallization, and T_g' is the glass transition temperature of the maximally freeze-concentrated solution.

Both variables (T_g' and w_g') are of paramount importance when analyzing the stability of frozen systems (Slade and Levine, 1991; Simatos and Blond, 1991; Kerr and Reid, 1994). In the present work, the thermal stability of several enzymes from different sources (malt extract, soy extract and honey) was analyzed in supercooled systems (marked as SC in Fig. 4.1) in relation to the sugar or water crystallization.

Figure 4.2 shows the remaining activity of the enzymes amylase, urease, and ASP in dilute solutions (w ~ 0.8–0.9) stored at −26°C (a, b), represented by point 1 in Fig. 4.1 and in freeze-dried systems of w ~ 0.05–0.15 containing trehalose at 55°C (c, d), in the SC region between points 5 and 6, respectively, in Fig. 4.1.

At the storage conditions, all systems were in the SC region during storage, and significant reduction of enzyme activity was verified during the storage time in all cases. Both in the frozen systems stored at −26°C or in the dehydrated systems treated at 55°C, the stability of amylase and urease from malt extract was higher than the stability of the enzymes from soy extract or honey.

ASP was the most labile of the studied enzymes in dehydrated and in frozen conditions. In consequence, amylase from honey and ASP were selected as model systems for the stability studies.

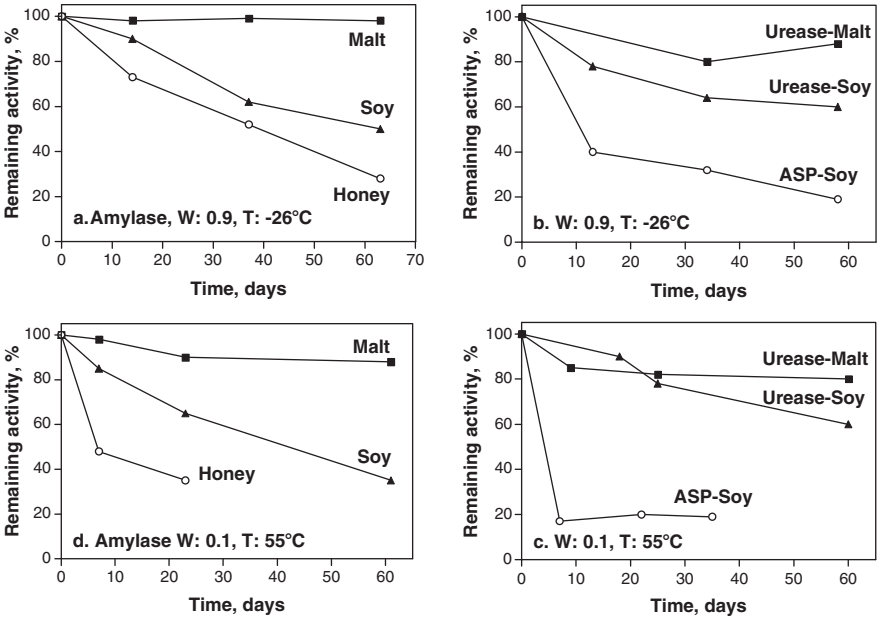

FIG. 4.2. Remaining activity of enzymes from different sources in dilute solutions (W= 0.9) stored at −26°C (a, b) or in dehydrated (W= 0.1) systems containing trehalose at 55°C (c, d). Sources: malt extract, soy extract and honey

The effect of cryo-concentration on the stability of the enzymes was studied in sugar and sugar-salt containing systems in relation to ice formation conditions and T_g.

In frozen systems, the amount of ice formed in each case, the amount of water associated with the amorphous phase, and mobility factors, represented by $T\text{-}T_g$ are the factors responsible for maintaining enzyme functionality.

Figure 4.3 shows the remaining activity of amylase from honey or honey-trehalose (in 2:1 solids ratio) systems after 60 days of storage at −26°C as a function of solid concentration in the initial solution. The remaining enzymatic activity decreased with dilution of the initial solution. It is interesting to note that the glass transition temperature of the maximally concentrated phase (T_g') does not vary for each particular system. The T_g' values reported are −46°C for honey (Rubin et al., 1990; Zoltan et al., 1999) and −44°C for trehalose systems (Mazzobre et al., 2001). However, the amount of ice formed, which was higher in the more diluted systems, may have affected protein stability. It is well known that not only do mobility factors, accounted for by ($T\text{-}T_g$') affect protein stability (Slade and Levine, 1991; Kerr et al., 1993), but, for a given formulation, the presence of surfaces or interfaces also have a deleterious effect (Privalov, 1990; Arakawa et al., 1993). Also, the points corresponding to honey-trehalose (at 2:1 solids ratio) systems, as seen in Fig. 4.3, reflect the same trend as those without trehalose,

FIG. 4.3. Remaining activity of amylase from honey or honey-trehalose systems after 60 days of storage at −26°C as a function of solid concentration in the initial solution

indicating that in these frozen honey systems, no special effect of trehalose, other than an increase of solids content, was observed.

When salts such as NaCit and NaCl were added to the enzymatic extracts in the absence of trehalose, both amylase and ASP stabilities were enhanced, compared to the enzyme extracts without salts. The recovered amylase and ASP activities were about 50 to 70% higher for NaCl and NaCit systems, respectively, compared to the activity recovered without salts. $CaCl_2$ had a lower effect, and $MgCl_2$ impaired the stability of both enzymes. Lecker and Arshad (1998) studied the effect of salts on amylase in liquid media, and they attributed deactivating effects to cations (Na and K) and stabilizing effects to anions (chlorides and citrates), as a result of the function of the salt concentration. On the other hand, when trehalose was present, the addition of salts had a negative effect on the stability of both enzymes at −26°C, compared to the trehalose-containing systems without salts (Fig. 4.4).

Figure 4.4 shows the results obtained for the remaining activity of ASP as a function of time of storage at −26°C in soy aqueous extract containing trehalose (20% w/w) or trehalose/salts (R = 5). The selected conditions of temperature (−26°C) and concentration chosen for the isothermal storage of the samples correspond to a region in the phase diagram where ice is expected to form readily, above T_g', and close to the zone of maximal ice formation (Roos and Karel, 1991b) (Fig. 4.1.).

Dynamic DSC thermograms were made to analyze the effect of salts on T_g and water crystallization/melting (Fig. 4.5). The systems were stored at −26°C for 60 days before the measurement (represented by point 1 in Fig. 4.1). These systems were cooled rapidly from −26°C to −160°C (point 2 in Fig. 4.1), and then scanned

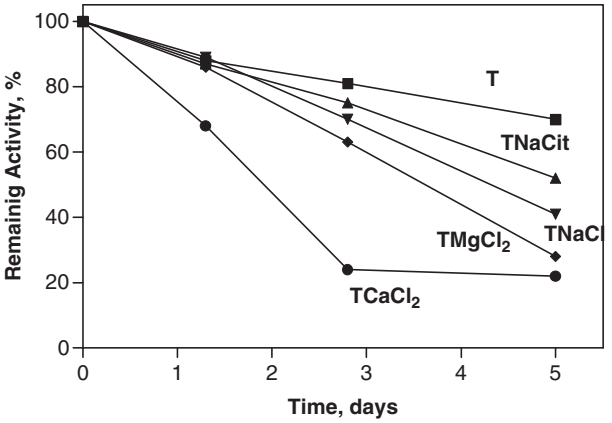

FIG. 4.4. Remaining activity (R.A.) of ASP as a function of time of storage at −26°C, in soy aqueous extract containing trehalose (W= 0.8) or trehalose in presence of different salts (R= 5). Salts: $Na_3C_6H_5O_7$ (NaCit), NaCl, $CaCl_2$ and $MgCl_2$

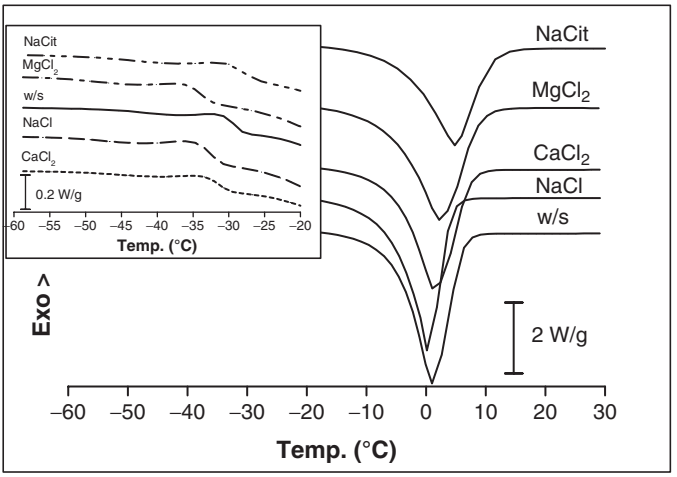

FIG. 4.5. Dynamic DSC thermograms for soy aqueous extract containing trehalose (W= 0.8) or trehalose in the presence of salts (R= 5). Salts: $Na_3C_6H_5O_7$ (NaCit), NaCl, $CaCl_2$ and $MgCl_2$. The systems were stored at −26°C for 60 days before measurement

over the supercooled region to analyze their ice-forming and melting properties up to room temperature (point 3 in Fig. 4.1). The endothermal baseline shifts depicted in Fig. 4.5 represent the glass transition temperatures and the exothermal or endothermal peaks that correspond to crystallization or melting of water, respectively. For all systems, a small exotherm was observed in the thermogram during the dynamic run (inset in Fig. 4.5), indicating that not all of the water had

crystallized with the time/temperature conditions employed at the storage conditions. The values obtained for the glass transition temperature (T_g), heats of crystallization (ΔH_{ic}) and heats of melting (ΔH_{im}) of water are shown in Table 4.1.

The ΔH_{im} values, which were lower for the trehalose/salt systems compared to those without salts, indicated that a lower amount of ice formed both during the previous storage at −26°C and during the dynamic run, which caused a higher amount of water present in the amorphous phase (or unfrozen water, W_{NF}) and concomitant lower T_g values.

After storage, in the systems under conditions of temperature, time and concentration that are favorable for water crystallization, the T_g values of the systems are close to those for T_g' predicted on the basis of phase/state diagrams (−44°C for trehalose, and −52.5°C for trehalose in the presence of $MgCl_2$; Mazzobre et al., 2001). It can be seen that the amount of non-frozen water also depends on the salt added.

A higher amount of water in the maximum concentrated amorphous phase may lead to increased molecular mobility in the trehalose-salt system, which is probably related to the negative effect of salts observed on enzyme stability to freezing (Fig. 4.4).

In freeze-dried enzymatic systems, different degrees of trehalose crystallization were attained after humidification of samples at mass fractions of water between 0.05 and 0.15. As discussed in previous papers (Mazzobre et al., 2001; Longinotti et al., 2002; Santagapita and Buera, 2007), the degree of sugar crystallization was different according to the presence and/or type of salt employed, and some salts (KCit, KAc, $MgCl_2$, $CaCl_2$) exerted an inhibitory effect on sugar crystallization. Some of them also provided enhanced protection of the enzyme, as compared to trehalose systems without salts.

Remaining enzymic activity was related to sugar crystallinity, as shown in Fig. 4.6 for the enzymes ASP and β-gal, and in Fig. 4.7 for amylases of different fonts.

It is to be noted that, for a given system, as the sugar crystallinity increased, the remaining enzymic activity decreased, but in the samples without salt, the enzymes were less sensitive to the degree of crystallinity, with the exception of honey amylase (Figs. 4.6 and 4.7).

The remaining amorphous phase, in partially crystalline systems without salts, could exert a protective action. However, as shown in Fig. 4.6, the protective

TABLE 4.1. Glass transition temperature (T_g), temperature of ice crystallization (ΔH_{ic}) and melting (ΔH_{im}), and the fraction of non-frozen water (W_{NF}) obtained by dynamic DSC for soy aqueous extract containing trehalose (W= 0.8) in the presence of different salts (R= 5) after storage at −26°C. Salts: $Na_3C_6H_5O_7$ (NaCit), NaCl, $CaCl_2$ and $MgCl_2$

Matrix system	T_g (°C, onset)	ΔH_{ic} (J/g)	ΔH_{im} (J/g)	W_{NF} (% of total water)
T	−47.7 ± 0.5	1.7 ± 0.5	250.0 ± 0.5	23 ± 2
T/$MgCl_2$	−56.1 ± 0.5	2.2 ± 0.5	239.5 ± 0.5	27 ± 2
T/NaCit	−52.2 ± 0.5	6.1 ± 0.5	221.5 ± 0.5	31 ± 2
T/NaCl	−53.3 ± 0.5	1.9 ± 0.5	225.8 ± 0.5	31 ± 2
T/$CaCl_2$	−56.4 ± 0.5	1.9 ± 0.5	240.0 ± 0.5	27 ± 2

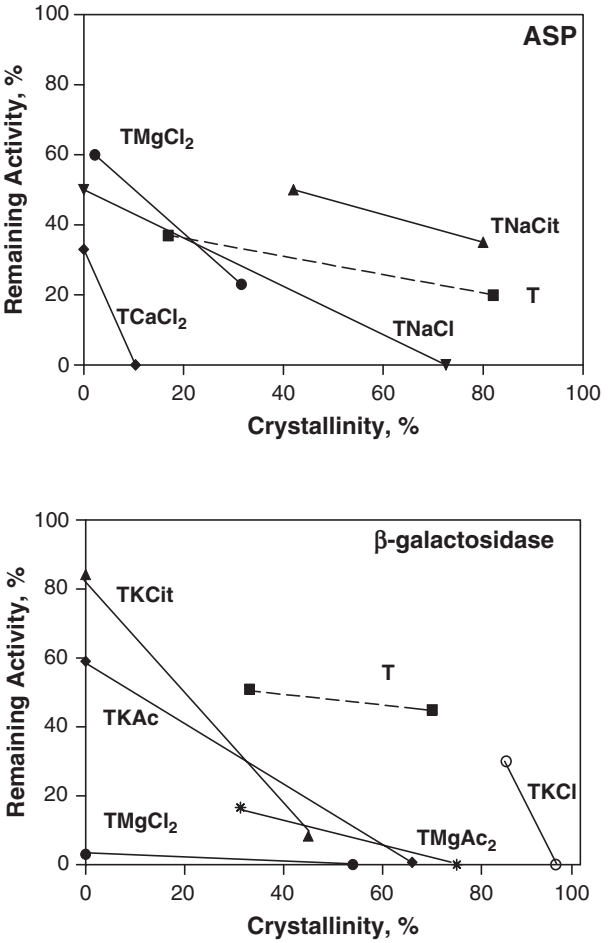

FIG. 4.6. Remaining enzymic activity as a function of the degree of trehalose crystallization. a) ASP, 20 days at 55°C; b) β-galactosidase, 48 h at 70°C. Mass fraction of water between 0.05 and 0.15

synergistic effect observed for some salts ($MgCl_2$ and NaCl for ASP; KCit and KAc for β-gal) at very low crystallinity degrees, is lost when about 30% of the sugar had crystallized. In Fig. 4.7, amylase activity was lower in $MgCl_2$ containing systems, but this effect was enhanced at 40% crystallinity degree. Upon sugar crystallization, the salts present are concentrated in the amorphous phase, negatively affecting enzyme stability, possibly by changes in pH and/or ionic strength. Negative effects of salts were also observed independently of their action on sugar crystallization: While $CaCl_2$ and $MgCl_2$ inhibited trehalose crystallization, they had a negative effect on ASP and β-gal stability, respectively, attributable to their interactions with the enzyme. On the other hand, NaCit was the only salt

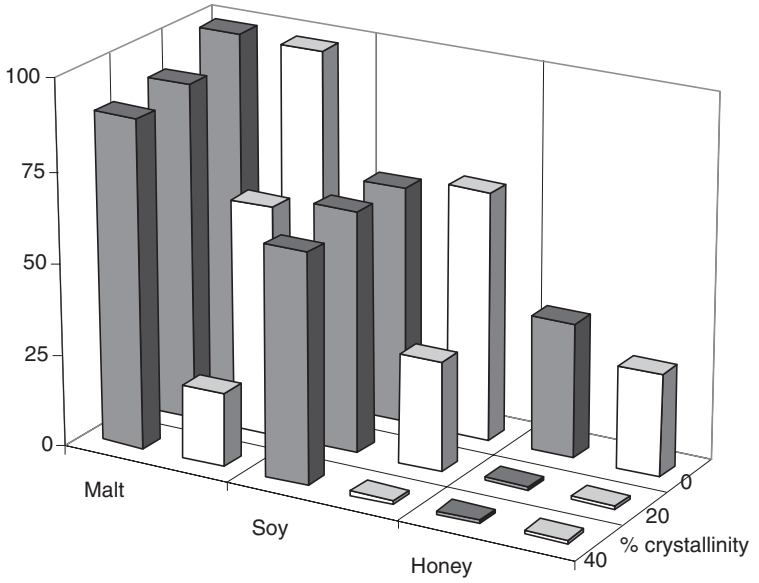

FIG. 4.7. Remaining amylase activity at 55°C for malt, soy and honey extracts in freeze-dried trehalose-containing systems with or without $MgCl_2$. The degree of trehalose crystallization is indicated. ▪without $MgCl_2$ ▫with $MgCl_2$

system that allowed retention of enzyme (ASP) activity at an 80% crystallinity degree. Although it would be concentrated in the amorphous phase, citrate may have a protective effect on ASP. On the other hand, when trehalose was present (Figs. 4.6 and 4.7), the addition of salts had a negative effect on the stability of both enzymes in the frozen systems. In this case, the salts were concentrated in the remaining amorphous phase, leading to negative effects on the enzyme. Lecker and Arshad (1998) reported that the citrate effect on amylase activity in liquid media may be beneficial or not, depending on the salt concentration.

4.4. Conclusions

In frozen systems, for a given composition, the water associated with the amorphous phase was constant, but the amount of ice formed in the diluted enzymatic extracts was higher than in more concentrated ones, which negatively influenced enzyme stability. Thus, the solid concentration of the extracts defined the kinetics of frozen enzyme inactivation. The amount of water associated with the amorphous frozen matrix increased when salts were present. Thus, enzyme stability was impaired due to the increased molecular mobility, and to the high concentration of salt in the unfrozen matrix.

In dehydrated systems, even when some salts improved the efficiency of trehalose as an enzyme protectant by delaying its crystallization, when about 30–50% trehalose crystallized, the protective effect of the sugar was lost, and the enzyme quickly became inactivated in almost all salt containing systems.

In order to optimize the efficiency of cryo- and dehydro-protectant agents of biomolecules, the construction of state diagrams are a good starting-point for the analysis of the dynamic of quality changes, but they must be complemented by the knowledge of intermolecular interactions that may take place. In the present work, electrolytes commonly present in biological media or food and pharmaceutical formulations-modified metastable systems affected the kinetics of water and sugar crystallization and enzyme inactivation, both by molecular and supramolecular interactions.

The effect of salts, regarding kinetics of ice and sugar crystallization and enzyme inactivation, seems to be connected with the magnitude of the effect of sugar on disrupting the tetrahedral hydrogen bond network of water and the reduction of freezable water. The distortion of water structure by the addition of sugars or salts to an aqueous solution is well known. It is generally accepted that a hydration sphere of water molecules surrounds the solvated ions, with the oxygen atoms oriented toward the cations, or the hydrogen atoms oriented to the anions. In this way, the self-association of the water molecules directly adjacent to the ion is interrupted because they are oriented in the electric field of the ion. This orientation induces different kinds of structuring in local water that depends on the size of the ions and on the extent of hydration. Ions that impose more local ordering to the surrounding water molecules and which strengthen the hydrogen bonds between them are known as structure making or kosmotropic, while structure breaking, or chaotropic ions increase disorder and weaken the hydrogen bonds between adjacent water molecules, increasing protein solubility and inducing protein denaturation. It is to be noted that the most important properties to define the effect of a given ion are charge, size and polarizability (Leontidis, 2002). Water structure makers (citrate > acetate; Mg^{+2}), are large, have large polarizability, enhance the tetrahedral coordinated hydrogen bond structure of water, and they are expected to have strong dispersion interactions with interfaces and to stabilize proteins. On the other hand, water structure breakers (K^{+}) disrupt the tetrahedral coordination of water, reducing the amount of freezable water, and increase protein denaturation. Some ions, such as Na^{+} or Cl^{-} are considered neutral (Calligaris and Nicoli, 2006). Proteins are generally stabilized by strong kosmotropic anions and destabilized by strong kosmotropic cations. Thus, optimal stabilization is achieved through the use of salts containing kosmotropic anions and chaotropic cations (Zhao et al., 2006), which play also a role in determining the amount of freezable water. Trehalose acts as a structure breaker, but it provides enzyme stabilization by strong hydrogen bonding interactions (Patist and Zoerb, 2005). In restricted water environments, such as in the frozen or dehydrated systems analyzed in the present work, the amount of water determines the kinetics of phase changes and of enzyme inactivation. Thus, the type of water-ion interactions are manifested in those dynamic changes, and the so called Hofmeister series (Calligaris and Nicoli, 2006) offers a wide possibility to aid in their description.

Acknowledgements The authors acknowledge financial support from Universidad de Buenos Aires (Project EX 226), CONICET (PIP 5977) and ANPCYT (PICT 20680 and 20545).

References

Acevedo, N., Schebor, C., and Buera M.P., 2006, Water-Solids Interactions, Matrix Structural Properties and the Rate of Non-Enzymatic Browning, *J. Food Eng*. (in press).

Amador, E., and Wacker W., 1962, Serum Glutamic Oxalacetic Transaminase Activity. A New Modification and an Analytical Assessment of Current Assay Technics, *Clin. Chem*. **8**:343.

Angyal S.J., 1973, Complex formation between sugars and metal ions, *Pure Appl. Chem*. **35**: 131.

Arakawa, T., Prestrelski, S.J., Kinney, W., and Carpenter J.F., 1993, Factors Affecting Short Term and Long Term Stabilities of Proteins, *Adv. Drug Delivery Rep*. **10**:1.

Arvanitoyannis, I., and Blanshard J., 1994, Rates of Crystallization of Dried Lactose-Sucrose Mixtures, *J. Food Sci*. **59**:197.

Buera, M.P., Schebor, C., and Elizalde B.E., 2005, Carbohydrate Crystallization Phenomena in Dehydrated Food and Ingredient Formulations. Involved Factors, Consequences and Prevention, *J. Food Eng*. **67**:157

Burin, L., Jouppila, K., Roos, J., Kansikas, J., and Buera P., 2004, Retention of β-Galactosidase Activity as Related to Maillard Reaction, Lactose Crystallization, Collapse and Glass Transition in Low Moisture Whey Systems, *Int. Dairy J*. **14**:517.

Calligaris, S., and Nicoli M.C., 2006, Effect of Selected Ions from Lyotropic Series on Lipid Oxidation Rate, *Food Chem*. **94**:130.

Carpenter, J.F., Crowe, J.H., and Arakawa T., 1986, Comparison of Solute-Induced Protein Stabilization in Aqueous Solution and in the Frozen and Dried States, *J. Dairy Sci*. **73**:3627.

Chinachotti, P., 1997, Water Migration and Food Storage, in: *Food Storage Stability,* A.I. Taub and R.P. Singh (eds.), CRC Press, Boca Raton, pp. 245–267.

Faulkner, W.R., and King J.W., 1970, Renal Function, in: *Fundamentals of Clinical Chemistry*. N.W. Tietz (ed.), W.B. Saunders Co., Philadelphia, pp. 12:718.

Gabarra, P., and Hartel, W., 1998, Corn Syrup Solids and Their Saccharide Fractions and Their Effect on Crystallization of Amorphous Sucrose, *J. Food Sci*. **63**:523.

Kerr, W.L, Lim, M.H., and Reid D.S., 1993, Chemical Kinetics in Relation to Glass Transition Temperature in Frozen Food Polymers Solutions, *J. Food Sci. Agric*. **61**:512.

Kerr, W.L., and Reid D.S., 1994, Temperature Dependence of the Viscosity of Sugar and Maltodextrin Solutions in Coexistence with Ice, *Lebensm. Wiss. U-Technol*. **27**:225.

Lecker. D.N., and Arshad K., 1998, Model for Inactivation of α-Amylase in the Presence of Salts: Theoretical and Experimental Studies, *Biotechnol. Prog*. **14**:621.

Leontidis E., 2002, Hofmeister Anion Effects on Surfactant Self Assembly and the Formation of Mesoporous Solids, *Curr. Opin. Colloid Interface Sci*. **7**:8.

Levine, H., and Slade L., 1988, Thermomechanical Properties of Small Carbohydrate–Water Glasses and "Rubbers," *J. Chem. Soc. Faraday Trans*. **84**:2619.

Longinotti, M.P., Mazzobre, M.F., Buera, M.P., and Corti H.R., 2001, Effect of Salts on the Properties of Aqueous Sugar Systems, in Relation to Biomaterial Stabilization. 2. Sugar Crystallization Rate and Electrical Conductivity Behaviour, *Phys. Chem. Chem. Phys*. **4**:533.

Mazzobre, M.F., and Buera M.P., 1999, Combined Effects of Trehalose and Cations on the Thermal Resistance of –Galactosidase in Freeze-Dried Systems, *Bioch. et Bioph. Acta* **1473**:337.

Mazzobre, M.F., Longinotti, M.P, Buera, M.P., and Corti H.R., 2001, Effect of Salts on the Properties of Aqueous Sugar Systems, in Relation to Biomaterial Stabilization. 1. Water Sorption Behaviour and Ice Crystallization/Melting, *Cryobiology* **43**:199.

Miller, D.P. de Pablo, J., and Corti H., 1997, Thermophysical Properties of Concentrated Aqueous Trehalose Solutions, *Pharm. Res*. **14**:578–59.

Morel-Desrosier, N., Lhermet, C., and Morel J.P., 1991, Interaction Between Cations and Sugars. Part 6. Calorimetric Method for Simultaneous Determination of the Stability Constant and Enthalpy Change for Weak Complexation, *J. Chem. Soc. Faraday Trans*. **87**:2173.

Natelson, S., Scott M.L., and Beffa C., 1951, A Rapid Method for the Estimation of Urea in Biologic Fluids, *Am. J. Clin. Pathol*. **21**:275.

Park, Y.K., de Santi, M.S.S., and Pastore G.M., 1979, Production and Characterization of β-Galactosidase from *Aspergillus Oryzae, J. Food Sci*. **44**:100.

Parker, R., and Ring S.G., 1995, A Theorical Analysis of Diffusion Controlled Reactions in Frozen Solutions, *Cryoletters* **16**:197.

Patist, A., and Zoerb H., 2005, Preservation Mechanisms of Trehalose in Foods and Biosystems, *Colloids Surf. B. Biointerfaces*. **40**:107.

Pikal M.J., 1999, Mechanisms of Protein Stabilization During Freeze-Drying and Storage: The Relative Impor-Tance of Thermodynamic Stabilization and Glassy State Relaxation Dynamics, in: *Freeze Drying/Lyio-philization of Pharmaceutical and Biological Products*, L. Rey and J.C. May (eds.), Marcel Dekker, Inc., New York, pp. 161–198.

Privalov P.L., 1990, Cold Denaturation of Proteins, *Crit. Rev. Biochem. Mol. Biol*. **25**:281.

Roos, Y., and Karel, M., 1991a, Amorphous State and Delayed Ice Formation in Sucrose Solutions, *Int. J. Food Sci. Technol*. **26**:553–566.

Roos, Y., and Karel, M., 1991b, Nonequilibrium Ice Formation in Carbohydrate Solutions, *Cryo-Letters* **12**: 367–376.

Rubin, C.E., Wasylyk, J.M., and Baust J.G., 1990, Investigation of Vitrification by Nuclear Magnetic Resonance and Differential Magnetic Resonance and Differential Scanning Calorimetry in Honey and Model Carbohydrate Systems, *J. Agric. Food Chem*. **38**:1824.

Santagapita, P.R., and Buera M.P., 2007, Trehalose-Water-Salt Interactions Related to the Stability of β-Galactosidase in Supercooled Media, *Food Biophysics*. (submitted).

Simatos, D., and Blond G., 1991, DSC Studies and the Stability of Frozen Foods, in: *Water Relationships in Foods*, H. Levine and L. Slade (eds.), Plenum, New York, pp. 139–155.

Slade, L., and Levine H., 1991, Beyond Water Activity: Recent Advances on an Alternative Approach to the Assessment of Food Quality and Safety, *Crit. Rev. Food Sci. Nutri*. **30**:115.

Slade, L., and Levine H., 1993, The Glassy State Phenomenon in Food Molecules, in: *The Glassy State in Foods*, J.M.V. Blanshard and P.J. Lillford (eds.), Nottingham University Press: Loughborough, Leicestershire, pp. 35–101.

Sun, W., and Leopold A., 1997, Cytoplasmic Vitrification and Survival of Anhydrobiotic Organisms, *Comp. Biochem. Physiol*. **117A**:327.

Suzuki, T., Imamura, K., Yamamoto, K., Satoh, T., and Okazaki, M., 1997, Thermal Stabilization of Freeze-Dried Enzymes by Sugars, *J. Chem. Eng. Japan* **30**:609.

Tietz, N., 1999, *Tietz Textbook of Clinical Chemistry,* 3rd ed., Saunders Co., Philadelphia.

Zhao, H., Olubajo, O., Song, Z., Sims, A.L., Person, T.E., Lawal, R.A., and Holley L.A., 2006, Effect of Kosmotropicity of Ionic Liquids on the Enzyme Stability in Aqueous Solutions, *Biorganic Chem*. **34**:15.

Zoltan, K., Pitsi, G., and Thoen. P., 1999, Glass Transition Temperature of Honey as a Function of Water Activity as Determined by Differential Scanning Calorimetry, *J. Agric. Food Chem*. **47**:2327.

5
Air Impingement Cooling of Cylindrical Objects Using Slot Jets

S.K. Singh and R. Paul Singh

5.1. Introduction

Impingement cooling is well known for its application in obtaining high rates of heat transfer, when temperature of the impinging fluid is different than that of the impingement surface. It involves a high velocity air jet (10–100 m/s) striking against an object to be cooled or heated. Applications of air jet impingement have been reported by many researchers (Li and Walker, 1996; Ovadia and Walker, 1998; Wählby et al., 2000; Nitin et al., 2001; Sarkar et al., 2004; Scott and Bradley, 2005). When food products are treated with air impingement, the stagnant boundary layer surrounding a food product is disrupted, resulting in increased surface heat transfer coefficient. Surface heat transfer coefficient during impingement can even reach as high as that for food being fried in oil (Ovadia and Walker, 1998). It is used extensively in industrial cooling of electronics components, textiles, paper pulp and food applications. In the food industry, impingement is used to accelerate freezing, baking, drying (Bórquez et al., 1999), cooling and thawing. With strict legislations for food processing temperatures in many countries becoming increasingly popular, the heat transfer rate has become an important part of food processing and handling. Raw or processed food must be stored at low temperature (normally 0–5°C). A longer processing time may result in potential microbial growth or weight loss due to mass transfer. Air impingement offers the potential to reduce the risk of microbial growth and increased processing rate.

5.2. Applications in the Food Industry

Smith (1975) developed a rapid food cooking technology based upon high velocity air jets striking the food product from above and below. Air jet impingement is currently used for heating, baking, browning, roasting and freezing in the food industry. Lujan et al. (1997) reported that increasing drying air temperature increased the drying rate significantly for air impingement dehydration of tortilla chips. Bórquez et al. (1999) studied the drying process of pressed fish cakes under

various conditions (mixing intensity, size of particle, and wall and air temperature) and reported that air temperature and particle diameter influenced the drying rate. Potato chips dried using superheated steam impingement had less color deterioration and fewer nutritional losses (Moreira, 2001).

In many non-food applications, the surface under impingement heating or cooling is flat. In food applications, often the object being cooled is not necessarily a flat surface. Most of the time it is either circular, elliptical or some other irregular shape. To compute heat transfer from impinging air to these types of objects, we must have a good understanding of the surrounding flow field. Our research is aimed at studying the effect of curvature of cylindrical products, jet exit-to-object distance, and cooling air stream velocity and turbulence on external flow field and surface Nusselt number.

5.3. Flow Under Air Jet Impingement

A high velocity jet of fluid flowing in a stagnant fluid medium can be categorized as a free jet or an impinging jet; when there is no target surface, it is called a free jet. Otherwise, it is called an impinging jet. Impinging jet flow can be divided into three basic components (Narayanan et al., 2004; Polat et al., 1989): free jet, stagnation flow and wall jet regions.

The flow immediately following the jet exit is similar to free jet flow; hence it is termed the free jet region (Ashforth et al., 1997). The free jet region consists of a potential core region, transition zone and a fully developed region, depending on the jet exit to surface spacing. In the potential core region, the jet maintains its exit velocity at the centerline. Typically, the length of the potential core varies from 5 to 6 times the slot width. The end of core is commonly assumed as the point where the jet velocity drops to 95% of the velocity at the jet exit ($U = 0.95U_e$). A potential core length of 6 nozzle diameters for a circular nozzle exit is suggested by Gauntner et al. (1970). In the transition region the constant core velocity starts dissipating. Velocity of the jet decreases and pressure increases as the flow approaches the surface. The velocity of air is zero in the region where the jet hits the surface orthogonally. This region is called the stagnation region (Fig. 5.1). The high pressure differences between the stagnation region and the surrounding air forces the air to accelerate in the radial direction.

Assuming no-slip condition, the air velocity is zero at the product surface, forming a boundary layer. This boundary layer resists the surface heat transfer. Boundary layer thickness increases from the stagnation point in a radial direction. For flows on the surface with concave curvature, the centripetal force due to curvature makes the flow unstable, and the so-called Taylor-Gortler type vortex is generated (Gau and Chung, 1991). It has its axis parallel to the flow direction and is known to enhance the momentum and energy transfer and thereby the surface heat transfer.

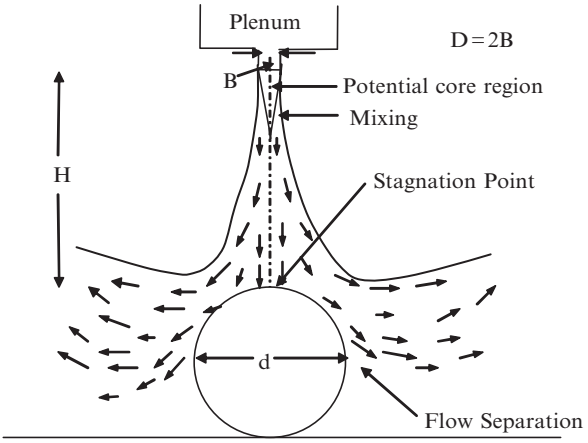

FIG. 5.1. Fluid flow under a slot jet impingement system over a cylindrical object (not drawn to scale)

5.4. Modeling Flow and Heat Transfer in Air Jet Impingement

Fluid flow and heat transfer can be described by three basic equations known as Navier-Stoke's equations. Navier-Stoke's equations describe conservation of mass, momentum and energy of a fluid flow. In turbulent flow, velocity magnitude fluctuates with time. This fluctuation is known as turbulence. Velocity in turbulent flow can be divided in to average velocity (U) and the turbulent component (u').

$$u_i = U_i + u_i'$$

When turbulence is added to the velocity term, Navier Stoke's equations can be expressed, as given by Tennekes and Lumley (1972):

Continuity
$$\frac{\partial \overline{U}_i}{\partial x_j} = 0 \tag{5.1}$$

Momentum
$$\frac{\partial \overline{U}_i}{\partial t} + \frac{\partial \overline{U_i U_j}}{\partial x} = -\frac{1}{p}\frac{\partial \overline{P}}{\partial x_i} + \frac{\partial}{\partial x_j}\left[v_f \left(\frac{\partial \overline{U}_i}{\partial x_j} + \frac{\partial \overline{U}_j}{\partial x_i} \right) - \overline{u_i' u'}_j \right] \tag{5.2}$$

Energy
$$\overline{\rho_f} c_v \frac{\partial \overline{T}}{\partial t} + \rho_f \overline{U}_j c_p \frac{\partial \overline{T}}{\partial x_j} = -\frac{\partial}{\partial x_j}\left[k_f \frac{\partial \overline{T}}{\partial x_i} + \overline{\rho_f} c_p \overline{u}' \overline{T}' \right] \tag{5.3}$$

Where,

$$\frac{\partial}{\partial x_i} = \frac{\partial}{\partial x}, \frac{\partial}{\partial y} \qquad i.e. \qquad x_1 = x, x_2 = y$$

$$\frac{\partial}{\partial x_j} = \frac{\partial}{\partial x} + \frac{\partial}{\partial y} \quad \text{and} \quad U_j \frac{\partial}{\partial x_j} = U_x \frac{\partial}{\partial x} + U_y \frac{\partial}{\partial y}$$

ν_f is the kinematic viscosity of the fluid (air, in the present case), ρ_f is the density of the fluid (kg/m^3), T is the temperature of the fluid (°C), T' is the fluctuating temperature of the fluid (°C), k_f is the thermal conductivity of the fluid (W/m°C), and c_p and c_v are the specific heat capacities of the fluid at constant pressure and volume, respectively. Equations (5.1)–(5.3) are known as Reynolds equations. The additional terms $\bar{u}'_i \bar{u}'_j$ in Reynolds equations make the number of unknowns greater than the number of equations. This is known as the closure problem. There are special turbulence models (κ-ε, κ-ω and Reynolds stress model) to handle this closure problem, as explained by Versteeg and Malalasekera (1995).

5.4.1. Turbulence Modeling

There are three popular turbulence models, κ-ε, κ-ω and Reynolds stress model, used to solve turbulence problems. Olsson et al. (2004) compared κ-ε, κ-ω and shear stress transport (SST) models with experimental data available in the literature. The κ-ω and SST models were found to be good in predicting the heat transfer in the upper part of the cylinder with a low Reynolds number. They found that the SST model was best suited to describe the flow around an object. Hofmann et al. (2004) recommended κ-ε with an RNG turbulence model for heat transfer predictions in impinging jet situations and concluded that none of available turbulence models could predict a Nusselt number near the stagnation point. They found that heat transfer near the stagnation point increased with increasing turbulence at the exit of the nozzle, and the effect of turbulence was negligible at some distance away from the stagnation point. Sarkar et al. (2004) and Singh (2005) used κ-ε with RNG turbulence models to solve the external flow for an impinging jet on a flat plate, and then used the external flow data to solve for boundary layer and heat transfer. The turbulence model used in this case is the κ-ε model. The κ-ε model contains two model equations for turbulence kinetic energy (κ) and turbulence dissipation energy (ε).

$$\frac{\partial(\rho\kappa)}{\partial t} + div(\rho\kappa U) = div\left[\frac{\mu_t}{\sigma_k} grad(\kappa)\right] + 2\mu_t E_{ij} . E_{ij} - \rho\varepsilon$$

$$\frac{\partial(\rho\varepsilon)}{\partial t} + div(\rho\varepsilon U) = div\left[\frac{\mu_t}{\sigma_\kappa} grad(\varepsilon)\right] + C_{1\varepsilon} \frac{\varepsilon}{k} 2\mu_t E_{ij} . E_{ij} - C_{2\varepsilon} \rho \frac{\varepsilon^2}{k} \qquad (5.5)$$

Where,

$$div(\vec{F}) = \nabla \cdot \vec{F} = \frac{\partial F_x}{\partial x} + \frac{\partial F_y}{\partial y} \quad \text{and} \quad grad(\vec{F}) = \nabla \vec{F} = \hat{t}\frac{\partial \vec{F}}{\partial x} + \hat{j}\frac{\partial \vec{F}}{\partial y}$$

$$\mu_t = C\rho\ell = \rho C_\mu \frac{k^2}{\varepsilon}$$

$= \kappa^{1/2}$ is velocity scale

$\ell = \frac{\kappa^{3/2}}{\varepsilon}$ is length scale and

$C_{\mu,} \sigma_{\varepsilon,} C_{1\varepsilon}$ and $C_{2\varepsilon}$ are constants

Equations for κ and ε contain five adjustable constants: C_μ = 0.09, σ_κ = 1.00, σ_ε = 1.30, $C_{1\varepsilon}$ = 1.44 and $C_{2\varepsilon}$ = 1.92. Values of these constants are determined by comprehensive data fitting for a wide range of turbulent flow, as presented by Versteeg and Malalasekera (1995).

5.4.2. *Boundary Conditions*

A computational fluid dynamics (CFD) solver requires well-defined boundary conditions of the grid, in order to simulate the flow and heat transfer. Boundary conditions for this case are shown in Fig. 5.2. Air velocity at the inlet was defined as 25 m/s with 10% turbulence. No-slip condition was adopted at the wall boundary of the cylinder. For unsteady state heat transfer, initial temperature of the cylinder was set to 70°C. For steady state heat transfer solutions, the cylinder surface was assumed to be isothermal at 70°C. Jet centerline and centerline between two nozzles were defined as symmetry. The outlet was declared as a pressure outlet. Heat transfer due to radiation from the cylindrical surface was neglected. Wall boundaries other than the cylindrical surface were assigned as zero heat flux boundaries. The wall boundary of the cylindrical surface was coupled with the external flow.

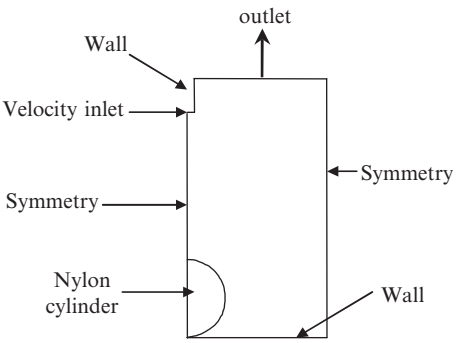

FIG. 5.2. Boundary conditions used in FLUENT simulation

5.5. Flow Measurements in Air Jet Impingement

Surface heat transfer depends upon the flow field around the object. Hence, it is important to measure the flow field characteristics of the impingement system. Bouchez and Goldstein (1975) performed flow visualization of a circular impingement jet using fog generated by dropping dry ice pellets into hot water in a pressurized vessel, and took pictures of the flow. Gau and Chung (1991) studied flow pattern using the entrained smoke particle method. The effect of curvature was difficult to determine because of poor resolution of the images. Cornaro et al. (1999) used smoke-wire flow visualization to study the effect of round jet impinging on convex and concave surfaces. The visualization of the jet showed initiation and growth of ring vortices in the jet shear layer and their interaction with the cylindrical surfaces. Marcroft and Karwe (1999) used two-dimensional laser doppler anemometry for velocity measurement. They used sublimed CO_2 (dry ice fog) to seed the flow. We have used particle image velocimetry technique in our research to measure the flow field.

5.5.1. Particle Image Velocimetry (PIV)

Particle image velocimetry (PIV) is a flow-field visualization technique providing instantaneous velocity vector measurements in a 2-dimensional cross-section of a flow field. The flow field is seeded with fine tracer particles flowing along with the fluid. The flow field is illuminated by a pair of pulsed laser sheets with certain time gap (Δt). Velocity vectors (U_x) are obtained by measuring the displacement of particles (Δx) between the two laser pulses ($U_x = \Delta x/\Delta t$).

PIV measures the velocity of seeding particles to determine actual fluid flow characteristics. Therefore, these seeding particles should be of a suitable size and density to follow the fluid flow closely and respond quickly to any change in velocity magnitude or direction. A lighter and smaller particle can follow the flow better for any abrupt change in magnitude or direction of flow. In our experiments, we used incense smoke as seeding particles. The target area in seeded flow is illuminated with two short duration laser flashes, and images of the flow field are captured by a charge-coupled device (CCD) digital camera. The CCD camera can capture each light pulse in separate image frames. The PIV setup is shown in Fig. 5.3.

These images are then divided into small subsections, called Interrogation Areas (IA). Interrogation areas can be rectangular or square. Typical sizes of these IAs are 16×16 or 32×32 pixels ranging from 8×8 to 256×256 pixels. The corresponding interrogation areas of frame A and B are cross-correlated with each other, pixel by pixel. The mathematical correlation analysis on cluster of particles results in a signal peak. Location of the highest peak and the correlation plane corresponds to the most likely average particle displacement in the interrogation area. This displacement can be divided by the time delay between two frames to get instantaneous velocity vector of particles in the interrogation area.

It would have been preferable to compare the flow along the surface of the cylinder. However, poor data immediately close to the surface due to reflection could

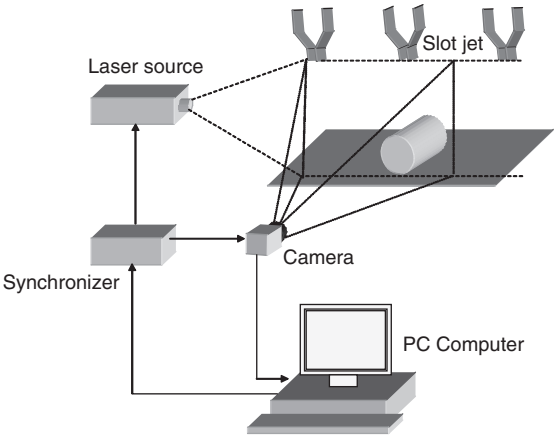

FIG. 5.3. PIV setup for flow measurement during impingement on cylindrical object

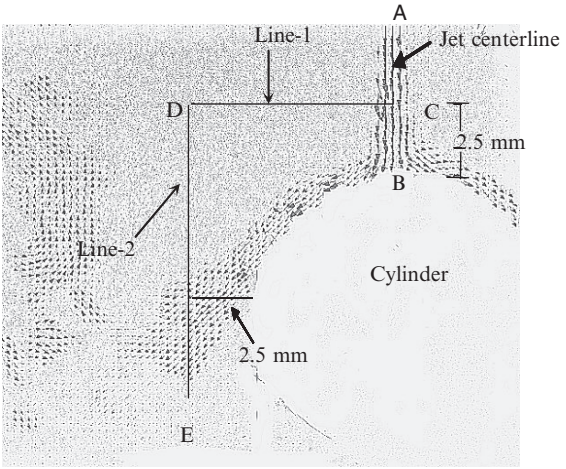

FIG. 5.4. Vector image from PIV (H/D=6, d=32mm)

not be used for flow validation. Instead, velocity profiles along three arbitrary lines in the flow field, close to the surface of the cylinder, were obtained. One along the jet centerline and two lines CD and ED, 2.5mm from the surface of the cylinder were selected, as shown in Fig. 5.4. The velocity profiles along these three lines measured by PIV were compared with the model predicted data (Fig. 5.5). The agreement was reasonably good within the experimental limits (15% of the simulated velocity). Velocity contours obtained from the CFD simulations were also compared with that obtained from PIV measurements (Fig. 5.6).

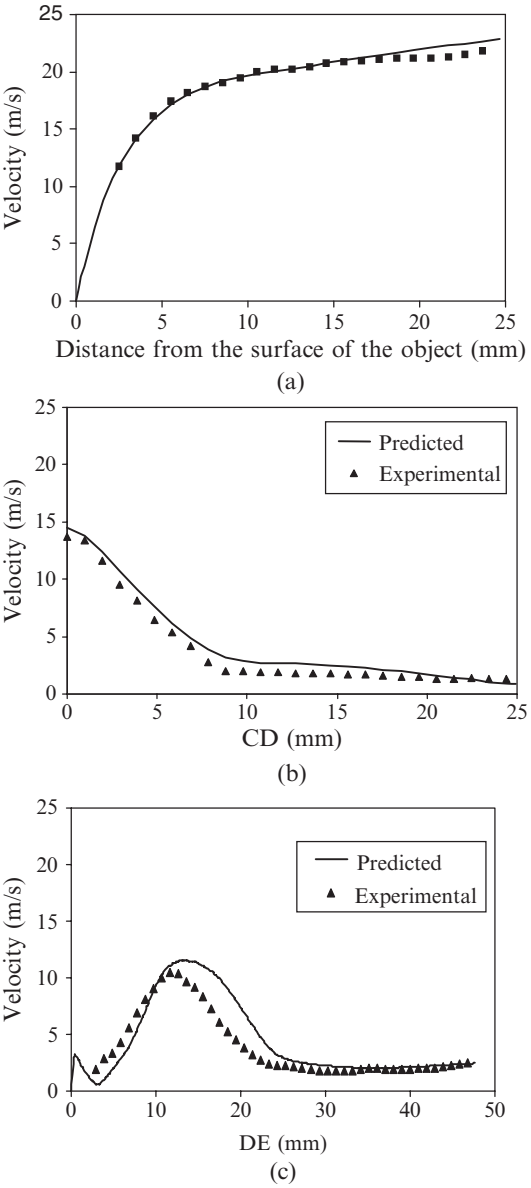

FIG. 5.5. Velocity profile along (a) jet centerline, (b) line-1 and (c) line-2

5.6. Heat Transfer Measurements in Air Jet Impingement

There is a considerable variation of heat transfer coefficients at various locations under impinging jets that may be studied experimentally. Various researchers have studied the spatial variations of heat transfer characteristics of circular and slot

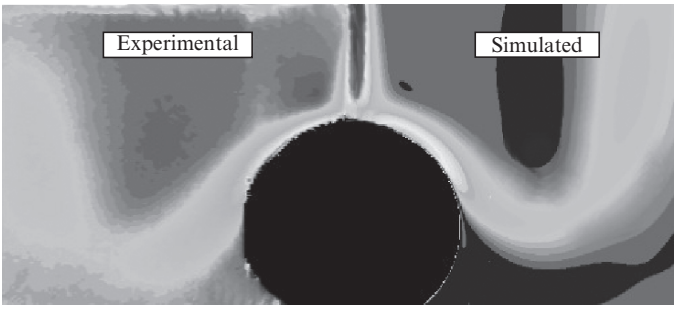

FIG. 5.6. Flow field comparison between experimental and simulated data. Left half of the image is obtained from PIV measurements and right half from FLUENT simulation. (H/D=6, d=25 mm and U=25 m/s)

jets impinging on flat and curved surfaces (Gardon and Akfirat, 1966; Polat et al., 1989; Jambunathan et al., 1992; Chan et al., 2002). In these studies, experimental techniques have been developed to study the spatial variation of convective heat transfer, and attempts have been made to develop conditions such that this variation is minimized, while maximizing the average heat transfer coefficients. More recently, researchers have extended the research on heat transfer measurements to food processing (Nitin and Karwe, 2001; Sarkar et al., 2004).

Traditionally, the lumped capacitance technique has been used to determine average convective heat transfer coefficients for food processing applications at high Reynolds number. In this technique, a transducer made of high thermal conductivity material is used to represent the product shape, and a temperature sensor is placed at its geometric center to determine the change in temperature. This method is simple to use and is good as an average estimate, but use of this technique for air impingement applications will not provide details of the spatial variations of heat transfer coefficients. Hence, there is a need to study the effect of spatial variation of heat transfer and its effects. For heat transfer studies, a material with well-known thermal properties was required. Nylon (6/6) has a low thermal conductivity (0.246 W/m K) and specific heat (1675 J/kg.K), and therefore slower heat transfer. Slower heat transfer helps in better spatial resolution of temperature. These properties made nylon (6/6) an ideal material for this work. Solid nylon cylinders of two diameters, 25 mm and 32 mm, were used. It was desired to compare the temperatures at locations close to the surface, between experimental and predicted values from the model. A T-type thermocouple (Omega Engineering Inc., part number TT-T-30SLE, Stamford, CT) was placed at a location 2 mm below the surface of the cylinder. A preheated cylinder was kept at different angular positions every time and cooled under an impinging jet. Time-temperature data at various locations along the circumference of the cylinder were recorded using a DASYLAB data acquisition system (IOtech, Inc., Cleveland, OH). The nylon cylinder was preheated inside a hot air oven. Temperature readings were scaled based upon the initial temperature of the cylinder (T_i) and cooling air temperature (T_{air})

$$T_{scaled} = T - T_{air} / T_i - T_{air} \tag{5.6}$$

where T is temperature reading at any time t. Scaled temperature profiles obtained from experiments were compared with the temperature profile obtained from unsteady state heat transfer simulation as shown in Fig. 5.7.

5.7. Effect of Various Impingement Parameters

Effective Nusselt number, a dimensionless representation of transient convective conductance, was used to study the effect of various flow parameters on heat transfer rate. The effective Nusselt number was calculated based on the hydraulic diameter of the slot and mean temperature of the air near the surface $[(T_{air}+T_s)/2]$

$$Nu = \frac{D}{\Delta T}\frac{dT}{dy} \tag{5.7}$$

where ΔT is the temperature difference between the air jet and the surface of the cylinder ($T_{air} - T_s$). A high heat transfer coefficient is observed at the stagnation

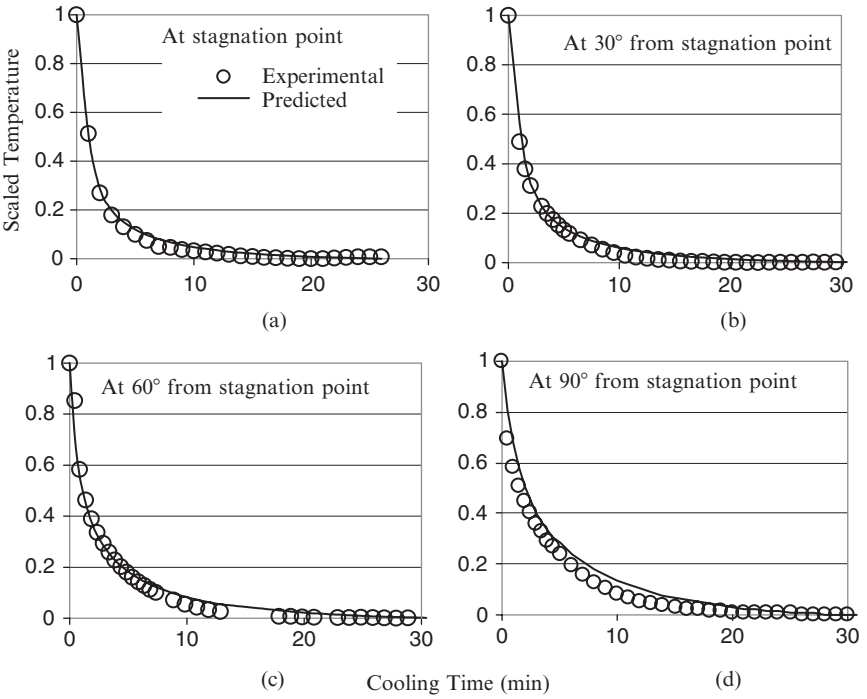

FIG. 5.7. Comparison between experimental and predicted temperature profiles at 2 mm below the surface, at different angular positions, under air impingement cooling of a nylon cylinder. d=25mm, Re=8000, H/D=6, turbulence intensity (I) = 5%

point, but the maximum Nusselt number occurred at some distance away from the stagnation point (angular position of around 10° from the stagnation point), as shown in Fig. 5.8. The Nusselt number profile along the curvilinear axis of the cylinder showed three maxima after the stagnation point. The first peak is the point of highest Nusselt number, and its location coincided with the region of flow-acceleration. Gardon and Akfirat (1965) suggested flow transition from laminar to turbulent as a reason for this peak just near the stagnation point for jet impinging on a flat plate. After the first peak, the surface Nusselt number decreased sharply until the position of the second peak. The position of this second peak coincides with the flow separation region (at an angular position of 60° to 90° away from the stagnation point). The region between the stagnation point and the second peak falls in the wall jet flow region, as shown in Fig. 5.8. Flow recirculation below the separation point results in the third peak.

5.7.1. Effect of H/D

Distance of the target surface from the jet exit plays an important role in deciding the flow characteristics around the object. Within the potential core region, the flow is laminar in nature. The jet becomes completely turbulent at the end of the potential core and turbulence increases further downstream. Heat transfer through a surface is higher in turbulent flow when compared to laminar flow. Placing an object in the potential core region gives a lower Nusselt number due to the laminar nature of the flow. The magnitude of jet velocity decreases with increasing *H/D*. Loss of kinetic energy of the jet due to shearing with surrounding stagnant fluid is the reason for this. Loss of kinetic energy of the jet means a decreased heat transfer. But at the same time, turbulence intensity of the flow increases with increasing *H/D*. Therefore, the effect of decreasing jet velocity and increasing turbulence

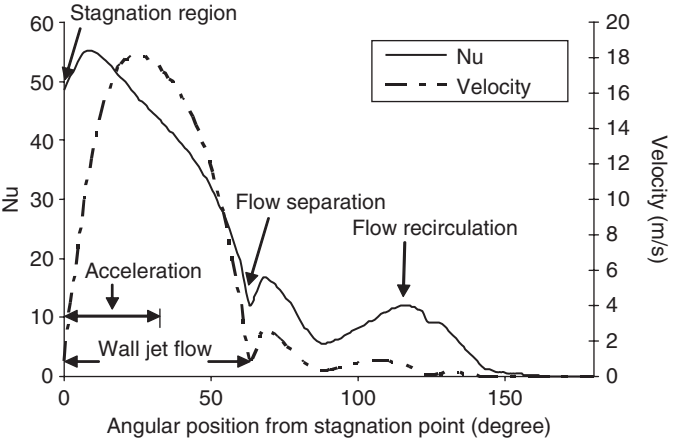

FIG. 5.8. Nusselt number and velocity distribution over the surface of the cylinder, under an impinging jet. *d*=25mm, *Re*=8000, *H/D*=6, turbulence intensity (*I*) = 5%. (Simulated)

tries to counterbalance, and at a specific *H/D* the heat transfer on the product surface is maximum. Downs and James (1987) suggested that the stagnation point Nusselt number is maximum at *H/D* of 4–7. Some authors have suggested *H/D* = 5–8 for maximum heat transfer rate (Lee et al., 1999; McDaniel , 2000; Chan et al., 2002; Gori and Bossi, 2003). Short jet exit-to-object distance results in a drop in heat transfer at a short distance from the stagnation point (Sarkar, 2004). Albertson et al. (1950) and Gardon and Akfirat (1965) reported that the potential core length is approximately five times the slot width for slot jet impingement. After potential core, the centerline velocity decreased with $\sqrt{1/H}$, less rapid than for circular jets, for which centerline velocity decreased with (*1/H*) after the potential core region. For *Re*=8000-16000, optimum *H/D* where stagnation point Nusselt number (Nu_{stag}) is highest, is near 3. In our work, the stagnation point Nusselt number was found to be maximum at H/D=3, as shown in Fig. 5.9.

5.7.2. Effect of Reynolds Number (Re)

The Reynolds number (*Re*) for slot jet impingement can be defined based on hydraulic diameter of the jet exit (Yang et al., 1999)

$$\mathrm{Re} = \frac{U\,2B}{\upsilon} \tag{5.8}$$

where *U* is velocity magnitude of the fluid (m/s), *B* is the width of the slot nozzle (m), and υ is the kinematic viscosity of the fluid (m^2/s).

Heat transfer characteristics of the impinging jet can be described by velocity alone for a very low Reynolds number, but at higher Reynolds number, turbulence generated by the jet plays an important role in heat transfer rate and distribution (Gardon and Akfirat, 1965). Heat transfer rate increases with increasing Reynolds number, but the increase is asymptotic. Sarkar (2004) observed that change in heat transfer coefficient is mainly at the stagnation point, and the effect remains

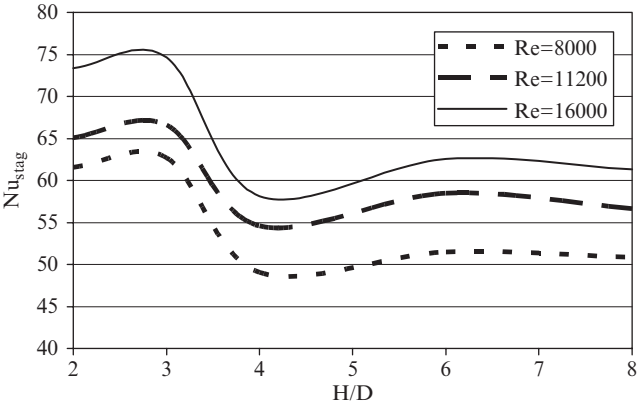

Fig. 5.9. Stagnation point Nusselt number variation with H/D for d=32mm and turbulence intensity (I)=5% (simulated)

for a very short distance from the stagnation point for impingement on a flat plate. The effect of curvature increased with increasing Reynolds number (Cornaro et al., 2001). For *Re* = 6,000 the effect of curvature diminishes, i.e. there is no difference in heat transfer profile around the objects of different curvatures.

In this work, Reynolds number of the flow was calculated based on the hydraulic diameter of the slot jet nozzle (*D*). Velocity profiles along the jet centerline were compared for the Reynolds number, varying from 3,200 to 16,000. It was observed that velocity magnitude decayed faster for low Reynolds number (Fig. 5.10.a). Potential core is the region where velocity remains greater than 95% of the velocity at the jet exit. The potential core was longer for higher Reynolds numbers. Nusselt number distribution over the surface of the cylinder shows an increasing trend with the Reynolds number (Fig. 5.10.b).

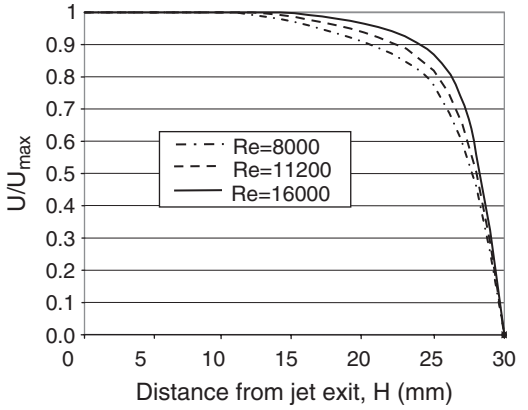

(a)

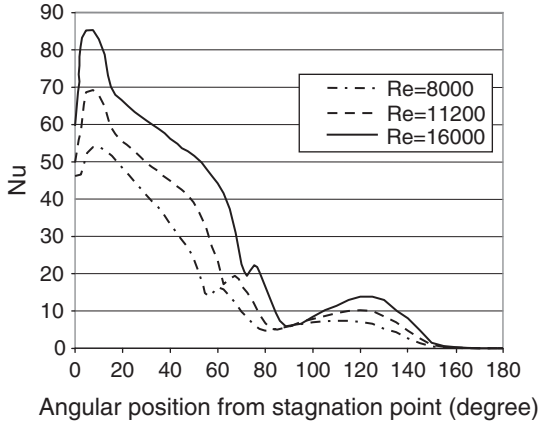

(b)

FIG. 5.10. (a) Effect of Reynolds number on flow along jet centerline and (b) Nusselt number distribution over the cylindrical surface for steady state condition for *H/D*=6, *d*=25mm and 5% turbulence intensity at jet exit (simulated)

5.7.3. *Effect of Surface Curvature (d/D)*

Surface curvature in this work is defined as the inverse of the cylinder diameter (*d*). Curvature was made dimensionless with hydraulic diameter of the slot jet (*D*). Gau and Chung (1991), Lee et al. (1997) and Cornaro et al. (2001) reported that Nusselt number increases at the stagnation point, with increase in curvature of the surface under impingement. Kornblum and Goldstein (1997) used high Reynolds number with small relative curvature (*D/d* = 0.019–0.038). Chan et al. (2002) observed that the decay in average circumferential Nusselt number around a convex surface was higher than that on a flat plate. This fast decay is due to decrease in energy and momentum transport due to centrifugal force along the circular surface (Schlichting, 1979).

As shown in Fig. 5.11.a, the value of maximum velocity increases with decreasing diameter (*d*) or increasing curvature of the cylinder (*D/d*). Surface heat transfer coefficient at any location depends upon the boundary layer characteristics (thickness and turbulence). Boundary layer characteristics are determined by local free stream velocity (velocity at the surface of the product at that location). Hence, it can be expected that higher surface curvature (smaller diameter) will have a higher overall surface heat transfer coefficient, as shown in Fig. 5.11.b.

The position of the first and second velocity peaks are displaced away from the stagnation point with increasing curvature (Fig. 5.11.a). At the stagnation point, velocity magnitude was zero, following acceleration in the air stream along the curvature until 20° to 30° from the stagnation point. Location of a separation point depends upon the surface curvature. For larger diameter cylinders with lower curvature, flow separation occurred earlier than that for smaller diameter cylinders.

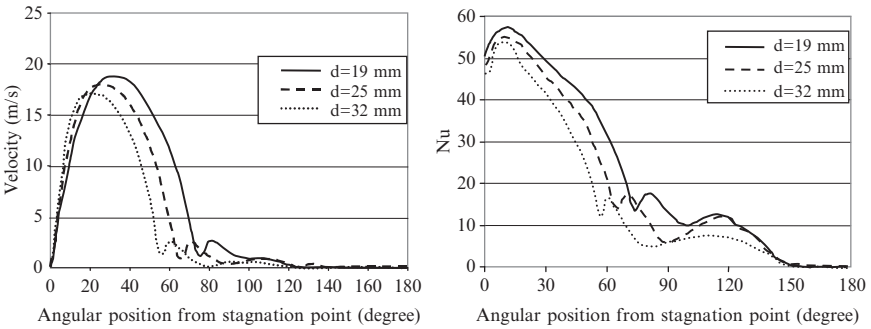

FIG. 5.11. (a) Velocity magnitude and (b) Nusselt number distribution over the surface of cylinder of different diameters. H/D=6, Re=8000, I=5% (simulated)

References

Albertson, M.L., Dai, Y.B., Jensen, R.A., and Rouse H., 1950, Diffusion of Submerged Jets, *Trans. Am. Soc. Civil Eng*. **115**(2409):639–697.

Ashforth, S.F, Jambunathan, K., and Whitney C.F., 1997, Velocity and Turbulence Characteristics of a Semiconfined Orthogonally Impinging Slot Jet, *Exp Thermal Fluid Sci*. **14**:60–67.

Bórquez, R., Wolf, W., Koller, W.D., and Spieb W.E.L., 1999, Impinging Jet Drying of Pressed Fish Cake, *J. Food Eng*. **40**(1-2):113–120.

Bouchez, J.P., and Goldstein J., 1975, Impingement Cooling From a Circular Jet In a Cross Flow, *Int. J. Heat Mass Transfer* **18**:719–730.

Chan, T.L., Leung, C.W., Jambunathan, K., Ashforth-Frost, S., Zhou, Y., and Liu M.H., 2002, Heat Transfer Characteristics of a Slot Jet Impinging on a Semi-Circular Convex Surface, *Int. J. Heat Mass Transfer* **45**:993–1006.

Cornaro, C., Fleischer, A.S., and Goldstein R.J., 1999, Flow Visualization of a Round Jet Impinging on Cylindrical Surfaces, *Exp. Therm. Fluid Sci*. 20:66–78.

Cornaro, C., Fleischer, A.S., Rounds, M., and Goldstein R.J., 2001, Jet Impingement Cooling of a Convex Semi-Cylindrical Surface, *Int. J. Therm. Sci*. **40**:890–898.

Downs, S.J., and James E.H., 1987, Jet Impingement Heat Transfer—A Literature Survey, *ASME Paper No 87-HT-35*.

Gardon, R., and Akfirat J.C., 1965, The Role of Turbulence in Determining the Heat Transfer Characteristics of Impinging Jets, *Int. J. Heat Mass Transfer* **8**:1261–1272.

Gardon, R., and Akfirat J.C., 1966, Heat Transfer Characteristics of Impinging Two Dimensional Air Jets, *J. Heat Transfer* **88**:101–108.

Gau, C., and Chung C.M., 1991, Surface Curvature Effect on Slot Air Jet Impinging Cooling Flow and Heat Transfer Processes, *ASME J. Heat Transfer* **113**:858–864.

Gauntner, J.W., Livingwood, J.N.B., and Hrycak P., 1970, *Survey of Literature on Flow Characteristics of a Single Turbulent Jet Impinging on a Flat Plate*, NASA TN D-5652.

Gori, F., and Bossi L., 2003, Optimal Slot Height in the Jet Cooling Of Cylinder, *Appl. Therm. Sci*. **23**:859–870.

Hofmann, H., Martin, H., and Matthias K., 2004, Numerical Simulation of Heat Transfer from an Impinging Jet on a Flat Plate. *Chem. Eng. Technol*. **27**(1):27–30.

Jambunathan, K., Lai, E., Moss, M.A., and Button B.L., 1992, Review of Heat Transfer Data for Single Circular Jet Impingement, *Int. J. Heat Fluid Flow* **13**(2):106-115.

Kornblum, Y., and Goldstein R.J., 1997, Impingement on Semicircular Concave and Convex Surfaces, Part Two: Heat Transfer, in: *Proceedings. International Symposium on the Physics of Heat Transfer in Boiling Condensation*, L. Bolshov publications, Moscow, pp. 603–608.

Lee, D.H., Chung, Y.S., and Kim M.G., 1999, Technical Note: Turbulent Heat Transfer from a Convex Hemispherical Surface to a Round Impinging Jet, *Int. J. Heat Mass Transfer* **42**:1147–1156.

Lee, D.H., Chung, Y.S., and Kim D.S., 1997, Turbulent Flow and Heat Transfer Measurements on a Curved Surface with a Fully Developed Round Impinging Jet, *Int. J. Heat Fluid Flow* **18**(1):160–169.

Li, A., and Walker C.E., 1996, Cake Baking in Conventional, Impingement and Hybrid Ovens, *J. Food Sci*. **61**(1):188–191, 197.

Lujan, J., Moreira, R.G., and Seyed Y.J., 1997, Air Impingement Drying of Tortilla Chips, *Drying Technol*. **15**(3–4):881–897.

Marcroft, H., and Karwe M.V., 1999, Measurement of Flow Field in a Jet Impingement Oven, Part II: Multiple Jets, *J. Food Process Preserv*. **23**:235–248.

McDaniel A.W., 2000, Slot Jet Impingement Heat Transfer from Circular Cylinders, *J. Heat Mass Transfer* 43:1975-1985.

Moreira R.G., 2001, Impingement Drying of Foods Using Hot Air and Superheated Steam, *J. Food Eng*. **49**(4):291–295.

Narayanan, V., Yagoobi, J.S., and Page R.H., 2004, An Experimental Study of Fluid Mechanics and Heat Transfer in an Impinging Jet Flow, *Int. J. Heat Mass Transfer* **47**:1827–1845.

Nitin, N., and Karwe M.V., 2001, Heat Transfer Coefficient for Cookie Shaped Objects in a Hot Air Jet Impingement Oven, *J. Food Process Eng*. **24**(1):51–69.

Olsson, E.E.M., Ahrne, L.M., and Tragrardh A.C., 2004, Heat Transfer from a Slot Air Jet Impinging on a Circular Cylinder, *J. Food Eng*. **63**:393–401.

Ovadia, D.Z. and Walker, C.E., 1998, Impingement in Food Processing, *Food Technol*. **52**(4):46–50.

Polat, S., Huang, B., Majumdar, A.B., and Douglas W.J.M., 1989, Numerical Flow and Heat Transfer Under Impinging Jets, in: *Annual Review of Numerical Fluid Mechanics and Heat Transfer*, Hemisphere Pub. Corp, Washington, pp. 157–197.

Sarkar A., 2004, Numerical Modeling and Experimental Studies on Air Impingement Freezing under Slot Jets, PhD thesis, Biological and Agricultural Engineering, University of California Davis, Davis.

Sarkar, A., Nitin, N., Karwe, M.V., and Singh R.P., 2004, Fluid flow and Heat Transfer in Air Jet Impingement in Food Processing, *J. Food Sci*. **69**(4):113–122.

Schlichting H., 1979, *Boundary Layer Theory*. 7th ed., McGraw-Hill, New York.

Scott, C M., and Bradley P.M., 2005, Condensing-Convective Boundary Conditions in Moist Air Impingement Ovens, *J. Food Eng*. **70**(1):101–108.

Singh S.K., 2005, Air Impingement Cooling of Cylindrical Objects Using Slot Jets, M.S. Thesis, Biological Systems Engineering, University of California Davis, Davis.

Smith N.R., 1975, United States Patent Number 3884213.

Tennekes, H., and Lumley J.L., 1972. *A First Course in Turbulence*, 1st ed. MIT Press, Cambridge, p. 300.

Versteeg, H.K., and Malalasekera W., 1995, *An Introduction to Computational Fluid Dynamics: The Finite Volume Method*, McGraw-Hill, Loughborough University.

Wählby, U., Skjoldebrand, C. and Junker E., 2000, Impact of Impingement on Cooking Time and Food Quality, *J. Food Eng*. **43**(3):179–187.

Yang, G., Choi, M., and Lee J.S., 1999, An Experimental Study of Slot Jet Impingement Cooling on Concave Surface: Effects of Nozzle Configuration and Curvature, *Int. J. Heat Mass Transfer* **42**:2199–2209.

6
New Technologies to Preserve Quality of Fresh-Cut Produce

G.A. González-Aguilar, S. Ruiz-Cruz, R. Cruz-Valenzuela, J.F. Ayala-Zavala, L.A. de la Rosa, and E. Alvarez-Parrilla

6.1. Introduction

Food preservation is critical for keeping the global food supply safe and available for consumers. Food scientists study production and processing to develop new technologies that improve the quality and quantity of healthy food products. The main goal is to safely increase yields with effective quality control and to preserve the environment and fulfill consumer expectations.

Both consumers and food producers require more research about fresh-cut produce. Producers demand inexpensive and effective technologies to safely preserve the quality of the products. In the same manner, consumers want quality low priced fresh-cut produce. Food scientists attempt to solve problems in fresh-cut processing and quality preservation.

In the past two decades, rapid advances in scientific knowledge on fresh-cut produce preservation have been developed. The present paper reviews technologies such as ultraviolet irradiation (UV-C), edible coatings, active packaging and volatiles, noting the areas in which information is still lacking and commenting on future trends.

6.2. UV-C Irradiation

Ultraviolet light (UV) is a type of non-ionizing radiation with wavelengths from 100 to 400 nm, which is usually classified in three types: UV-A (315–400 nm), UV-B (280–315 nm) and UV-C (100–280 nm). UV-C irradiation has its maximum at 254 nm and is, of the three, the one with the highest germicidal action, and therefore, the most studied (Bintis et al., 2000). Radiation has been used both to delay ripening associated processes and to reduce microorganism growth (Vicente et al., 2005a). Several studies have been published, and recently, UV-C has been used as an alternative treatment to preserve the quality of different fruits and vegetables (González-Aguilar et al., 2004a; Pan et al., 2004; Yaun et al., 2004). Pre-storage applications of UV-C reduced chilling injury in pepper (Vicente et al., 2005b), delayed senescence yellowing, chlorophyll degradation, and pheophytin

accumulation in broccoli (Costa et al., 2006), controlled storage rot in strawberry (Marquenie et al., 2002; Marquenie et al., 2003), reduced pathogen growth and induced disease resistance in the fruit tissue (Mercier et al., 2001).The mechanism by which UV-C radiation preserves fruit and vegetable quality has also been studied (Wright et al., 2000). UV-C treatments induced a stress that simulates the production of phenylalanine ammonia-lyase (PAL), an enzyme that plays a key role in the synthesis of phytoalexins, phenolic compounds that improve the resistance of fruits and vegetables to microorganisms (Guerrero-Beltrán and Barbosa-Cánovas, 2004). The UV-C treatment-induced phytoalexins have been identified in fresh-cut cantaloupe (Lamikanra et al., 2002) and fresh-cut pineapple (Lamikanra and Richard, 2004).

Exposure to UV-C delays fruit softening, one of the main factors determining fruit postharvest life. Barka et al. (2000) found that UV-C decreased the activity of enzymes involved in tomato cell wall degradation and delayed fruit softening. Reduction of strawberry fruit decay by UV-C application has also been reported (Vicente et al., 2004). Chilling injury symptoms and deterioration of "Tommy Atkins" mangoes was reduced by UV-C irradiation during storage at 5°C (González-Aguilar et al., 2001a).

In addition, UV-C irradiation reduced ethylene of apple slices and had minimal effect on the respiratory physiology of tissues (Gunes et al., 2000). Allende and Artés (2003) studied the effect of short UV-C doses (0.4 – 8.14 kJ/m^2) on the shelf-life of the fresh processed lettuce. They found that the use of these short doses is effective in delaying senescence and deterioration in fresh-processed lettuce and thereby maintaining the quality of the product.

6.3. Edible Coating

Edible coating has been used in a wide range of food products. It may be applied directly on the food surface by dipping, spraying or brushing, in addition to, or as a replacement for natural protective waxy coatings, to prevent water loss and gas exchange and to provide a micro-modified atmosphere around products that retards food deterioration (McHugh and Senesi, 2000). Edible Coatings also enhance food safety due to their natural biocide activity or as a consequence of the incorporation of antimicrobial compounds (Cha and Chinnan, 2004). It can be considered as a physical method to improve quality and extend shelf-life of fresh-cut fruits and vegetables (Salcini and Massantini, 2005). Its use has been discussed in several reports. McHugh and Senesi (2000) studied various edible coatings made from apple puree with different concentration of fatty acids, fatty alcohols, beeswax and vegetables. They found that edible coatings control browning of fresh-cut apple for 3 days at 5°C. In other studies, sensory evaluation confirmed that chitosan-coated longan fruit (Jiang and Li, 2001), and peaches (Li and Yu, 2000) had better quality compared to controls. These authors also observed a direct correlation between coating concentration and fruit quality.

Different compounds have been used as edible coating to prevent deterioration and extend shelf-life on cherries (Yaman and Bayindirh, 2002; Alonso and Alique, 2004), plum (Pérez-Gago et al., 2003), strawberries (Mali and Grossmann, 2003; Del-Valle et al., 2005), apple (Lee et al., 2003; Moldao-Martins et al., 2003) and avocado (Maftoonazad and Ramaswamy, 2005).

Chitosan, yam starch and *Aloe vera* gel were used for controlling microbial growth in carrot (Durango et al., 2006), grapes (Valverde at al., 2005) and raspberries (Han et al., 2004). Dong et al. (2004) studied the effect of chitosan based edible coatings at different concentrations on the shelf-life of peeled litchi fruits. They found that chitosan based edible coatings were used successfully to maintain quality attributes and extend shelf-life.

6.4. Active Packaging

Active packaging is an innovative concept in which the package, the product, and the environment interact to prolong shelf-life or enhance safety or sensory properties, while maintaining the quality of the product. This is particularly important in the area of fresh and extended shelf-life foods (Vermeiren et al., 2002). Active packaging (AP) can be divided in two groups. In the first group, the packaging material is modified in order to protect the product against microbial spoilage and enhance food quality, by adding oxygen scavengers, ethylene and water vapor absorbers, carbon dioxide and ethanol emitters, odor removers, aroma emitters, and system-to-release active compounds such as antimicrobials and antioxidants (Fernández, 2000). Special attention has been focused on antimicrobial (Appendini and Hotchkiss, 2002; Suppakul et al., 2003) and antioxidant packaging (Wessling et al., 2000). The second group is intelligent packaging (IP). Yam et al. (2005) defined IP as conservation method that can monitor the quality/safety condition of food products and provide early warning to food manufacturers. They believe that IP is a provider of enhanced communication and AP is a provider of enhanced protection; unfortunately, clear and unequivocal definitions are not yet available. In a typical IP system, multiple smart package devices are employed at several strategic locations throughout the supply chain; these include barcodes, radio frequency identification tags, time-temperature indicators, gas indicators and biosensors (Yam et al., 2005).

Two basic forms of making the active components available exist. They can be found in the interior of the active package (in small bags or envelopes) or may form part of the packing material. In this context, edible coating could be considered the best active packaging used to improve food safety by inhibition or delay of the growth of microorganisms in fruits and vegetables (Appendini and Hotchkiss, 2002).

6.4.1. Cyclodextrin

Cyclodextrins are naturally occurring cyclic carbohydrates extensively used in the food industry due to their ability to form stable complexes with organic

molecules. As a consequence of their complexation ability, cyclodextrins are used in the fresh-cut industry as release control materials of volatile compounds. An example of this release control ability is the complexation of 1-methylcyclopropene (1-MCP) by α-cyclodextrin derivatives. 1-MCP is encapsulated in a α-cyclodextrin polymer, without any degradation or loss due to evaporation. However, when dissolved in water, it is released from the complex into the air, over a period of 2 h (Blankenship and Dole, 2003). β-cyclodextrin has been described as a potent PPO inhibitor (Álvarez-Parrilla et al., 2005). This enzyme inhibition is explained in terms reduction of free substrate due to the complexation process between the CD and the PPO substrate. Hicks et al. (1996) observed a synergic effect on the browning prevention of apple juice for as long as 2–3 weeks at 4°C. However, they reported that CD was not effective in the prevention of fresh-cut apple browning, due to the small diffusion rate of CD inside apple tissue. Further studies have to be made in order to study the combined effect of cyclodextrin with other PPO inhibitors in the prevention of browning of fresh-cut fruits.

6.4.2. Volatiles

Volatiles are low molecular weight organic compounds (less 250 g/mol) with high vapor pressure at room temperature (Wills et al., 1998). Plants produce a wide range of volatile compounds, some of which are important flavor quality factors in fruits, vegetables, spices and herbs (Kays, 1991). A number of volatile compounds inhibit the growth of microorganisms (Fries, 1973; Azzouz and Bullerman, 1982; Linton and Wright, 1993). The presence of volatile compounds has also been hypothesized to play an important role in the defense systems of fresh produce against decay microorganisms (Fenwick et al., 1990; Ben-Yehoshua et al., 1998).

Over recent decades there has been increasing public pressure to reduce the use of synthetic food preservatives and fungicides in agriculture products and their presence in the environment. Moreover, concern has been raised about the health risk involved in the use of synthetic food preservatives and fungicides on fruits and vegetables shortly before consumption. Therefore, considerable research has been recently directed toward the development of effective alternative food preservatives. The European Commission has been actively promoting the development and commercial implementation of these new compounds, known as "Green Chemicals" (Gorris and Smid, 1995). The ability of plant volatiles to inhibit microorganism growth is one of the reasons why there is an increased interest in using them to control postharvest and postprocessing decay of fruits and vegetables (Wilson and Winiewski, 1989). An important factor is that plant volatiles have been widely used as food flavoring agents, and many are generally recognized as safe (GRAS).

6.4.3. Methyl Jasmonate

Methyl jasmonate (MJ) is a natural compound widely distributed in plants. It was first detected as a fragrant compound in *Jasminum* essential oil and other plant species (González-Aguilar et al., 2006). MJ is known to regulate plant development

and response to environmental stress (Sembder and Parthier, 1993; Creelman and Muller, 1995; González-Aguilar et al., 2006). MJ affects many biochemical and physiological reactions in intact and fresh-cut fruits and vegetables. Several lines of evidence suggest that jasmonates play a role as a signal molecule in climateric fruits by inducing defense responses and increasing resistance during storage of whole and fresh-cut fruits. MJ treatments have been shown to extend shelf-life of whole tomatoes, oranges, grapes, mangoes and guavas (D'Hallewin et al., 1999; Cantos et al., 2001; González-Aguilar et al., 2001b), reduce microbial contamination in fresh-cut celery and peppers, and alleviate symptoms of chilling injury in mangoes and guava (Meir et al., 1998; Buta and Moline, 1998; González-Aguilar et al., 2001b; 2004b). The use of MJ in conjunction with modified atmosphere packaging significantly reduced chilling injury symptoms and decay of "Sunrise" papaya during cold storage (González-Aguilar et al., 2003). In this study, the resistance induced by MJ treatment was positively correlated with higher levels of polyamines presented in the fruit tissue.

6.4.4. 1-methylcyclopropene (1-MCP)

1-methylcyclopropene (1-MCP) has been considered one of the best options for extending quality and shelf-life of fresh-cut fruits and vegetables (Blankenship and Dole, 2003). 1-MCP exerts its action by tightly binding ethylene receptors, preventing ethylene binding, and consequently, inhibiting its action (Sisler and Serek, 1997). Treatment can be applied to either whole or sliced fruit (Laurie, 2005) and therefore it has a potential use in modified atmosphere packaging systems. Recently some studies have focused on the effects of 1-MCP treatment of whole fruits on the quality and shelf-life of fresh-cut produce. In some fruits, like banana and persimmon, whole fruit showed better results than fresh-cut, in terms of texture preservation (Vilas-Boas and Kader, 2001). Several reports showed excellent results in fresh-cut apples (Jiang and Joyce, 2002; Bai et al., 2004; Calderón-López et al., 2005). Weight loss of 1-MCP-treated apple slices was less than 2% after 21 days, with improved firmness preservation (Calderón-López et al., 2005). Furthermore, the firmness of sliced tomatoes was improved and water soaking reduced by treating with 1-MCP (Jeong et al., 2004).

6.4.5. Ethanol

Ethanol, a GRAS compound, has shown to be effective for controlling decay of whole fruits and vegetables, inhibiting microbial growth (Feliciano et al., 1992; Lichter et al., 2002; Karabulut et al., 2004). However, there are few reports of treatment of fresh-cut fruits with ethanol vapors. The mode of action of ethanol is by interaction with the membrane of microorganisms. Several devices have been designed to control ethanol release in the headspace of packed fruit (Kalathenos and Russel, 2003), which could be applied in fresh-cut produce. Ethanol vapors applied to grapes decreased fungal development. Ayala-Zavala et al. (2005) reported that ethanol treatment in conjunction with MJ increased antioxidant capacity, volatile compounds and postharvest life of tomato fruits. Previous work

reported that acetaldehyde and ethanol treatment delayed color development and ripening, increasing carbon dioxide production of tomatoes (Beaulieu and Saltveit, 1997). Plotto et al. (2006) concluded that ethanol vapor applied for 20 h, prior to processing whole mangoes, did not delay ripening; however, shorter time of exposure (10 h) suppressed fruit ripening.

6.4.6. Acetic Acid

Acetic acid is one of the most common and inexpensive organic acids. Acetic acid and its derivates are known as GRAS by the regulatory agencies. These compounds have shown to be effective in controlling fungal development in whole apples, peaches, apricots and cherries (Sholberg and Gaunce, 1995). However, acetic acid was not as effective as essential oils treatment in preventing decay of fresh-cut kiwi (Wang and Buta, 2003).

6.4.7. Essential Oils

Essential oils (EOs) represent the most important aromatic fraction of plant and plant produce, constituted by a complex mixture of terpenes, alcohols, cetones, aldehydes and esters. Their antibacterial mode of action has been related to their individual active compounds. Plant EOs have shown a wide antimicrobial range of action against several bacteria and molds. Therefore, EOs present a huge potential as food preservatives, especially because most of them are classified as GRAS. However, EO's treatments can affect aroma and sensory properties of fresh-cut product. Citrus EO preserved the quality of fresh-cut fruit salads without affecting consumer acceptance of the product (Lanciotti et al., 2004). Mandarin, cider and lime EOs increased shelf-life of fresh-cut fruit salads delaying microbial growth and maintaining sensorial attributes (Lanciotti et al., 2004).

6.5. Future Research

Food science trends indicated that new technologies are useful tools for improving shelf-life, quality and safety of fresh-cut produce. However, more research is needed to identify the optimal operational conditions in which combinations among technologies are tested with different products. Every new technology must be focused in maintaining or improving sensorial, nutritional and microbiological quality of fresh-cut produce.

References

Allende, A., and Artés F., 2003, Combined Ultraviolet-C and Modified Atmosphere Packaging Treatments for Reducing Microbial Growth of Fresh Processed Lettuce, *Lebensm.-Wiss. U.-Technol*. **36**:779–786.

Alonso, J., and Alique R., 2004, Influence of Edible Coating on Shelf Life and Quality of "Picota" Sweet Cherries. *Eur. Food Res. Technol*. **218**:535–539.

Álvarez-Parrilla, E., de la Rosa, L.A., and Rodrigo-García J., 2005, Aplicaciones de las Ciclodextrinas en Alimentos, in: *Nuevas Tecnologías de Conservación de Vegetales Frescos Cortados*, G.A. González-Aguilar, A.A. Gardea and F. Cuamea-Navarro (eds.), Logoprint Digital, Guadalajara, pp. 359–380.

Appendini, P., and Hotchkiss J.H., 2002, Review of Antimicrobial Food Packaging, *Innovative Food Sci. Emerg. Technol*. **3**(2):113–126.

Ayala-Zavala, J.F., Wang, S.Y., Wang, C.Y., and González-Aguilar G.A., 2005, Methyl Jasmonate in Conjunction with Ethanol Treatment Increases Antioxidant Capacity, Volatile Compounds and Postharvest Life of Strawberry Fruit, *Eur. Food Res. Technol*. **221**(6):731–738.

Azzouz, M.A., and Bullerman L.B., 1982, Comparative Antimycotic Effects of Selected Herbs, Spices, Plant Components and Commercial Antifungal Agents, *J. Food Prot*. **45**:1298–1301.

Bai, J., Baldwin, E.A., Soliva-Fortuny, R.C., Mattheis, J.P., Stanley, R., Perera, C., and Brencht J.K, 2004, Effect of Pretreatment of Intact "Gala" Apple with Ethanol Vapor, Heat, or 1-Methylcyclopropene on Quality and Shelf Life of Fresh-Cut Slices, *J. Am. Soc. Hort. Sci*. **1**:583–593.

Barka, E.A, Kalantari, S., Makhlouf J., and Arul J., 2000, Impact Of UV-C Irradiation on the Cell Wall-Degrading Enzymes During Ripening of Tomato (*Lycopersicon Esculentum L*) Fruit, *J. Agric. Food Chem*. **48**:667–671.

Beaulieu, J.C., and Saltveit M.E., 1997, Inhibition or Promotion of Tomato Fruit Ripening by Acetaldehyde and Ethanol Is Concentration-Dependent and Varies with Initial Fruit Maturity, *J. Am. Soc. Hort. Sci*. **122**:392–398

Ben-Yehoshua, S., Rodov, V., and Peretz J., 1998, Constitutive and Induced Resistance of Citrus Fruit Against Pathogens, in: *Disease Resistance In Fruit, ACIAR Proceeding No. 80*, G.I. Johnson, E Highly, D.C. Joyce (eds.), Australian Centre for International Agricultural Research: Canberra, pp. 78–79.

Bintis, T., Litopoulou-Tzanetaki, E., and Ribinson R., 2000, Existing and Potential Applications of Ultraviolet Light in the Food Industry—A critical review, *J. Sci. Food Agric*. **80**:637–645.

Blankenship, S.M., and Dole J. M., 2003, 1-Methylcyclopropene: A Review, *Postharv. Biol. Technol*. **28**:1–25.

Buta, G., and Moline H.E., 1998, Methyl Jasmonate Extends Shelf Life and Reduces Microbial Contamination of Fresh-Cut Celery and Peppers, *J. Agric. Food Chem*. **46**:1253–1256.

Calderón-López, B., Bartsch, B.J.A., Lee, C.Y., and Watkins C.B., 2005, Cultivar Effects on Quality of Fresh Cut Apple Slices from 1-Methylcyclopropene (1-MCP)-Treated Apple Fruit, *J. Food Sci*. **70**:221–227.

Cantos, E., Spin, J.C., and Tomas-Barberan F.A., 2001, Postharvest Induction Modeling Method Using UV Irradiation Pulses for Obtaining Resveratrol Enriched Table Grapes: A New Functional Fruit, *J. Agric. Food Chem*. **49**:5052–5058.

Cha, D.S., and Chinnan M., 2004, Biopolymer-Based Antimicrobial Packaging: A Review, *Crit. Rev. Food Sci. Nutr*. **44**:223–237.

Costa, L., Vicente, A.R., Civello, P.M., Chaves, A.R., and Martínez G.A., 2006, UV-C Treatment Delays Postharvest Senescence in Broccoli Florets, *Postharvest Biol. Technol*. **39**:204–210.

Creelman, R.A., and Muller J.E., 1995, Jasmonic Acid Distribution and Action in Plants: Regulation During Development and Response to Biotic and Abiotic Stress. *Proc. National Acad. Sci. USA*. **44**:569–4114–4119.

Del-Valle, V., Hernández-Muñoz, P., Guarda, A. and Galotto M.J., 2005, Development of a Cactus-Mucilage Edible Coating (*Opuntia Ficus Indica*) and Its Applications to Extend Strawberry Shelf-Life, *Food Chem*. **91**:751–756.

D'Hallewin, G., Schirra, M., Manueddu, E., Piga, A., and Ben-Yehoshua S., 1999, Scoparone and Scopoletin Accumulation and Ultraviolet-C Induced Resistance to Postharvest Decay in Oranges as Influenced by Harvest Date, *J. Am. Soc. Hort. Sci*. **124**:702–707.

Dong, H., Cheng, L., Tan, J., Zheng, K., and Jiang Y., 2004, Effect of Quitosan Coating on Quality aand Shelf-Life of Peeled Litchi Fruit, *J. Food Eng*. **64**:355–358.

Durango, A.M., Soares, N.F.F., and Andrade N.J., 2006, Micribiological Evaluation of an Edible Coating on Minimally Processed Carrots, *Food Control*. **17**:336–341.

Feliciano, A., Feliciano, J., Vendruscuolo, J., Adaskaveg, J.E., and Ogawa J.M., 1992, Efficacy of Ethanol in Postharvest Benomyl-DCNA Treatments for Control of Brown Rot of Peach, *Plant Dis*. **76**:226–229.

Fenwick, G.R., Johnson, I.T. and Hedley C.I., 1990, Toxicity of Disease Resistant Plants Strains, *Trends Food Sci. Technol*. t. 23, pp. 23–25.

Fernández M., 2000, Review: Active Packaging, *Food Sci. Technol*. **6**(2):97–108.

Fries N., 1973, Effect of Volatile Organic Compounds on the Growth and Development of Fungi, *Trans. Brit. Mycol. Soc*. **60**:1–21.

González-Aguilar, G.A, Wang, C.Y., Buta, J.G., and Krizek D.T., 2001a. Use of UV-C Irradiation to Prevent Decay and Maintain Postharvest Quality of Ripe "Tommy Atkins" Mangoes, *Inter. J. Food Sci. Technol*. **36**(7):767.

González-Aguilar, G.A., Buta, J.G., and Wang C.Y., 2001b, Methyl Jasmonate Reduces Chilling Injury Symptoms and Enhances Color Development of "Kent" Mangoes, *J. Sci. Food Agric*. **81**:1244–1249.

González-Aguilar, G.A., Wang, C.Y., and Buta J.G., 2003, Methyl Jasmonate and Modified Atmosphere Packaging (MAP) Reduce Decay and Maintain Postharvest Quality of Papaya "Sunrise," *Postharv. Biol. Technol*. **28**:361–370.

González-Aguilar, G.A., Wang, C.Y., and Buta J.G., 2004a, UV-C Irradiation Prevents Breakdown and Chilling Injury of Peaches During Cold Storage, *J. Sci. Food Agric*. **84**(5):415–422.

González-Aguilar, G.A., Tiznado-Hernández, M.E., Zavaleta-Gatica, R., and Martínez-Téllez M.A., 2004b, Methyl Jasmonate Treatments Reduces Chilling Injury and Activates the Defense Response of Guava Fruits, *Biochem. Biophys*, *Res. Comm*. **313**:704–711.

González-Aguilar, G.A., Tiznado-Hernández, M., and Wang C.Y., 2006, Physiological and Biochemical Response of Horticultural Crops to Methyl Jasmonate, *Stewart Postharv. Rev*. **1**:1–9.

Gorris, L.G.M., and Smid E.J., 1995, Crop Protection Using Natural Antifungal Compounds, *Pestic. Outlook*. **6**:20–24.

Guerrero-Beltrán, J.A., and Barbosa-Cánovas G.V., 2004, Review: Advantages and limitations on Processing Foods by UV Light, *Food Sci. Technol. Int*. **10**(3):137–147.

Gunes, G., Watkins, C.B., and Hotchkiss J.H., 2000, Effects of Irradiation on Respiration and Ethylene Production of Apple Slices, *J. Sci. Food Agric*. **80**:1169–1175.

Han, C., Zhao, Y., Leonard, S.W., and Traber M.G., 2004, Edible Coatings to Improve Storability And Enhance Nutritional Value of Fresh and Frozen Strawberries and Raspberries, *Postharvest Biol. Technol*. **33**:67–78.

Hicks, K., Haines, R.M., Tong, C.B.S., Sapers, G.M., El-Atawy, Y., Irwin, P., and Seib P.A., 1996, Inhibition of Enzymatic Browning in Fresh Fruit and Vegetable Juices by Soluble and Insoluble Forms of β-ciclodextrin Alone or in Combination with Phosphates, *J. Agric. Food Chem*. **44**(9):2591–2594.

Jeong, J., Brecht, J.K., Huber, D.J., and Sargent S.A., 2004, 1-Methylcyclopropene (1-MCP) for Maintaining Textural Quality of Fresh-Cut Tomato, *Amer. Soc. Hort. Sci*. **39**:1359–1362.

Jiang, Y., and Li Y., 2001, Effects of Chitosan on Postharvest Life and Quality of Longan Fruit, *Food Chem*. **73**:139–143.

Jiang, Y.M., and Joyce D.C., 2002, 1-Methylyclopropene Treatment Effects on Intact and Fresh-Cut Apple, *J. Hortic. Sci. Biotechnol*. **77**:19–21.

Kalathenos, P., and Russell N.J., 2003, Ethanol as Food Preservative, in: *Food Preservatives*, N.J., Russell, and G.H., Gould, (eds), Springer, New Delhi, pp. 386.

Karabulut, O.A., Arslan, U., and Kuruoglu G., 2004, Control of Postharvest Diseases of Organically Grown Strawberry with Grapes Preharvest Applications of Some Food Additives and Postharvest Hot Water Dips, *J. Phytopathol*. **152**:224–228.

Kays S.J., 1991, *Postharvest Physiology of Perishable Plant Products*, Van Nostrand Reinhold, New York.

Lamikanra, O., Richard, O.A., and Parker A., 2002, Ultraviolet Induced Stress Response in Fresh-Cut Cantaloupe, *Phytochemistry*. **60**:27–32.

Lamikanra, O., and Richard O.A., 2004, Storage and Ultraviolet-Induced Tissue Stress Affects on Fresh-Cut Pineapple, *J. Sci. Food Agric*. **84**:1812–1816.

Lanciotti, R., Gianotti, A., Patrignani, F., Belletti, N., Guerzoni, M.E., and Gardini F., 2004, Use of Natural Aroma Compounds to Improve Shelf-Life and Safety of Minimally Processed Fruits, *Food Sci. Technol*. **15**:201–208.

Laurie S., 2005, Application of 1-Methylcyclopropene to Prevent Spoilage, *Stewart Postharv. Rev*. **1**(4):doi:10.2212/spr.2005.4.2

Lee, J.Y., Park, H.J., Lee, C.Y., and Choi W.Y., 2003, Extending Shelf-Life of Minimally Processed Apples with Edible Coatings and Antibrowning Agents, *Lebensm.- Wiss. U.-Technol*. **36**:323–329.

Li, H., and Yu T., 2000, Effect of Chitosan on Incidence of Brown Rot, Quality and Physiological Attributes of Postharvest Peach Fruit, *J. Sci. Food Agric*. **81**:269–274.

Lichter, A., Zutkhy, Y., and Sonego L., 2002, Ethanol Controls Postharvest Decay of Table Grapes, *Postharv. Biol. Technol*. **24**:301–308.

Linton, C.J., and Wright S.J.L., 1993, Volatile Organic Compounds: Microbiological Aspects and Some Technological Implications, *J. Appl. Bacteriol*. **75**:1–2.

Maftoonazad, N., and Ramaswamy H.S., 2005, Postharvest Shelf-Life Extension of Avocados Using Methyl Cellulose-Based Coatings, *Lebensm.- Wiss. U.-Technol*. **38**:617–624.

Mali, S., and Grossmann M.V.E., 2003, Effects of Yam Starch on Storability and Quality of Fresh Strawberry, *J. Agric. Food Chem*. **21**:7005–7011.

Marquenie, D., Michiels, C.W., Geeraerd, A.H., Schenk, A., Soontjens, C., Van Impe, J.F., and Nicolaí B.M., 2002, Using Survival Analysis to Investigate the Effect Of UV-C and Heat Treatment on Storage Rot of Strawberry and Sweet Cherry, *Int. J. Food Microbiol*. **73**:187–196.

Marquenie, D., Michiels, C.W., Van Impe, J.F., Schrevens, E., and Nicolaí B.N., 2003, Pulsed White Light in Combination with UV-C and Heat to Reduce Storage Rot of Strawberry, *Postharv. Biol. Technol*. **28**:455–461.

McHugh, T.H., and Senesi E., 2000, Apple Wraps: A Novel Method to Improve the Quality and Extend the Shelf Life of Fresh-Cut Apples, *J. Food Sci*. **65**(3):480–485.

Meir, S., Droby, S., Davidson, H., Alsevia, S., Cohen, L., Horev, B. and Philosoph-Hadas S., 1998, Suppression of *Botrytis* Rot in Cut Rose Flowers by Postharvest Application of Methyl Jasmonate, *Postharv. Biol. Technol*. **13**:235–243.

Mercier, J., Baka, M., Reddy, B., Corcuff, R., and Arul J., 2001, Shortwave Ultraviolet Irradiation for Control of Decay Caused by *Botrytis Cinerea* in Bell Pepper: Induced Resistance and Germicidal Effects, *J. Am. Soc. Hort. Sci*. **126**:128–133.

Moldao-Martins, M., Beirao-da-Costa, S.M., and Beirao-da-Costa M.L., 2003, The Effects of Edible Coatings on Postharvest Quality of the "Bravo de Esmolde" Apple, *Eur. Food Res. Technol*. **217**:325–328.

Pan, J., Vicente, A.R., Martínez, G.A., Chaves, A.R., and Civello P.M., 2004, Combined Use of UV-C Irradiation and Heat Treatments to Improve Postharvest Life of Strawberry, *J. Sci. Food Agric*. **84**:1831–1838.

Pérez-Gago, M.B., Rojas, C., and Del Río M.A., 2003, Effect of Hydroxypropyl Methylcellulose-Lipid Edible Composite Coatings on Plum Quality During Storage, *J. Food Sci*. **68**:879–883.

Plotto, A., Bai, J., Narciso, J.A., Brecht, J.K., and Baldwin E.A., 2006, Ethanol Vapor Prior to Processing Extends Fresh-Cut Mango Storage by Decreasing Spoilage, but Does Not Always Delay Ripening, *Postharv. Biol. Technol*. **39**:134–145.

Salcini, M.C., and Massantini R., 2005, Minimally Processed Fruits: An Update on Browning Control, *Stewar Postharv. Rev*. **1**(3):1–7.

Sembder, G., and Parthier B., 1993, The Biochemistry and the Physiological and Molecular Actions of Jasmonates, Annual Review, *Plant Physiol. Plant Molec. Biol*. **44**:569–589.

Sholberg, P.L., and Gaunce A.P., 1995, Fumigation of Fruit with Acetic Acid to Prevent Post Harvest Decay, *Hort. Sci*. **30**(6):1271–1275.

Sisler, E.C., and Serek M., 1997, Inhibitors of Ethylene Response in Lants at the Receptor Level: Recent Developments, *Physiol. Plantar*. **100**:577–582.

Suppakul, P., Miltz, J., Sonneveld, K., and Bigger S.W., 2003, Active Packaging Technologies with an Emphasis on Antimicrobial Packaging and Its Applications, *J. Food Sci*. **68**(2):408–420.

Valverde, J.M., Valero, D., Martínez-Romero, D., Guillén, F., Castillo, S., and Serrano M., 2005, Novel Edible Coating Based on *Aloe Vera* Gel to Maintain Table Grape Quality and Safety, *J. Agric. Food Chem*. **53**(20):7807–7813.

Vermeiren, L., Devlieghere, F., and Debvere J., 2002, Effectiveness of Some Recent Antimicrobial Packaging Concepts, *Food Add. Contamin*. **19**(Suppl.):163–171.

Vicente, A., Repice, B., Martíinez, G., Chaves, A., Civello, M., and Sozzi G., 2004, Maintenance of Fresh Boysenberry Fruit Quality with UV-C Light and Heat Treatments Combined with Low Storage Temperature, *J. Hortic. Sci. Biotech*. **79**:246–251.

Vicente, A.R., Civello, P.M., Martínez, G.A., Powell, A.L.T., Labavitch, J.M., and Chaves A.R., 2005a, Control of Postharvest Spoilage in Soft Fruit, *Stewart Postharv. Rev*. **1**(4):1–11.

Vicente, A.R., Pineda, C., Lemoine, L., Civello, P.M., Martíinez, G.A., and Chaves A.R., 2005b, UV-C Treatments Reduce Decay, Keep Quality and Alleviate Chilling Injury in Pepper, *Postharv. Biol. Technol*. **35**:69–78.

Vilas-Boas, E.V., and Kader A.A., 2001, Effect of 1-MCP on Fresh-Cut Fruits, *Perishables Handling Q*. **108:**25.

Wang, C.Y., and Buta J., 2003, Maintaining Quality of Fresh-Cut Kiwifruit with Volatile Compounds, *Postharv. Biol. Technol*. **28**:181–186.

Wessling, C., Nielsen, T., and Giacin J.R., 2000, Antioxidant Ability of BHT- and α-Tocopherol Impregnated LDPE Film in Packaging of Oatmeal, *J. Sci. Food Agric*. **81**:194–201.

Wills, R.B.H., McGlasson, B., Graham, D., and Joyce D., 1998, *Postharvest. An Introduction to the Physiology and Handling of Fruit, Vegetables and Ornamentals*, 4th ed. The University of New South Wales Press Ltd., Sydney, p. 262.

Wilson, C.L., and Winieski M.E., 1989, Biological Control of Postharvest Diseases of Fruits and Vegetables: An Emerging Technology. Annual Review. *Phytopathol*. **27**:425–441.

Wright, J.R., Sumner, S.S., Hackney, C.R., Pierson, M.D., and Zoecklein B.W., 2000, Efficacy of Ultraviolet Light for Reducing Escherichia Coli O157:H7 in Unpasteurized Apple Cider, *J. Food Protec*. **63**(5):563–567.

Yam, K.L., Takhistov, P.T., and Miltz J., 2005, Intelligent Packaging: Concepts and Applications, *J. Food Sci*. **70**(1):R1–R10.

Yaman, O., and Bayindirh L., 2002, Effects of an Edible Coating and Cold Storage on Shelf-Life and Quality of Cherries, *Lebensm.- Wiss. U.-Technol*. **35**:146–150.

Yaun, B.R., Sumner, S.S., Eifert, J.D., and Marcy J.E., 2004, Inhibition of Pathogens on Fresh Produce by Ultraviolet Energy, *Int. J. Food Microbiol*. **90**:1–8.

7
Advanced Food Products & Process Engineering (SAFES) I: Concepts & Methodology

P. Fito, M. Le Maguer, N. Betoret, and P.J. Fito

"In a complete theory there is an element corresponding to each element of reality."

(Einstein, 1935)

Nomenclature

Latin symbols

a_i	Activity of i-component	(dimensionless)
E	Internal Energy	(J)
E_i	Molar Internal Energy	(J/mol of i)
G	Gibbs' Free Energy	(J)
$\bar{G}_i$	Molar Gibbs' Free Energy for i component	(J/mol of i)
$\bar{G}_{i,j}$	Molar Gibbs' Free Energy for component i in the j phase	(J/mol of i)
H	Enthalpy	(J)
h_i	Molar Enthalpy	(J/mol of i)
J_i	Mass Flux of i-component	(Mol of i/ s m^2)
L_i	Phenomenological Coefficient for i-component flux	(Mol of i/s m^2 $\Delta\mu_i$)
$M_{n,\,n}$	Descriptive matrix of product flowing out of the stage of change n considering the overall mass in the system equal to $m_n/m_n = 1$	
$M_{n,\,n-1}$	Descriptive matrix of product flowing out of the stage of change n referred to the strain n−1 (considering the overall mass in the system equal to $m_n/m_{n-1} \neq 1$)	
$MC_{n-1,n}$	Matrix of changes produced when the strain m_{n-1} passes through the stage of change n	
MP_N	Descriptive matrix of one process with N stages of change	
m_n	Mass flux corresponding to strain n	(kg/s)
Δm_n	Mass gain in the Stage of Change n	(kg/s)
n	Number of moles	(dimensionless)

n_i	Number of moles of i-component	(dimensionless)
P	Pressure	(Pascal; N/m^2)
p_i	Partial pressure of i-component in a gas	(Pascal; N/m^2)
R	Universal gases constant	(N m/mol K)
P°_i	Vapour pressure of i-component	(Pascal; N/m^2)
S	Entropy	(J/K)
s_i	Molar Entropy	(J/ K mol of i)
T	Temperature	(K)
t	Time	(s)
V	Volume	(m^3)
v_i	Partial Molar Volume of i-component	(m^3/mol of i)
X_i	Molar fraction of component i	(mol of i / total mol)
x_i	Mass fraction of component I	(kg of i/ total kg)

Greek symbols

μ_i	Chemical potential of i-component	(J/mol of i)
μ_i^{ext}	Extended Chemical potential of i-component	(J/mol of i)
$\mu_i^{ext,0}$	Extended Chemical potential of i-component at reference conditions	(J/mol of i)
$\varphi_i = p_i / P^\circ_i$	(relative concentration of component i in a gas mixture referred to saturation; $0 \le \varphi_i \le 1$)	(dimensionless)
γ_i	Activity coefficient of component i	(dimensionless)
σ	Surface tension	(N/m)
ρ	Density	(kg/m^3)

Subscripts

i	some property referred to i-component
w	some property referred to water
s	some property referred to solutes

Superscripts

o	refer to some condition where the value of the function is supposed arbitrarily equal to zero

7.1. Introduction

Food quality and safety are the main concerns of consumers and the principal target of Food Industry processes. The concept of "food process engineering for product quality" has arisen in recent years with the aim of designing and controlling processes to produce food products with very specific properties of quality and safety, previously defined on the basis of market opportunities analysis (ETP, 2006).

The final properties of food products are the result of the changes produced in raw materials as a consequence of process treatments (Aguilera and Stanley,

1999). These changes may be observed as differences in quality factors, such as food composition, nutritional facts, taste and flavor, aspect, shape and size, colour, texture, etc. (Aguilera et al., 2003a, b). In the case of colloidal or cellular foods, these changes in food properties may be explained as the result of physical and chemical phenomena produced in line with the process progression such as structure deformations and relaxations (shrinking and swelling), chemical or enzymatic reactions, phase transitions, mass and energy transport phenomena, etc. (Aguilera and Baffico, 1997; Barat et al., 2001).

The models currently used in food process engineering usually oversimplify both the food system description and the mechanisms and rate equations of changes. Typically, the food system is supposed to be isotropous, homogeneous and continuous, with only two or three components, distributed in one or two phases (Crank, 1985). In this approach, thermodynamic and kinetic equations deduced for ideal gas or liquids in conditions close to equilibrium are applied to model food with colloidal or cellular structures and, of course, in conditions far away from the equilibrium (Bird et al., 2002). The typical approach used to model food drying operations is a good example of this methodology. Frequently, the models obtained in this way cannot accurately predict the changes in the food properties through the industrial processes when the range of values for the industrial process variables is different from those used in the experiments. In this sense, it is remarkable how scattered reported values in the literature for the experimental effective diffusivities are (Martínez et al., 1998).

Based on this remark, it is necessary to develop advanced concepts and methodologies in food process engineering (Marcotte and Le Maguer, 1991; Zhiming and Le Maguer, 1996). The new models for food and processes development must incorporate enough information about all of these aspects (thermodynamic, structural, chemical and biochemical, and even mechanics). Only in this way would they be able to calculate and predict the real changes in the quality of food product in line with the process pro-gression. The SAFES methodology (Systematic Approach to Food Engineering Systems) recognizes the complexity of the food system and allows coordination of information about food structure (Aguilera, 2006), composition, thermodynamics, etc., with adequate tools to develop real food and processes.

7.2. Food Product Engineering: Modelling of Food and Biological Systems

7.2.1. Structure of Food System: The Structure-Properties Ensemble

The food system is described as a volume of a universe full of matter and energy. The structure reflects the way in which matter and energy organize themselves inside the system volume. Some levels of complexity in matter condensation inside the system may be observed in Table 7.1 (in order of increasing complexity).

TABLE 7.1. Some levels of complexity in matter condensation

Level of complexity	Name of the structure	Structural features	Branch of science
Sub-atomic	Elemental particles	Subatomic particles	Physics
Atomic	Atomic structure	Nucleus and Electrons	Physics
Molecular	Molecular structure	Covalent or ionic bonds; ions	Chemistry
Polymeric	Macromolecular structure	Tertiary and quaternary structures	Science of polymers; Proteomics; Genomics
Colloidal	Colloidal structure	Colloids (suspensions, emulsions, foams, gels)	Colloids science
Cellular	Cellular structure	Cells	Cellular biology
Multi-cellular plants and animals	Live plants & animals	Tissues, organs, individuals	Biology

These levels of complexity in the structure of condensed soft matter are the results of the universe evolution. Each new level of complexity incorporates an improved level of functionality and results from the rearrangement of the previous, less complex structures. In this way, more complexity implies new and more powerful functionality. In the same way, the system functionality is appreciated by an observer as the system properties (ETP, 2006). As a consequence, complexity refers to level of structure as well as functionality refers to the system properties. Therefore, the concept of complexity-functionality is equivalent to those of structure-properties. The structure-properties ensemble refers to the knowledge of structure and properties in a system, as well as the understanding of the relationships existing between the two concepts and, of course, the capability to predict the changes in food properties produced when any change in food structure occurs (Aguilera et al., 2003a).

7.2.2. The SAFES Simplified Space of the Structured Phases and Components: Components, Structured Phases and Aggregation States.

In the food system observed in Fig. 7.1, a foam structure with a phase of gas bubbles dispersed in an emulsion (oil-water) containing fat granules and an aqueous solution as continuous phase may be observed. The description of such a complex product, as well as the analysis of its properties and changes throughout any process, implies the recognition of the phases that play some role in the product behavior. As a first approach, it would be convenient to include the following simplified "structured phases": gas, insoluble dispersed solids, liquid fat, solid fat and aqueous solution. The aggregation states, depending on temperature and concentration, may be solid, adsorbed, vitreous, rubbery, liquid and gas. Additionally, some characteristic dimensions of the different structural features must be included, e.g., the average diameter (or even diameter distribution) of gas bubbles and fat globules. Table 7.2 summarizes the elements included in the 3-dimension space.

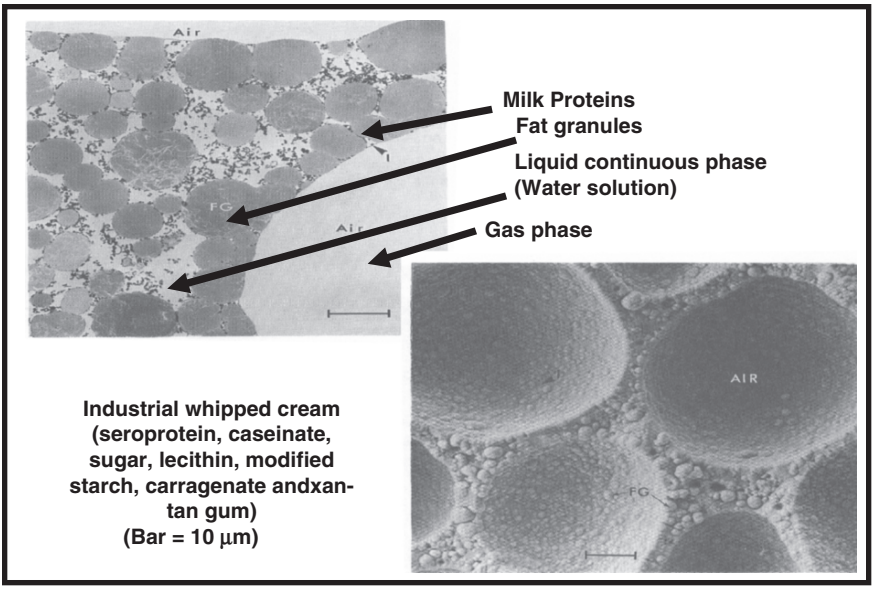

FIG. 7.1. Sample of an industrial whipped cream observed by Cryo-SEM (Right) and TEM (Left)

TABLE 7.2. Elements included in the 3-dimension (i, j, k) simplified space describing an industrial whipped cream

Components (i)	Structured Phases (j)	Aggregation State (k)
Water	Gas	Solid
Fat	Insoluble dispersed solids	Adsorbed
Air	Liquid fat	Vitreous
Seroprotein	Solid fat	Rubbery
Caseinate	Aqueous liquid solution	Liquid
Sucrose		Gas
Lecithin		
Modified Starch		
Carragenate		
Xantan gum		

B. - Figure 7.2 shows a magnification of parenchyma of apple *Granny Smith* observed by Cryo-SEM (Fito et al., 2001). Several cells may be observed (diameter ranging from 200 to 300 μm) showing their cell wall, cell membrane and medium lamella. All of these elements are insoluble in water and may be simplified as a *food insoluble matrix*. Inside the broken cells, a simplified *internal liquid phase* may be observed. Also, several intercellular spaces are filled both with some *extracellular liquid phase* and/or with a *gas phase*. In some cases (if the product will be air dried), a *solid solutes phase* may appear when the liquid phases in the food became saturated. Table 7.3 shows the different elements included in

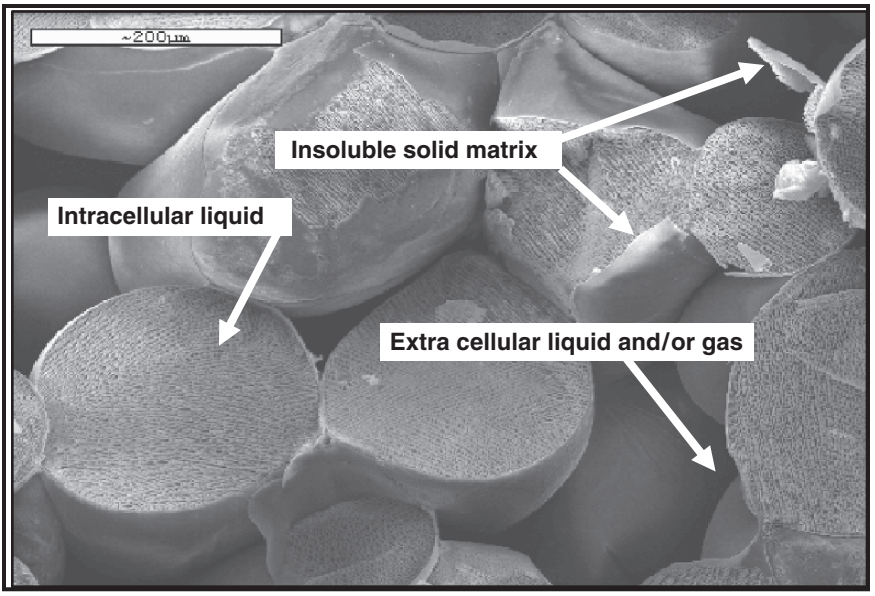

FIG. 7.2. Parenchyma tissue of apple *"Granny Smith"* observed by Cryo-SEM

TABLE 7.3. Elements included in the 3-dimensional simplified space (i,j,k) describing the parenchyma of apple *Granny Smith*

Components (i)	Structured Phases (j)	Aggregation State (k)
Water	Gas	Solid
Native solutes	Solid matrix	Adsorbed
Solid matrix	Intracellular liquid	Vitreous
Added solutes	Extracellular liquid	Rubbery
Gas	Solid solutes	Liquid
		Gas

the 3-dimensional simplified space of the structured phases and components. Additionally, the cell membrane is semi-permeable, allowing only water transport by osmotic mechanisms (Barat et al., 2001). Structural features may include the average diameters of cells and intercellular spaces, cell wall thickness, etc.

C. - Figure 7.3 shows a magnification of a typical salted dried meat, which is called "*tasajo*" in some countries of Latin-America. Sodium chloride crystals produced because the internal liquid phase in the salted meat became saturated (a_w= 0.75 and 0,245 kg salt/kg solution) throughout the drying operation may be observed. From this point onward, any additional loss of water produces more NaCl crystallization. In Table 7.4, the different components, structured phases and aggregation states included in the simplified space of phases and components may be observed.

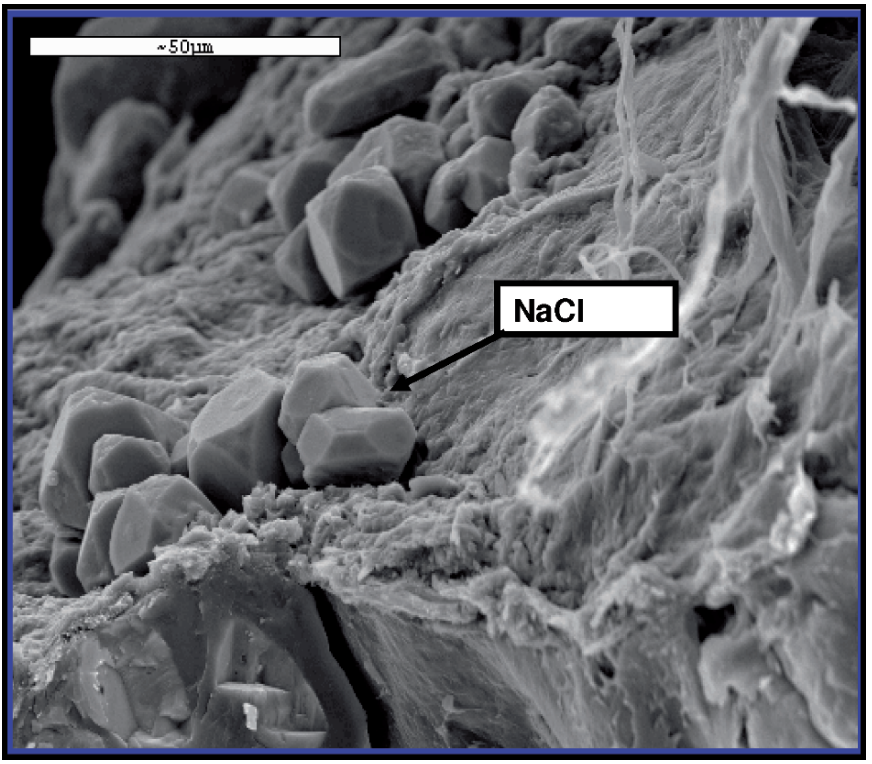

FIG. 7.3. Cryo-SEM observation of dried salted meat *tasajo*

TABLE 7.4. Elements included in the 3-dimensional simplified space (i,j,k) describing a typical salted dried meat

Components (i)	Structured Phases (j)	Aggregation State (k)
Water	Gas	Solid
Native solutes	Solid matrix	Adsorbed
Solid matrix	Intracellular liquid	Vitreous
NaCl	Extracellular liquid	Rubbery
Gas	Solid solutes (crystals)	Liquid
		Gas

D.- Figure 7.4 shows a Cryo-SEM observation of a cell of dried cassava. A typical feature in this product is the large amount of starch granules that may be observed inside the cell membrane. In such a product, an interesting question is the knowledge of the shared-out water between the starch granules and the liquid phase inside the cell. Different ways of sharing-out may result in different a_w values for the same water content due to the different isotherms for the liquid phase and for the solid matrix.

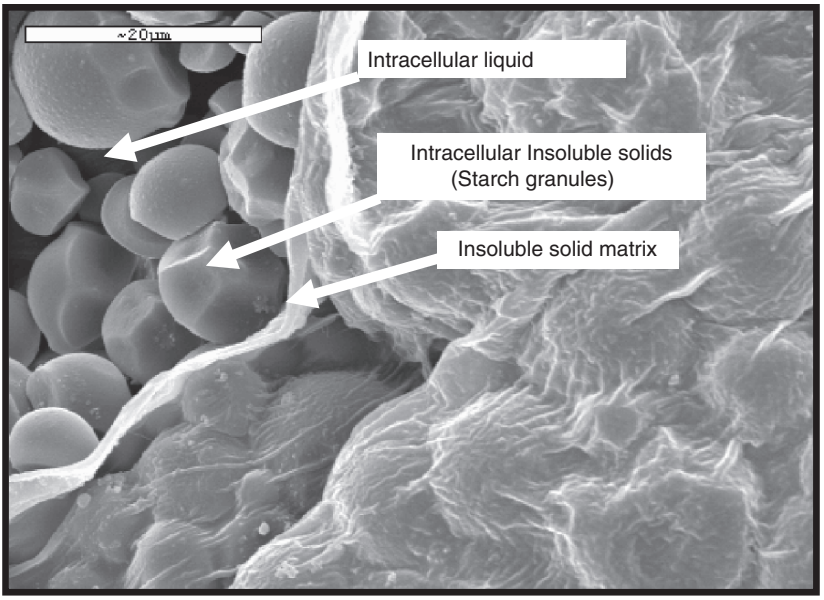

FIG. 7.4. Starch in cassava cells

7.2.3. The Descriptive Matrix: A Mathematical Tool to Describe the Food System. The State Variables: The Share-Out of Matter Among Components and Structured Phases

After defining the 3-dimensional space of phases and components (i, j, k), it is possible to include information about the state variables of the system in an ordered way. The state variables are P, T, V and the mass of any component in any phase and in any aggregation state. Usually, the chemical complexity of real food systems leads to the use of mass content (m) or mass fractions (x) instead number of moles (n). Then, the needed state variable information may be integrated as follows:

- The share-out of matter among phases, components and aggregation states (*the composition matrix*: $X^k_{i,j}$)
- The share-out of the system volume among phases (the *volume vector*: V_j)
- The value of P and T in the phases (the *Pressure and Temperature vectors*: P_j and T_j)

Then, the Descriptive Matrix of the product will be, provisionally:

$$M\,(x^k_{i,j};V_j;P_j;T_j) \tag{7.1}$$

The composition matrix $X^k_{i,j}$ may be represented as shown in Fig. 7.5. The components, phases and aggregation states are located on the three axes (i, j, k),

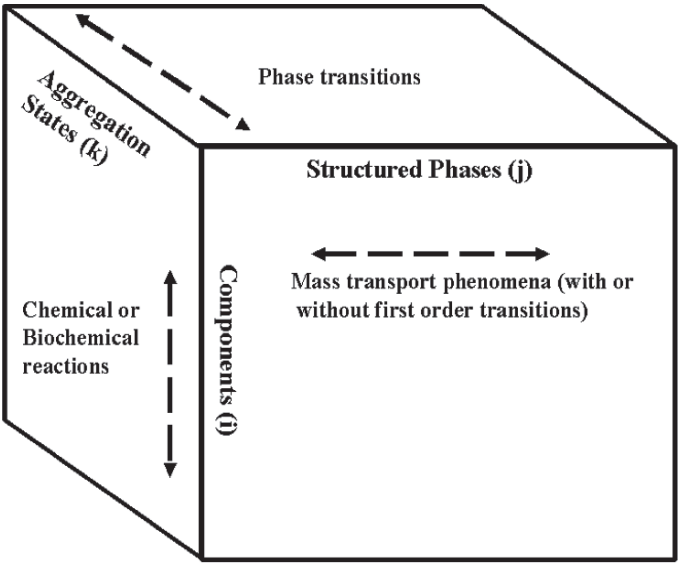

FIG. 7.5. Composition Matrix of Food System

TABLE 7.5. Elements included in the 3-dimensional simplified space (i,j,k) describing a typical salted dried meat

Components (i)	Structured Phases (j)	Aggregation State (k)
Water	Gas	Solid
Solutes	Solid matrix	Adsorbed
Solid matrix	Intracellular liquid	Vitreous
Starch	Extracellular liquid	Rubbery
Gas	Starch granules	Liquid
		Gas

respectively. In this arrangement, the dotted arrows show the possible changes in local values of X^k_{ij} produced by mass transport, phase transitions and /or chemical reactions inside the system.

Additionally, it is also possible to show the 3-dimensional data in a plane. In this way, the values of aggregation states (k) of each component are included in the plane (i,j), as described in Fig. 7.6. Now it is possible to show together both the composition matrix and the PVT vectors in a unified matrix: the *Descriptive Matrix*.

Some properties of the Descriptive Matrix are:

- The value $\sum_i \sum_j \sum_k x^k_{i,j} = m$ where m is the overall mass of the system:

  When m=1; values in $X^k_{i,j}$ are mass fractions (concentrations)
  When m≠1; values in $X^k_{i,j}$ are just the value of the mass of component i in phase j and in an aggregation state k.

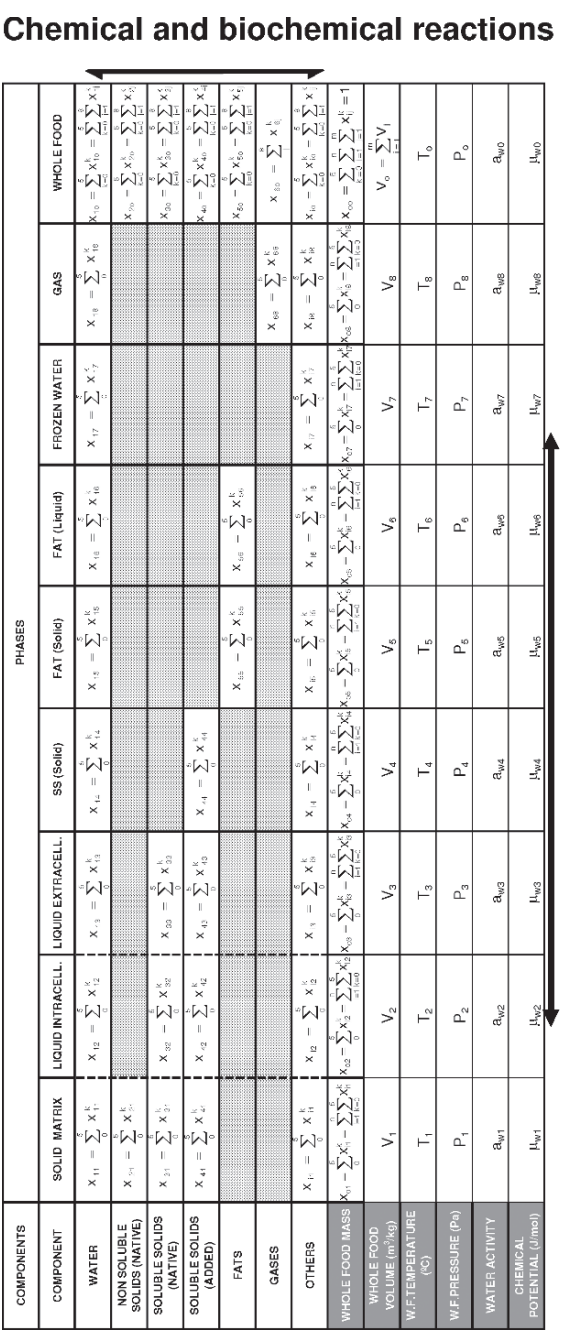

FIG. 7.6. Descriptive Matrix of Food System developed on a plane

- The ratio $\frac{V_j}{\sum_i \sum_k x_{i,j}^k}$ is the specific volume of phase j.

- The ratio $\frac{\sum_i \sum_j \sum_k x_{i,j}^k}{\sum_j V_j} = \rho$ is the food system average density.

- $\sum_j V_j$ is the volume of food system when m≠1

- $\sum_j V_j$ is the average specific volume of food system when m=1.

7.2.4. *Mass and Volume Balances Inside the Product*

- Mass Balance for each component: Vector of mass shared-out for each component among the phases. For the component 1:

$$x_{i=1} = \sum_k \sum_j x_{1j}^k \tag{7.2}$$

Mass Balance for each phase: Vector of overall mass shared-out among phases (last row of the concentration matrix). For phase 1:

$$x_{j=1} = \sum_k \sum_i x_{i1}^k \tag{7.3}$$

- Overall mass balance

$$x = \sum_i \sum_j \sum_k x_{ij}^k = 1 \tag{7.4}$$

- Overall volume balance

$$V = \sum_j V_j \tag{7.5}$$

7.2.5. *Energy Inside the System: Gibbs Free Energy*

The thermodynamic analysis of the energy, the equilibrium and fluxes analysis in food systems is usually made in terms of Gibbs free energy (Nicolis and Prigogine, 1977a,b).

For a closed system:

$$G = H - TS = E + PV - TS \tag{7.6}$$

and so:

$$dG = dH - TdS - SdT = VdP - SdT \tag{7.7}$$

In the food system the state variables have been included in the Descriptive Matrix as follows:

$$M(x^{k}_{i,j}, V_j, P_j, T_j) \tag{7.8}$$

But, we may change the units to describe the mass share-out in the system using moles instead kg, and then Eq. (7.8) becomes:

$$M(n^{k}_{i,j}, V_j, P_j, T_j) \tag{7.9}$$

Functions 7.8 and 7.9 are completely equivalent, depending only on the units used to define the mass in the system. Then, in any phase j of the system, it may be assumed that:

$$G_j = G_j\left(T_j, P_j, n^{k}_{i,j}\right) \tag{7.10}$$

It is supposed that the function G_j represents the total free energy in phase j, including those corresponding to the interactions of phase j with its interphases with its neighbor's phases. The function 7.10 allows the possibility that the values of G in the same phase would be different for one i-component at the different aggregation states k.

That means that there is a possibility of a non-equilibrium situation inside the same phase. This is possible only because we are working with simplified structured phases where sometimes we have included two or more real phases in the same simplified one. Anyway, if internal equilibrium in the phase is assumed, Eq. (7.10) simplifies as:

$$G_j = G_j\left(T_j, P_j, n_{i,j}\right) \tag{7.11}$$

Consequently, any differential change of G in the j-phase may be calculated by the equations:
From 7.10:

$$dG_j = \left(\frac{\partial G_j}{\partial T}\right)_{P_j, n^{k}_{i,j}} dT_j + \left(\frac{\partial G_j}{\partial P}\right)_{T_j, n^{k}_{i,j}} dP_j + \sum_i \sum_k \left(\frac{\partial G_j}{\partial n_{i,j}}\right)_{P_j, T_j, n \neq n^{k}_{i,j}} dn^{k}_{i,j} \tag{7.12}$$

From 7. 11:

$$dG_j = \left(\frac{\partial G_j}{\partial T}\right)_{P_j, ni, j} dT_j + \left(\frac{\partial G_j}{\partial P}\right)_{T_j, n_{i,j}} dP_j + \sum_i \left(\frac{\partial G_j}{\partial n_{i,j}}\right)_{P_i, T_{,}, n \neq n_{i,i}} dn_{i,j} \tag{7.13}$$

Obviously, for the whole food system, the change in the Gibbs free energy may be calculated by:

$$dG = \sum_j dG_j \tag{7.14}$$

Thus obtaining Eqs. (7.15) and (7.16), depending on the equilibrium situation inside the phases:

$$\mathrm{dG} = \sum_{\mathrm{j}} \left[\left(\frac{\partial \mathrm{G_j}}{\partial \mathrm{T}} \right)_{\mathrm{P_j}, \mathrm{n}^{\mathrm{k}}_{\mathrm{i,j}}} \mathrm{dT_j} \right] + \sum_{\mathrm{j}} \left[\left(\frac{\partial \mathrm{G_j}}{\partial \mathrm{P}} \right)_{\mathrm{T_j}, \mathrm{n}^{\mathrm{k}}_{\mathrm{i,j}}} \mathrm{dP_j} \right] + \sum_{\mathrm{i}} \sum_{\mathrm{j}} \sum_{\mathrm{k}} \left(\frac{\partial \mathrm{G_j}}{\partial \mathrm{n_{i,j}}} \right)_{\mathrm{P_j}, \mathrm{T_j}, \mathrm{n} \neq \mathrm{n}^{\mathrm{k}}_{\mathrm{i,j}}} \mathrm{dn}^{\mathrm{k}}_{\mathrm{i,j}} \tag{7.15}$$

$$dG = \sum_j \left[\left(\frac{\partial G_j}{\partial T} \right)_{P_j, ni, j} dT_j \right] + \sum_j \left[\left(\frac{\partial G_j}{\partial P} \right)_{T_j, n_{i,j}} dP_j \right] + \sum_i \sum_j \left(\frac{\partial G_j}{\partial n_{i,j}} \right)_{P_j, T_j, n \neq n_{i,j}} dn_{i,j} \tag{7.16}$$

Remembering the values of the first derivatives of the function G:

$$\left(\frac{\partial \mathrm{G}}{\partial \mathrm{P}} \right)_{\mathrm{T,\, n}} = \mathrm{V} \tag{7.17}$$

$$\left(\frac{\partial \mathrm{G}}{\partial \mathrm{T}} \right)_{\mathrm{P,n}} = -\mathrm{S} \tag{7.18}$$

$$\left(\frac{\partial \mathrm{G}}{\partial \mathrm{n_i}} \right)_{\mathrm{P,T,n} \neq \mathrm{n_i}} = \mu_{\mathrm{i}} \tag{7.19}$$

The Eqs. (7.12) and (7.13) became, respectively:

$$\mathrm{dG_j} = \mathrm{S_j dT_j} + \bar{\mathrm{V}}_{\mathrm{j}}\, \mathrm{dP_j} + \sum_{\mathrm{i}} \sum_{\mathrm{k}} \mu^{\mathrm{k}}_{\mathrm{i,j}}\, \mathrm{dn}^{\mathrm{k}}_{\mathrm{i,j}} \tag{7.20}$$

$$\mathrm{dG_j} = \mathrm{S_j dT_j} + \bar{\mathrm{V}}_{\mathrm{j}}\, \mathrm{dP_j} + \sum_{\mathrm{i}} \mu_{\mathrm{i,j}}\, \mathrm{dn_{i,j}} \tag{7.21}$$

We may use either Eq. (7.12) or (7.13) to calculate the Gibbs free energy in any j-phase, depending on the situation of internal equilibrium inside the phase. Both equations are different forms of representing the well known Gibbs-Duhem equation. In the same way, for the whole system, the two equations became, respectively:

$$\mathrm{dG} = \sum_{\mathrm{j}} \mathrm{dG_j} = \sum_{\mathrm{j}} \mathrm{S dT_j} + \sum_{\mathrm{j}} \bar{\mathrm{V}}\, \mathrm{dP_j} + \sum_{\mathrm{i}} \sum_{\mathrm{j}} \sum_{\mathrm{k}} \mu^{\mathrm{k}}_{\mathrm{i,j}}\, \mathrm{dn}^{\mathrm{k}}_{\mathrm{i,j}} \tag{7.22}$$

$$\mathrm{dG} = \sum_{\mathrm{j}} \mathrm{dG_j} = \sum_{\mathrm{j}} \mathrm{S dT_j} + \sum_{\mathrm{j}} \bar{\mathrm{V}}_{\mathrm{j}}\, \mathrm{dP_j} + \sum_{\mathrm{i}} \sum_{\mathrm{j}} \mu_{\mathrm{i,j}}\, \mathrm{dn_{i,j}} \tag{7.23}$$

Where the physical sense of $\mu_{i,j}$ (the chemical potential of i-component in j-phase) is the change in G_j produced by the loss (–) or gain (+) of one mol of one specific component i (J/mol) in conditions of P_j, T_j and $n_j \neq n_{i,j}$ constants. In conclusion, the value of G in the system is the sum of the values of G in every phase. It is very important to realize whether the phases are in internal equilibrium, and also if there are equilibrium among them. Obviously, a non-equilibrium situation, inside the phases or among them, implies the spontaneous appearance of internal transport of energy and/or mass.

7.2.5.1 Equilibrium and Driving Forces

The Gibbs energy defines the equilibrium and the events in the system.

Gradients of the intensive variables (T, P and μ^k_{ij}) represent driving forces responsible for fluxes of energy and/or matter (Fito and Pastor, 1994). Gradients of T usually result in heat transfer, while gradients of P result in deformations or/and bulk fluxes, depending on the viscoelastic properties of the system (Fito, 1994; Fito et al., 1996), whereas gradients of chemical potential produce mass transfer phenomena (Barat et al., 1998). Any change in the system that occurs at constant temperature (isothermal) and constant pressure (isobar) must result in a decrease in G if the process occurs naturally, or no change in G if the process is reversible. Taking into account Eqs. (7.20) and (7.21), we have the conditions for the equilibrium:

$$dG = 0;\ dT = 0;\ dP = 0 \text{ and } d\mu^k_{ij} = 0 \tag{7.24}$$

7.2.5.2 Transport Mechanisms and Rate equations.

The structure features in food may produce coupling of some of these transport phenomena (Gras et al., 2003). For instance, in cellular structures, the loss or gain of water by any individual cell is always coupled with deformations and relaxation phenomena in the insoluble matrix (cellular wall and membrane), promoting the use of an extended definition of chemical potential (Seguí et al., 2006):

$$\mu_i^{ext} - \mu_i^{ext,0} = RT\ln a_i + \overline{V}_i (P - P_0) \tag{7.25}$$

In these cases, it is possible to calculate the changes of G due to couplings of pressure and activities gradients, as well as the contribution of the different gradients (pressure or activities) to the global change of energy (Martínez-Monzó et al., 1998). These situations are usual in drying (both air drying and osmotic dehydration) of colloidal or cellular foods. In drying, for instance, the water flux between two points (1 and 2) inside the food system may be calculated by the Eq. (7.19) (Wesseling and Krishna, 1990):

$$J_w = -L_w (\mu_{w1} - \mu_{w2}) = -RT (\ln a_{w1} - \ln a_{w2}) \tag{7.26}$$

In this equation, the driving force is $(\ln a_{w1} - \ln a_{w2})$ and may be simplified as:

$$(1na_{w1} - 1na_{w2}) \cong x_{w1} - x_{w2} \tag{7.27}$$

only if and when the requirements below can be accepted as true:

- The activity coefficient (γ_w) for water is close to one:

$$a_w = \gamma_w x_w \approx x_w \tag{7.28}$$

- The values of a_{w1} and a_{w2} are very close (the system is close to equilibrium):

$$a_{w1} \approx a_{w2} \tag{7.29}$$

Only in this way does Eq. (7.26) become similar to the well known Fick equation, and the two conditions mentioned above determine the conditions for its use in a rigorous way.

When applying Eq. (7.26) to a system where the points 1 and 2 are separated by a membrane (which allows water to flow across it, but not to the solutes), it is necessary to use the extended definition of chemical potential (Eq. 7.25). In this case, Eq. (7.26) becomes:

$$J_w = -L_w(\mu_{w1}^{ext} - \mu_{w2}^{ext}) = -RT\left(\ln a_{w1} - \ln a_{w2}\right) - \bar{V}_w\left(P_1 - P_2\right. \tag{7.30}$$

The two terms on the right side of Eq. (7.30) allow us to understand how the mass transport may be driven by mechanical energy, even against the activities gradients (as is in the case of inverse osmosis) or, in other cases, chemical potentials gradients produce simultaneously mass transfer and mechanical deformations (as in cellular systems drying).

The definition of Descriptive Matrix may be defined as:

$$M\ (x_{i,j}^k; V_j; P_j; T_j; \mu_{i,j}^k) \tag{7.31}$$

If it is assumed that there are not gradients of P, T, μ_t inside any phase of the system, the Eq. (7.24) becomes:

$$M\ (x_{i,j}^k; V_j; P_j; T_j; \mu_{i,j}) \tag{7.32}$$

The equilibrium condition arises when grad P = 0; grad T=0; grad $\mu_{i,j}$=0, in any phase of the system.

Finally, the corresponding vectors $\mu_{i,j}$ applied to the components affected by mass transport phenomena may be included in the descriptive matrix (Gekas et al., 1998). In a situation with only water and solutes moving throughout the system, a complete Descriptive Matrix will result as follows:

$$M\ (x_{i,j}^k; V_j; P_j; T_j; \mu_{w,j}; \mu_{s,j}) \tag{7.33}$$

Where $\mu_{w,j}$ and $\mu_{s,j}$ are the chemical potential of water and solutes in all the phases of the system (where they may exist), respectively. In the case of air-drying or hydration, the simplification that only water may move inside the system may be considered. In this case, the Descriptive Matrix may be organized as:

$$M\ (x^{k}_{i,j};V_j;P_j;T_j;\ a_{w,j},\ \mu_{w,j}) \tag{7.34}$$

The two last lines in Fig. 7.6 have been occupied by the vectors $a_{w,j}$ and $\mu_{w,j}$.

7.3. Food Process Engineering: Modelling of Food Operations and Processes

We have introduced above the Descriptive Matrices (M) as a useful tool, both to describe food products by recognizing their structural features (physicochemical, thermodynamical and biological), and for explaining and understating their properties. In food processes, the food products suffer controlled changes that affect their structure and properties. The comparison between two Descriptive Matrices corresponding to products in two different points of a process permits one to identify when and where a change appears, as well as to analyze the mechanism(s) responsible for this change. This use of the properties of M in the analysis of food processes will be discussed in the following points.

7.3.1. Definition of Unit Operation and Stage of Change

The concept of Unit Operation came from the Chemical Engineering Processes Theory and some stages in a process where the product suffers one change in one physical or chemical property. Several unit operations constitute a process where the raw material becomes the desired final product throughout the successive changes. Very often in a real process, every unit operation is performed in a specific type of equipment (e.g., drying operation is performed in a drier). In this way, both concepts are frequently used (unit operation and the related equipment) as similar or even equivalents.

In Food Processes, the complexity of the food systems usually results in some different changes suffered by the food in the same equipment. Sometimes the major macroscopic change identified in the product (e.g., loss of water in drying) results from several important changes in the system (in the state variables, in the structure, etc.). Sometimes these changes occur, but in other cases, they are consecutive in time. Then it is convenient to introduce a new concept, *Stage of Change*, defined as one stage of the process where the product suffers a significant change only in its properties. According to this definition, one unit operation may refer to one or more Stages of Change, and the same applies to the specific equipment used to perform this operation. Some examples of phenomena that demand defining a Stage of Change may be:

- When a phase of the system disappears or a new one arises, as, for instance, when in drying operations, the loss of water by the product causes the disappearance of the food liquid phase, and only adsorbed water remains in the solid
- When a phase transition occurs because the physical and transport properties of the food changes, sometimes dramatically
- When the pattern of the mass and energy transport phenomena changes, e.g., change of the mechanisms responsible for these phenomena
- When the pattern of the chemical or microbiological reactions changes because of changes in temperature, pH, activation or inactivation of enzymes, etc.

In conclusion, one process will be represented as a series of stages of change in order to analyze the changes undergone by the product after any one of those changes.

7.3.2. Mass Balances and Transformed Matrices: Matrix of Changes

Considering one process with N Stages of Change and N+1 different products flowing in the N+1strains (being m_0 the raw material and m_N the final product), it must be considered:

N Stages: $\{1,2,3,.....,n\text{-}1, n, n+1, ...,N\}$

N+1 Strains $\{m_0, m_1, ..., m_{n-1}, m_n, m_{n+1}, ..., m_N\}$

In Fig. 7.7 three Steps of Change of this process may be observed (n−1, n, n+1).

The subscripts of any matrix (vs. $M_{a,b}$) indicates: The first one (a) is the subscript of the corresponding strain, and the second one (b) indicates the strain of reference. Therefore, the value of the overall mass of the system is always fixed as:

$$x_a = \left[\sum_i \sum_j \sum_k x_{i,j}^k\right]_a = \frac{b}{a} \tag{7.35}$$

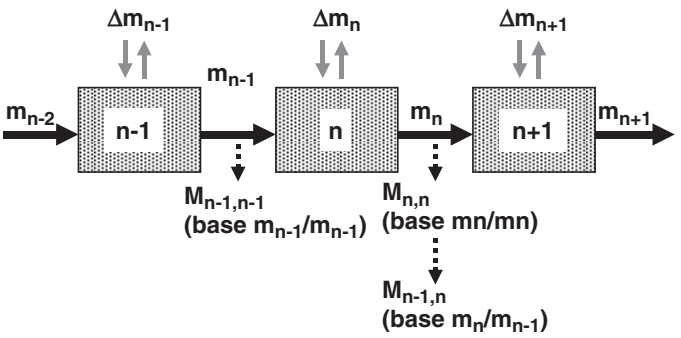

FIG. 7.7. Different Stages of Change

The overall mass balance for the n stage will be:

$$m_n - m_{n-1} = \Delta m_n \tag{7.36}$$

If the value of Δm_n is negative, it means a loss of matter by the system. As a consequence, the values of the ratio [b/a] would be 1 for any descriptive matrix, but to compare with any other, it is necessary to calculate one transformed matrix with different values for a and b.

As an example, for the Stage n may be defined:

The descriptive matrix for strain m_{n-1} $M_{n-1,\,n-1}$
The descriptive matrix for strain m_n $M_{n,\,n}$
The transformed matrix of strain m_n referred to the strain m_{n-1} $MC_{n,n-1}$

The Descriptive Matrices of products corresponding to these strains will be as follow:

$$x_{n,n} = \left[\sum_i \sum_j \sum_k x_{ij}^k\right]_{n,n} = \frac{m_n}{m_n} = 1 \tag{7.37}$$

$$x_{n\text{-}1,n\text{-}1} = \left[\sum_i \sum_j \sum_k x_{ij}^k\right]_{n.1,n-1} = \frac{m_{n\text{-}1}}{m_{n\text{-}1}} = 1 \tag{7.38}$$

where the overall mass distributed in the system has been arbitrarily considered as 1 kg. In this way, the physical meaning of x_{n-1} and $x_{n,n}$ would be the mass fraction of total mass corresponding to any component I in any phase j and in any aggregation state k. In order to compare the two mass distribution matrices in a balance Eq. (7.36) the values of $x_{n,n}$ must be transformed by multiplying by the ratio $m_{n-1}/m_n \neq 1$, defining:

$$x_{n,\,n\text{-}1} = \left[\sum_i \sum_j \sum_k x_{ij}^k\right]_{n,n-1} = \frac{m_{n\text{-}1}}{m_n} \neq 1 \tag{7.39}$$

We obtain the Transformed Mass Share-out matrix of strain m_n referred to those of the strain m_{n-1}:

$$\left[x_{i,j}^k\right]_{n,n-1} = \left(\frac{m_{n\text{-}1}}{m_n}\right)\left[x_{i,j}^k\right]_{n,\,n} \tag{7.40}$$

Therefore, the Descriptive Matrix and the Transformed Descriptive Matrix of the product flowing throughout the **n** stage of change of the process will be:

$$M_{n,n}(x_{i,j}^k; V_j; P_j; T_j; \mu_{i,j}) \tag{7.41}$$

$$M_{n\text{-}1,n}\left[(m_{n\text{-}1}/m_n)x_{i,j}^k; V_j; P_j; T_j; \mu_{i,j})\right] \tag{7.42}$$

And also the matrix of changes:

$$MC_{n,n-1} = M_{n-1,n} - M_{n-1,n-1} \tag{7.43}$$

$$MC_{n,\,n-1}\left(\Delta x^{k}_{i,j};\Delta P_j;\Delta T_j;\Delta V_j\right) \tag{7.44}$$

7.3.3. The Process Matrix

In Fig. 7.8 we may observe the flow diagram of a process with nine stages of change. There are 10 strains of matter (m_0, m_1,….m_8 ,m_9).

The description of the product of each strain may be represented by the corresponding Descriptive Matrices ($M_{0,0}$, $M_{1,1}$, ……., $M_{9,9}$).

The Matrix of Process (MP) is represented in Fig. 7.8. The cells in the diagonal of this MP are occupied by the ten descriptive matrices corresponding to the ten process strains. The cells corresponding to the right-up side of the diagonal would be occupied by the Transformed Matrices and the left-down side of the diagonal by the Matrices of Change. The matrix $MC_{9,0}$ would be the result of the accumulated changes suffered by the strain (m_0) after passing through the nine stages of change of the process, and has been calculated as:

$$MC_{9,0} = M_{0,9} - M_{0,0} \tag{7.45}$$

In other words, the differences between the final product (m_9) and the raw material (m_0) would be represented by this matrix of changes. Obviously, these

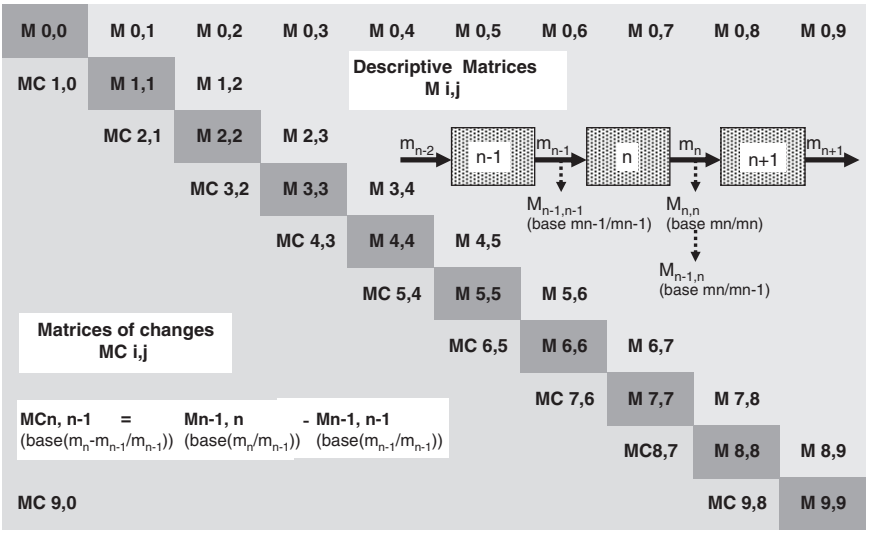

FIG. 7.8. The Matrix of Process (MP)

"overall" values of change have lost much significant information about what has really happened in each one of the stages. For this reason, the analysis of the changes in every stage is of great interest in order to know what elements do change in the food descriptive matrix, after passing through the stage, and to quantify the level of change, as well as to identify the mechanisms responsible for these changes. In conclusion, the Matrix of one Process with N Stages of Change would be made up from $(N+1)^2$ matrices distributed as follow:

- N+1 Descriptive Matrices
- $0{,}5[(N+1)^2 - (N+1)]$ Transformed Matrices
- $0{,}5[(N+1)^2 - (N+1)]$ Matrices of Change

7.4. Conclusions

Nowadays, food quality and safety (food properties) are major concerns of consumers and the food industry, and targets for product and process design.

Structured foods are dissipative structures (Nicolis and Prigogine, 1977b) with a high level of complexity. Therefore, the mathematical models of food behavior through operations and processes must include all of the information about food characteristics, as well as that regarding the different phenomena occurring during the processes: transport phenomena, chemical reactions, phase transitions, structure changes, etc.

To simplify foods as continuous (monophasic) and homogeneous systems will only result in the loss of much relevant information about their properties concerning their quality and security factors.

The SAFES methodology provides tools to describe, to calculate and to develop food products and processes with enough information to predict their food quality and safety.

Acknowledgement The authors acknowledge the grants received from the Spanish Ministry of Science and Education.

References

Aguilera J.M., 2006, Seligman Lecture 2005 Food Product Engineering: Building the Right Structures, *J. Sci. Food Agric*. **86**(8):1147–1155.

Aguilera, J.M., and Baffico P., 1997, Structure-Mechanical Properties of Heat-Induced Whey Protein/Cassava Starch Gels, *J. Food Sci*. **62**(5):1048–1053.

Aguilera, J.M., Chiralt, A., and Fito P., 2003a, Food Dehydration and Product Structure, *Trends Food Sci. Technol*. **14**:432–437.

Aguilera, J.M., Chiralt, A., and Fito P., 2003b, Process, Structure and Functionality, Special Issue on the International Conference Iberdesh 2002, *Food Sci. Technol. Int*. **9**:135.

Aguilera, J.M., and Stanley D.W., 1999, *Microstructural Principles of Food Processing and Engineering*, 2nd ed., Aspen Publishers Inc., Maryland.

Barat, J.M., Chiralt, A., and Fito P., 1998, Equilibrium in Cellular Food-Osmotic Systems: The Role of the Structure, *J. Food Sci*. **63**:836–840.

Barat, J.M., Fito, P., and Chiralt A., 2001., Modelling of Simultaneous Mass Transfer and Structural Changes in Fruit Tissues, *J. Food Eng*. **49**:77–85.

Bird, R.B., Stewart, W.E., and Lightfoot E.N., 2002, *Transport Phenomena*, 2nd ed., John Wiley & Sons, Inc., New York.

Crank J., 1985, *The Mathematics of Diffusion*, Oxford University Press, New York.

Einstein, A., Podolsky, B., and Rosen N., 1935, Can Quantum-Mechanical Description of Physical Reality Be Considered Complete? *Phys. Rev*. **47**:777–780.

ETP, Food for Life, 2006. The Vision for 2020 and Beyond. Confederation of the Food and Drink Industries of the EU. (October 27, 2006) www.ciaa.be.

Fito, P., 1994, Modelling of Vacuum Osmotic Dehydration of Foods, *J. Food Eng*. **22**:313–318,

Fito, P., Andrés, A., Chiralt, A., and Pardo A., 1996, Coupling of Hydrodynamic Mechanism and Deformation-Relaxation Phenomena During Vacuum Treatments in Solid Porous Food-Liquid Systems, *J. Food Eng*. **27**:229–240.

Fito, P., Chiralt, A., Betoret, N., Gras, M., Cháfer, M., Martínez-Monzó, J., Andrés, A., and Vidal D., 2001, Vacuum Impregnation and Osmotic Dehydration in Matrix Engineering: Application in Functional Fresh Food Development, *J. Food Eng*. **49**:175–183.

Fito, P., and Pastor R., 1994, On Some Non-Diffusional Mechanism Ocurring During Vacuum Osmotic Dehydration, *J. Food Eng*. **21**:513–519.

Gekas, V., González C., Sereno A., Chiralt, A., and Fito P., 1998, Mass Transfer Properties of Osmotic Solutions. I. Water Activity and Osmotic Pressure, *Int. J. Food Prop*. 1(2):95–112.

Gras, M.L., Vidal, D., Betoret, N., Chiralt, A., and Fito P., 2003, Calcium Fortification of Vegetables by Vacuum Impregnation. Interactions with Cellular Matrix, *J. Food Eng*. **56**(2–3):279–284.

Marcotte, M., and Le Maguer M., 1991, Mass Transfer in Cellular Tissues. Part 1. The Mathematical Model, *J. Food Eng*. **13**;199.

Martínez, N., Andres, A., Chiralt, A., and Fito P., 1998, *Termodinámica y Cinética de Sistemas Alimento – Entorno*, Editorial UPV, Valencia.

Martínez-Monzó, J., Martínez-Navarrete, N., Chiralt, A., and Fito P., 1998, Mechanical and Structural Changes in Apple (Var. Granny Smith) Due to Vacuum Impregnation with Cryoprotectant Agents, *J. Food Sci*. **63**:499–503.

Nicolis, G., and Prigogine I., 1977a, *Die Erforschung des Komplexen. Auf dem Weg zu Einem Neuen Verständnis der Naturwissenschaften,* R. Piper GmbH & Co. KG., München.

Nicolis, G., and Prigogine I., 1977b, *Self Organization in Non Equilibrium Systems. From Dissipative Structures to Order Through Fluctuations*, John Wiley & Sons, Inc., New York.

Seguí, L., Fito, P.J., Albors, A., and Fito, P., 2006, Mass Transfer Phenomena During the Osmotic Dehydration of Apple Isolated Protoplasts (*Malus Domestica* Var. Fuji), *J. Food Eng*. 77(1):179.

Wesseling, J.A., and Krishna R., 1990, *Mass Transfer,* Ellis Horwood Limited, England.

Zhiming, Y., and Le Maguer M., 1996, Mathematical Modelling and Simulation of Mass Transfer in Osmotic Dehydration Processes. Part I: Conceptual and Mathematical Models, *J. Food Eng*. **29**(3):349–360.

8
Phase Transitions and Hygroscopicity in Chewing Gum Manufacture

J. Welti-Chanes, F. Vergara-Balderas, E. Pérez, D. Bermúdez, A. Valdez-Fragoso, and H. Mújica-Paz

8.1. Introduction

Confectionery products constitute a very important branch in the food industry. There are several confectionery products: chewing gum, candy, and chocolate among others. Beside chocolate, chewing gum is one of the most consumed products in the world. Chewing gum is a product made with natural or man-made gums, polymers, and copolymers, added with other ingredients and food additives.

Traditionally, chewing gum was made of natural gums, although for reasons of economy and quality, many modern chewing gums use synthetic gums. These have proven beneficial in providing high consistency of chewing quality. To obtain acceptable products, gum properties must be maintained during manufacture of chewing gum. Most chewing gums are manufactured according to the following steps: The gum base is melted; other ingredients are added and mixed. The blended gum passes onto cooling belts and is bathed in currents of cool air to reduce its temperature; after this, the gum is extruded and flattened into thinner and thinner sheets. The gum passes into the scoring machine. The scored sheets are conditioned ("set" in an air-conditioned room) and then, candy-coated. Finally, the chewing gum is wrapped.

In order to assure product quality, specifications for the final product must be met. If the product is out of specifications, losses are generated. During chewing gum manufacture, several alterations can be presented. Among these are elasticity loss, unsuitable porosity, texture changes, etc. These alterations lead to difficult handling during manufacture, provoking undesirable characteristics of candy-coated pellet gum (deformed or ruptured pellets, inadequate coating, grainy surface, etc.). These defects are related to poor coating due to texture problems of pellets before coating.

During chewing gum manufacture, several moisture and temperature conditions are handled; these conditions can provoke changes in the gum base, passing from a solid state into a "rubber" state. During this transition, the moisture of the gum can be changed and the texture modified, causing an inadequate coating. According to this, preparation of uncoated pellets is a critical step in chewing gum manufacture.

This contribution presents some general information about water sorption properties, textural and thermo-physical characteristics of the "gum base" and its relation to process conditions and quality of candy-coated chewing gum.

8.2. Description of Chewing Gum Manufacture Process

According to Mexican regulations, chewing gum is defined as a gum base (chewable synthetic polymer) subjected to several changes to obtain a product with a rubbery structure and a pleasant taste. The gum base or synthetic polymer in a solid state suffers several changes during chewing gum manufacture.

In Fig. 8.1., a flow diagram for chewing gum manufacture is presented. The following steps can be identified: melting of the gum base, adding and mixing of other ingredients to form the chewing gum, sheet formation, scoring to obtain pellets of specified dimensions, and coating with sugar syrups; finally, the product is packaged and traded.

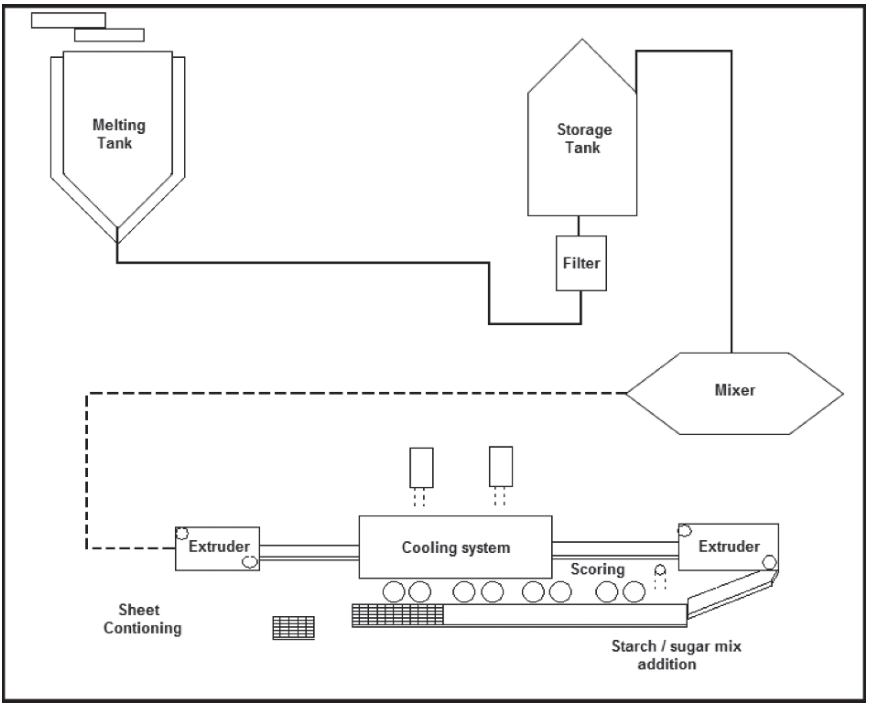

FIG. 8.1. Flow diagram for chewing gum manufacture

8.2.1. The Steps of Chewing Gum Manufacture

Following is a brief review of the main steps of chewing gum manufacture, emphasizing uncoated pellet formation due to its importance on the product final quality.

8.2.1.1. Melting

The gum base or synthetic polymer in solid state is melted, usually in large, hot water- or steam-jacketed kettles where the gum achieves the consistency of thick fluid. It is important to reach the fusion temperature to obtain a fluid with suitable viscoelastic characteristics. This fluid must be around the softening point (temperature to maintain polymer in a "rubbery" state) to mix the gum base with other ingredients to yield the chewing gum.

8.2.1.2. Mixing

The melted gum is mixed with other ingredients: sugar, glucose (or corn syrup), natural or artificial flavoring, and other products, including reprocessed material (candy-coated gum and pellets). To obtain a homogenous mix, time, temperature and other parameters must be met. The temperature must be around the softening point (temperature between the glass transition temperature and the fusion point).

8.2.1.3. Sheet Formation

The blended gum is handled to make it much smoother and finer in texture. It passes to a series of rollers, and the gum is flattened into thinner and thinner sheets. The final dimensions and weight of the sheet are determined by the type of gum it is to be. Sheet formation uses cooling belts with currents of cool air to reduce gum temperature as well as extruders, rollers, and cutting and scoring machines.

8.2.2. Extruders

Extruders are machines to mold and transport the blended gum into a cooling system. The temperature must be controlled during this operation, and it can be done by means of hot and cold water. In this step, gum texture and elasticity are modified.

8.2.3. Cooling System

Gum temperature must be lowered so scoring can be done. In addition, a lower temperature helps to control pellet dimensions and weight, and it has an important effect on hardness, consistency and firmness of gum. Heat must be removed from gum sheets for an adequate pellet coating.

8.2.4. Scoring

The gum destined for candy-coating is scored into small square or oblong pellets. Stick gum, ball gum, and other forms are scored in a different way. For sheet formation, a mix of sugar and starch is added to the gum. In addition, to prevent problems during pellet formation, the temperature must be controlled.

8.2.5. Sheet Conditioning

The scored gum sheets are set aside in an air-conditioned room (with temperature and moisture control) and after a 24-to-48 h storage period, the sheets must reach an appropriate hardness value so the pellet can be coated. Hardness is a typical mechanical property of polymers and other materials, related to plastic deformation resistance when a material is subjected to a penetration force. Also, the term hardness is used to describe material resistance to abrasion, scratching, cutting, and folding.

A hardness measurement is a simple way of obtaining a measure of the elastic modulus of a rubber by determining its resistance to a rigid indentor to which a force is applied. Indentation involves deformation in tension, shear and compression. Hardness is a very important parameter for establishing whether the pellet is ready to be coated; During coating, pellets are subjected to drastic conditions of moisture and temperature, as well as strokes inside the coating pan. In addition, an adequate hardness helps the coating adhere more firmly. If a gum sheet does not remain long enough inside the conditioning room, it will not achieve adequate hardness, and defects will appear.

Pellets are ready for coating when hardness values are around 16–20 °Shore. Pellets are coated with sugar syrup which is prepared in a jacketed kettle. Pellets are put inside coating pan and syrup is added to coat them. During coating, pellets are air-dried at specified relative humidity and temperature. Finally, the coated gum is whirled with a wax product. This process provides candy-coated chewing gum with its characteristic sheen. Then the gum is packaged.

8.3. Chewing Gum Ingredients and Their Function

8.3.1.1. Gum Base

As mentioned earlier, the gum base is a chewable synthetic polymer. There are two groups of base gums: chewing gum and bubble gum. The difference between them is the capacity to form bubbles according to the content of natural latex or high molecular weight polymers. A higher proportion of these polymers provokes a higher elasticity and hence the capacity to form bubbles.

The chewable gum base has no taste, and it imparts flexibility and malleability to the gum mix. It must be even and soft, with the capacity to retain aroma and malleability after processing, so that a mouth pleasant sensation is achieved. Polymer malleability and flexibility is achieved adding another type of polymers, the elastomers.

Table 8.1. Composition of a typical gum base

Component	Function
Elastomers and polyvinyl acetate	Chewable synthetic material
Resins	Plasticizing agent
Waxes and fats	Softening/emulsifying agent
BHT	Antioxidant

Table 8.1 shows components of a typical gum base and their function.

The gum base is made with a thermoplastic polymer that can be melted and solidified. These thermoplastic polymers are made of large interlinked chains; at low temperatures they are rigid, but when heat is applied, they soften and are malleable when they reach the glass transition temperature (Tg). Below this temperature, the polymer is brittle (a glassy solid state), but if the temperature is above Tg, the product is flexible and malleable (a rubbery state). This is a desirable characteristic of chewing gum.

One of the polymers used in chewing gum is polyvinyl acetate (PVA); its glass transition temperature is slightly higher than ambient temperature (28–30°C) (Rodríguez, 1984). This causes a hard and stable material at ambient temperature, but it becomes fluid and sticky when the temperature is increased. This low molecular weight polymer behaves as a rubber when it is chewed; moisture content affects some physical properties, for instance, stickiness and resistance. Most available PVA emulsions have been prepared by polymerization (Billmayer, 1978).

Several studies have emphasized the miscibility of this amorphous polymer, reporting Tg values around 35 °C, but depending on mix components, this value can change (Liu and Mathr, 2003).

It is possible to modify the polymer behavior used in the gum base by means of one type of additives: the plasticizers. A plasticizer is a small molecule that promotes a more flexible polymer. They are added to the polymer, which changes the polymer Tg and hence, transforms a glassy, hard and brittle material into a soft and flexible product. To be useful, a plasticizer must be compatible and miscible with the polymer (Billmayer, 1978).

Waxes are used as softeners in the gum base. They must be hard, with a high fusion temperature. In gum formulation it is common practice to use both natural and synthetic microcrystalline waxes.

In addition, the gum base contains antioxidants, for instance, butylated-hydroxytoluene (BHT), butylated -hydroyanisole (BHA), or tocoferol used to protect gum base components. If necessary, gums can be produced without antioxidants, but it can shorten gum shelf-life (Billmayer, 1978).

8.3.1.2. Glucose

The glucose used in chewing gum formulation usually comes in the form of clear syrup (corn syrup) and has several functions:

- It keeps the gum moist and pleasant to chew and helps the sugar (sucrose) to combine easily with the gum base

- It prevents growing of sugar crystals, avoiding a grainy texture
- It maintains flexibility and moistness of the gum

Glucose is subjected to phase transitions, from a viscous fluid (syrup) into a glassy solid at temperatures around 20–35 °C; if it is subjected to high temperatures, it collapses and turns sticky because of moisture gain.

8.3.1.3. Sucrose

Sucrose is a sweetener and, in combination with starch, it is used to bathe the gum sheet, modifying the gum's hygroscopicity. It is necessary to use sugar that is free of impurities; its moisture content must be low, and it must have a low level of inverted sugar. Sucrose must be powdered because particle size has a definite effect on the brittleness or flexibility of the final product.

8.3.1.4. Starch

Starch acts as humectant for the polymer. Usually, a modified starch is used, and it is applied on the surface of scored gum sheets. The starch, with a sugar mix, helps to absorb moisture in the gum, modifying its hardness. In addition, starch helps to incorporate added components during the final coating of pellets.

8.3.1.5. Flavorings

Either natural or artificial flavoring, whichever is desired and to whatever taste, is added to the gum base. In addition, flavorings act as gum softeners, affecting chewing gum texture. Flavorings contain essential oils; they are the best gum base plasticizers. However, they are not enough to soften the gum, so other plasticizers must be added to obtain a good chewing quality.

8.4. Final Quality of Pellets

In order to be coated, pellets must meet some requirements:

- Sheet specifications: There are predetermined values for sheet length, width and weight. Sheets out of specifications lead to difficult slipping when they are piled up; in addition, deformation and other defects may be present.
- Pellet specifications: There are predetermined values for pellet dimensions and weight before and after conditioning; besides, a predetermined hardness value must be met.
- Final chewing gum pellet specifications: There are predetermined values for pellet dimensions, coating thickness, and hardness.

If gum sheet conditioning is deficient or the coating process is inadequate, defective gum pellets are generated. Some of these defective products are shown in Fig. 8.2.

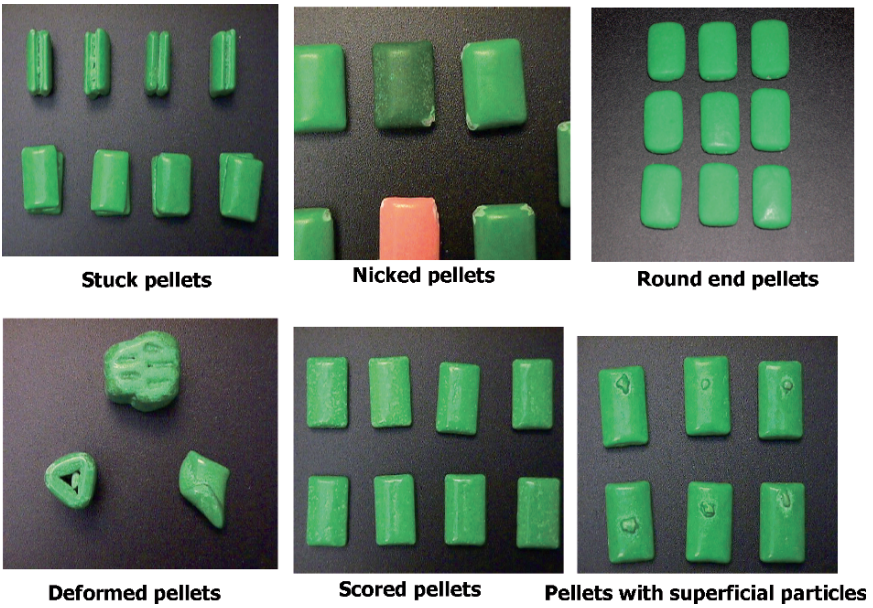

FIG. 8.2. Typical defective chewing gum pellets

8.5. Process Variables

Control of process variables is essential for chewing gum manufacture. Important variables are temperature, moisture, and air velocity during gum conditioning. Temperature is a very important process factor because high temperatures are required to melt the gum base; on the other hand, low temperatures are required to form sheets and coat gum. These drastic temperature changes must be controlled to avoid damage in texture, consistency and elasticity due to transitions in gums and other components (Fried, 1995).

Ambient relative humidity provokes changes in gum that must be controlled to avoid viscosity modifications leading to a sticky gum, making for difficult handling during processing. In addition, final gum texture may be affected by these changes.

Air velocity and distribution are important factors during gum cooling. Several desirable gum characteristics are developed in this stage, in a way similar to the cooling of chocolate to improve firmness and scoring.

Air temperature and relative humidity affect gum moisture and water activity. Water activity of gum has a very low value, around 0.2, and moisture content is lower than 1%; during chewing gum manufacture, these values increase due to the ingredients added and the moisture gained. The changes in moisture and water activity values must be controlled to assure the final quality of gum pellets.

8.6. Moisture, Water Activity and Texture of Chewing Gum

According to the preceding concepts, it is clear that knowledge about chewing gum moisture variations to evaluate gum hygroscopicity (by means of moisture sorption isotherms) is necessary in order to establish relationships among texture changes and moisture content (or water activity) during the process of manufacturing chewing gum. Table 8.2 shows representative information about values of temperature, moisture and water activity of the gum base during several stages of gum conditioning, previous to gum coating. It can be noticed that the initial gum base or synthetic polymer, with low moisture content and water activity, is mixed with several ingredients and transformed into gum sheets, modifying product moisture content and thus provoking changes in hardness and malleability. In addition, temperature changes are necessary to obtain the final coated pellet.

A way to describe the relationship between moisture content of a system (gum) and physical state of water in the system is by means of a moisture sorption isotherm. A moisture sorption isotherm relates moisture against water activity in a system, and it defines solvent availability for several purposes, including one related to phase transitions and texture (hardness) in the system. Figures 8.3 and 8.4 show moisture sorption isotherms at 25, 35 and 45°C of an extruded gum

TABLE 8.2. Average characteristics of gum base during conditioning stages

Type of gum	Temperature (°C)	Moisture (g H2O/100 g d.s)	a_w
Gum base	69	0.20	0.213
Melted gum	74	0.40	0.280
Gum after mixing	48	2.20	0.520
Extruded gum	48	2.20	0.520
Gum after cooling	46	2.50	0.563
Scored sheets (with starch/sugar mix)	41.6	1.30	0.401

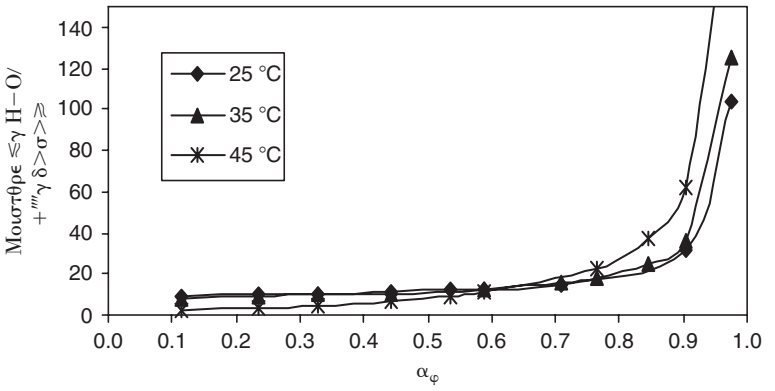

FIG. 8.3. Moisture sorption isotherms at 25, 35, and 45 °C of extruded gum

and gum sheets bathed with a starch/sugar mix, respectively. In the case of the extruded gum (Fig. 8.3), it can be seen that for a_w levels up to 0.75 there is no clear effect of temperature on gum moisture sorption ability; also, in this a_w range, the gum has a poor ability to retain water in its structure, maintaining moisture levels lower than 20 g H_2O/100 g d.s. When a_w is higher, moisture that can be incorporated by the gum increases dramatically; also, if the temperature increases, it generates higher moisture levels for systems with the same a_w. This behavior is "abnormal" in biological systems, as in the case of foods. This behavior can be explained because the gum base (polymer) has a rigid and compact structure at low temperatures; however, when the temperature is increased, polymer changes from a rigid structure into a rubbery one where water can penetrate and mix with the gum, creating higher moisture contents. When the starch/sugar mix is added (Fig. 8.4), the moisture isotherm has a different form. In this figure, temperature effect is noticeable in the whole a_w range. At higher temperatures, the gum capacity to retain water is higher at the same a_w level, generating a softer product, because of the combined action of temperature and water inside the gum.

In addition, it is clear in Fig. 8.4 that when the temperature is 25 °C (and probably at lower temperatures), there is a minimum moisture gain in the a_w range 0.0–0.5, which indicates that in this range, moisture plays a less important role as a solvent and plasticizer, and temperature is more important in gum texture changes during conditioning.

Figure 8.5 shows a_w values as a function of conditioning time in a cooling room for gum pellets bathed with a sugar/starch mix. The conditioning process is used to generate adequate pellet texture for coating. As can be seen in Fig.8.5, gum pellets enter the cooling room with an a_w value around 0.41, and after 48 hours the value is around 0.45; equilibrium is not reached between the gum and the surrounding air, which has a relative humidity of 50 %. With these data and referring to Fig. 8.4,

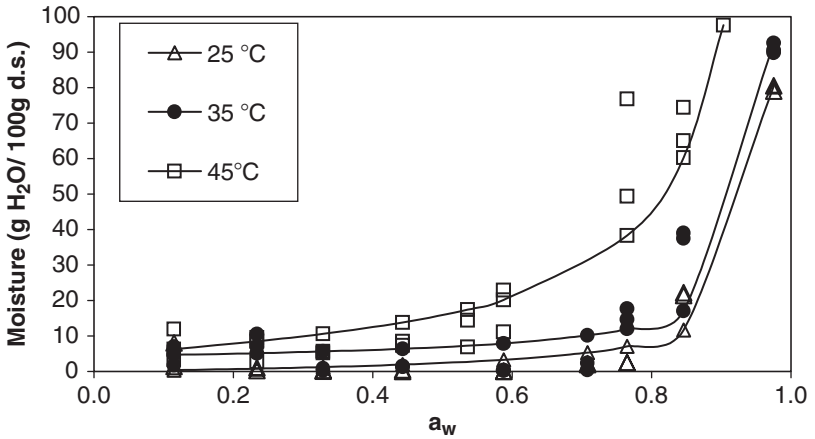

FIG. 8.4. Moisture sorption isotherms at 25, 35, and 45°C of gum sheets bathed with a sugar/starch mix

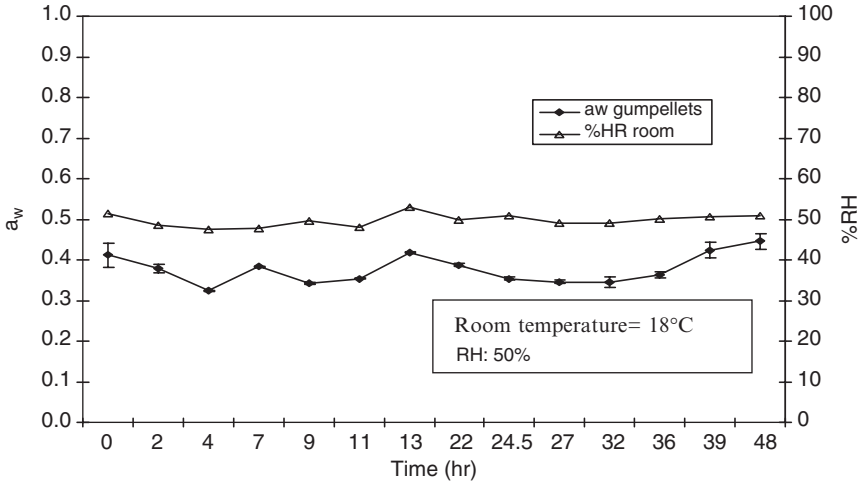

FIG. 8.5. Evolution of a_w of gum pellets in a cooling room

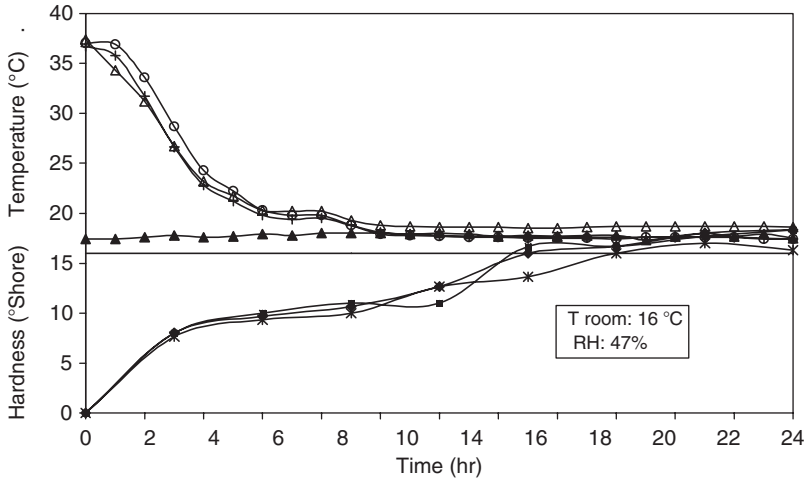

FIG. 8.6. Relationship between gum sheet temperature and gum hardness

it can be concluded that during this time moisture changes in gum pellets are small and hence, gum thermal and textural properties are only slightly affected due to its water content.

On the other hand, the temperature decrease of the gum pellet in the conditioning room seems to be the main factor related to texture (hardness) changes, as can be seen in Fig. 8.6. Gum pellets enter the cooling room almost at 40 °C, and a low hardness value (it is not possible to measure the hardness value with the systems

normally used in the confectionery industry); however, after 6 hours in the cooling room, a temperature of 20°C is reached and pellet hardness is 10 °Shore; after 16 hours, a temperature of 16–18°C is reached, with a hardness value of 16 °Shore (this value is in the desirable range for gum hardness).

After this time, temperature and hardness changes are very small, and after 48 hours in the cooling room, hardness increases to 22 °Shore; at this value, pellet coating can be applied without problems. However, if pellet hardness reaches values above 22 °Shore, the pellets are fragile and difficult to coat. In order to know if hardness changes due to temperature effects are related to glass transitions of chewing gum, studies must be conducted. Differential scanning calorimetry (DSC) is a tool that can be used to carry out these studies.

8.7. Phase Transitions of Chewing Gum

Phase transitions studies in foods are relatively new; however, their importance in controlling processes and products has been demonstrated (Roos, 1995). Physical structure of a chemical or biological system, as in the case of chewing gum, is important from a functional and a sensorial point of view. Usually, this structure is modified by changes in a_w because moisture is gained or lost. For example, caking of powders is due to sugar and oligosaccharides transition into an amorphous-crystalline state; this happens when a_w increases to values above those corresponding to glass transition at ambient temperature (a_w around 0.3–0.4) (Saltmarch and Labuza, 1980). There are several examples where application of knowledge about phase transitions in foods generates improvements in process techniques; for instance, the control of molten properties of comestible fats (cocoa), control of caking of powders, control of texture (related to ice crystal formation) in ice cream, control of stickiness in chewing gum, evaluation of the mechanism of marshmallow hardening, etc. (Chiralt et al., 1998; Lim, et al., 2006).

8.7.1.1. Glass Transition

Most food products with low moisture content are not in a crystalline state. Their state depends on whether the temperature of observation is below or above their glass transition temperature (Tg) (Simatos et al., 1995). Each substance has a characteristic Tg; at temperatures below Tg the substance is an amorphous, glassy solid of extremely high viscosity; on the other hand, at temperatures higher than Tg a transition into a rubbery state is produced. The most important consequence of glass transition is an increment in molecular mobility and free volume above Tg (Zaritzky, 1997).

The relevance of Tg and of the plasticizing effect of water in foods may be shown in state diagrams based on curves of Tg as a function of water content. For instance, crispy products, such as breakfast cereals or extruded flat bread, are in the glass domain; they lose their crispness (they change into rubber) if their water content increases (Simatos et al., 1995).

8.7.1.2. Polymer Transitions

The physical state of polymer molecules can be partially crystalline (adequate structure) or completely unordered; it can be a melted material with viscosity characteristics of a liquid, or with elasticity associated with a rubbery solid (Rodríguez, 1984).

Polymers can exist in several states, depending on rotation and conformation of chains forming their molecules that are trying to reach a thermodynamic equilibrium condition, for instance, the solid crossing from an equilibrium state to a non-equilibrium state when heat is applied (Chiralt et al., 1998). When a polymer is melted, molecular motion increases as a result of temperature increments; on the other hand, if the temperature is low enough, rotation around a single bond is impossible due to energy barriers, and polymer molecules are trapped in a chaotic, unordered and entangled state, generating a glass. If the temperature is lower, intermolecular barriers for rotation are bigger and the crystal is more stable (Rodríguez, 1984).

8.7.1.3. DSC Thermograms of Gum Base or Synthetic Polymers

The gum base is a polymer mix; the most abundant polymer in the mix is polyvinyl acetate (PVA) which is responsible for most gum characteristics. Figure 8.7 shows the DSC thermogram of a gum base sample with a heating rate of 10 °C/min, and then cooled at the same rate. The region of possible phase transitions (glassy to rubbery) and the fusion peak (endothermic peak) can be seen, as well as the change in heat capacity (Cp). According to thermograms for similar materials (Liu and Mathr, 2003), a crystallization peak is not detected because PVA and elastomers in the mix are amorphous polymers with more molecular mobility, where crystallization is not noticeable. First Tg is observed around 5.65 ± 0.21 °C. The onset point of this transition is around 1.15 °C ± 0.21 °C and the end is around 10.15 ± 0.636 °C. The Cp change during this transition is 2.16 ± 0.74 J/g °K. The second Tg (Tg2) is observed around 17.5 ± 1.56 °C with an onset point of 14.10 ± 1.98 °C and the end at 20.90 ± 1.31 °C, with a Cp change of 0.33 ± 0.14 J/g °K. This temperature range is of interest during chewing gum conditioning in order to reach adequate hardness for coating.

Melting of the gum base is shown in thermograms as a peak with maximum heat absorption (endothermic peak) at temperature (Tm) around 50.5 ± 0.2 °C; the onset point for this transition is around 37.95 ± 0.1 °C, and the end is around 59.55 ± 0.55 °C, and the fusion enthalpy is 22.81 ± 0.61 J/g.

On the other hand, Liu and Mathr (2003) evaluated miscibility and morphology of a similar polymer in a mix with a semi-crystalline polymer and reported that PVA alone is amorphous and that peak positions are slightly displaced when another polymer is added; the polymer fusion temperature is around 40–60°C, which is in agreement with information reported here, indicating that this peak possibly represents PVA. Also, Fig. 8.7 shows that the point where the viscosity of the gum base falls is in the range 60–80°C; in the chewing gum industry this point is called the “drop softening point.”

When all other ingredients are added to the gum base (including the sugar/starch mix), and the obtained mix is adjusted to several a_w values, thermograms like the one in Fig. 8.8 are obtained. It can be observed that there is a different form for each thermogram with a tendency to lose the polymer fusion peak due to displacement of fusion temperature that is reduced when a_w is increased;

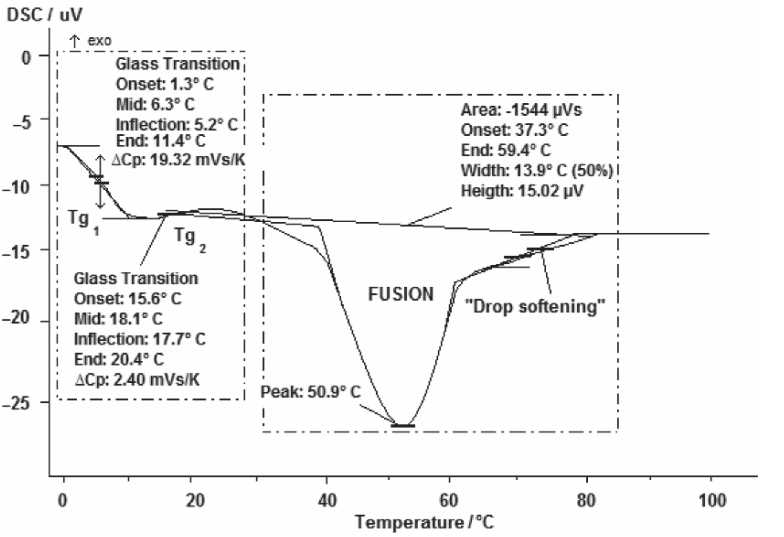

FIG. 8.7. DSC thermogram of chewing gum base

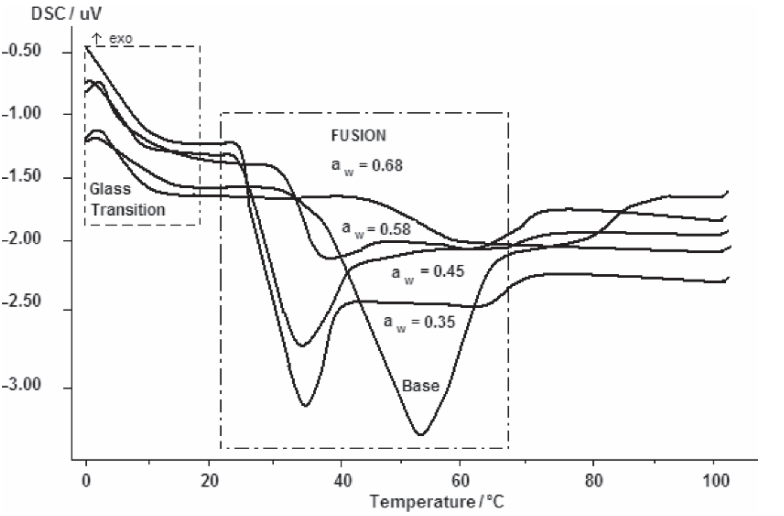

FIG. 8.8. DSC thermograms of chewing gum base mixed with other ingredients at several a_w values

however, the phase transition zone is not affected when other ingredients are added or a_w is changed in this range (0.35–0.68); it is still present at around 14–21 °C. These results show the importance of polymer type and temperatures applied to gum before coating to generate the adequate hardness for subsequent handling of the gum.

8.8. Final Remarks

The chewing gum industry has many similarities with processes and conditions applied in the food industry, and in this sense many of the scientific developments could be considered for their applications and to improve old processes currently used in that industry. This contribution shows some basic information about the interaction of water, polymers and other ingredients and their relation with textural and phase changes during different steps of chewing gum manufacture.

Knowledge of hygroscopicity and phase transitions of chewing gum and its ingredients is essential to understand the manufacturing process. This knowledge can be an important tool to improve processes and products in this industry, not only from a quality point of view; also, it can have an important role from the economics point of view.

Additionally, light and lower-calorie products represent an important sector of the confectionary industry. Processing of these products follows the same principles used to process "regular" products. However, ingredients to prepare these products are different; there is a necessity to understand the behavior of these ingredients so that high quality products can be obtained.

Acknowledgements Thanks are due to Cadbury Adams Mexico for their support of this research project.

References

Billmayer R., 1978, Tecnología de los Plásticos, in: *Ciencia de los Polímeros*, 2nd ed., Reverte, Barcelona, pp. 122–125, 420–421, 502–503.

Chiralt, A., Fito, P., and Martínez N., 1998, Transiciones de Fase en Alimentos, in: *Termodinámica y Cinética de Sistemas de Alimentos y Su Entorno*, Universidad Politécnica de Valencia, Valencia, pp. 66, 156–179, 225–257.

Fried J.R. (ed.), 1995, The Solid-State: Properties of Polymers, in: *Polymer Science and Technology*, Prentice Hall. Cincinnati, pp. 146–155.

Lim, M.H., Jia, Y., and Heenan S., 2006, The Mystery of Marshmallow Hardening, in: *Water Properties of Food, Pharmaceutical, and Biological Materials*, M.P. Buera, J. Welti-Chanes, P.J. Lillford, and H.R. Corti (eds.), CRC Taylor & Francis, Boca Raton, pp. 325–342.

Liu C., and Mathr P., 2003, *Thermomechanical Characterization of Blends of Poly (vinyl acetate) with Semicrystalline Polymers for Shape Memory Applications*, 1962-ANTEC 2003, Connecticut.

Rodríguez F. 1984. *Principios de Sistemas de Polímeros*, 2nd ed., El Manual Moderno, México, pp. 35–55, 490–495.

Roos Y., 1995, Water Activity and Glass Transition Temperature: How Do They Complement and How Do They Differ? in: *Food Preservation by Moisture Control: Fundamentals and Applications,* G.V. Barbosa-Cánovas and J. Welti-Chanes (eds.), Technomic Publishing Co., Lancaster, pp. 133–151.

Saltmarch, M., and Labuza, T.P., 1980, Influence of Relative Humidity on the Physicochemical State of Lactose in Spray-Dried Sweet Whey Powders, *J. Food Sci.,* **45**(5):1231–1236.

Simatos, D., Blond, G., and Pérez J., 1995, Fundamentals of Water in Foods: Basic Physical Aspects of Glass Transition, in: *Food Preservation by Moisture Control: Fundamentals and Applications*, G.V. Barbosa-Cánovas and J. Welti-Chanes (eds.), Technomic Publishing Co., Lancaster, pp. 3–30.

Zaritzky N. 1997, Transición Vítrea y Congelación de Alimentos, in: *Temas de Tecnología de Alimentos*, Instituto Politécnico Nacional, México, pp. 180–183.

9
Exploring The Linear Viscoelastic Properties Structure Relationship in Processed Fruit Tissues

S.M. Alzamora, P.E. Viollaz, V.Y. Martínez, A.B. Nieto, and D. Salvatori

9.1. Introduction

Texture is a quality attribute that is critical in determining the acceptability of raw and processed fruits, so it is of primary concern in product development and/or preservation techniques design. Texture is a sensory attribute that can only be sensed by people. Perceived texture results from an array of sensory inputs, arising before and during consumption (Jack et al., 1995). As a rule, one texture property is based on various physical properties. However, product texture is closely related with product rheology, and this is one of the most obvious reasons for studying fruit rheology.

Mechanical properties of biologic tissues depend on contributions from the different levels of structure: the molecular level (i.e., the chemicals and interactions between the constituting polymers), the cellular level (i.e., the architecture of the tissue cells and their interaction) and the organ level (i.e., the arrangement of cells into tissues and their chemical and physical interactions) (Ilker and Szczesniak, 1990; Waldron et al., 1997; Jackman and Stanley, 1995a; Alzamora et al., 2000). Fruits are composite materials and consist of various structural elements with different mechanical properties. The edible portion of most plant foods is predominantly composed of parenchymatous tissue. The parenchyma cells, approximately 50–500 μm across and polyhedral or spherical in shape, show, from out to inner, the middle lamella that glue adjacent cells; the primary cell wall with the plasmodesmata; the plasma membrane; a thin layer of parietal cytoplasm containing different organelles (mitochondrias, spherosomes, plastids, chloroplasts, endoplasmic reticulum, nucleus and so on); and, bound by the tonoplast membrane, one or more vacuoles that contain a watery solution of organic acids, salts, pigments, and flavors that are responsible for the osmotic potential of the cell. Cells and intercellular spaces are arranged into tissues, and these last into the final organ (Brett and Waldron, 1996).

The three major structural aspects that contribute to textural properties of plant-based foods are *turgor*, the force exerted on the cell membrane by intracellular fluid, *cell wall rigidity,* and *cell-cell adhesion,* determined by the integrity of the middle lamella and the plasmodesmata. In addition, the relative percentage of

the different tissues, size and shape of the cells, ratio of cytoplasm to vacuoles, volume of intercellular spaces (which may contain either fluids or interstitial air), type of solutes present, and presence of starch and its state are also important (Ilker and Szczesniak , 1990; Alzamora et al., 2000). The plant cell wall is a strong fibrillar network that gives each cell its stable shape. Various alternative models of cell wall structure have been proposed based on indirect evidence and biochemical hunches (Cosgrove, 1997; 1998). In general, the models postulate that three intertwined networks, stuck together perhaps by various non-covalent adhesions and entanglements, are responsible for bearing tensile stresses within the wall: 1) a stretch resistant, load-bearing cellulose/hemicelluloses network, where the hemicelluloses are thought to form a hydrogen-bonded surface coat over the microfibrils and may bridge between microfibrils; 2) a compression-resistant pectic polysaccharide network, where the junction zones are originated by calcium cross-linking and by ester linkages with dihydroxy-cinnamic acids; and 3) a third network consisting of structural proteins covalently linked by oxidative phenolic cross-bridges and other linkages (Carpita and Gibeaut, 1993). The cellulose microfibrils (with crystalline and amorphous regions) are remarkably stable and usually undergo negligible breakdown under stress, playing a major role in determining the strength and structural bias of the cell wall; the disposition of microfibrils in space also determines many of the mechanical properties of the wall. Pectins make up a hydrophilic phase with gel-like properties situated in the space between microfibrils, preventing aggregation and collapse of the cellulose network and allowing for easy slippage between the celluloses and hemicelluloses. The wall matrix is approximately 75% water by mass, resembling a very dense aqueous gel.

The macro-, micro- and ultrastructure of tissues are affected by processing, with several modifications that influence the mechanical behavior and the perceived texture. Thus, establishing and understanding a relation between texture and instrumental mechanical parameters also requires determining what the most essential structural elements are, and to which fundamental rheologic parameters they are primarily linked. Knowledge resulting from investigations on plant cell structure during processing and its influence on viscoelastic behavior (determined by small deformation tests) and failure properties (determined by large deformations methods) can be utilized for the development of tailor-made technologies or the optimization of existing techniques for the production of processed fruits with specific mechanical properties (Kunzek et al., 1999).

At the macroscopic level, fruits are viscoelastic systems that exhibit a combination of elastic and viscous behavior under mechanical loading, which means that force, distance and time, in the form of rate, extent and duration of load, determine the value of measurements (Pitt, 1992). Determining the structural characteristics of polymers has long been the main focus of linear viscoelastic tests (Ferry, 1980). It is assumed that these techniques are very sensitive means of studying microstructure. However, the use of linear viscoelastic data for characterizing food materials has just begun in the last fifteen years, and research

efforts today are focused on correlating transient or dynamic methods to sensory characteristics and structure of foods (mainly dairy products and gels). Until now, these tests have not been very much used to elucidate the structure-function correlation in vegetable tissues.

This chapter is part of a comprehensive study on the relationship between structure, rheology and texture of raw and minimally processed fruit. With this aim, this chapter is intended to explore the correlation between the linear viscoelastic (oscillatory shear and creep) properties and the microstructure/ultrastructure of selected fruits (melon, apple), as affected by osmotic dehydration and/or calcium incorporation.

9.2. Linear Viscoelastic Behavior and Modelling

Dynamic oscillatory shear, relaxation and creep/recovery tests are usually used to determine material properties in the linear viscoelastic regimen (Ferry, 1980).

In dynamic tests, the strain (or the stress) is varied periodically, usually with a sinusoidal alternation at a frequency ω, and the response can be subdivided vectorially in two components, one in phase with the stimulus (the shear storage modulus $G'(\omega)$), and the other 90° out of phase (the shear loss modulus $G''(\omega)$). G' is directly proportional to the energy storage in a deformation cycle and provides information about the elastic nature of the material. G'' is proportional to the dissipation of energy as heat in a cycle of deformation, and characterizes the viscous nature of the material. Dynamic measurement provides data on viscosity and elasticity, which is especially valuable for small values of time, and the dynamic mechanical spectrum (i.e., a plot of G' and G'' moduli as a function of frequency) appears to represent a signature of the static microstructure of the material. Dynamic rheology allows characterization of microstructures without disrupting them in the process (Khan et al., 1997).

On the other hand, creep tests (in which a shear stress is instantaneously applied to the specimen and then maintained constant) allow elastic, viscoelastic and viscous flow characteristics to be predicted separately (Sherman, 1970; Ferry, 1980). Deformation and compliance (i.e., the ratio of the strain to the constant shear stress) increase as a function of time. In the initial states of shear, the material behaves as a solid, and subsequently exhibits fluid behavior.

The viscoelastic characterization of fruits presented in this chapter involved oscillatory shear and creep recovery tests. Dynamic oscillatory tests were performed in the controlled strain mode at 20°C in a Paar Physica CR 300 rheometer (Anton Paar GmbH, Graz, Austria) with 30 mm diameter parallel plate geometry. Prior to a frequency sweep, a strain sweep was carried out at an angular frequency of $10\,s^{-1}$ to determine the linear viscoelastic range. The conditions for linear viscoelasticity are that the stress be linearly proportional to the imposed strain and that the torque response involves only the first harmonic. Thereafter, storage (G') and loss (G'') moduli and loss tangent ($\tan \delta = G''/ G'$) were recorded in the

frequency range 0.1 to 100 s^{-1} using a strain amplitude value of 0.05% (within the limits of linearity previously established).

Creep recovery tests were conducted at 20 °C by applying a constant shear stress of 15 Pa (melon) or 35 Pa (apple) for 60 sec. After this time, the shear stress was switched off and the sample recovery was registered for an additional period of 120 sec. Prior to the creep recovery assay, the samples were exposed to various loading and unloading cycles to remove any surface irregularities in the specimen and to provide consistent results in identical tests (Mittal and Mohsenin, 1987).

The theory of viscoelasticity is well developed for small stresses and deformations. Different approaches to the analytical modeling of the rheological behavior of a linear viscoelastic system are available in the literature, such as standard mechanical models, fractional derivate models and power-law models (Tshoegl, 1989; Park, 2001). The classical approach uses mechanical models comprised of two (or their combinations) primary elements: the elastic element (referred as the Hookean or spring element), and the viscous element (referred as the Newtonian or dashpot element) (Ferry, 1980).

The mechanical models, characterized by a discrete number of time constants, have long been used to express the material functions of linear viscoelastic media, and the related topics, including fitting and interconversion, are well known. In particular, the mechanical model analogs have been shown to accurately describe the broad-band rheological behavior of agricultural products by a number of authors (Chappel and Hamann, 1968; De Baerdemaeker and Segerlind, 1976; Datta and Morrow, 1983; Jackman et al., 1992).

In this chapter, compliance data from creep experiments were fitted by a mechanical model consisting of a spring connected in a series with two Voigt elements (each Voigt element has a spring and a dashpot in parallel) and a dashpot element (Fig. 9.1.), described by the equation (Sherman, 1970; Jackman and Stanley, 1995b):

$$J\left(t,\sigma_c\right) = \left(J_o\right) + \sum_{i=1}^{2}\left(J_i\right)\left(1-e^{-t/\lambda_i}\right) + t/\eta_N \tag{9.1}$$

where J (t, σ_c) is the creep compliance (= γ(t) / σ_c, with γ (t) being the strain at time t, and σ_c the constant stress applied); J_o is the instantaneous compliance at t=0; J_i are the retarded compliances; λ_i (= $\eta_i \times J_i$) are the retardation times, and η_i are the coefficients of viscosity associated with the Voigt elements; η_N is the coefficient of viscosity associated with Newtonian flow, and its inverse is the steady-state fluidity of the material.

The model allows viscoelastic material functions to be readily determined from the experimental data. J_o is related to those bonds of structural units that are stretched elastically when stress is applied and show instantaneous and complete recovery when the stress is removed. J_i parameters are related to bonds that break and reform at different rates; the weaker bonds break at smaller values of time than do the stronger ones. They show retarded elastic recovery.

The linear region of Newtonian compliance t/η_N is related to those bonds that are ruptured during the shear creep step, and the time required for them to reform

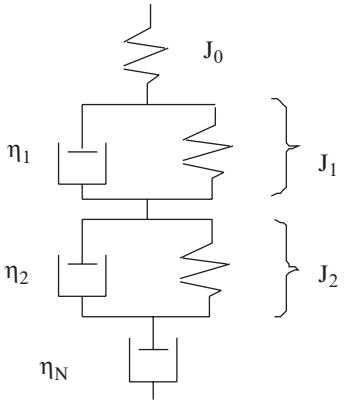

FIG. 9.1. Mechanical model for describing creep behavior of fruits

is longer than the creep recovery period; the released units will flow, and part of the structure will not be recovered.

One difficulty encountered in measuring and characterizing the physical properties of fresh or minimally processed plant tissues is that they are usually alive and respiring, and also they can be dehydrated during measurement, changing very rapidly and requiring tissue extension to be observed in short periods of time. Thus, the interpretation of creep behavior in this chapter ascribes considerable importance to the time scale over which creep occurs.

9.3. Variability Associated with Linear Viscoelastic Functions

Fruit tissues are anisotropic, and there is differentiation between the flesh close to the skin and the flesh close to the core of the fruit. Thus, rheological parameters and microscopic observations vary within sampling regions and with regional sampling depths (Petrell et al., 1979). Even within fairly homogeneous tissues of a sampling region, cells exhibit different turgidity, osmotic pressure, elasticity, composition and wall structure, and we should consider a distribution of rheologic properties in this apparently homogeneous cell population. Physical and chemical differences also depend on fruit cultivar, agronomic practices and time of harvest in the field. Also, growing cell walls show distinctive rheological properties. At very early stages of development, structure and bio-chemistry of walls are varied and dynamic. For cells to develop their functional form and individuality, they must elongate and differentiate; this expansion and differentiation is achieved by modification of the structure of a developing wall. During acid growth, the wall is transformed from a viscoelastic solid to a viscoelastic liquid, and extends rapidly by a form of polymer creep, permitting cell enlargement. As plant cells begin to mature, their walls become inextensible and resistant to disassembly (Cosgrove, 1997, 1998; Carpita and Gibeaut, 1993; Brownleader et al., 1999). In addition,

differences between samples of a particular fruit or vegetal are normally larger that those between locations of the same sample.

This enormous variability within and between fruits is of particular concern in creep experiments, and a sufficient number of replicates is necessary to obtain an acceptable level of confidence in fundamental parameters determined by instrumental tests. Moreover, not only are the average mechanical properties a product characteristic, but also the variation between samples (van Vliet, 2002).

Data variability is exemplified in Fig. 9.2, where the creep recovery strain curves and the corresponding average creep compliance function (usually used in calculations instead of a distribution function as a matter of simplicity) are represented for samples of different raw apples of the same lot. As can be seen, departure from the assumption of homogeneity was in some cases quite large. Not only were strain magnitudes different, but also the creep strain patterns. In the time domain analyzed, some apple samples exhibited an equilibrium compliance

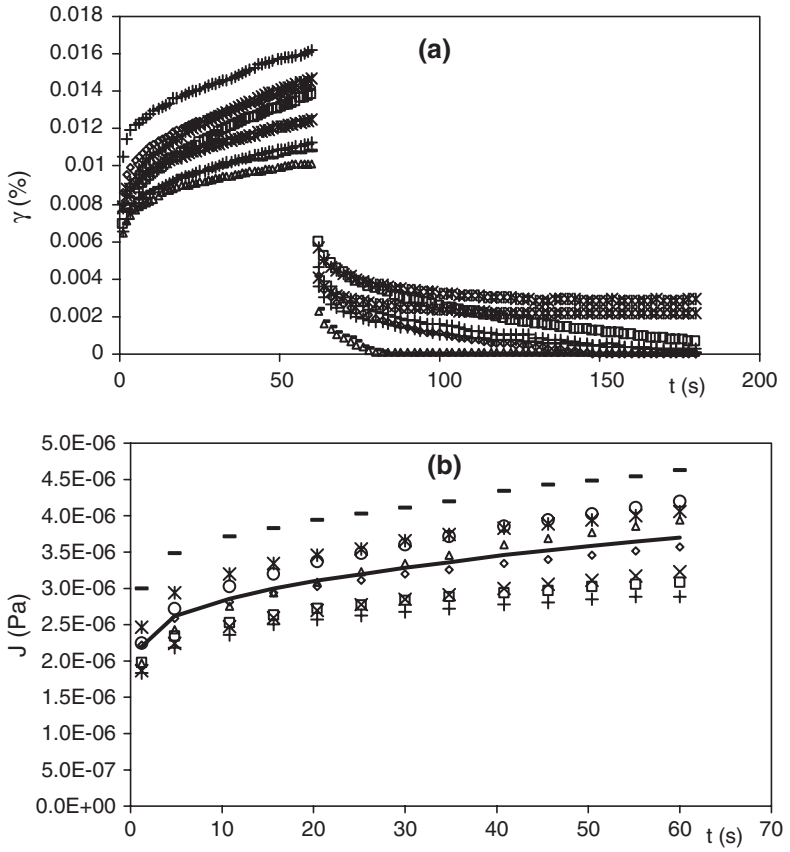

FIG. 9.2. Creep/recovery time curves for parenchymatous tissue of different raw apples: a) strain during creep and recovery phases; b) creep compliance, experimental values (points) and average creep compliance, mean of 8 samples (line)

(i.e., a residual reverse strain still persisted at the end of the recovery phase), and a situation of steady-state flow was eventually attained, governed by a Newtonian viscosity η_N. On the other hand, other apple samples gradually returned toward their initial state after the load was removed. It is to be noted that this last behavior (shear creep followed by complete creep recovery) was only shown by some samples of raw apples. All treated apple and melon samples, as well as raw melon tissues, showed a small residual strain at the end of the recovery stage. For this reason, and to facilitate the comparison between fresh and treated fruits, creep curves were analyzed using the mechanical model previously described, where a final dashpot takes into account the viscous contribution.

The relatively large standard deviations associated with creep data of plant tissues are so not uncommon and, on the contrary, expected. From this information, it becomes apparent that, when examining the effect of treatment on structure and viscoelasticity of fruit tissues, the specific rheologic parameters have less importance than the comparison of parameters between treatments.

9.4. Relation Between Structure and Viscoelastic Parameters

9.4.1. General Viscoelastic Behavior of Melon and Apple Fruits

The different dynamic mechanical spectra of raw and treated melon and apple samples revealed a change in the microstructure of the materials due to processing. However, the pattern for all G' and G'' - ω curves appeared to represent rather well the microstructure of a colloidal dispersion with strongly attractive inter-particle forces and high particle concentrations with significant flocculation of the system (that is, systems with a network-type microstructure) (Khan et al., 1997).

The elastic modulus greatly exceeded the viscous modulus ($G''/G' \cong 0.10-0.30$) for all the fruit samples assayed, but the loss modulus G'' and the storage modulus G' were reduced due to processing. Both G' and G'' moduli for fresh and treated tissues showed a weak dependence on the frequency of the oscillations. G' magnitudes slightly increased as the angular frequency increased, with greater slope of the G' - ω lines for treated samples.

The lesser frequency dependence of raw fruits would indicate more elasticity in the fresh fruits than in the treated ones. The frequency dependence of G'' was more complex. The curves of G'' versus ω consisted of one shallow negative slope (nearly a plateau) at low frequencies and a positive slope at high frequencies (see Fig. 9.4 as an example of moduli behavior in melon).

Treatments also caused significant changes in both creep strain and residual strain after recovery. Comparing the compliance curves of fresh tissues with those of treated ones, one obvious difference between them was the increase in the overall compliance at the end of the creep phase.

For all melon and apple samples, the relative magnitude of the retardation time λ_1 was approximately ten times that of the retardation time λ_2. As these parameters represent the time required for the strain on structural elements associated with viscoelastic behavior to reach 63% of their maximum strain, the shorter retardation time of the second Voigt unit reflected the viscoelastic behavior of tissues over relatively short times. Thus, for both raw and treated tissues, the structural elements associated with this second Voigt unit would reach equilibrium faster than those contributing to the first Voigt unit.

For all fruit tissues assayed, the magnitudes of the viscoelastic compliances J_1 and J_2 were almost alike, indicating a similar elasticity of the structural elements involved. Light microscopy (LM), transmission electronic microscopy (TEM) and environmental electronic microscopy (ESEM) observations of raw and treated fruit tissues revealed many structure changes. Some results intended to relate structure changes with measured linear viscoelastic properties are next presented.

9.4.2. Melon: Effect of Osmotic Dehydration and Calcium Incorporation.

Some techniques for obtaining minimally processed high moisture fruit products with characteristics close to fresh ones are based on a combination of blanching, a slight reduction of water activity (a_w), control of pH, and incorporation of antimicrobial agents and other additives to improve color and texture (Alzamora et al., 1995). Water activity depression is usually performed by osmotic dehydration in concentrated sugar aqueous solutions with simultaneous incorporation of additives achieving final values after equilibration of $a_w = 0.94–0.98$. Osmotic dehydration processes at atmospheric pressure (AOD), under vacuum conditions (VOD) or by a combination of vacuum impregnation followed by large periods at atmospheric pressure, may be employed to reduce a_w and simultaneously incorporate additives. During AOD, plant cellular structure acts as a semi-permeable membrane, and water and solutes fluxes are usually considered as diffusion driven. When a porous fruit tissue is immersed in a solute concentrated solution under vacuum conditions, air is extracted from the pores and then, when atmospheric pressure is restored, the impregnation solution penetrates the intercellular spaces by capillary action and by pressure gradients (i.e., the hydrodynamic mechanism, HDM) that are imposed to the system, helping incorporation of solutes and additives and moisture removal (Fito, 1994). The substitution of internal gases by a liquid phase of adjustable composition allows direct formulation of a food by expeditious compositional modifications of the solid matrix, without exposing the food structure to the eventual stress due to long exposure to gradient solute concentration, as in the atmospheric process (Fito and Chiralt, 1997).

Water significantly affects wall rheology. As a solvent and a lubricant, water reduces physical interactions between wall polymers, thus facilitating wall creep. The hydration properties of cell wall materials are also expected to

influence their rheological behavior, since suspensions of cell wall materials with a high water binding capacity form suspensions with a high yield stress, high apparent viscosity and high elastic shear modulus (Kunzek et al., 1999).

Next, we would like to comment briefly on the micro and ultrastructure changes of melon tissues as affected by osmotic dehydration and the influence of these changes on rheological characteristics.

9.4.2.1. Treatment

In this example, melon (*Cucumis melo* L., Honey Dew variety) was hand peeled, and cut in half longitudinally. After discarding the central part and the part near the hull, melon halves were cut longitudinally into plates (≅ 60 mm × 60 mm × ≥ 6 mm). For osmotic dehydration at atmospheric pressure (AOD), samples were immersed in a 20% w/w aqueous glucose solution at 25°C to reach equilibrium a_w of 0.98. A large weight ratio of syrup/fruit (30:1) was used in the osmotic treatment to minimize the dilution effect on the glucose solution by water and glucose transport. In some experiments, calcium lactate (1000 ppm) was included in the osmotic medium.

For vacuum glucose impregnation (VOD), fruit samples were immersed in a 55% w/w aqueous glucose solution (weight ratio of syrup /fruit ≈ 15:1) at 25°C. The pH of the solution was adjusted with citric acid to a value of 1.7 to attain an average pH of 3.5 in the system after treatment. In order to inhibit microbial growth, 2000 ppm potassium sorbate were incorporated in the solution. A pressure equal to 35 Pa was applied to the system for 10 min, and then atmospheric pressure was restored for 10 min (final equilibrium a_w = 0.98) (Martínez et al, 2005). After osmotic treatment, melon samples were withdrawn from the osmotic medium, immersed in distilled water for 20 s, and put on blotting paper three times to eliminate superficial syrup.

9.4.2.2. Structural Changes

Microscopic studies revealed that the effect of osmotic dehydration to reduce a_w to 0.98 on melon tissue structure depended on the pressure and on the presence of calcium in the osmoticum (Mastrángelo et al., 2000; Martínez et al., 2005). As seen in LM (micrographs not shown), fresh tissue was composed of isodiametric cells in transversal sections of two size groupings, with moderate intercellular spaces, densely stained cell walls and parietal cytoplasm.

Treatments resulted in compression and deformation of cells, sinuous cell walls and increased intercellular contact, particularly in atmospheric treated tissue without calcium addition. Treated cells appeared less turgid and more polyhedral, with broken membranes in atmospheric infused tissues and plasmolysis of cytoplasm in vacuum treated samples.

Ultrastructural studies of the melon flesh in the fresh fruit demonstrated darkly stained cell walls with greater intensity toward the margin and in the central zone of the middle lamella, and a loose intermixed microfibrilar structure (Fig. 9.3A, B).

The arrangement of cytoplasm was marginal, with numerous invaginations of the plasma membrane. Tonoplast and plasmalemma appeared intact. Atmospheric osmotic dehydration caused folding and rupture of cell walls (microphotographs not shown) and breakage of cellular membranes with formation of coarse granules that were assembled along cell walls (Fig. 9.3C). Cell walls appeared with very much reduced staining in the central zone (putting into evidence a severe loss of material except near the wall surface) with disorganized microfibrils. When

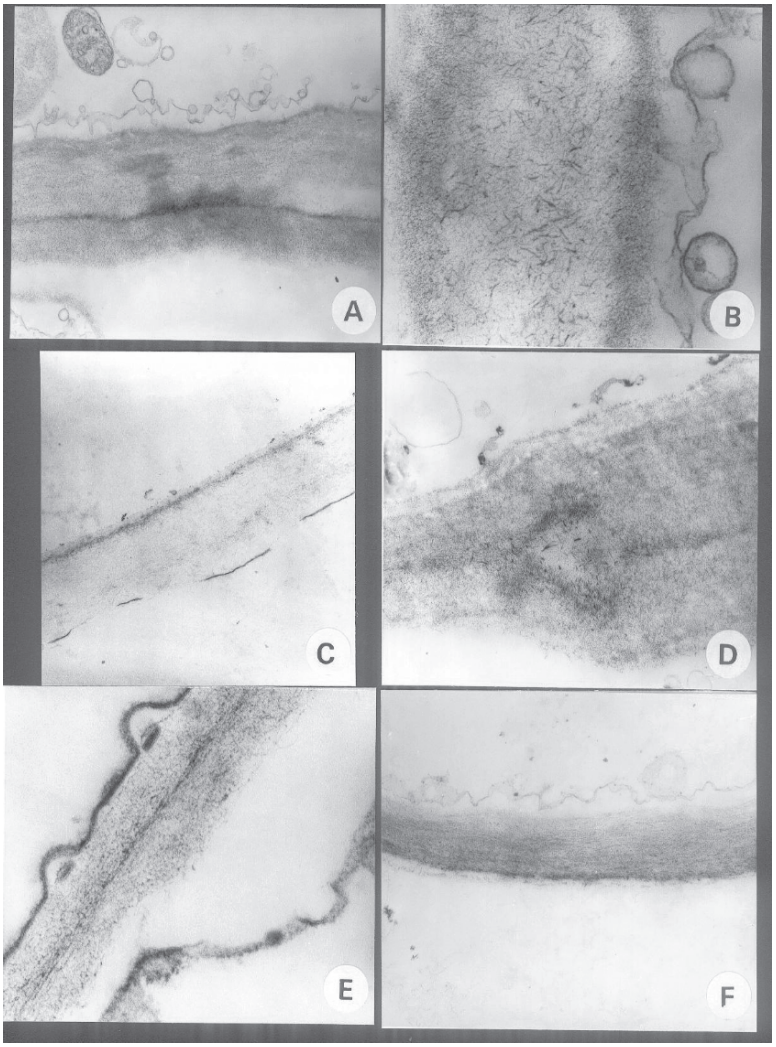

Fig. 9.3. TEM micrographs of melon flesh as affected by osmotic dehydration in a 20% w/w glucose aqueous solution at 20°C. A,B: fresh control; C,D: atmospheric treatment; E,F: vacuum treatment. C,E: without calcium; D,F: with calcium. Scale: A,C,D,F: 500 nm; B,E: 100 nm (adapted from Alzamora et al., 2000; Martinez et al., 2005)

atmospheric osmotic dehydration was performed in the presence of calcium, the cells showed walls with good electron density, a clear reticulate pattern, and broken membranes with vesicle formation (Fig. 9.3D).

Vacuum treatment caused slight plasmolysis of cellular membranes, but cell walls appeared with good electron density, with dense longitudinal fibrous staining and a notorious middle lamella (Fig. 9.3E). Addition of calcium during vacuum provoked a very dense longitudinal staining fiber pattern (Fig. 9.3F).

9.4.2.3. Viscoelastic Behavior

At any frequency, the storage and loss moduli of treated melon samples were smaller than those of the raw fruit (Fig. 9.4). Osmotic dehydration (at atmospheric

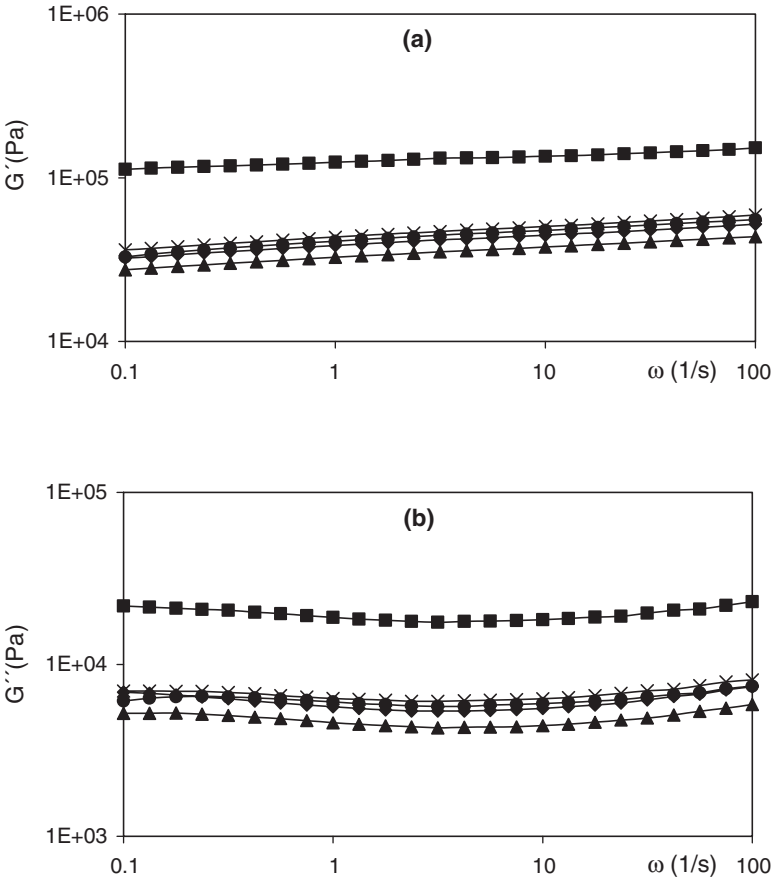

FIG. 9.4. Average complex modulus for fresh and osmotically dehydrated melon tissue in the frequency domain at a strain of 0.05 % (values represent mean of ≥ 12 determinations); a) storage modulus (G′); b) loss modulus (G″). ■: fresh; ▲: AOD; ●: AOD + calcium; ♦: VOD; ×: VOD + calcium

pressure or under vacuum, and with or without calcium incorporation) caused an approximately 3-fold decrease in G' of the tissue relative to the untreated melon. There were no significant differences ($p<0.05$) in the storage modulus of osmotically dehydrated tissues at atmospheric pressure or in vacuum. In the same way, calcium incorporation in the osmotic medium did not change the dynamic elastic modulus of tissues subjected to osmosis.

In general, the tan δ (G''/G') was not sensitive for distinguishing physical differences between raw or osmotically dehydrated melon tissues, or between osmotic treatments. At low frequency ($0.1 s^{-1}$), the tan δ was similar for all melon samples; at higher frequencies (1, 10 or $100 s^{-1}$), the small differences observed in tan δ values did not show any clear trend.

Creep compliance curves for melon exposed to the different treatments are presented in Fig. 9.5. Table 9.1 supplies the physico-mechanical parameters that defined the creep behavior of melon tissue obtained by applying Eq. (9.1) to the creep phase. The instantaneous elastic compliance J_0 increased significantly in value for osmotically dehydrated tissues relative to untreated tissue, revealing a decrease in the instantaneous elastic modulus E_0 (=1/ J_0). J_0 of melon subjected to osmotic dehydration at atmospheric pressure without calcium incorporation was greater ($p<0.05$) than that of melon osmotically dehydrated under vacuum (with or without calcium) or at atmospheric pressure with calcium in the osmoticum.

The viscoelastic compliances J_1 and J_2 of the recoverable regions of the creep compliance curves significantly increased in value ($p<0.05$) after the osmotic treatments. However, although calcium presence did not change the behavior observed in the sample upon vacuum, there were significant differences between osmotic dehydration treatments at atmospheric pressure with or without calcium in the osmotic medium.

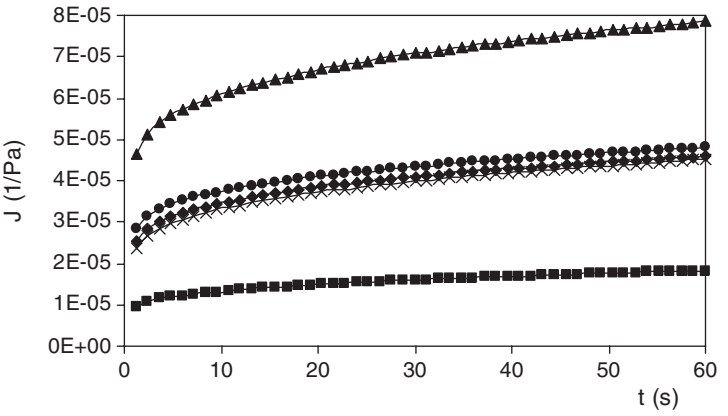

FIG. 9.5. Average creep compliance time curves for fresh and osmotically dehydrated melon tissue. ■: fresh; ▲: AOD; ●: AOD + calcium; ♦: VOD; ×: VOD + calcium. (Values represent mean of ≥ 12 determinations)

TABLE 9.1. Viscoelastic creep parameters* and relative contribution** of each type of compliance to overall compliance for fresh and osmotically dehydrated melon tissues

Sample	J_0 (1/Pa) ($\times 10^5$)	J_1 (1/Pa) ($\times 10^5$)	J_2 (1/Pa) ($\times 10^5$)	λ_1(s)	λ_2(s)	η_N(Pa.s) ($\times 10^{-6}$)
Fresh	0.7 ± 0.35 [a] (40)	0.4 ± 0.15 [a] (22)	0.3 ± 0.14 [a] (17)	14 ± 3.3 [a]	1.1 ± 0.37 [a]	16 ± 7.6 [a] (21)
AOD	4 ± 1.6 [d] (49)	1.6 ± 0.68 [c] (19)	1.4 ± 0.61 [d] (17)	15 ± 1.9 [a]	1.5 ± 0.17 [b]	5 ± 1.8 [b] (15)
AOD + Ca^{2+}	2.2 ± 0.56 [c] (45)	1.0 ± 0.23 [b] (20)	0.9 ± 0.24 [c] (17)	14 ± 1.4 [a]	1.4 ± 0.09 [b]	8 ± 3.7 [b] (15)
VOD	1.9 ± 0.19 [c] (42)	1.1 ± 0.46 [b] (24)	0.8 ± 0.19 [c] (18)	14 ± 1.6 [a]	1.4 ± 0.16 [b]	8 ± 0.4.5 [b] (16)
VOD + Ca^{2+}	1.8 ± 0.55 [c] (39)	1.1 ± 0.52 [b] (23)	0.9 ± 0.3 [c] (19)	14 ± 3.3 [a]	1.4 ± 0.27 [b]	7 ± 3.8 [b] (18)

* Parameters derived by fitting Eq (1) to compliance curves from the creep phase
Means in the same column with the same superscripts were not significantly different ($p<0.05$)
** Numbers in brackets express the relative contribution (%) of each type of compliance to the overall compliance at the end of the creep phase

Osmotic treatment at atmospheric pressure in the glucose solution without addition of calcium resulted in a melon tissue with higher J_1 and J_2 values, reflecting lower elasticity or stiffness associated with this process. A significant increase in the steady-state viscous compliance ($1 / \eta_N$) occurred in the samples exposed to the different osmotic treatments (the values of η_N were roughly 1/3–1/5 of the value of raw melon). In general, the greatest changes in the contribution of each type of compliance to overall softening process due to treatments were observed in the steady-state viscous properties and in the instantaneous elastic component; an increase in J_0 participation occurred concomitant with a reduction in the fluidity contribution. Retardation time λ_1 was not significantly affected by the different treatments, while retardation time λ_2 slightly increased for osmotically dehydrated tissues.

All of the treatments provoked a loss of cell turgidity due mainly to plasmolysis of cytoplasm and /or disruption of cellular membranes, but a significant difference in wall staining was observed among tissues subjected to atmospheric osmosis without calcium and the other osmotic treatments. Paradoxically, the rheological characteristics measured via dynamic oscillatory shear tests did not reveal any difference in the ultrastructure of the samples with different osmotic dehydration treatments. The considerable degradation of cell wall of melon tissue exposed to atmospheric osmotic dehydration could not be detected through G' and G'' values. In contrast, the instantaneous compliance (J_0) and the retarded compliances (J_1 and J_2) were the most sensitive parameters for distinguishing cell wall structural differences among osmotic treatments, and seemed to be the most useful tool in understanding cell wall structure of melon.

The elastic response of plant tissues has been attributed to: 1) cellulose, the main component of the cell wall, which provides individual cells with rigidity

and resistance to rupture (John and Dey, 1986; Pitt, 1992); 2) the occluded air in the porous matrix; and 3) the turgor pressure (i.e., the outwardly directed pressure exerted by the content of the cell on the wall), which leads to the rigidity of plant cells and tissues, and, together with the cell wall, provides the mechanical support for maintaining cell and tissue shape (Bourne, 1976; Alzamora et al., 2000). A linear relation has been previously observed between turgor and the dynamic elastic modulus (G) of tomato, kiwifruit, potato and apple (Lin and Pitt, 1986; Jackman et al., 1992; Rojas et al., 2001). In melon, the turgor pressure and the air of intercellular spaces (induced elasticity of cells and tissues) could largely be responsible for G' values. All osmotic treatments provoked loss of turgor and a decrease in intercellular spaces and occluded air, diminishing in a similar way G' values. The loss of elasticity could partially be explained by the air-liquid exchange, because the air (elastic character) was substituted by an incompressible liquid during the osmotic process. The apparent modification in the disposition of microfibrils of cell wall by the treatments, mainly AOD, was not reflected in this parameter, and/or its effect was masked by the large standard deviation due to tissue variability. Various structural modifications may contribute to disassembly and loosening of primary cell walls and cell turgidity of fruits during processing, affecting creep response. The complexity of these changes has made it difficult to determine the significance of the individual structural elements on creep parameters. Jackman and Stanley (1995b) proposed an interpretation of a similar 6-element creep model with respect to cell wall structure and biochemical changes in tomato pericarp tissue during ripening. This interpretation could be adapted for melon behavior as follows. Instantaneous elastic compliance J_0 could be related to the combination of turgor and primary cell wall strength as dictated by cellulose. Viscoelastic compliances J_1 and J_2 could be attributed to time-dependent changes in pectins and hemicelluloses, respectively. Steady-state viscosity could be related to cell wall fluidity arising from exosmosis and/or solubilization and degradation of polymers and less water binding capacity due to treatments.

9.4.3. Apple: Effect of Osmotic Dehydration Time

Mass transfer during osmotic dehydration of fruit tissues takes place simultaneously with physical, microstructural and macrostructural modifications, and transport mechanisms are difficult to clarify because of the complex morphology of plant tissues.

Water plays a key role in determining perceived fruit texture. Much of the past work on osmotic dehydration has focused on the kinetics of solute/water exchange in and out of tissue. Although various data published in the literature reveal that osmotic dehydration strongly affects the mechanical properties of plant tissues, there is sparse information on the way the mechanical properties of plant tissues (especially at small deformations) change through osmotic treatment. Knowledge of these relations would provide an important tool in understanding the mechanical response of apple tissue to water stress and solute uptake.

In this example, the evolution of linear viscoelastic properties and ultrastructure and macrostructure (porosity, solid-liquid and bulk densities) features of apple parenchymatous tissue undergoing osmotic process at atmospheric pressure was described (Nieto et al., 2004; Martinez, 2005).

9.4.3.1. Treatment

Fresh apples (*Malus pumila*, Granny Smith cultivar; 86 % w/w moisture content, wet basis; soluble solids content ≅ 12 °Brix) were hand peeled, cut parallel to the main axis using a lathe to obtain outer parenchyma slabs (≅ 60 mm × 60 mm × ≥ 6 mm for rheological tests and approximately 60 mm × 60 mm × 4 mm for structure examinations) and subjected to osmotic process. Osmotic dehydration was performed by immersing the apple slabs of fresh fruit in a 25.0% w/w glucose aqueous solution with forced convection at atmospheric pressure and 20°C to reach equilibrium at a_w of 0.97.

The agitation level was chosen in order to make the surface mass transfer resistance negligible. A large weight ratio of syrup/apple (60/1) was used in osmotic treatment to minimize the dilution effect on the glucose solution by water and glucose transport. Apple samples were taken out of the osmotic medium at selected time intervals up to 360 min, immersed in distilled water for 20 s, and put on blotting paper to eliminate superficial syrup.

9.4.3.2. Structural Features

The solid-liquid density of apple tissue (ρ_s) increased slowly but steadily throughout the osmotic process. However, during the early drying stages, the bulk density (ρ_b) increased up to a certain value until 50 min and then decreased with increasing time. Accordingly, a decrease in porosity (ε) was observed at approximately 50 min. After this period of time, a recovery in sample porosity was noted, although the values were lower than for fresh fruit.

The evolution of ρ_b and ε values could be clearly correlated with microscopic observations and explained by considering the structural tissue alterations associated with the osmotic process (Nieto et al., 2004). Apple tissue structure depended on the time of osmotic dehydration. As seen in LM (micrographs not shown), cells and intercellular spaces in the fresh tissue were loosely arranged in a net-like pattern that was inhomogeneous and anisotropic. The cell wall and the middle lamella were observed as a unique markedly electron-dense region between cells. Turgor pressure forced the plasma membrane tightly against the cell wall. The large amount of cell volume was occupied by the central vacuole and the protoplasm, bounded by the plasmalemma and the tonoplast, was present as a thin layer lining the cell surface. After 50 min of osmotic dehydration in the glucose solution, cell structure appeared clearly affected by plasmolysis. There was shrinkage of the tissue and reduction of intercellular spaces, phenomena that would contribute to a decrease in porosity, and cell-to-cell contact increased. In some cells, rupture of cellular membranes was also noted.

Folding of cell walls was observed, indicating some ultrastructural cell wall impact by the treatment. At 125 min immersion, cells seemed to partially recover their shape. Finally, at 200 min treatment, tissue arrangement was observed to be more similar to the control. The cells recovered their shape and looked even more rounded than in the control, and an increase in the size of intercellular spaces occurred. Plasmalemma was apparently intact in many cells, although plasmolysis was maintained. Cell walls also appeared intact, but with lower density of staining. Bulk density exhibited a maximum at around 50 min of treatment (and in consequence, porosity value would present a minimum), when micrographs sustained significant cell collapse and reduced intercellular spaces.

Figure. 9.6 shows the ultrastructural modification of apple tissue at selected times of immersion in 25.0% (w/w) glucose aqueous solution monitored by ESEM and clearly illustrates some of these findings. Tissues of the fresh sample showed conspicuous intercellular spaces (Fig. 9.6A). Cells appeared turgid with an apparent consistent cell wall structure. In some areas, a well defined middle lamella between cells was also observed. Cells were more or less regular in shape, in general, isodiametric, arranged in a loose pattern and attached along extended contact areas.

Samples treated during 50 min showed a general collapse of tissues and folding of cells walls (Fig. 9.6B). An important reduction in intercellular spaces was also observed. At 200 min immersion, cells recovered their shape (some of them appeared more rounded than in the fresh sample), tissue arrangement was similar to the control, and the size of intercellular spaces increased (Fig. 9.6C).

This structure behavior was mainly explained by considering osmosis as a multicomponent diffusion process through porous media and due to the relaxation of the viscoelastic shrunken cell walls, since osmoregulation could not explain cell shape recovery except at the beginning of the osmotic process (Nieto et al., 2004).

9.4.3.3. Viscoelastic Behavior

Osmotic treatment significantly ($p < 0.05$) influenced the oscillatory strain properties of outer apple parenchyma tissue. Both dynamic moduli were reduced due to processing; the fruit softened and became less viscous and less elastic. Samples osmotically dehydrated during 40 min showed a 2-fold decrease in G' as compared with the fresh tissue.

There were no significant differences ($p < 0.05$) in the storage modulus between samples treated during 40, 55 or 90 min at an angular frequency of $0.1\ s^{-1}$ and between samples treated during 40 and 55 min or 40 and 90 min at higher frequencies (1, 10 and $100\ s^{-1}$). However, G' values of samples treated during 55 min were significantly higher than those corresponding to 90 min treated apples at 1, 10 and $100\ s^{-1}$.

Thereafter, G' values steadily decreased with osmosis treatment time until they reached a plateau (approximately 4 or 5-fold decrease) at nearly 180 minutes of osmosis. At the lower testing frequency, the phase angle appeared not to

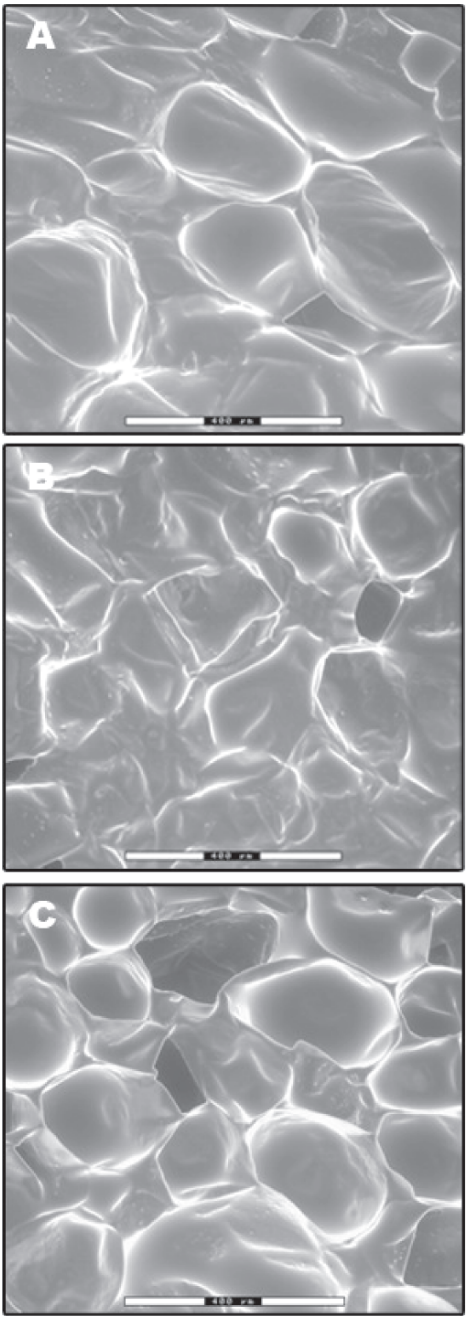

FIG. 9.6. ESEM micrographs of parenchyma tissue of apple illustrating the effect of osmotic dehydration time in a 25% w/w glucose aqueous solution at 30°C. A: fresh; B: after 50 min; C: after 200 min. Scale: 400 nm

be influenced by the osmotic treatment, excepting for 40 and 55 min processed apples, which exhibited a greater viscous effect on the complex modulus than the fresh fruit. In contrast, at angular frequency of 100, 10 and 1 s^{-1}, the loss and storage moduli did not change proportionately to each other. It is to be noted that in the early stages of the process (approximately 40 min), a faster water loss and solids uptake were observed, followed by a gradual change in both parameters as osmosis proceeded. Up to 360 min of contact time, moisture and soluble solids content of apple slices continued changing (Martinez, 2005).

The creep compliance curves for apple samples exposed to different times of osmosis are shown in Fig. 9.7, and the physico-mechanical parameters that defined creep behavior are supplied in Table 9.2.

After 40 min treatment, the instantaneous and fully recoverable elastic compliance, J_0, and the discrete retarded elastic or viscoelastic compliances, J_1 and J_2, for osmotically dried apples showed a significant increase relative to untreated tissues. Afterwards, J_0 and J_2 parameters continued increasing until 360 min of osmosis, while J_1 value showed a slight decrease at 90 min of osmosis as compared with the one registered at 55 min of osmosis. On the other hand, the instantaneous compliance J_0 was approximately two to three folds that of J_1 and J_2, so the retarded viscoelastic elements had a greater elasticity than the instantaneous element. There were no significant differences ($p < 0.05$) between steady-state viscous compliance ($1/\eta_N$) values of apples subjected to glucose impregnation for different times, but these values were significantly greater than that of fresh apple. However, when only apples subjected to osmotic treatment were compared, there were significant differences between the steady-state viscous compliance of apples treated 55 min and the rest (statistical data not shown).

In general, the greatest changes in the contribution of each type of compliance to the overall softening process due to osmosis were observed in samples treated during 40, 55 and 90 min. For greater times of treatment, the relative

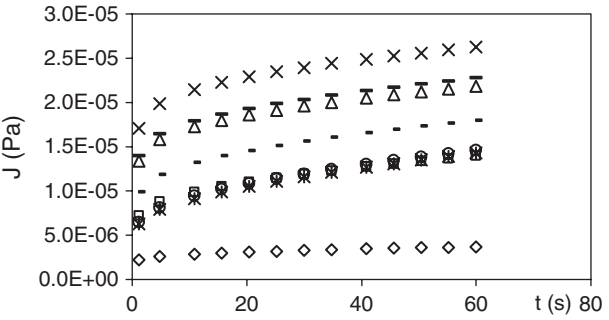

FIG. 9.7. Average creep compliance time curves for apple tissue as affected by glucose osmotic treatment ◊: fresh; osmotically dehydrated: *: 40 min; ○: 55 min; □: 90 min; –: 120 min; △: 180 min; —: 255 min; ×: 360 min. (Values represent mean of ≥ 12 determinations)

TABLE 9.2. Viscoelastic creep parameters*, plasticity (P) and relative contribution ** of each type of compliance to overall compliance of apple tissue as affected by osmotic dehydration time at atmospheric pressure

AOD (min)	J_0 (1/Pa) ($\times 10^6$)	J_1 (1/Pa) ($\times 10^6$)	J_2 (1/Pa) ($\times 10^6$)	λ_1 (s)	λ_2 (s)	η_N (Pa s) ($\times 10^{-7}$)	P (%)
Fresh	1.7 ± 0.4^{a} (49)	0.6 ± 0.1^{a} (17)	0.6 ± 0.2^{a} (17)	13 ± 2.9^{a}	1.2 ± 0.2^{a}	11 ± 4^{a} (16)	15.9
40	4.6 ± 0.6^{b} (35)	2.7 ± 0.5^{b} (20)	2.0 ± 0.2^{b} (15)	14.3 ± 0.9^{abc}	1.38 ± 0.07^{bc}	1.5 ± 0.2^{b} (30)	30.2
55	5.4 ± 0.3^{bc} (32)	3.3 ± 0.3^{cd} (19)	2.20 ± 0.09^{bc} (13)	15.0 ± 0.9^{bc}	1.5 ± 0.1^{c}	0.98 ± 0.07^{b} (36)	36.1
90	6.3 ± 0.9^{cd} (45)	2.5 ± 0.3^{b} (17)	2.2 ± 0.2^{bc} (16)	14.4 ± 1.0^{abc}	1.39 ± 0.08^{bc}	1.9 ± 0.2^{b} (22)	22.4
120	7.6 ± 0.9^{d} (46)	2.9 ± 0.4^{bc} (17)	2.7 ± 0.3^{c} (16)	15 ± 1.4^{c}	1.43 ± 0.04^{c}	1.8 ± 0.3^{b} (20)	20.2
180	10 ± 1.6^{e} (48)	3.2 ± 0.4^{cd} (15)	3.8 ± 0.6^{d} (18)	13 ± 1.5^{ab}	1.3 ± 0.2^{ab}	1.6 ± 0.3^{b} (18)	18.1
255	11 ± 1.9^{f} (49)	3.5 ± 0.6^{d} (15)	4.1 ± 0.6^{d} (18)	15 ± 0.3^{abc}	1.3 ± 1.1^{ab}	1.5 ± 0.3^{b} (18)	17.7
360	14 ± 1.6^{g} (51)	4.2 ± 0.7^{e} (15)	5.2 ± 0.8^{e} (19)	12.7 ± 0.7^{a}	1.3 ± 0.4^{ab}	1.4 ± 0.2^{b} (15)	15.5

* Parameters derived by fitting Eq (1) to compliance curves from the creep phase
Means in the same column with the same superscripts were not significantly different ($p < 0.05$)
** Numbers in brackets express the relative contribution (%) of each type of compliance to the overall compliance at the end of the creep phase

contribution of each type of compliance exhibited a similar pattern as in the fresh fruit. Degree of plasticity P (i.e., the ratio of unrecoverable or permanent deformation to the total deformation) is also shown in Table 9.2. All apple samples exhibited plastic strain, which remained unrecovered in the creep recovery test. Apple tissues subjected to 40 and 55 min osmosis underwent considerable plastic deformation. Thereafter, osmosis treatment provoked a gradual reduction of unrecovery deformation, with the plasticity of 360 min-treated apples being similar that of raw apple.

The overall compliance at the end of the creep phase in general showed an increase throughout osmotic drying, but at 40 and 120 min treatment, the values were slightly lower as compared with samples corresponding to 55 min osmosis.

As can be observed in Fig. 9.6, for short times of osmosis, there was a collapse of the tissue immersed in glucose aqueous solution, and cells showed shrinkage and folding and deformation of walls. Toward the end of treatment, cells appeared more rounded, and the cell arrangement was more similar to the fresh sample, indicating a shape recovery, though plasmolysis increased steadily as moisture content decreased. These structural changes observed at short-term osmotic dehydration process were reflected in the rheological properties. Between 40 and 90 min of osmosis, many rheological parameters (G' at frequencies in the range 1–100 s^{-1}; loss tangent at 0.1 s^{-1}, J_1, relative contribution

of each type of compliance, η_N, plasticity and overall compliance) showed a turning point, fluctuations or the greatest changes in the evolution along treatment. The times at which this behavior was observed were slightly greater than those at which considerable contraction and posterior re-swelling of tissue were detected in microscopic experiments because of the greater thickness of apple slices used in rheological analysis.

Both employed tests, oscillatory and creep recovery, were sensitive for distinguishing cell wall structure changes during osmotic dehydration, but only the creep test was sensitive enough until the end of the osmosis, since G' values reached a plateau at aproximately 180 min, while compliance values continued varying as with moisture and soluble solids contents.

Many mechanisms (in series and/or in parallel, acting in different periods of osmosis), such as cell homeostasis, multicomponent diffusion and tissue relaxation, could be responsible for the shrinking and posterior re-swelling of the cells (Nieto et al., 2004). Assuming G' is related to turgor pressure, the slight fluctuations of the parameter observed at 40–90 min osmosis could be partially due to the turgidity recovery by living cells by basal permeability. The cell viability of 0.6 cm thick apple slices was also monitored by LM observations with fluorescein diacetate (Martinez, 2005). Fluorescence steadily decreased from 0 to 55 min osmotic treatment, indicating a reduction in the fraction of viable cells. At 90 min of osmosis, fluorescence was no longer detected. After 90 min, as the air in the intercellular spaces continued decreasing and the turgor pressure was reduced due to cell death, G' decreased.

Increased cell wall fluidity at short times of osmosis could be the result of: a) the greater amount of apoplastic water due to plasmolysis or membrane breakage, and b) the solubilization and depolymerization of pectins and hemicelluloses during immersion in the aqueous solution. It is well known that the degree of polymerization of any polymer is generally of importance on the viscosity (Ferry, 1980), and this property may decrease rapidly after degradation of only a few glycosidic linkages. The greater plasticity exhibited after 40 to 55 min would be related to the high amount of water lost to apoplast at the beginning of the process. Afterwards, as water re-entered into the shrunken cells, the unrecovered strain decreased.

9.4.4. Apple: Effect of Calcium Fortification

The promotion of foods enriched with minerals is increasing because of the high consumer interest in products that improve the capacity to resist disease and enhance health (Gibson and Williams, 2000). Adequate calcium intake has been associated with reduced risk of osteoporosis, hypertension, colon cancer, kidney stones and lead absorption (Goldberg, 1994). Because of their appreciated sensory, nutritional and functional properties, fruits and vegetables might be ideal matrices for calcium fortification. Some previous studies have demonstrated the feasibility of these matrices (apple, eggplant, mushroom, carrot, melon, etc.) to support vacuum and/or atmospheric impregnation techniques with bioactive compounds,

providing novel functional product categories and new commercial opportunities (Betoret et al., 2001; Mújica-Paz et al., 2002; Alzamora et al., 2005; Ortiz et al., 2003; Tapia et al., 2003; Gras et al., 2002, 2003; Anino et al., 2006). Calcium impregnation capability of parenchymatous apple tissue by different impregnation techniques and the effect of these treatments on mechanical properties at large deformations were studied by Anino et al. (2002, 2006). The effect of calcium fortification on the viscoelastic linear behavior of apple tissue using oscillatory shear and creep tests was next analyzed.

9.4.4.1. Treatment

Apples (Granny Smith var.; a_w 0.98; 11.6 °Brix and pH 3.4) were peeled and cut into slabs (0.60 ± 0.03 cm thickness).

Calcium impregnation experiments were performed at room temperature and atmospheric pressure by immersing the fruit into agitated isotonic glucose aqueous solutions containing 5.24% (w/w) Ca^{++} salts. A mixture of Ca^{++} lactate and Ca^{++} gluconate was chosen because of its relatively high solubility at room temperature and the neutral taste imparted to the food. Potassium sorbate (1500 ppm) was added to all of the systems and the pH was adjusted to 3.5 by the addition of citric acid to inhibit and/or retard microbial growth.

Calcium impregnation was conducted under conditions of internal control. Samples were withdrawn from the solutions at different times (0, 2, 6, 10 and 22 h), put on blotting paper to eliminate superficial solution, cut into discs (3 cm in diameter) with a cork borer and analyzed for rheological and structural characteristics.

9.4.4.2. Structural Features

Calcium incorporation resulted in many structural changes. Some LM and TEM microphotographs of 2 h, 6 h and 22 h treated apples, as compared with fresh fruit, are shown in Fig. 9.8. In the fresh tissue, arrangement of cells and intercellular spaces was inhomogeneous and anisotropic (Fig. 9.8A). Cells showed central vacuoles, parietal cytoplasmic layers and darkly stained walls with a tight longitudinal fiber pattern (Fig. 9.8C). Some cells exhibited a very neat middle lamella (micrographs not shown). After 2 h immersion in the calcium-containing isotonic solution, the wall looked reinforced in the region of the middle lamella, probably due to calcium-pectin interaction (Fig. 9.8D).

Crystals of calcium salts also appeared between the cell wall and the plasmalemma, detaching the cytoplasm and pushing it further into the cell. After 6 h immersion in calcium-containing solution, the cytoplasm appeared separated from the wall and in some cells membranes looked broken with vesicle formation (Fig. 9.8E).

Despite that calcium incorporation resulted in darkly stained cell walls with a middle lamella clearly reinforced in some regions, extensive folding of cell walls occurred. Crystals of calcium salt appeared located not only

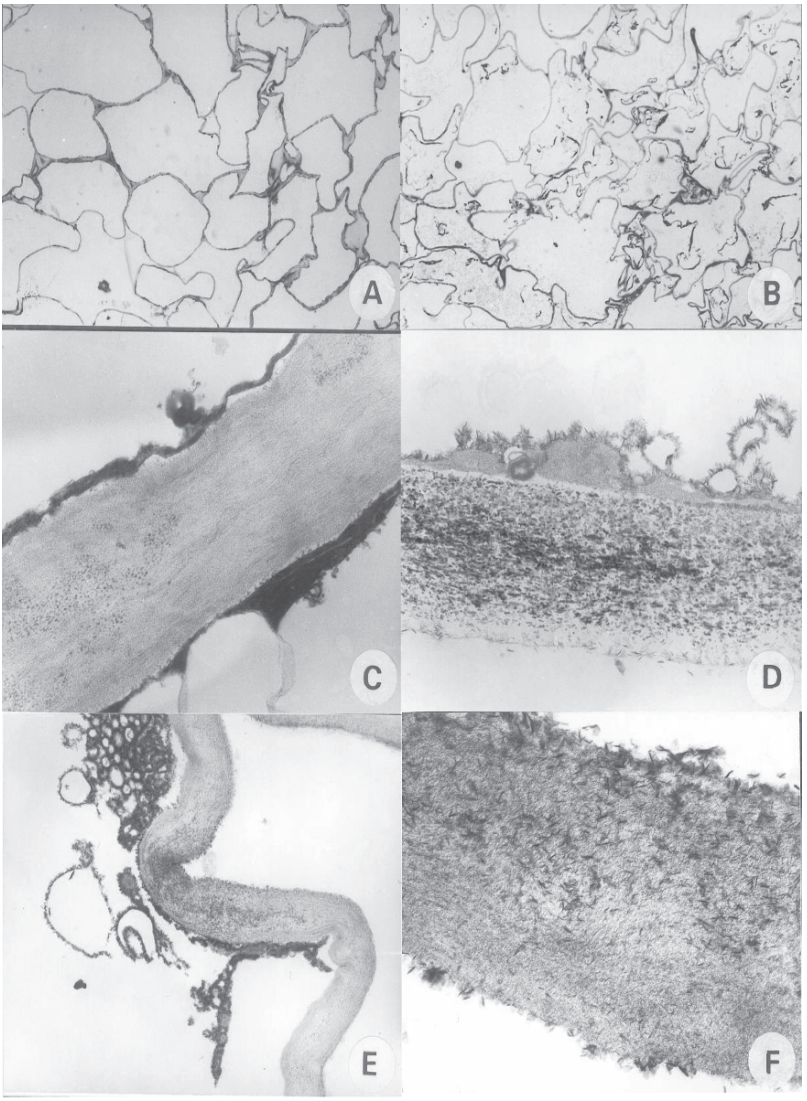

FIG. 9.8. LM and TEM microphotographs of apple tissue subjected to calcium fortification in an isotonic glucose solution at atmospheric pressure. A,B: LM; C-F: TEM. A,C: fresh apple; D: 2 h immersion; E: 6 h immersion; F: 22 h immersion. Scale: A,B: 100 μ; C,D,F: 200 nm; E: 500 nm

between the cell wall and the plasmalemma, but also in the other side of the plasmalemma and into the cytoplasm, so that deposition of calcium could be seen in the intercellular spaces, along the walls and in the lumen of the cells of impregnated apples (micrographs not shown).

After 22 h immersion, cell walls appeared with a very high electronic density, although with loose intermixed network pattern, very different from the longitudinal one of the fresh fruit (Fig. 9.8F). Membranes were completely disrupted and cells appeared deformed with folded and angular walls (Fig. 9.8B).

9.4.4.3. Viscoelastic Behavior

The elastic modulus G' diminished with impregnation time until 6 h treatment and then, as calcium impregnation proceeded, remained constant. The viscous modulus G" also decreased along the process until 6 h immersion, but to a lesser extent than G' (data not shown). This fact would indicate that apple matrix became less elastic as treatment proceeded.

A similar trend with calcium impregnation time was shown by creep compliance curves (Fig. 9.9). Fresh tissue exhibited lower values of compliances (instantaneous and viscoelastic) and fluidity than calcium-fortified samples (Table 9.3). An increase in J_0, J_1 and J_2 values with process time was observed until 6 h treatment, with no significant differences between compliances of tissues impregnated for long periods of time (6 h to 22 h). Retardation times λ_1 and λ_2 did not change by the treatments. There were no significant differences ($p < 0.05$) between steady-state viscous compliance ($1/\eta_N$) values of apples treated for different times, but these values were significantly greater than that of fresh apple.

The presence of calcium in the wall matrix helped to maintain middle lamella integrity, since it promoted cross-linking of pectic polymers, as demonstrated by LM and TEM photographs. In addition, calcium would make pectic macromolecules of the cell wall less soluble through the formation of bridges

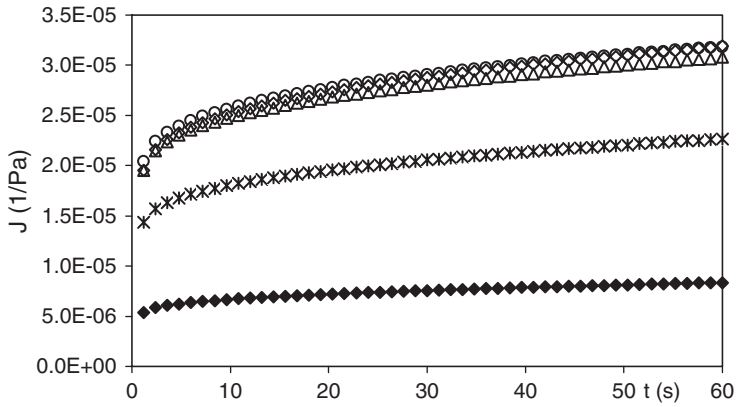

FIG. 9.9. Average creep compliance time curves for apple tissue as affected by calcium impregnation in an isotonic glucose solution. ♦: t = 0 (fresh); ∗: 2 h immersion; ○: 6 h immersion; ◊: 10 h immersion; △: 22 h immersion. (Values represent mean of ≥ 12 determinations)

TABLE 9.3. Viscoelastic creep parameters* of apple tissue as affected by different exposure times to calcium

Treatment	J_0 (1/Pa) ($\times 10^6$)	J_1 (1/Pa) ($\times 10^6$)	J_2 (1/Pa) ($\times 10^6$)	λ_1(s)	λ_2 (s)	η_N (Pa s) ($\times 10^{-7}$)
Raw tissue	4.1 (0.3)[a]	1.52 (0.12)[a]	1.70 (0.2)[a]	19 (3)[a]	1.31 (0.15)[a]	60 (34)[a]
2 h	11.8 (1.1)[b]	3.5 (0.3)[b]	3.8 (0.3)[b]	13.1 (0.5)[a]	1.4 (0.05) [a]	1.73 (0.13)[b]
6 h	16.3 (0.6)[c]	5.2 (0.3)[d]	6.1 (0.3)[c]	12.8 (0.6)[a]	1.27 (0.05)[a]	1.27 (0.09)[b]
10 h	15.2 (0.8)[c]	5.3 (0.2)[d]	6.2 (0.3)[c]	13.1 (0.5)[a]	1.30 (0.06)[a]	1.17 (0.06)[b]
22 h	15.6 (1.0)[c]	4.9 (0.3)[d]	5.8 (0.3)[c]	12.9 (0.4)[a]	1.33 (0.04) [a]	1.32 (0.06)[b]

*Parameters derived by fitting Eq. (1) to compliance curves from the creep phase
Means in the same column with the same superscripts were not significantly different ($p < 0.05$)
Numbers in brackets express the standard error

between them. This fact would also help to counteract the solubilization and depolymerization of pectins and hemicelluloses of the wall occurring during immersion in the aqueous solution. The extension of these reactions increased with immersion time, contributing to wall loosening and disintegration. However, the penetration of calcium also provoked a severe internal disruption in the cell, and a considerable loss of tissue rigidity occurred. As calcium incorporation proceeded, the number of cells that lost turgidity due to breakage of membranes by calcium crystals increased. Accordingly, G' values diminished with immersion time until 6 h treatment, when a generalized rupture of tonoplast and plasmalemma was observed. Further exposure to calcium solution did not modify the value of the storage modulus.

Moreover, in spite of the clearly stained cell walls and of the high calcium concentration achieved in the matrix (approximately 1300 ppm, 1600 ppm and 3100 ppm after 6, 10 and 22 h immersion, respectively) (Anino et al., 2006), the extensive folding of cell walls indicated that the wall network of treated tissues had a mechanical resistance very much reduced as compared with that of raw fruit. This change in wall characteristics will result in greater compliance values.

9.5. Conclusions

Understanding fruit rheology is of major concern, since the mechanical properties of fruits are linked to the perceived texture. The present chapter constitutes clear experimental evidence of the significance of tissue structure in linear viscoelastic properties of processed fruits.

Plant tissues are very complex, and establishing a causal relation between main fruit structure elements and viscoelastic parameters determined by instruments is a complicated work.

Mechanical models, due to their simplicity, sound physical basis and remarkable computational efficiency, could be a good alternative, not only in

the characterization of viscoelastic fruit tissues, but in developing a structural model of cell rheological behavior.

References

Alzamora, S.M., Castro, M.A., Nieto, A.B., Vidales, S.L., and Salvatori D.M., 2000, The Role of Tissue Microstructure in the Textural Characteristics of Minimally Processed Fruits, in: *Minimally Processed Fruits and Vegetables,* S.M. Alzamora, M.S. Tapia and A. López-Malo (eds.), Aspen Publishers Inc., Gaithersburg, pp. 153–171.

Alzamora, S.M., Cerrutti, P., Guerrero, S., and López-Malo A., 1995, Minimally Processed Fruits By Combined Methods, in: *Food Preservation by Moisture Control: Fundamentals and Applications,* G.V. Barbosa-Cánovas, and J. Welti-Chanes (eds.), Technomics Publishing Co., Lancaster, pp. 463–492.

Alzamora, S.M., Salvatori, D.M., Tapia, M.S., López-Malo, A., Welti-Chanes, J., and Fito P., 2005, Novel Functional Foods from Vegetable Matrices Impregnated with Biologically Active Compounds, *J. Food Eng*. **67**:205.

Anino, S.V., Salvatori, D.M., and Alzamora S.M., 2006, Changes in Calcium Level and Mechanical Properties of Apple Tissue Due to Impregnation with Calcium Salts, *Food Res. Int*. **39**:154.

Anino, S., Salvatori, D.M., Castro, M.A., and Alzamora S.M., 2002, Cambios Estructurales en Tejido de Manzana Fortificado con Calcio, *IX Congreso Argentino de Ciencia y Tecnología de Alimentos. Asociación Argentina de Tecnólogos Alimentarios*, Buenos Aires.

Betoret, N., Fito, P., Martínez-Monzó, J., Gras, M.L., and Chiralt A., 2001, Viability of Vegetable Matrices as Support of Physiologically Active Components, in: *Proceedings of the International Congress on Engineering and Food (ICEF 8)*, vol. II, J. Welti-Chanes, G.V.Barbosa-Cánovas, and J.M. Aguilera, (eds.), Technomic Publishing Co., Inc., Lancaster, pp. 1366–1371.

Bourne M.C., 1976, Texture of Fruits and Vegetables, in: *Rheology and Texture in Food Quality,* J.M. DeMan, P.W. Voisey, V.F. Rasper, and D.W. Stanley (eds.), Van Nostrand Reinhold/AVI, New York, pp. 275–307.

Brett, C.T., and Waldron K.W., 1996, *Physiology and Biochemistry of Plant Cell Walls,* 2nd ed., Chapman & Hall, London.

Brownleader, M.D., Jackson, P., Moabsheri, A., Pantelides, A.T., Sumar, S. Trevan M., and Dey P.M., 1999, Molecular Aspects of Cell Wall Modifications During Fruit Ripening, *Crit. Rev. Food Sci. Nutr*. **39**:149.

Carpita, N.C., and Gibeaut D.M., 1993, Structural Models of Primary Cell Walls in Flowering Plants: Consistency of Molecular Structure with the Physical Properties of the Walls During Growth, *Plant J*. **3**:1.

Cosgrove D.J., 1997, Relaxation in a High-Stress Environment: The Molecular Bases of Extensible Cell Walls and Cell Enlargement, *Plant Cell* **9**:1031.

Cosgrove D.J., 1998, Cell Wall Loosening by Expansions, *Plant Physiol*. **118**:333.

Chappell, T.W., and Hamann D.D., 1968, Poisson's Ratio and Young's Modulus for Apple Flesh Under Compresive Loading, *Trans. Am. Soc. Agric. Eng*. **11**:608.

Datta, A., and Morrow C.T., 1983, Graphical and Computational Analysis of Creep Curves, *Trans. Am. Soc. Agric. Eng*. **26**:1870.

De Baerdemaeker, J.G. and Segerlind L.J., 1976. Determination of Viscoelastic Properties of Apple Fresh, *Trans. ASAE* **19**:346, 353.

Ferry J.D., 1980, *Viscoelastic Properties of Polymers,* 3rd ed., Wiley, New York.
Fito P., 1994, Modelling of Vacuum Osmotic Dehydration of Foods, *J. Food Eng*. **22**:313.
Fito, P., and Chiralt A., 1997, An Approach to the Modeling of Solid Food-Liquid Operations: Application to Osmotic Dehydration, in: *Food Engineering 2000,* P. Fito, G. Barbosa-Cánovas, and E. Ortega, (eds.), Chapman & Hall, New York, pp. 231–269.
Gibson, G.R., and Williams C.M., 2000, *Functional Foods. Concept to Product*, Woodhead Publishing Limited, Cornwall, pp. 1–27.
Goldberg I., 1994, *Functional Foods, Designer Foods, Pharmafoods, Nutraceuticals*, Chapman & Hall., New York, USA.
Gras, M., Vidal-Brotons, D., Betoret, N., Chiralt, A., and Fito P. 2002, The Response of Some Vegetables to Vacuum Impregnation, *Innov. Food Sci. Em. Technol*. **3**:263.
Gras, M.L., Vidal, D., Betoret, N., Chiralt, A., and Fito P., 2003, Calcium Fortification of Vegetables by Vacuum Impregnation Interactions with Cellular Matrix, *J. Food Eng*. **56**:279.
Ilker, R., and Szczesniak A.S., 1990, Structural and Chemical Bases for Texture of Plant Foodstuffs, *J. Text. Stud*. **21**:1.
Jack, F.R., Paterson, A., and Piggot J., 1995, Perceived Texture: Direct and Indirect Methods for Use in Product Development, *Int. J. Food Sci. Technol*. **30**:1.
Jackman, R.L., Marangoni, A.G., and Stanley D.W., 1992, The Effects of Turgor Pressure on Puncture and Viscoelastic Properties of Tomato Tissue, *J. Text. Stud*. **23**:491.
Jackman, R.L., and Stanley D.W., 1995a, Perspectives in the Textural Evaluation of Plant Foods, *Trends Food Sci. Technol*. **6**:187.
Jackman, R.L., and Stanley D.W., 1995b, Creep Behaviour of Tomato Pericarp Tissue as Influenced by Ambient Temperature Ripening and Chilled Storage, *J. Text. Stud*. **26**:537.
John, M.A., and Dey P.M., 1986, Postharvest Changes in Fruit Cell Walls, *Adv. Food Res*. **30**:139.
Khan, S.A., Roger, J.R., and Raghavan S.R., 1997, Rheology: Tools and Methods, in: *Aviation Fuels with Improved Fire Safety,* Proceedings.The National Academy of Sciences USA, Washington D.C., pp. 39–46.
Kunzek, H., Kabbert, R., and Gloyna D., 1999, Aspects of Material Science in Food Processing: Changes in Plant Cell Walls of Fruits and Vegetables, *Z. Lebensm. Unters Forsch. A*. **208**:233.
Lin, T.T., and Pitt R.E., 1986, Rheology of Apple and Potato Tissue as Affected by Cell Turgor Pressure. *J. Text. Stud*. **17**:291.
Martinez, V.Y., 2005, Alteraciones Microestructurales y Ultraestructurales de Tejidos Vegetales Mínimamente Procesados. Impacto en las Características Mecánicas. Thesis, University of Buenos Aires.
Martínez, V.Y., Nieto, A.B., Viollaz, P.E., and Alzamora S.M., 2005, Viscoelatic Behaviour of Melon Tissue as Influenced by Blanching and Osmotic Dehydration, *J. Food Sci*. **70**:12.
Mastrángelo, M.M., Rojas, A.M., Castro, M.A., Gerschenson, L.N., and Alzamora S.M., 2000, Texture and Structure of Glucose-Infused Melon, *J Sci. Food Agric*. **80**:769.
Mittal, J. P., and Mohsenin N.N., 1987, Rheological Characterization of Apple Cortex, *J. Text. Stu*. **18**:65.
Mújica-Paz, H., Hernández-Fuentes, M.A., López-Malo, A., Palou, E., Valdez-Fragoso, A., and Welti-Chanes J., 2002, Incorporation of Minerals to Apple Slabs Through Vacuum

Impregnation and Osmotic Dehydration, in: *2002 IFT Annual Meeting Book of Abstracts*, Anaheim, pp. 74, 306–22.

Nieto, A., Salvatori, D., Castro, M.A., and Alzamora S.M., 2004, Structural Changes in Apple Tissue During Glucose and Sucrose Osmotic Dehydration: Shrinkage, Porosity, Density and Microscopic Features, *J. Food Eng*. **61**:269.

Ortiz, C., Salvatori, D., and Alzamora S.M., 2003, Fortification of Mushroom with Calcium by Vacuum Impregnation, *Latin Amer. Appl. Res*. **33**:191.

Park S.W., 2001, Analytical Modelling of Viscoelastic Dampers for Structural and Vibration Control, *Int J. Sol. Struct*. **38**:8065.

Petrell, R.J., Mohsenin, N.N., and Wallner S., 1979, Dynamic Mechanical Properties of the Apple Cortex in Relation to Sample Location and Ripening, *J. Text. Stu*. **10**:217.

Pitt R.E., 1992, Viscoelastic Properties of Fruits and Vegetables, in: *Viscoelastic Properties of Foods,* M.A. Rao, and J. F. Steffe (eds.), Elsevier Science, Amsterdam, pp. 49–76.

Rojas, A.M., Gerschenson, L.N., and Marangoni A.G., 2001, Contributions of Cellular Components to the Rheological Behaviour of Kiwifruit, *Food Res. Int*. **34**:189.

Sherman P., 1970, *Industrial Rheology*, Academic Press, London.

Tapia, M.S., Schulz, E., Gómez, V., López-Malo, A., and Welti-Chanes J., 2003, A New Approach to Vacuum Impregnation and Functional Foods: Melon Impregnated with Calcium and Zinc, in: *IFT Annual Meeting Book of Abstracts,* Institute of Food Technologists, Chicago, p. 158, Abstract 60D-2.

Tshoegl N.W., 1989, *The Phenomenological Theory of Linear Viscoelastic Behavior,* Springer, Berlin.

Van Vliet T., 2002, On the Relation Between Texture Perception and Fundamental Mechanical Parameters for Liquids and Time Dependent Solids, *Food Qual. Pref*. **13**:227.

Waldron, K.W., Smith, A.C., Parr, A.J., Ng, A., and Parker M.L., 1997, New Approaches to Understanding and Controlling Cell Separation in Relation to Fruit and Vegetable Texture, *Trends Food Sci. Technol*. **8**:213.

10
Bubbles in Foods: Creating Structure out of Thin Air!

K. Niranjan and S.F.J. Silva

10.1. Introduction

Bubbles are always perceived to represent the best in food and drink. Their presence and characteristics have dominated our perception of the quality of bread, champagne, ice creams, and let's not forget the good olde beer! In recent years, there has been a constant flow of new bubble-containing snack foods into our supermarkets—whipped cream, chocolate, wafers, cakes, meringues, extruded snacks and sparkling drinks—all of which have very novel structures and are perceived to offer lighter alternatives in terms of calories. Figure 10.1 shows a selection of bubble-containing food products currently available in supermarkets in the UK. Most products manage to gain a positive market image by highlighting bubbles, which is beneficial to manufacturers. From a consumer's point of view, too, there are advantages. Bubble-included products are normally perceived to have a sophisticated mouth-feel, and this is achieved by using gases which, although not formally recognized, represent a zero calorie ingredient. The high ratio of volume to the amount of material normally associated with such products can also be beneficial to consumers who are struggling to control their amount of food intake.

Despite widespread practice, bubble inclusion into foods has received relatively little research attention as a processing operation. This paper will aim to demonstrate how food structure can be created by using gases. Using real but adequately characterized examples such as cake batter, whipped cream and chocolates, the paper will present experimental data on bubble hold-up and bubble size distributions. The relationship between operating variables (such as pressure, temperature and level of mechanical power dissipation) and the dispersion properties will be modelled and explained in the context of the rheological and interfacial characteristics of the continuous phase.

Bubble-included structures can be formed in any of the following ways:

- Agitation of a given amount of liquid or a continuous phase in an unlimited amount of gas (e.g., whipping of cream in a bowl);

FIG. 10.1. A selection of bubble-containing food products

- Agitation of gas and continuous phases (e.g., ice cream) which is normally carried out by passing the two phases at specified rates through a mixing head;
- Gas generation within a continuous phase either by the desorption of a previously dissolved gas by releasing pressure (e.g., fizzy drinks) or by a chemical or biochemical reaction (e.g., fermentation or thermal breakdown of baking powders).

10.1.1. Methods of Forming Bubble-Included Structures

Campbell and Mougeot (1999) also suggest a similar classification of foaming processes. The first two processes are based on mechanical agitation, and this can be carried out either by using an impeller (e.g., a whisk; see Fig. 10.2) or by sparging steam into the continuous phase.

A number of foamed coffee products are produced by steam injection. In practice, however, processors tend to combine the above methods. The gas and the continuous phases are passed through a mixing head running under pressures up to 10 bar. The mechanical agitation breaks up the gas into fine bubbles which lose some of the gas into the continuous phase by dissolution. The bubble-containing dispersion that is formed when the pressure is released is a result of the expansion of bubbles present in the continuous phase as well as desorption of the dissolved gas. The relative contribution of each mechanism depends on the operating

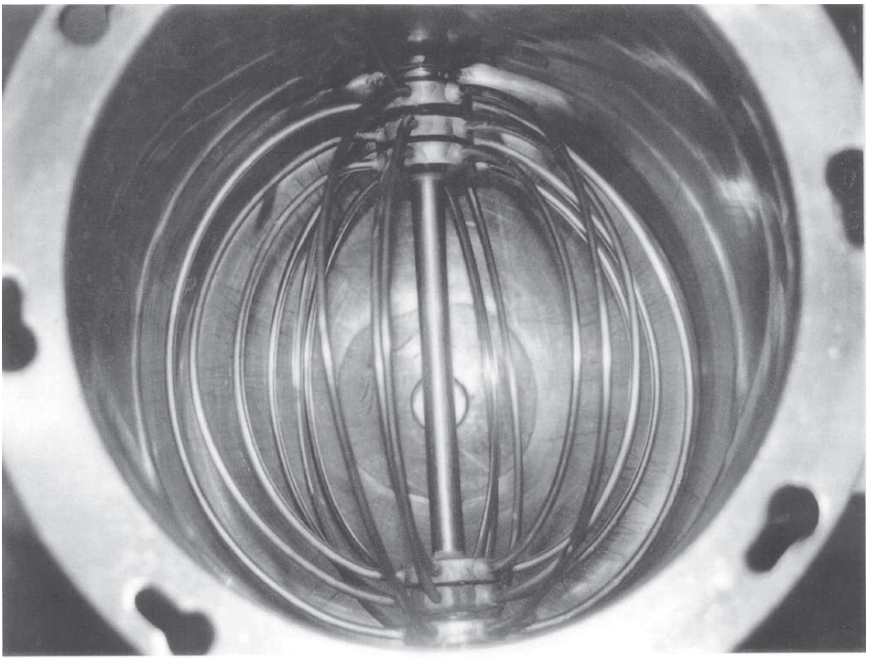

FIG. 10.2. A view of a commercial whisk

conditions used and the solubility of the gas in the continuous phase. The latter mechanism tends to dominate when highly soluble gases are used. It is implicitly assumed here that bubble inclusion processes involve the use of a variety of gases, which, indeed, is the case. For example, fizzy drinks and sparkling wines use carbon dioxide, whereas low reactivity gases such as nitrogen, helium, argon, etc. are used particularly when the continuous phase is sensitive to oxidation and air cannot be used (e.g., bubble inclusion into fat-sugar mixtures used in cream biscuits; see Fig. 10.3).

It is implicitly assumed here that bubble inclusion processes involve the use of a variety of gases, which, indeed, is the case. For example, fizzy drinks and sparkling wines use carbon dioxide, whereas low reactivity gases such as nitrogen, helium, argon, etc., are used particularly when the continuous phase is sensitive to oxidation and air cannot be used (e.g., bubble inclusion into fat-sugar mixtures used in cream biscuits; see Fig. 10.3). The structures of the products as well as their mouth-feel are both critically influenced by the chemical nature of the gas used in the process of bubble inclusion. The temperature at which the dispersion is formed is also very critical. For example, carbon dioxide is dissolved into syrups in the manufacture of fizzy drinks at relatively low temperatures, around 5°C, in order to exploit high gas solubility at these temperatures. On the other hand, bubble inclusion into fat-sugar mixtures has to be carried out above the

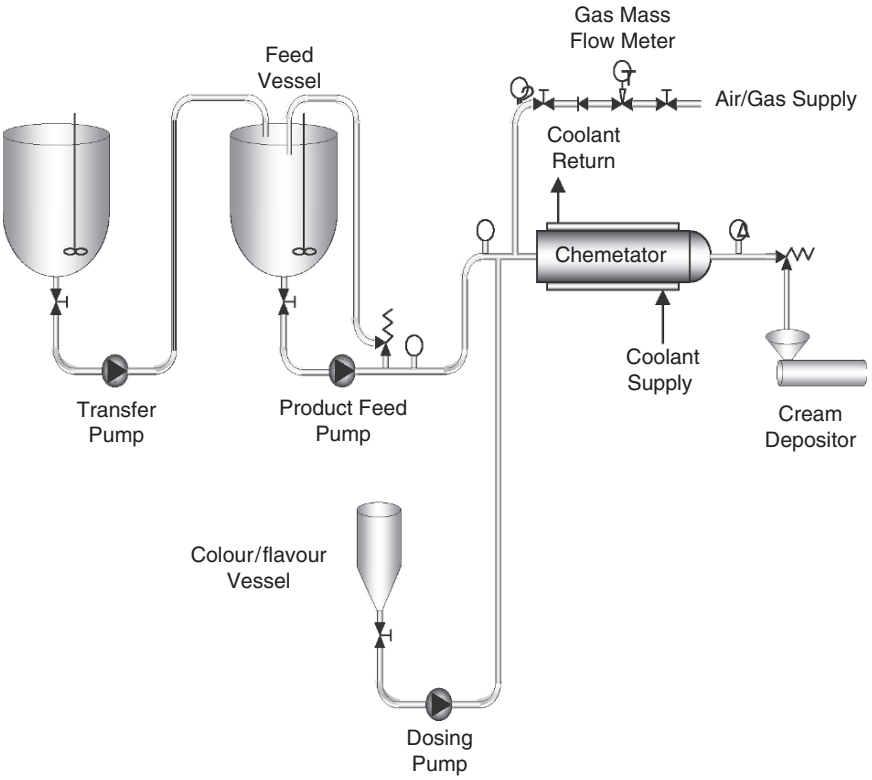

FIG. 10.3. Biscuit cream line (Courtesy—Chemtech International, Reading, UK)

melting point of the fat. In this case, it is very important to set the dispersion by cooling it as soon as possible, so that the escape of gas during setting can be minimized.

Regardless of the methods used to form dispersions, it is absolutely critical to understand bubble mechanics in food systems. There are a number of reasons to do so, which have already been discussed by Niranjan (1999). Since bubble mechanics determines the relationship between aerating conditions and dispersion characteristics, its study will enable us to optimize process design. It should therefore be possible for us to select the right type of equipment, to size it correctly, and to optimize its performance in order to produce the desired dispersion. Bubble mechanics also determines how long a given dispersion can remain stable. This information can be directly used to estimate the shelf-life of products. One of the most important, and perhaps the least understood, applications of bubble mechanics is in the area of texture and sensory analysis. The textural appearance and mouth-feel of "bubbly" products is a direct consequence of the complex

interactions between bubble mechanics and our senses. Our knowledge of the fundamental mechanisms governing the formation and stability of bubble-containing food dispersions is still patchy, although it is encouraging to note the increasing level of research interest in this area. The next section of this paper will consider the fundamental characteristics of bubble-containing food dispersions.

10.1.2. Characterization of Bubble-Containing Food Dispersions

10.1.2.1. Gas Hold-Up:

Gas hold-up (ε) is a common measure of the level of bubble inclusion. It is normally defined as the volume fraction of gas based on the dispersion volume, and estimated from density measurements before and after aeration, as follows:

$$\varepsilon = 1 - \frac{\rho\,\text{dispersion}}{\rho\,\text{continuous phase}} \tag{10.1}$$

Within a bubble-including device, the gas hold-up constantly changes with time. It is therefore necessary to consider the desired gas hold-up in a product as a design parameter, and accordingly adjust its residence time within the device. Figure 10.4 shows typical transient variations of gas hold-up observed in two different systems: whipping of cream and cake batter. It is clear that the gas hold-up increases initially, reaches a peak and then drops. In the case of cake batters, the hold-up attains a constant value after decreasing for some time. Massey (2002) proposed a mechanistic model for the time dependency of gas hold-up. This model successfully described experimental data for a range of whisk speeds and headspace pressures. The model accounts for air entrainment and disentrainment during whisking, considering two mechanisms of bubble formation: a primary mecha-nism, where entrapped bubbles are directly entrained from the headspace, and a second-dary mechanism involving the breakup of larger bubbles entrained from the headspace. The primary mechanism is considered to be a zero order process, whereas the secondary mechanism is considered to be exponentially decaying with time (due to changes in the properties of the continuous phase). Disentrainment of bubbles is considered to occur mainly due to coalescence of entrapped bubbles that subsequently get released from the system; hence it can be assumed to be proportional to the gas hold-up at any instant. On the basis of these assumptions, Massey (2002) showed that the gas hold-up at any time could be correlated by the following equation:

$$\varepsilon_g = \frac{k_1}{k_4} + \frac{k_2}{k_4 - k_3} e - k_3 t - \left(\frac{k_1}{k_4} + \frac{k_2}{k_4 - k_3} \right) e k_4 t \tag{10.2}$$

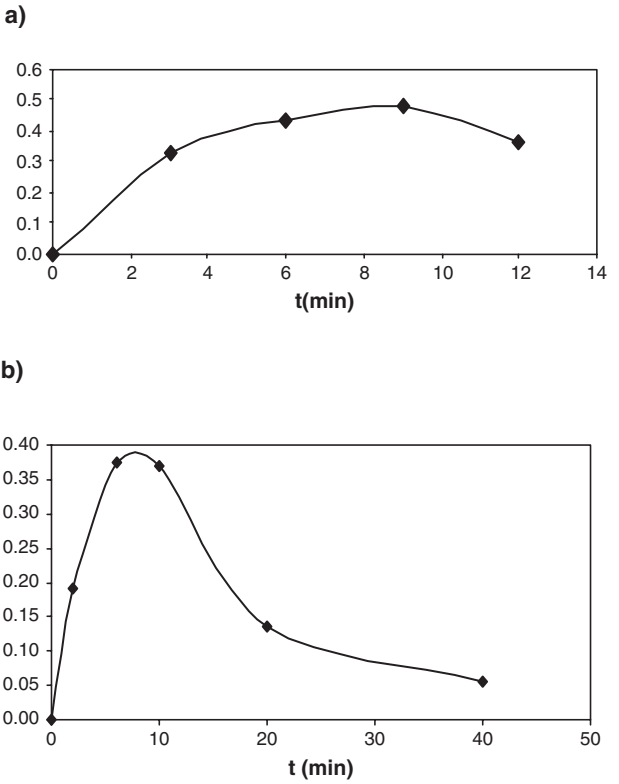

FIG. 10.4. Effect of aeration time on the gas hold-up of entrapped bubbles in: **a)** cream whipped at atmospheric pressure and 380 rpm; **b)** cake batter aerated at 3 bar, 5 rps (Recipes described by Massey et al. (2000) and Jakubczyk and Niranjan (2006)

with k_1, k_2, k_3 and k_4 as model parameters. Massey (2002) also observed that whisk speed only influenced the time taken by the batter to acquire a steady state gas hold-up, and not the hold-up itself.

Jakubczyk and Niranjan (2006) investigated the variation of gas hold-up with time when cream was whipped. Table 10.1 shows hold-up values after 3, 6, 9 and 12 min. The hold-up increased initially, and the highest value was observed after 9 min. Between 3 and 6 min of whipping, the hold-up increased by about 35%, whereas it only increased by 18% between 6 and 9 min. The cream whipped for 12 min had a significantly lower hold-up than the cream whipped for 9 min. Birkett (1985) noticed that maximum overrun corresponded with maximum stability and stiffness of the foam, and all air bubbles at this point were encapsulated by coalesced fat droplets which adsorbed at the air/serum interface. The decline in hold-up after 9 min of whipping was probably caused by fat-globules aggregating, which caused the foam to collapse partially.

TABLE 10.1. Effect of whipping time on gas hold-up in UHT cream (35% milk fat and 5.3% solids not fat) using a domestic whipping device (model A 700, Kenwood) running at 380 rpm

Whipping time (min)	*Gas hold-up (%)*
3	33.1 ± 0.2
6	43.3 ± 0.45
9	48.5 ± 0.4
12	36.8 ± 19

During the process of generating bubbles in tempered chocolate by applying vacuum, Haedelt (2005) observed that the gas hold-up increased when higher vacuum levels were applied. This was explained by the mechanism of bubble formation under vacuum: gas solubility in the chocolate decreased proportionally to the pressure, which in turn increased the volume of gas desorbed from the chocolate (Haedelt, 2005). The hold-up of bubbles trapped within the chocolate is a balance between the volume desorbed and the volume of gas escaped during the setting of the chocolate. The latter, obviously, depends on the rapidity of the setting process. Generally, chocolate is set as rapidly as possible in order to minimize gas loss. Table 10.2 shows the gas hold-up data obtained at different vacuum levels under very rapid setting conditions.

10.1.2.2. Bubble Size Distribution

Bubble sizes have traditionally been examined by taking photographs of dispersions and analyzing them using image analysis software. For instance, Massey (2002) analyzed the bubble size distributions in cake batter by spreading out a thin film of aerated batter (less than 2 mm thick) and imaging the film by using a microscope-linked camera. The image was then presented to image analysis software which provided details of the bubble size distribution. Jakubczyk and Niranjan (2006) also used a similar technique to investigate the bubble size distributions in whipped cream. Haedelt (2005) found that this technique was unsuitable for measuring bubble sizes in chocolates because thin sections could not easily be formed for the purpose of imaging. Instead, the chocolate was imaged using X-ray tomography, which has proved to be a valuable tool for imaging a number of cellular food products such as strawberry mousse and chocolate muffins (Lim, 2004). An X-ray micro-tomography system described by Jenneson et al. (2003) was used by Haedelt (2005) to characterize cross-sections taken along specific planes passing through a cylindrical sample of bubble-containing chocolate. This technique is non-invasive and avoids laborious sample treatments, and it is particularly appropriate for analyzing fragile bubble-containing foods. Used in conjunction with an appropriate image analysis software (e.g., Imagine Pro®Plus Software, The Proven Solution™), it can successfully visualize bubble-containing sections, giving information on bubble numbers and size distribution (see images in Table 10.2). While this technique is useful in terms of characterizing dispersions, it is necessary to note that the method only represents a two-dimensional

analysis of what is essentially a three-dimensional structure, because it relies on observing a plane sliced (in real or virtual terms) through a sample. Haedelt (2005) has succeeded in reconstructing a virtual 3-D image by combining a number of two-dimensional sections, and characterized the bubble size distributions based on the reconstructed image. This approach, although tedious, gives a realistic idea of the bubble size distribution prevailing in any sample.

Regardless of the technique used, it is necessary to note that the bubble size distribution is essentially dependent on the method used to include bubbles, the operating conditions and the chemical nature of the gas. Massey (2002) examined the transient development of bubble size distribution in a standard cake batter and found that the mean bubble size decreased initially with agitation time. It then attained a minimum value before increasing to reach a steady value (Fig. 10.5.) The time at which this minimum in the mean size

TABLE 10.2. Effect of vacuum level on gas hold-up and dimensions of bubble sections in a standard chocolate recipe (Haedelt, 2005)

Effect of pressure on gas hold-up and dimensions of bubble sections					
Pressure	0.01bar	0.0125 bar	0.02 bar	0.05 bar	0.1bar
X-ray Image	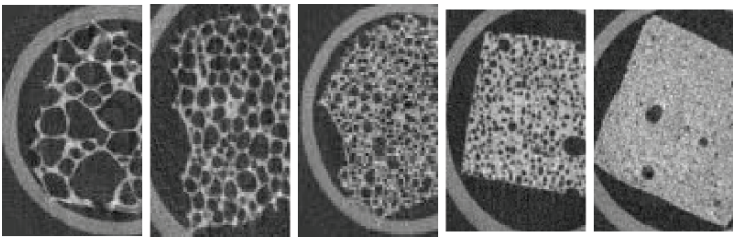				
ε (%)	67.1 +/– 0.1	65.6 +/– 0.1	54.8 +/– 0.1	28.8 +/– 0.1	21.6 +/– 0.1
d_{mean} (mm)	1.33 +/– 1.09	0.85 +/– 0.4	0.43 +/– 0.33	0.39 +/– 0.16	0.37 +/– 0.19
Number of bubbles in 1.65cm^2	48 +/– 5	61 +/– 5	243 +/– 16	154 +/– 13	38 +/– 12

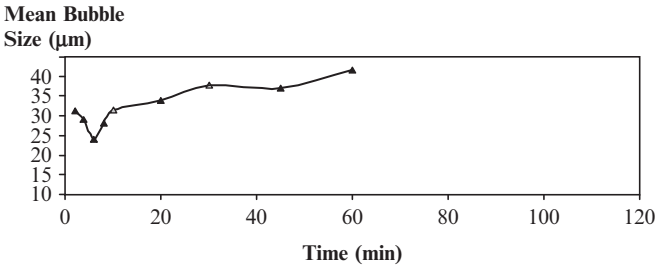

FIG. 10.5. The transient variation in mean bubble size observed in a cake batter whipped at 300 rpm at a pressure of 3 bar

was observed, interestingly, corresponded to the time at which the maximum gas hold-up was recorded (Fig. 10.4b). Massey (2002) also showed that the bubble size distribution in cake batters under any given set of conditions could be described by log normal distribution curves with mean size and standard deviation representing the two parameters characterizing the distribution. The standard deviation indicates the spread in the bubble size distribution. In another study, Niranjan and Khare (2002) found that a more uniform bubble size distribution increased batter stability and improved baking properties. Whisk speed was found to have little effect on mean bubble size; however, it was observed that speed enhanced bubble breakup and coalescence rates, lowering the time required to achieve a given mean size. Progressive whipping of dairy cream was also found to result in the formation of smaller bubbles, until a maximum hold-up was attained. Prolonged whipping caused the bubble size distribution to change from being log-normal to bi-modal (Jakubczyk and Niranjan, 2006).

10.1.2.3. Rheological Studies

Haedelt et al. (2005) suggest that rheology can be a useful tool in the assessment of structural changes occurring in bubble-containing products. Dynamic oscillatory tests have been performed on whipped cream and cake batters, not only to assess their rheological properties, but also to trace the way these properties change during the course of bubble inclusion (Massey, 2002; Jakubczyk and Niranjan, 2006). Although such data provide insight into the structural changes occurring in these products during bubble inclusion, there is hardly any study that attempts to relate multi-phase rheology with mouth-feel. All dairy creams studied by Jakubczyk and Niranjan (2006) exhibited viscoelastic behavior with elastic modulus, G', exceeding the viscous modulus, G'', which suggests that viscoelasticity played a dominant role in characterizing whipped cream. Whipping was observed to alter the cream properties significantly; the elastic modulus, after 3 min of whipping, varied between 9 and 17 times that for unwhipped cream, whereas the viscous modulus varied between 10 and 14 times the same parameter. The increase in moduli was attributed to the presence of bubbles and to the clustering of fat globules. The whipped samples also exhibited a more distinct separation between G' and G'' at all frequencies. These results are also consistent with the study of Massey (2002), who noted that bubble inclusion created a stronger viscoelastic system in cake batter. The results also agreed with Bee and Prins (1986), who, during the aeration of maltodextrin solutions, observed an increase in storage and loss modulus (the fractional increase in the storage modulus being approximately 4 times greater than the increase in viscous modulus). In general, it is relatively difficult to undertake rheological measurements on food foams, because of the narrow range of applied shear stress/strain over which a given foam is stable. Regardless, it is still reliable and conveys very useful information that can be used as a measure of the foam texture.

10.1.2.4. Concluding Remarks

This article has illustrated how air and other gases can be used to create novel food structures and textures without adding calories. A detailed understanding of the process, and the relationship between process parameters and product characteristics, are only just being unravelled, with increasing research attention being paid to this area. The mechanism of bubble inclusion and the factors governing the stability of the resulting dispersion are both complicated, with ingredients, particularly those that are interfacially active, playing a decisive role.

References

Bee, R.D.C., and Prins A., 1986, Behaviour of an Aerated Food Model, in: *Food Emulsions and Foams*. E. Dickinson (ed.), Royal Society of Chemistry.

Birkett R.J., 1985, Role of Interfacial Processes in the Whipping of Dairy Cream, in: *Int. Union Food Sci. Technol*, pp. 149–150.

Campbell, G.M., and Mougeot E., 1999, Creation and Characterisation of Aerated Food Products, *Trends Food Sci. Technol*. **10**(9):283–296.

Haedelt J., 2005, *An Investigation into Bubble Inclusion in Liquid Chocolate*. PhD Dissertation, University of Reading.

Haedelt, J., Pyle, D.L., Beckett, S.T., and Niranjan K., 2005, Vacuum-Induced Bubble Formation in Liquid-Tempered Chocolate, *J. Food Sci*. **70**(2):E159-E164.

Jakubczyk, E., and Niranjan K., 2006, Transient development of whipped cream properties, *J. Food Eng*. **77**(1): 79–83.

Jenneson P. M., Gilboy W. B.,,Morton, E. J., and Gregory, P. J., 2003. An X-ray microtomography system optimised for the low-dose study of living organs, *Appl. Radiat. Isot*. **58**: 177–181.

Lim KS, B. M., 2004. X-ray micro-computed tomography of cellular food products, *Food Res. Int.,* **37**(10): 1001–1012.

Massey, A., 2002, *Air Inclusion Mechanisms and Bubble Dynamics in Intermediate Viscosity Food Systems*. PhD dissertation, University of Reading.

Niranjan, K., 1999, *An Iintroduction to Bubble Mechanics in Foods. Bubbles in Food*. G. M. Campbell, C. Webb, S. Pandiella and Niranjan K., (eds.), Eagan Press, St. Paul: 3–9.

Niranjan, K. and Khare A., 2002, Unpublished work.

11
Films Based on Biopolymer from Conventional and Non-Conventional Sources

P. Sobral, J. de D. Alvarado, N.E. Zaritzky, J.B. Laurindo, C. Gómez-Guillén, M.C. Añón, P. Montero, G. Denavi, S. Molina Ortiz, A. Mauri, A. Pinotti, M. García, M.N. Martino, and R. Carvalho

11.1. Introduction

Edible films are thin materials based on biopolymers. These films are also biodegradable and because of that, these materials have attracted the attention of the food science academic community in the last decades. The main biopolymers used in the edible films production are polysaccharides (Nisperos-Carriedo, 1994) and proteins (Gennadios et al., 1996).

The polysaccharide most used in edible film technology is starch, because it is produced abundantly and is inexpensive. But other polysaccharides, such as chitosan and some cellulose derivates, have been also studied. Normally, proteins produced industrially, such as soja and gelatin from mammals, are largely applied in film production. However, some proteins from less conventional sources, such as muscle proteins, gelatin from fish, and feather keratins, have also been studied in the last several years. Thus, this work will present and discuss some aspects of edible and/or biodegradable film technology based on biopolymers from conventional or less conventional resources.

11.2. Films Based on Chitosan Produced on Laboratory Scale

Chitosan is a polymer derived from chitin partially or totally deacetylated. Usually it comes from the chitin found in fungi, crustaceans, molluscs, or annelids; however, in general, crab, lobster or shrimp shells are used because they are industrial wastes (Shepherd et al., 1997).

Chitin ($C_8H_{13}O_5N$) is a polymer formed by units of 2-acetamide-2-deoxiglucose linked by 1,4-beta-glucosidic of cellulose. It is insoluble in water, diluted acids and alkalis, alcohol, and organic solvents; it is soluble in general with some degradation in concentrate mineral acids. By acid hydrolysis, it is degraded to glucose amine; the alkaline hydrolysis deaceylates it extensively, with some reduction of chain length, forming chitosan (Kirk and Othmer, 1970).

Chitosan [β-(1,4)-2-amino-2-deoxy-D-glucopyranose] is an amorphous white solid, insoluble in water, soluble in acids, whose crystalline structure is substantially the same as the original purified chitin. At extreme conditions of deacetylation, chitosan keeps the amino groups, and that confers enormous possibilities for chemical modification because they have positive ionic links that react to substances negatively charged as fats, cholesterol, basic ions and proteins (Argukelles et al., 1998). The multiple applications of chitosan allow it to be used in agriculture, medicine, effluent treatment and in foods. According to Devlieghere et al. (2004), chitosan can be use in foods as an antimicrobial agent, a clarifying agent for juices, an antioxidant in sauces, an inhibitor of enzymatic browning in apples and potatoes, and additionally as films for fresh fruit and vegetable covering; it can also act as an enzyme inhibitor. Han et al. (2005) established that chitosan films behave as adequate covering material for strawberries due to their antimicotic properties; however, solutions of chitosan diluted in acid become bitter and astringent and therefore less practical for the real market.

11.2.1. Chitosan Production

To obtain chitosan, the group N-acetyl is removed without polysaccharide hydrolysis; that is why the alkaline methods are the most used. Several authors (Ramírez et al., 1998; Taboada et al., 2003) obtain chitosan by the chemical modification of chitin; the acetyl units are eliminated with long treatments in highly concentrate alkalis.

Pinelli et al. (1998) showed a recompilation of methods to obtain chitosan from shrimp shells; they adapted a method to obtain chitosan from chitin and pointed out the importance of the initial control of the shells by thermal treatment for the inactivation of the hydrolytic enzymes, tunnel drying and milling. According to the technology developed by Almeida and Arancibia (2005), chitosan was obtained from the chitin extracted from Ecuadorian shrimp shells by a previous protein removal done with diluted solutions of sodium hydroxide at 80°C for 30 min and then a second protein removal done thrice with solutions 3% (w/w) of sodium hydroxide at 80°C. The process continued with the demineralization using HCl 2N for 60 min at temperatures around 20°C. At last, the obtained chitin was deacetylated to obtain chitosan by chemical treatment, using 50% (w/w) sodium hydroxide solution at 100 °C for 60 min. Alvarado et al. (2006) modified the method to eliminate protein removal, obtaining chitosan directly without getting the chitin, by a severe alkaline treatment, showing the utility of the obtained product to produce edible films.

11.2.2. Chitosan Film Production and Characteristics

Film formation is based on the biopolymer dispersion or solution in a solvent and additives use (plastificants, link agents), obtaining a dispersion or a solution. After preparing the suspension, these undergo processes of lamination and drying in

order to get the films. In this step the biopolymer concentration increases because of the solvent evaporation and, as a consequence, molecule aggregation occurs, forming a tri-dimensional network (Gontard et al., 1995).

As chitosan is soluble in organic solvents, several authors have worked with organic acid solutions. Caner et al. (1998) prepared chitosan films using acetic, lactic and formic acids with different concentrations of the plastificant and molding them in glass dishes. Alvarado et al. (2005) used Petri boxes in which they put the chitosan suspension and let it dry at temperature of 20 ± 5 °C for 48 h; finally, the films were removed by using NaOH 0.1% (w/w) solution. Other samples were prepared on clean and dry acrylic plaques measuring 10 × 20 cm, where the chitosan solution was poured; the films dried at a temperature of 20 ± 5 °C for 48 h and were removed by releasing them from the acrylic without using the NaOH solution. The best results were obtained in acrylic plaques without NaOH.

The applications of films depend principally of their barrier properties to water and to gases, and their mechanical characteristics, solubility, and optical and thermal properties. Those characteristics depend on the polymer type, polymer obtaining process, film conditioning, drying and film thickness (Galed et al., 2000; Srinivasa et al., 2004). The interest in chitosan films for foods is based on their capacity as an oxygen barrier (Caner et al., 1998) and carbon dioxide barrier (Choi et al., 2002). The methods used to determine film properties are derived from the classic methods applied to synthetic material; these methods were adapted to the characteristics of biopolymers, particularly due to their great sensitivity to relative humidity and temperature (Issam et al., 2005).

One of the fundamental properties is the permeability to water vapor (WVP). Buonocore et al. (2005) established that chitosan films showed less permeability to water vapor compared to films made with casein and alginate; they pointed out that this is due to their low affinity with water and less macromolecular mobility. According to this, chitosan films can act as adequate barriers to water vapor; they used a mathematical model to describe the barrier properties of these films. Caner et al. (1998) worked with chitosan films treated with several acid solutions and plastificants. They reported values from 0.535 to 1.320 [g/m day at] at 25 °C between 50%–100% of relative humidity; they did not establish changes on the mass transfer properties during nine weeks storage. Alvarado et al. (2005) published values of permeability to water vapor (WVP) in a range of 0.097 up to 0.227 [g mm/kPa h m^2]. Values increased while the concentration of chitosan increased, and therefore, the film thickness; these values correspond to the low permeability of films to water vapor in relation to other biodegradable films, but to high permeability in relation to plastic inorganic films.

Tensile strength and elongation at break are among the more known mechanical properties. Miranda et al. (2004) reported the following ranges: tensile strength from 7.23 to 48.3 [MPa] and elongation at break expressed as percentage from 22.9 to 167.2% for chitosan films. Tanveer et al. (2003), for chitosan films, published several values of tensile strength from 59.87 to 67.11 [N/$(mm)^2$] and elongation percentage to rupture from 21.35 to 67.10%. Caner et al. (1998), for chitosan films made with four organic acid suspensions, published values of

resistance to tension from 6.85 to 31.88 [MPa], and the elongation percentage varied from 14 to 70%, decreasing while the time of storage increased.

Alvarado et al. (2006) published data for chitosan films made with two organic acid suspensions, acetic and lactic. The films obtained were compact, lightly permeable to water vapor, medium strong, and transparent, and their thickness increased while the chitosan concentration increased in the suspension. The films made with the suspensions of chitosan in acetic acid are less hygroscopic, show less permeability to water vapor, and are more resistant to traction but less elastic; they behave as partial crystalline materials and are opaque. The films elaborated with chitosan suspensions in lactic acid are more hygroscopic, more permeable, less resistant and more elastic; they behave as crystalline materials and are transparent.

11.3. Composite Films Based on Chitosan and Methylcellulose

Cellulose derivatives are also interesting biomaterials for film technology; they are polysaccharides composed of linear chains of β (1–4) glucosidic units with methyl, hydroxypropyl or carboxyl substituents. Methylcellulose (MC) has excellent film-making properties, high solubility and efficient oxygen and lipid barrier properties (Park et al., 1993; Donhowe and Fennema, 1993a,b; Nisperos-Carriedo, 1994).

Besides, chitin and its deacetylated product, chitosan, have received much interest for their application in agriculture, biomedicine, biotechnology and the food industry due to their biocompatibility, biodegradability and bioactivity (Muzzarelli et al., 1988; Tharanathan and Kittur, 2003). Among potential applications, the use of chitin and chitosan as food antimicrobials and biopesticides are especially attractive (Wu et al., 2005). Due to its antifungal, good mechanical and oxygen barrier properties (Chen et al., 1996; Caner et al., 1998), chitosan film is a promising packaging material that can be included in the active film category (Vermeiren et al., 1999). In the absence of additives, films made from these polysaccharides are brittle. Plasticizers are necessary to enhance flexibility and to improve mechanical properties. Hydrophilic compounds such as polyols are commonly used as plasticizers in hydrophilic film formulations.

11.3.1. Film Production

Commercial methylcellulose (A4M, Methocel, Dow, USA) with a substitution degree of 27.5% was purchased from Colorcon (Argentina). Commercial chitosan from crab shells with a minimum deacetylation degree of 85% was purchased from Sigma (St. Louis, USA). Solutions of 1% (w/w) of methylcellulose (MC), and 2% (w/w) of chitosan were prepared. Chitosan (CH) was solubilized in 1% (v/v) acetic acid solution, followed by a vacuum filtration to eliminate insolubles. Mixture solutions were prepared with the following (w/w) CH:MC proportions: 25:75, 50:50 and 75:25. In all cases, to obtain films, 40 g of solutions were poured

on rectangular acrylic plates (10×20 cm). The solutions were dried at 60 °C in a ventilated oven to constant weight. Films were stored under controlled temperature and relative humidity conditions (20 °C and 65% RH).

Equilibrium moisture content: Water content of the films was determined by measuring weight loss of films upon drying in an oven at 110 °C until constant weight (dry sample weight). Thickness of the films was determined using a digital coating thickness gauge Elcometer A 300 FNP 23 (England) for non-conductive materials on non-ferrous substrates. Film solubility in water was determined using film pieces of 2×3 cm; samples were weighed to the nearest 0.0001 g and placed into test beakers with 80 ml deionizated water. The samples were maintained under constant agitation at 200 rpm for 1 h at room temperature (approximately 25 °C). After soaking, the remaining pieces of film were collected by filtration and dried again in an oven at 60 °C to constant weight. The percentage of total soluble matter (% solubility) was calculated.

For film microstructure analysis, scanning electron microscopy (SEM) analysis was performed with a JEOL JSPM 100 electron microscope (Japan). Film pieces were mounted on bronze stubs using a double-sided tape and then coated with a layer of gold (40–50 nm), allowing surface and cross-section visualization. All samples were examined using an accelerating voltage of 5 kV. Water vapor permeability tests were conducted using a modified ASTM (1996) method E96, as described in a previous work (García et al., 2004) using an especially designed permeation cell that was maintained at 20 °C. After steady state conditions were reached (about 2 h), eight weight measurements were made over 24 h. A driving force of 1753.55 Pa, expressed as water vapor partial pressure, was used. Tensile tests were performed in a texturometer TA.XT2i (Stable Micro Systems, England), as described in a previous work (García et al., 2004) using a tension grip system A/TG and probes of 6 cm in length and 0.7 cm width. Puncture tests were performed using a cylindrical probe 2 mm in diameter at a constant rate of 1 mm/s. Tests were carried out with samples of 3×3 cm from each film formulation. Curves of force (N) as a function of deformation (mm) were automatically recorded by the Texture Expert Exceed software. Maximum breaking force (N), tensile strength (MPa), deformation at break (mm), percent of elongation at break (%) and elastic modulus (N/mm) were calculated according to the ASTM D4092 method (1996).

11.3.2. Characterization of Composite Films Based on Chitosan and Methylcellulose

Flexible, homogeneous, thin, and transparent films were obtained from MC, CH and mixture solutions. Visually, MC films were colorless, and chitosan films had a slightly yellow appearance, increasing yellowness with chitosan concentration for composite films—even though the intensity of the yellowness is negligible when compared to values reported for whey protein based films (Trezza and Krochta, 2000). All films were easily removed from the cast plate, and no pores

or cracks were detected as seen by SEM (Fig. 11.1), although film formulation did not include a plasticizer. In addition, a compact structure was observed, (Fig. 11.1). Composite films showed multilayer structures (Fig. 11.1c). This could possibly be attributed to the limited chain mobility, even though both CH and MC are compatible polymers. As shown in Table 11.1, thickness of films varied between 14.12 ± 1.59 and 26.07 ± 3.17 μm. CH films obtained from a 2% solution were thicker than MC film obtained from 1% solution; this was also evidenced by SEM observations (Figs. 11.1a and 11.1b). Composite films exhibited intermediate thickness values within the range of those of one component film (Table 11.1). All films reached low moisture after drying; MC films exhibited the lowest equilibrium moisture, while the highest value was observed for CH films (Table 11.1). MC films were completely soluble in water, while CH films had lower solubility values. Composite films had intermediate water solubilities, decreasing film solubility with increasing chitosan proportion (Table 11.1). Thus, by controlling CH concentration in film formulation, solubility can be tailored, enhancing the applications of these materials.

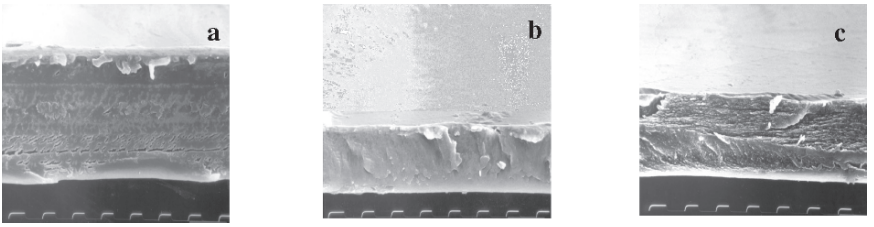

FIG. 11.1. SEM micrographs of the cross-section of: a) CH, b) MC and c) 50:50 CH:MC films. Magnification: 10μm between marks

TABLE 11.1. Film solubility in water, equilibrium moisture content, thickness and water vapor permeability of CH-MC films

Film Composition	g CH: g MC	Film solubility in water (%)	Equilibrium moisture content (g water/ 100 g film)	Film thickness (μm)	WVP × 10^{11} (g m^{-1} s^{-1} Pa^{-1})
MC	1:0	98.4 ± 2.2[b]	0.91 ± 0.16	16.32 ± 2.46	7.55 ± 0.60
25:75[a]	0.5: 0.75	40.7 ± 6.3	1.12 ± 0.01	21.22 ± 0.68	6.77 ± 0.92
50:50	1:0.5	27.7 ± 1.6	2.41 ± 0.16	23.35 ± 2.72	6.67 ± 0.74
75:25	1.5: 0.25	14 ± 2.1	2.22 ± 0.01	22.75 ± 1.69	7.24 ± 0.35
CH	2:0	9.3 ± 0.9	6.33 ± 0.58	26.07 ± 3.17	7.24 ± 0.81

[a] CH:MC (w/w) proportion in film formulation, [b] value ± standard deviation

Table 11.1 shows WVP values of individual and composite films. CH and MC films showed lower WVP values than those of some protein films and even lower than other polysaccharide based films reported in the literature (Krochta and De Mulder Johnston, 1997; Mali et al., 2002). Our obtained results are in agreement with those of Park et al. (1993), Wong et al., (1992) and Caner et al. (1998).

Permeability of composite films did not differ significantly from the values of one component film (Table 11.1). Since permeability is the contribution of diffusivity and solubility of the permeant through the solid matrix, the obtained results for composite films indicate that the developed matrix should be similar to those of the individual component matrixes, as seen by X-ray diffraction analysis. Chitosan films were shown to be good barriers to oxygen permeation in comparison to commercial polymers, but exhibited relatively low water vapor permeabilities.

WVP values of our composite CH-MC films were higher than other synthetic films like low density polyethylene (LDPE), with a WVP value of 9.14×10^{-13} $gm^{-1}s^{-1}Pa^{-1}$ (Smith, 1986), although CH-MC films had WVP values similar to those of cellophane, as expected, due to the similar chemical structure of both polymers. According to Shellhammer and Krochta (1997), cellophane exhibited a WVP value of 8.4×10^{-11} $gm^{-1}sec^{-1}Pa^{-1}$.

MC and CH films showed different behavior patterns under tensile tests; both films showed high resistance, but MC films were more flexible (Fig. 11.2). Percent elongation values of films were 12.7% for MC and 3.9% for CH, and intermediate values were obtained with composite films (Fig. 11.8a). Similar mechanical properties were found in the literature for MC films (Donhowe and Fennema, 1993a,b; Park et al., 1993; Debeaufort and Voilley, 1997). For CH films, data reported in the literature for tensile test were higher than those obtained in the present work; differences may be due to CH composition and suppliers, plasticizer presence and film preparation (Chen and Lin, 1994; Butler et al., 1996; Caner et al., 1998). The main differences may be attributed to plasticizer type and content; Caner et al. (1998) reported a wide range of elongation (14–70%), depending on storage time, plasticizer and type of acid used in chitosan solubilization.

In composite films, tensile strength and elastic modulus increased with CH concentration, leading to stronger films, (Fig. 11.2b). Accordingly, a decreasing deformation trend was observed with CH concentration, indicating a reduction in film flexibility (Fig. 11.2a).

Mechanical properties of CH-MC films were comparable to many medium strength commercial polymer films like cellophane. However, synthetic polymers like LDPE and HDPE exhibit similar tensile strength to those obtained in the present work, but higher elongation (Cunningham et al., 2000).

With regard to puncture tests, elastic modulus showed the same trend as in tensile tests (Fig. 11.2b). However, all films had a similar value of deformation at break, about 2 mm, regardless of the CH:MC ratio (Fig. 11.2a). Thus, CH may replace MC, maintaining puncture resistance of films with economical benefits.

In conclusion, physical properties of composite films showed intermediate (solubility and mechanical properties) values compared to those of individual

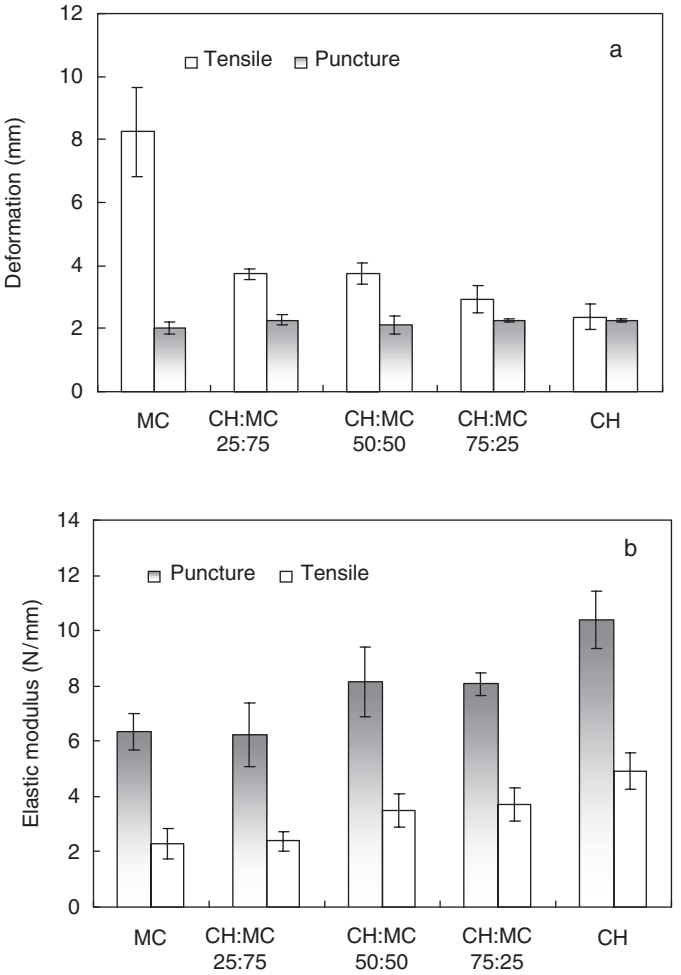

FIG. 11.2. Mechanical properties of MC, CH and composite films with different CH:MC ratios. Tensile and puncture tests: a) deformation at break and b) elastic modulus

component films or did not differ significantly (WVP), reinforcing the idea of compatibility of CH and MC polymer.

These combined biodegradable films with good water vapor barrier properties have the possibility to tailor mechanical and solubility properties, within a range, based on polymer ratio composition. CH imparts rigid characteristics to composite films (high elastic modulus and small elongation), while MC contributes to a higher elongation and lower elastic modulus, increasing solubility as well. Thus, MC-CH edible films can lead to many possible applications in food, pharmaceutical and cosmetic industry considering the natural origin of both polymers.

11.4. Films Based on Muscle Proteins from Cultivated Fishes

Some years ago, Cuq et al. (1995), working with Atlantic sardines, demonstrated that myofibrillar proteins had the capacity to form transparent and resistant films. In fact, numerous works are encountered in the specialized literature about the elaboration and characterization of films based on the myofibrillar proteins obtained from *post rigor mortis* muscles of Atlantic sardine (*Sardina pilchardus*) (Cuq et al., 1995, 1996a,b, 1997), *anten rigor mortis* muscles of Nile tilapia (*Oreochromis niloticus*) (Monterrey-Quintero, 1999, 2000; Sobral, 2000; Sobral et al., 2002), and bovine meat (*Bos taurus taurus*) (Sobral et al., 1998; Sobral and Ocuno, 2000; Souza et al., 2004). Myofibrillar proteins are insoluble in water, but can be made soluble by adjusting the pH of the solution. These proteins are fully stretched and closely associated with each other in parallel structures (Iwata et al., 2000). Probably as a function of this, these proteins are capable of forming a continuous matrix during drying of the solution (Cuq et al., 1995; Monterrey-Quintero and Sobral, 2000; Sobral et al., 1998). Contrary to the most important commercial vegetal proteins, myofibrillar proteins have to be prepared adequately before being used in the film elaboration process. In this case, after fish slaughter and evisceration, the muscles are ground and washed to eliminate the sarcoplasmic proteins. Then, the material is minced and passed through a screen to separate the connective tissue (insoluble proteins) (Cuq et al., 1995; Monterrey-Quintero and Sobral, 2000). Possibly, the elimination of the connective tissue could be due to its completely insoluble character, which could affect the homogeneity of films. The separation of sarcoplasmic proteins was made due to its bad flavor and principally because these proteins have a low molecular weight.

Fifty years ago, Japanese researchers demonstrated that sarcoplasmic proteins are also capable of forming flexible films, in spite of its low molecular weight. Iwata et al. (2000) and Tanaka et al. (2001) developed and characterized films based on sarcoplasmic proteins extracted from blue marlin (*Makaira mazara*) muscle. Contrary to the myofibrillar proteins, the sarcoplasmic proteins are globular proteins, which in general have to be thermally denatured to form a continuous matrix (Iwata et al., 2000). Heating modifies the three-dimensional structure of the globular proteins, causing exposition of the SH groups, and consequently producing S-S bonds among adjacent protein chains, also promoting the exposition of hydrophobic groups which proportionate hydrophobic interactions during drying (Perez-Gago and Krochta, 2001). Considering that the sarcoplasmic proteins also have the capacity to form a continuous matrix, Paschoalick et al. (2003) supposed that edible films could be produced by the mixture of these proteins with myofibrillar proteins, avoiding the washing process of the muscles. Thus, these authors developed flexible films based on Nile tilapia muscle proteins, i.e., containing myofibrillar and sarcoplasmic proteins. After that, others' work on production and characterization of films based on muscle proteins of fishes were published (Sobral et al., 2004, 2005; Garcia and Sobral, 2005).

11.4.1. Some Characteristics of Fish Muscle Proteins

According to Table 11.2, the polar ionic amino acids (aspartic acid, glutamic acid, arginine and lysine) are in high concentration in both the muscle proteins (Paschoalick et al., 2003) and the myofibrillar (Monterrey-Quintero and Sobral, 2000) proteins from Nile tilapia. The difference between the compositions of these proteins may be explained by the presence of sarcoplasmatic proteins in the muscle proteins.

These freeze-dried proteins, produced by Paschoalick et al. (2003) and Monterrey-Quintero and Sobral (2000), showed an interesting fluidity, i.e., without a characteristic of agglomeration. However, the muscle proteins were not as bright as the myofibrillar proteins of Nile tilapia, which were almost white.

11.4.2. Some Characteristics of Fish Muscle Proteins

The control of film thickness is very important and difficult, principally in the processes of production by casting. The fish muscle proteins, when made soluble by decreasing pH, provide extremely viscous colloidal solutions (Cuq et al., 1995). In high protein concentrations, the film-forming solution behaves as fluid of Bingham, which means that it does not flow over the force of its own weight. In this case, the solution can be spread with adequate equipment, controlling the height of the solution in the support, which allows knowledge of the thickness of the film after drying. This technique allows good thickness control, but the high

Table 11.2. Amino acid composition (g amino acids/100 g of protein) for tilapia proteins

Amino acid	Muscle proteins[1]	Myofibrillar proteins[2]
Alanine	5.50	5.00
Arginine	6.15	2.71
Aspartic acid	9.20	12.08
Glutamic acid	14.69	12.20
Phenylalanine	3.55	4.07
Cystine	0.78	0.67
Glycine	3.97	4.35
Histidine	2.05	2.57
Isoleucine	4.19	5.86
Leucine	7.35	8.36
Lysine	8.65	10.30
Methionine	2.30	3.15
Proline	3.03	8.95
Serine	3.48	4.41
Tyrosine	2.84	3.43
Threonine	4.18	4.63
Valine	4.29	6.22

[1] From Paschoalick et al. (2003); [2] From Monterrey-Quintero and Sobral (2000)

viscosity allows the production of bubbles and foams in the solution, decreasing the homogeneity of films after drying.

An important alternative is to work with diluted solutions. In this case, the solution is cast on a support, and control of the thickness may be made by controlling the weight of the solution applied in the support (Fig. 11.3A).

Practically, the thickness of films affects all physical properties of films (Cuq et al., 1996a; Sobral, 2000), and also the water vapor permeability (Fig. 11.3B), contrary to what could be expected (Sobral and Ocuno, 2000).

Among other factors, the physical properties of films based on fish muscle proteins may be affected by the plasticizer concentration and by thermal treatments of the film-forming solution (Paschoalick et al., 2003). The reduction of the puncture force with the increase of the plasticizer concentration is typical behavior of films based on proteins (Cuq et al., 1995; Gontard et al., 1993). The presence of plasticizers and water molecules—considering that increasing the glycerin

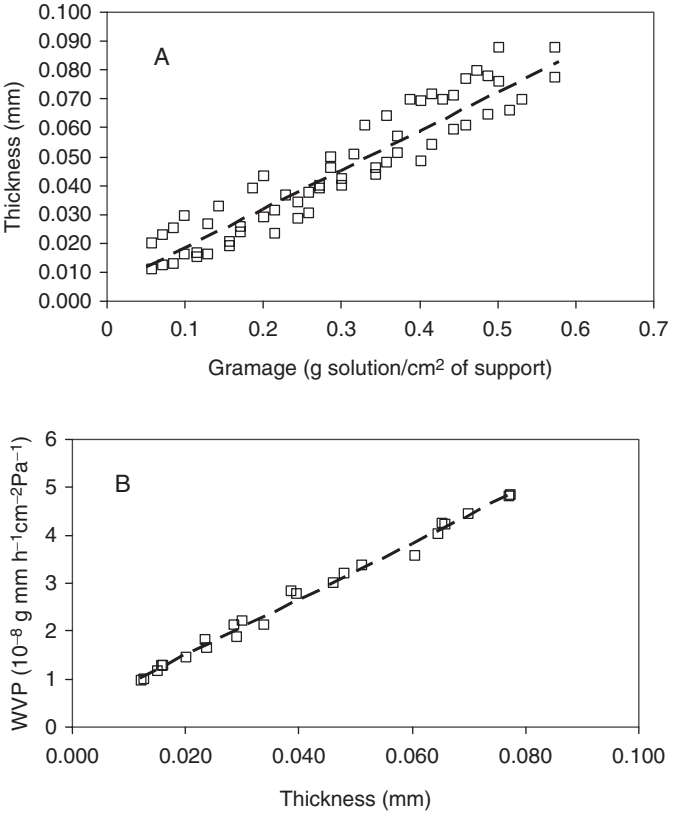

FIG. 11.3. Average thickness (A) and Water Vapor Barrier Properties (B) of films based on myofibrillar proteins from Nile tilapia (from Sobral, 2000)

content increased the final humidity of the films—decreased the protein-protein interactions, increasing the mobility of polypeptide chains and allowing the films to become less resistant and more elastic. On the other hand, Garcia and Sobral (2005) observed that the increase of the thermal treatment from 40 °C/30 min to 65°C/30 min increased the resistance to the puncture of films based on muscle proteins from tilapia. This behavior was possibly due to the formation of sulfite bonds between adjacent protein chains that proportioned more resistant films (Perez-Gago and Krochta, 2001; Choi and Han, 2002). However, increasing the treatment to 90 °C/30 min reduced the resistance of films, principally in low plasticizer concentration (Paschoalick et al., 2003). This last behavior may have occurred because the more intensive thermal treatment caused protein denaturation and consequently bury free –SH groups in the hydrophobic pockets such that they may remain unavailable for disulfide bond formation (Monahan et al., 1995).

Films produced by tilapia muscle proteins are practically colorless. The films produced with muscle proteins from Thai and Nile tilapia (Garcia and Sobral, 2005) presented color difference comparable to the color of soybean protein films ($\Delta E^* = 8.5–11.6$) (Kunte et al., 1997), but it was more colored than some films based on Nile tilapia myofibrillar proteins ($\Delta E^* = 7–8$) (Sobral, 2000), egg albumins ($\Delta E^* = 1.7–2.3$) (Gennadios et al., 1996), and pigskin gelatin ($\Delta E^* < 3$) (Sobral, 1999). On the other hand, films produced by Garcia and Sobral (2005) were more opaque than the films of pigskin gelatin (Y= 0.5) which were extremely transparent (Sobral, 1999), and than those based on Nile tilapia myofibrillar proteins (Y= 3.5) (Sobral, 2000). Monterrey-Quintero and Sobral (2000) studied the denaturation of Nile tilapia muscle proteins by differential scanning calorimetry and determined that the sarcoplasmic proteins of these fish denatured at around 41°C. Therefore, in some manner, the denaturation of sarcoplasmic proteins occurred during the thermal treatments (≥40°C/30 min) and must have caused the increase of opacity.

11.5. Edible Films From fish Gelatin

The volume of gelatin used annually by the food industry worldwide is considerable and growing. Gelatin is used not only for its functional properties, but also to increase protein content. It can enhance the elasticity, consistency and stability of food products, and it may also be used as an outer film to protect against drying, light and oxygen. Its use for encapsulation and film formation also makes it of interest to the pharmaceutical and photographic industries.

Gelatin and collagen have been extensively selected for the development of edible films and coatings. Protein-based films are generally superior to polysaccharide-based films in their mechanical and barrier properties (Cuq et al., 1998). This is attributed to a wide range of potential functionalities due to their specific structure. A stronger intermolecular binding potential via covalent bonds has been found in protein-based films, rather than in the films from homopolymer

polysaccharides (Cuq et al., 1995). Gelatin is a protein compound derived by hydrolysis of animal collagen contained in bones and skins. The source, age of the animal, type of collagen and extracting conditions all influence the properties of the gelatin (Johnston-Banks, 1990). For type A gelatins, the collagen rod is extracted in acid and solubilized without altering its original triple-helix configuration. Subsequent thermal treatment cleaves hydrogen and covalent bonds; this destabilizes the triple helix by means of a helix-to-coil transition, leading to conversion into soluble gelatin (Djabourov et al., 1993). Gelatin is normally manufactured from the waste generated during animal slaughter and processing, especially bovine and porcine. However, due to bovine illness (ESB) and religious objections to consuming food from pig origin, the production of fish gelatin is increasing.

11.5.1. Fish gelatin

The waste from fish filleting can account for as much as 75% of the total catch weight (Shahidi, 1994). This waste is an excellent raw material for the preparation of high-protein foods, besides helping to eliminate harmful environmental aspects and improve quality in fish processing. About 30% of such waste consists of skin and bone with high collagen content. A mild acid pre-treatment is normally used for collagenous material containing a low concentration of intra- and interchain nonreducible cross-links, as with fish skins (Norland, 1990). The main drawback of fish gelatins is that gels based on them tend to be less stable and to have worse rheological properties than gelatins from land mammals. This has been largely related to the considerably lower number of pro-rich regions of the collagen or gelatin molecule in cold water fish than in warm blooded animals (Ledward, 1986).

Skins from tropical fish species, such as tilapia, have been described as an optimal raw material for gelatin production (Grossman and Bergman, 1992). However, gelatin extracted from cod skin shows poor rheological properties (Gudmundsson and Hafsteinsson, 1997). Thus, the use of fish for gelatin production has to take into account the wide diversity among fish species, which present intrinsic differences in the collagen molecules present in their skin. In addition, the nature of the collagenous material from fish skins makes them more susceptible to degradation, in contrast to the more stable collagen from mammals (Asghar and Henrickson, 1982). As reviewed by Johnston-Banks (1990), the physical properties of gelatin depend not only on the amino acid composition, but also on the relative content of α-chains, β- or γ-components and higher molecular weight aggregates, as well as on the presence of lower molecular weight protein fragments.

In recent years a considerable effort is being conducted in the search for different fish species and extracting conditions to improve the properties of the resulting gelatins. Gelatins with high gelling capacity were obtained from the skin of flat-fish species, such as megrim and sole (Gómez-Guillén et al., 2002).

Other fish species have also been reported as a source for gelatin extraction, for example, pollock (Zhou and Regenstein, 2005), shark (Cho et al., 2004), Nile perch (Muyonga et al., 2004), yellowfin tuna (Cho et al., 2005) and bigeye snapper (Jongjareonrak et al., 2005). Modifications in the extraction process were introduced by the use of different organic acids in the pre-treatment of skins (Gómez-Guillén and Montero, 2001; Giménez et al., 2005b), different salts in the washing of skins (Giménez et al., 2005a), or even by the application of a high pressure treatment (Gómez-Guillén et al., 2005).

11.5.2. Gelatin Based Film

Numerous works in the recent literature are available concerning the use of gelatin, alone or combined with other biopolymers, to obtain edible and biodegradable films (Arvanitoyannis and Biliaderis, 1998; Menegalli et al., 1999; Sobral et al., 2001; Simon-Lukasik and Ludescher, 2004; Bertan et al., 2005). An exhaustive and well-documented review about properties of gelatin and gelatin films was reported by Arvanitoyannis (2002). However, this information is related to commercial gelatin from mammals. Although considerable attention to research on fish gelatin films is starting, until now the information available is very limited.

Gelatin films from skins of Nile perch, a warm water fish species, were reported to exhibit stress and elongation at break similar to that of bovine bone gelatin (Muyonga et al., 2004). On the contrary, Nile perch bone gelatin, consisting of a high proportion of low molecular weight fractions as a result of the more severe heat treatment needed for extraction, offered considerable lower film strength but higher elongation than the corresponding films from skin. Similarly, in a study comparing mechanical properties of gelatin films from tuna and halibut skins, the lower average molecular weight of halibut gelatin was related to a lower breaking force and noticeably higher elongation of the resulting films (Gómez-Guillén and Montero, 2003; Thomazine et al., 2005a). Dynamic-viscoelastic studies of 6.67% solution of both type of gelatins showed a melting temperature of ≈10°C and 25°C for halibut and tuna gelatins, respectively (Habitante et al., 2005). The melting temperatures of both types of gelatin were a direct consequence of differences in molecular weight distribution. The corresponding films obtained with both fish gelatins, using sorbitol as plasticizer, were found to be less resistant but more elastic than with more conventional gelatins from bovine or pig skin using a comparable amount of plasticizer (Sobral et al., 2001). Studies performed with two halibut gelatins, having slightly different average molecular weight, showed that films from the higher molecular weight gelatin, which, as observed by DSC studies, also showed a higher glass transition temperature, were significantly more resistant, more rigid and less elastic than the film from the lower molecular weight gelatin (Thomazine et al., 2005a). Halibut skin gelatin films were also characterized by lower water vapor permeability (WVP) than that reported for mammalian gelatin films in Sobral et al. (2001) or Vanin et al. (2005). Films from tuna skin gelatin plasticized with glycerol have also been shown to present

lower WVP than that reported in pig skin gelatin (Montero and Gómez-Guillén, 2005). Sobral et al. (2001) reported WVP in pig skin gelatin films to increase linearly using sorbitol in a concentration ranging from 15 to 65 g/100 g gelatin. When using 25 g glycerol/100 g pig skin gelatin, WVP was found to be considerably higher (Thomazine et al., 2005). Glycerol is well recognized as presenting a higher plasticizing effect than sorbitol, causing an increase in film flexibility, but a reduced resistance and WVP (Gennadios et al., 1996).

Thomazine et al. (2005b) explained this behavior in terms of molecular weight and number of molecules of plasticizers in the films. Similar findings have been recently reported working with different concentrations and types of plasticizers in films from skin gelatin of bigeye snapper and brownstripe red snapper (Jongjareonrak et al., 2006a), showing the latter generally higher mechanical properties at any protein and glycerol concentrations tested than the former (Jongjareonrak et al., 2006b). The tendency of fish gelatin films to exhibit lower WVP than that of land animal gelatin films could be explained in terms of aminoacid composition, since fish gelatins are known to be less rich in proline and hydroxyproline (Norland, 1990), thus increasing their hydrophobicity as compared to mammal gelatins. As in the case of other films of protein nature, fish gelatin films also represent a good barrier against UV light. Jongjareonrak et al. (2006b) reported that differences in light transmission between the films from bigeye snapper and brownstripe red snapper might be due to differences in composition, density and the aggregation or alignment of gelatin molecules in the film. Tuna and halibut skin gelatin films also presented high light barrier properties, especially those from tuna gelatin, having higher molecular weight (Habitante et al., 2005).

The properties of fish skin gelatin-based films, especially water vapor permeability, have been shown to improve by the addition of fatty acids or their sucrose esters (Jongjareonrak et al., 2006c). These authors also observed that light transmission and tensile strength of films was decreased by increasing the amount of fatty acids. However, incorporation of the sucrose esters generally increased tensile strength and reduced elongation at break. Tuna skin gelatin has also been used to produce transparent and flexible films with added aqueous plant extracts, without significantly modifying mechanical and vapor barrier properties (Montero and Gómez-Guillén, 2005). The resulting films were characterized by an increased antioxidant capacity as a result of the high content of polyphenolic compounds. In this connection, gelatin films enriched with oregano or rosemary aqueous extracts have been successfully applied to improve the conservation of cold-smoked fish by significantly reducing lipid oxidation during chilled storage (Gómez-Estaca et al., 2006). On the other hand, the unique property of gelatin to produce thermoreversible gels upon cooling also makes it an adequate material to produce coatings for preservation of foodstuffs under refrigerated conditions. In this sense, fish hamburgers coated with a blend of fish gelatin and chitosan have been reported to show a noticeable reduction in microbial growth during chilled storage, without altering rheological properties (Lopez-Caballero et al., 2005).

11.6. Feather Keratin Films

Feathers are an important waste disposal of the poultry industry and are basically composed of structural proteins, the keratins, which have a great ability to form films. It has been known that the stability of the keratin in the solid state is due to cross-linking produced by the formation of cystine disulphide bonds, hydrogen bonds and to salt linkages (Schrooyen et al., 2001b). It is possible to dissolve keratin using solvents that break the –S–S– bonds and the hydrogen bonds (Schrooyen et al., 2000, 2001a). The sodium dodecyl sulfate (SDS) can be used to obtain a stable dispersion of keratins (Yamauchi et al., 1996; Schrooyen et al. 2000, 2001a).

The regeneration of disulfide bonds in these materials during the drying of film forming dispersion may be used as a method to impart water insolubility and good mechanical properties to the films. The aim of this study was to prepare and characterize some properties of feather keratin films.

11.6.1. Preparation and Characterization of Feather Keratin Films

Keratin was extracted from white chicken feathers. Freshly plucked wet feathers were cleaned according to ASTM (1997), dried in a ventilated oven at 40°C for 72 h and cut into small filaments (75–700 μm). This material was treated in a Soxhlet device for 12 h with petroleum ether to remove grease. The keratin extraction was performed according to the method proposed by Schrooyen et al. (2000) and Yamauchi et al. (1996), with some modifications (Martelli et al., 2006). Fifty ml of the aqueous dispersion of the reduced keratins (7 g keratin/100 ml dispersion) were mixed with glycerol in the following concentrations: 0.01, 0.03, 0.05, 0.07 and 0.09 g/g of keratin, which were used to prepare the films by the casting procedure. Prior to properties determinations, films were conditioned at 35 °C and 75% relative humidity (RH) for 48 h. Film solubility (%) in water and film swelling (SW) were determined according to the methods proposed by Turhan and Sahbaz (2004) and Lee et al. (2004). The mechanical properties of the films were determined by tensile tests with a texturometer TA.XT2i (SMS, Surrey, UK). Thermal properties of films were studied using DSC analyses.

11.6.2. Some Characteristics of Feather Keratin Films

The extracted keratin presented a high content of sulfured amino acids, namely cysteine and methionine (Moore et al., 2006). These results agree with those found in the literature for wool keratin (Yamauchi et al., 1996) and for feather keratin from fowl (Arai et al., 1983). On the other hand, it can be observed that the polar amino acids, ionizable (4.7% aspartic acid, 7.7% glutamic acid and 5.4% arginine) or not ionizable (9.3% serine, 8.8 proline and 3.5% threonine), represent almost 40% of the total content of amino acids. Films properties are

TABLE 11.3. Film solubility, film swelling index in water, glass transition temperature and mechanical properties of keratin films

Glicerol concentration (g glycerol /g keratin)	Film solubility in water (%)	Swelling index (%)	Glass transition temperature of dry films (°C)	Mechanical properties		
				Tensile strength (MPa)	Elongation at break (%)	Young module (Mpa/%)
0.0	30.7±1.5	155±7	70	16.6±5.5	1.7±0.2	10.2±7.1
0.01	–	–	–	6.3±0.7	11.9±2.6	2.0±0.8
0.03	37.0±1.3	182±2	67.5	7.6±0.6	13.8±2.4	2.1±0.6
0.05	40.6±3.8	191±35	64.5	5.3±0.7	19.8±4.1	1.2±0.2
0.07	48.3±2.7	207±15	56.3	5.4±0.5	30.5±7.7	0.9±0.6
0.09	50.7±1.0	110±13	–	2.0±0.2	31.9±4.5	0.2±0.0

shown in Table 11.3. Water solubility increased from 30% for films without plasticizer to about 51% for films prepared with 0.09 g glycerol/g keratin. The relatively low solubility (30%) of keratin films without plasticizer suggest that some -S-S- bridges were formed during drying of films, although other interactions such as hydrogen bonds and electrostatic and hydrophobic interactions could also be improved. The results also indicated that the addition of glycerol avoided the formation of these bridges, increasing the films' solubility. Swelling was 155% for films without glycerol, increasing to 207% for films with 0.07 g glycerol/g keratin. Yamauchi and Yamauchi (2002) reported swelling data of 140% for films of wool keratin plasticized with 50 g glycerol/100 g keratin.

Films without plasticizers showed brittle characteristics. The addition of 0.01 g glycerol/g keratin decreased the tensile strength by about 38% when compared with the value found for the films without glycerol, while the addition of 0.09 g glycerol/g keratin decreased this property by 8.3 times, which represents about 12% of the tensile strength for the non-plasticized films. Similar results were observed with the Young Modulus, which decreased from 10.18 to 0.21 MPa when 0.09 g glycerol/g keratin was added to the films. On the other hand, glycerol had a positive effect on the films' elongation, which increased about 7 and 18.8 times for films prepared with 0.01 and 0.09 g glycerol/g keratin, respectively. Yamauchi and Yamauchi (2002) found values ranging between 5 MPa (films conditioned at 85% RH) and 11 MPa (films conditioned at 65% RH), for films plasticized with 0.5 g glycerol/g keratin. As expected, the glass transition temperatures (Tg) decreased with the increase of glycerol. The values of Tg obtained in this work implies that the dry films were in the glass state when conditioned at room temperature (T<Tg), but these films with plasticizer constituted flexible materials. This behavior has also been reported for other protein-based films (Sobral et al., 2001, 2005). In conclusion, it is possible to prepare films with good properties from keratin extracted from chicken feathers. Low glycerol concentrations are enough to significantly modify the films' mechanical properties. These films showed relatively low water solubility when compared with the values of other protein-based films presented in the literature.

11.7. Edible Films Based on Soy Proteins

11.7.1. Soybean Proteins

Protein accounts for approximately 38–44% of soybean composition, and 7S and 11S globulins constitute the 90% of the total proteins (Fukushima, 1991). The 7S globulin or β-conglycinin is a trimeric glycoprotein of 150 to 200 kDa, while the 11S globulin or glycinin is a heterogeneous oligomeric protein of 360 kDa (Lawrence et al., 1994). Based on protein content, soy proteins used in the food industry are classified as soy flours (50–59%), soy concentrates (65°72%) or soy isolates (more than 90%).

Physicochemical and functional properties of soy globulins have been widely studied. Both globulins (7S and 11S) are soluble in water and neutral saline solutions and develop an extensive range of functional properties. From all of these properties, those that are dependent on molecular superficial characteristics (capability to form foams and emulsions) and on protein–protein interactions (capability to form networks, particularly gels and films) are the ones that present bigger perspectives to their development.

The development of edible films from plant proteins represents an interesting way to increase the utilization of these proteins, as well as to reduce environmental problems generated by the accumulation of synthetic polymers (Gennadios, 2002).

11.7.2. Soy Protein Isolate (SPI) Films

A native SPI (SPIn), which was obtained in the laboratory from soybean defatted flour by alkaline extraction and isoelectric precipitation, was used as raw material (Petruccelli and Añón, 1995). The relationship among structural, mechanical and physical properties of soy protein isolate films was studied using the pH of initial film forming solutions as a variable, because pH affects the protein charge and the degree of protein denaturation. Films were obtained by casting from aqueous dispersions of 5% w/v SPI and 2.5% w/v of glycerol (used as plasticizer) at pH 2, 8 and 11, and dried at 60 °C. DSC studies showed that proteins retained their native conformation in films at pH 8, but were partially or extensively denatured at pH 11 and 2. Once unfolded, protein chains could interact strongly, mainly through disulfide bonds, and SEM verified production of denser protein networks. These films, at pH 2 and 11, showed a greater tensile strength—by about 1.05 MPa, and a higher Young's modulus—by at least 0.15 MPa, than the film made from the pH 8-SPI solution. However, films formed at alkaline pHs (8 and 11) exhibited about 70% greater deformation than films at pH 2. It seems that the native proteins may unfold during the mechanical test, providing a greater deformation before breaking (Table 11.4).

Solubility assays in buffers with different chemical activity (water, phosphate, with urea, SDS and urea-SDS-mercaptoethanol) and the analysis of the electrophoretic profiles of the soluble protein fractions, showed that at pH 2 the protein networks were mainly stabilized by hydrogen and disulfide bonds,

TABLE 11.4. Mechanical properties, WVP and thickness of SPIn films at pH 2, 8 and 11, SPIc at pH 10.5, and bilayers films

Film	TS (MPa)	E (%)	WVP.10^{10} $gm^{-1}s^{-1}Pa^{-1}$	Thickness (μm)
SPIn Ph 2	1.50 ± 0.09	92.64 ± 13.72	3.52 ± 0.21	114.6 ± 6.2
SPIn pH 8	0.45 ± 0.05	163.59 ± 14.91	2.86 ± 0.58	94.6 ± 8.0
SPIn pH 11	1.90 ± 0.28	205.41 ± 25.67	2.84 ± 0.25	105.1 ± 9.3
SPIc pH 10.5	1.86 ± 0.32	144.9 ± 18.3	2.28_{s} ± 0.66	62.8 ± 10.3
SPIc-Beeswax	2.70 ± 0.19	197.9 ± 23.4	0.12 ± 0.08	87.9 ± 13.9
SPIc-Sunflower	2.28 ± 0.21	173.9 ± 9.9	1.23_{s} ± 0.08	80.2 ± 13.0
SPIc-Carnauba	2.18 ± 0.34	177.6 ± 33.6	0.76 ± 0.38	94.0 ± 9.62

and that when the pH of the initial solution was increased, the hydrophobic interactions also become important. Films at acid pH had a higher water vapor permeability (WVP) and lower Tg than the films obtained at alkaline pH (Table 11.4), confirming than polymers linked by hydrogen bonds are more susceptible to moisture.

The effect of storage on the films' properties was studied. Films remained stable for long periods of time (at least up to 120 days at 20 °C and 59% RH), as no variations in their mechanical and barrier properties or in their color parameters were observed.

11.7.3. Soy Globulins Films

Film formation from the 7S and 11S pure globulins was studied in order to know the role of each fraction in SPI films. These proteins were obtained in the laboratory from defatted soy flour, as described by Nagano et al. (1992).

It was observed that the 7S film differs from 11S, especially in their mechanical properties, but not in their WVP, as has also been observed by other authors (Cho and Rhee, 2004; Kunte et al., 1997). Figure 11.4 shows the stress-strain curves obtained by tensile tests for 7S, 11S and SPIn films at pH 2 and 10.5.

In films at acidic pH, proteins were totally denatured and could interact chain to chain easily and strongly, producing denser films with higher tensile strength and lower elongation than basic films. 7S films were more elastic, while the 11S were more resistant due to their higher tendency to form disulfide bonds.

At alkaline pH, this effect was not so evident because of the 11S lower capacity to be deformed and the stress-strain behavior. The high tensile strength of 7S could in part be attributed to the presence of 11S as an impurity in the 7S-enriched fraction when it is obtained by the Nagano procedure, as demonstrated by DSC and electrophoretic assays. The mix of both globulins in SPIn improved the film mechanical properties, showing a synergic effect of both globulins. SPI films presented similar elongations to the 7S samples and tensile strength to the 11S films, indicating the presence of interactions between both fractions in SPI films.

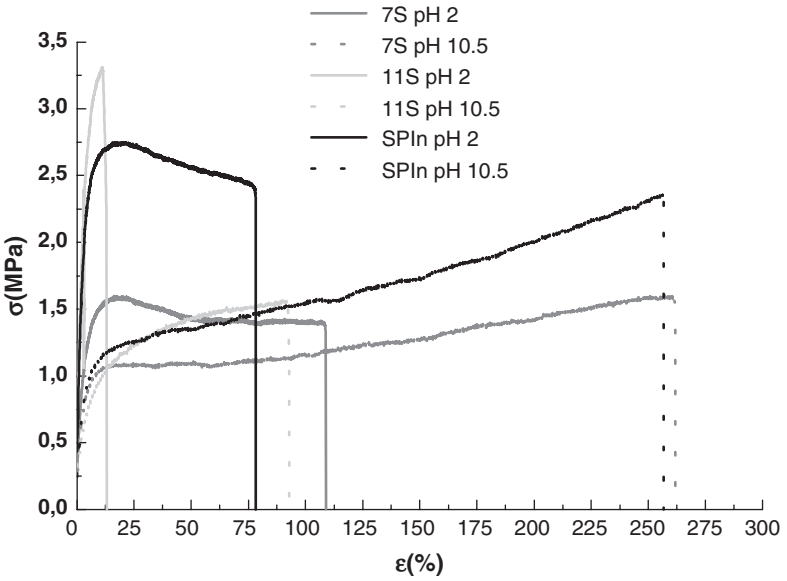

FIG. 11.4. Stress-strain curves of SPIn, 7S and 11S films at pH 2 and 10.5 obtained by tensile test

11.7.4. Soy Protein Isolates-Waxes Bilayers Films

In order to improve WVP of SPI films, lipids were included in their formulation. Waxes of different origin (bees, carnauba and sunflower) were used as lipid material (Gontard et al., 1994), and a commercial SPI (SPIc, Samprosoy 90 EG, Bunge Alimentos) as a protein source.

Bilayer films were obtained, spreading a thin layer of the molten waxes on a protein film, which was previously made by casting from soy protein isolates dispersions, using glycerol as plasticizer. All composite films showed a higher yellowness color and a higher opacity (as was demonstrated by the increase in the Hunter Parameter b and the decrease of L), lower water vapor permeabilities and higher tensile strengths than soy protein films, without modifying their elongation at break. Beeswax films presented the best properties (WVP 19 times lower and tensile strength 45% higher than protein films), probably because they contained a higher amount of lipid compounds in their formulation and their lipid layer was more homogeneous than those formed by the other waxes (as was seen by SEM) (Table 11.4).

Beeswax-SPI film showed a great stability during storage at 20°C and 75% relative humidity. At 120 days, WVP and tensile strength did not change.

As plasticizer concentration plays an important role in protein film behavior, it was used as a variable to evaluate the role of each component (proteins and lipids)

in the functionality of these bilayer films. Bilayer films were formed, applying the melted beeswax on SPIc films containing sorbitol or glycerol as plasticizers, in the different concentrations used (1, 1.5, 2, 2.5 and 5%) and were compared with the corresponding protein film.

As was expected, the increment in plasticizer concentration increased the elongation, WVP and moisture content of protein films, while decreasing their puncture and tensile strength—these effects being greater for glycerol than for sorbitol. The increase of plasticizer concentration showed the same tendency in mechanical properties for bilayer films. No differences in strength and elongation were found between the bilayer film and its corresponding protein films (both with the same type of plasticizer and concentration). WVP did not show differences among bilayer films with different plasticizer concentrations or between films with glycerol and sorbitol, but it was significantly lower in bilayers than in SPI film.

These studies suggest that the protein film dominates mechanical properties, as differences were not seen either in deformation or in strength between films, with or without the wax layer. Furthermore, the beeswax layer determines the WVP and the color of the bilayer films, since both parameters do not vary with the type or concentration of plasticizer.

11.8. Edible Films from Amaranth

Protein films are made of raw materials of high molecular weight such as gelatin, myobrillar proteins, gluten, and whey protein, among others. These films are characterized by good mechanical properties, although they are usually quite permeable to water vapor and gases (McHugh and Krochta, 1994).

Starch films have also received interest, since they are very low cost materials, the most abundant and important polysaccharide in nature. Numerous studies have been reported on its film forming capabilities and industrial applications. Also, various studies have attempted to improve the functional properties of these films by using mixtures of protein and starch as the raw material for the formation of edible films (Parris et al., 1997, Arvanitoyannis et al., 1996, 1997).

However, when raw cereals are used, it is not necessary to extract neither the starch nor the proteins for film production. Rayas et al. (1997) prepared edible films from three types of wheat flours, and more recently, Mariniello et al. (2003) used whole soy flour and apple pectin as the raw materials for producing edible films.

It is interesting to investigate other new renewable resources for the production of edible and biodegradable materials. The use of natural blends of protein, polysaccharides and lipids directly obtained from agricultural sources, which take advantage of each component in the original system, appears to be a new opportunity for material in the area of edible films. *Amaranthus cruentus* flour can be considered as such a natural mixture and, consequently, an interesting source of raw material for edible film technology.

Amaranth is a pseudocereal of rapid growth, with a high tolerance to arid conditions and poor soils where traditional cereals cannot be grown, so many countries have been adapting certain varieties to their soils. The main cultivars used are *Amaranthus hipochondriacus, Amaranthus cruentus* and *Amaranthus caudatus*.

The grain composition is a function of the cultivars and of the environmental conditions of culture (Saunders and Becker, 1984). Amaranth (*Amaranthus* spp.) is a tiny grain (~1 mm diameter) typically from South America, of which the species *Amaranthus cruentus* is composed of 15–22% protein (rich in lysine), 3.0–11.5% fat and 9–16% dietary fiber, depending on cultivation technique and environmental effects. The main constituent of amaranth is starch, 48–62%, with small granule size (< 1μm), a characteristic that allows easier dispersion; hence, it may yield good properties for resultant films.

11.8.1. Films Based on Amaranth Flours

Tapia-Blácido et al. (2005a,b) and Tapia-Blácido, 2006) obtained films using amaranth flour of two varieties, *A. caudatus* and *A. cruentus*. The amaranth flours were produced by the alkaline wet milling method. The chemical compositions of both materials are shown in Table 11.5. The *cruentus* variety has higher amylose content and lower lipid content than *caudatus*. Analysis of fatty acids content revealed a major fraction, up to 92% of linoleic acid (C18:2), oleic acid (C18:1), palmitic acid (C16:0), with composition depending on variety (Tapia-Blácido, 2006).

These authors obtained films using the casting process with glycerol (*caudatus*) and sorbitol (*cruentus*) as plasticizers. The influence of the most relevant variables of the process of film production on film properties were studied by a full factor design. The influence of plasticizer content, pH, temperature of heating process, and temperature and relative humidity (RH) of the air during film drying on mechanical and barrier properties were evaluated, and the optimal process conditions were found in each case.

The best mechanical properties and lower solubility were found for films made with *A. caudatus* flour, at a process temperature of 82°C, dried at 40°C and 55% RH, glycerol content 22.5% and pH of 10.7 (Tapia-Blácido et. al, 2005a). Meanwhile, the optimal process conditions for the *A. cruentus* films were obtained at 75°C and 20.02% of glycerol content. Table 11.6 shows the properties of films measured at those conditions (Tapia-Blacido, 2006).

Table 11.5. Composition of Amaranth varieties

Component (g/100g dried mass)	Amaranth flour (Amaranthus cruentus)	Amaranth flour (Amaranthus caudatus)
Ashes	2.10 ± 0.03	2.11 ± 0.03
Lipids	7.96 ± 0.19	8.93 ± 0.03
Protein	14.08 ± 0.	14.21 ± 0.32
Starch	75.07 ± 0.25	74.75 ± 0.25
Amylose	11.89 ± 0.26	7.58 ± 0.77

TABLE 11.6. Properties of amaranth flour films

Properties	Flour film (A.caudatus)[1]	Flour film (A.cruentus)[2]
Solubility (%)	42.25 ± 1.82	40.64 ± 2.36
Puncture test		
Force (N)	2.34 ± 0.09	4.09 ± 0.37
Deformation (%)	15.62 ± 0.65	4.91 ± 0.79
Tensile test:		
Tensile strength (MPa)	1.455 ± 0.045	5.35 ± 0.85
Elongation at break (%)	83.736 ± 5.107	12.93 ± 5.23
Young Modulus (MPa)	21.50 ± 1.40	252.00 ± 12.40
Water permeability ($g\ m^{-1}\ s^{-1}Pa^{-1}$)	$(8.20 \pm 0.15) \times 10^{-11}$	$(3.76 \pm 0.22) \times 10^{-10}$
Oxygen permeability ($cm^3.\mu m/m^2.dia.kPa$)	5.63 ± 3.68	22 ± 0.71
Optical properties		
a*	−1.16 ± 0.01	−1.16 ± 0.01
b*	8.09 ± 0.49	12.44 ± 0.24
L*	89.97 ± 0.28	87.28 ± 0.15
ΔE*	8.89 ± 0.62	13.35 ± 0.28
Opacity	15.24 ± 0.90	17.04 ± 0.84

[1]Films made with 22.5% glycerol (g glycerol/100 g flour)
[2]Films made with 20.02% glycerol (g glycerol/100 g flour)

Films are not very tough, and their properties are function of cereal variety. Nevertheless, these films furnish better barrier properties than other edible films. This was an unexpected fact, as the major constituent of amaranth is a waxy starch. The presence of native lipids and proteins in its formulation may explain the lower permeabilities of these materials. However, some noticeable differences between both varieties are verified that are not completely defined by differences in composition of both materials. Therefore, the interaction between the components may differ in both materials, resulting in diverse structures.

The changes in plasticizers also result in differences in process conditions and properties. Tapia-Blácido (2006) made films with amaranth flour (*A. cuentus*), plasticized with glycerol and sorbitol. The optimal conditions with glycerol and sorbitol were 20.02 and 29.6% for plasticizer content and 75 °C of process temperature. The drying condition also varied with the change of plasticizer. The optimal drying conditions were: 46.8 °C and 74.7% of relative humidity when glycerol was used and 28.6 °C e 72.5% for sorbitol. Table 11.7 show properties of the films as a function of the plasticizer used. Better water vapor and oxygen barrier and mechanical properties were verified using sorbitol, although solubility was higher when using sorbitol as a plasticizer.

Figure 11.5 shows the structure of both films, formed by a protein network (dark zones), linked to lipid globules, and dispersed through the starch phase (gray surfaces).

The lipid phase reduced permeabilities and also acts as plasticizer. Some improvements of properties can be obtained if additional lipids are mixed into the flour.

TABLE 11.7. Film properties with glycerol and sorbitol as plasticizer

Properties	Films of flour with glycerol	Films of flour with sorbitol
Solubility	40.64 ± 2,36	50.79 ± 4,35
Tensile strength (Mpa)[1]	4.09 ± 0,37	6.72 ± 0,43
Elongation (%)*	4.91 ± 0,79	2.82 ± 0,32
Water Permeability	3.761×10^{-10}	3.10×10^{-10}
(g.m.s-^{1}m-^{2}.Pa^{-1})	$\pm 2.25 \times 10^{-11}$	$\pm 1.95 \times 10^{-11}$
Oxygen permeabilidade		
(cm^{3}.µm/m^{2}.24h.kPa)	22 ± 0.71	13.5 ± 1.77

[1]Tensile test at break, measured at 57% relative humidity

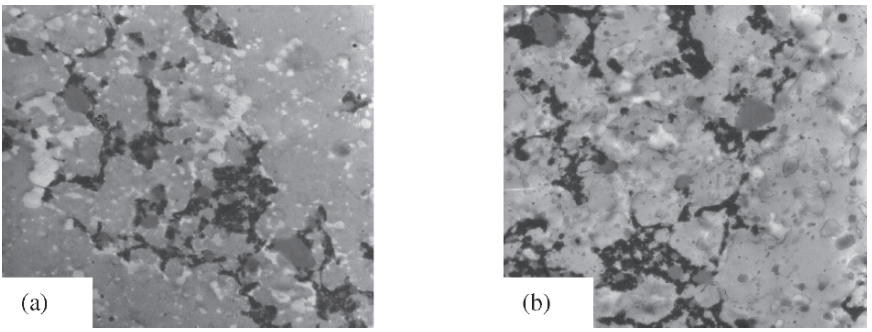

FIG. 11.5. TEM micrographs of films plasticized with glycerol (a) and sorbitol (b)

The feasibility of producing composite films of amaranth flour and stearic acid with improved water vapor barrier, low oxygen permeability and acceptable mechanical properties was demonstrated by Colla et al. (2006). The addition of stearic acid to films of amaranth flour (*Amaranth cruentus*) decreases solubility up to 15.2% and water permeability to 8.9×10^{-11} g/m s Pa. The optimal conditions of the process were: stearic acid concentration: 10 g/100 g flour; glycerol concentration: 26 g/100 g flour and stirring speed: 12000 rpm.

It can be concluded that amaranth flour seems to be an interesting material for the formulation of coatings and edible films.

Acknowledgement To CYTED (Project XI.20). The authors acknowledge the financial support from Agencia Nacional de Promoción Científica y Tecnológica (ANPCyT), Universidad de Buenos Aires (UBA), Universidad Nacional de La Plata (UNLP), Consejo Nacional de Investigaciones Científicas y Técnicas (CONICET) and Fundación Antorchas, from Argentina; to FAPESP, CAPES and CNPq, from Brazil; to FUNDACYT-UTA from Ecuador.

References

Almeida, A.V., and Arancibia M.Y., 2005, *Desarrollo de Una Tecnología para la Obtención de Quitina y Quitosano a Partir del Caparazón de Camarón (Penaeus Vannamei)*. Thesis, Universidad Técnica de Ambato-Facultad de Ciencia e Ingeniería en Alimentos, Ambato. p110.

Alvarado, J. de D., Almeida, A.V., and Arancibia M.Y., 2005, Permeabilidad al Vapor de Agua de Películas Biodegradables de Quitosano Obtenido de Caparazones de Camarón, *Ciencia y Tecnología* **4**(2):39–47.

Alvarado, J. de D., Almeida, A., Arancibia, M., Aparecida de Carvalho, R., Sobral, P.J. A.,Quinta Barbosa Habitante, A.M., Monterrey-Quintero, E.S., and Sereno A., 2006, Método Directo para la Obtención le Quitosano de Desperdicios de Camarón para la Elaboración de Películas Biodegradables, *Pesquisa Agropecuária Brasileira* (submitted).

Arai, K.M., Takahashi, R., Yokote, Y., and Akahane K., 1983, Amino-Acid Sequence of Feather Keratin from Fowl, *Eur. J. Biochem*. **32**:501–510.

Argukelles, W., Monal, F., Goycoolea, C., Peniche, I., and Higuera C., 1998, Rheological Study of The Chitosan/Glutaraldehyde Chemical Gel System, *Polymer Gels Netw*. **6**:429–440.

Arvanitoyannis I.S., 2002, Formation and Properties of Collagen and Gelatin Films and Coatings, in: *Protein-Based Films and Coatings*. A. Gennadios (ed.), CRC Press, Boca Ratón, pp. 275–304.

Arvanitoyannis I., and Biliaderis C.G., 1998, Physical Properties of Polyol-Plasticized Edible Films Made from Sodium Caseinate and Soluble Starch Blends, *Food Chem*. **6**(3):333–342.

Arvanitoyannis, I., Psomiadou, E., and Nakayama A., 1996, Edible Films Made from Sodium Caseinate, Starch, Sugars or Glycerol. Part. 1. *Carbohydr. Polym*. **31**:179–192.

Arvanitoyannis, I., Psomiadou, E., Nakayama, A., and Yamamoto N., 1997, Edible Films Made from Gelatin, Soluble Starch and Polyols, Part. 3. *Food Chem*. **60**:593–604.

Asghar, A., and Henrickson, R L., 1982, Chemical, Biochemical, Functional, and Nutritional Characteristics of Collagen in Food Systems, in: *Advances in Food Research*, vol. 28. Academic Press, London, pp. 232–372.

ASTM, 1996, Standard Test Methods for Water Vapor Transmission of Material, E96–95. *Annual book of ASTM*. Philadelphia.

ASTM, D584–96, 1997, Standard Test Methods for Wool Content of Raw Wool, in: *Annual Book of ASTM Standards*, (1-5), ASTM, Philadelphia.

ASTM, D4092, (1996), Standard Terminology: Plastics: Dynamic Mechanical Properties, ASTM, Philadelphia.

Bertan, L.C., Tanada-Palmu, P.S., Sian, A.C., and Grosso C.R.F., 2005, Effect of Fatty Acids and *Brazilian elemi* on Composite Films Based on Gelatin, *Food Hydrocolloid*. **19**(1):73–82.

Buonocore, G.G., Conte, A., and Del Nobile M.A., 2005, Use of a Mathematical Model to Describe the Barrier Properties of Edible Films, *J. Food Sci*. **70**(2):E142–E147.

Butler, B., Vergano, R., Testin, R., Bunn, J., and Wiles J., 1996, Mechanical and Barrier Properties of Edible Chitosan Films as Affected by Composition and Storage, *J. Food Sci*. **61**(5):953–961.

Caner, C., Vergano, P., and Wiles J., 1998, Chitosan Film Mechanical and Permeation Properties as Affected by Acid, Plasticizer, and Storage, *J. Food Sci*. **63**(6):1049–1053.

Chen, M., Yeh, H., and Chiang B., 1996, Antimicrobial and Physicochemical Properties of Methylcellulose and Chitosan Films Containing a Preservative, *J. Food Process. Preserv*. **20**:379–390.

Chen, R.H., and Lin J.H., 1994, Relationships Between the Chain Flexibilities of Chitosan Molecules and the Physical Properties of Their Casted Films, *Carbohydr. Polym*. **24**:41–46.

Cho, S.M., Gu, Y.S., and Kim S.B., 2005, Extracting Optimization and Physical Properties of Yellowfin Tuna (*Thunnus Albacares*) Skin Gelatin Compared to Mammalian Gelatins, *Food Hydrocoloid*. **19**(2):221–229.

Cho, S.M., Kwak, K.S., Park, D.C., Gu, Y.S., Ji, C.I., Jang, D.H., Lee, Y.B., and Kim S.B., 2004, Processing Optimization and Functional Properties of Gelatin from Shark (*Isurus oxyrinchus*) Cartilage. *Food Hydrocoloid*. **18**(4):573–579.

Cho, S.Y., and Rhee C., 2004, Mechanical Properties and Water Vapor Permeability of Edible Films Made from Fractions Soy Proteins with Ultrafiltration, *Lebensm.- Wiss. U.-Technol*. **37**:833–839.

Choi, W., Park, H., Ahn, D.J., Lee, J. and Lee C., 2002, Wettability of Chitosan Coating Solution on "Fuji" Apple Skin, *J. Food Sci*. **67**(7):2668–2672.

Choi, W.S., and Han, J.H., 2002, Film-Forming Mechanism and Heat Desnaturation Effects on the Physical and Chemical Properties of Pea-Protein-Isolate Edible Films, *J. Food Sci*., **67**:1399–1406.

Colla, E., do Amaral Sobral, P.J., and Cecília Menegalli F., 2006, *Amaranthus cruentus* Flour Edible Films: Influence of Stearic Acid Addition, Plasticizer Concentration, and Emulsion Stirring Speed on Water Vapor Permeability and Mechanical Properties, *Agric. Food Chem*. **54** (18):6645–6653.

Cunningham, P., Ogale, A., Dawson, P., and Acton J., 2000, Tensile Properties of Soy Protein Isolate Films Produced by a Thermal Compaction Technique, *J. Food Sci*. **65**(4):668–671.

Cuq, B., Aymard, C., Cuq, J.L., and Guilbert S.,1995, Edible Packaging Films Based on Fish Myofibrillar Proteins: Formation and Functional Properties, *J. Food Sci*. **60**:1369–1374.

Cuq, B., Gontard, N., Cuq, J.L., and Guilbert S., 1996a, Stability Of Myofibrillar Protein-Based Biopackagings During Storage, *Lebensm.-Wiss.-und-Tech*. **29**:344–348.

Cuq, B., Gontard, N., Cuq, J.L., and Guilbert S., 1996b, Functional Properties of Myofibrilar Protein-Based Biopackaging as Affected by Film Thickness, *J. Food Sci*. **61**:580–584.

Cuq, B., Gontard, N., Cuq, J.L., and Guilbert S., 1997, Selected Functional Properties of Fish Myofibrillar Protein-Based Films as Affected by Hydrophilic Plasticizers, *J. Agric. Food Chem*. **45**:622–626.

Cuq, B., Gontard, N., and Guilbert S., 1998, Proteins as Agricultural Polymers for Packaging Production, *Cereal Chem*. **75**:1–9.

Debeaufort, F., and Voilley A., 1997, Methylcellulose-Based Edible Films and Coatings: 2. Mechanical and Thermal Properties as a Function of Plasticizer Content, *J. Agric. Food Chem*. **45**:685–689.

Devlieghere, F., Vermeulen, A., and Debevere J., 2004, Chitosan: Antimicrobial Activity, Interactions with Food Components and Applicability as a Coating on Fruit and Vegetables. *Food Microbiol*. **21**:703–714.

Djabourov, M., Lechaire, J. and Gaill F., 1993, Structure and Rheology of Gelatin and Collagen Gels, *Biorheology* **30**:191–205.

Donhowe, I.G., and Fennema O., 1993a, The Effects of Plasticizers on Crystallinity, Permeability and Mechanical Properties of Methylcellulose Films, *J. Food Process. Preserv*. **17**:247–258.

Donhowe, I.G., and Fennema, O., 1993b, The Effects of Solution Composition and Drying Temperature on Crystallinity, Permeability and Mechanical Properties of Methylcellulose Films, *J. Food Process. Preserv*. **17**:231–246.

Fukushima D., 1991, Recent Progress of Soybean Protein Foods: Chemistry, Technology, and Nutrition, *Food Rev. Intern*. **7**:323–351.

Galed, G., Martínez, A. García, C., and Heras A., 2000, Relationship Between Physicochemical Characteristics and Functional Properties of Different Chitosans, in: *Memorias del Primer Simposio Latinoamericano de Quitina y Quitosano*, La Habana. pp. 400–405.

Garcia, F.T., and Sobral P.J.A., 2005, Effect of the Thermal Treatment of the Filmogenic Solution on the Mechanical Properties, Color and Opacity of Films Based on Muscle Proteins of Two Varieties of Tilapia, *Lebensm.-Wiss.-und-Tech*. **38**(3):289–296.

García, M.A., Pinotti, A., Martino, M., and Zaritzky N., 2004, Characterization of Composite Hydrocolloid Films, *Carbohydr. Polym*. **56**(3):339–345.

Gennadios A., 2002, *Protein Based Films and Coatings*, CRC Press., USA.

Gennadios, A., Weller, C.L., Hanna, M.A., and Froning G.W., 1996, Mechanical and Barrier Properties of Egg Albumen Films, *J. Food Sci*. **61**(3):585–589.

Giménez, B., Gómez-Guillén, M.C., and Montero, P., 2005a, The Role of Salt Washing of Fish Skins in Gelatin Extraction, *Food Hydrocolloid*. **19**:951–957.

Giménez, B., Turnay, J. Gómez-Guillén, M.C., and Montero P., 2005b, Use of Lactic Acid for Extraction of Fish Skin Gelatin, *Food Hydrocolloid*. **19**:941–950.

Gómez-Estaca, J., Gómez-Guillén, M.C., and Montero P., 2006, *Alta Presión y Películas Protectoras para Mejorar la Calidad del Pescado Ahumado en Frío*, CYTALIA. X Congreso Anual de Ciencia y Tecnología de los Alimentos, Madrid.

Gómez-Guillén, M.C., Giménez, B., and Montero P., 2005, Extraction of Gelatin from Fish Skins by High Pressure Treatment, *Food Hydrocoloidl*. **19**:923–928.

Gómez-Guillén, M.C., and Montero, P., 2001, Extraction Of Gelatin from Megrim (*Lepidorhombus boscii*) Skins with Several Organic Acids, *J. Food Sci*. **66**(2):213–216.

Gómez-Guillén, M.C., and Montero P., 2003, *Potencial del Empleo de Gelatinas de Nuevos Orígenes en la Tecnología de Películas Flexibles*, IV Iberoamerican Congress on Food Engineering, Valparaíso.

Gómez-Guillén, M.C., Turnay, J., Fernández-Díaz, M.D., Olmo, N., Lizarbe, M.A., and Montero P., 2002, Structural and Physical Properties of Gelatin Extracted from Different Marine Species: A Comparative Study, *Food Hydrocolloid*. **16**:25–34.

Gontard, N., Duchez, C., Cuq, J.L., and Guilbert S., 1994, Edible Composite Films of Wheat Gluten and Lipids: Water Vapour Permeability and Other Physical Properties, *Int. J. Food Sci. Technol*. **29**:39–50.

Gontard, N., Guilbert, S., and Cuq J.L., 1993, Water and Glycerol as Plasticizers Affect Mechanical and Water Vapor Properties An Edible Wheat Gluten Film, *J. Food Sci*. **58**(1):206–211.

Gontard N., Marchesseau, S., Cuq, J.L., and Guilbert S., 1995, Water Vapour Permeability of Edible Bilayer Films of Wheat Gluten and Lipids, *Int. J. Food Sci. Technol*. **30**: 49–56.

Grossman, S., and Bergman M., 1992, *Process for the Production of Gelatin from Fish Skins*. U.S. Patent 5,093, 474.

Gudmundsson, M., and Hafsteinsson H., 1997, Gelatin from Cod Skins as Affected by Chemical Treatments, *J. Food Sci*. **62**:37–39.

Habitante, A.M., Montero, P., Gómez-Guillén, M.C., Sobral, P., and Carvalho R., 2005, Desarrollo de Películas Comestibles Basadas en Gelatinas de Piel de Pescados: Atún Y Fletán, V Iberoamerican Congress on Food Engineering, Puerto Vallarta.

Han, C., Lederer, C., McDaniel, M., and Zhao Y., 2005, Sensory Evaluation of Fresh Strawberries (*Fragaria ananassa*) Coated with Chitosan-Based Edible Coatings, *J. Food Sci*. **70**(3):172–178.

Issam, S., Martial-Gros, A., Carnet-Pantiez, A., Grelier, S., and Coma V., 2005, Chitosan Polymer as Bioactive Coating and Film Against *Aspergillus Niger* Contamination, *J. Food Sci*. **70**(2):101–105.

Iwata, K., Ishizaki, S., Handa, A., and Tanaka M., 2000, Preparation and Characterization of Edible Films from Fish Water-Soluble Proteins, *Fisheries Sci*. **66**:372–378.

Johnston-Banks F.A., 1990, Gelatin, in: *Food Gels*. P. Harris, (ed.), Elsevier Applied Science Publishers, London. pp. 233–289.

Jongjareonrak, A., Benjakul, S., Visessanguan, W., and Tanaka M., 2005, Isolation and Characterization of Collagen from Bigeye Snapper (*Priacanthus macracanthus*) Skin, *J. Sci. Food Agr*. **85**(7): 1203–1210.

Jongjareonrak, A., Benjakul, S., Visessanguan, W., and Tanaka, M., 2006a, Effects of Plasticizers on the Properties of Edible Films from Skin Gelatin of Bigeye Snapper and Brownstripe Red Snapper. *Eur. Food Res. Technol*. **222**(3-4):229–235.

Jongjareonrak, A., Benjakul, S., Visessanguan, W., and Tanaka M., 2006b, Characterization of Edible Films from Skin Gelatin of Brownstripe Red Snapper and Bigeye Snapper, *Food Hydrocolloid*. **20**(4):492–501.

Jongjareonrak, A., Benjakul, S., and Visessanguan W., 2006c, Fatty Acids and Their Sucrose Esters Affect the Properties of Fish Skin Gelatin-Based Film, *Eur. Food Res. Technol*. **222**(5–6):650–657.

Kirk, R., and Othmer N., 1970, *Enciclopedia de Tecnología Química*. Editorial Hispano Americana, México, 13: 423–428.

Krochta, J.M., and De Mulder-Johnston C., 1997, Edible and Biodegradable Polymer Films: Challenges and Opportunities, *Food Technol*. **51**(2): 61–77.

Kunte, L.A., Gennadios, A., Cuppett, S.L., Hanna, M.A., and Weller C.L., 1997, Cast Films from Soy Protein Isolates and Fractions, *Cereal Chem*. **74**:115–118.

Lawrence, M.C., Izard, T., Beuchat, M., Blagrove, R.J., and Coleman P.M, 1994, Structure of Phaseolin At 2.2 Angstroms Resolution: Implications for a Common Vicilin/Legumin Structure and the Genetic Engineering of Seed Storage Proteins, *J. Mol. Biol*. **238**:748–776.

Ledward, D.A. 1986. Gelation of Gelatin, in: *Functional Properties of Food Macromolecules*, J.R. Mitchell, and D.A. Ledward (eds.), Elsevier Applied Science Publishers, London. pp: 171–201.

Lee, K.Y., Shim, J., and Lee H.G., 2004, Mechanical Properties of Gellan And Gelatin Composite Films, *Carbohydr. Polym*. **56**:251–254.

López-Caballero, M.E., Gómez-Guillén M.C., Pérez-Mateos, M., and Montero P., 2005, A Chitosan-Gelatin Blend As A Coating For Fish Patties, *Food Hydrocolloid*. **19**:303–311.

Mali, S., Grossmann, M.V., García, M.A., Martino, M.N., and Zaritzky N.E., 2002, Microstructural Characterization of Yam Starch Films, *Carbohydr. Polym*. **50**(4):379–386.

Mariniello, L., Di Pierro, P., Esposito, C., Sorrentino, A., Masi, P., and Porta R., 2003, Preparation and Mechanical Properties of Edible Pectin-Soy Flour Films Obtained in the Absence or Presence of Transglutaminase, *J. Biotechnol*. **102**(2): 191–8.

Martelli, S.M., Moore, G.P.R., Paes, S.S., Gandolfo, C.A., and Laurindo J.B., 2006, Influence of Plasticizers on the Water Sorption Isotherms and Water Vapor Permeability of Chicken Feather Keratin Film, *Lebensm.- Wiss. U.-Technol. - Food Sci.Technol*. **39**:292–301.

McHugh, T.H., and Krochta J.M., 1994, Sorbitol vs. Glycerol Plasticized Whey Protein Edible Films: Integrated Oxygen Permeability and Tensile Property Evaluation, *J. Agric. Food Chem*. **42**(4):841–845.

Menegalli, F.C., Sobral, P.J.A., Roques, M.A., and Laurent S., 1999, Characteristics of Gelatin Biofilms in Relation to Drying Process Conditions Near Melting, *Drying Tech*. **17**(7–8):1697–1706.

Miranda P., Garnica, S., and Lara-Sagahon O., 2004, Water Vapor Permeability and Mechanical Properties of Chitosan Composite Films, *J. Chilean Chem. Soc*. **49**(2):173–178.

Monahan, F.J., German, J.B., and Kinsella J.E., 1995, Effect of Ph and Temperature on Protein Unfolding and Thiol/Disulfide Interchange Reactions During Heat-Induced Gelation of Whey Proteins, *J. Agric. Food Chem*. **43**:46–52.

Montero, P., and Gómez-Guillén M.C., 2005, Función Protectora de Películas y Coberturas Basadas en Gelatina de Pescado, V Iberoamerican Congress on Food Engineering, Puerto Vallarta.

Monterrey-Quintero, E.S., and Sobral P.J.A., 1999, Caracterização de Propriedades Mecânicas E Óticas de Biofilmes À Base de Proteínas Miofibrilares de Tilápia do Nilo Usando Uma Metodologia de Superfície-Resposta. *Ciên. e Tecn. de Alim*. **19**(2):294–301.

Monterrey-Quintero, E.S., and Sobral P.J.A., 2000, Preparo E Caracterização de Proteínas Miofibrilares de Tilápia do Nilo (Oreochromis Niloticus) para Elaboração de Biofilmes. *Pesq. Agropec. Bras*. **35**(1):179–189.

Moore, G.R.P., Martelli, S., Gandolfo, C.A, Sobral, P.J.A., and Laurindo J.B., 2006, Influence of the Glycerol Concentration on Some Physical Properties of Feather Keratin Films Food Hydrocolloids, *J. Food hydrocolloid*. **20**(7):975–982

Muyonga, J.H., Cole, C.G.B., and Duodu K.G., 2004, Extraction and Physico-Chemical Characterisation of Nile Perch (Lates niloticus) Skin and Bone Gelatin, *Food Hydrocolloid*. **18**(4):581–592.

Muzzarelli, R., Baldassarre, V, Conti, F., Ferrara, P., Biagini, G., Gazzanelli, G., and Vasi V., 1988, Biological Activity of Chitosan: Ultrastructural Study, *Biomaterials*, **9**(3):247–252.

Nagano, T., Motohiko, H., Mori, H., Kohyama, K., and Nishinari K., 1992, Dynamic Viscoelastic Study on the Gelation of Conglycinin Globulin from Soybeans, *J. Agric. Food Chem*. **40**:941–944.

Nisperos-Carriedo M.O., 1994, Edible Coatings and Films Based on Polysaccharides, in: *Edible Coatings and Films to Improve Food Quality*, J.M. Krochta, E.A. Baldwin and M.O. Nisperos-Carriedo (eds.), Technomic Pub., Lancaster. pp. 305–330.

Norland, R.E., 1990, Fish Gelatin, in: *Advances in Fisheries Technology and Biotechnology for Increased Profitability*, M.N. Voight, and J.K. Botta (eds.), Technomic Publishing Co., Lancaster. pp: 325–333.

Paschoalick, T.M., Garcia, F.T., Sobral, P.J.A., and Habitante A.M.Q.B., 2003, Characterization of Some Functional Properties of Edible Films Based on Muscle Proteins of Nile Tilapia, *Food Hydrocolloid*. **17**(4):419–427.

Park, H, Weller, C., Vergano, P., and Testin R., 1993, Permeability and Mechanical Properties of Cellulose-Based Edible Films, *J. Food Sci*. **58**(6):1361–1364, 1370.

Parris N., Dickey, L., Kurantz, M.J., Moten, R.O., and Craig J.C., 1997, Water Vapor Permeability and Solubility of Zein/Starch Hydrophilic Films Prepared from Dry Milled Corn Extract, *J. Food Eng*. **32**:199–207.

Perez-Gago, M.B., and Krochta, J.M., 2001, Denaturation Time and Temperature Effects on Solubility, Tensile Properties, and Oxygen Permeability of Whey Protein Edible Films, *J. Food Sci*., **66**:705–710.

Petruccelli, S., and Añón M. C., 1995, Partial Reduction of Soy Proteins Isolate Disulfide Bonds, *J. Agric. Food Chem*. **43**:2001–6.

Pinelli Saavedra, A., Toledo Guillén, A., Ezquerra Brauer, I., Luviano Silva, A., and Higuera Ciapara I., 1998, Métodos de Extracción de Quitina a Partir de Cáscara de Camarón, *Arch. Lat. Nutr*. **48**(1):58–61.

Ramírez, M., Rodríguez, A., and Cárdenas R., 1998, Preparación de Hidrolizados Bioactivos de Quitosana a Partir de Diferentes Fuentes. Instituto Nacional de Ciencias Agrícolas, San José de las Lajas (April 30, 2004) http://www.inca.edu.cu.

Rayas, L.M., Hernández, R.J., and Ng P.K.W., 1997, Development and Characterization of Biodegradable/Edible Wheat Protein Films, *J. Food Sci*. **62**(1):160–162.

Saunders, R.M., and Becker R., 1984, Amaranthus: A Potential Food and Feed Resource, *Adv. Cereal Science Technol*. **6**:357–396.

Schrooyen, P.M.M., Dijkstra, P.J., Oberthür, R., Bantjes, A., and Feijen J., 2000, Partially Carboxymethylated Feather Keratins. 1. Properties in Aqueous Systems, *J. Agric. Food Chem*. **48**:4326–4334.

Schrooyen, P.M.M., Dijkstra, P.J., Oberthür, R., Bantjes, A., and Feijen J., 2001a, Partially Carboxymethylated Feather Keratins. 2. Thermal and Mechanical Properties of Films, *J. Agric. Food Chem*. **49**:221–230.

Schrooyen, P.M.M., Dijkstra, P.J., Oberthür, R., Bantjes, A., and Feijen J., 2001b, Stabilization of Solutions of Feather Keratins by Sodium Dodecyl Sulfate, *J. Colloid Interface Sci*. **240**:30–39.

Shahidi F., 1994, Seafood Processing By-Products, in: *Seafoods Chemistry, Processing, Technology and Quality*, F. Shahidi and J.R. Botta (eds.), Blackie Academic & Professional, Glasgow. pp. 320–334.

Shellhammer, T.H., and Krochta J.M., 1997, Whey Protein Emulsion Film Performance as Affected by Lipid Type Amount, *J. Food Sci*. **62**(2):390–394.

Shepherd, R., Reader, S., and Falshaw A., 1997, Chitosan Functional Properties, *Glycoconjugate J*. **14**:535–542.

Simon-Lukasik, K.V., and Ludescher R.D., 2004, Erythrosin b Phosphorescence as a Probe of Oxygen Diffusion in Amorphous Gelatin Films, *Food Hydrocol*. **18**(14):621–630.

Smith S.A., 1986, Polyethylene, Low Density, in: *The Wiley Encyclopedia of Packaging Technology*, M. Bakker (ed.), John Wiley & Sons, New York. pp. 514–523.

Sobral, P.J.A., 2000, Influência da Espessura Sobre Certas Propriedades de Biofilmes À Base de Proteínas Miofibrilares, *Pesq. Agropec. Bras*. **35**(6):1251–1259.

Sobral, P.J.A., 1999, Propriedades Funcionais de Biofilmes de Gelatina em Função da Espesura, *Ciên. Eng*. **8**(1):60–67.

Sobral, P.J.A., Garcia, F.T., Habitante, A.M.Q.B., and Monterrey-Quintero E.S., 2004, Propriedades de Filmes Comestíveis Produzidos com Diferentes Concentrações de Plastificantes e de Proteínas do Músculo de Tilápia-do-Nilo, *Pesquisa Agropecuária Brasileira* **39**(3):255–262.

Sobral P.J.A., Menegalli, F.C., Hubinguer, M.D. and Roques M.A., 2001, Mechanical, Water Vapor Barrier and Thermal Properties of Gelatin Based Edible Films, *Food Hydrocolloid*. **15**: 423–32.

Sobral, P.J.A., Monterrey-Quintero, E.S. and Habitante A.M.Q.B., 2002, Glass Transition of Nile Tilapia Myofibrillar Protein Films Plasticized by Glycerin and Water, *J. Thermal Anal. Calor*. **67**: 499–504.

Sobral, P.J.A., and Ocuno D., 2000, Permeabilidade ao Vapor de Água de Biofilmes À Base de Proteínas Miofibrilares de Carne, *Braz. J. Food Techn*. **3**:11–16.

Sobral, P.J.A, Ocuno, D., and Savastano Jr, H., 1998, Preparo De Proteínas Miofibrilares de Carne E Elaboração de Biofilmes com Dois Tipos ce Ácidos: Propriedades Mecânicas, *Braz. J. Food Techn*. **1**:(1/2)44–52.

Sobral, P.J.A., Santos, J.S. and Garcia F.T., 2005, Effect of Protein and Plasticizer Concentrations in Film Forming Solutions on Physical Properties of Edible Films Based on Muscle Proteins of a Thai Tilapia, *J. Food Eng*. **70** (1):93–100.

Souza, S.M.A., Sobral, P.J.A., and Menegali F.C., 2004, Extração de Proteínas Miofibrilares de Carne Bovina para Elaboração de Filmes Comestíveis, *Ciência e Tecnologia de Alimentos* **24**(4):619–626.

Srinivasa, P.C., Ramesh, M., Kumar, K, Tharanathan, R., 2004, Properties of Chitosan Films Prepared Under Different Drying Conditions, *J. Food Eng*. **63**:79–85.

Taboada, E., Cabrera, G. and Cardenas G., 2003, Retention Capacity of Chitosan for Copper and Mercury Ions, *J. Chilean Chem. Soc*. **48**(1):7–12.

Tanaka M., Iwata K., Sanguandeekul R., Handa, A., and Ishizaki S., 2001, Influence of Plasticizers on the Properties of Edible Films Prepared from Fish Water-Soluble Proteins, *Fisheries Sci*. **67**(2):346–351.

Tanveer, A.K., Kok, K.P. and Hung S.C., 2003, Mechanical, Bioadhesive Strength and Biological Evaluations of Chitosan Films for Wound Dressing, *J. Pharm. Pharmaceut. Sci*. **3**(3):303–311.

Tapia-Blácido D., 2006, Biofilms Based In Amaranth Flour, PhD. Thesis, School of Food Engineering, Unicamp, Brazil.

Tapia-Blacido, D., Sobral, P.J., and Menegalli F.C., 2005a, Development and Characterization of Biofilms Based on Amaranth Flour (*Amaranthus caudatus*), *J. Food Eng*. **67**:215–223.

Tapia-Blacido, D., Sobral, P.J., and Menegalli F. C., 2005b, Effect of Drying Temperature and Relative Humidity on Mechanical Properties of Amaranth Flour Films Plasticized with Glycerol, *Braz. J. Chem. Eng*. **22**:249–256.

Tharanathan, N.R. and Kittur S.F., 2003, Chitin—The Undisputed Biomolecule of Great Potential, *Crit. Rev. Food Sci*. **43**:61–83.

Thomazine, M., Carvalho, R.A., and Sobral P.I.A., 2005a. Physical Properties of Gelatin Films Plasticized by Blends of Glycerol and Sorbitol, *J. Food Sci*. **70**(3):172–176.

Thomazhine, M., Carvalho, R., Habitante, A.M., Sobral, P., Montero P., and Gómez-Guillén M.C., 2005a, Desarrollo de Películas Comestibles Basadas en Gelatinas de Piel de Fletán, V Iberoamerican Congress on Food Engineering, Puerto Vallarta.

Trezza, T.A., and Krochta J.M., 2000, Color Stability of Edible Coatings During Prolonged Storage, *J. Food Sci*. **65**(7):1166–1169.

Turhan, K.N., and Sahbaz F., 2004, Water Vapor Permeability, Tensile Properties and Solubility of Methylcellulose-Based Edible Films, *J. Food Eng*. **61**:459–466.

Vanin, F.M., Sobral, P.J.A., Menegalli, F.C., Carvalho, R.A., and Habitante A.M., 2005, Effects of Plasticizers and Their Concentrations on Thermal and Functional Properties of Gelatin-Based Films, *Food Hydrocolloid*. **19**(5):899–907.

Vermeiren, L., Devlieghere, F., van Beest, M., de Kruijf, N., and Debevere J., 1999, Developments in the Active Packaging of Foods, *Trends Food Sci. Technol*. **10**:77–86.

Wong, D.W.S., Gastineau, F.A., Gregorski, K.S., Tillin, S.J., and Pavlath A.E., 1992, Chitosan Lipid Films: Microstructure and Surface Energy, *J. Agric. Food Chem*. **40**:540–544.

Wu, T., Zivanovic, S., Draughon, F.A., Conway, W.S., and Sams C.E., 2005, Physicochemical Properties and Bioactivity of Fungal Chitin and Chitosan, *J. Agric. Food Chem*. **53**:3888–3894.

Yamauchi, A., and Yamauchi K., 2002, Formation and Properties of Wool Keratin Films and Coatings, in: *Protein Based Films and Catings*, A. Gennadios (ed.), CRC Press, Boca Raton. pp. 253–274.

Yamauchi, K., Yamauchi, A., Kusunoki, T., Kohda, A., and Konishi Y., 1996, Preparation of Stable Aqueous Solution of Keratins, and Physiochemical and Biodegradational Properties of Films, *J. Biomed. Mater. Res*. **31**:439–444.

Zhou, T., and Regenstein J. M., 2005, Effects of Alkaline and Acid Pretreatments on Alaska Pollock Skin Gelatin Extraction, *J. Food Sci*. **70**(6):392–396.

12
Edible Coating as an Oil Barrier or Active System

M. García, V. Bifani, C. Campos, M.N. Martino, P. Sobral, S. Flores, C. Ferrero, N. Bertola, N.E. Zaritzky, L. Gerschenson, C. Ramírez, A. Silva, M. Ihl, and F. Menegalli

12.1. Introduction

Edible coatings have long been known to protect perishable food products from deterioration by retarding dehydration, suppressing respiration, improving textural quality, helping to retain volatile flavor compounds and reducing microbial growth (Mauer et al., 2000; Yang and Paulson, 2000; Peressini et al., 2003; Han et al., 2004). Also, they can be used as a vehicle for incorporating functional ingredients, such as antioxidants, flavor, colors, antimicrobial agents and nutraceuticals (Kester and Fennema, 1989; Guilbert et al., 1997; Bifani et al. 2006).

Antimicrobial edible films and coatings are used for improving the shelf life of food products without impairing consumer acceptability (Baker et al., 1994). They are not designed to totally replace traditional packaging, and might be used as a stress factor in minimally processed foods in order to prevent surface contamination while providing a gradual release of the antimicrobial.

Another application of edible films or coatings is as barrier to lipid absorption by food during deep fat frying. Oil uptake in fried foods has become a health concern; high consumption of lipids has been related to obesity and other health problems such as coronary heart disease. Reducing the fat content of fried foods by application of coatings is an alternative solution to comply with both health concerns and consumer preferences. Food coatings may become a good alternative to reduce oil uptake during frying. The effectiveness of a coating is determined by its mechanical and barrier properties, which depend on its composition and microstructure, and on the characteristics of the substrate.

Some fried products may contain fat up to 50% of the total weight (Pinthus et al., 1993). Some of these lipids were not in the food before frying. For example, the lipid content of french fries increases from 0.2% to 14 %, and lipid content may reach 40% in potato chips; raw fish with 1.4% reach 18% fat after frying (Smith et al., 1985; Mackinson et al., 1987). Several hydrocolloids with thermal gelling or thickening properties, such as proteins and carbohydrates, have been tested to reduce oil and water migration (Debeaufort and Voilley, 1997; Williams and Mittal, 1999).

Thus, the objective of this work is to present and discuss some potentiality or applications of edible films or coatings and to examine its possible uses to improve the quality and lengthen the shelf life of foods.

12.2. Use of a Tapioca Starch Edible Film Containing Potassium Sorbate to Extend the Shelf Life of Minimally Processed Pumpkin

Starch is a natural biopolymer very commonly used to constitute film matrices (Durango et al., 2005). In particular, tapioca starch is a promising alternative due to its low price in the world market when compared to starches obtained from other sources (FAO, 2004). These film matrices are commonly used with additives that provide an extra protection against surface contamination of some microorganisms. Sorbic acid and its potassium salt (sorbates) are GRAS (generally regarded as safe) additives and are active against yeasts, molds and many bacteria (Sofos, 1989). Addition of potassium sorbate to edible films has been proposed as a way of minimizing surface microbial contamination (Cagri et al., 2001).

Pumpkin is a seasonal crop used as human food. It covers a wide number of species of the family *Cucurbitaceae*, most of them with an economic potential due to low price in the world market and the fact that it is a good source of nutrients, especially β-carotene (Hels et al., 2004). Therefore, in this work the possibility of controlling microbial growth and lengthening the shelf life of minimally processed pumpkin is studied.

12.2.1. Film Preparation and Application on Minimally Processed Pumpkin

The film was prepared using a mixture of tapioca starch, glycerol, sorbates and water (5.0:2.5:0.15:92.35 in weight). Starch was gelatinized by heating on a hot plate with magnetic stirrer at a constant rate of 1.8 °C/min for approximately 30 min. After gelatinization, films were cast over glass plates and dried at 50 °C for two h. The drying process was completed in a chamber (Velp, Italy) at 25 °C. Once constituted, films were peeled from the glass plates. Before using to wrap pumpkin, sample films were conditioned at 25 °C over a saturated solution of NaCl (water activity, $a_W = 0.755$) for 4 days.

Pumpkin (*Curcumis moschata*, Duch.) was purchased at a local supermarket, then washed and cut into cylinders of 16 mm length and 23 mm diameter employing a metallic cork borer. The pumpkin was then cooked in water vapor at 100 °C for 10 min and rapidly cooled with water, drained and introduced in a glucose osmotic solution of 0.895 a_w acidified to 3.0 with citric acid and containing 0.02% (w/w) of vanillin (ratio of pumpkin cylinders:solution, 2:5). The system was stored at 8 °C for 4 days; pumpkin cylinders reached a 0.938 a_w and 4.4 pH. Portions constituted by four pumpkin cylinders were then wrapped with film and

packed into gas impermeable bags (PET/ Al/PE), which were sealed and stored at 25 °C for 21 days. Pumpkin cylinders without edible film wrapping, packed as previously stated, were also stored as controls for comparison purposes.

12.2.2. Microbiological and Chemical Analyses

To evaluate the effect of the potassium sorbate wrapping on the development of food microbiota, microbiological analyses of aerobic mesophilic and lactic acid bacteria, yeast and molds were carried out on the surface of the film and in the pumpkin tissue after removing the film. Analyses were performed according to the methodology described by the Compendium of Methods for the Microbiological Examination of Foods (Vanderzant and Splittstoesser, 1992). Non-coated samples were used as controls. Three bags from each treatment were sampled at time zero and after 21 days of storage at 25°C.

The evolution of pH and water activity (a_w) in the film and in the pumpkin after removing the film was determined. Weight loss of samples was also determined. Potassium sorbate concentration in the film and in the pumpkin after removing the film was evaluated according to AOAC method (1990), which includes steam distillation of the preservative followed by oxidation to malonaldehyde and measurement at 532 nm of the pigment formed between malonaldehyde and thiobarbituric acid.

All determinations were performed in triplicate and means are reported. A "t" test was performed to determine significant differences between parameters ($\alpha = 0.05$).

12.2.3. Storage Tests

The level of aerobic mesophiles and lactic acid bacteria, yeasts and molds in the surface of the film-wrapped pumpkin cylinders was below 42 CFU/cm^2 at time zero and after 21 days of storage, showing that the film carried a low microbial load and demonstrating that the film used is an efficient barrier to prevent external contamination.

Figure 12.1 shows the evolution of native flora in the pumpkin after removing the film. It can be seen that levels of mesophilic aerobes after storage decreased 2 log cycles. In the case of yeasts and molds and lactic acid bacteria, initial populations in pumpkin were approximately 150 CFU/g; after storage, the microorganism's counts decreased significantly in all cases. It must be mentioned that for control samples the level of mesophilic aerobes after storage was similar to the initial level. However, samples had an unacceptable appearance; the surface was spoiled by molds and the tissue had an aqueous aspect. This behavior was related to the high counts of yeast, molds and lactic acid bacteria (Fig. 12.1).

The pH of the product decreased to 3.3 in controls (Table 12.1) as a result of lactic acid bacteria metabolism. Moreover, a_w increased to 0.951, probably as a consequence of changes induced by metabolic activity of microbial flora. Otherwise, the pH of the pumpkin wrapped with the film reached a value of 5.1, and a_w decreased to 0.918 because of the contact with edible films of pH 6.3 and a_w of 0.753.

These results demonstrated that depression of a_w to 0.938, adjustment of pH to 4.4 with citric acid, together with the use of an impermeable packaging were not

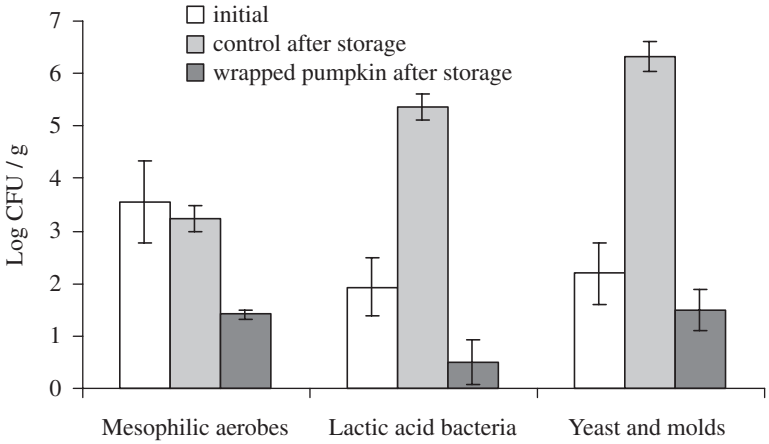

FIG. 12.1. Evolution of native flora in samples of processed pumpkin. Bars followed by the same letter are not significantly different (P>0.05)

TABLE 12.1. pH and water activity of pumpkin samples

	Initial	21 days	
		Control	Treatment
pH	4.4 ± 0.1	3.3 ± 0.3	5.1 ± 0.1
a_w	0.938 ± 0.004	0.951 ± 0.002	0.918 ± 0.003

Reported values are the mean of three measurements. Standard deviations are also shown

enough to preserve pumpkin, and demonstrated the need for an additional stress factor, such as the addition of a preservative agent that could be supported in an edible film, as is proposed in this work.

Weight loss for wrapped pumpkins at the end of the experiment was 15.1±1.8%. This behavior can be attributed, at least partially, to water transfer from pumpkin to film, since higher water content and a_w value (0.902) was noted for the edible films used. Weight loss reported here is similar to the values reported by Garcia et al. (1998) for starch-coated strawberries. For control samples, weight loss could not be determined because of the high degree of tissue spoilage.

Antimicrobial migration from film to pumpkin was verified by measurement of potassium sorbate content in wrapped pumpkin cylinders. Concentration observed was 2588 ± 85 ppm after 21 days, which represents approximately 40% of total potassium sorbate contained initially in the film (15,000 ppm). It must be mentioned that the content of the preservative in the film after storage was 7140 ± 770 ppm, suggesting that part of the potassium sorbate initially contained in the film was lost throughout storage, probably as a result of oxidation. It is well documented that potassium sorbate suffers autoxidative degradation in model systems and in food products, and that the magnitude of this reaction depends on system composition (Gerschenson and Campos, 1995).

In relation to the physico-chemical changes mentioned, the edible film formulation proposed must be modified in order to avoid the increase in pH in order to minimize weight losses and to ensure sorbate content in the pumpkin is in accordance with maximum values allowed by food legislation of the country of application.

Results reported here demonstrate that the use of tapioca starch edible films containing potassium sorbate to wrap pumpkin cylinders can act as a physical barrier to exclude the entrance of microorganisms, provide a source of preservative that can prevent microbial growth at the surface and, at the same time, control spoilage flora in the pumpkin tissue, since part of the antimicrobial was released to the food.

12.3. Edible Cellulose Derivative Coatings to Reduce Oil Uptake in Fried Products

The application of edible coatings on the surface of foods is an interesting technique that has not been studied extensively. Mallikarjunan et al. (1997), working with mashed potato balls, reported a reduction, compared to uncoated balls, of 14.9%, 21.9% and 31.1% in moisture loss, and of 59.0%, 61.4% and 83.6% in fat uptake for samples coated with corn zein, hydroxypropylmethylcellulose (HPMC) and methylcellulose (MC) films, respectively. Williams and Mittal (1999) also found that MC films showed the best barrier properties, reducing fat uptake more than hydroxypropylcellulose (HPC) and gellan gum films applied to a pastry mix.

Cellulose derivatives, including MC and HPMC, exhibit thermal gelation. When suspensions are heated, they form a gel that reverts to below the gelation temperature, and the original suspension viscosity is recovered (Grover, 1993). These cellulose derivatives reduce oil absorption through film formation at temperatures above their incipient gelation temperature, or they reinforce the natural barrier properties of starch and proteins, especially when they are added in dry form (Meyers, 1990).

The objective of this study was to apply coatings based on cellulose derivatives and plasticizer in order to reduce oil uptake in fried potato strips and pastry products, optimizing their formulations.

12.3.1. Preparation of Suspension of Edible Coating

Cellulose derivatives (Methocel), K100LV and E15LV (two different hydroxypropylmethylcelluloses, HPMC) and A4M (methylcellulose, MC), were provided by Dow Chemical (USA). Concentrations of aqueous cellulose derivative suspensions of 1% and 2% were tested to select appropriate formulations for coating applications. Plasticizer effect of sorbitol on the selected cellulose derivative formulations was analyzed. Sorbitol (Merck, USA) concentrations assayed in the suspensions were 0.25, 0.50, 0.75 and 1% (w/w) (Garcia et al., 2002).

Rheological characterization of the cellulose derivative suspensions was performed in a Haake RV2 (Haake, Germany) rotational viscometer, at controlled

constant temperature (20 °C). An NV type sensor system of coaxial cylinders was used for all measurements. Rheological curves were obtained after a stabilization time of 3 min at 20 °C. Shear stress was determined as a function of shear rate between 0 and 1382 s^{-1} with the following program: 3 min to attain the maximum shear rate, 1 min at the maximum shear rate and 3 min to attain 0 shear rate. Apparent viscosities were calculated at 64 rpm (345.6 s^{-1}) and 128 rpm (691.2 s^{-1}). Apparent viscosities of 1% A4M at 20 °C were 138.1 ± 5.2 and 138.1 ± 5.2 mPa.s at shear rates of 345.6 and 691.2 s^{-1}, respectively. These values were significantly higher than the apparent viscosities of 2% K100LV and E15LV solutions.

According to the manufacturer's description, A4M is a modified cellulose that contains only methyl groups as substituents, allowing stronger interactions between hydrocolloid chains; thus, it should yield high viscosity solutions even at concentrations of 1%. K100LV and E15LV are hydroxypropylmethyl derivatives of cellulose containing both substituents: methyl and hydroxypropyl groups. In these cases, the interaction between chains may be hindered by steric impediment. Thus, K100LV should yield medium viscosity solutions and E15LV with a higher percentage of hydroxypropyl groups, and more steric impediments should yield lower viscosity solutions.

Thermal gelation was also analyzed; clouding point was 70 °C for 1%A4M, 80 °C for 2% K100lLV and 60 °C for 2%E15LV al. Similar results were found by Mallikarjunan et al. (1997). According to Grover (1993), thermal gelation is produced because thermal treatments induce perturbations in the hydration layers of the macromolecules, leading to an increase in hydrophobic interpolymeric interactions. Thermal gelation temperature increased with sorbitol concentration; this was attributed to a more difficult hydrocolloid chain association.

12.3.2. Frying Tests

Frying tests were performed with potato strips (0.7 × 0.7 × 5 cm) and commercial dough discs of wheat flour (Pillsbury, Argentina) measuring 3.7cm in diameter and 0.3 cm high. Samples were dipped in the coating suspensions for 10 sec and immediately fried.

Coated and uncoated (control) samples were fried in a controlled temperature deep-fat fryer filled with 1.5 L of commercial sunflower oil. Oil composition was 99.93% lipids, with 25.71% mono-unsaturated and 64.29% poly-unsaturated fatty acids. Used oil was replaced by fresh oil after four frying batches. In each batch, six potato samples or four dough discs were fried. A variety of constant frying temperatures was tested to select the working frying conditions according to sample characteristics. These temperatures ranged between 150 ± 0.5 °C and 170 ± 0.5 °C for dough and between 170 ± 0.5 °C and 190 ± 0.5 °C for potatoes; frying times ranged between 2 and 5 min in both cases. Optimum time-temperature frying conditions were determined by both instrumental color and sensory analysis; a non-trained panel judged color, flavor, texture and overall appearance (Garcia et al. 2002, 2004).

Colorimetric measurements were carried out with a Minolta colorimeter CR 300 Series (Japan). The Hunter scale was used, and lightness (L) and chromaticity parameters a* (red – green) and b* (yellow – blue) were measured. Samples were analyzed in triplicate, recording four measurements for each sample.

Instrumental surface color showed no significant differences ($P > 0.05$) between fried potato strips processed for 5 min at 170 °C or 4 min at 180 °C, or for dough discs processed between 2.5 min at 160 °C and 3 min at 150 °C. However, sensory analysis (color, flavor, texture and overall appearance) determined that 4 min at 180 ± 0.5 °C for french fried potatoes and 3 min at 150 ± 0.5 °C for dough discs were the best frying conditions. Accordingly, these parameters were selected as operative conditions for further determinations.

Water content (WC) was determined by measuring the weight loss of fried products upon drying in an oven at 110 °C until constant weight. Relative variation of water retention % (WR) in the coated product relative to the uncoated product was calculated as follows:

$$WR = \left(\frac{WCcoated}{WCuncoated} - 1 \right) \times 100 \tag{12.1}$$

Lipid content (LC) of fried products was determined on dried samples using a combined technique of successive batch and semi-continuous Soxhlet extractions. The first batch extraction was performed with petroleum ether:ethylic ether (1:1), followed by a Soxhlet extraction with the same mixture and another Soxhlet extraction with n-hexane. Oil uptake relative variation % (OU) in the coated product relative to the uncoated product was calculated as follows:

$$OU = \left(\frac{LCcoated}{LCuncoated} - 1 \right) \times 100 \tag{12.2}$$

For each coating formulation, results were obtained using all samples from two different batches.

The cellulose derivative was selected from experiments done with fried potato strips. Water and oil contents of the control sample were 62.62 ± 0.92 g water/100 g (dry basis) and 4.43 ± 0.74 g oil/100g (dry basis), respectively. Coatings with cellulose derivatives without plasticizer applied on potato strips reduced oil uptake and led to a higher retention of moisture content during deep fat frying (Table 12.2). As water content in the coated product was higher than in the uncoated product, the WR was always positive and higher for MC than for the HPMC coatings. The oil uptake was always negative because the lipid content of the coated sample was lower than the uncoated sample (Garcia et al., 2002).

MC coating was selected because it showed the highest oil uptake reduction compared to HPMC coatings. This could be attributed to the differences in suspension viscosities, which is related with the covering capacity of coatings. HPMC coatings did not show noticeable differences with regard to oil uptake; the presence of hydroxypropyl groups may limit film-forming capacity through steric hindrances. Mallikarjunan et al. (1997), working with potato balls, found

Table 12.2. Characterization of fried potato strips coated with different formulations

Coating formulation (without plasticizer)	Relative variation of oil uptake (OU) % Eq. (12.2)	Relative variation of water retention (WR) % Eq. (12.1)
Control	–	–
1% MC (A4M)	−15.53 ± 0.79	2.14 ± 0.49
2% K100LV	−6.30 ± 0.21	0.49 ± 0.21
2% E15LV	−7.60 ± 0.74	1.00 ± 0.15

Value ± standard deviation

that MC coatings have better moisture barrier performance than HPMC coatings, due to the lower hydrophilic character of MC. In addition, Holownia et al. (2000) reported that MC and HPMC films applied on chicken strips decreased oil uptake and the degradation of frying oil, thus extending the useful life of the product.

Coating presence significantly ($P<0.05$) modified surface color parameters of potato slices. Chromaticity parameter a^* of samples with different coatings and the uncoated samples were significantly different ($P<0.05$). Even though instrumental color parameters showed differences, all samples were accepted by the non-trained panel. Sensory analysis and L values showed that control samples were darker and more opaque than coated samples.

12.3.3. Effect of Sorbitol Addition to the Coating Formulation on Oil Absorption and Water Retention

The initial water and oil contents of potato strips before frying were previously reported. For dough discs, the initial water content before frying was 35.72 ± 0.64 g/100 g (dry basis) and the lipid content was 4.00 ± 0.10 g/100 g (dry basis). After frying, the oil content of dough samples without coating (control) was 18.42 ± 1.77 oil/100 g (dry basis) and the water content was 17.12 ± 1.43 g water/100 g (dry basis). For potato samples without coating (control), values were 3.49 ± 0.21 oil/100 g (dry basis) and 63.97 ± 2.54 g water/100 g (dry basis), respectively.

Table 12.3 shows values obtained for the relative decrease of oil uptake and increase of water retention of fried dough and potato strips coated with MC formulations.

MC coating treatment significantly ($P<0.05$) reduced oil uptake and increased water retention of both fried potato and dough samples compared to uncoated samples. Similar results were obtained by other researchers who applied cellulose derivative coatings on different products (Mallikarjunan et al., 1997; Balasubramaniam et al., 1997; Holownia et al., 2000).

Sorbitol addition improved the barrier properties of coatings by decreasing oil content and increasing moisture retention compared to control and coated samples without plasticizer. ANOVA analysis ($P<0.05$) showed that the most effective sorbitol concentrations to reduce oil uptake were 0.5% for potato strips and 0.75% for dough discs (Table 12.2). Considering that the plasticizer increases the elasticity of the coating (Donhowe and Fennema, 1993), and that the dough discs expanded during the frying process, a higher sorbitol concentration was required

TABLE 12.3. Relative variation of oil uptake and water retention of fried dough discs and potato strips coated with methylcellulose (MC) and sorbitol (S) formulations

Sample	Formulation	Relative decrease of oil uptake (OU), (%) Eq. (12.2)	Relative increase of water retention (WR), (%) Eq. (12.1)
Dough discs	Control (without coating)[1]	0	0
	1% MC	14.20±0.14[3]	10.34±0.09
	1% MC + 0.25% S	27.53±0.09	27.93±0.16
	1% MC + 0.5% S	25.65±0.07	23.68±0.11
	1% MC + 0.75% S	35.23±0.06	25.75±0.12
	1% MC + 1% S	29.03±0.08	22.87±0.14
Potato strips	Control (without coating)[2]	0	0
	1% MC	15.53±0.23	2.14±0.08
	1% MC + 0.25% S	26.60±0.18	5.61±0.03
	1% MC + 0.5% S	40.62±0.13	6.31±0.04
	1% MC + 0.75% S	23.69±0.15	6.98±0.04
	1% MC + 1% S	15.58±0.27	7.65±0.03

[1] Oil content of dough control sample= 18.42±1.77oil/100g (dry basis); water content= 17.12±1.43 g water/100 g (dry basis)

[2] Oil content of potato control sample= 3.49±0.21oil/100 g (dry basis); water content = 63.97±2.54 g water/100 g (dry basis)

[3] Value ± standard deviation

for dough samples. Similarly, Rayner et al. (2000) reported that the performance of soy protein film applied on dough discs increased by the addition of glycerin as plasticizer, reducing the food fat uptake.

Dough discs coated with MC and 0.75% sorbitol showed a 35.2% reduction of oil absorption and a 25.7% increase of moisture retention compared to control samples. For potato strips coated with MC and 0.5% sorbitol, oil absorption decreased 40.6% and moisture retention increased 6.3% compared to control samples. Pinthus et al. (1993) reported that the addition of methylcellulose in dough formulation significantly reduced the oil uptake of doughnuts in the case of dry addition.

Coating integrity was analyzed by stereomicroscopy observation (Leitz Ortholux II, Germany), staining sample surfaces with toluidine blue. Scanning electron microscopy (SEM) of coated and uncoated samples was performed with a JEOL JSMP 100 scanning electron microscope (Japan). Coated pieces were mounted on bronze stubs using double-sided tape and then coated with a layer of gold (40–50 nm). All samples were examined using an accelerating voltage of 5 kV.

Staining with toluidine blue only helped to visualize coated dough samples under light microscopy; the similar chemical structures of the potato matrix and cellulose derivatives did not allow effective differentiation of the coating in french fries.

Fried samples with unplasticized coatings showed cracks that may reduce barrier properties of the coating. Mallikarjunan et al. (1997) attributed the reduction in oil uptake and moisture loss to the formation of a protective layer

on the surface of the samples during the initial stages of frying due to thermal gelation above 60 °C. This protective layer inhibits the transfer of moisture and fat between the sample and the frying medium. Coating integrity is an important factor, since the presence of cracks may reduce barrier properties of coatings and may limit coating applications (Donhowe and Fennema, 1993). In the case of frying applications, coating integrity also depends on the substrate. While most potato fries maintained their shape and volume after frying, dough discs increased their volume and modified the shape. Observations by both SEM and stereomicroscope of stained dough discs showed cracks in the coatings without plasticizer, evidencing the fragility of the coating structure.

Addition of plasticizer (sorbitol) to MC coatings was necessary to achieve coating integrity (Fig. 12.2). A similar trend was observed by Rayner et al. (2000), working on deep-fat fried potato discs coated with plasticized soy protein films. Formation of a uniform coating on the surface of the sample is essential to limit mass transfer during the frying process (Huse et al., 1998).

MC is characterized by its thermogelation properties, i.e., the gel formed upon heating above 60 °C (Meyers, 1990; Grover, 1993; Garcia et al., 2002). The fact that a layer corresponding to the coating was seen after frying indicated that dehydration also took place on the coating. Absorption of oil on the surface of the fried product occurs when samples are removed from the frying medium; oil that remains on the piece surface enters into the product (Ufheil and Escher, 1996; Aguilera and Gloria, 1997; Aguilera and Gloria-Hernandez, 2000; Mellema, 2003). According to these authors, oil does not invade the sample itself, so no oil uptake occurs during frying. Conditions at which potato slices are removed from the frying oil seem decisive for the uptake of oil; this is related to adhesion of oil to the surface and draining phenomena. Two main mechanisms are proposed to explain oil uptake: condensation and capillary mechanisms. In both cases, oil penetrates through the pores to the inside of the product (Mellema, 2003). Thermogelling of the coating could lead to a stronger barrier that would limit oil uptake after that frying process.

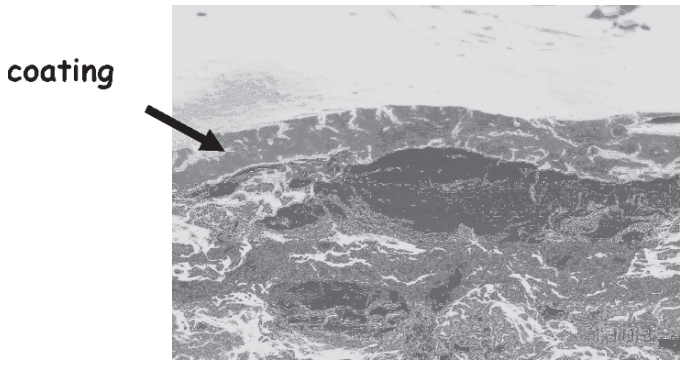

Fig. 12.2. SEM Micrograph of fried dough disc coated with 1% methylcellulose (MC) with 0.75% sorbitol. Magnification: 100μm between marks

The breaking force of samples was measured by puncture test using a texture analyzer TA.XT2i—*Stable Micro Systems* (Haslemere, Surrey, UK) with a 5 kg cell. Samples were punctured with a cylindrical plunger (2 mm diameter) at 0.5 mm/sec. Maximum force at rupture was determined from the force-deformation curves. At least 10 samples were measured in each assay. Samples were allowed to reach room temperature before performing the tests.

Table 12.4 shows breaking force results for dough discs and potato strips with and without coatings. Coating did not significantly ($P > 0.05$) modify the texture of fried products. Instrumental results of breaking force agree with sensory analysis data. Similar results were obtained by Rayner et al. (2000), working on deep-fat fried potato discs coated with plasticized soy protein films. In addition, Funami et al. (1999), working on doughnuts, found that MC addition had no effect on the breaking stress of samples.

After frying, dough discs showed a volume increase that was quantified by the linseed method. Samples coated with MC and sorbitol showed a significantly ($P<0.05$) lower volume increase than uncoated samples. Samples coated with MC solutions plasticized with 0.5% sorbitol showed a higher density value (0.95 ± 0.05 g/mL) than the uncoated samples (0.70 ± 0.05 g/mL). With regard to volume, samples coated with MC without plasticizer did not differ significantly ($P > 0.05$) than those of uncoated samples. This could be attributed to the more elastic layer of coating, which limits the development of the dough network (Normen et al., 1998).

Color of potato strips did not show significant differences ($P > 0.05$) between uncoated samples and those with unplasticized coatings (Table 12.4). However, for dough discs, significant differences ($P < 0.05$) in lightness and chromaticity a^* parameter were found between the uncoated samples and those with unplasticized coatings. In any case, all samples were accepted by the sensory panel. Sorbitol addition showed a highly significant ($P < 0.01$) effect on chromaticity parameters a^* and b^* for both potato and dough fried samples. In the case of lightness, the presence of sorbitol was significant ($P < 0.01$) only for potato strips (Table 12.4). Samples coated with MC and sorbitol showed a lighter color, which could be associated with a lower cooking time, even though all samples were cooked for

TABLE 12.4. Texture and color parameters of fried dough discs and potato strips

			Surface color (Hunter units)		
Sample	Formulation	Breaking force (N)	L	a^*	b^*
Dough discs	Control	6.69 ± 2.97[1]	54.83 ± 3.85	−2.11 ± 2.54	33.67 ± 2.33
	1% MC [2]	4.81 ± 1.53	61.68 ± 3.34	−7.15 ± 1.85	31.62 ± 2.31
	1% MC + 0.75% S[3]	5.33 ± 1.58	62.58 ± 1.62	−10.03 ± 0.62	27.77 ± 1.78
Potato strips	Control	2.57 ± 0.64	51.09 ± 3.62	6.21 ± 2.39	36.22 ± 1.68
	1% MC	2.77 ± 0.44	52.73 ± 4.08	4.32 ± 2.58	34.92 ± 1.86
	1% MC + 0.5% S	2.66 ± 0.30	46.91 ± 3.58	8.86 ± 1.78	33.29 ± 3.29

[1] Value ± standard deviation

[2] MC = methylcellulose

[3] S = sorbitol

the same time period. The panelists did not detect flavor or texture differences between coated and control samples.

French fries and fried dough discs coated with the selected formulations were evaluated by a non-trained sensory panel of 22 members. Two triangular tests were performed to determine whether consumers could distinguish between coated and uncoated samples. Each sample was randomly numbered and presented to the panel members with the instruction to pick the two equal samples out of three. A hedonic panel was also performed with the same panelists, who evaluated texture, color, flavor and overall characteristics. A hedonic 4-point scale was used: 1= dislike, 2= acceptable, 3= like and 4= like very much.

The triangular test showed no significant differences ($P > 0.05$) between samples coated with MC and sorbitol and the uncoated controls for both fried products. Panelists did not reject any sample; in all cases, scores were higher than 2 (acceptable). Texture was the lowest scored parameter (2.2) with regard to color and flavor; however, texture scores of coated samples were similar to control scores. Flavor scores of coated samples were the highest, and similar to the control values; these results were of great significance because no off flavors were detected considering the presence of the coating. Mallikarjunan et al. (1997) reported that HPMC coatings improved the sensory attributes of fried chicken nuggets and marinated chicken strips, even more so when HPMC was incorporated into the breading mix.

In conclusion, methylcellulose (MC) and hydroxypropylmethylcellulose (HPMC) were used in coating formulations to reduce oil uptake in deep-fat fried potato strips and dough discs. MC coatings were more effective in reducing oil uptake than HPMC coatings, and the cellulose derivative was selected for coating formulations. The addition of a plasticizer (sorbitol) was necessary to maintain coating integrity and improve barrier properties. The most effective coating formulations were 1% MC and 0.75% sorbitol for dough discs and 1% MC and 0.5% sorbitol for potato strips. For these formulations, oil uptake reduction was 35.2% and 40.6% for dough discs and potato slices, respectively, compared to the uncoated samples, and the increase in water content of the same products was 25.7% and 6.3%, respectively.

All samples were accepted by the panelists, although color differences between coated and uncoated samples were detected by instrumental analysis. Coating application did not modify texture characteristics of fried samples. This is a favorable result, since our goal was to incorporate the coating to decrease oil uptake without having a significant impact on the sensory characteristics of the fried products.

12.4. Incorporation of Natural Antioxidants on Carboxy-Methylcellulose Based Edible Films

Traditionally, the hot water extract of leaves from a plant native to the south of Chile, known as “murta” or “murtilla” (*Ugni molinae* Turcz), is highly valued as a folk medicine by the indigenous Chilean Mapuche for its physiological benefits,

mainly for its kidney-protection effect (Montenegro, 2002). Due to this interest, the germoplasm of this plant has been collected and characterized (Seguel et al., 2000). Methanolic, ethanolic and water extracts of the leaves were found to be high in polyphenols content and antioxidant abilities, as measured through DPPH and TBARS (Rubilar et al., 2006). Finally, through reverse phase HPLC-MS analysis of the aqueous extracts, it was shown that the main difference between the polyphenol content of the two ecotypes studied, Pumalal Soloyo Grande (SG) and Soloyo Chico (SC), is the flavonol derivatives myricetin dirhamnoside, myricetin glucoside or myricetin galactoside and quercetin dirhamnoside (Bifani et al., 2006).

The use of edible films prepared with the aqueous extracts of murta leaves is an interesting alterative to give additional antioxidant properties to the films and therefore improve the coatings. But the presence of polyphenols may affect the polymeric matrix, changing some physical properties of the films; there is a need to study their effect on rheological characteristics of the film forming solutions and on physical characteristics of the edible films.

12.4.1. Films Production

Using 2 g L^{-1} of carboxymethylcellulose as a structural basis of the film forming solutions, the addition of the leaf extract of each murta ecotype was done without dilution (SC-100 and SG-100), mixing 50% extract with 50% water (SC-50 and SG-50), and 100% distilled water (control); 0.4 g L^{-1} of glycerol and 0.5 g L^{-1} of sunflower oil were always added as plasticizers (Table 12.5).

The CMC solutions behave as pseudoplastic fluids and can be described through the Power Law Model. SG samples always show a higher resistance to the deformation than the SC samples. For both ecotypes, the consistency coefficient *K* decreased when the extract concentration in the sample was increased, being one order of magnitude higher for SG than for SC samples. The flow behavior index *n* for the SG samples was always higher than for the SC ecotype; it increased with concentration for both samples, but was always lower than 1, corroborating the pseudoplastic behavior of the CMC solution (Vais et al., 2002). Both the shear storage modulus G′ (or elastic modulus) and the shear loss modulus G″ (or viscous modulus) in the lineal range of viscoelasticity were performed to evaluate the viscoelastic behavior of the filmogenic solutions.

Table 12.5. Composition of forming solution of carboxymethylcellulose-based edible film with murta (*Ugni molinae* Turcz) leaf extract (Bifani et al., 2006)

Sample	Extract concentration [g/100g]	CMC [g]	Glycerol [mL]	Sun flower oil [mL]	Water [mL]	Soloyo Chico extract [mL]	Soloyo Grande extract [mL]
SC50	48.57	2.000	0.40	0.50	0.00	100.00	0.00
SC100	97.18	2.000	0.40	0.50	50.00	50.00	0.00
SG50	48.57	2.000	0.40	0.50	0.00	0.00	100.00
SG100	97.18	2.000	0.40	0.50	50.00	0.00	50.00
Control	0.00	2.000	0.40	0.50	100.00	0.00	0.00

The shear storage modulus (G') and also the shear loss modulus were higher for the SG samples than for the SC samples. In all of the analyzed conditions, the results were in the so-called initial region of low frequency or diluted state, where G" is higher than G', indicating that the samples were more viscous than elastic. The chains are not more imbricated on these frequencies, and therefore, the solution can flow more easily. The gel point, where values of G' and G" are the same, were observed only for SG samples, with a displacement to the left; therefore, the addition of murta leaf extracts of SG led to higher molecular weight of the solution (De Matos, 1997) (Table 12.6).

12.4.2. Film Characteristics

Using dynamic mechanical analysis (DMA), viscoelastic properties of the films were studied. The shear loss modulus G" was always smaller than the shear storage modulus G'; this is a characteristic of physical gels, and means that gels which most of the time behave as solids, instead behave as liquids (Paschoalick et al., 2003).

Water vapor permeability (WVP), measured by the method described in Mali et al. (2002), was significantly lower ($p \leq 0.05$) for SG films than control and SC films, without any significant difference ($p > 0.05$) between WVP for control and SC films (Table 12.7). Carbon dioxide (CO_2) and oxygen (O_2) permeabilities of the films were assessed by the accumulation method (Garcia et al., 2000). Carbon dioxide permeability of SG films was significantly higher ($p \leq 0.05$) than control and SC films; oxygen permeability of SG films was significantly lower ($p \leq 0.05$) than SC films, and both films showed significantly lower ($p \leq 0.05$) oxygen permeability than the control (Bifani et al., 2006).

In conclusion, the addition of aqueous murta leaf extract with different concentrations of the same polyphenols as a CMC-based film-forming solution not only affects the physical properties of these solutions, but also affects the physical properties of formed films, in particular important physical properties such as water vapor and gases (CO_2 and O_2) permeability. It is necessary to know the behavior of CMC chains with polyphenols present in the water extract of murta leaves that have different distribution of components to predict the physical properties of edible films. This conclusion is not only valid for CMC-based films added with murta extract, but also for the addition of any natural extract of any carbohydrate or protein-based films.

Table 12.6. Rheological properties of film-forming solution of carboxymethylcellulose-based edible film with murta (*Ugni molinae* Turcz) leaf extract[a]

Sample	Extract concentration [g/100g]	Consistency coefficient K	Flow behavior index n	Elastic modulus G′ [Pa]	Viscous modulus G″ [Pa]
SC50	48.57	6.87	0.56	6.50 – 7.56	15.04 – 17.00
SC100	97.18	2.66	0.67	2.30 – 2.60	7.97 – 8.97
SG50	48.57	28.72	0.35	36.86 – 43.05	40.21 – 47.18
SG100	97.18	23.89	0.41	31.77 – 34.63	38.69 – 39.94

[a]Means value of two replicates

TABLE 12.7. Water vapor and gases permeability of CMC based edible films with murta leaf extract (Bifani et al. 2006)

Extract concentration [g/100g]	Water vapor permeability $\times 10^{11}$ [g m^{-1} s^{-1} Pa^{-1}]		CO_2 permeability $\times 10^{10}$ [cm^3 m^{-1} s^{-1} Pa^{-1}]		O_2 permeability $\times 10^{10}$ [cm^3 m^{-1} s^{-1} Pa^{-1}]	
	Soloyo Grande	Soloyo Chico	Soloyo Grande	Soloyo Chico	Soloyo Grande	Soloyo Chico
0	7.144 ± 0.130[a] Aa[b]	7.144 ± 0.130 Aa	4.092 ± 0.095 Aa	4.092 ± 0.095 Aa	8.096 ± 0.077 Aa	8.096 ± 0.077 Aa
48.57	6.738 ± 0.032 Bb	7.200 ± 0.038 Aa	7.485 ± 0.002 Bb	3.914 ± 0.486 Aa	3.260 ± 0.035 Ab	2.344 ± 0.011 Cb
97.18	5.655 ± 0.049 Cc	7.188 ± 0.064 Aa	6.850 ± 0.007 Cc	3.551 ± 0.093 Aa	4.382 ± 0.078 Ac	5.941 ± 0.141 Bc

[a] Means value ± standard deviations of two replicates

[b] For each property, means in the same row with different capital letters are significantly different ($p \leq 0.05$); means in the same column with different small letters are significantly different ($p \leq 0.05$)

Acknowledgements To CYTED (Project XI.20). The authors acknowledge the financial support from Agencia Nacional de Promoción Científica y Tecnológica (ANPCyT), Universidad de Buenos Aires (UBA), Universidad Nacional de La Plata (UNLP), Consejo Nacional de Investigaciones Científicas y Técnicas de la República Argentina (CONICET) and Fundación Antorchas; Universidad de La Frontera (Temuco, Chile). To Fapesp and CNPq (Brazil).

References

Aguilera, J. M., and Gloria, H., 1997, Determination of oil in fried potato products by differential scanning calorimetry, *J. Agric. Food Chem*. **45**(3): 781–785.

Aguilera, J.M., and Gloria-Hernandez H., 2000, Oil Absorption During Frying of Frozen Parfried Potatoes, *J. Food Sci*. **65** (3):476–479.

AOAC, 1990, Official Methods of Analysis, 13th ed., Association of Official Analytical Chemists, Washington, DC.

Baker, R., Baldwin, E., and Nisperos-Carriedo M., 1994, Edible Coatings and Films for Processed Foods, in: *Edible Coatings and Films to Improve Food Quality*, J.M. Krochta, E.A. Baldwin, and M.O. Nisperos-Carriedo (eds.), Technomic Publishing Co. Inc., Lancaster, pp. 89–104.

Balasubramaniam, V.M., Chinnan, M.S., Mallikarjunan, P., and Phillips R.D., 1997, The Effect of Edible Film on Oil Uptake and Moisture Retention of a Deep-Fat Fried Poultry Product, *J. Food Process Eng*. **20**:17–29.

Bifani, V., Ramírez, C., Ihl, M., Rubilar, M., Garcia A., and Zaritzky N., 2006, Effects of Murta (*Ugni molinae* Turcz) Extract On Gas And Water Vapor Permeability of Carboxymethylcellulose Based Edible Films, *Lebensm.- Wiss. U.-Technol*. (In press).

Cagri, A., Ustunoi, Z., and Ryser E.T., 2001, Antimicrobial, Mechanical, and Moisture Barrier Properties of Low Ph Whey Protein-Based Edible Films Containing Aminobenzoic or Sorbic Acids, *J. Food Sci*. **66**(6):865–870.

Debeaufort, F., and Voilley A, 1997, Methylcellulose-Based Edible Films and Coatings: 2. Mechanical and Thermal Properties as a Function of Plasticizer Content, *J. Agric. Food Chem*. **45**:685–689.

De Matos, V., 1997, *Caracterização Reológica de Soluções de CMC: Viscoelasticidade e Influência de Características da Molécula*, Tese de Mestre em Engenharia de Alimentos, Universidade Estadual de Campinas, Campinas.

Donhowe, I.G., and Fennema O.R., 1993, The Effects of Plasticizers on Crystallinity, Permeability, and Mechanical Properties of Methylcellulose Films, *J. Food Process. Preserv*. **17**:247–257.

Durango A.M., Soares N.F.F., and Andrade N.J., 2005, Microbiological Evaluation of an Edible Antimicrobial Coating on Minimally Processed Carrots, *Food control* (In press).

FAO, 2004, Global Cassava Market Study Business Opportunities for The Use of Cassava, in: *Proceedings of the Validation Forum on the Global Cassava Development Strategy*, Volume 6, International Fund for Agricultural Development, Rome.

Funami, T., Funami, M., Tawada, T., and Nakao Y., 1999, Decreasing Oil Uptake Of Doughnuts During Deep-Fat Frying Using Curdlan, *J. Food Sci.,* **64**(5):883–888.

Garcia, A., Ferrero C., Bertola N., Martino, M., and Zaritzky N., 2002, Edible Coatings from Cellulose Derivatives to Reduce Oil Uptake in Fried Products, *Innov. Food Sci. Emerging Technol*. **3**(3):391–397.

Garcia M., Ferrero, C., Campana A., Bertola, N., Martino, M., and Zaritzky N., 2004, Methylcellulose Coating Applied to Reduce Oil Uptake in Fried Products, *Food Sci. Technol. Int*. **10**(5):339–346.

Garcia, M., Martino, M., and Zaritizky N., 1998, Plasticized Starch Based Coatings to Improve Strawberry (*Fragaris Ananassa*) Quality And Stability, *J. Agric. Food Chem*. **46**(9):3758–3767.

Garcia, M.A., Martino, M.N., and Zaritzky N.E., 2000, Lipid Addition to Improve Barrier Properties of Edible Starch-Based Films and Coating, *J. Food Sci*. **65**(6):941–946.

Gerschenson, L., and Campos C.A., 1995, Sorbic Acid Stability During Processing and Storage of High Moisture Foods, in: *Food Preservation by Moisture Control. Fundamentals and Applications*, G. Barbosa-Cánovas and J. Welti-Chanes (eds.), Technomic Publishing Co., Inc., Lancaster, pp. 761–790.

Grover J.A., 1993, Methylcellulose and Its Derivates, in: *Industrial Gums*, R.L. Whistler and J.N. Be Miller (eds.), Academic Press, San Diego, pp. 475–504.

Guilbert, S., Cuq, B., and Gontard N., 1997, Recent Innovations in Edible and/or Biodegradable Packing Materials, *Food Addit. Contam*. **6**(6–7):741–751.

Han, C., Zhao, Y., Leonard, S.W., and Traber M.G., 2004, Edible Coatinga Improve Storability and Enhance Nutritional Value of Fresh Strawberries (*Fragaria x ananassa*) and Raspberries (*Rubus ideaus*), *Postharvest Biol. Technol*. **33**(1):67–78.

Hels, O., Larsen Christensen, L., Kidmose, U., Hassan, N., and Haraksingh Thilsted S., 2004, Contents of Iron, Calciumzinc and -Carotene in Commonly Consumed Vegetables in Bangladesh, *J. Food Compos. Anal*. **17**(5):587–595.

Holownia, K.I., Chinnan, M.S., Erickson, M.C., and Mallikarjunan P., 2000, Quality Evaluation of Edible Film-Coated Chicken Strips and Frying Oils, *J. Food Sci*. **65**(6):1087–1090.

Huse, H.L., Mallikarjunan, P., Chinnan, M.S., Hung, Y.C., and Phillips R.D., 1998, Edible Coatings For Reducing Oil Uptake In Production Of Akara (Deep-Fat Frying Of Cowpea Paste), *J. Food Process. Preserv*. **22**:155–165.

Kester, J.J., and Fennema O.R., 1989, An Edible Film of Lipids and Cellulose Ethers: Barrier Properties to Moisture Vapor Transmission and Structural Evaluation, *J. Food Sci*. **54**(6):1383–1389.

Mackinson, J.H., Greenfield, H., Wong, M.L., and Willis R.B.H., 1987, Fat Uptake During Deep-Fat Frying Of Coated And Uncoated Foods, *J. Food Compos. Anal*. **1**:93–101.

Mali, S., Grossmann, M.V.E., García, M.A., Martino, M.N., and Zaritzky N.E., 2002, Microstructural Characterization of Yam Starch Films, *Carbohyd. Polym*. **50**:379–386.

Mallikarjunan, P., Chinnan, M.S., Balasubramaniam, V.M., and Phillips, R.D., 1997, Edible Coatings for Deep-Fat Frying of Starchy Products. *Lebensm.-Wiss. U Technol*. **30**:709–714.

Mauer, L.J., Smith, D.E., and Labuza T.P., 2000, Water Vapor Permeability, Mechanical, and Structural Properties of Edible β-Casein Films, *Int. Dairy J*. **10**(5–6):353–358.

Mellema M., 2003, Mechanism and Reduction of Fat Uptake in Deep Fat Fried Foods, *Trends Food Sci. Technol*. **14**: 364–373.

Meyers M.A., 1990, Functionality of Hydrocolloids in Batter Coating Systems, in: *Batters and Breadings in Food Processing*, K. Kulp and R. Loewe (eds.), American Association for Cereal Chemists, St. Paul, pp. 17–142.

Montenegro G., 2002, *Ugni molinae* Turcz, in: *Chile Nuestra Flora Útil. Guía de Uso Apícola, Medicinal Folclórica, Artesanal y Ornamental*, G. Montenegro and B.N. Timmermann, Ediciones Universidad Católica de Chile, Santiago, pp. 241–242.

Normen, E., Rovedo, C.O., and Singh, R.P., 1998, Mechanical Properties of an Immersion Fried Potato Starch-Gluten Gel During Postfrying Period, *J. Texture Stud*. **29**:681–697.

Paschoalick, T.M., Garcia, F.T., Sobral, P.J.A., and Habitante A.M.Q.B., 2003, Characterization of Some Functional Properties of Edible Films Based on Muscle Proteins of Nile Tilapia, *Food Hydrocolloids* **17**:419–427.

Peressini, D., Bravin, B., Lapasin, R., Rizzotti, C., and Sensidoni A., 2003, Starch-Methylcellulose Based Edible Films: Rheological Properties of Film-Forming Dispersions, *J. Food Eng*. **59**(1):25–32.

Pinthus, E.J., Weinberg, P., and Saguy I.S., 1993, Criterion for Oil Uptake During Deep-Fat Frying, *J. Food Sci*. **58**:204–205, 222.

Rayner, M., Ciolfi, V., Maves, B., Stedman, P., and Mittal G.S., 2000, Development and Application of Soy-Protein Films to Reduce Fat Intake in Deep-Fried Foods, *J. Sci. Food Agric*. **80**:777–782.

Rubilar, M., Pinelo, M., Ihl, M., Scheuermann, E., Sineiro, J., and Núñez M.J., 2006, Murta Leaves (*Ugni molinae* Turcz) as a Source of Antioxidant Polyphenols, *J. Agric. Food Chem*. **54**(1):59–64.

Seguel, I., Peñalosa, E., Gaete, N., Montenegro, A., and Torres A., 2000, Colecta y Caracterización Molecular de Germoplasma de Murta (*Ugni molinae* Turcz.) en Chile, *Revista Agro Sur*, **28**(2):32–41.

Smith, L.M., Clifford, A.J., Creveling, R.K., and Hamlin C.L., 1985, Lipid Content and Fatty Acid Profiles of Various Deep-Fat Fried Foods, *JAOCS*. **62**:996–999.

Sofos J.N., 1989, *Sorbate Food Preservatives*. CRC Press Inc., Boca Raton, pp. 111–129.

Ufheil G. and Escher F., 1996, Dynamics of Oil Uptake During Deep-Fat Frying of Potato Slices, *Food Sci. Technol.- Lebensm.-Wiss. U Technol*. **29**(7):640–644.

Vais, A., Palazoglu, T., and Sandeep K., 2002, Rheological Characterization of Carboxymethylcellulose Solution Under Aseptic Processing Condition, *J. Food Process. Eng*. **25**:41–46.

Vanderzant, M., and Splittstoesser R., 1992, *Compendium of the Methods for the Microbiological Examination of Foods*, 4th ed., American Public Health Association, Washington.

Williams, R., and Mittal G.S., 1999, Water and Fat Transfer Properties of Polysaccharide Films on Fried Pastry Mix, *Lebensm.-Wiss. U Technol*. **32**:440–445.

Yang, L., and Paulson A.T., 2000, Mechanical and Water Vapor Barrier Properties of Edible Gellan Films, *Food Res. Int*. **33**(7):563–570.

13
From Powders End Use Properties to Process Engineering

E. DUMOULIN

13.1. Introduction

Food processes are designed to create final products with specific properties (composition, structure and functionality, with reproducibility), with respect to quality, security and environment along the production chain.

Food powders are dried or semi-dried products with different shapes and composition (Bimbenet et al, 2002). They are used from manufacturer to consumer as additives, ingredients or solid food.

Powders are usually characterized at two levels, individual particles and powder in bulk, which is different from liquid or gas products. The physical characteristics of the individual particles are mainly determined by the materials from which they are made and the process by which they are formed (Peleg, 1983).

13.2. Looking for Powder End-Use Properties in Food

13.2.1. Why Produce Powders?

The production of food powders is interesting for stabilization (dried), storage (delayed use), transport (reduced weight, volume), for an easy dosage or instant properties, while retaining nutritional and functional properties (Schubert, 1993).

Food powders are added directly to a dish in a small quantity (e.g., salt, pepper, garlic, sugar, aromas). They may also be consumed or processed with other constituents in a solvent (e.g., water, milk, oil): milk and derivatives, flour, purée, cocoa, sugar (crystallized), coffee, soup, vegetables, meat, fish, sauce mix, vending machine powders, ingredients (colorings, enzymes, yeasts), etc.

Powders exist in other fields with similar objectives and processes, but their composition (constituents, solvents) and uses are different. For example, in the different industrial sectors we find: in agriculture, coated grains and fertilizers; in cosmetics, make-up; in pharmaceutics, capsules, tablets, patches, and aerosols; in chemicals, paints, detergent, plaster, concrete, adsorbents, explosives and catalysts (Chulia et al., 1994; Rhodes, 1998).

More generally, the initial liquid/solid mixture is associated with a specific process, generating powders with specific properties; the main parameters are temperature, time and relative humidity.

Particle properties are linked to the bulk powder behavior, but the relationship is not easy to predict. Environmental conditions such as pressure, atmosphere and other particles play an important role, both on each particle and on the powder as an assembly of particles. In order to use powders more efficiently, some properties will have to be considered more carefully (Table 13.1).

13.2.2. Examples Of Relationship Between Powder Properties And Production Process Conditions

Size (nm to mm) and *shape* are linked to physical and functional powder properties such as flowability, density, solubility and wettability. Size, shape and surface properties influence the powder color aspect. Stirring a mixture of two free-flowing powders of different sizes may result in segregation rather than improved mixture quality. In the spray drying process, if the viscosity of the sprayed solution is high, the drop size is large, corresponding to a final larger size for dry particles.

Density has an economical importance, given the cost of transport and the packaging volume. The bulk density represents the total of the true absolute density, the air included inside particles and the interstitial air. In the case of large size distribution, small particles may enter the interstices, leading to a denser powder.

TABLE 13.1. Influence of process, storage and powder properties in final dried products

Powder properties measured In bulk or on particles	Process, storage (environment), final use
Size, size distribution, density, porosity, specific area Angle of repose, flowability Friability, compressibility	*Powders mixing, packaging, Handling, filling, dosage Storage, mechanical resistance →influence on demixing, dust*
Image analysis, MEB images; + RX, IR Composition (water, dry matter) a_w, sorption isotherm, Reactivity, wettability, dispersibility, solubility	*Aspect, regularity shape, surface composition → influence on properties Dosage, stability Rehydration, dissolution (in liquid), instantization*
Melting, glass transition temperature, sticky point, Tcrystallization	*Sticking, caking → influence on stability during process/storage*
Presence of microorganisms	*Quality/security*
Sensorial aspects	*Color, taste, odor* (±), *granular*
Component diffusion from/in particle	*Encapsulation, controlled release (polymer barrier)*
After dissolution/dispersion => viscosity, emulsion size, surface tension	*Composition, stability, processability*

Composition (including water content) influences density. In the spray drying process, when formulating the solution/emulsion to dry, air may be incorporated when mixing, leading to less dense powder. For milk products the foaming capacity is related to the protein state and content. Composition and process influence the processability of powder. In cheese making, "low heat milk" powder (produced by ultrafiltration or microfiltration) is used to enable controlled protein coagulation.

Linked with composition, the *affinity of powder components for water*, i.e., the possible access for water in terms of *powder structure* (porosity, capillarity), contributes to modification of powder properties. Powder solubility is decreased by thermal denaturation (i.e., soluble proteins) or by decrease of water transfer (hygroscopicity gradients).

Dispersibility is improved by increasing particle size (with a narrow distribution and optimal size (e.g., 200 microns), or using thermal treatment at low temperature, in relation to solubility and wettability. The wettability depends on favorable porosity and capillarity, and on the presence of specific components (fat (<0), lactose, and minerals (>0) in the case of milk).

Powder hygroscopicity in the presence of air (with controlled relative humidity) is influenced by surface contact and by the presence of amorphous components. The final rehydration may be improved by pretreatments (like steam for freeze-dried vegetables).

Isotherms of sorption give the equilibrium relationship between water content and water activity, $X = f(a_w)$ at a given temperature. Adsorption of water (vapor) at the surface of a food product depends on the behavior of each constituent in the presence of water (equilibrium with different kinetics). These isotherms may be used to choose storage conditions avoiding chemical and microbiological denaturation. They are used to predict caking or spontaneous agglomeration and plasticization, especially with amorphous constituents (changes in crystallinity) (Mathlouti and Rogé, 2003). For example, stable water content will be different for skimmed milk ($\leq 4\%$) and whole milk ($\leq 2.5\%$), with a water activity inferior to 0.2 of a_w increases, crystallization of amorphous lactose is observed, favorable to Maillard reactions and to liberation of molecules entrapped in the amorphous structure (like aromas) (Senoussi et al., 1995).

Plasticization may also be obtained by heating in the presence of amorphous and/or crystallized constituents. The viscous behavior may be characterized by temperatures (domains of temperature), which depend on water content: sticking point temperature (Ts), collapse temperature (Tc), glass transition temperature (Tg) and crystallization temperature (Tcrystallization). In addition, time is an important parameter for the temperature measurement method or for the process which is being investigated: Is there establishment of equilibrium? What are the reaction kinetics? (Figs. 13.1 and 13.2). Sugar was stored in silos (several Mt) at a constant temperature (20 °C) for several years, using blowing of filtered air with controlled relative humidity. Other conditions may be used to improve storage, such as the addition of an anticaking agent or multicellular silos for better control.

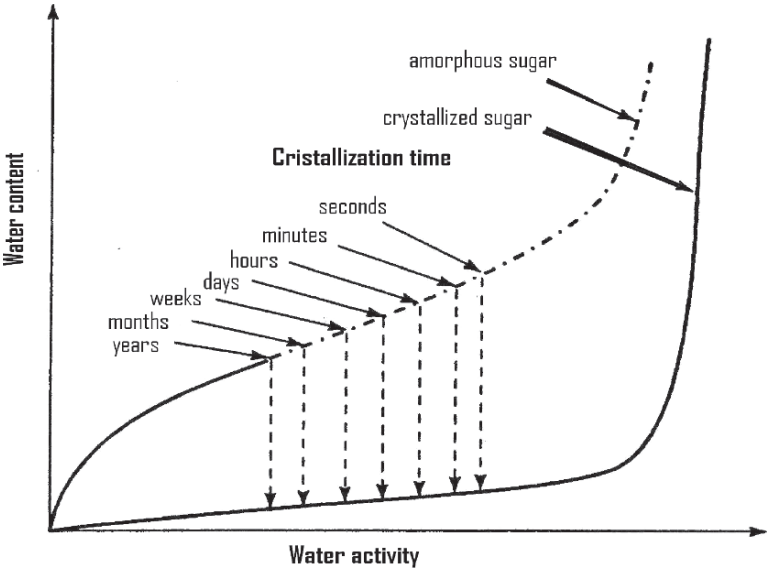

FIG. 13.1. Crystallization of amorphous sugars versus time beyond critical a_w (adapted from Roos, 1995)

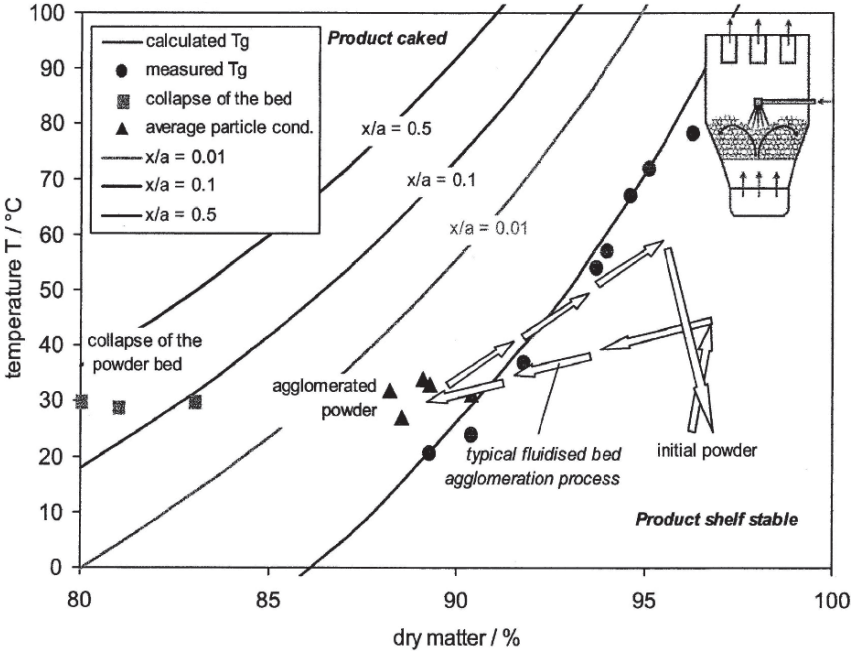

FIG. 13.2. Fluidized bed agglomeration of dextrose (DE 20–23) in the moisture/temperature diagram: x, a, bridge and particle diameters (adapted from Palzer, 2005)

The *flowability* and cohesiveness of the bulk powder (free flowing to cohesive, even sticky) depend on the relative humidity and temperature of the surrounding atmosphere, on particle size and size distribution, on surface properties (smooth, porous, etc.), and on density. Different measurements are possible: flow rate through a funnel, angle of repose, microscopic observation, and flow function (Jenike cell). However, the influence of the different parameters on the flow properties is difficult to predict. Some conditions improve flowability, such as particle agglomeration, low fraction of fine particles, low percentage of free fat, or the presence of additives.

For milk powder production by spray drying, a better flowability is observed when using a spray nozzle instead of rotative disk, or when drying is done in two steps (multistage dryer), improving particle flow and modifying particle properties (humidity, shape, surface).

Handling, pouring and processing cause particles to segregate according to size and, to a lesser extent, density and shape. Consequently, sampling is especially difficult (static or dynamic? manual or non-manual?). In all cases, a good scientific knowledge of the product is necessary to estimate the risks.

How *to prepare a sample* (1mg, 1g) representative of bulk powder placed in a big bag or in a silo (several tons) (Gy, 1982). If sampling is done on-line, the operation must be integrated as soon as the line is designed.

13.3. The Processes and Formulation

13.3.1. Powders Production

The final powder product may be either the end of one process (e.g., sugar from crystallization of sugar beet juice, flakes of potato purée dried on a drum), or a simple mix of different powders (e.g., dry soup), or the mix may be processed. For example, a baby mix is prepared as a dosed mix of powders (starch, milk, fruits, vegetables, vitamins, iron, and minerals) added with water, then cooked and drum dried.

The initial preparation is a key step that takes into account final objectives and choice of process and constituents. Different types of food ingredients (polysaccharides, proteins, lipids, gums, celluloses and minerals) are used with possible interactions and with positive or negative consequences during processing and storage.

The properties of components such as solubility, stability (temperature, water), drying behavior, structure modification (crystallization), and emulsifying properties, must be understood in relation to the process conditions (time, temperature, pressure, transport of fluids, atmosphere in contact) and for their variation (in the complex medium) along process/storage (quality losses).

Powders may be prepared from liquids, pastes or solids:

a) Formulated *liquid/emulsion/suspensions* generate humid solid particles that require further drying and separation. In *spray drying*, small drops of liquid (usually solution or emulsion) are formed with an atomizer in hot air (180–250 °C).

The high contact surface for heat/mass transfer corresponds to a rapid drying process with high capacity, creating fine particles (50–100 microns) (Dumoulin and Bimbenet, 1998).

The *freeze drying* of a formulated liquid (or paste) includes a freezing step, followed by the sublimation of ice, usually under vacuum, leading to a final porous structure.

The *precipitation* phenomenon may occur for conditions where the particles are not soluble in the liquid solvent. By *crystallization* of a saturated solution, modifying the temperature, the pH, the ionic forces or by solvent evaporation, it is possible to create an organized solid structure. If the solvent is a supercritical fluid (e.g., CO_2), the particles are very fine and monodisperse.

By the liquid *coacervation* process, it is possible to coat a liquid particle (e.g., aroma in emulsion) with a film of polymer before separation and drying.

b) Powders may be prepared by *extrusion*, applying pressure to a *paste* mixture in a special reactor with screws, or by drying a *layer* on a belt in a tunnel (with microwaves and vacuum) or onto a drum dryer. The dry thread/layer will yield different millimetric final shapes such as spheres, pellets, and flakes (mm).

c) Fruits and vegetables in small *solid* pieces may be dried using convective drying (low pressure) with hot gas (air or superheated steam) or by using *freeze drying*.

Grinding, agglomeration (compaction, fluidized bed) are used to create new sizes, new surfaces and properties (instantization, flowability, density) (Turchiuli et al., 2005a). The *coating* of particles in fluidized beds or pans represents a process to modify the particles surface properties, and therefore the contact with environment. Coating can be used for preservation or to provide some new functionality with the added coating layer.

13.3.2. Example of Industrial Animal Feed Process

The objectives of animal feed processing are to produce powders, pellets (compressed powder), stable dehydrated products (several months at ambient temperature) with well defined composition, enriched in vitamins and minerals.

The animal feed composition varies with type of animal, as some components are toxic for specific animals. For end use, the farmer will ask for a dosed product that is easy to handle, with good solubility, flowability, without dust, which is easy to store. For feed production it is also important to keep in mind the security aspect because of possible subsequent use for human food, such as milk, eggs, and meat.

Different operations enter into the process at an industrial scale (batches of several tons) (Melcion and Ilari, 2003) and are described as follows.

The *mixing/grinding* of the different ingredients may involve either the pregrinding of each component followed by a batch mixing (2–5 t) or a premixing with the dosage of each constituent before grinding (2–5 t). In all cases this means high energy consumption (21MJ/t).

The final product granulometry is related to digestibility, depending on the type and size of the animal. The grinding operation may develop interfaces by breaking, with risks of reactions, and of interactions between ingredients.

Density and water activity of constituents are various and must be considered to get a good dosage and storage without caking and demixing. Difficulties may occur when constituents do not have the same behavior due to different size, density, hygroscopicity.

To improve the quality of mixing some possible recommendations may be given: to have a low number of constituents to mix; to use flowability additives; to prepare the powder from a liquid mixture instead of mixing powders and to realize intermediate mixings. Furthermore, the addition of the constituents (vitamins, minerals) with low concentration (<0.5%) represents a difficulty in achieving homogeneity. Powder additives like vitamins A, E and B2, amino acids, minerals (Fe, Cu) are specifically prepared. They must be stable in the medium to which they will be added (a_w, T, pH, oxidation), digestible and bioavailable, with non-toxic dosage adapted to the animal. Premixing with a major constituent is recommended.

By *compression/extrusion,* powders are mixed, with addition of liquid (molass, vinass) or steam, to facilitate the compression. The process works with a continuous flow of powders, with possible increase of temperature (60–80 °C). It is difficult to control temperature homogeneity inside the bulk of powder, and residence time distribution in the equipment. At the exit of the die, pellets may be coated with additives like fat, aromas, and enzymes.

Storage of final bulk products is done in silos, or in bags (big bags). From those storage silos or bags, containers must be filled, frequently by using air pneumatic transport. These operations are possible with good properties of flowability and mechanical resistance for the powder and specific conditions for silos design (wall surface, geometry).

The separation of air and powder is provided by gravity with controlled air rate (if <10 (1) microns => air rate < 3 (0.03) mm/s), or through filter bags. The vibrations at the origin of any possible demixing may be avoided by controlling powders properties such as density, shape, surface state, size and distribution of size.

For all processes involving powders, *dust* represents losses, hazardous risks for people and the environment, and risks of explosion and toxic cross contamination. The dust generation may contribute to microorganism dissemination. Additionally, dust means difficulties in cleaning, in packaging (i.e., clean sealing of polyethylene bags) and a need for etancheity of equipments and filtration for gas. As for other food process lines, a *hygienic process design* is needed, using mainly gravity flow (better than horizontal flow), with late introduction of sensible components and use of efficient process control.

13.4. Some Trends in Research

13.4.1. General Comments on Research Studies

Usually conducted on a pilot scale, research studies are performed for one specific product, often as a batch process, using experimental design. Extrapolation to industrial production, in batch or continuous, often introduces new parameters.

Modeling helps to better understand mechanisms, and to determine the influence of each parameter. Models are built on heat and mass transfer equations, fluid dynamics, population balances and neural networks, with some coupling between models. Often based on an experimental approach, established models are valid for one specific product, and generalization is difficult because of the complexity of these phenomena.

13.4.2. Example of Encapsulation of Active Component in a Powder

The research objective was the encapsulation of oil in powder using spray drying and fluidized bed agglomeration. The vegetable oil (VO) content was 5% w/w in a matrix made of maltodextrin (MD DE 12) and acacia gum (AG) with a mass ratio 3MD /2AG. This ratio was determined in a previous study on aroma (oil) encapsulation by spray drying (Senoussi et al., 1995).

The searched end-use properties of the powder were:

- water content suitable for no sticking during production process, and for stability during storage
- good dispersion properties in water
- controlled size, size distribution and density to facilitate mixing with other powders, without fine particles
- known composition adapted for dosage and limited oil oxidation during storage
- good flowability for handling and transfer (e.g., in capsules)

Three ways of operation were tested for encapsulation of vegetable oil (5%) in powder MD/AG, with different results (Fuchs et al, 2006; Turchiuli et al, 2005b):

- spray drying of a formulated emulsion MD / AG / VO leading to a dosed powder (A) with a mean particle size inferior to 50 microns
- agglomeration of this spray-dried fine powder (A) in an air fluidized bed giving agglomerated products (B) of 200 microns, with good wettability, but poor mechanical resistance
- direct agglomeration of MD in a fluidized bed by spraying a formulated emulsion AG / VO performed to elaborate agglomerates (C) of 240 microns with both good flowability and mechanical resistance

The three types of powders, A, B and C, were well dosed in oil (5%), with low losses of oil during the different processes, and an efficient protection of oil against oxidation.

Such techniques are suitable for encapsulation of other components such as aromas, antioxidants or other oil substances. Higher concentrations in oil may be envisaged. Other possible constituents for the matrix may replace maltodextrin and acacia gum, such as modified starch, proteins, gums or other protective agents.

13.4.3. Example of Coating of Solid Particles in Fluidized Bed

The objectives in particle coating are to totally cover the surface of solid particles (0.1 to 1 mm) with a layer (usually 10–100 microns) of polymer with different aims:

- to give new properties such as regular shape, size and composition to improve dosage, mixing, flowability and density
- to modify aspect, texture and hardness to avoid dust and sticking
- to build a barrier for active component and/or control the release of an active component, with a controlled rate (time, quantity) in a specific medium (pH, pressure, solution, etc.).
- to improve stability within environment (oxygen, humidity, other constituents) during storage or during subsequent use (e.g., powder enriched with Fe, stable in fat medium).

Coating of solid particles may be realized by progressively spraying a coating solution on the particle surface, followed by hot gas (air) drying. A regular coating is formed when assuring a regular movement of individual particles in a fluidized bed or a pan. The quality of coating depends on the particles composition and surface properties, and the composition of the coating as well as on process parameters.

Guignon et al. (2003) tested feasibility and modeling of particles coating in a fluidized bed (Wurster mode) with different model particles and coating solutions:

- particles of glass, aluminum, polymethyl methacrylate (pmma), resin and semolina (125 to 1250 microns)
- coating of aqueous solutions of NaCl, acacia gum and maltodextrin (20% w/w dry matter)

Optimal operating conditions were defined for particles circulation and coating without agglomeration, and minimal losses of coating. The coating deposit rate was found to be proportional to the duration of pulverization, representing a layer of 23 microns of acacia gum on aluminum beads after 25min. Coating of glass beads with NaCl was limited after 10 min, due to crystallization, but the addition of acacia gum to the salt solution (50/50) gave a regular deposit during 65 min of pulverization.

A model describing 4 zones in the process was built, taking into account the particle trajectory (position, moving) for one particle, and the mass transfer of water to the air. It was possible to calculate the mean thickness of coating and the efficiency of the process (% deposit) as a function of reactor geometry, operating conditions, and properties of particles and coating solution (composition, viscosity, surface tension).

13.5. Conclusion

As usual in process engineering, powder production requires scientific knowledge in various disciplines such as chemistry, biochemistry, mechanics, physics and engineering.

Design of process lines must integrate the specificity of powder technology, keeping in mind the relationship between the physicochemical characteristics of the initial mixture, the various operations involved in the process, and the final use of powders, in order to reach the final objectives for industry and for consumers.

Topics of interest for further research are traceability, control of dust; control of sticking during process wanted or not (agglomeration) and during storage; criteria for choice of matrix constituents to answer a given problem, e.g., particles able to retain taste or mask intense odor or bad taste, or to keep nutritional value.

In summary food process engineering must help to produce *intelligent particles* with individual and bulk behavior that are easy to predict in various environments, and able to protect and/or to release a specific constituent when and where it is needed.

References

This text was based on our experience in research, complemented with some general publications on powders.

Bimbenet, JJ., Bonazzi, C., and Dumoulin E., 2002, Drying of Foodstuffs, in: *Drying 2002*, A.S. Mujumdar (ed.) Beijing, vol.A, 64–80.

Chulia, D., Deleuil, M., and Pourcelot Y., 1994, *Powder Technology and Pharmaceutical Processes. Handbook of Powder Technology*, Elsevier, Amsterdam, London, New York, Tokyo, vol. 9, 557p.

Dumoulin, E., and Bimbenet J.J., 1998, Spray Drying and Quality Changes, in: *The Properties of Water in Foods – ISOPOW 6*, D.S. Reid (ed.) Blackie Acad. & Prof, London, pp. 209–232.

Fuchs, M., Turchiuli, C., Bohin, M., Cuvelier, M.E., Ordonnaud, C., Peyrat-Maillard, M.N., and Dumoulin E., 2006, Encapsulation of Oil in Powder Using Spray Drying and Fluidized Bed Agglomeration, *J. Food Engineering* **75**(1):27–35.

Guignon, B., Regalado, E., Duquenoy, A., and Dumoulin E., 2003, Helping to Choose Operating Parameters for a Coating Fluid Bed Process, *Powder Technology* **130**:193–198.

Gy P., 1982, *Sampling of Particulate Materials. Theory and Practice*, 2nd ed., Elsevier, Amsterdam, p. 431

Mathlouti, M., and Rogé B., 2003, Water Vapour Sorption Isotherms and the Caking of Food Powders, *Food Chemistry* **82**:61–71.

Melcion J.P., and Ilari J.L., 2003, *Technologie des Pulvérulents dans les IAA*, Tec & Doc Lavoisier, Londres-Paris-New York. p. 814

Palzer S., 2005, Controle de L'agglomeration de Polymeres de Dextrose par L'application du Concept de la Transition Vitreuse, *Ind. Alim. Agr*. **122**(12):20–27.

Peleg M., 1983, Physical Characteristics of Food Powders, in *Physical Properties of Foods*, M. Peleg and E.B. Bagley (eds.) Avi Pub Co, New York, pp. 293–321.

Rhodes M., 1998, *Introduction to Particle Technology*, Wiley, Chichester, p. 320.

Roos Y., 1995, Activité de L'eau et Transitions de Phase Dans les Aliments Riches en Sucres, 4th colloque CEDUS Alliance 7, Paris.

Schubert H., 1993, Instantization of Powdered Food Products, *Int. Chem. Eng*. **33**(1):28–45.

Senoussi, A., Dumoulin, E., and Berk Z., 1995, Retention of Diacetyl in Milk During Spray Drying and Storage, *J. Food Science*, **60**(5):894–897, 905.

Turchiuli, C., Eloualia, Z., El Mansouri, N., and Dumoulin E., 2005a, Fluidized Bed Agglomeration: Agglomerates Shape and End-Use Properties, *Powder Technology* **157**:168–175.

Turchiuli, C., Fuchs, M., Bohin, M., Cuvelier, M.E., Ordonnaud, C., Peyrat-Maillard, M.N., and Dumoulin E., 2005b, Oil Encapsulation by Spray Drying and Fluidized Bed Agglomeration, *Innovative Food Science and Emerging Technologies* **6**, 29–35.

14
Towards an Integrated Approach to Food Engineering: Structure-Function Relationships And Convective Drying

G.F. Gutiérrez-López, L. Alamilla-Beltrán J. Chanona-Pérez, E. Parada-Arias, and C. Ordorica-Vargas

14.1. Introduction: Food Engineering, Opportunities and Challenges of an Integrated Approach

Food engineering is a multidisciplinary activity in which many subjects converge and play important roles. Preparation of foodstuffs for consumption for a growing and wide range of needs should include novel approaches to product development, engineering and equipment design, as well as the usage of advanced algorithms for establishing operating conditions of emerging processing technologies such as high hydrostatic pressure and pulsed electric fields rigs.

The knowledge base for achieving reasonable product engineered processing includes, in addition to traditional physical and chemical backgrounds, advanced non-linear dynamics, solid state physics, biotechnology, nanoscience and nanotechnology and novel interpretation of traditional concepts such as interfaces, as well as computer vision tools and product architecture. All of these components of an integrated approach to food engineering play a key role on the production of successful foodstuffs through innovation; thirty years ago, the food industry directed attention to production, whereas at present much more attention has been given to the manufacture of healthy, more natural, fresher, easier to use and tastier products with declared beneficial attributes. This tendency has increased the speed at which innovation in food industrial activities is carried out, and the time of product development has decreased from 10 years in 1970s to 2 years in the year 2000 (Bruin and Jongen, 2003).

Development and implementation procedures of knowledge-base manufactured foodstuffs have reached commercial levels while, on the other hand, processing engineering know-how of equipment and process design is not well established. Practical application has moved ahead from a fundamental understanding of engineering.

Examples of this situation include many separation processes that are made up of combined operations, and emerging technologies for the design of structures and architecture of materials, as well as for nanotechnology and nanoscience-based products or nano-foods. Proteomics, genomics, metabolomics and, in general,

so-called "omics" sciences will have important roles in the manufacture of molecular-biology based materials for food processing (Dettmer and Hammock, 2004). Also, systems biology, defined as the quantitative analysis of the dynamic interactions between components of a biological system, aims to understand the behavior of the systems as a whole as opposed to the behavior of its individual constituents (Dollery and Kitney, 2007), will have more importance in applied engineering fields in the years to come, including food engineering science.

The above described situations have several implications within the frame of food engineering and may raise questions regarding engineering activity, such as the examples depicted below, and which are recommended to bear in mind when attempting to perform food processing:

- Do we actually design products/processes considering advanced available engineering capabilities?
- Are we contributing to the provision of fundamental solutions to turbulent-regimes based processing?
- Do we produce foodstuffs with maximum achievable processing efficiency?
- Are we aware that production lines often have more than one bottleneck? Can we suppress them and not create others?
- Having a production line delivering *n*-products and involving *n*-production operations, are we able to increase/decrease individual production rates without affecting overall plant efficiency and the delivery of any of the *n*-products involved?
- How well do we handle the fundamental basis of unit and combined operations involved in processing?
- Do we know that, very often, combined operations such as pervaporation, inverse micelization and affinity pertraction will have an increasingly important role in food related areas?
- Up to what extent are we conscious of the increased importance of engineered-based products and of product engineering for innovation?

Answers to the above questions are not readily available, and food engineers should tackle processing by considering each case separately and resolving particular problems by taking into consideration integrated approaches and working with multidisciplinary teams.

It is always advisable to bear in mind that no matter the complexity of problem, rigorous solutions offer advantages over simplified solutions, and they may represent an important reference for decision making.

Food engineering science attempts to open what engineers have called processing "black boxes" in order to understand the fundamental basis of manufacturing. However, entering food processing black boxes gives rise to the formulation of new questions, and new black boxes appear. As a consequence, engineering teams find a continuous gap between utilitarian application and generation of fundamental knowledge.

14.2. Experimental and Mathematical Techniques with a Concourse in Food Engineering Practice

Given the multi- and inter-disciplinary nature of food production, processing activity has imported a number of analytical techniques, both experimental and mathematical, that were originally developed and designed within other scientific fields. Engineers face a huge challenge in using these techniques in a sensible way, integrating results and providing a rational description of phenomena in heterogeneous and complex systems. Some techniques are:

- Nuclear magnetic resonance: high and low resolution
- X-ray spectroscopy
- Ultrasound imaging
- Microscopy: scanning electron, transmission, fluorescence, atomic force, transmission electron and co-focal
- Computer vision systems
- Differential scanning calorimetry
- Image and fractal analysis
- Statistical mathematical tools such as Weisbull distribution and Montecarlo analysis
- Computer fluid dynamics (CFD)
- Non-linear dynamics
- Deterministic chaos
- Immunological and molecular biology based techniques such as ELISA and PCR tests
- Cell and tissue culture

Many of the above techniques/methodologies may render experimental data which, without a correct interpretation, could turn experimentation into a monotonous, frustrating activity consisting of accumulating and reporting results that have little relation to a sound and sensible integrative food engineering scope. Integration has to build bridges between processes and their fundamental basis; experimental and analytical-mathematical tools should give consideration to data that would contribute to the interpretation of phenomena and thus increase the knowledge base that will help to open processing black boxes (Fig. 14.1).

Foods are heterogeneous materials in which a multiplicity of components interact and may mask the actual phenomena under study. The above situation leads to the development of descriptive models for interpretation of different phenomena associated with food production and processing (Caro-Corrales et al., 2002).

Aiming to present a revision of attempts to integrate food engineering knowledge, comments on recent works made by our research team on the dehydration operation is presented next within the frame of fractal and image analysis and non linear dynamics.

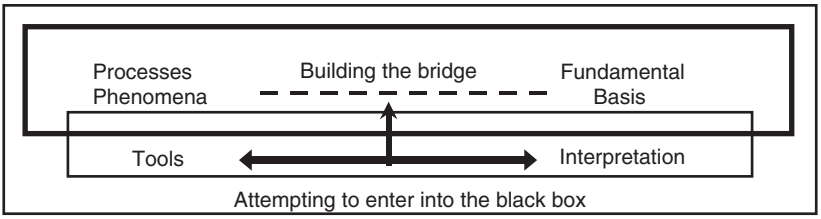

FIG. 14.1. Task: to build the bridge (dotted line) between processes and phenomena and their fundamental basis, aiming to enter into the processing black box. Tools (mathematical, experimental) allow placement of bi-directional interaction

14.3. Convective Drying, Structure and Function Relationships

In Fig. 14.2, a diagram illustrating the interaction between processing, functionality and structure is presented to introduce this section within an integrative frame.

It has been demonstrated that surface temperature (ST) distribution of a slab-shaped food model presented three regions or stages when subjected to hot air drying under various drying conditions: 45–65 °C, 1–3 m/s (Chanona et al., 2003). The first region has been related to the presence of a *strange* attractor that was evident when plotting defaced surface-slab temperatures with in-face temperatures during drying. This *strange* attractor is characteristic of deterministic chaos; the second stage has a fractal surface temperature (ST) distribution, showing a region of invariance of the characteristic fractal dimension of ST distributions, and the third one corresponds to equilibrium conditions when ST did not show any further change. Ruggedness of material increased with drying time, and heterogeneous surface morphology was related to homogeneous ST distributions. A pictorial representation of the above depicted phenomena is presented in Fig. 14.3.

Alamilla et al. (2005) reported the fractal dimension of spray dried maltodextrin particles subjected to two-fluid nozzle co-current spray drying at high (200/173°C), intermediate (170/145 °C) and low (110/74°C) drying air inlet/outlet temperatures. Fractal dimensions of projected perimeter of particles were obtained for the three temperature combinations. Mainly, broken hollow particles were obtained by drying at high temperatures (highest fractal dimension), while hollow and some broken particles were obtained at intermediate temperature conditions (lowest value of fractal dimension), and the formation of collapsed solid spheres was observed at low temperatures (intermediate values of fractal dimension). These results were also related to particle moisture content and droplet size profiles into the drying chamber, thus giving a description of product quality operating conditions of a complex operation. Additionally,

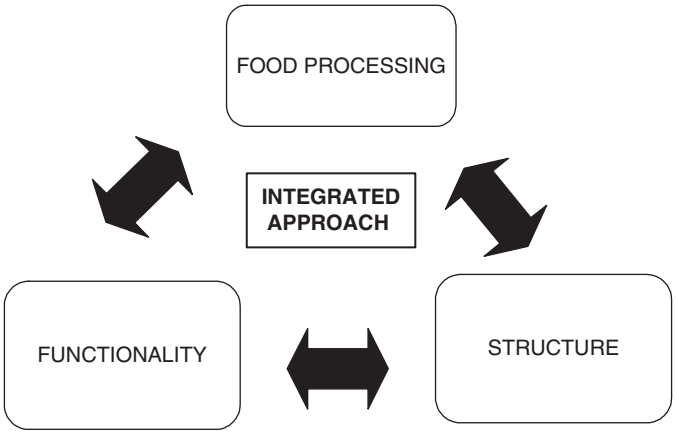

FIG. 14.2. Interaction frame among the three main components of the integrated approach to processing: structure, functionality and food processing

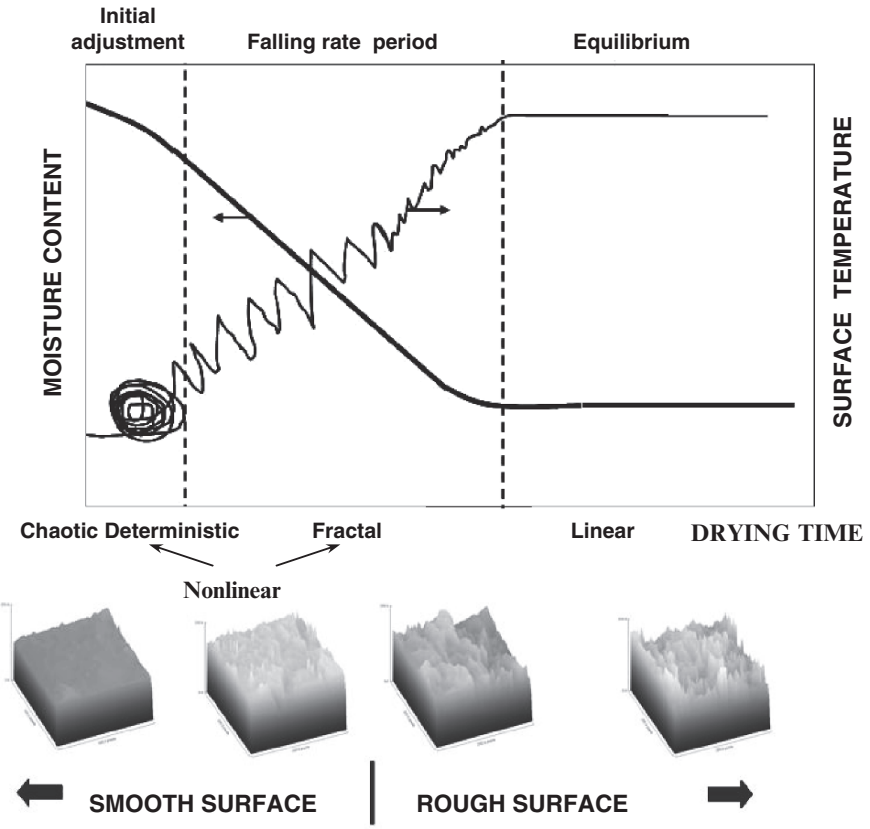

FIG. 14.3. Drying kinetics: proposed stages related to non-linear behavior. The first stage may be related to the presence of a deterministic chaotic attractor, the second stage was characterized by a fractal dimension before reaching equilibrium (third stage). Also, pictorial representation of surface irregularity during dehydration is depicted

reports on convective drying of macroscopic spheres as related to spray drying performance have been carried out in relation to fractal dimension of dried materials (Chanona-Pérez et al., 2006).

Regarding convective drying of vegetable tissues, Campos-Mendiola et al. (2007) reported the microscopic and morphological features of potato slabs subjected to hot air drying. It was concluded that deformation followed patterns which were controlled by fibers alignment. Also, it was observed that the fractal dimension of relative projected areas showed two peaks during drying; the first peak corresponded to extra-cellular water removal, while the second peak was characteristic of intra-cellular water evaporation, thus giving a perspective of morphology-drying conditions relationships associated with potato slab preparation techniques.

In another work, Villalobos et al. (2005) prepared edible films with hydroxypropyl methylcellulose with various solids contents, which were studied by means of light microscopy, atomic force microscopy and scanning electron microscopy. Fractal analysis was applied to the microscopy images to quantify the film microstructure complexity. Apparent fractal dimensions from LM and AFM images were well correlated with transparency and gloss parameters of the films, respectively.

The above described works may give the reader an insight on integrated approaches to convective drying, solid-moisture interactions and structure-function relationships. These results were obtained thanks to integrative approaches to food-engineering-related topics, in which a single operation (dehydration) is analyzed from various perspectives and using several experimental and mathematical analytical tools that give an overall appraisal not only of the products under study but also of the unit operation itself, and reach a complementary non-linear description of the stages of drying kinetics.

14.4. Opportunities for Food Engineers

It is important to point out that many aspects related to non-linear dynamics in food engineering situations still need to be further investigated. Foods are very complex materials and most phenomena related to product engineering, processing design, materials handling and end-product delivery are non-linear. Some examples of this area are described in Chapter 2 of this book. Also, sensible inclusion of analytical and mathematical techniques for process design, optimization and increasing of yields will augment professional areas in which food engineering may develop.

Opportunities for a rational food engineering activity are discussed in leading chapters of this book and comments on this topic are given in Table 14.1.

TABLE 14.1. Leading chapters in this book; comments on their contribution to integrated approach of food engineering

Title of chapter	Contribution towards an integrated approach of food engineering
• Food sterilization by combining high pressure and thermal energy	• Application and fundamentals of emerging technologies; consideration of complex variables involved
• Non-linear kinetics: principles and potential food applications	• Exploring novel solutions to complex phenomena
• Consequences of matrix structural changes on chemical and functional stability of enzymes as affected by electrolytes	• Solute-solvent interactions, implications in enzyme kinetics
• Air impingement cooling of cylindrical objects using slot jets	• Novel applications and scope to transport phenomena
• New technologies to preserve quality of fresh-cut produce	• Approaches to new production techniques
• Advanced food products & process engineering (safes) i: concepts & methodology	• New approach to integrated analysis of processing
• Phase transitions and hygroscopicity in chewing gum manufacture	• Analysis of production of a complex-based food related material
• Exploring the linear viscoelastic properties structure relationship in processed fruit tissues	• Integrated approach to textural studies
• Bubbles in foods: creating structure out of thin air!	• Novel approach to description of gas-liquid-solid interactions
• Films based on biopolymers from conventional and non conventional sources	• Example of integrated approach to applied surface processing
• Edible coating as oil barrier or active system	• Complex system application to food related processing
• From powders end use properties to process engineering	• Powder technology: integrated description
• Towards food product design	• Scope of manufacturing tendencies within an integrated frame

14.5. Final Remarks

By trying integrated approaches to food processing, engineers may improve the long term efficiency of production. It is advisable to prepare young engineers to design with rigorous criteria, no matter how complex the production problem may seem. Inclusion of multidisciplinary teams for solving food product engineering situations is also advisable, and the main goal within this context nowadays is to be prepared to design strong knowledge-based production platforms for delivering pre-designed food commodities that are directed toward very demanding consumer needs. This situation, illustrated in Fig. 14.4, is the challenge imposed by strongly globalized and highly competitive markets.

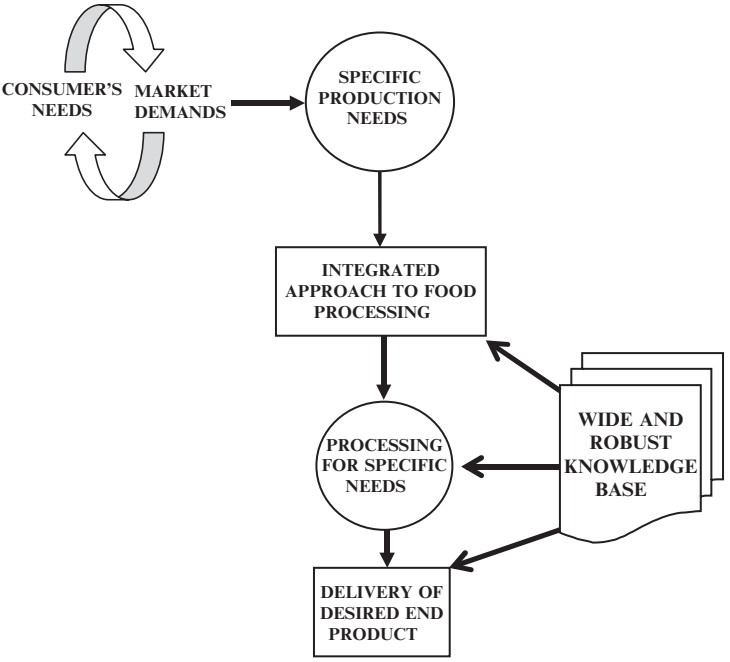

FIG. 14.4. From Consumer demands to end product pathway: Generation of specific production needs requires solving technical issues such as appropriate processing equipment, adequate quality control, specific analytical techniques, etc., and the concourse of an integrated approach to the problem throughout the input of a wide and robust knowledge base

References

Alamilla-Beltrán, L., Chanona-Pérez, J.J., Jiménez-Aparicio, A.R., and Gutiérrez-López G.F., 2005, Description of Morphological Changes of Particles Along Spray Drying, *J. Food Eng*. **67**: 79–184.

Bruin, S., and Jongen T.R.G., 2003, Food Process Engineering: The Last 25 Years and Challenges Ahead, *Comprehensive Reviews Food Sci.& Food Safety* **2**:42–81.

Campos-Mendiola, R., Hernández-Sánchez, H., Chanona-Pérez, J.J., Alamilla-Beltrán, L., Jiménez-Aparicio, A., Fito, P., and Gutiérrez-López G.F., 2007, Non-Isotropic Shrinkage and Interfaces During Convective Drying of Potato Slabs Within the Frame of the Systematic Approach to Food Engineering Systems (SAFES) Methodology, *J. Food Eng*. (In press).

Caro-Corrales, J., Cronin, K., Abodayeh, K., Gutiérrez-López, G., and Ordorica-Falomir C., 2002, Analysis Of Random Variability In Biscuit Cooling, *J. Food Eng*. **54**(2):147–156.

Chanona, P.J.J., Alamilla, B.L., Farrera, R.R.R., Quevedo, R., Aguilera, J.M., and Gutiérrez L.G.F., 2003, Description of the Convective Air-Drying of a Food Model by Means of The Fractal Theory, *Food Sci. Technol. Int*. **9**(3): 207–213

Chanona-Pérez, J.J., Alamilla-Beltrán, L., Farrera-Rebollo, R.R., and Gutiérrez-López G.F., 2006, Evaluation of Morphological and Microstructural Changes During Air Drying of Spheres Using Fractal Analysis and Relationships with Spray Drying, in: *Water Properties of Food, Pharmaceutical and Bilological Materials*, M. P. Buera, J. Welti-Chanes, P.J. Lillford, and H.R. Corti (eds.), CRC Taylor & Francis, Boca Raton, pp. 519–524

Dettmer, K., and Hammock B.D., 2004, Metabolomics—A New Exciting Field Within the "Omics" Sciences, *Environ. Health Perspect*. **112**(7):A396–A397

Dollery, C., and Kitney R., 2007, Systems *Biology: A Vision for Engineering and Medicine*. A Report from the Academy of Medical Sciences and The Royal Academy of Engineering, UK.

Villalobos, R., Chanona, J., Hernández, P., Gutiérrez, G., and Chiralt, A., 2005, Gloss and Transparency of Hydroxypropyl Methylcellulose Films Containing Surfactants as Affected by Their Microstructure, *Food Hydrocolloid*. **19**: 53–61

15
Towards Food Product Design

J.M. Aguilera

15.1. Abstract

Most quality and acceptability traits of foods are derived from their unique microstructures. Food microstructure is imparted by nature or by processing and plays an important role in physical, engineering, sensorial and nutritional properties. Thus, food technology may be regarded as a controlled effort to preserve structure, or to transform it into palatable products by processing. The application of scientific knowledge and advanced tools that probe the microstructure of foods has resulted in major advances in our understanding of how microstructure in processed products is developed and broken down. Changes in consumer demand towards health and wellbeing are finding an appropriate response in the design and delivery of novel food systems.

Keywords: Foods, food engineering, microstructure, materials science, quality.

15.2. Introduction

The structure of all foods, whether consumed with minimal preparation or imparted by processing, comes from nature. According to the valuable structural components that give desirable textures to foods, natural raw materials may be classified into four broad categories: i) encapsulated dry embryos of plants (e.g., grains and pulses) that contain a dispersion of starch granules, protein assemblies and/or lipid bodies within cells bounded by cell walls containing cellulose and other biopolymers; ii) fleshy materials from plants that are hierarchical composites of turgid cells (filled with water) bonded together at the cell walls (e.g., fruits and vegetables, tubers); iii) fibrous proteinaceous structures assembled hierarchically for specific body functionality (i.e., movement) from macromolecules into fibrils, fibers and then tissue (e.g., muscle) and held together at different levels by specific interfacial interactions; and, iv) a unique complex fluid called milk, intended for nutrition of the young mammal, containing nutrients in a state of colloidal liquid dispersion (casein micelles, fat globules) or solution (lactose, soluble whey proteins).

Even today, most food consumed around the world undergoes minimal or reduced transformation, as is the case of cooked grains and pulses (or their flours), fresh fruits and vegetables, meat and fluid milk. Ninety-one percent of the world's agricultural production depends on only 24 different domesticated plant species. One cereal grain, rice, provides 23% of the calories derived from foods worldwide, and when corn and wheat are added, they account for most of the world's caloric intake. However, in industrialized countries and most urban areas of the Third World, processed foods with unique man-made structures abound in local supermarkets. Food structure is also transformed on a large scale in restaurants, fast food outlets, and by street vendors. The overall outcome is that the food industry has the largest annual sales turnover of any manufacturing industry, approximately US $3.5 trillion (Bauer, 2004).

15.3. Why Structure Foods?

Throughout evolution, humans have ingested nutrients in the form of palatable products called foods, which are easily recognized by their structure and the sensations experienced during mastication, for example, their texture and flavor. Changes in the natural structure of foods have evolved through time, first as a result of preservation (e.g., drying, natural freezing) and then by cooking. The discovery of basic culinary transformations (e.g., baking, fermentation, frying) brought further modifications that significantly altered the structure of foods. The initiation of gastronomy in the 16th century, with the incorporation of spices and products of the new worlds (Asia and America) greatly augmented the diversity of food structures and tastes (Fig. 15.1).

Industrial food processing started at the beginning of the 19th century in small canning factories and continued with the later development of freezing plants and cool storage. The merit of the food industry of the 20th century was scaling-up processes developed by artisans into fabrication lines that consistently produced thousands of units per hour of microbiologically safe and nutritious foods. Supermarkets proliferated in the United States with the growth of suburban areas after World War II, and today there are more than 85,000 grocery stores in that country alone. With this growth came the need for product diversification and product development that added convenience and lowered the price of foods. The food trade (which presently amounts to almost 20% of food production worldwide), the introduction of ethnic foods and globalization of tastes, the advent of modern gastronomy, and new demands for healthy foods have greatly expanded the offerings of food structures and flavors.

There are several reasons why the food industry continues to develop food textures and structures that we enjoy (Aguilera, 2005): i) expanding the variety and appeal of food sources (e.g., ice cream, snacks, ready-to-eat products); ii) improving the stability and convenience of products (e.g., dried, frozen, instant and precooked meals); iii) adding value to ingredients and byproducts (e.g., extruded products, processed meats); and iv) emulating existing products with

specific nutritional or functional properties (e.g., dietetic foods, food analogs). A special case of structuring foods using nature is the introduction into the human food chain of inedible or underutilized sources of nutrients, as is the case of rearing meat animals in pastures and salmon in sea cages.

Driven by new scientific knowledge and consumer demand for health and wellbeing, a paradigmatic shift is occurring in the way food engineers develop new foods. The top-down approach to product development (i.e., *mix and see*) is being replaced by the bottom-up approach to structuring and food product design. Modern food product design recognizes that food structures start at the molecular level and continue through molecular assembly processes at the mesoscale (e.g., 10 nm to 1 μm). The typical morphology of a processed food is the outcome of a specific kinetics mediated by momentum (shear), heat, and mass transfer, resulting in formation of structural elements that give foods their desirable properties: oil droplets, bubbles, ice and fat crystals, pores, etc. The final structure is stabilized by a mechanism that can be understood by using concepts from physical chemistry and polymer science. Use of this approach and of scientific knowledge makes the quest for new structures faster, more rational and efficient. New opportunities for product design come from the increased understanding of the relation between diet and health, the potential to tailor-make foods based on human genomics (*nutrigenomics*), and changes in raw materials achieved through plant and animal biotechnology (Fig. 15.1).

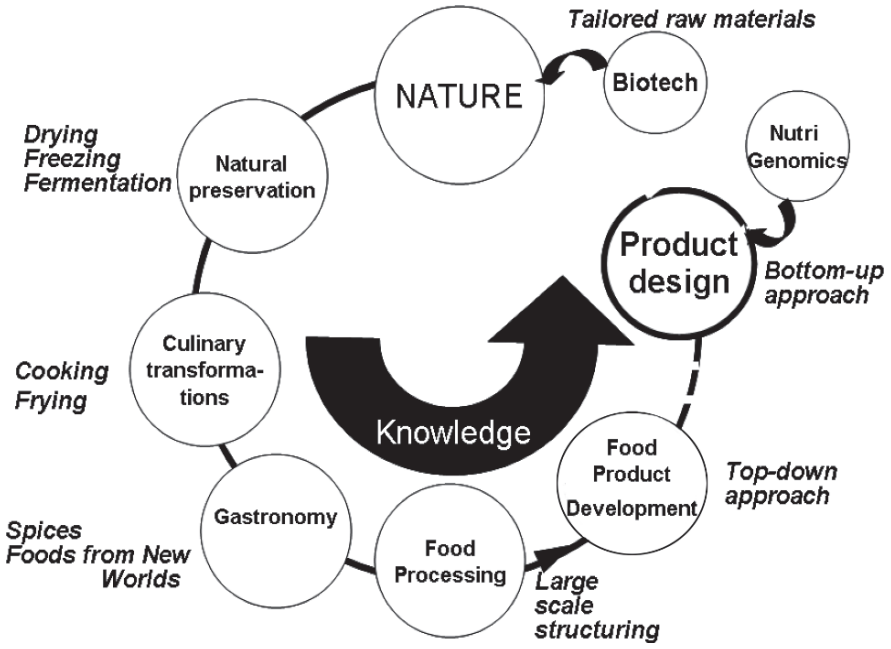

FIG. 15.1. The evolution of food structuring through times and key milestones

To be widely available as foods, the "natural" structures of fruits, vegetables, and muscle tissues first need to be *preserved* for transport, storage, processing and consumption. Preservation of the natural structure of these foods means reducing the rates of detrimental biochemical reactions and microbial proliferation. Post-harvest and post-mortem technologies are mostly based on reducing the temperature (refrigeration), controlling the composition of the atmosphere surrounding the foods (fruits and some vegetables, meat and fish), removing water by drying (grains and pulses), immobilizing water as ice (freezing of plant and animal tissues) and proper packaging.

Versatility of processed foods is derived not so much on molecular variability, but on mixing of refined fractions. C*ontrolled destruction* of structure means fractionation and separation of raw materials into valuable components, considering the intrinsic tissue archi-tecture in which they are dispersed. These operations result in the ingredients of processed foods: oils and special fats (e.g., cocoa butter), sugar and starches, flours and grits, hydro-colloids from plants and algae, etc. Hydrolysis using enzymes or acid may further reduce the molecular structure for added functionality. More recent separation technologies make use of membrane processing to fractionate proteins from milk and the use of supercritical CO_2 extraction to extract nutraceuticals from plants. But what is central to the food industry is the *transformation* of these ingredients by mixing, shearing and heating/cooling into recognizable and desired shapes and textures. Some of the microstructural elements in processed foods that contribute to their sensorial identity and quality are gas bubbles, oil droplets, hydrated starch granules, debonded cells, fibers, gel and crystal networks, particulate solids, crystals of many types, and assemblies of colloidal nature, among others.

15.4. Structuring for Designed Properties

Controlling microstructure has been central to the processed food industry in the last 40 years. The length scales involved vary from those of interfacial phenomena in the nanometer range (e.g., surfactants stabilizing emulsions) to the millimeter size in solid foams (e.g., bubbles in cereal snacks). It is amazing that the chemical engineering profession has ignored advances in the manufacture of structured food products now that they realize that creams and foams, pastes, catalysts, new drugs, cements and ceramics, artificial tissues, etc. are complex multiphase products whose most valuable properties are not determined by composition, but rather by their unique microstructure formed in the 0.1 to 100 μm range (Hill, 2004; Cussler and Wei, 2003; Villadsen, 1997). The past and present contribution of food engineers to structural product design became more evident at the recent International Congress of Engineering and Food (ICEF 9) held in Montpellier (March, 2004). The theme with the largest number of papers presented was *Processing and Characterization of Polyphasic Structured Systems*, surpassing classical subjects such as *Tools and Methods for Food Engineering* and *Emerging Technologies*. Figure 15.2 shows some of the desirable properties in designed foods.

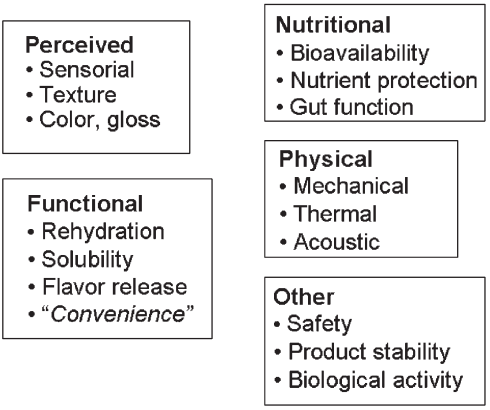

FIG. 15.2. Some of the desirable properties of processed foods

15.5. Microstructure and Materials Science over the Years

Although systematic investigation of food structure began recently, scientists have been looking through lenses or down microscopes at foods for much longer than that. During the 17th and 18th centuries, a great deal of descriptive anatomy was conducted on plants and animal tissues used as foods. Perhaps the first practical application of micros-copy in the food industry was in quality control to detect adulteration of ingredients and admixing. However, it was not until the late 1970s that a book was published that included the contribution of many researchers from industry, research stations and universities, which demonstrated how microscopy could be used to investigate the microstructure of raw materials and processed foods—among the latter, chocolate, ice cream and extruded soy (Vaughan, 1979).

It is likely that the earliest publication in which food structure was brought into the main scene of food engineering was the proceedings of a conference on drying held in Aberdeen in 1958, organized by the Society of Chemical Industry (Singh, 1958). The first two chapters addressed the subjects of *Plant Structure and Dehydration* and *The Structure of the Animal Tissues and Dehydration*. The effect of structure on the rate of air drying and freeze-drying was addressed by several authors for many food materials.

At the risk of making unforgivable omissions, a short narrative of the main scientific events that have shaped what is now known as food materials science and the microstructural view of food engineering is presented. The work on freeze-drying in the 1960s and early 1970s is perhaps the best representation of the early recognition by food engineers that product structure played a crucial role in heat and mass transfer during processing and in the quality of foods. Work in the U.S. by the groups of C.J. King at Berkeley (King, 1971) and M. Karel at MIT (1970), and in Europe by the groups of H.A.C. Thijssen at TU Einhoven (1971) and L. Rey at Nestle (1966), among others, clearly established that drying rates, aroma retention

and collapse during freeze-drying were decisively influenced by the structure and properties of the dry matrix. The debate was about how aroma molecules—those in pure state are more volatile than water—were largely retained during drying. Both the selective diffusion mechanism as well as the microregion entrapment concepts are now understood by the formation of vitreous domains of low mobility that restrict the diffusion of large flavor molecules within the dry matrix.

Most foods are dispersed systems containing substantial amounts of water. Thus, surface phenomena and colloidal interactions, as well as other physicochemical phenomena, received much attention from the 1970s onwards, particularly in the study of milk as a complex system (Walstra, 2002). The *polymer science approach* to the study of foods emerged strongly in the late 1980s, highlighted by Levine and Slade (then at Nabisco), although the first mention of the glass transition in foods appeared in the literature in the 1960s (Levine and Slade, 1986; Slade and Levine, 1991). This approach recognized that water in low-moisture foods acts as a plasticizer that increases the mobility of the matrix, negatively affecting the quality, stability and safety of foods. Thus, the glass transition concept complemented the water activity notion introduced by microbiologists in the mid-1950s to assess the microbial stability of foods at intermediate and high moisture contents. For many situations, state diagrams have been constructed that separate different regions according to the physical state of the matrix as a function of moisture and temperature. These diagrams are used to predict changes in material properties during processing and in assessing product stability (Roos and Karel, 1991; Kokini et al., 1994).

The first version of the book *Microstructural Aspects of Food Processing and Engineering* (Aguilera and Stanley, 1991) attempted to put together several ideas about food microstructure and food structuring that had been set forward by many authors up until that time. Unit operations of food dehydration and solvent extraction were revisited, considering structure as a key parameter. The authors were particularly critical of the widespread use by food engineers of the *effective diffusivity* concept as the sole parameter to describe mass transfer in structured foods. Recently, it has been realized that other mass transport modes, particularly capillarity and pressure-driven phenomena, have significant contributions in food products, for example, in oil uptake by fried products (Mellema, 2003), moisture release during baking and extrusion (Fu et al., 2003), powder rehydration (Saguy et al., 2005) and possibly in fat migration in particulate materials such as chocolate (Aguilera et al., 2004). In the second edition (Aguilera and Stanley, 1999), basic concepts of physical chemistry, polymer science and colloid science were presented as the basis of food structuring processes, and the potential of image analysis to quantify microstructure was highlighted.

The text on transport phenomena by Gekas (1991) emphasized that chemical engineering principles applied to foods should consider the structured nature of foods and biological materials. In this context, physical properties of foods have practical meaning once the proportion and architecture of the different phases or structural elements have been resolved in the actual product (Saravacos and

Maroulis, 2001). The work on osmotic dehydration in the 1990s was particularly enlightening to demonstrate that both diffusion and the so-called hydrodynamic flow were acting in parallel in cells and pores, respectively (Fito, 1994). Since we have borrowed and successfully applied concepts of polymer physics, such as the glass transition, we will be in a position to derive scaling laws that link physical magnitudes at the nano- or microscale with product properties at the macroscale. An excellent example of this is the work on fat crystal networks by Marangoni's group at University of Guelph (Narine and Marangoni, 1999). Table 15.1 presents a summary of research topics and some of the groups that have made significant contributions to the development of food structuring and food materials science.

TABLE 15.1. A concise guide of some of the research topics on food microstucture, institutions and useful references

Subject	Institution	References
Food microstructure and relation texture, physical and transport properties and food product engineering	Dept. Chemical & Bioprocess Engng, Univ. Católica (Chile)	Aguilera and Stanley, 1999; Aguilera, 2005
Generation of structures by processing, and effect of process parameters (shear, heating/cooling) on structure engineering and microstructures	Swedish Institute of Technology (SIK)	Hermansson, 2000
Microstructure of disperse systems as the characteristic feature and link between the process and properties of the final product	University of Karlsruhe, Germany	Schubert, et al., 2003
State of aggregation or dispersion of food components and dependence of functional properties on specific interactions of various structural elements	Unilever Research Laboratory, Vlaardingen	Heertje, 1993
Relations between lipid structures at various levels and fat crystal networks on desirable properties of fat-containing products; use of fractal analysis	Dept. Food Science, University of Guelph, Canada	Marangoni, 2005
The "bottom-up" approach to food fabrication; relevant scales in future food structure research and role of the "nano-level" in generating a multi-scale food colloid science	Nestle Research Centre, Switzerland	Leser et al., 2003
Principles in trapping a structure by phase-separation and gelation of mixed food polymer mixtures	Unilever R&D Colworth, UK	Norton and Frith, 2003
Understanding the science of nanoscale particles, properties and applications of materials emerging from food nanotechnology	Rutgers University, NJ	Moraru et al., 2003
Image acquisition and enhancement, selection of specific features in images, measurement of size and shape of objects and many applications to foods	University of North Carolina	Russ, 2004

(continued)

TABLE 15.1. (continued)

Subject	Institution	References
Mesoscopic physics (scale 1nm–100 μm), e.g., liquid crystalline bilayers structured to provide a specific rheological behavior	Food Physics Group, Wageningen Univ., The Netherlands	van der Linden, 2000
Controlling crystallization (e.g., crystal size and morphology) involves selection of ingredients and process conditions to promote desirable product properties	Dept of Food Science, University of Wisconsin	Hartel, 2001
Dependence of rheological parameters on the structure of dispersed food systems and modeling; applications to food processing	ETH Zurich, Switzerland	Windhab, 1995
Rheology and microstructure of gels and emulsions, and mixed systems	University of Leeds, UK	Dickinson, 2000
Processing of chocolate is presented as a sequence of mixing, shearing, heating/cooling steps to give the right structure	University of Birmingham, UK	Fryer and Pinschower, 2000

15.6. Stabilizing Food Structures

The concept of structure was not fundamental in chemical engineering, except perhaps when dealing with porous solids (e.g., catalysts), where the parameters of porosity and tortuosity were sufficient to describe transport processes in these materials. Many food processing operations create a microstructure that provides products with desirable traits and functional properties. Food structure engineering is defined as the generation of microstructures in foods based on fundamental knowledge (e.g., colloid science, polymer science), use of appropriate ingredients and controlled application of processing variables, such as shear and temperature gradients (Aguilera, 2000; Hermansson, 2000).

Structure generation usually starts as a kinetic process, during which the key structural elements are formed. This is the case of bubble production in aerated products, gluten-starch interactions in baked products, droplet formation in emulsions, etc. Design variables are the formulation, the rates of shear and heat transfer, weight ratio of each of the phases, etc. The appropriate structure is then "frozen" in thermodynamic terms (e.g., crystal formation), or more generally as a metastable state (e.g., glass) (Fig. 15.3). Main shape stabilization mechanisms in foods are not different from those in polymers: vitrification, phase dispersion/phase separation, crystallization, and network formation.

15.7. Impact on Academia and Education

Food engineering departments (and ChemE departments as well) worry that graduates leave ill-prepared to enter companies whose value is in rapidly responding

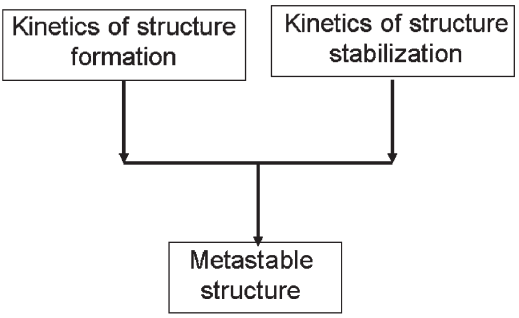

FIG. 15.3. Food structures are generally the result of two kinetic processes: structure formation and structure stabilization

to consumer demands and trends by launching innovative products. What do we have to offer compared to other fashionable engineering careers? The invitation is to work with edible soft matter, dispersed systems and structured products, to learn about emerging technologies such as microfabrication, to understand the interfaces with nutrition and health, and to participate in biotechnology by improving those structural components in raw materials that will redound in better texture, improved stability, higher functionality, less processing and reduced waste. Developing food product design and reinventing food product engineering will require a broader scientific base to include materials science, advanced methods used in physics, medicine and biological sciences, nutrition and the gut function, information science, and even notions of neurobiology.

15.8. Conclusions

Changes in consumers' needs and perceptions about foods are shifting the emphasis from processes to products. In the era of structured products, this is the birth of food product design.

There is ample evidence (although still mostly of qualitative nature) linking food microstructure to many desirable properties of foods (sensorial, physical and nutritional).

The foundation for finding meaningful product-property relationships is the sound application of scientific knowledge (e.g., food materials science), utilization of probing techniques at different length and time scales, the generation of numerical data from images, and the development of scaling laws or models linking the micro- and macrolevels.

Changes are needed in academia and education to cope with this trend, including broadening of the scientific base, acquaintance with new instrumental techniques, development of predictive models and emphasis on multidisciplinary work. Consumers are now the focus of all production chains, and they expect that food products will contribute to their health and well-being, with high quality and safety. The emphasis is shifting from processes to products, in particular, structured products that deliver taste, nutrition and wellness. There is a lot of science and engineering to put into food products!

Acknowledgements Research on food microstructure at the Biomaterials Laboratory has been financed by contracts from Nestle Research Centre (Switzerland) and grants from FONDECYT Project 1030339) and the Alexander von Humboldt Foundation (Germany).

References

Aguilera J.M., 2000, Microstructure and Food Product Engineering, *Food Technol*. **54**(11):6–58, 60, 62, 64, 66.

Aguilera J.M., 2005, Why Food Microstructure? *J. Food Eng*. **67**:3–11.

Aguilera, J.M., Mayor, G., and Michel M., 2004, Fat Migration in Chocolate: Diffusion or Capillary Flow in a Particulate Medium? *J. Food Sci*. **69**:R167–74.

Aguilera, J.M., and Stanley D.W., 1991, *Microstructural Principles of Food Processing and Engineering*, 1st ed. Elsevier Applied Science, London.

Aguilera, J.M., and Stanley D.W., 1999, *Microstructural Principles of Food Processing and Engineering,* 2nd ed. Aspen Publishers Inc., Gaithersburg.

Bauer W., 2004, The Importance of Engineering for Competitivity in the Food Industry. Plenary lecture, ICEF 9, Montpellier, France.

Cussler, E.L., and Wei J., 2003, Chemical Product Engineering. *AIChE J*.**49**:1072–1075.

Dickinson E., 2000, Rheology and Structure of Aggregated Particle Networks and Emulsions. *Proc, 2nd. Int. Symp. Food Rheology & Struct*., Zurich, pp. 3–12.

Fito P., 1994, Modelling of Vacuum Osmotic Dehydration of Food, *J. Food Eng*. **22**:313–328.

Fryer, P., and Pinschower K., 2000, The Materials Science Of Chocolate, *MRS Bulletin* **25**(12):25–29.

Fu, Y.C., Tong, C.H., and Lund D.B., 2003, Moisture Migration in Solid Food Matrices, *J. Food Sci*. **68**:2497–2503.

Gekas V., 1991, *Transport Phenomena of Foods and Biological Materials*, CRC Press, Boca Raton.

Hartel R.W., 2001, *Crystallization in Foods,* Aspen Publishers, Inc., Gaithersburg, MD.

Heertje I., 1993, Structure and Function of Food Products: A Review, *Food Struct*. **12**:343–364.

Hermansson A.M., 2000. Structure Engineering. *Proceedings of the 2nd International Symposium on Food Rheology and Structure,* Zurich, Switzerland, pp. 47–56.

Hill M., 2004, Product and Process Design for Structured Products. *AIChE J*., **50**:1656–1661.

Karel. M., 1970, Effect of Process Variables on Retention of Volatiles in Freeze Drying, *J. Food Sci*. **35**:444.

King J.C., 1971, *Freeze-Drying of Foods*. CRC Press, Cleveland.

Kokini, J.L., Cocero, A.M., Madeka, H., and de Graaf E., 1994, The Development of State Diagrams, *Trends Food Sci. & Technol*. **5**:281–288.

Leser, M.E., Michel, M., and Watzke H.J., 2003, "Food Goes Nano"—New Horizons for Food Structure Research, in: *Food Colloids. Biopolymers and Materials*, E. Dickinson and T. van Vliet (eds.), pp. 3–13. Royal Society of Chemistry, Cambridge.

Levine, H., and Slade L., 1986, A Polymer Physico-Chemical Approach to the Study of Commercial Starch Hydrolysis Products (SHPs), *Carbohydr. Polym*. **6**:213–244.

Marangoni A.G., 2005, *Fat Crystal Networks*, Marcel Dekker, New York.

Mellema, M., 2003, Mechanism and Reduction of Fat Uptake in Deep-Fat Fried Foods, *Trends Food Sci. & Technol*. **14**:364–373.

Moraru, C.I., Panchapakesan, C.P., Huang, Q., Takhistov, P., Liu, S., and Kokini J., 2003, Nanotechnology: A New Frontier in Food Science, *Food Technol*. **57**(12):24–29.

Narine, S.S., and Marangoni A.G., 1999, Relating Structure of Fat Crystal Networks to Mechanical Properties: A Review, *Food Res. Int*. **32**:227–248.

Norton, I.T., and Frith W.J., 2003, *Food Colloids. Biopolymers and Materials,* Royal Society of Chemistry, Cambridge. pp. 282–297.

Rey L. (ed.), 1966, *Advances in Freeze Drying*, Hermann, Paris.

Roos, Y., and Karel M., 1991, Applying State Diagrams to Food Processing and Development. *Food Technol*. **45**:66, 68–71, 107.

Russ, J.C., 2004, *Image Analysis of Food Microstructure*. Boca Raton: CRC Press.

Saguy, I.S., Marabi, A., and Wallach R., 2005, New Approach to Model Rehydration of Dry Food Particulates Utilizing Principles of Liquid Transport in Porous Media. *Trends Food Sci. & Technol*. **16**:495–506.

Saravacos, G.D., and Maroulis Z.B., 2001, *Transport Properties of Foods*, Marcel Dekker, Inc., New York. pp. 29–61.

Schubert, H., Ax, K., and Behrend O., 2003, Product Engineering of Dispersed Systems, *Trends Food Sci. & Technol*. **5**:289–293.

Singh, R.P. (ed.), 1958, *Fundamental Aspects of the Dehydration of Foodstuffs*. Society of Chemical Industry, London.

Slade, L., and Levine H., 1991,. Beyond Water Activity: Recent Advances Based on an Alternative Approach to the Assessment of Food Quality and Food Safety, *Crit. Rev. Food Sci. Nutr*. **30**:115–360.

Thijssen H.A.C., 1974, Freeze Concentration, in: *Advances in Preconcentration and Dehydration of 24 Foods*, A. Spicer (ed.), John Wiley and Sons, New York, pp. 114–119.

van der Linden E., 2000, Mesoscopic Physics and Functional Properties of Foods, Imperial College Press, Singapore, pp. 214–223.

Vaughan J. G., 1979, *Food Microscopy,* Academic Press, London.

Villadsen J., 1997, Putting Structure into Chemical Engineering, *Chem. Eng. Sci*. **17**:2857–2864.

Walstra P., 2002, *Physical Chemistry of Foods*. Marcel Dekker Inc., New York.

Windhab E.J., 1995, Rheology in Food Processing, in: *Physico-Chemical Aspects of Food Processing*, S.T. Beckett (ed.), Blackie Academic & Professional, York.

16
Image Processing Methods and Fractal Analysis for Quantitative Evaluation of Size, Shape, Structure and Microstructure in Food Materials

J. Chanona-Pérez, R. Quevedo, A.R. Jiménez Aparicio, C. Gumeta Chávez, J.A. Mendoza Pérez, G. Calderón Domínguez, L. Alamilla-Beltrán, and G.F. Gutiérrez-López

16.1. Introduction

In recent years, image analysis methods have been applied for quantitative evaluation of morphology, structure and microstructure of foodstuffs. Image processing techniques usually consist of five steps (Castleman, 1996; Pedreschi et al., 2004; Du and Sun, 2004), which are: 1) image capture, 2) pre-processing, 3) image segmentation, 4) feature extraction and 5) classification. In food engineering applications, some or all of these steps have been used to extract information from food images captured with different acquisition systems. The extracted information is useful to translate the food system complexity to numeric data that shall be analyzed to improve the understanding of structure-function relationships of complex systems, such as food and biological materials. On the other hand, fractal analysis has been successfully applied for quantitative evaluation of irregular surfaces and textures of biological materials (Quevedo et al. 2002; Chanona et al., 2003; Villalobos et. al, 2005), and also to characterize ruggedness and geometric complexities of different food particles, such as instant coffee, skim milk, potato starch powder, maltodextrin particles and others (Peleg and Normand, 1985; Barletta and Barbosa, 1993; Shafiur, 1997; Alamilla et al., 2005). The key to quantifying the irregularity of the contours and surfaces in food materials is to evaluate the apparent fractal dimension (FD) by extracting it from the images of structural and microstructural features. Results from fractal analysis are important in examining the architecture and structure-functionality properties of food products.

The objective of this contribution was to provide a brief description of diverse methods for image processing and fractal analysis of acquired data in our laboratory for quantitative evaluation of size, shape, structure and microstructure in different biological/food materials.

16.2. Methodology

Instant coffee (Nescafe-Nestle-Mexico) and maltodextrin (Arancia Corn Products-México) were chosen as food powder examples. Tissues from the *Agave atrovirens* Karw were cut transversely and longitudinally using a slicing device to obtain 3 mm thick slices. These pieces were used as a model for evaluating the changes in size, morphology and microstructure during convective drying of material. Cellular aggregates of *Beta vulgaris* were grown in shaking flasks and used as a biological model, and their morphological changes during growth were evaluated. A French bread slice was selected to evaluate the bread-crumb features in the central field of view (FOV) of the slice. In all the examples, a general methodology for image processing was conducted. Table 16.1 shows the different methods used during image processing and FD estimation.

Image processing was performed using the public domain program NIH ImageJ 1.34s (National Institute of Health, USA, available from: http://rsb.info.nhi.gov/ij/) combined with other commercial software, such as SigmaScan Image 1.20 and Sigma ScanPro 5 (Jandel Scientific Corp., USA). Several ImageJ codec or plug-ins were used to compute the FD and morphology features, and other software used for image analysis are indicated in Table 16.1.

16.3. Results And Discussion

Figure 16.1 presents a general diagram showing the basic steps of image processing, taking as example particles of commercial instant coffee. Extracted parameters from the binary images were area, perimeter, shape factor and FD evaluated with the relationship proposed by Olsen et al. (1993). Extracted parameters allowed us to obtain criteria for classification of food particles obtained or processed by different technologies. These morphological parameters, and especially the FD, may be useful to establish relationships with other physical properties such as rehydration and packing properties that are of importance in the control of quality and processing parameters during the production of agglomerates and powders. Packing and instant properties have a strong dependence with shape and roughness of the food powders.

The concept of the apparent fractal dimension can be used successfully to quantify the morphological characteristics of food particles (Shafiur, 1997; Peleg and Normand, 1985).

FD could be evaluated from the contours of food particles and agglomerates; theoretically, FD of a two-dimensional profile ranges from 1 to 2. Fractal value close to 1 indicates that the border of the analyzed object has smooth boundaries, and a value close to 2 indicates a high degree of tortuosity or roughness (Barletta and Barbosa, 1993). Consequently, FD values estimated from digital images of food powders allow characterization of changes of shape and roughness of materials during processing, such as those shown in Fig. 16.2, in which scanning electron

TABLE 16.1. Image processing and FD methods used for quantitative evaluation of size, shape, structure and microstructure in selected food materials

Material	Image capture	Pre-processing	Segmentation Processing	Geometric features extracted	FD method/software	References
Instant coffee particles	Light stereomicroscopy-CCD camera	Cropped, Filtered Images conversion (transfer) from RGB to grey level	Semiautomatic binarization with threshold tool	Area, Perimeter, Shape Factor, FD of particles obtained from the projected perimeter and area	FD = 2[ln(P/4)/ln(A)] ImageJ 1.34s	Olsen et al., 1993
Maltodextrin particles	Scanning electron microscopy (SEM)	Cropped	Manual	Mean particle size, FD of projected perimeter	Box counting/ Sigma Scan Image 1.20, Corel Photo Paint 11.6	Alamilla et al., 2005
Agave slices	Light stereomicroscopy and computer vision system	Image conversion from RGB to grey level	Semiautomatic binarization with threshold tool	FD of projected perimeter, FD texture	Box counting to contour and Scanning Differential Box counting (SDBC) to surfaces ImageJ 1.34s, Adobe Photo-Shop 7.0	Handen, 2006
Cellular aggregates	Light stereomicroscopy	Image conversion from RGB to grey level Contrast optimization	Manual	FD (ln P *vs* ln A), FD (ln L vs ln A)	SigmaScan Pro 5.0	Kenkel and Walker, 1996; Chakraborti et al., 2003
Bread slices	Computer vision system	Cropped and image conversion from RGB to gray level	Semiautomatic binarization with threshold tool and gray level histogram	FD of pores obtained from the projected perimeter and area, FD texture	FD = 2[ln(P/4)/ ln(A)], SDBC to surfaces ImageJ 1.34s, SigmaScan Pro 5.0	Olsen et al., 1993; Handen, 2006

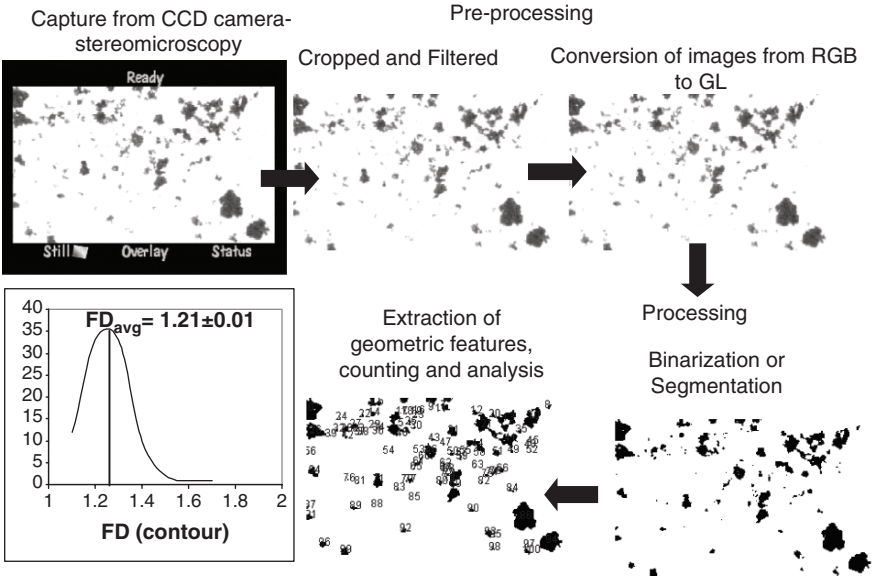

FIG. 16.1. Steps used to image processing of instant coffee particles from light stereomicroscopy images (30X) and average values for the FD of particles

microscopy (SEM) images of maltodextrin particles dried by spray drying under two different process conditions are shown. These figures were analyzed using image processing methodology and fractal analysis (Alamilla et al., 2005). According to these authors, when droplets are dried at low temperatures (110/74 °C), shrinkage is greater than samples observed at higher drying temperatures (170/ 145 °C).

This behavior could be associated with more drastic shrinkage and deformation mechanisms under these process conditions, causing the water diffusion in the material to be slower and allowing the deformation process in the particles to be more pronounced. Consequently, it was possible to observe a more drastic collapse and shrinking of particles when drops were dried at low temperatures. In Table 16.2 it can be observed that low drying temperatures generate smaller particles that are rougher and less spherical than when the drying proceeds under high temperatures. Image processing allows characterization of size, shape factor and FD of the particles under two different drying conditions. Also, it was evident that the fractal texture of the surface particles was smoother at low temperatures than when the process was performed at high temperatures.

Morphological parameters extracted from images and fractal analysis can be useful for establishing relationships among the process conditions and physical, microstructural, morphological and several other particles properties. Also, these

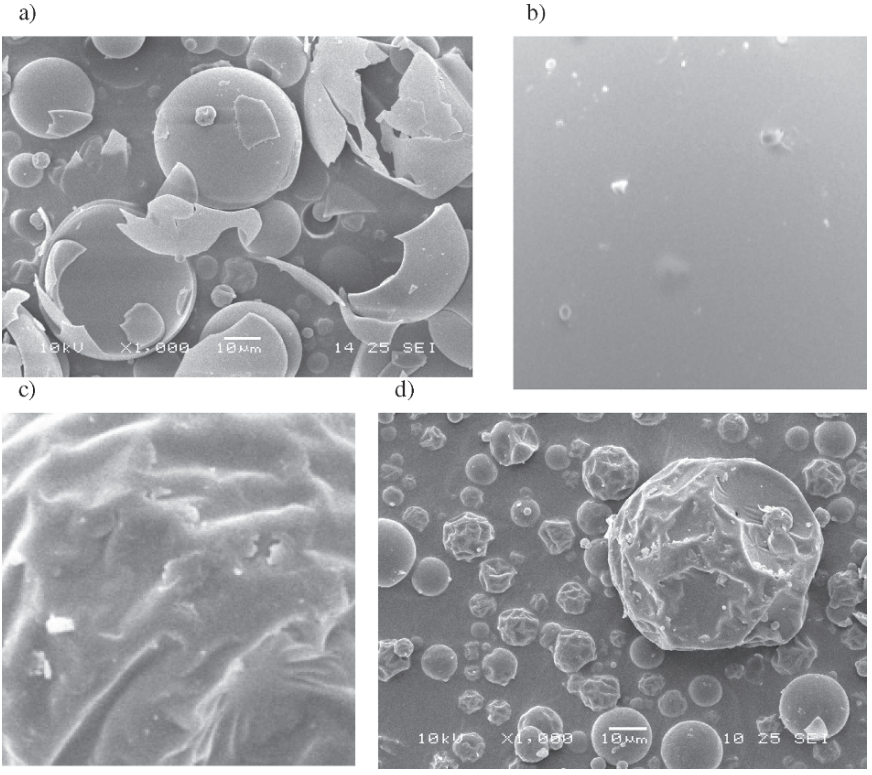

FIG.16.2. SEM images of maltodextin particles (1000X) and zooming (5000X) of their surface at two spray drying conditions (inlet/outlet temperatures) at 170/ 145 °C: a)-b), and at 110/74 °C: c)-d)

TABLE 16.2. Fractal and morphological parameters of maltodextin particles and their surface at two spray drying conditions

Drying Condition	Particle Size (mm)	FD (contour)	Shape Factor	FD (texture)
110/74 °C	11.87 ± 0.58	1.19 ± 0.004	0.81 ± 0.006	2.31 ± 0.016
170/145 °C	18.91 ± 1.24	1.15 ± 0.006	0.85 ± 0.006	2.14 ± 0.011

properties can be related with the instant properties of powders such as wetting, submerging, dispersing and dissolving. Relationships found among morphological and instant properties can help to improve the efficiency of the transformation process and quality properties of food particles obtained by spray drying.

Image analysis and FD concept also provide advantages for studying the shrinkage and deformation phenomena during the drying of vegetable tissues, such as the tissue obtained from long spiked leaves of the agave plant (*A. atrovirens* Karw). Due to its high amount of cellulose and lignin and the ability to grow in arid zones, this plant represents an attractive source for extraction of these important compounds for the paper and food industries (Idarraga et al., 1999).

Also, during the extraction process of cellulose and lignin by a non-conventional method (organosolve), a previous process of convective drying is applied because it has been proposed as playing an important role in extraction efficiency, since the drying conditions and the form of cutting the tissue can generate materials that present a denser microstructure and a higher grade of deformation when they are dehydrated. In Fig. 16.3 it can be observed that the longitudinal cut from tissue of *A. atrovirens* Karw presents a smaller shrinkage and deformation than the transversal cut of the same tissue. Consequently, FD values for contours from the superior and lateral views of lengthwise cut slices also present smaller FD values than the slices obtained by traversal cutting. A similar effect was observed for the fractal texture values of the slices.

In this kind of tissue, the evaluation of the shrink, deformation and microstructural changes during the drying process are important, because a drastic shrinkage and deformation can represent a barrier to solvent diffusion during the extraction process of cellulose and lignin. Consequently, this can cause a decrease in extraction efficiencies. Thus, the applications of image processing and fractal analysis for evaluating the changes of shape, size and microstructure throughout the drying process will allow us to obtain quantitative criteria for selecting operation conditions for processed biological materials in order to promote major efficiency in later processes.

Almost in the same context, another example of application for image and fractal analysis was performed in order to evaluate the changes during growth of cellular aggregates of *Beta vulgaris* in shaking flasks (Fig. 16.4a). The morphological

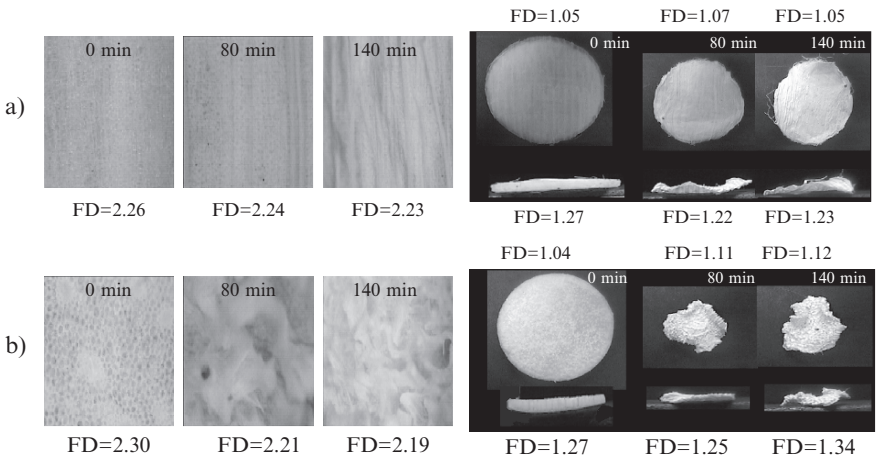

FIG. 16.3. Microstructure images from slices (lateral and superior side) of *A. atrovirens* Karw were taken with a light microscopy (10X) and captured with a computer vision system (CVS) at selected times of drying (drying conditions 3 m/s and 60 °C). a) Longitudinal cut and b) transversal cut. FD of texture and FD of contours are indicated next to the image

characterization can be evaluated by bilogarithmic relationships such as ln(Perimeter) vs. ln(Area) or ln(Area) vs. ln(major longitude). Bilogarithmic plots obtained from a set of aggregates allow us to obtain the fractal dimensions of perimeter and area, respectively. In the case of fractal dimension of landscape perimeters or a set of aggregates composed with perfectly square or Euclidian objects (perimeter:area low ratio) both examples will have a fractal dimension of the perimeter = 1, while those containing highly complex convoluted objects (perimeter:area high ratio) usually have fractal dimensions approaching 2.

In the case of fractal dimension for the area, landscapes with objects more branching (area:major longitude low ratio) will have a fractal dimension of the area = 1, because the set objects do not fill the two-dimensional Euclidian space efficiently. On the other hand, landscapes with objects less branching (area:major longitude high ratio) will have a fractal dimension of the area = 2, because the set objects do fill two-dimensional Euclidian space. Consequently, the FD of the perimeter indicates that as tortuosity of the perimeter and the FD of the area increase the density of the set of objects also increases. Figures 16.4b and 16.4c show the behavior of the FD values for the perimeter and area of the cellular aggregates of *Beta vulgaris*. During their growth, the FD values show an opposed behavior between the two different FD mentioned above. This indicates that when in an initial stage of the growth the agglomerated present an irregular perimeter (high values for FD of the perimeter) and when the growth proceeds, the empty places are filled by new cells, and the contour becomes smoother, providing low values for FD of the perimeter. The cycle repeats until the end of the growth kinetics (Fig. 16.4b). Inverse behavior was observed for FD values of the area. Fractal dimension concepts have allowed us to associate the FD values with the traditional stages of kinetic growth in these types of cells. Also, it has been possible to associate the values of FD with biomass generation and aggregate size; it has provided useful criteria for improving the production processes of these colorant cell producers

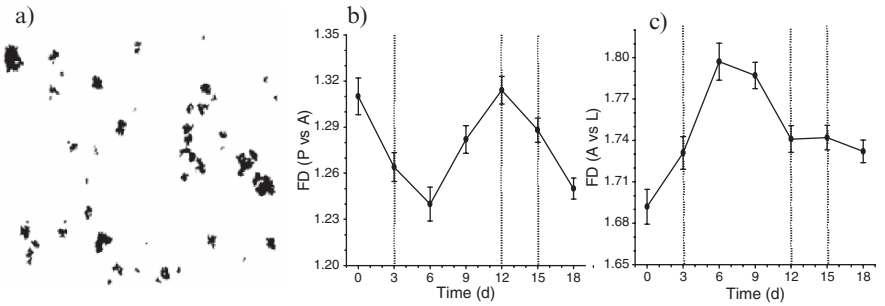

FIG. 16.4. Shows in A) Binary image of *Beta vulgaris* cellular aggregates at 7 days of growing in shaking flask; image was captured since light stereomicroscopy at 1X; B) FD change during growth of cellular aggregates obtained from the slope of ln(P) *vs*. ln (A) plot; C) FD change during growth of cellular aggregates obtained from the slope of ln(A) *vs*. ln (L) plot. Indicated values correspond to 1000 aggregates ± standard error

with proper applications for the cosmetic, food and pharmaceutical industries. As a last example, image analysis has been proposed for use in the breadmaking industry for quality control of bread crumbs in several bakery products (Sapirstein et al., 1994; Zghal et al., 1999; Crowley et al., 2000; Scanlon and Zghal, 2001; Zghal et al., 2001). On the other hand, research applying fractal geometry has been performed less frequently in these kinds of products (Riva and Fessas, 1999; Riva and Liviero, 2000; Scher and Hardy, 2002; Scher et al., 2004).

When analyzing bread crumbs by image analysis, the most critical aspect is the selection of the threshold method. Several algorithms have been applied, and the most reported ones are the Otsu method, isodata, k-means clustering and the manual method (Gonzalez-Barron and Butler, 2006). In this context, ImageJ offers different algorithms that allow performing the threshold of the bread crumb pores in a very simple way. Indeed, the most mentioned method for bread crumb is k-means clustering, because of its high efficiency for pore segmentation (Gonzalez-Barron and Butler, 2006). The obtained information from the image and fractal analysis allows evaluation of the quality of the bread crumbs and screening the effect of adding food additives, or the bakery procedure conditions. Figure 16.5 shows an example of a French bread crumb where the FD values for the crumb texture and the pore contour can be observed. These FDs were obtained from gray level and binary images, respectively. These data could complement studies on the bread making process and help in the evaluation of additives or other substance effects during the process.

16.4. Conclusion

Image processing and fractal geometry could be auxiliary tools for understanding and characterizing complex systems such as food and biological materials. The

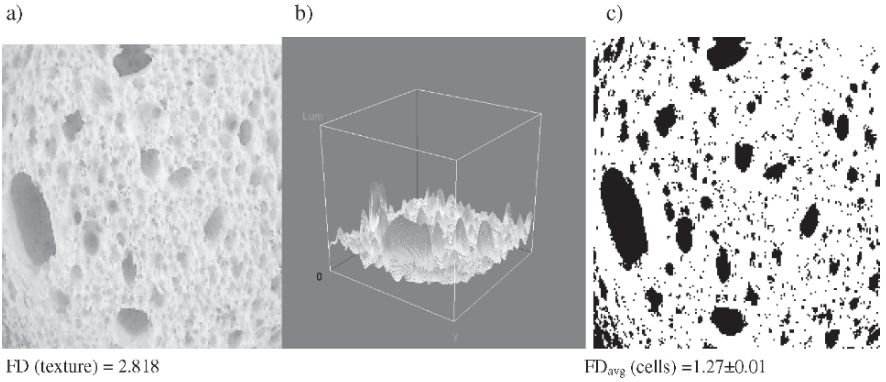

FIG. 16.5. a) Gray level image of French bread crumb and its corresponding FD texture value; b) surface intensity plots obtained from gray level image; c) Binary image obtained from gray level image and the corresponding FD of cells' average value

presented examples show the versatility of application of these tools and how they can be applied to evaluate form changes, size, structure and microstructure in processes and evaluation of food quality. On the other hand, fractal dimension concept offers important advantages for quantitative description of complex materials because it provides numeric data of irregular shape and complex texture of food materials. The obtained data extracted from image analysis and fractal geometry may provide valuable information to understand the role of structure with respect to product functionality. In consequence, these mathematical tools could supplement carrying out improvements in food processing.

Acknowledgements The authors acknowledge financial support from Instituto Politécnico Nacional. Grants: EDI, COFAA, COTEPABE, PIFI. Projects SIP-IPN: 20060370, 20060627 and 2006; CONACYT: 2004-C01-48061.

References

Alamilla, B.L, Chanona, P.J.J., Jiménez, A.A.R., and Gutiérrez L.G.F., 2005. Desciption Of Morphological Changes Of Particles Along Spray Drying, *J. Food Eng*. **67**:179–184.

Barletta, B.J., and Barbosa C.G.V., 1993, Fractal Analysis to Characterize Ruggedness Changes in Tapped Agglomerated Food Powders, *J. Food Sci*. **58**(5):1030–1035, 1046.

Castleman K.R., 1996, *Digital Image Processing*. Prentice Hall, Englewood Cliffs, pp. 667.

Chakraborti, R.K., Gardner, K.H., Atkinson J.F., and Van Benschoten J.E., 2003, Changes in Fractal Dimension During Aggregation, *Water Res*. **37**:873–883.

Chanona, P.J.J, Alamilla, B.L., Farrera, R.R.R., Quevedo, R, Aguilera, J.M., and Gutiérrez L.G.F., 2003, Description of the Convective Air Drying of a Food Model by Means of the Fractal Theory, *Food Sci. Technol. Int*. **9**(3):207–213.

Crowley, P. Grau, H., and Arendt E.K., 2000, Influence of Additives and Mixing Time on Crumb Grain Characteristics of Wheat Bread, *Cereal Chem.* **77**(3):370–375.

Du, C., and Sun D., 2004, Recent Developments in the Applications of Image Processing Techniques for Food Quality Evaluation, *Trends Food Sci. Technol*. **15**:230–249.

Gonzalez-Barron, U., and Butler F., 2006, A Comparison of Seven Thresholding Techniques with the K-Means Clustering Algorithm for Measurement of Bread-Crumb Features by Digital Image Analysis, *J. Food Eng*. **74**:268–278.

Handen P., 2006, Scanning Differential Box counting (SDBC) codec, version 1.0. Plug-in of ImageJ. (June 2006); http://rsb.info.nhi.gov/ij/.

Idarraga, G., Ramos, J., Zuñiga, V., Sahin, T., and Young R.A., 1999, Pulp and Paper from Blue Agave Waste From Tequila Production, *J. Agric. Food Chem*. **47**:4450–4455.

Kenkel, N.C., and Walker D.J., 1996, Fractals in the Biological Sciences. [On-line] (June 1, 2006): http://www.umanitoba.ca/faculties/science/botany/labs/ecology/fractals/fractal.html.

Olsen, E R, Ramsey, R.D., and Winn D.S., 1993, A Modified Fractal Dimension as a Measure of Landscape Diversity*, Photogramm. Eng. Rem. S*. **59**:1517–1520.

Pedreschi, F., Mery, D., Mendoza, F., and Aguilera, J.M., 2004, Classification of Potato Chips Using Pattern Recognition*, J. Food Sci*. **69**:E1–E7.

Peleg, M., and Normand M.D., 1985, Characterization of the Ruggedness of Instant Coffee Particles by Natural Fractals, *J. Food Sci*. **50**(3):829–831.

Quevedo, R., López, G.R., Aguilera, J.M., and Cadoche L., 2002, Description of Food Surfaces and Microstructural Changes Using Fractal Image Texture Analysis, *J. Food Eng*. **53**:361–371.

Riva, M., and Fessas D., 1999, New Physical Approach to Sliced Toasted Bread Characterization, *Ind. Aliment.-Italy* **38**(381):521–526.

Riva, M., and Liviero S., 2000, Image Analysis Approach to Characterize the Bread Cooking Kinetic, *Ind. Aliment.-Italy* **39**(395):593–660.

Sapirstein, H.D., Roller, R., and Bushuk W., 1994, Instrumental Measurement of Bread Crumb Grain by Digital Image Analysis, *Cereal Chem*. **71**(4):383–391.

Scanlon, M.G., and Zghal M.C., 2001, Bread Properties and Crumb Structure, *Food Res. Int*. **34**:841–864.

Scher, J., and Hardy J., 2002, A New Approach of Sensorial Evaluation of Cooked Cereal Foods: Fractal Analysis of Reological Data, *EPJ Applied Physic*, **20**(2):159–163.

Scher, J., Berton, B., and Hardy J., 2004, Mechanical and Sensory Characterization of Died Bread-Crumbs: Application of Fractal Concept, *Sci. Aliment*. **24**(4):279–287.

Shafiur R.M., 1997, Physical Meaning and Interpretation of Fractal Dimensions of Fine Particles Measured by Different Methods, *J. Food Eng*. **32**:447–456.

Villalobos, R. Chanona, J., Hernández, P., Gutiérrez, G., and Chiralt A., 2005, Gloss and Transparency of Hidroxypropyl Methylcellulose Films Containing Surfactants as Affected by Their Microstructure, *Food Hydrocollid*. **19**:53–61

Zghal, M.C., Scanlon, M.G., and Sapirstein H.D., 2001, Effects of Flour Strength, Baking Absorption, and Processing Conditions on the Structure and Mechanical Properties of Bread Crumb, *Cereal Chem*. **78**(1):1–7.

Zghal, M.C., Scanlon, M. G., and Sapirstein H.D., 1999, Prediction of Bread Crumb Density by Digital Image Analysis, *Cereal Chem*. **75**(5):734–742.

17
Scanning Electron Microscopy of Thermo-Sonicated *Listeria Innocua* Cells

D. Bermúdez and G.V. Barbosa-Cánovas

17.1. Abstract

Listeria innocua cell structure was studied after conducting thermo-sonication treatments (24 kHz, 400 W, 120 µm, 63°C) in order to establish a possible mechanism of cell inactivation. Raw and whole cow's milk was used as the medium of treatment, and samples were analyzed after 10 min of thermo-sonication. Scanning electron microscopy (SEM) was used to identify possible injuries in cells after the treatment. The control sample showed complete integrity and non-disruption of the cell membrane, the characteristic rod shape of *Listeria* cells could be seen, and a smooth surface was clearly observable. After 10 min of sonication, the lethal effects of caviation were observed as the presence of small holes in the cell surface, perforations outside the cell wall, surface granules and disruption of the cell membrane. These preliminary effects are responsible for cell inactivation during the first minutes of treatment, and they increase the lethality of the sonication with longer treatment times.

17.2. Introduction

Listeria monocytogenes was discovered more than 90 years ago, and it has been recognized as one of the most important food-borne pathogenic microorganisms. Some of its characteristics are its small size (0.5–2.0 µm in length and 0.4–0.5 µm in diameter); it is Gram-positive, facultative anaerobic, non-spore forming and has a coccid rod shape (Martin and Fisher, 2000); and it is able to survive in a wide range of temperatures (1°C to 45°C) and pH values (4.1–9.6) (Jay, 1992). This microorganism has become one of the most important emerging pathogens in the food industry because of the feasibility of growth under very different and wide conditions. Outbreaks related with the presence of *Listeria monocytogenes* are associated with salads, pasteurized milk, raw fish, oysters, rice salad, Mexican-style soft cheese, and other cheeses (Martin and Fisher, 2000), raw milk, pork, raw poultry, ground beef and some vegetables (Jay, 1992). Some recognized

species of *Listeria* belong to the pathogenic variety, while others, such as *Listeria innocua*, show many of the characteristics and resistance of *Listeria monocytogenes*, but without the pathogenic behavior; for that reason, it is often used in research as a surrogate for the pathogen.

The so-called emerging technologies are looking into alternatives to conventional thermal processing approaches, and these new technologies include the utilization of nonthermal or "new" thermal stress factors, as well as sound combinations of preservation strategies. It is expected that food products processed by these emerging technologies will have a very reasonable cost and better quality attributes than those attained by conventional ones. Pressure, electricity, sound and light have shown inactivation effects in microorganisms and enzymes when applied alone or in combination with other preservation factors. Ultrasound has two ranges of application in the food industry: high frequency, which is used as a non-invasive technique focused mainly on quality control issues, and low frequency or power ultrasound, which has the capacity to disrupt cells and promote chemical reactions. Power ultrasound is based on the propagation of sound waves through a liquid medium generating a physical phenomenon called cavitation. This phenomenon is related to the production of small bubbles generated by compression and rarefaction cycles in the medium, and it is considered to be one the main reasons for the breakage of the cell membrane. During cavitation bubbles collapse and high pressures and temperatures are produced, and cell wall structures are disrupted or particles are removed from surfaces (Earnshaw et al., 1995). Despite that, there have been several inactivation reports (Raso et al., 1998; Pagán et al., 1999; Mañas et al., 2000; Cabeza et al., 2004) that have considered ultrasound in microbiology and enzymatic activity, in which the main mechanism of cell inactivation has only been suggested (Earnshaw et al., 1995), but not clarified.

The objective of this work was to study the microstructure of *Listeria innocua* cells following thermo-ultrasonic treatments in order to establish a possible mechanism of cell inactivation using scanning electron microscopy.

17.3. Materials and Methods

17.3.1. Milk Sample

Raw whole milk was obtained from Washington State University's Creamery. Milk was kept in refrigeration at 4°C until it was used. Inoculation of *Listeria innocua* was carried out in a ratio of 1:100 (Inoculum:milk; V/V). A control sample (15 ml) was taken and poured into a disposable 15 ml sterile plastic conical test tube.

17.3.2. Listeria innocua Cells

Two ml of unfrozen *Listeria innocua* cells (ATCC 51742) (one ml of microorganism grown in the early stationary phase plus one ml of sterile glycerol) stored at −21°C were added to 100 ml tryptic soy broth (TSB) with 0.6% yeast extract

(TSBYE). The microorganism was kept in a bath shaker at 37°C and 218 rpm until it reached the early stationary phase, after approximately 11 h.

17.3.3. Thermo-Sonication Treatment

A sterile double-walled beaker (500 ml), 8 cm in diameter and 13.5 cm in depth, was used as a reactor. An ultrasonic processor manufactured by Hielscher USA, Inc. (Ringwood, NJ) model UP400S (400 W, 24 kHz, 120 microns) with a 22 mm diameter probe was used at the maximum amplitude (100%). Raw and whole milk (500 ml) was used as the medium of treatment. Temperature was set up and kept constant (63 ± 0.5°C) via a refrigerated bath (VWR Scientific Model 1166, Niles, IL). A thermocouple was used to monitor the temperature; when it was stable, the inoculum was added to the milk and a magnetic stirrer was used to make sure that the treatment was homogeneous throughout the treatment time. Samples were taken after 10 and 30 min of thermo-sonication and transferred to disposable 15 ml sterile plastic conical test tubes.

17.3.4. Scanning Electron Microscopy (SEM)

Inoculated raw milk with *Listeria* cells and thermo-sonicated milk samples were centrifuged at 1500 rpm for 5 min at 10°C. The supernatant was discarded and the cells were re-suspended in 15 ml of sterile TSBYE. Centrifugation was performed again. The supernatant was discarded and the cells were transferred with a sterile Pasteur pipette to disposable 1.5 ml sterile plastic microcentrifuge tubes. Fixation was made with 2% glutaraldehyde, 2% paraformaldehyde in 0.1 M phosphate buffer (pH 7.2) at 4°C for 24 h, followed by 2% osmium tetroxide in cacodylate buffer 0.1 M at 4°C for 24 h. Dehydration was carried out with serial dilution of ethanol solution and afterwards HMDS (hexamethyldisilazane) drying was performed. Samples were mounted in aluminum stubs, and gold plating was used as a final step. Samples were analyzed with a scanning electron microscope (Hitachi S-570, Tokyo, Japan) at 20 KV at the Electron Microscopy Center at Washington State University (Pullman, WA).

17.4. Results and Discussion

In Fig. 17.1, the control sample showing intact cells of *Listeria innocua* is shown. These cells were inoculated in raw whole milk and processed to be observed under SEM. The characteristic rod-shape of these bacteria and their size, as described by Martin and Fisher (2000), are shown. The texture of the surface looks smooth, and the continuity of the cell membrane is clear in each individual cell. No effect that could suggest cell injuries is observed.

In Fig. 17.2, cells exposed to thermo-sonication treatments are shown. All of the cells in this picture have visible injuries because of cavitation. The cell at the top of the image has a couple of orifices along the cell wall, creating the possibility of

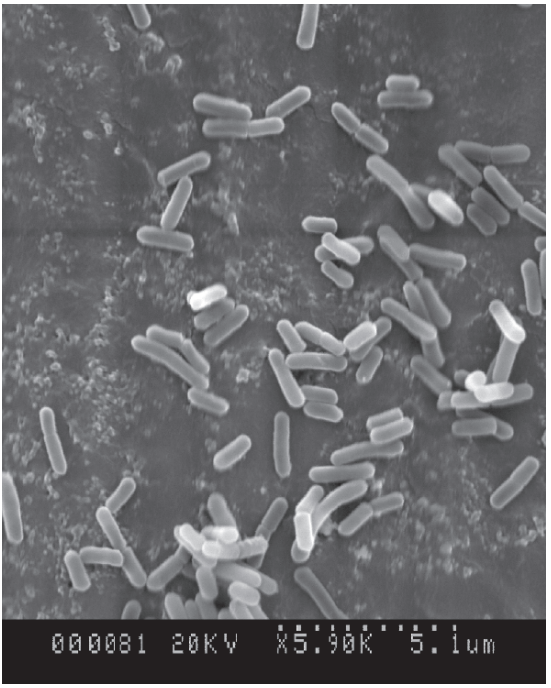

FIG. 17.1. *Listeria innocua* cells without treatment (control sample) inoculated in raw whole milk. 20 kV, magnification 5.90 K and 5.1 µm

leakage of cytoplasmatic material to the environment and allowing the interchange of material inside the cell. In the left corner of the same figure, three cells show similar effects; two present surface granules, and the third has a discontinuity of the cell wall. All these effects could be explained on the basis of cavitation theory. Cavitation takes place when sound waves across a liquid medium, and thousands of bubbles or cavities are generated inside the medium. But caviation could be grouped into two different types, depending on the physical effects that are generated in the liquid. According to Earnshaw et al. (1995) cavitation can be classified as stable or transient. During stable cavitation, the presence of small bubbles dissolved in the liquid is observed, and the force generated in the medium is caused by the formation of strong eddies that generate micro-currents; this physical phenomenon is called micro-streaming. Explosions are not produced in this cavi-tation, and the main lethal effect could be the force that rubs the surface and damages the cell membrane. This effect of stable cavitation is observed in the presence of small holes in the cells; micro-streaming causes a friction effect in the surface, breaking down the cell wall and producing orifices. But the effects of stable cavitation are not isolated from transient cavitation. Both mechanisms take place at the same time, and the lethal effect is the combination of both.

Transient cavitation could be considered more active, lethal and with stronger effects. During transient cavitation, one of the main effects is the presence of

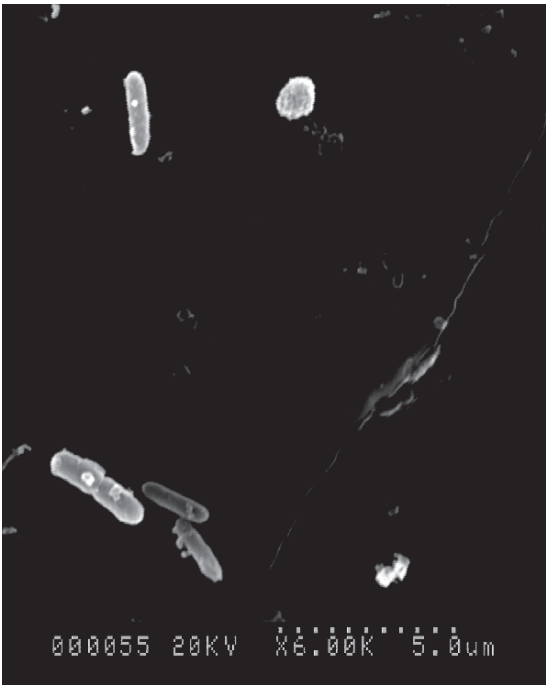

FIG. 17.2. *Listeria innocua* cells after 10 min of thermo-sonication treatment (63°C and 120 μm) showing perforation, surface granules and disruption of the cell membrane 20 kV, magnification 6.00 K and 5.0 μm

explosions. The collapse of bubbles is produced in the medium due to rapid change in the bubble size; the intensity of this phenomenon is variable. One of the characteristics of this cavitation is the increase of temperature and pressure generated by the collapse of bubbles. Pressure inside the medium could be as high as 100 MPa, and the temperature could rise up to 5000 K. According to Earnshaw et al. (1995), tem-perature and pressure affect the cells and remove particles from the surface. This effect is observed in one of the cells in Fig. 17.2, which shows the presence of granules on the surface. These granules could come from the same cell, because the material that was removed from the site showing perforations could be moved to another part of the cell and be present as a granule; otherwise, this material could come from other damaged cells.

In Fig. 17.3, a closer view of a single *Listeria* cell is shown. This picture shows the cell at a magnification higher than 21 K, and the damage in the upper left corner is readily observed. The cell membrane is disrupted and broken down, with the consequent loss of cytoplasmatic material. Pitting on the cell surface can also be observed. Besides the physical effects of cavitation, some chemical effects take place under sonication. One of the most important effects is the sonolysis of water, which is related to the separation of the components of water molecules in free radicals like OH^- and H^+. Tsukamoto et al. (2004a; 2004b) mention

FIG. 17.3. Closer view of *Listeria innocua* cell after 10 min of thermo-sonciation (63 °C and 120 μm) showing the disruption of the cell wall in the upper left corner. 20 kV, magnification 21.9 K and 1.37 μm

that these free radicals attack the cell membrane, producing a primary biocidal effect. After the recombination of free radicals in the medium, the production of oxidants is generated that is called the secondary biocidal effect. Thus, another factor that could promote microbial inactivation is the presence of free radicals in the medium freely entering into the cells through the perforations generated in the membrane.

In Fig. 17.4, more damaged cells are shown with similar characteristics in the surface, that is, the presence of perforations generated by the physical effects of cavitation. This research was conducted to establish some of the possible effects of thermo-sonication in cells that are responsible for microbial inactivation. On the basis of these images, the effects can be separated into two groups according to the type of cavitation. First, the effects generated by the friction of the bubbles generated by stable cavitation which causes an abrasive effect in the membrane and break-down of the cell membrane can be seen as disrupted membranes and perforations outside the cell wall.

The second event, which could be classified as more violent, is generated by transient cavitation, with explosions generated and important increases of temperature

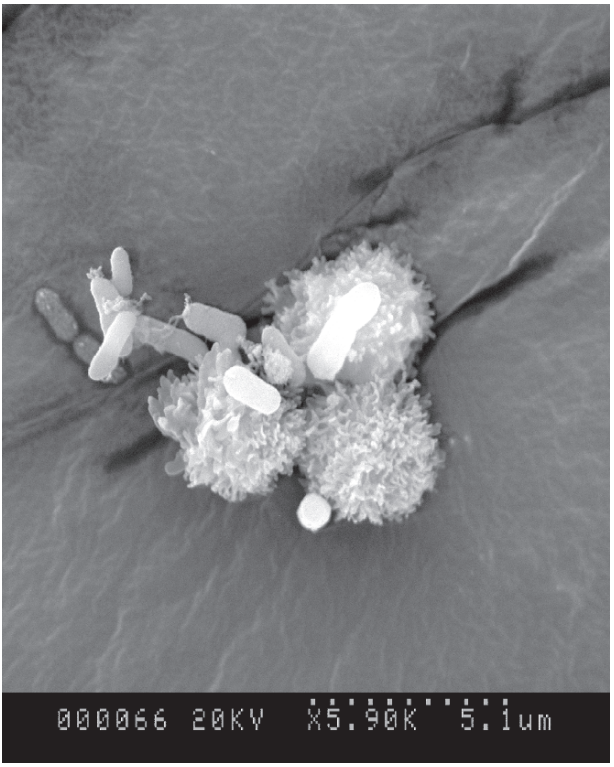

FIG. 17.4. *Listeria innocua* cells after 10 min of thermo-sonication treatment (63°C and 120 μm) showing pitting outside the cell wall. 20 kV, magnification 5.90 K and 5.1 μm

and pressure that attack the cells. Those effects are responsible for removing cellular material from the surfaces and for generating sound waves to move the material through the medium. These effects could be assigned as the main physical damages in cells after sonication, although it is important to highlight that these cells represent the injured microorganisms after 10 min of treatment, suggesting higher damage with longer times. Results after 10 min of thermo-sonication under the same conditions used in this work showed 5-log reduction of *Listeria* cells in raw whole milk (Bermúdez-Aguirre et al., 2005); for that reason, it can be assumed in this work that some of the cells shown in the different images represent death cells. If treatment times are longer than 10 min, the cells could probably be broken in several pieces because of more intense cavitation.

17.5. Conclusions

This study to describe a possible mechanism of inactivation of *Listeria* cells under thermo-sonication showed that the physical damages generated by cavitation

lead to different representations, such as perforations or orifices in the cell wall, surface granules, cell wall deformation and cell membrane breakage. These cells were exposed to very hard conditions of ultrasound for 10 min. Longer times would generate more injuries in the cell. Another lethal factor that could help in cell inactivation is the production of free radicals due to the sonolysis of water.

References

Bermúdez-Aguirre, D., Mobbs, T., Versteeg, K., and Barbosa-Cánovas G.V., 2005, Inactivation of *Listeria innocua* by Ultrasound of Low Frequency in Raw Whole Milk, in: *2005 IFT Annual Meeting Book of Abstracts*. Institute of Food Technologists, New Orleans, 16–20.

Cabeza, M.C., Ordóñez, J.A., Cambero, I., De la Hoz, L., and García M.L., 2004, Effect of Thermoultrasonication on *Salmonella Enterica Serovar Enteridits* in Distilled Water And Intact Shell Eggs. *J. Food Protect*. **67** (9):1886–1891.

Earnshaw, R.G., Appleyard, J., and Hurst R.M., 1995, Understanding Physical Inactivation Processes: Combined Preservation Opportunities Using Heat, Ultrasound and Pressure, *Int. J. App. Microbiol*. **28**:197–219.

Jay J., 1992, *Modern Food Microbiology*. 4th ed., Van Nostrand Reinhold, New York.

Mañas, P., Pagán, R., and Raso J., 2000, Predicting the Lethal Effect of Ultrasonic Waves Under Pressure Treatments on *Listeria monocytogenes* ATCC 15313 by Power Measurements. *J. Food Sci*. **65** (4):663–667.

Martin, S.E., and Fisher C.W., 2000, *Listeria monocytogenes*, in: *Encyclopedia of Food Microbiology*, R.K. Robinson, C.A. Batt and P.D. Patel (eds.), Academic Press, Great Britain, Vol. 2, pp. 1228.

Pagán, R., Mañas, P., Alvarez, I., and Condón S., 1999, Resistance Of *Listeria monocytogenes* to Ultrasonic Waves Under Pressure at Sublethal (Manosonication) and Lethal (Manothermosonication) Temperatures. *Food Microbiol*. **16**:139–148.

Raso, J., Pagán, R., Condón, S., and Sala F.J., 1998, Influence of Temperature and Pressure on the Lethality of Ultrasound. *Appl. Environ. Microb*. **64** (2):465–471.

Tsukamoto, I., Constantinoiu, E., Furuta, M., Nishimura, R., and Maeda Y., 2004a, Inactivation effect of Sonication and Chlorination on *Saccharomyces cerevisiae*. Calorimetric Analysis. *Ultrason. Sonochem*. **11**:167–172.

Tsukamoto, I., Constantinoiu, E., Furuta, M., Nishimura, R., and Maeda Y., 2004b, Inactivation of *Saccharomyces cerevisiae* by Ultrasonic Irradiation. *Ultrason. Sonochem*. **11**:61–65.

18
Sorption Properties of Dehydrated Model Systems and Their Relationship to the Rate of Non-Enzymatic Browning

N.C. Acevedo, C. Schebor, and M. del P. Buera

18.1. Introduction

The non-enzymatic browning (NEB) reaction is one of the most important chemical reactions that occur in foods during heating and storage. The NEB rate is known to be affected by physico-chemical factors such as concentration and the chemical nature of the reactants, pH, relative humidity, temperature, and time of heating (Labuza and Baisier, 1992). In dehydrated systems, NEB is a diffusion limited reaction, due to mobility restrictions of the reactants; therefore, it can also be affected by the glass transition (Buera and Karel, 1995). Although there are many ways in which water can influence the kinetics of the reaction, some of these influences have been neglected. It is also important to note that water, being a product of the NEB reaction, acts as an inhibitor (Acevedo et al., 2004; 2006). Thus, the purpose of the present work was to analyze the combined effects of several water–solids interactions and the structural properties of model systems on the NEB rate, and the counteracting effects of water as an inhibitor of the browning reaction and its compromise with the solid matrix.

18.2. Methodology

The following matrices were employed: polyvinylpyrrolydone (PVP, MW: 34 000) obtained from ISP Technologies, Inc. (Wayne, NJ); trehalose and a mixture 2:1 (in weight) of trehalose obtained from Hayashibara Co. Ltd. (Okayama, Japan); and gelatinized wheat starch (obtained from Sigma Chemical Co., St. Louis, USA). Wheat starch was previously gelatinized by heating an aqueous suspension for 15 min at 80°C. Samples were prepared by freeze-drying aqueous solutions of the corresponding matrices in phosphate buffer 0.175 M, pH 6, containing 15% (w/w) of the matrix material and the browning reactants, glycine and glucose, both of 0.5% on a solid basis. Glycine and glucose were analytical grade (obtained from Merck Darmstadt, Germany and Andrea San Fernando, Argentina, respectively). Aliquots of 1 ml of each solution were placed in 3 ml

glass vials and frozen at −20°C for 24 h. The freeze-drying process lasted 48 h. A Heto-Holten A/s cooling trap model CT110 freeze drier (Heto Lab Equipment, Denmark) was used; it was operated at −110°C, at a chamber pressure of 4.10^{-4} mbar. After freeze-drying, the samples were equilibrated over saturated salt solutions (in a range of 11–75% R.H.) in vacuum desiccators for 15 days to obtain the desired water contents (Greenspan, 1977).

The water content was determined by difference in weight before and after vacuum drying over magnesium perchlorate at 70 °C for 48 h. After equilibration, the vials were hermetically sealed and placed in forced air ovens at 70 °C ± 1°C. The model systems were reconstituted to their original volume. Browning was determined by measuring absorbance at 445 nm.

Thermal transitions were determined by differential scanning calorimetry (DSC; onset values) using a DSC 822^e Mettler Toledo (Schwerzenbach, Switzerland).

18.3. Results and Discussion

Figures 18.1 and 18.2 show the water sorption isotherm at 20°C (solid line) and the NEB rate at 70°C (dotted line) as a function of water activity (a_w) for polymeric and trehalose containing systems, respectively. The water sorption isotherms were adjusted with the GAB model (van den Berg and Bruin, 1981) and two important zones were identified: the monolayer values (m_0) and the water activity above which water incipiently manifests solvent properties (*I*). The *I* value was obtained from the second inflection point of the sorption isotherm. The maximum NEB rate in the PVP system was observed at a_w 0.33 (Fig. 18.1a, gray zone). A maximum NEB rate at a_w 0.33 was also reported for PVP systems of MW 1 200 000 (Acevedo et al., 2004), MW 40 000 (Bell, 1996) and MW 24 000 (Buera and Karel, 1995). It can be observed that in this system the maximum NEB rate occurs at a water content close to the m_0 value. Table 18.1 shows the glass transition temperatures (T_g) values corresponding to all of the analyzed systems in a wide range of a_w. The presence of Maillard reagents and buffer affected the T_g values; thus, they were lower than those reported in the literature for the pure PVP and trehalose matrices. The T_g value for the PVP systems at a_w 0.33 (Table 18.1) was close to the storage temperature. Above a_w 0.33, the PVP system in the supercooled state readily collapsed, and the NEB rate decreased. According to White and Bell (1999), the decrease in NEB rate can be attributed in part to the structural collapse of the samples, which may cause elimination of preferential sites for the reaction.

In the gelatinized starch system (Fig. 18.1b), the maximum NEB rate was located at a_w 0.52 in the supercooled state (Table 18.1), and was also close to the monolayer value. The NEB rate values, however, were about one order lower than those observed for the PVP systems (Fig. 18.1a). These results suggest that the nature of the polymeric matrix strongly affects the development of the browning reaction and the specific influence of water. Figure 18.1c shows the behavior of a mixture of PVP and gelatinized starch (2:1 ratio). The maximum NEB rate was

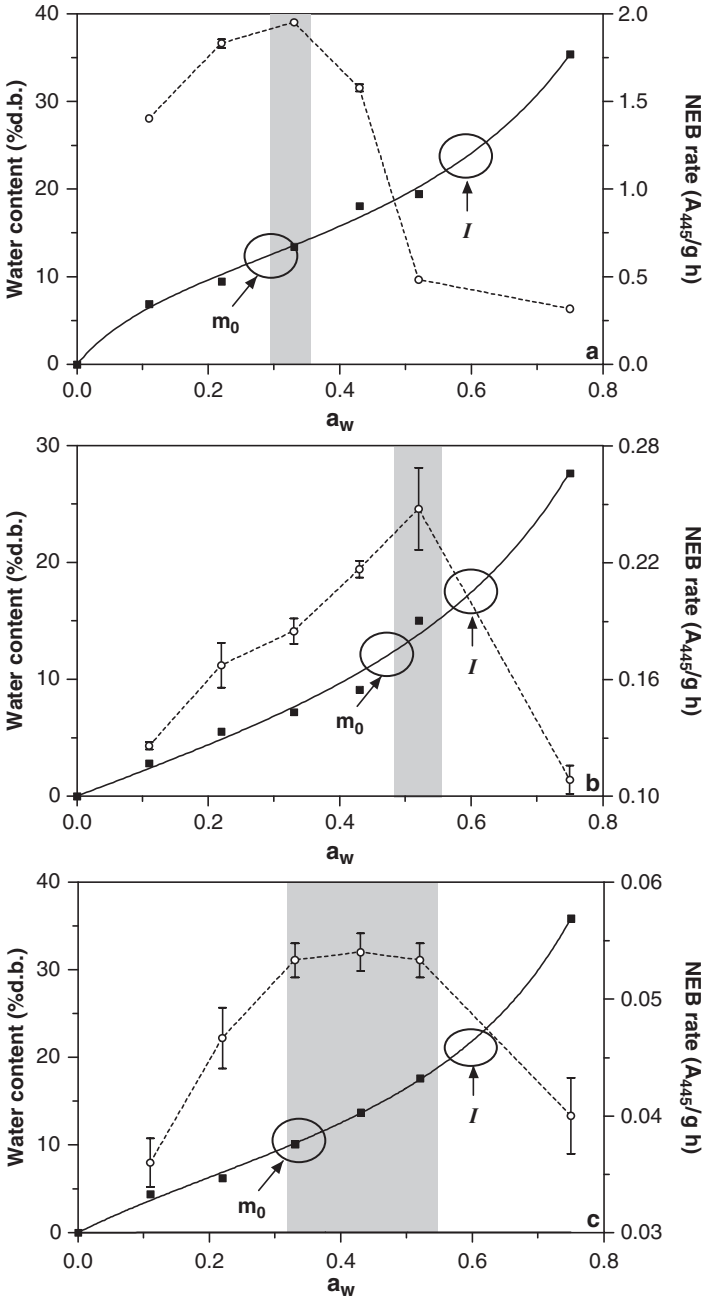

FIG. 18.1. Water sorption isotherm at 20 °C (left axis, solid line) and NEB rate (70 °C) versus a_w (right axis, dotted line) for PVP (a), gelatinized starch (b), and PVP-gelatinized starch 2:1 (c). The maximum NEB rate is indicated by a gray zone. The m_0 and *I* values are indicated as circles on the isotherm curves

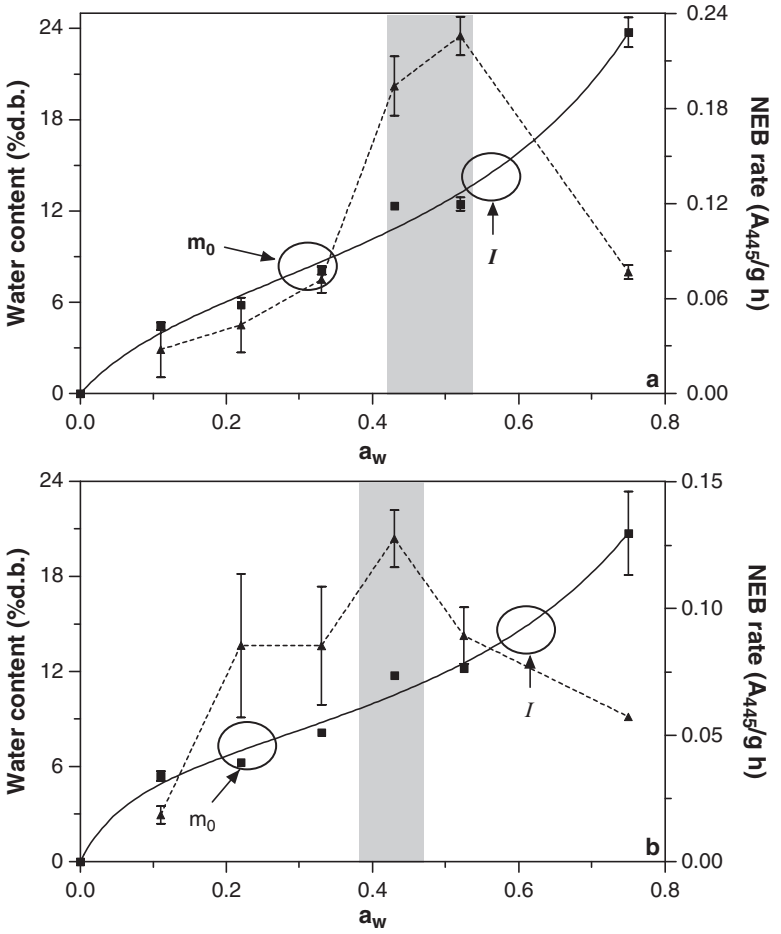

FIG. 18.2. Water sorption isotherm at 20 °C (left axis, solid line) and NEB rate (70 °C) versus a_w (right axis, dotted line) for trehalose (a), and trehalose-gelatinized starch 2:1 (b). The maximum NEB rate is indicated by a gray zone. The m_0 and *I* values are indicated as circles on the isotherm curves

observed in a range between a_w 0.33 and 0.52, which corresponds to the two a_w values for the maximum rates for each individual matrix. The PVP-starch matrix manifested structural collapse at and above a_w 0.52, showing a much stable structure than the PVP system, which collapsed at a_w 0.33.

The NEB rate values in the mixture were at least five orders lower than those for the individual components, suggesting that this reaction is less favored in the mixture, probably due to mobility restrictions or water availability.

For the starch containing matrices (Fig.18.1b and 18.1c), the decrease in NEB rate occurs at a_w values at which the solvent properties of water start to increase (indicated as *I* values). For the PVP system, however, the NEB rate decreased at

TABLE 18.1. Glass transition temperatures for model systems at different a_w values. CR: crystallized system

	Glass Transition Temperature (T_g)				
a_w	PVP	Starch	PVP/Starch	Trehalose	Trehalose/Starch
0.11	96	104	95	43	28
0.22	80	–	84	38	23
0.33	64	58	67	12	13
0.43	47	44	41	CR	−11
0.52	42	42	36	CR	−12
0.75	−7	−4	−11	CR	−44

a_w values lower than the *I* value. This could be due, on one hand, to the fact that the browning development was noticeably higher for the PVP systems, producing a high amount of water that could inhibit browning as a product of the reaction. On the other hand, the multilayer of water present in the PVP system may not be attached so strongly to the matrix, again rendering available water for the inhibition of the reaction.

The trehalose system (Fig. 18.2a) showed a maximum NEB rate between a_w 0.43 and 0.52, above the monolayer value. At this a_w range, trehalose was completely crystallized (Table 18.1). The decrease in NEB rate occurred in the presence of water available as a solvent, as indicated by the *I* value in the isotherm. The maximum NEB rate for the trehalose-gelatinized starch system was observed at a_w 0.43, well above the monolayer value, and in the supercooled state (Fig. 18.2b). The addition of gelatinized starch to the trehalose matrix reduced the maximum rate values and delayed sugar crystallization (Table 18.1).

18.4. Conclusions

The location of the maximum NEB rate on the a_w scale strongly depended on the type of system. In the case of trehalose, it could be related to the crystallization of sugar. Upon crystallization, the reagents could concentrate in the non-crystalline region of the matrix, increasing the reaction rate. The type of system also affected the NEB rate values along the a_w scale. The addition of gelatinized starch affected NEB kinetics of the polymeric and sugar systems analyzed. The presence of starch reduced NEB rates in the mixtures, modified the location of the maximum NEB rate in the a_w scale, and delayed structural collapse and sugar crystallization. The NEB rate in the a_w scale could be related to the water sorption properties of the systems, described in this work by m_0 and *I*: the maximum NEB rate always occurred close to (at or above) the m_0 value, and the rate dramatically decreased after the second inflection point of the isotherm, when the solvent properties of water were incipiently developing. These results reinforce the highly inhibitory character of water on the NEB reaction and suggest that the water sorption characteristics of the systems has information on water-solids interactions which, besides thermal properties and structural characteristics, can predict a_w for the maximum NEB rate.

Acknowledgements The authors acknowledge financial support from Universidad de Buenos Aires (UBACYT X226), ANPCYT (PICT 20545), CONICET (PIP 3066) and CONICET (PIP 02734).

References

Acevedo, N.C., Schebor, C., and Buera M.P., 2004, Prediction of The Relative Humidity for the Maximum Rate of Non-Enzymatic Browning in Food Systems, *Res. Adv. Food Sci*. **4**:2004.

Acevedo, N.C., Schebor, C., and Buera M.P., 2006, Water-Solids Interactions, Matrix Structural Properties and The Rate of Non-Enzymatic Browning, *J. Food Eng*. **77**:1108.

Bell, L., 1996, Kinetics of Non-Enzymatic Browning in Amorphous Solid Systems: Distinguishing the Effects of Water Activity and the Glass Transition, *Food Res. Int*. **28**:591.

Buera, M.P., and Karel M., 1995, Effect of Physical Changes on the Rates of Nonenzymic Browning and Related Reactions, *Food Chem*. **52**:167.

Greenspan L., 1977, Humidity Fixed Points of Binary Saturated Aqueous Solution, *J. Res. Nat. Bureau Stand. – A – Phys. Chem*. **81**:89.

Labuza, T., and Baisier, W.M., 1992, The Kinetics of Nonenzymatic Browning, in: *Physical Chemistry of Foods,* H. Schwartzberg and R. Hartel (eds.), Marcel Dekker, M., New York, pp. 595–649.

van den Berg, C., and Bruin S., 1981, Water Activity and Its Estimation in Food Systems Theoretical Aspects, in: *Water Activity Influences on Food Quality,* L.B. Rockland, and G.E. Stewart (eds.), Academic Press, New York, pp. 185.

White, K., and Bell L., 1999, Glucosa Loss and Maillard Browning in Solids as Affected by Porosity and Collapse, *J. Food Sci*. **64**:1010.

19
Drying of Porous Materials: Experiments and Modelling at Pore Level

L.A. Segura

19.1. Introduction

Drying of porous materials is important in the processing industry, mainly in food manufacturing. The classical drying theory has been widely studied (Barbosa-Cánovas and Vega-Mercado, 1996). This approach is based on experimental determination of the effective diffusion coefficients as a function of water saturation. A different approach is based on the study of drying mechanisms at pore level (Segura and Toledo, 2005a; Segura and Toledo, 2005b; Laurindo and Prat, 1998). Provided pore geometry, pore topology and wall composition of the porous medium, these coefficients can be predicted. In this work we studied isothermal drying of non-hygroscopic porous media with a mechanism based computer facilitated model of pore-level drying.

Simulation results of pore-level drying of non-hygroscopic rigid liquid-wet porous media are presented. Two and three-dimensional pore networks represent pore spaces.

Here, I report results of experiments and distributions of liquid and vapor as drying time advances. For the calculation of transport properties, details of pore space and displacement were subsumed in pore conductances (Segura and Toledo, 2005b). Solving for the pressure field in each phase, vapor and liquid, I found a single effective conductance for each phase as a function of liquid saturation. Along with the effective conductance for the liquid-saturated network, the diffusivity of liquid and diffusivity of vapor were calculated.

19.2. Experiments of Drying at Pore Level

Several experiments have been performed in micromodels to determine the mechanisms that occur on drying at pore level (Shaw, 1987; Laurindo and Prat, 1998).

Figure 19.1 shows drying fronts in a bead pack. The medium is homogeneous, dense and random packing of 0.4 μm mean diameter silica spheres, sandwiched in a 15 μm × 2.5cm × 4.0cm gap between two glass slides (Segura and Toledo,

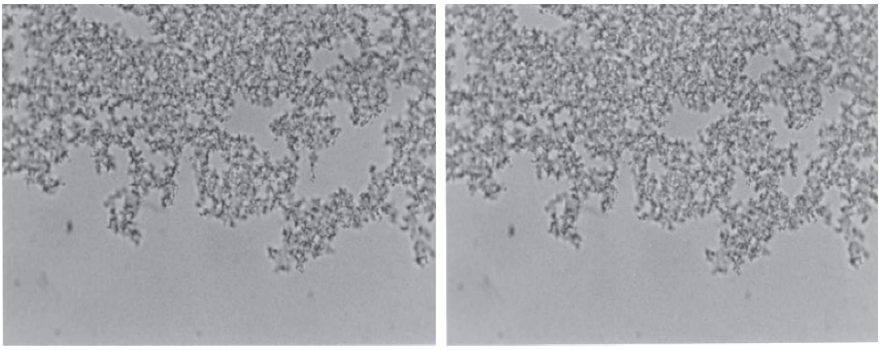

(a) (b)

FIG. 19.1. Drying fronts in a bead pack (Segura and Toledo, 2001)

2001). In an optical microscope, silica spheres saturated with water appear transparent, and dried zones appear dark. After packing the cell with spheres and filling it with distilled water, three edges of the cell were sealed. Drying was initiated by allowing the water to evaporate from the open edge. As air invaded the packing during drying, the cell became opaque. This allowed the drying front to be directly imaged in an optical microscope using transmitted light. The experiment was carried out at room temperature (18°C). The cell was used in horizontal position. Shaw (1987) first conducted a similar experiment. Photographs a and b were taken with a difference of 30 s.

19.3. Modeling of Drying at Pore Level

Porous media were represented by rigid two-dimensional square and three-dimensional cubic networks of prismatic pore bodies connected by narrow pore throats of rectangular cross section circumscribing circles of given radii and depth.

Initially, the network was fully saturated with liquid. Evaporation took place by allowing the liquid to evaporate into the air from an open edge of the network. At the top of this edge a stream of air and evaporating species mixture flowed past slowly. The other edges of the network were sealed.

Network orientation with respect to gravity was horizontal. Liquid perfectly wet the solid surfaces; thus, the contact angle, measured through the wetting phase, was zero. Menisci movement was considered quasistatic and capillary-controlled. Liquid accumulation in pore corners allowed for liquid connectivity throughout the network no matter how high the capillary pressure was. Details of pore network and drying model were presented in a previous work (Segura and Toledo, 2005a; Segura and Toledo, 2005b).

Fick's first law defines the effective diffusivity of the evaporating species in the gas phase (Segura and Toledo, 2005a; Segura and Toledo, 2005b):

$$D_v = \frac{Q_v}{A}\left(\frac{RTd}{M}\right)\left(\frac{L}{\Delta p}\right)_v \tag{19.1}$$

Where Q_v is the volumetric flow rate of the evaporating species in the gas phase, M and d are, respectively, the molecular weight and density of the evaporating species, R is the ideal gas constant, T is the temperature, $(\Delta p/L)_v$ is the pressure gradient on vapor in the direction of the main flow, and D_v is the vapor effective diffusivity.

Liquid Diffusivity is defined by (Toledo *et al*., 1995):

$$D_l = -\frac{k_h}{\mu_l}\left(\frac{dP_c}{dS_l}\right) \tag{19.2}$$

where D_l is the liquid effective diffusivity , k_h is the hydraulic conductivity, μ_l is the liquid viscosity, and dP_c/DS_L is the variation of capillary pressure with liquid saturation.

19.4. Results and Discusion

Results are presented for 2D and 3D pore networks of pore bodies connected by narrow pore throats distributed by a log-normal distribution. Networks were disposed horizontally; thus, gravity was not a factor. The liquid used was hexane.

Figure 19.2 shows drying curves. Here we compare the results of Laurindo and Prat's (1998) experiments and simulation with our simulations. Our model captured the essence of the experiments.

Figure 19.2 displays drying curves from two-dimensional simulations on 140×140-pore networks saturated with hexane. Results are compared with experimental data from a micromodel of the same size (Laurindo, 1996) and simulation results of Laurindo (1996) (see also Laurindo and Prat, 1998) in the same network. Laurindo's (1996) results are the one realization of the log-normal pore size distribution. Our results correspond to five realizations of the same pore size distribution.

The experimental drying curve has the typical monotonic decreasing form. The lack of a plateau at early times in the drying process is explained by the two-dimensional nature of the micromodel and network replicas.

Figure 19.2 reveals that not enough liquid remains in the narrow outer surface to produce a constant period of drying. The experimental curve suggests two distinct regimes: a fast drying rate period followed by a significantly slower rate period. The arrow in Fig. 19.2 signals the change of rate in the simulated drying curve.

Figure 19.3 shows a comparison of experimental and simulated morphologies of drying fronts and corresponding saturations at equivalent drying times. Drying fronts move from the right. Pores filled with hexane vapor are shown in black; regions filled with liquid hexane are shown in white. Upper and lower boundaries are sealed. The left column in Fig. 19.3 displays a sequence of images from a

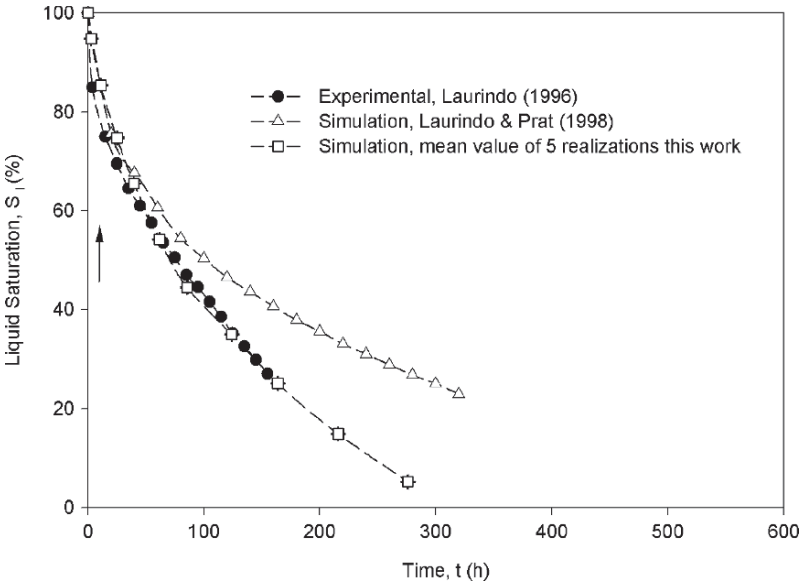

FIG. 19.2. Drying curves for 2D network (140×140)

100×60 pore micromodel (Laurindo, 1996). The right column in Fig. 19.3 displays the corresponding sequence obtained with our model in a computer replica of the micromodel, which is a 100×60 pore network. The sequence shows that at early stages of the process, when the average velocity of the drying front is high, a roughly compact front forms. As the front velocity slows, the size of the front roughness increases, and capillary fingers develop. Islands of liquid of various sizes appear. Notable is the compact front that evolves behind the rough front.

Similar analysis has been offered by Shaw (1987) and Laurindo and Prat (1998). Important is the striking resemblance of the simulated drying pattern when compared to the experimental pattern at the same drying time. The model also reproduces saturations, as Fig. 19.3 shows.

According to the model, the drying pattern at the beginning of the process is determined by capillary pumping, then by interplay between pumping and evaporation, and later, when only islands of liquid remain, by evaporation. The compact front behind the rough front is determined almost exclusively by evaporation. Our model successfully captures the physics of the drying process in the micromodel.

Figure 19.4 shows vapor diffusivity and liquid diffusivity curves from simulations in 2D and 3D pore networks saturated with hexane. Initially drying was governed by hydraulic flow, i.e., the liquid was eliminated to the outer surface of the network by liquid flow, where the liquid evaporated.

As liquid saturation diminished, liquid diffusivity diminished as well. Almost 90% of the liquid saturation in the network was unable to support liquid flow,

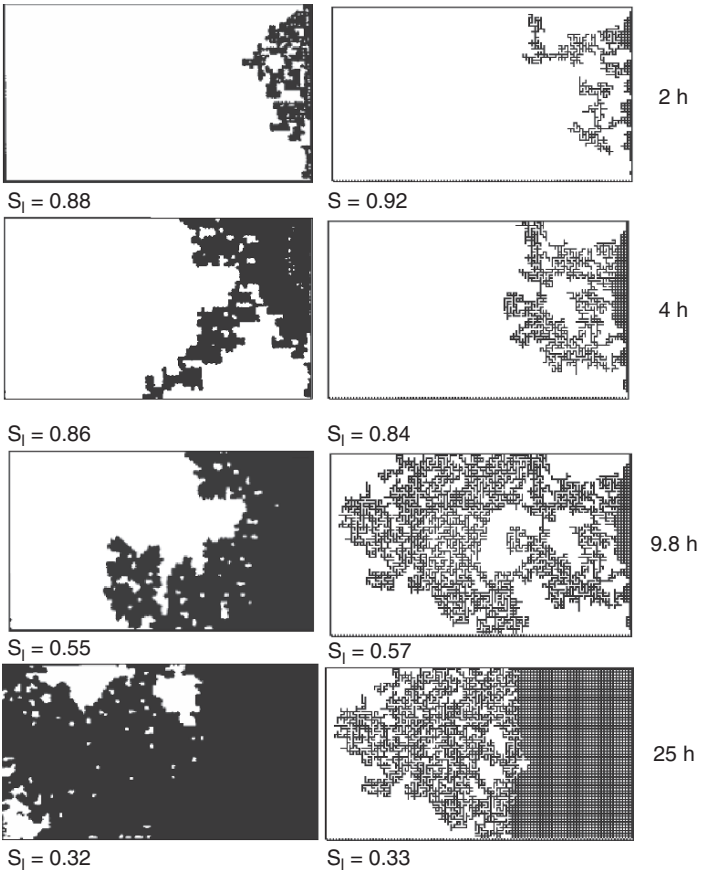

FIG. 19.3. Comparison of experimental and simulated morphologies of hexane drying fronts and corresponding saturations at equivalent drying times. Left column displays a sequence of images from a micromodel (Laurindo, 1996). Right column displays the corresponding sequence obtained with our model in a computer replica of the micromodel

and evaporation occurred inside the networks. At first, vapor coefficient diffusion increased because the interface liquid-gas increased. The vapor flux also increased; as liquid saturation decreased, both the vapor flux and the vapor diffusivity also diminished.

19.5. Conclusions

A mechanistic pore-level model of drying incorporating viscous flow and evaporation in two and three-dimensional networks is used to determine pore-level drying curves and vapor and liquid diffusivity as a function of liquid content.

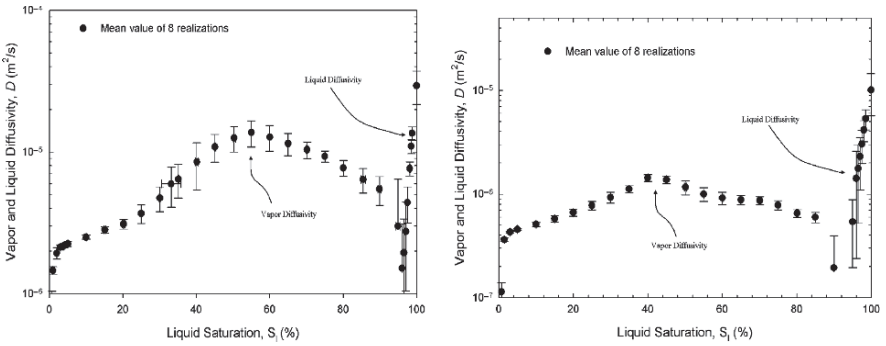

FIG. 19.4. Vapor and liquid diffusivity for 2D (a) and 3D (b) pore network

Initially, drying is governed by hydraulic mechanism, and then the water is eliminated by a combination of local evaporation and hydraulic flow. Finally, drying is governed by local evaporation of liquid clusters.

Acknowledgements This work is a natural continuation of the doctoral thesis of the author of the present work, and I appreciate very much the contribution of Dr. Pedro Toledo.

Financial support from University Bío-Bío through project DIUBB 053921 2/R is greatly appreciated.

References

Barbosa-Cánovas, G., and Vega-Mercado H., 1996, *Dehydration of Food,* Chapman & Hall, New York.

Laurindo J.B. 1996, *Evaporation en Milieu Poreux. Etude Expérimentale sur Milieux-Modèles et Modélisation de Type Percolation*, INPT Thesis, Toulouse.

Laurindo, J.B., and Prat M., 1998, Numerical and Experimental Network Study of Evaporation in Capillary Porous Media Drying Rates, *Chem. Eng. Sci.,* **53**:12, 2257.

Segura, L.A., and Toledo P.G., 2001, Monte Carlo Simulations and Experiments of the Isothermal Drying of Porous Materials: Humidity Curves and Maps, in: *Proceedings of III Congreso Iberoamericano de Ingeniería en Alimentos*, Valencia.

Segura, L.A., and Toledo P.G., 2005a, Pore-Level Modeling of Isothermal Drying of Pore Networks. Evaporation and viscous flow, *Lat. Am. Appl. Res*. **35**:43.

Segura, L.A., and Toledo P.G., 2005b, Pore-Level Modeling of Isothermal Drying of Pore Networks. Pore Shape and Size Distribution Effects on Saturation and Transport Parameters, *Chem. Eng. J*. **111**:2–3, 237.

Shaw T.M., 1987, Drying as an Immiscible Displacement Process with Fluid Counterflow, *Phys Rev. Lett*. **59**:1671.

Toledo, P.G., Davis, H T., and Scriven L.E., 1995, Hyperdispersive Flow Liquid Thin Films in Fractal Porous Media, *Colloids Surf*. **104**:73.

20
Rheological Description of the Disorder-Order Transition of Gellan Without Added Counter-Ions

B.E. Sánchez-Basurto, M. Ramírez-Gilly, and A. Tecante

20.1. Introduction

Gellan is a microbial anionic heteropolysaccharide with a repeating unit of tetrasaccharide formed by glucose, glucuronic acid and rhamnose in a 2:1:1 molar ratio, respectively. In native gellan, the repeating unit contains one O-acetyl and one O-L-glyceril in positions C6 and C2, respectively, in one of the glucose molecules. Removal of these substituents results in low acyl gellan, which together with the high acyl form are commercialized as gelling agents. However, each form produces gels with different textures (Sanderson, 1990).

Gellan forms gels with mono and divalent ions. Gelation occurs via a two-step mechanism that involves formation of a double helix from two random coils, followed by aggregation of double helices that gives rise to a three-dimensional network. The coil-helix transition defines the sol form while double helix aggregation characterizes the gel condition (Milas et al., 1990).

The sol-gel transition is thermoreversible (i.e., it occurs on cooling and heating) and takes place over a temperature range in which there is a peak temperature normally considered the transition temperature. However, when gellan concentration is low and ions are not added, only the coil-helix transition takes place upon cooling hot solutions. This transition is also thermoreversible.

The sol-gel transition with added ions has been studied using techniques that include optical rotation (Milas et al., 1990), ultrasound (Tanaka et al., 1993), DSC (Miyoshi et al, 1994; Izumi et al., 1996; Miyoshi et al., 1996; Amici et al., 2001), capillary viscometry (Sakurai et al., 1995) and analysis of viscoelastic moduli (Nakamura et al., 1993; Nakamura et al., 1996). In these works, transition temperatures for gellan without added ions are also provided, but mainly for polymer concentrations higher than 0.5%.

In this work we report on the viscoelastic behavior of gellan solutions at different temperatures without added ions. The disorder-order transition is described by a method based on the variation with temperature of the frequency at which $\tan \delta = 1$. The method from which transition temperatures were determined was validated by comparison with DSC measurements, and its applicability was tested

with guar and kappa-carrageenan solutions without added ions. Our purpose is to understand the behavior of gellan under non-gelling conditions in order to identify possible applications where the presence of salts is not possible or even undesirable.

20.2. Materials and Methods

20.2.1. Materials

Food grade low acyl gellan (Kelcogel, CPKelco, San Diego, USA) was used without further treatment. Its ion content (%), as determined by atomic absorption, was: Ca^{+2} = 0.42 ± 0.028; Mg^{+2} = 0.15 ± 0.070; Na^{+} = 0.74 ± 0.13 and K^{+} = 3.5 ± 0.078.

20.2.2. Gellan solutions

Gellan was dispersed in distilled and deionized water at room temperature (25 ± 2°C) under vigorous magnetic stirring. The resulting dispersion was heated to 75°C and kept 15 min at this temperature. Water was added to compensate for evaporation losses. The hot solutions were handled as described in the next section. Gellan concentrations were 0.1, 0.2, 0.3, 0.4, 0.5 and 0.65% on a dry weight basis.

20.2.3. Rheology

The disorder-order transition was examined by cooling the hot gellan solutions in a double wall Couette fixture (cup diameter, mm: inside = 27.94, outside = 34; bob diameter, mm: inside = 29.5, outside = 32; bob length, mm = 31.98) of a strain rheometer (ARES-RFSIII, TA Instruments, USA). Hot gellan solutions were equilibrated in the fixture previously heated to 60°C. Then, temperature was lowered to 45, 40, 35, 30, 25, 20, 15, 10, 5 and 1°C. At each of these temperatures, strain and frequency sweeps were carried out with the same sample. Strain sweeps were run at a constant oscillation frequency of 6.38 rad/s to find the zone of linear viscoelasticity. Frequency sweeps from 0.1 to 100 rad/s were carried out at a constant strain within this zone. The sample was covered with paraffin oil to avoid evaporation losses. Tests were run at least in duplicate with freshly prepared solutions. The frequency of G′and G″ overcrossing (i.e. tan δ = 1) was determined using an interpolation routine included in the rheometer software (Orchestrator V. 8.03).

20.2.4. Differential Scanning Calorimetry

DSC tests in a microcalorimeter (Setaram DSC III, France) were run to confirm the existence of the disorder-order transition in gellan solutions. Solutions were heated and cooled at a rate of 1°C/min from 5 to 60°C.

The peak temperature in the resulting thermographs was taken as the disorder-order transition temperature (DOTT).

20.3. Results and Discussion

Figure 20.1 shows the variation with frequency of dynamic moduli and loss angle for 0.65% gellan at 1, 25 and 45°C. At 45°C the behavior is typical of a macromolecular solution with $G' \propto \omega^{1.7}$, $G'' \propto \omega^{1.0}$, $G'' > G'$, between 1 to 30 rad/s, and an overcrossing at about 40 rad/s. The marked decrease with frequency of the loss angle above 1 rad/s (Fig. 20.1b) is typical of increasingly elastic disordered chains. Below 1 rad/s, the measured torques were lower than the detection limit of 0.4 μN.m. At 25 °C, $G'' \approx G'$, $G' \propto \omega^{0.58}$, $G'' \propto \omega^{0.55}$, and moduli overcrossed at about 60 rad/s. The loss angle was about 45° and independent of frequency. At 1°C, $G' \propto \omega^{0.32}$, $G'' \propto \omega^{0.34}$, and $G' > G''$ resulted in loss angles of about 26°. Cooling resulted in an increase of five orders of magnitude in moduli and changes in their dependence with frequency and shifting, but without gel formation. This is ascribed to the existence of a disorder-order (i.e., coil-helix) transition confirmed by DSC (Fig. 20.2). The DOTT on cooling (Fig. 20.2a) was 26.92°C, while that on heating was 26.81°C (Fig. 20.2b), which indicates the absence of hysteresis.

Plotting the overcrossing frequency, ω_C, against temperature resulted in a maximum at 30°C, as shown in Fig. 20.3 for 0.65% gellan. This temperature is about 3 °C greater than that determined by DSC. It is worth noticing that the appearance of a maximum, like that shown in Fig. 20.3, makes possible the DOTT

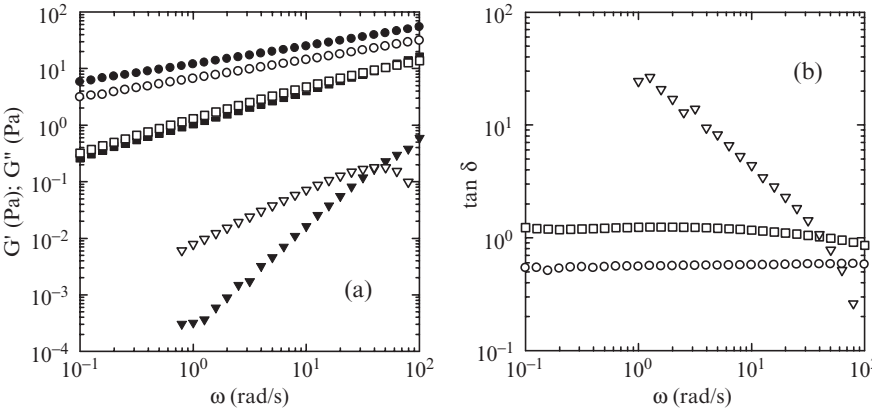

FIG. 20.1. Variation with frequency of (a): G′ (black symbols), G″ (white symbols) and (b): loss angle for 0.65% gellan at 1°C and 1% strain (circles), 25°C and 10% strain (squares) and 45 °C and 50% strain (inverted triangles)

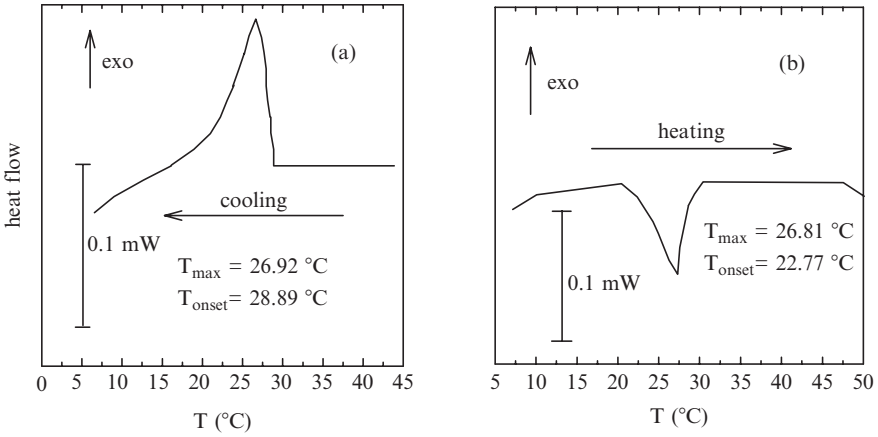

FIG. 20.2. Thermoreversible conformational transition for 0.65% gellan without added ions

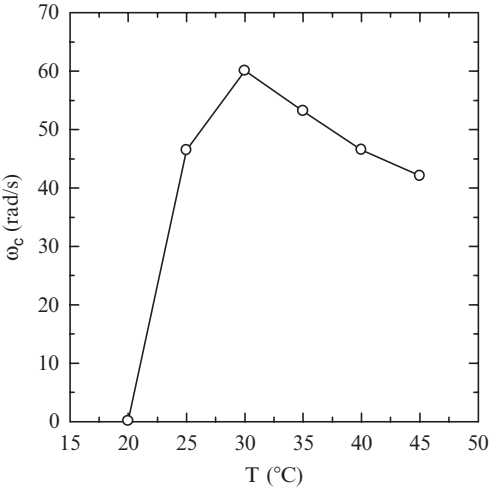

FIG. 20.3. Variation with temperature of ω_C during cooling of a 0.65% gellan solution

to be determined. To the best of our knowledge, this procedure has not been used before. The applicability of the method was tested with guar and κ-carrageenan without added ions. The former is a non-ionic polysaccharide for which a conformational transition is not expected, as it adopts a random coil conformation regardless of temperature. The latter has a gelling mechanism similar to gellan and also shows thermoreversible conformational transitions depending on its concentration and added ions content. For 0.5% guar, the variation with frequency of the dynamic moduli (data not shown) over the experimental temperature range was similar to that for 0.65% gellan at 45°C (Fig. 20.1a). This means that regardless of temperature, guar behaved as a macromolecular solution in which moduli

overcrossing resulted in an increase in ω_C with temperature without a maximum. Therefore, no conformational transition took place.

Figure 20.4 shows the behavior of 0.4% κ-carrageenan without added ions. A maximum in ω_C occurred at about 15°C (Fig. 20.4a). DSC confirmed the presence of a transition during cooling, with a peak temperature of 13.48°C. The transition on heating (signal not shown) occurred at 14.68°C. The difference among these temperatures is not greater than 1.5°C. Therefore, it is possible to conclude that the overcrossing method yields reliable values of DOTT.

Figure 20.5 shows the variation with temperature of ω_C for the other gellan solutions. DSC confirmed transition temperatures only for 0.5% gellan, because lower concentrations produced weak signals. For 0.5% gellan, the peak temperature was 25°C, which agrees quite well with 25.32°C from DSC. The DSC peak temperature on heating was 25.20°C. The DOTT decreases with decreasing gellan concentration. We have taken peak temperatures both in DSC and rheology just for comparison purposes, but it is clear that transition takes place over a temperature range.

Figure 20.6 shows the transition temperatures obtained by our procedure, together with those reported in the literature for gellan without added ions and determined only from rheological data (Nakamura et al., 1993; 1996). Gellan concentration, C_P (%), is plotted against the reciprocal of absolute temperature. The agreement of our data with those reported is excellent. This representation allows identification of the concentration and temperature for which the disordered and ordered states exist. For example, at a constant gellan concentration of 0.5% and 0.0032 1/K (39°C), the coil conformation exists, while at the same concentration but 0.0036 1/K (4.6°C), the double helix conformation is adopted.

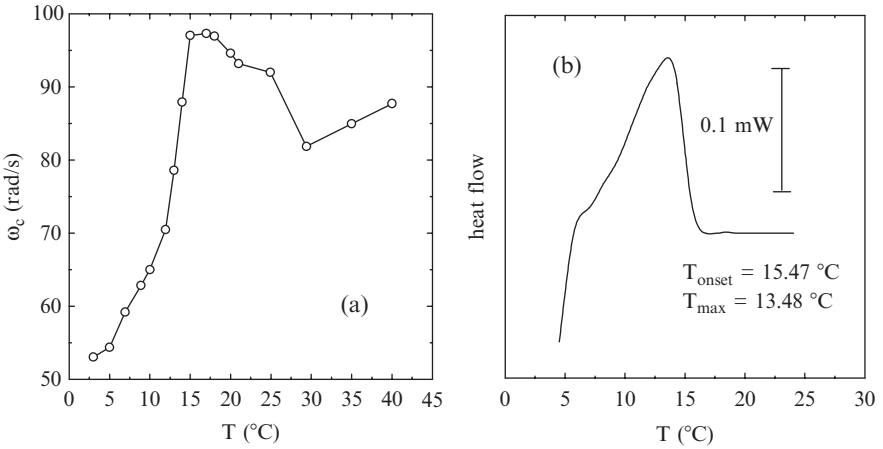

FIG. 20.4. (a): Variation with temperature of ω_C, and (b): DSC signal during cooling of a 0.40% κ-carrageenan solution without added ions

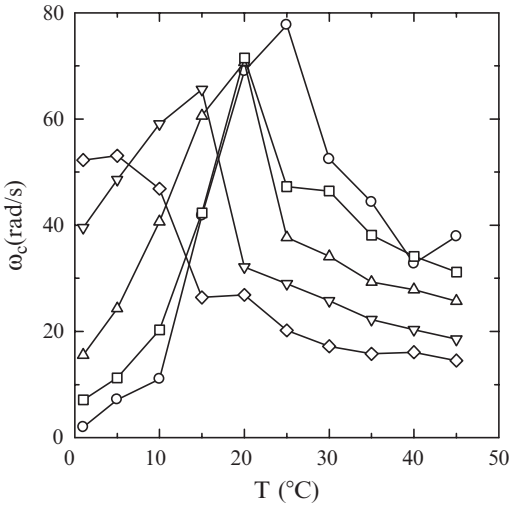

FIG. 20.5. Variation with temperature of ω_C for: 0.5 (circles), 0.4 (squares), 0.3 (triangles), 0.2 (inverted triangles) and 0.1% (diamonds) gellan solutions

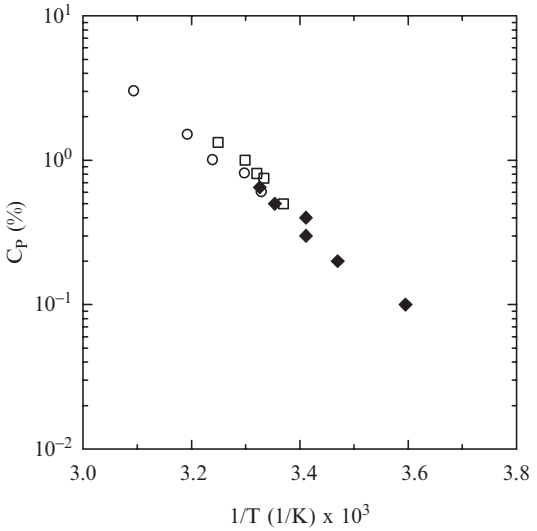

FIG. 20.6. Conformational transition diagram for low acyl gellan without added ions. Comparison of our data (black diamonds) with data from rheological techniques: squares (Nakamura et al. 1993) and circles (Nakamura et al., 1996)

20.4. Conclusions

The DOTT in gellan solutions without added ions can be determined from displacement with temperature of the frequency at which the dynamic moduli overcross. The agreement of transition temperatures with DSC measurements confirmed the validity of this method. Examination of the behavior of guar and kappa-carrageenan without added ions proved the applicability of the method.

Acknowledgements We express our gratitude to María del Carmen Núñez-Santiago for helping us with DSC measurements and to Professor Ruth Pedroza-Islas for allowing us the use of the micro-calorimeter.

References

Amici, E., Clark, A.H., Normand, V., and Johnson N.B., 2001, Interpenetrating Network Formation in Agarose-Sodium Gellan Gels Composites, *Carbohydr. Polym*. **46**:383.

Izumi, Y., Kikuta, N., Sakai, K., and Takezawa H., 1996, Phase Diagrams and Molecular Structures of Sodium-Salt-Type Gellan Gum, *Carbohydr. Polym*. **30**:121.

Milas, M., Shi, X., and Rinaudo M., 1990, On the Physicochemical Properties of Gellan Gum, *Biopolym*. **30**:451.

Miyoshi, E., Takaya, T., and Nishinari K., 1994, Gel-Sol Transition in Gellan Gum Solutions. II. DSC Studies on the Effects of Salts, *Food Hydrocoll*. **8**:529.

Miyoshi, E., Takaya, T., and Nishinari,K., 1996, Rheological and Thermal Studies of Gel-Sol Transition in Gellan Gum Aqueous Solutions, *Carbohydr. Polym*. **30**:109.

Nakamura, K., Harada, K., and Tanaka Y., 1993, Viscoelastic Properties of Aqueous Gellan Solutions: The Effects of Concentration on Gelation, *Food Hydrocolloid*. **7**:435.

Nakamura, K., Tanaka, Y., and Sakurai M., 1996, Dynamic Mechanical Properties of Aqueous Gellan Solutions in the Sol-Gel Transition Region, *Carbohydr. Polym*. **30**:101.

Sakurai, M., Tanaka, Y., and Nakamura K., 1995, Viscosities, Densities and Sound Velocities of Dilute Aqueous Gellan Solutions, *Food Hydrocoll*. **9**: 189.

Sanderson, G.R., 1990, Gellan Gum, in: *Food Gels*, P. Harris (ed.), Elsevier Applied Food Science, New York, pp. 201–232.

Tanaka, Y., Sakurai, M., and Nakamura N., 1993, Ultrasonic Velocities in Aqueous Gellan Solutions, *Food Hydrocolloid*. **7**: 407.

21
Advanced Food Products and Process Engineering (SAFES) II: Application to Apple Combined Drying

P. Fito, N. Betoret, P.J. Fito, and A. Andrés

Nomenclature

D_e: effective moisture diffusivity
K_s, K_{s0}, K_w, K_{w0}: kinetic parameters
l: characteristic dimension
m: mass
[OS]: osmotic solution concentration
P: pressure
r: radius
ρ: density
ρ_a: apparent density
ρ_r: real density
T: temperature
t: time
V: volume
v: air velocity
X_w: moisture content (as mass fraction)
X_{ss}: soluble solids content (as mass fraction)
X_1: volumetric fraction of liquid incorporated in the first stage of VI step
X_2: volumetric fraction of liquid incorporated in the second stage of VI step
γ_1: volumetric deformation in the first stage of VI step
γ_2: volumetric deformation in the second stage of VI step
ε: effective porosity
ΔM_w: relative increment in water mass
ΔM_{ss}: relative increment in soluble solids mass

21.1. Introduction

Different dehydration techniques are widely used to stabilize fruits. Numerous papers about dehydration methods such as air drying (AD) or osmotic dehydration (OD) are being published around the world. Vacuum impregnation (VI)

pre-treatment may be used as a tool both to improve mass transfer and to develop engineered products (Fito et al., 2001).

In this paper, a solid food is considered as a monophasic and homogenous system, and product humidity is considered as the main variable related to quality characteristics of the final product being correlated with process conditions (mainly air temperature and velocity).

Nowadays, consumers are much more demanding, calling for products with good texture, color and nutritional value. Quality is becoming a more complex concept that affects the functionality of the product (Fito and Chiralt, 2003). In this situation, foods have to be defined by considering some of the structural, sensorial, physical-chemical and nutritive aspects.

The changes in every considered characteristic, along with drying processes, need to be taken into account, and mechanistic correlations among these characteristics and process variables must be established (Torreggiani and Bertolo, 2001).

A new methodology that allows us to consider structural, physical-chemical and nutritive aspects when defining a fruit, while also analyzing phase transitions, structural changes and transport phenomena in a systematic way (SAFES) (Fito et al., 2006) has been applied to dehydration of apple by combined methods.

21.2. Materials and Methods

SAFES methodology was conceived to describe food by considering its structural, thermodynamic and physico-chemical complexity in the simplest possible way so as to detect the changes food can suffer as a result of a series of changes.

SAFES methodology is based on mathematic matrices designed for mass balances that include food components in different aggregation states in rows and food phases in columns (Fito et al., 2006).

A descriptive matrix (DM) defines a product, while the difference between two DMs defines a matrix of changes (MC), which reflects phase transitions, compositional and structural changes, and the transport phenomena involved in a stage of changes or in a basic operation.

DM and MC are identified with two subscripts; the first indicates the position of the product (DM) or the stage considered (MC) in the global process (represented by a flux diagram), and the second is a reference to specify the mass basis to which values are referred in the matrix.

Apple *var. Granny Smith* was analyzed; a dehydration process that includes VI, OD and AD as basic operations was considered. Data from the literature have been used, and some hypotheses related to composition and water distributions have been established to define DM. Data, hypotheses, and the sequence of calculations to construct DM and MC are included in Fig. 21.1.

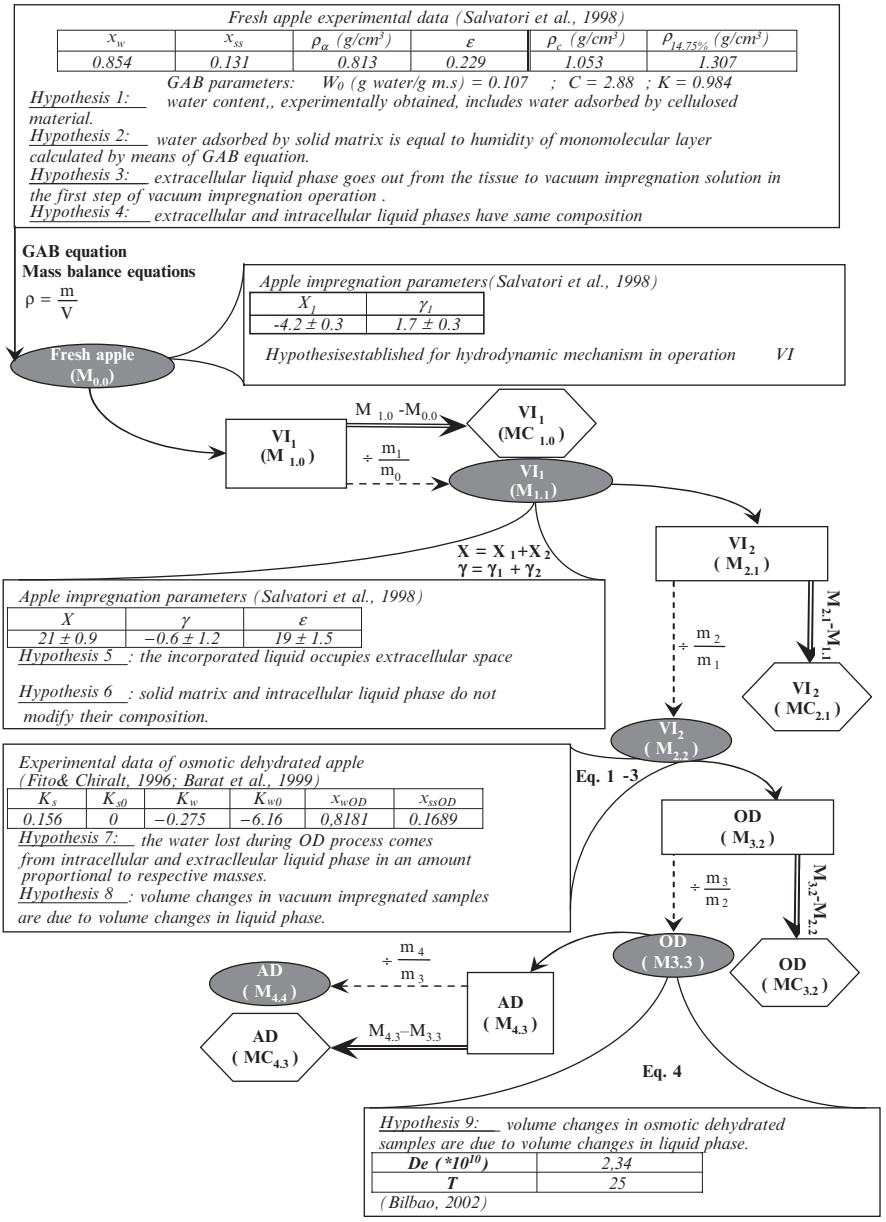

FIG. 21.1. Data, hypothesis and the sequence of calculations to build up DM and MC for each stage of changes

21.3. Results and Discussion

21.3.1. The Concept of Stage of Changes: Application to the Process of Dehydration of Apple by Combined Methods

The concept of basic operation (BO), inherited from chemical engineering, has been used in food engineering for a long time. The SAFES methodology has defined the concept of "stage of changes (SC)", in order to, specifically, identify each one of the changes that a product undergoes through a BO, as well as the mechanisms responsible for them. An SC can be defined as the time span during which a food system undergoes some relevant change (e.g., in state variables, structure, composition, aggregation states, etc.) (Fito et al., 2006).

In the process of dehydration by combined methods considered in this work, VI operation has been divided in two SC, while OD and AD have been analyzed as unique operations. Figure 21.2 shows the flow chart, including operation conditions.

In operation of VI, the direction of the pressure gradients that act as driving forces in stage at atmospheric pressure determines the direction of the flows and deformations in the product, making it necessary to analyze each one independently.

It is well known that in AD operations different mechanisms (osmotic, diffusion, hydrodynamic, etc.) are responsible for water removal depending on the presence of a liquid phase. As a consequence, the drying rate is affected. In accordance with both periods, the operation has been divided in two SC. OD has been analyzed as a unique SC because the time considered (three hours) is too short.

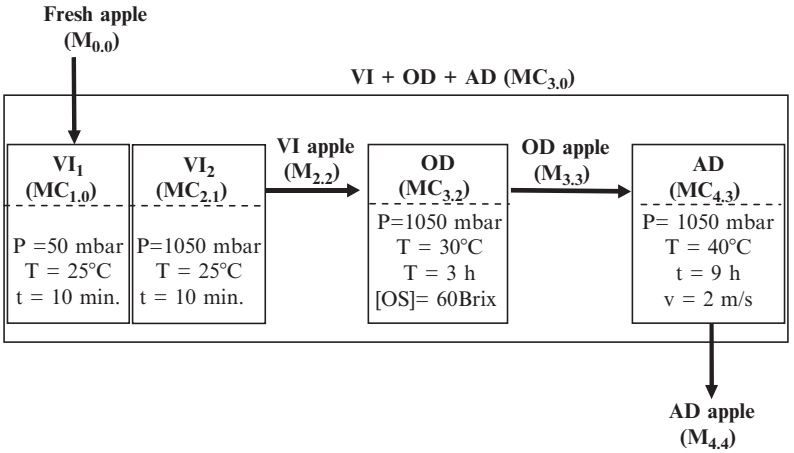

FIG. 21.2. Flow chart of the process of dehydration by combined methods analyzed in this work. Conditions of each SC have been specified and the calculated matrices are referred in brackets

21.3.2. Phases, Components and Aggregation States in Fresh and Dried Fruits: The Descriptive Matrix (DM)

Fruits and vegetables are biological systems constituted by cells that are assembled to configure a parenquimatic tissue that includes intercellular connections, intercellular spaces and pores taken up by gas or native liquid to quite an extent (Trakoontivakorn et al., 1988). This structure largely conditions fluxes and kinetics in processing operations and the quality of final product (rehydration and instant properties, flavor retention and sensorial attributes such as color and texture). In addition, some changes in an operation may only affect some components included in a limited area or some specific structures; therefore, those changes have to be considered when describing a raw material, an intermediate product in a process or a final product. Some phenomena affecting one specific phase in VI, OD and AD operations are:

- VI operation produces the partial release of gas from pores and its replacement by an external liquid that affects physico-chemical and structural properties of raw material and the subsequent behavior of OD and AD operations (Fito et al., 2001).
- In OD operation, when there is liquid in the pores, the force balance on the double layer plasmalema cell wall leads to layer separation while the plasmalema shrinks in line with water loss with scarce deformation of the cell wall. However, when a gas phase occupies the intercellular space, the plasmalema shrinks together with the cell wall that deforms greatly as the process progresses (Barat et al., 1999).
- In AD processes of fruit and vegetables, the transport rate is greatly affected by the tissue structure and composition, both defining the effective values of its transport properties (thermal properties and water effective diffusion coefficient) (Fito et al., 2001). Moreover, large moisture content gradients coexist during drying, meaning that rubber and glassy states may be present simultaneously inside a finite food piece.

In order to control changes that occur only in a specific phase or component, a matrix that includes phases, components and aggregation states has been designed to describe a food. This matrix may include mass values, energy values or any other state variable or thermodynamic variable that is interesting for evaluating changes in a product or in a process.

As has been indicated in the Materials and Methods section, the matrix including mass values (as mass fractions), volume values and temperature and pressure vectors has been named the descriptive matrix (DM).

Five phases (solid matrix, SM; intracellular liquid, IL; extracellular liquid, EL) soluble solids in solid state (SSs) and gas (G)) and five components (water, insoluble solids, soluble solids (native), soluble solids (added) and gases) have been considered in the DM of fresh, impregnated, osmotic dehydrated and air dried apple.

The space of phases and components defined in this way (as a matrix) includes cells that are thermodynamically possible (white cells) and cells that are not

(pointed cells). Figure 21.3 shows this space suitably configured for apple in the process of drying by combined methods (AD, OD and VI

Experimental data and the four hypotheses (Fig. 21.1) mainly referred to water sharing among the different phases and to the composition of intracellular and intercellular liquid phases for fresh apple used to define the DM of fresh apple (Fig. 21.4).

Values of X_l and γ_l of apple (*Granny Smith*), experimentally calculated by Salvatori et al. (1998), have been used with hypothesis 3 to quantify liquid that takes up extra-cellular spaces.

21.3.3. A Procedure To Quantify Changes in an SC: The Matrix of Changes (MC)

Using this methodology to describe fresh, intermediate or final products in a process, it is easy to detect the mass fluxes, phase transitions and biochemical reactions that one SC produces in a product. These changes appear automatically reflected in the MC, which is calculated by the difference between the DM of the products involved in the SC process.

COMPONENTS		DESCRIPTIVE MATRIX (DM)						
		Solid Matrix (**SM**)	Intracellular Liquid (**IL**)	Extracellular Liquid (**EL**)	Soluble Solids (solid) (**SSs**)	Gas (**G**)	Whole Food (**WF**)	External Phase (**EP**)
Water	**G**							
	L							
	A							
	R							
	V							
	K							
	TOTAL							
Non Soluble Solids (native)	**L**							
	A							
	R							
	V							
	K							
	TOTAL							
Soluble Solids (native)	**L**							
	A							
	R							
	V							
	K							
	TOTAL							
Soluble Solids (added)	**L**							
	A							
	R							
	V							
	K							
	TOTAL							
GAS	**TOTAL**							
WF (Mass)								
WF (Volume) cm^3								
Temperature (**K**)								
Pressure (mbar)								

FIG. 21.3. The space of phases and components suitably configured for apple in the process of drying by combined methods

COMPONENTS		FRESH APPLE ($M_{0,0}$)						
		Solid Matrix (SM)	Intracellular Liquid (IL)	Extracellular Liquid (EL)	Soluble Solids (solid) (SSs)	Gas (G)	Whole Food (WF)	External Phase (EP)
Water	G					0	0	
	L		0,7110	0,0464			0,7573	0,8500
	A	0,0967			0		0,0967	
	R							
	V							
	K							
	TOTAL	0,0967	0,7110	0,0464	0	0	0,8540	0,8500
Non Soluble Solids (native)	L							
	A							
	R	0,0150					0,0150	
	V	0					0	
	K	0					0	
	TOTAL	0,0150	0	0	0	0	0,0150	
Soluble Solids (native)	L		0,1230	0,0080			0,1310	
	A	0					0	
	R				0		0	
	V				0		0	
	K							
	TOTAL	0	0,1230	0,0080	0	0	0,1310	
Soluble Solids (added)	L		0	0			0	0,1500
	A	0					0	
	R				0		0	
	V				0		0	
	K				0		0	
	TOTAL	0	0	0	0	0	0	0,1500
GAS	TOTAL	0	0	0	0	0	0	0
WF (Mass)		0,1116	0,8340	0,0544	0	0	1,0000	1,0000
WF (Volume) cm^3		0,0854	0,7893	0,0515		0,2817	1,2300	0,9464

FIG. 21.4. DM of fresh apple

COMPONENTS		VI_1 ($MC_{1,0}$)						
		Solid Matrix (SM)	Intracellular Liquid (IL)	Extracellular Liquid (EL)	Soluble Solids (solid) (SSs)	Gas (G)	Whole Food (WF)	External Phase (EP)
Water	G					0	0	
	L		0	−0,0464		HDM	−0,0464	0,0464
	A	0			0		0	
	R							
	V							
	K							
	TOTAL	0	0	−0,0464	0	0	−0,0464	0,0464
Non Soluble Solids (native)	L							
	A							
	R	0					0	
	V	0					0	
	K	0					0	
	TOTAL	0	0	0	0	0	0	0
Soluble Solids (native)	L		0	−0,0080			−0,0080	
	A	0					0	
	R				0	HDM	0	
	V				0		0	
	K							
	TOTAL	0	0	−0,0080	0	0	−0,0080	0
Soluble Solids (added)	L		0	0			0	0,0080
	A	0					0	
	R				0		0	
	V				0		0	
	K				0		0	
	TOTAL	0	0	0	0	0	0	0,0080
GAS	TOTAL	0	0	0	0	0	0	0
WF (Mass)		0	0	−0,0544	0	0	−0,0544	0,0544
WF (Volume) cm^3		0	0	−0,0515	0	0,0946	0,0209	0,0515

FIG. 21.5. MC of VI_1 stage

The MC of each SC included in the flow chart represented in Fig. 21.2 is represented in Figs. 21.5 to 21.8. Each one of the fluxes and phase transitions that appear reflected in each of the matrices is described in the next paragraphs according to the hypothesis pre-established and the mechanism involved.

21.3.3.1. The MC of VI_1 Stage ($MC_{1.0}$)

Figure 21.5 shows MC of VI_1 stage. Values in this matrix reflect that in the stage VI of operation that occurs at vacuum pressure (VI_1 stage), there is a flux of liquid (water and soluble solids) from the extracellular liquid phase to the external phase. As described by Fito et al. (1996), this flux occurs as a consequence of pressure gradients. The mechanism responsible for this gradient was called hydrodynamic mechanism (HDM), and it is coupled with deformation-relaxation phenomena that affect the structure and modify the volume of the sample. The extent of deformations, as well as the degree of impregnation reached in this type of operation, depends essentially on the structure of the material and its mechanical properties and, of course, on operating conditions. Tissue structure plays a very important role, not only due to the total porosity, but also to the size and shape distribution of pores and the communications between themselves and with the external liquid (Fito et al., 1996). The last row of the MC of VI_1 stage shows a positive value in the cell of whole food volume; that means that the volume of the sample increases in this stage. This increase in the volume is the consequence of gas expansion inside extracellular spaces (Fito et al., 1996).

21.3.3.2. The MC of VI_2 Stage ($MC_{2.1}$)

Figure 21.6 shows the MC of VI_2 stage. Values in this matrix reflect changes produced in the fruit after atmospheric pressure is restored. As Fito et al. (1996) explained, when the atmospheric pressure is restored in the system, forces due to differences between external and internal pressures may produce both solid

COMPONENTS		VI2 (MC2.1)						
		Solid Matrix (SM)	Intracellular Liquid (IL)	Extracellular Liquid (EL)	Soluble Solids (solid) (SSs)	Gas (G)	Whole Food (WF)	External Phase (EP)
Water	G					0	0	
	L		0	0,2701		HDM	0,2701	–0,2701
	A	0			0		0	
	R							
	V							
	K							
	TOTAL	0	0	0,2701	0	0	0,2701	–0,2701
Non Soluble Solids (native)	L							
	A							
	R	0					0	
	V	0					0	
	K	0					0	
	TOTAL	0	0	0	0	0	0	0
Soluble Solids (native)	L		0	0			0	
	A	0					0	
	R				0		0	
	V				0		0	
	K							
	TOTAL	0	0	0	0	0	0	0
Soluble Solids (added)	L		0	0,0477		HDM	0,0477	–0,04767
	A	0					0	
	R				0		0	
	V				0		0	
	K				0		0	
	TOTAL	0	0	0,0477	0	0	0,0477	0
GAS	TOTAL	0	0	0	0	0	0	0
WF (Mass)		0	0	0,3178	0	0	0,3178	–0,3178
WF (Volume) cm³		0	0	0,3008	0	–0,3221	–0,0214	–0,3522

FIG. 21.6. MC of VI_2 stage

matrix deformations and the fluxes induced by HDM. The net liquid penetration by HDM and the solid matrix deformation (X and γ) in apple *(var. Granny Smith)* were experimentally evaluated by Salvatori et al. (1998). As represented in Fig. 21.1, these values have been used to build $MC_{2.1}$ where no null values reflect liquid (water and soluble solids) penetration from external fluid to extracellular liquid phase. The last row shows a negative value in the cell of whole food volume, which means the volume of the sample decreases in this stage.

21.3.3.3. The MC of OD stage ($MC_{3.2}$)

Experimental kinetic data for osmotic dehydration operations obtained according to Eqs. (21.1)–(21.3) (Fito and Chiralt, 1996) and Hypothesis 7 (Fig. 21.1) have been used to obtain DM for osmotic dehydrated apple. Equations used were included in a model deduced by Fito and Chiralt (1996) that takes into account:

- Thermodynamic aspects in terms of the chemical potential of components in the present phases at equilibrium;
- Kinetic analysis of mass transfer for each component, taking into account pseudo-Fickian (osmotic and diffusion), vaporization-condensation, HDM, as well as the role of structure in their coupling;
- Prediction of the liquid retention capacity of the solid matrix.

MC associated with the OD stage reflects compositional changes originated in the product as a consequence of this basic operation (under conditions specified) (Fig. 21.7). The sign of the values and its position in the configured matrix allow

COMPONENTS		OD ($MC_{3.2}$)						
		Solid Matrix (SM)	Intracellular Liquid (IL)	Extracellular Liquid (EL)	Soluble Solids (solid) (SSs)	Gas (G)	Whole Food (WF)	External Phase (EP)
Water	G					0	0	
	L		−0,0725	−0,0260		MPD	−0,0985	0
	A	0		MO	0		0	
	R							
	V							
	K							
	TOTAL	0	−0,0725	−0,0260	0	0	−0,0985	0
Non Soluble Solids (native)	L							
	A							
	R	0					0	
	V	0					0	
	K	0					0	
	TOTAL	0	0	0	0	0	0	0
Soluble Solids (native)	L		0	0			0	
	A	0					0	
	R				0		0	
	V				0		0	
	K							
	TOTAL	0	0	0	0	0	0	0
Soluble Solids (added)	L		0	0,0209		MPD	0,0209	0
	A	0					0	
	R				0		0	
	V				0		0	
	K				0		0	
	TOTAL	0	0	0,0619	0	0	0,0209	0
GAS	TOTAL	0	0	0	0	0	0	0
WF (Mass)		0	−0,0725	−0,0051	0	0	−0,0776	0
WF (Volume) cm3		0	−0,0727	−0,0133	0	0	−0,0860	0

FIG. 21.7. MC of OD stage

us to know fluxes and mechanisms involved in the operation. Water flows from intracellular liquid to extracellular liquid and from there to the external phase, and soluble solids flow from the external phase to the extracellular liquid phase. Considering that during an OD operation there are normally no pressure gradients except for the contribution from cell turgor, which is supposed to disappear in the first stages of the process. Mechanisms depending on water activity gradients are responsible for these fluxes. These mechanisms have been named "pseudodiffusional" mechanisms, which include Fickian and osmotic mechanisms that involve individual cell interaction, cells in the external surface of the solid external solution and cells in the internal surface of the pores. As no pressure gradients have been considered, volume changes are only due to volume changes in liquid phase. Null values for every component in the external phase are the result of a mass relation of 20 between external phase and vacuum impregnated apple.

21.3.3.4. The MC of AD Stage ($MC_{4.3}$)

Drying of cellular tissues produces several chemical (browning and other reactions) and physical (color, texture, shape, porosity, etc.) changes that are not independent, but that are related in some complex ways. The most commonly examined properties of dried products are usually classified into two major categories: engineering and quality properties. For the chemical engineer, the critical parameters derived from the drying process are the drying rate and the effective moisture diffusivity of the product. Although these parameters do not provide information about the final quality of the product, they are the most

COMPONENTS		AD (MC4.3)						
		Solid Matrix (SM)	Intracellular Liquid (IL)	Extracellular Liquid (EL)	Soluble Solids (solid) (SSs)	Gas (G)	Whole Food (WF)	External Phase (EP)
Water	G					0	0	0
	L		−0,5400	−0,1940		MPD	−0,7340	
	A	0	MO		0		0	
	R							
	V							
	K							
	TOTAL	0	−0,5400	−0,1940	0	0	−0,7340	0
Non Soluble Solids (native)	L							
	A							
	R	0					0	
	V	0					0	
	K	0					0	
	TOTAL	0	0	0	0	0	0	0
Soluble Solids (native)	L		−0,1070	0			−0,1070	
	A	0					0	
	R				0		0	
	V				0,1070		0,1070	
	K							
	TOTAL	0	−0,1070	0	0,1070	0	0	0
Soluble Solids (added)	L		0	−0,0619			−0,0619	
	A	0					0	
	R				0		0	
	V				0,0619		0,0619	
	K				0		0	
	TOTAL	0	0	−0,0619	0,0619	0	0	0
GAS	TOTAL	0	0	0	0	0	0	0
WF (Mass)		0	−0,6470	−0,2559	0	0	−0,7340	0
WF (Volume) cm^3		0	−0,6079	−0,2330	0	−0,0623	−0,3773	0

FIG. 21.8. MC of AD stage

widely reported. In order to show that SAFES methodology is useful to know the mechanisms involved in mass transfer phenomena, apparent moisture diffusivity of apple (Bilbao et al, 2002) has been used to obtain the DM of air dried apple and the MC associated with this SC in the process considered in this study. MC associated with the AD stage is shown in Fig. 21.8. It can be observed that all the water in the liquid phase has been eliminated and has, necessary, flowed from intracellular liquid to extracellular liquid and from the last to the external phase (as in the OD stage). The mechanisms involved are the same as those in the OD stage. Positive and negative values in cells for soluble solids reflect that the water loss has induced phase transitions in every soluble solid.

Changes in volume appear as a consequence of the water loss and the viscoelastic matrix contraction into the space previously occupied by the water removed from the cells (Aguilera, 2003).

References

Aguilera J.M., 2003, Drying and Dried Products Under the Microscope, *Food Sci. Technol. Int*. **9**(3):137–143.

Barat, J.M., Albors, A., Chiralt, A., and Fito P., 1999, Equilibration of Apple Tissue in Osmotic Dehydration: Microstructural Changes, *Drying Technology* **17**(7):1375–1386.

Bilbao, C., 2002, *Estudio del Secado Combinado Aire/Microondas en Manzana Granny Smith*. Tesis doctoral – UPV, UPV, Valencia.

Fito, P., Andrés, A., Chiralt, A., and Pardo A., 1996, Coupling of Hydrodynamic Mechanism and Deformation-Relaxation Phenomena During Vacuum Treatments in Solid Porous Food-Liquid Systems, *J. Food Eng*. **27**:229–240.

Fito, P., and Chiralt A., 1996, Osmotic Dehydration, an Approach to Modelling of Solid Food–Liquid Operations, in: *Food Engineering 2000*, Chapman and Hall, London.

Fito, P., and Chiralt A., 2003, Food Matrix Engineering: The Use of the Water-Structure-Functionality Ensemble in Dried Food Product Development. *Food Sci. Technol. Int*. **9**(3):151–156.

Fito, P., Chiralt, A., Barat, J.M., Andrés, A., Martínez-Monzó, J., and Martinez-Navarrete N., 2001, Vacuum Impregnation for Development of New Dehydrated Products, *J Food Eng*. **49**: 297–302.

Fito, P., LeMaguer, M., Betoret, N., and Fito P.J., 2006, An Advanced Food Process Engineering to Design Real Food and Processes: The SAFES Methodology, *J. Food Eng*. (In Press).

Salvatori, D., Andrés, A., Chiralt, A., and Fito P., 1998, The Response of Some Properties of Fruits to Vacuum Impregnation. *J. Food Process Eng*. **21**:59–73.

Torreggiani, D., and Bertolo G., 2001, Osmotic Pre-Treatments in Fruit Processing: Chemical, Physical and Structural Effects, *J. Food Eng*. **49**(2/3):247–253.

Trakoontivakorn, G., Patterson, M.E., and Swanson B.G., 1988, Scanning Electron Microscopy of Cellular Structure of Granny Smith and Red Delicious Apples, *Food Microstructure* **7**:205–212.

22
Simple, Practical and Efficient on-Line Correction of Process Deviations in Batch Retort Through Simulation

R. Simpson, I. Figueroa, and A. Teixeira

22.1. Introduction

The basic function of a thermal process is to inactivate pathogenic and food spoilage-causing bacteria in sealed containers of food by using heat treatments at temperatures well above the ambient boiling point of water in pressurized steam retorts (autoclaves). Excessive heat treatment should be avoided because it is detrimental to food quality, wastes energy, and under-utilizes plant capacity. Therefore, the accuracy of the methods used for this purpose is of importance to food science and engineering professionals working in this field.

Control of thermal process operations in food canning factories has consisted of maintaining specified operating conditions that have been predetermined from product and process heat penetration tests, such as the process calculations for the time and temperature of a batch cook. Sometimes, unexpected changes can occur during the course of the process operation such that the pre-specified processing conditions are no longer valid or appropriate. These types of situations are known as process deviations. Because of the important emphasis placed on the public safety of canned foods, processors must operate in strict compliance with the US Food and Drug Administration's Low-Acid Canned Food (FDA/LACF) regulations. A succinct summary and brief discussion of these regulations can be found in Teixeira (1992). Among other things, these regulations require strict documentation and record-keeping of all critical control points in the processing of each retort load or batch of canned product. Particular emphasis is placed on product batches that experience an unscheduled process deviation, such as when a drop in retort temperature occurs during the course of the process, which may result from loss of steam pressure. In such a case, the product will not have received the established scheduled process, and must be either fully reprocessed, destroyed, or set aside for evaluation by a competent processing authority. If the product is judged to be safe, then batch records must contain documentation showing how that judgment was reached. If judged unsafe, then the product must be fully reprocessed or destroyed. Such practices are costly. Based on observations and record review of various retort control systems, the US Food and Drug Administration (FDA) concluded that the design of alternative-schedule retort control systems (table-lookup method) meet

the overall intent of the FDA Low-acid Canned Food (LACF) regulations at 21 CFR 113, and appear to provide safeguards which are sufficiently equivalent to the safeguards provided by the mandatory provisions of these regulations. Table-lookup methods are easily implemented in any cannery plant, and are a safe FDA-approved on-line procedure for correcting process deviations. However, they are a very inefficient way to correct a deviation because they often result in extensive over-processing, resulting in poor product quality and costly disruption of cook room retort operating schedules. In order to avoid these inefficient corrections, processors tend to operate at 1 or 2 °C, and sometimes at 3 to 4 °C over the registered retort temperature. Therefore, processors are able to minimize, and even reduce to zero, the occurrence of deviant processes, but at the cost of exposing every batch to an over-processing situation. The aim of this research was the development of a safe, simple, efficient and easy-to-use procedure to manage on-line corrections of unexpected process deviations in any canning plant facility. Specific objectives were to:

- Develop strategies to correct the process deviation by an alternative "proportional-corrected" process that delivers no less than final target lethality, but with near minimum extended process time at the recovered retort temperature.
- Demonstrate strategy performance by comparing "proportional-corrected" with "commercial-corrected" and "exact-corrected" process times.
- Demonstrate consistent safety of the strategy through an exhaustive search over an extensive domain of product and process conditions to find cases in which safety is compromised.

22.2. Methodology

22.2.1. Scope of Work

To reach the objectives stated above, the approach to this work was carried out in three tasks, in support of each objective.

22.2.2. Task 1—Proportional Correction Strategy Development

The objective for the strategy required in this task was to accomplish an on-line correction of an unexpected retort temperature deviation by an alternative process that delivers final target lethality, but with minimum extended process time at the recovered retort temperature. This would be accomplished by using the same alternative process "look-up tables" that would normally be used with currently accepted methods of on-line correction of process deviations, but with a "proportional correction" applied to the alternative process time that would reduce it to a minimum without compromising safety. In order to fully understand this strategy, it will be helpful to first review the currently accepted method that is in common practice throughout

the industry. Commercial systems currently in use for on-line correction of process deviations do so by extending process time to that which would be needed to deliver the same final lethality had the entire process been carried out with an alternative lower constant retort temperature equal to that reached at the lowest point in the deviation. These alternative retort temperature-time combinations that deliver the same final process lethality (F_0) are called equivalent lethality processes. When these equivalent time-temperature combinations are plotted on a graph of process time versus retort temperature, they fall along a smooth curve called an equivalent lethality curve. These curves are predetermined for each product from heat penetration tests and thermal process calculations carried out for different retort temperatures.

In practice, the new process times obtained from these curves at such low alternative temperatures can be as much as two or three times longer than the originally scheduled process time required to reach the same final target lethality, resulting in considerable quality deterioration and costly disruption to scheduled retort operations. Nonetheless, these systems are versatile because they are applicable to any kind of food under any size, type or container shape, as well as mode of heat transfer (Larkin, 2002). These consequences are particularly painful when, as in most cases, the deviation recovers quickly, and the alternative extended process time is carried out at the recovered original retort temperature. Canned food products subjected to such "corrected" processes become severely over-processed, with final lethalities far in excess of that required and quality deterioration often reaching levels below consumer acceptance (a safe correction, but by no means optimal or efficient: Alonso et al., 1993; Von Oetinger, 1997; Simpson, 2004). To avoid these painful corrections, processors normally operate at retort temperatures 3 to 4 °C over the registered retort temperature.

The "proportional-correction" strategy developed in this research significantly avoids such excessive over processing by taking advantage of the short duration of most recovered retort temperature deviations and the lethality delivered by carrying out the corrected process at the recovered retort temperature. The strategy calculates the corrected process time (t_D) as a function of the temperature drop experienced during the deviation, but also the time duration of the deviation. The following expression illustrates mathematically how this "proportional-corrected" process time would be calculated for any number (n) of deviations occurring throughout the course of a single process:

$$t_D = t_{TRT} + \sum_{i=1}^{n} \left(t_{D_i} - t_{TRT}\right) \frac{\Delta t_i}{t_{TRT}}; \quad t_{D_i} \geq t_{TRT} \tag{22.1}$$

where n is the number of deviations occurring during the process, t_D is the corrected process time, t_{TRT} is the pre-established process time at retort temperature TRT, Δt_i is the duration of deviation i, t_{Di} is the process time at the deviation temperature TRT_i, TRT_i is the lowest temperature during the deviation i, and TRT is the retort temperature.

For example, in the case of a single deviation, the corrected process time would be calculated by first finding the alternative process time that would be required to deliver the same final lethality had the entire process been carried out with an alternative lower constant retort temperature equal to that reached at the lowest point in the deviation (t_D). This would be done by use of the equivalent lethality process curve or look-up table described earlier. The difference between this longer alternative process time and the originally scheduled process time (t_D–t_{TRT}) is the extra time that would normally be added to the original process time to correct the process according to current industry practice. However, in the new strategy proposed here, this extra process time differential (t_D–t_{TRT}) is multiplied by a proportionality factor consisting of the ratio, [time duration of the deviation]:[originally scheduled process time], or expressed mathematically as ($\Delta t/t_{TRT}$). This proportionality factor is always less than or equal to one, and always results in a corrected process that delivers no less than the final target lethality specified for the original process, but with near minimum extended process time.

22.2.3. Task 2—Performance Demonstration

This task consisted of demonstrating the performance of these strategies by simulating the occurrence of process deviations occurring at different times during the process (early, late and randomly) to both solid and liquid canned food products, calculating the alternative corrected process times, and predicting the outcomes of each corrected process in terms of final lethality and quality retention. For each deviation, three different alternative corrected process times were calculated:

- "Exact correction," giving corrected process time to reach precisely the final target lethality specified for the scheduled process, using computer simulation with heat transfer models;
- "Proportional correction," using the strategy described in this research with look-up tables; and,
- "Commercial correction," using current industry practice with look-up tables (manually or computerized).

The heat transfer models were explicitly chosen to simulate the two extreme heat transfer cases encountered in thermal processing of canned foods. The rationale behind this decision was that canned foods possess heating characteristics between these two extreme situations. Conclusions extracted from these simulations will be extended to all canned foods. First was the case of pure conduction heating of a solid product under a still-cook retort process. The second was the case of forced convection heating of a liquid product under mechanical agitation. In both cases, the container shape of a finite cylinder was assumed, typical of a metal can or wide-mouthed glass jar. However, suitable models appropriate for true container shapes can be used as required for this purpose. Examples of such models can be found in the literature (Teixeira et al., 1969; Manson et al., 1970; Manson et al., 1974; Datta et al., 1986; Simpson et al., 1989; Simpson, 2004). The product and process conditions chosen to carry out the demonstrated simulations for each case are given in Table 22.1.

22.2.4. Task 3—Demonstration of Safety Assurance by Complex Optimization Search Routine

This on-line correction strategy was validated and tested for safety assurance by executing a strict and exhaustive search routine with the use of the heat transfer models selected in Task 2 on a high-speed computer.

The problem to be solved by the search routine was to determine whether the minimum final lethality delivered by all the corrected processes that could be found among all the various types of deviations and process conditions considered in the problem domain met the criterion that it had to be greater than or equal to the lethality specified for the original scheduled process. This criterion can be expressed mathematically:

$$\underset{U}{\text{Min}}\left[F_{proportional} - F_{Tol}\right] \geq 0 \tag{22.2}$$

where $F_{\text{proportional}}$ is the F-value calculated with the proportional correction, F_{Tol} is the F-value specified for normal scheduled process, and U is the universe of feasible process conditions in the search routine.

The search routine was designed as an attempt to find a set of conditions under which the required search constraint was not met.

22.3. Results And Discussions

22.3.1. Equivalent Lethality Curves

Look-up tables were used to find the alternative process time for the corrected process and can be presented graphically as "equivalent process lethality curves" for each scheduled product/process. Therefore, equivalent process lethality curves were constructed. An example for pure conduction is shown in Fig. 22.1.

TABLE 22.1. Product and process conditions used for on-line correction strategy simulations

	Dimensions (cm)			Properties		Normal Process	
Product simulated	Major	Intermedium	Minor	Alfa (m^2/s)	fh (min)	Time (min)	TRT (°C)
Pure conduction can, Biot > 40	11.3	-	7.3	1.70E-07	44.4	64.1	120
Forced convection can, Biot<1	11.3	-	7.3	-	4.4	15.6	120

22.3.2. Performance Demonstration

Figures 22.2 and 22.3 show results from the product/process simulations carried out to demonstrate the performance of these strategies. The figures contain retort temperature profiles resulting from on-line correction of process deviations occurring at early times during the process to both solid and liquid canned food products.

Each figure shows the "normal" constant retort temperature profile expected for the originally scheduled process, along with the occurrence of a deviation (sudden step-drop in retort temperature for short duration) relatively early in the process.

In addition, for each deviation (one in each figure), three different alternative corrected process times are shown resulting from different strategies: "exact correction," "proportional correction" and "commercial correction."

In both cases, the extended process time required by the "commercial correction" strategy is far in excess of the extended times called for by the other two strategies. Moreover, the new "proportional correction" strategy results in extending process time only slightly beyond that required for an "exact correction," and will always do so. These results are summarized in Table 22.2, along with results from predicting the outcomes of each corrected process in terms of

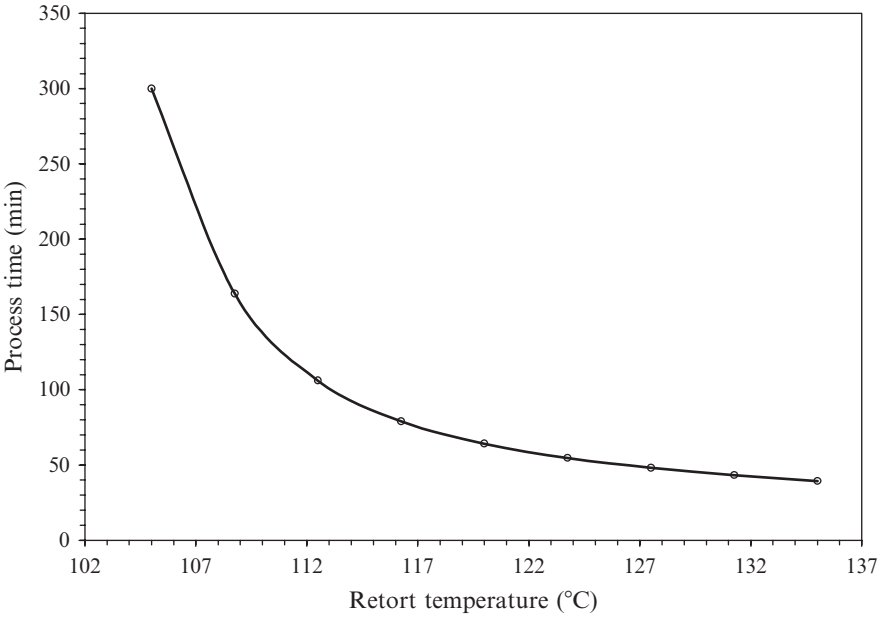

FIG. 22.1. An example of equivalent process lethality curve for simulated solid product under pure conduction heating, showing retort temperature / process time combinations that deliver the same final target lethality

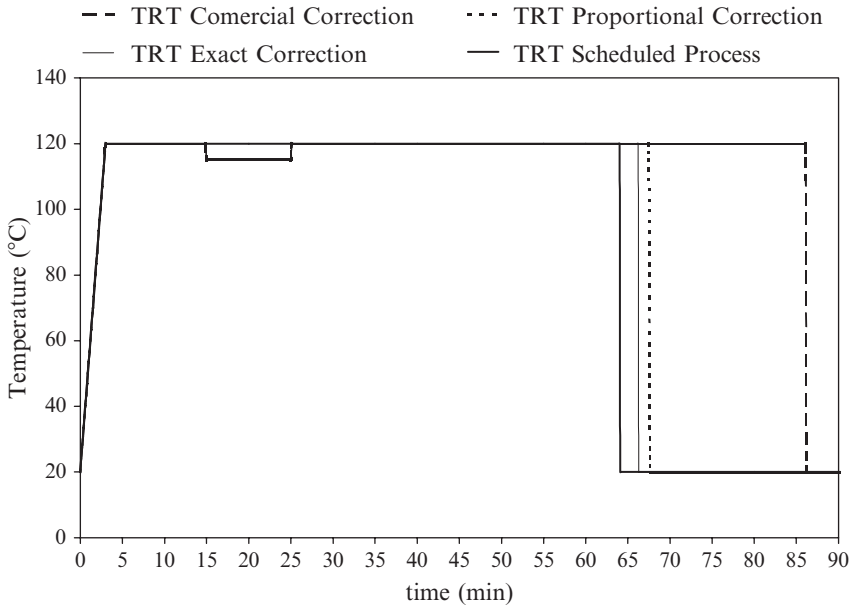

FIG. 22.2. Pure conduction simulation for on-line correction of an unexpected retort temperature deviation occurring early into the scheduled process for a cylindrical can of solid food under still cook

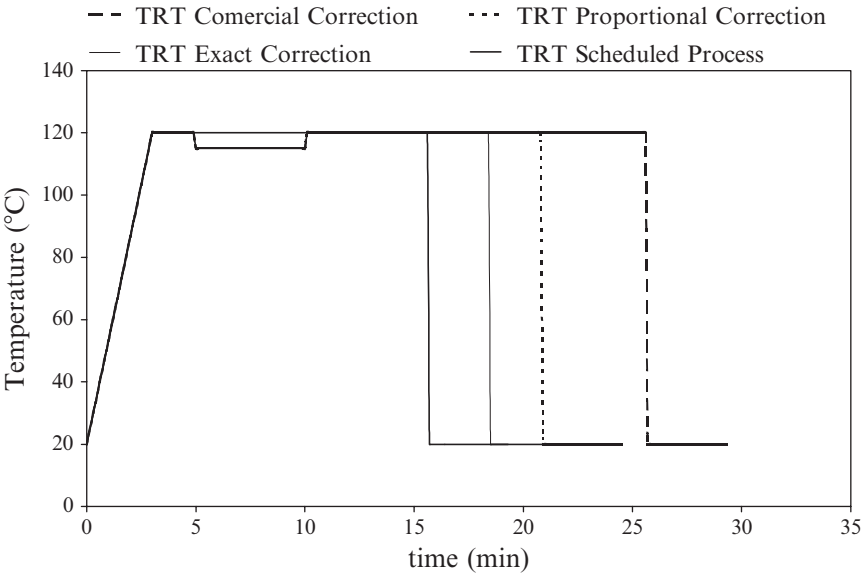

FIG. 22.3. Forced convection simulation for on-line correction of an unexpected retort temperature deviation occurring early into the scheduled process for a cylindrical can of liquid food under agitated cook

TABLE 22.2. Outcomes of each corrected process deviation described in Figs. 22.2 and 22.3 in terms of final process time, lethality and quality retention for the three different alternative correction methods

	Early deviation			Late deviation		
	Time (min)	F_0 (min)	Nutrient retention (%)	Time (min)	F_0 (min)	Nutrient retention (%)
Pure conduction						
Scheduled process	64.1	6.0	72.7	64.1	6.0	72.7
Exact correction	66.3	6.0	72.9	66.8	6.0	72.7
Proportional correction	67.5	6.5	72.2	67.5	6.2	72.3
Commercial correction	86.2	16.3	62.3	86.2	14.4	62.8
Forced convection						
Scheduled process	15.6	6.0	92.4	15.6	6.0	92.4
Exact correction	18.4	6.1	91.5	19.6	6.0	90.9
Proportional correction	20.8	8.0	89.7	20.8	7.0	89.9
Commercial correction	25.6	11.8	86.2	30.6	14.7	82.8

final process times required and final lethality and quality retention achieved (using product/process data presented in Table 22.1).

It is interesting to compare the improvement in nutrient (quality) retention resulting from the commercial correction (current industry practice) to the dramatic improvement resulting from either of the other two strategies.

22.3.3. Demonstration of Safety Assurance by Complex Search Routine

This on-line correction strategy was validated and tested for safety assurance by executing an exhaustive search routine with the use of the heat transfer models. Recall that the problem to be solved by the search routine was to determine if the minimum final lethality delivered by all of the corrected processes that could be found among the various types of deviations and process conditions considered in the problem domain met the criterion that it had to be greater than or equal to the lethality specified for the original scheduled process.

The search routine was designed to find a set of conditions under which the required search constraint was not met. No such conditions could be found.

22.4. Conclusions

This study has described a practical, simple and efficient strategy for on-line correction of thermal process deviations during retort sterilization of canned foods.

The strategy is intended for easy implementation in any cannery around the world. This strategy takes into account the duration of the deviation in addition

to the magnitude of the temperature drop. It calculates a "proportional" extended process time at the recovered retort temperature that will deliver the final specified target lethality with very little over-processing in comparison to current industry practice.

Results from an exhaustive search routine using the complex method support the logic and rationale behind the strategy by showing that the proposed strategy will always result in a corrected process that delivers no less than the final target lethality specified for the originally scheduled process.

Acknowledgements Author Ricardo Simpson is grateful for the financial support provided by CONICYT through the FONDECYT project number 1050810.

References

Alonso, A., Banga, J., and Perez-Martin R., 1993, A New Strategy for the Control of Pressure During the Cooling Stage of the Sterilization Process in Steam Retorts. Part I. A Preliminary Study. Food and Bioproducts Processing, *Trans IchemE* **71**(c):197-205.

Datta, A.K., Teixeira, A.A., and Manson J.E.,1986, Computer-Based Retort Control Logic for On-Line Correction of Process Deviations, *J. Food Sci*. **51**(2):480-483, 507.

Larkin J, 2002, Personal Communication. Branch Chief, National Center for Food Safety and Technology, Food and Drug Administration (FDA/NCFST), Chicago.

Manson, J.E., Zahradnik, J.W., and Stumbo C.R., 1970, Evaluation of Lethality and Nutrient Retentions of Conduction-Heating Food in Rectangular Containers, *Food Technol*. **24**(11):1297-1301.

Manson, J.E., Zahradnik, J.W., and Stumbo C.R. 1974. Evaluation of Thermal Processes for Conduction Heating Foods in Pear-Shaped Containers, *J. Food Sci*. **39**:276-281.

Simpson R., 2004, Control Logic for On-Line Correction of Batch Sterilization Processes Applicable to Any Kind of Canned Food, in: *Symposium of Thermal Processing in the 21st Century: Engineering Modeling and Automation*, IFT Meeting, Las Vegas.

Simpson, R., Aris, I., and Torres J.A., 1989, Sterilization oof Conduction-Heated Foods in Oval-Shaped Containers, *J. Food Sci*., **54**(5):1327-1331, 1363.

Teixeira, A.A., 1992, Thermal Process Calculations, in: *Handbook of Food Engineering*, D.R. Heldman and D.B. Lund (eds.), Marcel Dekker, Inc. New York, pp. 563-619.

Teixeira, A., Dixon, J., Zahradnik, J., and Zinsmeiter G.., 1969, Computer Optimization of Nutrient Retention in the Thermal Processing of Conduction-Heated Foods, *Food Technol*. **23** (6):845-850.

Von Oetinger K., 1997, *Lógica para el Control en Línea del Proceso de Esterilización Comercial*, Tesis Escuela de Alimentos. Pontificia Universidad Católica de Valparaíso, Valparaíso, Chile.

23
Effect of Capsicum Extracts and Cinnamic Acid on the Growth of Some Important Bacteria in Dairy Products

L. Dorantes, J. Araujo, A. Carmona, and H. Hernández-Sánchez

23.1. Introduction

Capsicum species have been the object of different studies (Dorantes et al., 2000; Careaga et al., 2003; Acero-Ortega et al., 2005) in order to determine their antimicrobial activity, the compounds that would be responsible for it, and the microorganisms that could be affected by it, finding that *Staphylococcus aureus, Salmonella tiphymurium, Listeria monocytogenes, Pseudomonas aureaginosa* and *Bacillus cereus* are susceptible to inhibition by *Capsicum* extracts. Some of the active compounds responsible for the inhibitory action are *t*-cinnamic acid and its derivatives, which are intermediate compounds in phenylpropanoids pathway. *Capsicum annuum* oleoresins are "generally recognized as safe" (GRAS) by the FDA, and so their use as natural antimicrobials is safe. However, it is important to know through predictive microbiology and modeling the quantitative effect of the *Capsicum* extracts, the active compounds, and the interactions with other factors such as pH and temperature.

One of the food products that has been involved in outbreaks is fresh rennet-curdled cheese, which has a rich nutrient content, a high water activity and low acidity, which make it an adequate culture medium for the growth of a wide variety of bacteria. Some of these bacteria are known to cause food-borne illness, such as *Staphylococcus aureus*. It has been estimated that consumption of foods contaminated by this microorganism is responsible for 185,060 illnesses, 1,753 hospitalizations and two deaths per year in the United States. In the United Kingdom since 1980, numbers of reported cases have not exceeded 189 per year, although this is only a small percentage of actual cases (Sutherland and Varnam, 2002). *S. aureus* has also been involved in food-borne diseases in México, especially in the consumption of milk products. Staphylococcal enterointoxication (staphylococcal food poisoning) results from the ingestion of enterotoxins that are synthesized during growth of *S. aureus* in foods. *S. aureus* is capable of producing an enterotoxin in conditions such as: water activity >0.85, a range of pH between 4 to 9.8, temperatures from 10 to 48 °C and a good nutrient supply such as that provided by fresh cheese and other milk products (Halpin-Dohnalek and Marth, 1989).

Another pathogenic bacteria causing food-borne illness is *Listeria monocytogenes*. In an outbreak that occurred in Los Angeles, 181 mother-infant pairs

were involved; the vehicle was determined to be Mexican-style cheese (Jones, 1992). *Listeria* is able to grow in wide ranges of temperature (−1.5 to 45 °C), pH (4.39–9.4) and osmotic pressures (NaCl concentrations over 10%), besides being an anaerobic facultative microorganism. The pathogen is particularly problematic for the food industry because of its wide environmental distribution, since it has been found in humans, waste water and milk (Acero-Ortega et al., 2005).

On the other hand, lactic acid bacteria are considered beneficial to humans, due to the production of lactic acid, which helps in the preservation of foods, maintaining of the gut microbiota and promotion of good digestion of foods. They also enhance the flavor and texture of milk products. *Lactobacillus plantarum* is a widespread member of the genus *Lactobacillus*, commonly found in sauerkraut, pickles and other fermented or decaying plant material. *L. plantarum* and related lactobacilli are unusual in that they can breathe oxygen but have no respiratory chain or cytochromes; the consumed oxygen ultimately ends up as hydrogen peroxide.

The peroxide probably acts as a weapon to exclude competing bacteria from the food source. In place of the protective enzyme superoxide dismutase, which is present in almost all other oxygen-tolerant cells, this organism accumulates millimolar quantities of manganese polyphosphate. Because the chemistry by which manganese complexes protect the cells from oxygen damage is subverted by iron, these cells contain virtually no iron atoms; in contrast, a cell of *Escherichia coli* of comparable volume contains over one million iron atoms (CDC, 2006).

Given the fact that food safety is required for the well-being of humans, the present study implies three aspects: 1) The first objective of this work was to use the principles of "hurdle technology" to inhibit the growth of *Staphylococcus aureus* in fresh cheese (stored at a non-shock temperature) by adding *Capsicum* extract and modifying the pH value. The cheese was stored at a non-shock temperature to enhance the risk in the challenge test, since we know that in developing countries there is lack of refrigeration in small towns. A response surface analysis was employed to have a secondary modeling of the effect of the two factors involved in the experiment; 2) The second aspect implied the evaluation of survival of a beneficial bacteria such as *Lactobacillus plantarum* when inhibitory concentration (as determined by response surface) of *Capsicum* extract was present; 3) The third objective was the evaluation of the effect of concentration of *t*-cinnamic acid on the survival of the pathogenic bacteria *Listeria monocytogenes* and a non-pathogenic bacteria (*Lactobacillus plantarum)*.

23.2. Materials And Methods

23.2.1. Inhibition of Staphylococcus aureus by Capsicum Extracts at a Non-shock Temperature Using Response Surface Analysis

Staphylococcus aureus (ATCC 29213) was obtained from the Medical Bacteriology Laboratory at the Instituto Politécnico Nacional, México City, México. The *Capsicum* extract was obtained from fresh bell peppers, as described by Dorantes et al., 2000.

The cheese was elaborated in the following manner: pasteurized milk was adjusted to the desired value of pH with lactic acid, then the *Capsicum* extract and the *Staphylococcus aureus* (100 cells/mL) were added. The inoculated milk was heated to 30 °C and rennet was added to achieve coagulation. The curd was cut and allowed to stand at 30 °C for 1.5 h; after this, the whey was drained, 2% (w/w) salt was added and then the curd was pressed at 5 °C for 20 h. The final product was stored in hermetically sealed polyethylene bags for 7 days at 20 °C. Colony counts for *S. aureus* were made at days 0, 3, 5, and 7. For the pH test the procedure was the same, except for the addition of a sterile solution of lactic acid 1 M to the milk, in the amounts required to achieve the following pH values: 5.0, 5.5, and 6.0. By surface response experimental design, 13 runs with different combinations of pH and extract concentration were obtained, as follows (pH: % extract):

pH	%	Repetitions
5.0	1	2
5.5	1	2
6.0	5	2
5.5	5	2
5.5	3	2
5.0	3	2

The adequate amount of bacteria to be used as a starter culture in the cheese was determined to be 100 bacteria/mL in the inoculum. This amount was calculated from preliminary tests.

23.2.2. Survival of a Beneficial Bacteria at Inhibitory Concentration of Capsicum Extract

Lactobacillus plantarum NRRL B-4496 (originally isolated from pickled cabbage) was used. To standardize the inoculum, the bacterium was cultured in Mann Ragosa Sharpe Agar (MRS, Difco, México City, México) for 18 h at 32 °C. Aliquots were taken and serial decimal dilutions were carried out using fresh broth until an absorbance of 1.3 at 590 nm was reached, to give a standard inoculum of about 10^7 CFU/mL. Mixture of MRS and 5% *Capsicum* extract was sterilized at 121 °C for 15 min and cooled at room temperature. The mixture was then inoculated with *Lactobacillus plantarum*, followed by incubation at 32 °C. Serial dilutions of samples were plated on MRS, incubated at 32 °C for 24 h and typical colonies were counted.

23.2.3. Effect of the t-cinnamic Acid on the Growth Curve of the Test Microorganisms

Listeria monocytogenes Scott A was obtained from the Sanitary Microbiology Laboratory of the Instituto Politécnico Nacional, México City, and was maintained on trypticase soy agar plates (TSA, Difco, Mexico City, México) at

4 °C until use. Flasks containing 99 mL of TSB and different concentrations of *t*-cinnamic acid (0 to 1.5%) were prepared, sterilized at 121 °C for 15 min and cooled down to 35-37 °C. The media were inoculated with 1 mL of the bacterial culture that contained 10^7 CFU/mL, followed by incubation at 35-37 °C for 24 h. Afterwards, colonies produced by *L. monocytogenes* were counted. All experiments were done in triplicate.

23.3. Results and Discussion

Regarding the inhibition of *Staphylococcus* by *Capsicum* extracts at 20 °C in fresh cheese, we found that the equation from the surface response analysis, which describes the growth of *S. aureus* (log (N/No)) under the different conditions of the experiments is the following:

$$Log\left(\frac{N}{N_0}\right) = 1.39 + 3.12\,pH - 4.84(\%\ extract)$$

The effect of pH values 5 and 5.5, on *S. aureus* is significant. In fresh cheese with no *Capsicum* and pH 6 the number of *Staphylococcus aureus* increased rapidly. The first day of storage, the number of cells increased from 2 to 6 logs. The optimum pH value for its growth is 6 to 7, as reported in the literature. As pH decreases, the microbial growth slows down. On the other hand, the *C. annuum* concentration that resulted in the strongest inhibition was 5% of extract in cheese (w/w), as observed in Fig. 23.1. The surface response analysis (Fig. 23.1) shows that when pH values are low and concentrations of extract are high, the maximum inhibitory effect is achieved. Such results are probably due to the inhibitory action of the active compounds that include *t*-cinnamic, o-cumaric, m-cumaric, ferulic, and caffeic acids, which can be classified as weak lipophilic acids. The antimicrobial activity of these compounds is due to their non-dissociated molecules. Rico-Muñoz et al. (1987) emphasized the effect of some phenolic compounds on the membrane-bound adenosine triphosphatase of *Staphylococcus aureus*.

All the combinations of pH and *Capsicum* extract showed some antimicrobial effect, the most effective being the combination of pH 5 and 5% *Capsicum* extract, showing a significant inhibitory effect along seven days of storage at 20 °C, when compared with the blank. According to the above, there is a synergistic effect between pH and the extract concentration. Such an effect has been observed on other natural compounds by some researchers (Acero-Ortega et al., 2005; Rauha et al., 2000).

It may be concluded from this challenge test that the *Capsicum annuum* extract at pH5 showed a bacteriostatic effect against *Staphylococcus aureus* in fresh cheese, after three days of storage, at a non-shocking temperature of 20 °C. This is important when no refrigeration is available, and hence the period of consumption must be short.

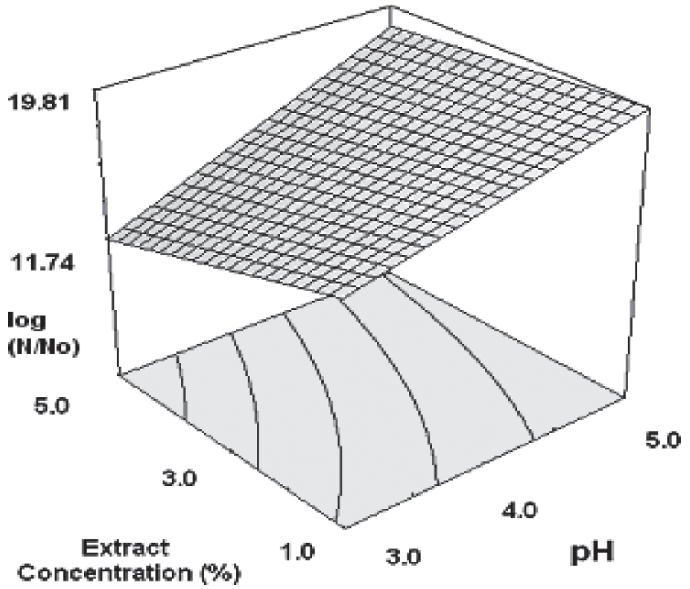

FIG. 23.1. Response surface of the effect of *Capsicum* extract concentration (%) and pH on the growth of *Staphylococcus aureus*

23.3.1. Survival of Lactobacillus plantarum at Inhibitory Concentration of Capsicum Extract

With the aim of knowing if the conditions that inhibit Listeria would affect the growth of beneficial bacteria, the survival of the *Lactobacillus* was determined at 5% *Capsicum* extract and pH5. A control (without *Capsicum* extract added) was run at the same time. Mean of triplicates of log CFU versus time, is shown in Fig. 23.2. It may be observed that *Lactobacillus plantarum* was not significantly ($\alpha > 0.05$) inhibited by *Capsicum* extract. These results suggest that bell pepper extract may be used to inhibit *Listeria monocytogenes*, without affecting the growth of the beneficial lactic bacteria.

23.3.2. Effect of the Concentration of t-cinnamic Acid on the Survival of Listeria monocytogenes and Lactobacillus plantarum

Given the results described above, it was interesting to find out if one of the active compounds (*t*-cinnamic acid) found in bell pepper extracts affect in different form the growth of the pathogenic bacterium and the beneficial one. The population of *Listeria* in the control after 24 h of incubation was of 10^{11} CFU/mL. The acid

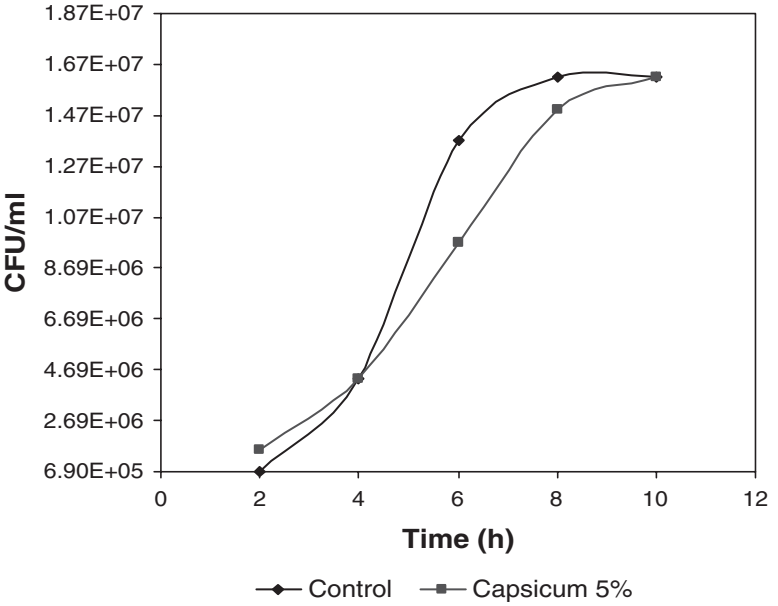

FIG. 23.2. Survival of Lactobacillus plantarum at 5% bell pepper extract

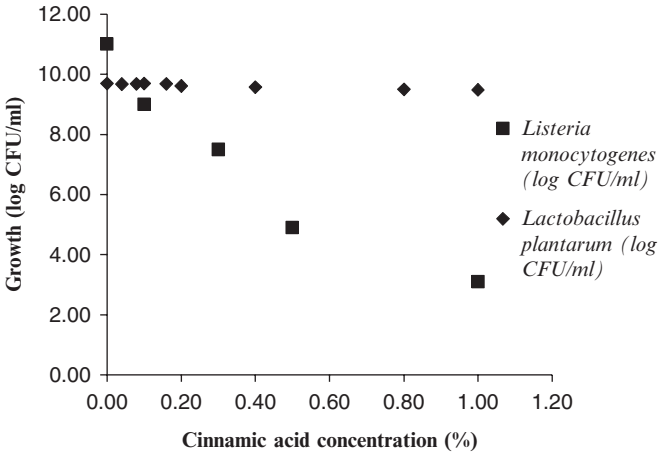

FIG. 23.3. Effect of *t*-cinnamic acid on the growth of *Listeria monocytogenes* and *Lactobacillus plantarum* after 24 h

proved to have a strong inhibitory action against *L. monocytogenes*, as shown in Fig. 23.3. The bacterial population decreased in direct proportion with the active compound concentration, as reported by Acero-Ortega et al. (2005). Kouassi and Shelef (1998) found that *t*-cinnamic acid had a higher antilisterial activity

than benzoic acid. As it is known, benzoic acid and its salts are widely used as preservatives in foods.

Given the results described above, it was interesting to find out if one of the active compounds (*t*-cinnamic acid) found in bell pepper extracts affects in different form the growth of the pathogenic bacterium and the beneficial one. The population of *Listeria* in the control after 24 h of incubation was of 10^{11} CFU/mL. The acid proved to have a strong inhibitory action against *L. monocytogenes*, as shown in Fig. 23.3. The bacterial population decreased in direct proportion with the active compound concentration, as reported by Acero-Ortega et al. (2005). Kouassi and Shelef (1998) found that *t*-cinnamic acid had a higher antilisterial activity than benzoic acid. As it is known, benzoic acid and its salts are widely used as preservatives in foods.

On the other hand, no inhibition of the growth of *Lb. plantarum* by *t*-cinnamic acid was found. This is very important, because it supports the idea of using this active compound in preserving dairy products, without the inhibition of beneficial bacteria such as *L. plantarum*. Among the cinnamic acids, *t*-cinnamic is the one with the lowest toxicity, it has an acceptable daily intake level of 1.25 mg/kg, and it has been approved for food use by the FDA (2003).

References

Acero-Ortega, C., Dorantes, L., Hernandez-Sanchez, H., Tapia, M.S., Gutierrez-Lopez, G., Alzamora, S., and Lopez-Malo A., 2005, Response Surface Analysis of the Effects of *Capsicum* Extract, Temperature and Ph on the Growth and Inactivation of *Listeria monocytogenes, J. Food Eng*. **67**:247.

Careaga, M., Fernandez, E., Dorantes, L., Mota, L., Jaramillo, M.E., and Hernandez-Sanchez H., 2003, Antibacterial Activity of *Capsicum* Extract Against *Salmonella typhimurium* and *Pseudomonas aeruginosa* Inoculated in Raw Beef Meat, *Int. J. of Food Microbiol*. **83**:331.

C.D.C., 2006, Coordinating Center for Infectious Diseases/Division of Bacterial and Mycotic Diseases, CDC, Atlanta, GA. (September 24, 2006); http://www.cdc.-gov/nci-dod/dbmd/diseaseinfo/ escherichiacoli_g_sp.htm.

Dorantes, L., Colmenero, R., Hernandez, H., Mota, L., Jaramillo, M.E., Fernandez, E., and Solano C., 2000, Inhibition of Growth of Some Foodborne Pathogenic Bacteria by *Capsicum annuum* Extracts, *Int. J. of Food Microbiol*. **57**:125.

Food and Drug Administration (FDA), 2003, Essential Oils, Oleoresins (Solvent Free), And Natural Extractives Including Distillates, in: *Code of Federal Regulations*, FDA Washington, **21**:4-1–03.

Halpin-Dohnalek, M.I., and Marth E.H., 1989. *Staphylococcus aureus*: Production of Extracellular Compounds and Behavior in Foods—A Review, *J. Food Protect*. **52**:267.

Jones M.J., 1992, *Food Safety*, Eagan Press, St. Paul, pp. 127–128.

Kouassi, Y., and Shelef L.A., 1998, Inhibition of *Listeria monocytogenes* by Cinnamic Acid: Possible Interaction of the Acid with Cysteynil Residues, *J. Food Saf*., **18**:231.

Rauha, J.P., Remes, S., Heinonenn, M., Hopia, A., Kahokonen, M., Kujala, T., Pihlaja, K., Vuorela, H., and Vuorela P., 2000, Antimicrobial Effects of Finish Plant Extracts Containing Flavonoids and Other Phenolics Compounds. *Int. J. Food Microbiol*, **56**:3.

Rico-Muñoz, E., Bargiota, E.E., and Davidson P.M., 1987, Effect of Selected Phenolic Compounds on the Membrane-Bound Adenosine Triphosphatase of *Staphylococcus aureus. Food Microb*. **4**:239.

Sutherland, J., and Varnam A., 2002, Enterotoxin-Producing *Staphylococcus, Shigella, Yersinia, Vibrio, Aeromonas* And *Plesiomonas*, in: *Foodborne Pathogens*, W. Blackburn and P.J. McClure (eds.), Woodhead Publishing Limited, Cambridge, pp. 385–415.

24
Predictive Equations to Assess the Effect of Lactic Acid and Temperature on Bacterial Growth in a Model Meat System

F. Coll Cárdenas, L. Giannuzzi, and N.E. Zaritzky

24.1. Introduction

Meat microflora is mainly composed of *Acinetobacter, Moraxella, Brochothrix termosphacta, Lactobacillus, Pseudomonas* and *Enterobacteriaceae* family genera, such as *Klebsiella sp*. and *E. coli*. In natural conditions meat pH can range from about 6.0 (being close to the optimum level for most pathogenic and alteration-causing bacteria) to values close to 5.5, at which microbial growth rate decreases significantly. Combining low pH with other factors such as low temperatures can almost completely prevent microbial growth from occurring. Muscle pH variation is highly dependent on the tissue glycogen level at the time of slaughter.

Weak organic acids tend to be more effective as antimicrobials than strong acids because they acidify the interior of the cell (Anderson et al., 1987). Antimicrobial activities exerted by organic acids depend upon i) pH reduction, ii) minimizing dissociation of the acid and iii) maximizing toxicity of the acid molecule (Anderson et al., 1987). Lactic acid produces an inhibitory effect because of the decrease in pH; this acid could act both on the meat muscle flora itself and on that of the fat, although such antimicrobial effect varies, not only according to the type of acid used, but also according to the microbial variety to be treated. Sometimes it could be bacteriostatic and sometimes it could have a bactericidal action. High efficiency in meat surface sanitization due to lactic acid addition has been widely reported (Nakai and Siebert, 2004).

The use of organic acids as decontaminants is an emerging preventive procedure, despite the fact that this application is not new. However, for reasons of solubility, taste and low toxicity, the short chain organic acids are more commonly used as preservatives or acidulating systems. Nevertheless, despite its effectiveness as a decontaminant, acetic acid has been considered unacceptable because of its pungent odor and its discoloration of the meat surface. Gil and Badoni (2004) have studied the effect of a 0.02% peroxyacetic acid solution, 0.16% sodium chloride with 2% and 4% lactic acid on the natural flora of the distal surfaces of chilled beef carcasses.

Peroxyacetic acid and the acidified sodium chloride solution had little effect on the number of aerobes, coliforms or *E. coli* on meat, and were less effective than 4% lactic acid for reducing the number of bacteria on meat. Lactic acid is an acceptable decontaminant because it is a natural, non-toxic, physiological product produced naturally in meat products, and it offers the possibility of reducing the contamination of carcasses, cuts and products. According to Snijders et al. (1984), the use of lactic acid as a terminal decontaminant in combination with perfect slaughter line hygiene produces both bactericidal and bacteriostatic effects that result in extended shelf life of meat.

Cudjoe (1988) studied the effect of lactic acid sprays on meat keeping qualities during storage. The spraying of the meat surface of a skinned cow head with 1% V/V lactic acid resulted in a significant reduction in total viable counts of bacteria during storage at 4°C, 15°C and 20°C. The shelf life of all sprayed heads was observed to have been extended to about three days at 4 °C and to one day at both 15°C and 20°C.

Predictive microbiology is a powerful tool for predicting microorganism growth rate under ambient conditions, with the aim of guaranteeing food quality and thereby determining its effective life. One of the most frequently used mathematical models is that of Gompertz (Gibson et al., 1988; Giannuzzi et al., 1998), which describes the microorganism response under different combinations of factors (Andrés et al., 2001). This model permits estimate parameters such as lag phase duration (LPD), specific growth rate (μ) and maximum cell concentration (MDP) of microorganisms under such conditions.

The objective of this work is to analyze and mathematically model the effect of storage temperatures (0°C, 4°C and 10°C) on the growth of three microorganisms isolated from beef samples: *Klebsiella sp., E. coli* and *Pseudomonas sp*., inoculated in a culture broth with different concentrations of lactic acid leading to pH values ranging between 5.6 and 6.1.

24.2. Materials and Methods

24.2.1. Isolation and Identification of the Microorganisms

Isolations were carried out using beef samples (about 100 g each), obtained in local markets, aseptically treated and collected in sterile bags. The samples were immediately carried to the laboratory, where 20 g of sub-samples were aseptically and randomly taken. Sub-samples were placed in sterile bags with 180 ml peptone water in 0.1% w/v solution (Merck KGaA, Darmstadt, Germany) and were homogenized for 1 min in Stomacher equipment (Model 400, Seward Medical, London, UK).

The isolations were performed using: i) bile agar red violet glucose culture medium (37°C for 24 h), and characterized through Gram coloration, catalase and oxidase, plus biochemical tests: Sensident EM-Iden Enterobacteriaceae (Merck KGaA, Darmstadt, Germany), according to MacFaddin (1979); ii) Agar Masurovsky (Masurovsky et al., 1965). The microorganisms were then

characterized through Gram coloration, oxidase test and oxide fermentation assay; iii) AOAC Method 46016 (AOAC, 1984), and isolated in lauril sulfate triptose (Merck KGaA, Darmstadt, Germany) at 37 °C for 48 h. Microorganisms giving positive results with the above techniques were inoculated in MacConkey broth (Merck KGaA, Darmstadt, Germany) as well as in EC (*Escherichia coli*) broth (Merck KGaA, Darmstadt, Germany), with incubation at 37 and 44.5 °C, respectively, for 48 h. Positive tubes were spread with EMB (Eosyn methylene blue) (Merck KGaA, Darmstadt, Germany) (37 °C, 48 h); typical metallic brightness colonies were isolated in nutritive agar (37 °C, 48 h) which were then identified through corresponding biochemical tests (IMViC) Indole, methyl red, Voges Proskauer, and Citrate (MacFaddin,1979).

24.2.2. Meat Model Broth System

A model system was prepared from a 2% meat extract solution (Merck), to which different lactic acid volumes were added to reach lactic acid concentrations of 0.28, 0.39 and 0.58 M. After sterilization, the pH values were 6.10, 5.80 and 5.60, respectively. The control medium at pH=7 (without acid addition) was also inoculated. Cell suspensions between 10^7 and 10^8 CFU/ml from each of the isolated bacteria were inoculated separately in 50 ml of the model system reaching up to concentrations ranging between 10^4 to 10^6 CFU/ml. Inoculated culture media were incubated at three storage temperatures (0°C, 4°C and 10°C) without agitation; at different storage times, aliquots were taken and microbial counts were determined in Agar Plate Count (37 °C, 48 h).

24.2.3. Mathematical Modeling

Mathematical models allow description of the effect of the main factors affecting microbial growth parameters. One of the most recommended models (Gibson et al., 1988; Andrés et al., 2001) is the Gompertz modified equation, the expression of which is:

$$\log N = a + c \exp(-\exp(-b(t-m))) \quad (24.1)$$

where log N is the decimal logarithm of microbial counts [log ($CFU.ml^{-1}$)] at time t, a is asymptotic log count as time decreases indefinitely (approximately equivalent to log of the initial level of bacteria) [log($CFU.ml^{-1}$)], c is log count increment as time increases indefinitely [log ($CFU.ml^{-1}$)], b [log ($CFU.ml^{-1}$ $days^{-1}$)] is the maximum growth rate at time m, and m is the time required to reach maximum growth rate (days). From these parameters, the following derived parameters were obtained: specific growth rate μ = b.c/e [log ($CFU.ml^{-1}$) $days^{-1}$] with e = 2.7182; lag phase duration LPD = m - (1/b) [days], maximum population density MPD= a + c [log ($CFU.ml^{-1}$)].

The Gompertz model was fitted to experimental values using a statistical software package (Systat Inc., 1990). The Systat software calculates the set of

parameters with the lowest residual sum of squares (RSS) and their 95% confidence interval.

The log linear regression model was applied when microbial counts in food remained constant or decreased during storage, as follows:

$$\log N = \log N_0 + \mu t \tag{24.2}$$

where log N [log (CFU.ml^{-1}) is the logarithm of the microbial counts at time t [days], N_0 is the initial microbial count, and μ is the regression slope [(CFU.ml^{-1})$^{-1}$days^{-1}] (Whiting, 1995), which is negative when there is a bactericidal effect. It was considered that microorganisms are in the lag phase when the slope gets a value lower than 0.01(CFU.ml^{-1})$^{-1}$days^{-1}, or when the difference between the final and the initial counts is lower than 0.5 logarithm cycle. Lag phase was calculated as the time necessary to increase initial microbial counts in 0.5 log cycle (LPD = 0.5/μ).

24.2.4. Experimental Design and Statistical Analysis

A full factorial analysis (4×3×3) was performed using four pH values in the meat broth (7.0, 6.1, 5.8 and 5.6), three storage temperatures (0°C, 4°C and 10°C) and three different inoculated microorganisms. Each set of experiments was run on duplicate samples. Analysis variance and comparison tests according to the Fisher significant differences table (LSD) were applied, with significance levels of 0.05 and 0.01.

24.3. Results and Discussion

24.3.1. Identification of the Isolated Bacteria

Isolated bacteria were identified as: i) *Klebsiella sp*., growing in bile agar red violet glucose culture medium, Gram negative, positive catalase, negative oxidase and subsequent identification through biochemical tests; ii) *Pseudomonas sp*., growing in Masurovsky agar, Gram negative, positive oxidase, not fermentative and with an oxidative metabolism; and iii) *E. coli* growing in EMB agar, Gram negative, lactose and glucose fermentative and characterized on the basis of biochemical tests IMViC.

24.3.2. Modeling of Klebsiella sp., Escherichia coli and Pseudomonas sp. Growth in Meat Broth Systems

Figure 24.1a, b and c shows an example of microbial counts of *Klebsiella sp*. inoculated in the meat broth with different added lactic acid concentrations and stored at 0°C, 4°C and 10°C. As can be observed, linear and non linear

(Gompertz) regressions applied to the bacterial count. Gompertz, derived parameters, and linear regression coefficients for the three bacteria are shown in Table 24.1. In all cases, the decrease in temperature and the added lactic acid led to a decrease in growth rate (μ), as well as a decrease in maximum population density (MPD) and a progressive increase of the lag phase (LPD).

Growth rate values for *Klebsiella* notably decreased along with the decrease in temperature; at pH 5.6 and at 10°C, a μ value of 0.60 log (CFU/ml) days^{-1} was obtained; at 4°C such value decreased 3 times, and at 0°C a maximum reduction in growth rate of up to 10 times was observed for this bacterium.

Lag phase values range proximately 33.3 days at 0°C; at 4°C, lag phase ranged between 2.51 and 2.62 days, and at 10°C it ranged from 0.62 to 4.14 days for the different pH values assayed. *E. coli* did not grow at 0°C and 4°C; at 10°C, lag phase varied between 3.00 and 6.57 days at pH 7.0 and 5.6, respectively.

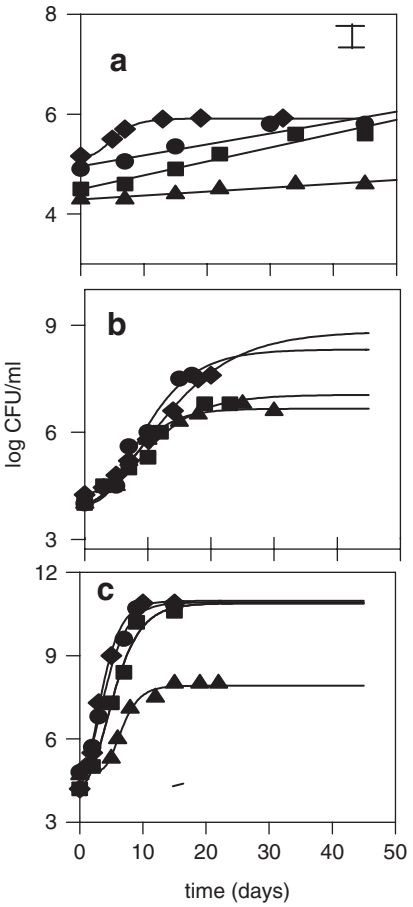

FIG. 24.1. Effect of temperature and pH (reached by addition of lactic acid) on the growth of *Klebsiella sp*. in a meat model system. Full lines correspond to Gompertz or linear model at a) 0°C, b) 4°C;c) 10°C, at different pH values: ♦7.0, ■ 6.10, ● 5.80, ▲ 5.6

TABLE 24.1. Application of Gompertz equation and the linear model to assess the effect of pH and temperature on microbial growth of *Klebsiella sp., Pseudomonas sp.* and *Escherichia coli* in a model meat system

		Gompertz parameters				Derived parameters			
T°C	pH	a	c	b	m	μ	LPD	MPD	$t10^6$(days)
				Klebsiella sp.					
0	7.0	5.15±0.01	0.76±0.01	0.42±0.01	4.46±0.01	0.12	2.1	6.77	28
	6.1	—	—	—	—	0.03	16.6	—	>50
	5.8	—	—	—	—	0.02	25.0	—	>50
	5.6	—	—	—	—	0.015	33.3	—	>50
4	7.0	4.12±0.15	4.71±0.63	0.13±0.02	10.21±0.82	0.22	2.51	8.82	10.9
	6.1	3.93±0.41	4.39±1.40	0.19±0.11	7.85±1.64	0.20	2.54	8.32	9.35
	5.8	3.97±0.22	3.08±0.43	0.18±0.05	8.05±0.94	0.19	2.55	7.05	12.9
	5.6	3.96±0.13	2.70±0.16	0.26±0.04	6.46±0.48	0.19	2.62	6.66	11.4
10	7.0	4.08±0.43	6.88±0.53	0.49±0.08	2.65±0.33	1.24	0.62	10.97	2.2
	6.1	4.69±0.34	6.23±0.48	0.43±0.08	3.28±0.34	0.98	0.96	10.92	2.2
	5.8	4.18±0.55	6.70±0.87	0.35±0.10	4.28±0.69	0.86	1.43	10.88	3.6
	5.6	4.83±0.13	3.09±0.17	0.53±0.18	6.03±0.27	0.60	4.14	7.92	6.1
				Escherichia coli					
0	7.0	—	—	—	—	0.013	38	—	>50
	6.1	—	—	—	—	0.006	50	—	>50
	5.8	—	—	—	—	0.003	50	—	>50
	5.6	—	—	—	—	0.003	50	—	>50
4	7.0	—	—	—	—	0.05	10.0	—	>50
	6.1	—	—	—	—	0.04	12.5	—	>50
	5.8	—	—	—	—	0.03	16.6	—	>50
	5.6	—	—	—	—	0.02	25.0	—	>50
10	7.0	4.24±0.21	4.41±0.27	0.58±0.14	4.85±0.28	0.95	3.00	8.65	5.0
	6.1	4.32±0.45	4.14±0.57	0.51±0.23	4.94±0.70	0.80	3.00	8.46	5.2
	5.8	4.20±0.43	4.20±0.54	0.51±0.27	5.20±0.64	0.80	3.27	8.40	5.5
	5.6	4.39±0.001	1.77±0.001	0.6±0.001	8.09±0.001	0.43	6.57	6.16	12.4

				Pseudomonas sp.					
0	7.0	4.33±0.03	1.06±0.06	0.10±0.01	21.21±1.30	0.08	11.2	5.40	>50
	6.1	4.25±0.08	1.16±0.16	0.10±0.03	2 1.50±3.12	0.04	11.5	5.41	>50
	5.8	4.40±0.06	1.00±0.15	0.08±0.02	22.86±2.80	0.03	11.7	5.40	>50
	5.6	3.89±0.02	1.11±0.05	0.14±0.03	22.19±1.60	0.05	15.0	5.01	>50
4	7.0	3.40±0.40	6.05±0.62	0.16±0.03	11.65±1.44	0.36	4.99	9.45	12.8
	6.1	3.48±0.28	6.11±0.43	0.14±0.02	12.23±1.03	0.32	5.04	9.59	13.1
	5.8	3.44±0.22	5.62±0.31	0.15±0.02	11.43±0.69	0.30	5.53	9.06	13.1
	5.6	3.25±0.48	5.05±0.71	0.12±0.07	11.53±1.64	0.22	6.45	8.30	15.7
10	7.0	3.51±0.85	5.89±1.02	0.26±0.07	3.89±1.240	0.56	0.04	9.40	4.5
	6.1	3.26±0.80	6.12±0.90	0.25±0.07	3.90±1.120	0.56	0.06	9.38	4.8
	5.8	2.73±0.39	6.13±0.49	0.24±0.03	4.54±0.590	0.55	0.45	8.86	6.6
	5.6	2.74±0.65	5.69±1.19	0.25±0.12	8.09±1.470	0.54	4.15	8.43	10.5

a: log(CFU/ml), c: log (CFU/ml), b: $days^{-1}$, m: days, μ: log (CFU/ml)$days^{-1}$, MPD: (log(CFU/ml), LPD: (days). A line in the table indicates that a linear regression was applied in this case

MPD values for the two *Enterobateriaceae* (*Klebsiella sp*. and *Escherichia coli*) diminished with decrease in temperature and pH; thus, for *Klebsiella sp*. at pH 5.6 and at 10°C, LPD was 7.92 log (CFU/ml), decreasing to 6.66 log (CFU/ml) at 4°C. *Pseudomonas* also showed low μ values at 0°C increased between 4 and 10 times at 4°C and between 7 and 18 times at 10°C; for the lag phase, values between 11.2 and 15.0 days at 0°C were obtained, decreasing between 5.00 and 6.45 days at 4°C and reaching the lowest values of 0.04 and 4.15 days at 10°C.

In addition, both at 10°C and at 4°C, maximum population densities did not show great variation between them, ranging between 8.30 and 9.59 log (CFU. ml^{-1}). None of the tested conditions showed bactericidal effect.

24.3.3. Effect of Temperature on Specific Growth Rate (μ)

The effect of temperature on specific growth rate (μ) was modeled through an Arrhenius type equation:

$$\mu = A.\exp(-E\mu/RT) \tag{24.3}$$

where T is the temperature in °K, Eμ is the activation energy (KJoule/mol), A is a pre-exponential factor and R is the gas constant (8.31 KJoule/°K mol). Activation energy (E_μ) can be considered as sensitivity of specific growth rate to thermal changes. E_μ values and regression coefficients for *Klebsiella sp., E. coli* and *Pseudomonas sp*. at the different tested pH are shown in Table 24.2.

Table 24.2. Application of the Arrhenius type equation to evaluate the effect of temperature on the specific growth rate (μ) of *Klebsiella sp., Pseudomonas sp*. and *E. coli* at different pH values

pH	LnA[ln(CFU/ml)days^{-1}]	Eμ[KJoule/mol]	R^2 coefficient of determination
	Klebsiella sp.		
7.0	90.55	210.8±8.8	0.89
6.1	137.9	320.2±1.5	0.99
5.8	149.1	347.4±4.2	0.99
5.6	178.1	416.5±1.1	0.96
	Escherichia coli		
7.0	105.1	244.4±6.1	0.96
6.1	104.3	242.4±7.3	0.95
5.8	140.1	332.4±9.0	0.99
5.6	194.2	451.4±5.9	0.99
	Pseudomonas sp.		
7.0	120.54	279.3±8.2	0.99
6.1	106.11	257.8±10.5	0.94
5.8	117.23	273.4±8.8	0.93
5.6	94.07	277.2±12.1	0.99

Activation energy values (E_μ) for each microorganism were affected by the different pH, thus obtaining the lower E_μ values at pH 7 for *E. coli* and *Klebsiella sp*. E_μ values for *Pseudomonas sp*. did not show significant variations at the different pH values, ranging between 257.8 and 279.3 KJoule/mol. The effect of pH on decreasing E_μ was more notable for the *Enterebacteriaceae* than for *Pseudomonas sp*.

24.3.4. Effect of Undissociated Acid Concentration on the Derived Parameters μ and LPD

Antimicrobial effect of organic acids is mainly due to its undissociated fraction rather than hydrogen ions. Undissociated acid concentration (uac) from a monoprotic acid such as lactic acid can be calculated through the following expression:

$$[uac] = Ca\ [H^+]/ ([H^+] + K) \tag{24.4}$$

where Ca is the added acid total concentration (0.29, 0.39 and 0.58M), $[H^+]$ is the proton concentration and K the lactic dissociation constant ($10^{3.86}$); uac values, calculated by applying Eq. (24.4) for the different pH (6.10, 5.80 and 5.60) are $1.66.10^{-3}$, $4.42.10^{-3}$ and $1.01.10^{-2}$ M, respectively; at pH = 7, without added lactic acid (Ca=0) and uac =0.

Fig. 24.2a, b and c shows the effect of uac on μ values at the three studied temperatures for *Klebsiella sp., E. coli* and *Pseudomonas sp*., respectively. In all cases the parameter μ decreased when uac increased. It can be observed that for the three microorganisms *Klebsiella sp., E. coli* and *Pseudomonas sp*. at 0°C and 4°C, there were no variations in μ values with an increase of the undissociated acid concentration (uac), whereas at 10°C a variation in the μ values was evidenced with an increase in uac. A linear regression was applied to μ values as a function of the undissociated acid concentration (uac) according to the following equation:

$$\mu = p + q\ .\ (uac) \tag{24.5}$$

A linear correlation between μ values and uac was obtained for the three bacteria. The coefficients p and q of Eq. (24.5) and the determination coefficients (R^2) for each linear regression are shown in Table 24.3. It can be observed that the specific growth rate values of the analyzed enterobacteria (*Klebsiella sp*. and *E. coli*) were more dependent on pH than in the case of *Pseudomonas sp., which is* in agreement with the results reported by Gill and Newton (1982), who used lactic acid for adjusting pH to 5.5 and 6.0 with an incubation temperature of 2 °C; the values measured in the present work were 0.01 log (CFU/ml) $days^{-1}$ at pH 5.6 and 0.03 log (CFU/ml) $days^{-1}$ at pH 6.1 for the particular case of *Klebsiella sp*., while μ values ranged between 0.003 and 0.006 log (CFU/ml) $days^{-1}$ at pH 5.6 and 6.1, respectively, for *E. coli*.

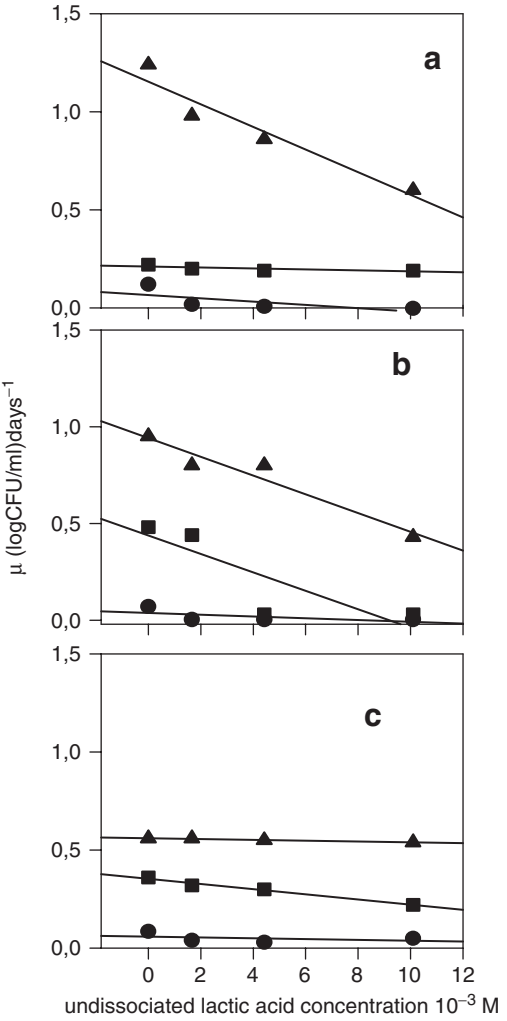

FIG. 24.2. Effect of the undissociated acid concentration (uac) on μ values at different temperatures: ● 0°C, ■ 4°C, ▲ 10 °C; a) *Klebsiella sp*., b) *Escherichia coli, c*) *Pseudomonas sp*.

The parameter LPD increased along with the increasing of uac for the three bacteria. The highest LPD values were obtained for *E. coli*, followed by *Pseudomonas* and *Klebsiella*. At 0°C *Klebsiella sp*. was the most affected by pH variation; thus, at pH 7, LPD value was 2.1 days, whereas with 10.1 mM undissociated lactic acid (pH=5.6), LPD value was 33.3 days. For this microorganism lag phase duration was the most affected by lactic acidity. A linear regression

between LPD values and the undissociated acid concentration (uac) was applied according to the following equation:

$$LPD = p' + q' \, (uac) \tag{24.6}$$

Satisfactory linear regressions between LPD and uac values were obtained for the three bacteria. The coefficients of the linear regressions (p′, q′) for each microorganism are shown in Table 24.3. As can be observed, LPD values of *Klebsiella sp*. and *E. coli* were the most sensitive to the pH given by added lactic acid.

The simultaneous effects of both storage temperature and undissociated acid concentration (uac) on μ values for each microorganisms are shown in Fig. 24.3a, b, and c. From the obtained Gompertz parameters it was possible to estimate the time necessary to reach microbial counts of 10^6 CFU/ml under different tested conditions, noting that a temperature of 0°C and pH of 5.6 by addition of lactic acid extends this time to more than 50 days.

24.4. Conclusions

In the present work, the growth of three isolated bacteria from beef (*Klebsiella sp., Escherichia coli* and *Pseudomonas sp*.) were analyzed in a meat broth system and modeled at different temperatures (0°C, 4°C and 10°C) and pH levels (7.0, 6.1, 5.8 and 5.6) reached by adding different concentrations of lactic acid. The

TABLE 24.3. Coefficients of the linear regressions obtained for μ (specific growth rate, p, q) and LPD (lag phase duration, p′, q′) as functions of the undissociated lactic acid concentration (uac) at 0°C, 4°C and 10°C for *Klebsiella sp., Escherichia coli* and *Pseudomonas sp*. p and q are the coefficients of the linear regression given by Eq. (24.5). p′ and q′ are the coefficients of the linear regression given by Eq. (24.6)

Temperature (°C)	p	q	R^2	p′	q′	R^2
			Klebsiella sp.			
0	0.09	−0.008	0.86	8.21	2.64	0.86
4	0.20	−0.008	0.89	2.51	0.01	0.97
10	1.15	−0.057	0.93	0.36	0.35	0.95
			Escherichia coli			
0	0.94	−0.048	0.94	44.72	0.69	0.67
4	0.43	−0.048	0.77	10.02	1.48	0.99
10	0.038	−0.004	0.79	2.47	0.37	0.87
			Pseudomonas sp.			
0	0.56	−0.002	0.96	10.80	0.38	0.91
4	0.35	−0.001	0.98	4.89	0.15	0.98
10	0.059	−0.002	0.73	0.35	0.35	0.89

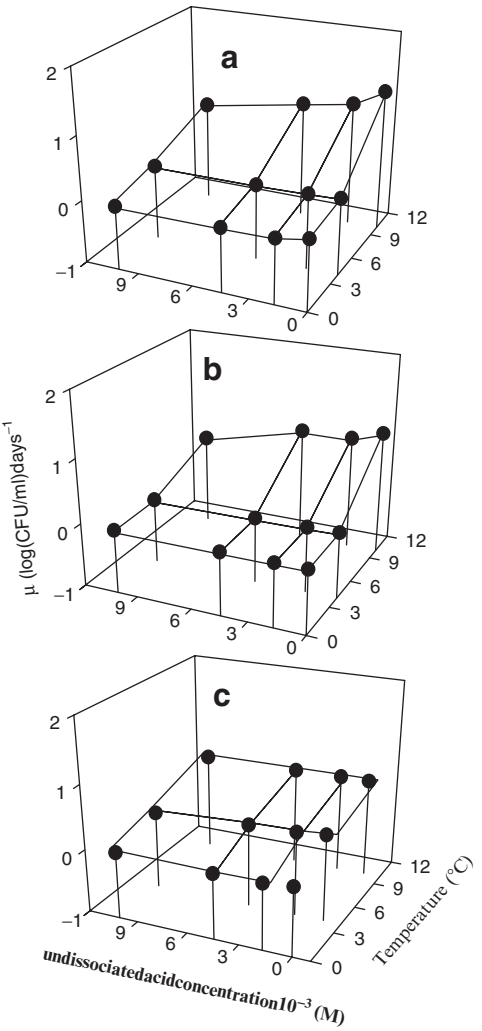

FIG. 24.3. Simultaneous effect of temperature and undissociated acid concentration (uac) on μ values for a) *Klebsiella sp*., b) *Escherichia coli, c*) *Pseudomonas sp*.

highest values of μ and LPD were observed for *Klebsiella sp*. and *Pseudomonas sp*., respectively. LPD of *Klebsiell*a *sp*. was the most affected by lactic acidity.

The effect of temperature on μ values was modeled through an Arrhenius type equation, determining the corresponding activation energies. The highest activation energy was obtained for *Klebsiella sp*. at pH 6.1 and 5.6.

Satisfactory correlations between μ and LPD with the undissociated acid concentration were obtained for the three microorganisms at the tested temperatures.

Lactic acid is a natural non-toxic decontaminant that can be applied in the food industry for the sanitization of meat surfaces.

Acknowledgements The authors gratefully acknowledge the financial support given by the Universidad Nacional de La Plata, CONICET and the Agencia Nacional de Promoción Científica y Tecnológica of Argentina.

References

Anderson, G.R., Vanderzant, C., Savell, J.W., Jones, D.R., Griffin, D.K., and Ehlers J.D., 1987, Effect of Decontamination of Beef Subprimal Cuts on the Microbiological and Sensory Characteristics of Steaks. *Meat Science* **19**:217–226.

Andrés, S., Giannuzzi, L., and Zaritzky N.E., 2001, Mathematical Modelling of Microbial Growth in Packaged Refrigerated Orange Juice Treated with Chemical Preservatives, *J. Food Sci*. **66**:724–728.

AOAC, 1984, *Official Methods of Analysis*. 14th ed. Assoc. Official Agric. Chemists. Washington, D.C.

Cudjoe, K., 1988, The Effect of Lactic Acid Sprays on the Keeping Qualities of Meat During Storage, *Int. J. Food Microbiol*. **7**:1–7.

Giannuzzi, L., Pinotti, A., and Zaritzky N., 1998, Mathematical Modelling of Microbial Growth in Packaged Refrigerated Beef Stored at Different Temperatures, *Int. J. Food Microbiol*. **39**:101–110.

Gibson, A.M., Bratchell, N., and Roberts, T.A., 1988, The Effect of Sodium Chloride and Temperature on Rate and Extent of Growth of *Clostridium botulinum* Type A in Pasteurized Pork Slurry, *J. Appl. Bacteriol*. **62**:479–490.

Gill, C., and Newton K., 1982, Effect of Lactic Acid Concentration on Growth on Meat of Gram–Negative Psychrotrophs from a Meatworks, *Appl. Environ. Microbiol*. **43**:284–288.

Gill, C.O., and Badoni M., 2004, Effects of Peroxyacetic Acid, Acidified Sodium Chlorite or Lactic Acid Solutions on the Microflora of Chilled Beef Carcasses, *Int. J. Food Microbiol*. **91**:43–50.

MacFaddin, J.F., 1979, *Biochemical Test for Identification of Medical Bacteria*. Baltimore: The Williams & Wilkins Company.

Masurovsky, E.B., Goldblith, S.A., and Voss J., 1965, Differential Medium for Selection and Enumeration of Members of the *Pseudomonas, J. Bacteriol*. **85**: 722.

Nakai, S.A., and Siebert K.J., 2004, Organic Acid Inhibition Models for *Listeria innocua, Listeria ivanovii, Pseudomonas aeruginosa* and *Oenococcus oeni, Food Microbiol*. **21**(1):67–72.

Snijders, J.M.A., van Logtestijn, T.G., Mossel, D.A.A., and Smulders F.T.M., 1984, Conditions for the Use of Lactic Acid as a Decontaminant in the Meat Industry, *Proc. Eur. Meet. Meat Res. Work* **30**:232–233.

Whiting, R., 1995, Microbial Modeling in Foods, *Food Sci. Nutr*. **35**:467–494.

25
Free-Choice Profiling of Passion Fruit Juice Processed by High Hydrostatic Pressure

R. Deliza, L.H.E.S. Laboissiere, A. Rosenthal,
A.M. de B. Marcellini, and R.G. Junqueira

25.1. Introduction

High hydrostatic pressure (HHP) refers to the process that subjects food to pressures ranging from 100 MPa to 900 MPa and, in commercial systems, between 300 MPa and 700 MPa (San Martín et al., 2002). The use of HHP has been explored extensively in the food industry and related research institutions due to increased consumer demand for improved nutritional and sensory characteristics of food without loss of "fresh" taste (Rosenthal and Silva, 1997; Tewari et al., 1999; Deliza et al., 2005). Heat leads to quality deterioration in certain foods by producing undesirable changes in their sensory and nutritional characteristics due to the slow heating and cooling rates (Thakur and Nelson, 1998). At ambient temperatures, application of pressures in the range of 300–500 MPa inactivates vegetative microorganisms and reduces the activity of enzymes, combined with the retention of small molecules responsible for taste, color and many vitamins. This process yields a pasteurized product that can be stored for a considerable time at 4–6 °C (Cheftel, 1995). The non-thermal pasteurization of fruit products using HHP offers the chance of producing food of high quality, greater safety and increased shelf-life (Butz et al., 2003).

Passion fruit is an ovoid shaped fruit that yields a juice with a very strong, exotic flavor and a bright orange color. Despite being marketed worldwide, few articles on this fruit have been reported in the literature (Deliza et al., 2004). The evaluation of the sensory quality of passion fruit is essential to facilitate its use in juice formulations. This evaluation can be carried out using conventional profiling techniques, such as Quantitative Descriptive Analysis (QDA), or, alternatively, Free Choice Profiling (FCP). QDA involves discriminating and description of both the qualitative and quantitative sensory components of a product by trained panels of judges (Stone and Sidel, 2004). The qualitative aspects of a product include appearance, aroma, flavor and texture. By using Quantitative Descriptive Analysis (QDA), trained panelists characterize and quantify the sensory properties of a food. However, this methodology is time consuming because assessors are trained to use a common "frame

of reference" to define product attributes (Jahan et al., 2005). Free Choice Profiling (FCP) is a sensory methodology where untrained assessors are allowed to use their own vocabulary for characterizing and scoring samples (Williams and Langron, 1984). FCP is a sensory methodology developed to avoid two major conventional flavor profiling disadvantages: the necessity of having a common vocabulary of attributes to describe the samples, and a pre-established measure of agreement among the panelists on their interpretation and meaning of the terms they will employ. The terms used by panelists vary, based on individual experience and familiarity with the product. FCP is similar to traditional profiling in the sense that assessors must be able to detect differences between the samples, verbally describe the perceived attributes, and quantify them (Oreskovich et al., 1991).

FCP was created to assist the demands of marketing and product development teams, which required information on consumers' perceptions of a product rather than the more technical description typically produced by trained panels (Murray et al., 2001). Several studies on different products have been carried out using this method (Deliza et al., 2004; Jahan et al., 2005; Vi as et al., 2001; Piggott et al., 1991). The aim of this study was to obtain a consumer vocabulary from FCP of natural and HHP processed passion fruit juices as well as five commercial thermally treated juices.

25.2. Passion Fruit Purée High Pressure Processing

Passion fruit purée was collected in a fruit juice factory before any thermal treatment, and conditioned in 500 mL plastic bottles. The purée was immediately transported to Embrapa Food Technology at 5 ± 2°C, and the bottles were stored in the freezer at −18°C after arrival, until the day before the beginning of the study. Commercial sugar was added to the passion fruit purée to obtain the basis for a ready-to-drink juice. Fruit juice consumers determined the optimum passion fruit juice sugar level according to Deliza (2001). The sweetened purée was packed in polyethylene bags, heat sealed (Fig. 25.1) and stored at 4 ± 2°C until the pressurization treatment.

Pressurization of samples at 300 MPa for 5 min at room temperature was carried out using a Stansted Food Lab 9000 (Stansted Fluid Power Ltd., England) isostatic high-pressure chamber and yielded the sample designated "pressurized." Details of the process can be found in Rosenthal et al. (2005).

25.3. Free-Choice Profiling

Seven fruit juice samples comprising pressurized passion fruit juice, non-treated passion fruit juice (from the non-pressurized purée), and five commercial thermally processed juices available in the Brazilian market were evaluated using FCP. The commercial products were coded as C1, C2, C3, C4 and C5.

FIG. 25.1. Detail showing heat-sealing of polyethylene bags with passion fruit purée

HHP treated passion fruit purée was diluted with water at a previously determined ideal dilution level (Laboissiere et al., 2005). The FCP was carried out in two sessions. During the first session, eight consumers (two males and six females recruited from the Embrapa Food Technology staff) were asked to observe, smell and taste the seven different passion fruit juices and to describe, using their own words, the appearance, aroma, flavor and consistency of samples. Samples were served at 8 ± 1°C in 50 mL transparent plastic cups. During the second session, each consumer was asked to define the list of descriptive terms created in the first session, and to evaluate samples using his/her own terms. Individual score cards were prepared, and each assessor evaluated the intensity of each descriptor by placing a mark in an unstructured 9 cm line scale, anchored with the words "weak" and "strong" (Oreskovich et al., 1991). In profiling, seven juices were scored monadically per session in sensory booths, in triplicate, using a balanced presentation order design (MacFie et al., 1989) over three days. Samples were presented at 8 ± 1°C in 50 mL transparent plastic cups coded with three digit numbers. Water and unsalted biscuits were provided for cleansing the palate.

Generalized Procrustes Analysis (GPA) was carried out on the consumer data using the XLSTAT software, and a consensus matrix was obtained by mathematical data operations (translation, rotation/reflection and scaling analysis) according to Arnold and Williams (1986). The optimum consensus is the average of all transformed configurations that show minimum overall deviation. It summarizes the information about samples and replaces the panel mean (Deliza et al., 2004; Langron et al., 1984).

Participants in this study generated 1 to 6 attributes for appearance, 1 to 10 for aroma, 2 to 9 for flavor, and 1 to 4 for consistency. The most cited attributes were:

orange color and presence of particles for appearance; natural and artificial for aroma; and natural, artificial, characteristic, sweet and sour for flavor.

Figures 25.2 and 25.3 show the results for the aroma and flavor evaluation, respectively. First and second dimensions explained 83.9% total variance for

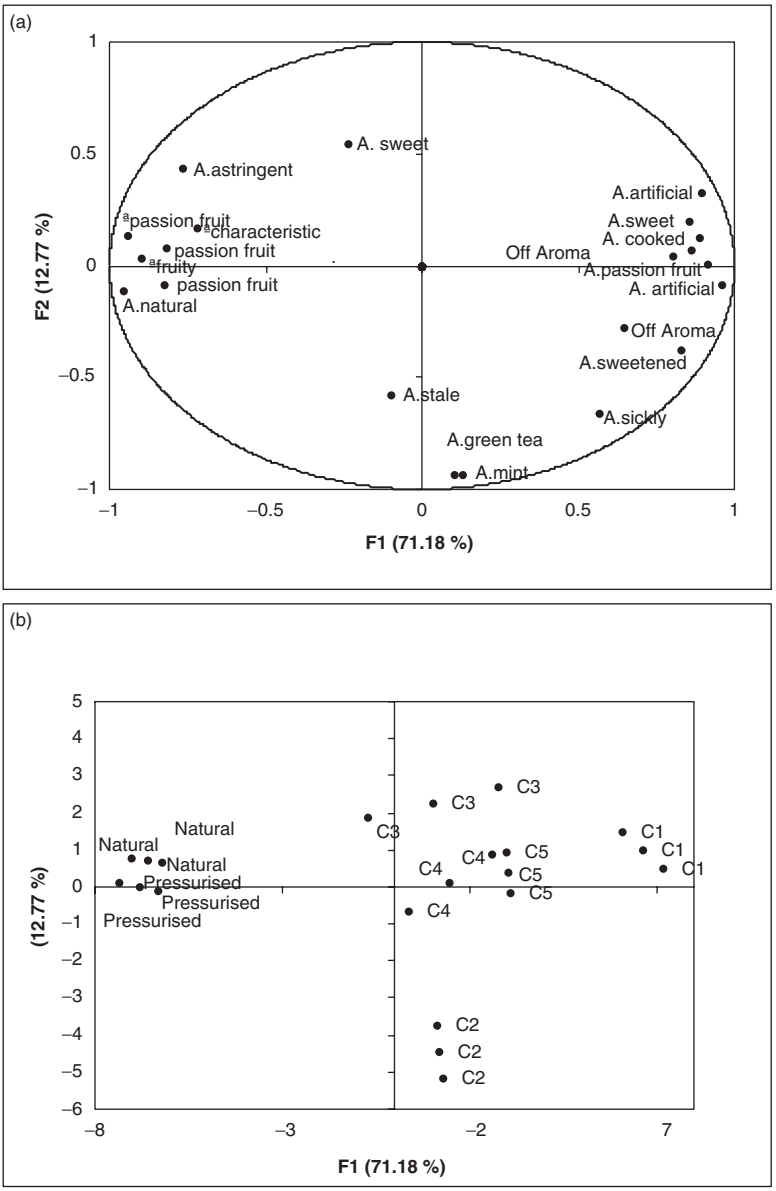

FIG. 25.2. GPA product space from FCP of passion fruit juices: (a) aroma attributes, (b) product space for aroma, in the plane defined by the first two dimensions of the consensus configuration

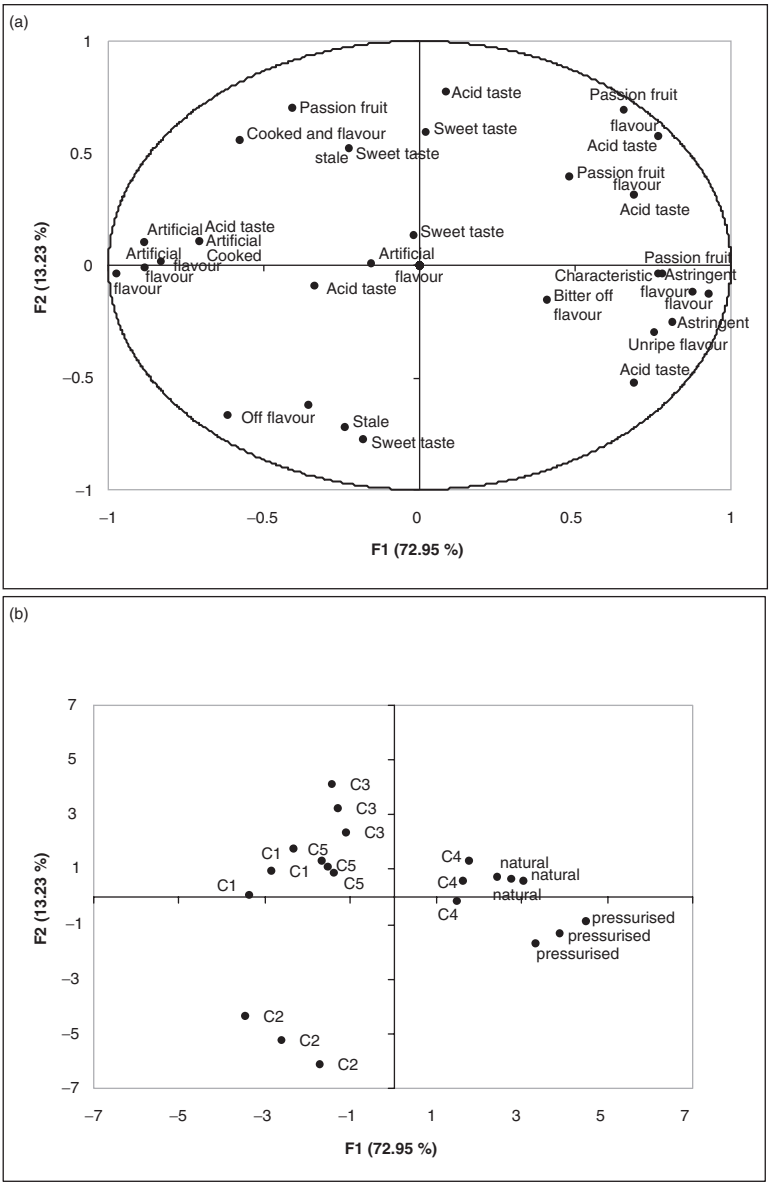

FIG. 25.3. GPA product space from FCP of passion fruit juices: (a) flavor attributes, (b) product space for flavor, in the plane defined by the first two dimensions of the consensus configuration

aroma. Looking at the attribute space (Fig. 25.2a) and the product space (Fig. 25.2b) for aroma, one can see that the juices prepared with the pressurized purée and the non-treated purée were perceived as having aroma characteristics of passion fruit and natural aroma. On the other hand, all commercial

juices (C1–C5) were described by assessors as artificial, cooked, stale, and having off-aroma.

Regarding the flavor results, the first and second dimensions accounted for 86.2% of the variance. Figure 25.3 shows that pressurized and non-treated juices were described with the attributes of acid taste, unripe, astringent, characteristic of passion fruit, and passion fruit. The commercial heat-treated passion fruit juices were perceived as artificial, having a stale flavor, cooked, and off-flavor. Juice C4 presented flavor attributes more similar to the pressurized and natural juices.

Taking into account the appearance and consistency product attributes, the results have shown high similarity between the juice prepared with the pressurized purée and the non-treated passion fruit juice. Sensory differences among these two juices and the commercial juices were perceived and described by consumers.

The results of this study allow one to conclude that samples were well separated in the plan defined by the first and second dimensions, demonstrating that assessors could discriminate pressurized and natural juices from the commercial thermally treated juices. This result suggests that FCP was an adequate tool to describe and quantify yellow passion fruit juice sensory attributes. Pressurized juice presented sensory attributes similar to the natural sample, ratifying the advantage of using high pressure on the product sensory attributes.

Acknowledgements The authors would like to thank Prodetab and CNPq for their financial support.

References

Arnold, G.M., and Williams A.A., 1986, The Use of Generalized Procrustes Techniques in Sensory Analysis, in: *Statistical Procedures in Food Research*, J.R. Piggott (ed.), Elsevier, London, pp. 233–253.

Butz, P., Fernández García, A., Lindauer, R., Dieterich, S., Bognár, A., and Tauscher B., 2003, Influence of Ultra High Pressure Processing on Fruit and Vegetable Products, *J. Food Eng*. **56**:233.

Cheftel J.C., 1995, High Pressure, Microbial Inactivation and Food Preservation, *Food Sci. Technol*. **1**:75.

Deliza R., 2001, The Use of Ideal Point Scale to Determine the Best Sugar and Dilution Levels of Passion Fruit Juice by Consumers, *Alimentaria*, **38**:109.

Deliza, R., MacFie, H., and Hedderley D., 2004, The Consumer Sensory Perception of Passion–Fruit Juice Using Free–Choice Profiling, *J. Sens. Stud*. **19**:577.

Deliza, R., Rosenthal, A., Abadio, F.B.D., Silva, C.H.O., and Castillo C., 2005, Application of High Pressure Technology in the Fruit Juice Processing: Benefits Perceived by Consumers, *J. Food Eng*. **67**:241.

Jahan, K., Paterson, A., and Piggott J.R., 2005, Sensory Quality in Retailed Organic, Free Range and Corn–Fed Chicken Breast, *Food Res. Internat*. **38**:495.

Laboissiere, L.H.E.S., Deliza, R., Rosenthal, A., Junqueira, R.G., and Barros A.M., 2005, Optimum Yellow Passion Fruit (*Passiflora edulis* Sims f. flavicarpa Degener)

Juice Formulation Based on Consumer Evaluation, in: *6th Pangborn Sensory Science Symposium*, Rubes Editoial S. L., Minneapolis, p. 119.

Langron, S.P., Williams, A.A., and Collins A.K., 1984, A Comparison of the Consensus Configuration from a Generalised Procrustes Analysis with the Untransformed Panel Mean in Sensory Profile Analysis. *Lebensm.–wiss. U. Technol*. **17**:296.

MacFie, H.J.H., Bratchell, N., Greenhoff, K., and Vallis L.V., 1989, Designs to Balance the Effect of Order of Presentation and First–Order Carry–Over Effects in Hall Tests, *J. Sensory Stud*. **4**:129.

Murray, J.M., Delahunty, C.M., and Baxter I.A., 2001, Descriptive Sensory Analysis: Past, Present And Future, *Food Res. Int*. **34**:461.

Oreskovich, D.C., Klein, B.P., and Sutherland J.W., 1991, Procrustes Analysis and Its Application to Free Choice and Other Sensory Profiling, in: *Sensory Science Theory and Application in Foods*, H.T. Lawless and B.P. Klein (eds.), Marcel Dekker, New York, pp. 353–394.

Piggott, J.R., Sheen, M.R., and Apostolidou S.G., 1991, Consumers' Perceptions of Whiskies and Other Alcoholic Beverages, *Food Quality and Preference* **2**:177.

Rosenthal, A., Deliza, R., Siqueira, R.S., Laboissiere, L.H.E.S., Camargo, L.M.A., and Marcellini A.M.B., 2005, Polpa de Maracujá Processada por Alta Pressão Hidrostática, Rio de Janeiro: Embrapa Agroindústria de Alimentos, 2005. (Embrapa Agroindústria de Alimentos. *Comunicado Técnico*, 91).

Rosenthal, A., and Silva J.L., 1997, Alimentos Sob Pressão, *Engenharia de Alimentos* **14**:37.

San Martín, M.F., Barbosa–Cánovas, G.V., and Swanson B.G., 2002, Food Processing by High Hydrostatic Pressure, *Crit. Rev. Food Sci. Nutr*. **42**:627.

Stone, H., and Sidel J., 2004, *Sensory Evaluation Practices*, Academic Press, London, p. 311.

Tewari, G., Jayas, D.S., and Holley R.A., 1999, High Pressure Processing of Foods: An Overview, *Sci. des Aliments* **19**:6*19*.

Thakur, B.R., and Nelson P.E., 1998, High–Pressure Processing and Preservation of Food, *Food Rev. Int*. **14**:427.

Vi as, M.A.G., Garrido, N., and Penna W., 2001, Free Choice Profiling of Chilean Goat Cheese, *J. Sensory Stu*. **16**:239.

Williams, A.A., and Langron S.P., 1984, The Use of Free Choice Profiling for Evaluation of Commercial Ports, *J. Sci. Food Agric*. **35**:558.

26
Effect of High Temperature on Shrinkage and Porosity of Crispy Dried Bananas

K. Hofsetz, C. Costa Lopes, M.D. Hubinger, L. Mayor, and A.M. Sereno

26.1. Introduction

The most common drying method employed for food materials is hot air drying. This process involves high temperatures and long drying times, which can lead to considerable shrinkage of the final product.

Freeze-drying yields products with high quality and little or no shrinkage, but it is more expensive than hot air drying (Ratti, 2001; Lozano and Saca, 1992; Jayaraman and Das Gupta, 1992).

Another alternative, and a cheaper one, for producing materials with quality similar to freeze-dried products is called "puffing." A puffing process involves the release or expansion of a vapor or gas within a product, either to create an internal structure or to expand or rupture an existing one.

Methods to obtain puffing include explosion puffing, high temperature fluidized beds, extrusion, the application of vacuum drying and a high temperature pulse combined with conventional hot air drying.

During high temperature application, the moisture turns into vapor that builds up pressure, forcing the walls from the inside out, creating a porous structure and increased volume (Varnalis et al., 2001; Payne et al., 1989), which must be further air-dried to reduce water activity to the range of values that does not allow microbiological activity and where the chemical and biochemical reactions rates are reduced to their minimum (Toledo, 1991; Katz and Labuza, 1981).

Therefore, the objectives of this work were: (1) to study the effect of HTST pulse on shrinkage and porosity of bananas; (2) to study the effect of the conventional air drying process (ADP) on shrinkage and porosity of bananas and to compare with the results obtained in (1); (3) to observe structural changes in the banana for both processes, and to try to relate these changes to shrinkage-porosity interaction.

26.2. Methodology

26.2.1. Materials

The equipment consisted of a stainless steel tray dryer with a 0.17 m inner diameter and a capacity to accommodate one circular tray with 0.15 m diameter. An upward air flux flowed perpendicularly on the tray. An electric resistance block heated the air with a variable input from 2 kW to 18 kW. A thermostatic controller controlled the air temperature from 30 °C up to 180 °C. A 0.5 Hp centrifugal fan controlled the air speed. Experiments were done at 3 m/s.

Banana fruits, originally from Madeira Island (Portugal), with an initial moisture content of 70–75% (kg water/100 kg wet solid) and 20° Brix were used in this study. Both ends of the fruits were removed and discarded. Bananas were peeled and cut into discs with a thickness of one centimeter; each disc was cut in quarters and placed in the tray dryer in a single layer.

26.2.2. Drying Experiments

Based on previous experiments (Hofsetz and Lopes, 2005), a drying time of 12 min at 150 °C for HTST pulse was chosen and used. The total drying time required to produce crispy banana pieces was reached with a cooling period (from the end of the HTST pulse up to the beginning of the AD stage) of 25 min, and finally an AD stage (70 °C) of 5 h. For the conventional air drying process (ADP), samples were dried at 70 °C for eight h. At the end of the process, equilibrium was attained and water activity (a_w) was below 0.3. Four samples were taken out at different drying times for physical characterization (Table 26.1).

26.2.3. Experimental Determinations

Soluble solids of fresh samples were determined with an Abbe refractometer (Abbe-3L, Bausch and Lomb, Rochester, NY, USA) at 25 °C. Dried banana a_w was determined with a Decagon CX-2T hygrometer (Aqualab-Decagon Devices Inc., Pullman, WA, USA) at 25 °C. The particle volume (V_p [m^3]) was measured in a gas pycnometer, built to work with wet solids, according to methodology proposed by Sereno et al. (2007). The bulk volume (V_b [m^3]) was determined from the buoyant forces of the samples when immersed in n-heptane (Lozano et al., 1980). Porosity was calculated from the bulk and particle volume, as shown in Eq. (26.1).

$$\text{Porosity } (\%) = [1-(V_p/V_{b)}]*100 \tag{26.1}$$

Volume change was expressed as a bulk shrinkage ratio of the sample volume at a certain drying time to its initial volume, as in Eq. (26.2). The subscript 0 refers to the fresh sample, V_b.

$$\text{Shrinkage} = V_b/V_{b0} \tag{26.2}$$

TABLE 26.1. Drying conditions and sampling times for the HTST/AD and for the ADP

HTST/AD		ADP	
Drying condition	Sampling Times	Drying condition	Sampling Times
Fresh	0 min	Fresh	0 min
HTST pulse (150 °C −12 min)	1 min		15 min
	3 min		30 min
	7 min		45 min
	9 min		1 h
	12 min		1 h 15 min
Cooling period (25 min)	17 min	Air Drying Process (ADP) (70 °C −8 h)	1 h 30 min
	22 min		1 h 45 min
	27 min		2 h 15 min
	32 min		3 h
	37 min		
AD stage (70 °C −5 h)	1 h 37 min		5 h
	2 h 37 min		6 h
	3 h 37 min		7 h
	4 h 37 min		8 h
	5 h 37 min		-

The solids content was determined in a vacuum oven (Vaciotem J.P. Selecta S.A. Abrera, Barcelona, Spain) at 70 °C for 48 h, following AOAC methods (AOAC, 1984). Microimages of the samples were taken with a stereomicroscope (Olympus SZ-11, Tokyo, Japan) and were calibrated with a stage micrometer of 2 mm length and divisions of 0.01 mm (Leitz Wetzlar, Germany). Paint Shop Pro 4.12 software was used for image processing.

26.3. Results and Discussion

Figure 26.1 presents the time dependence of experimental normalized moisture content of bananas for the two tested drying treatments. The combined HTST/ADP required 5.6 h of total drying time (a_w = 0.276; standard deviation of 0.003); this association saved at least 30% in drying time. The ADP samples presented surface hardening, probably caused by a too long drying time, and a_w values did not reach a reduction below 0.3 after 8 h of processing (a_w = 0.386; standard deviation of 0.001). In the dehydration process for bananas by explosion puffing pulse (Lozano and Saca, 1992), the final drying stage was twice as fast as the conventional air drying (4.4 h for the first and 2 h for the last). Kim and Toledo (1987), observed a similar behavior using high temperature fluidized bed (HTFB) drying for rabbiteye blueberries (1.1 h for HTFB and 12.5 h for air dehydration).

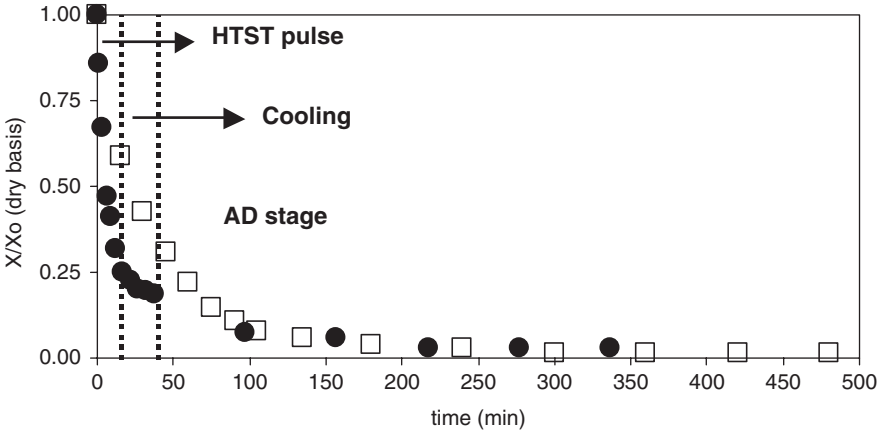

FIG. 26.1. Experimental normalized moisture content of banana versus time (● HTST/AD, □ ADP)

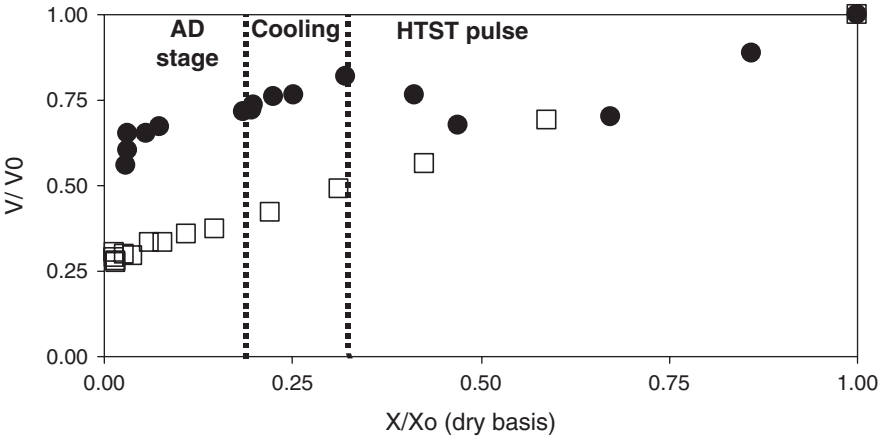

FIG. 26.2. Experimental shrinkage data of banana versus normalized moisture content (● HTST/AD, □ ADP)

Figure 26.2 shows the experimental shrinkage data as a function of dimensionless moisture. Initially, the volume decreased linearly, then increased again and finally decreased up to the end of the process, reaching 60% of the initial volume. The volume shrinkage of bananas during the ADP decreased almost linearly with the decrease in moisture content. This linear behavior was also reported for fresh apples (Mayor et al., 2005), air-dried bananas (Katekawa and Silva, 2004), as well as in many other food materials.

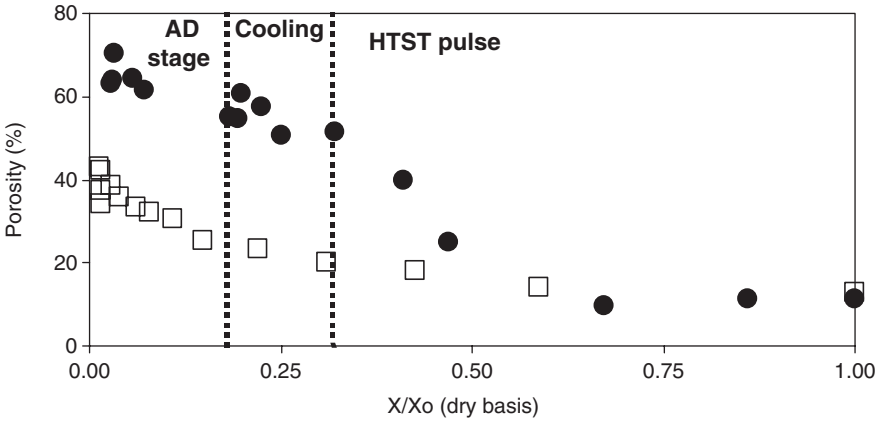

FIG. 26.3. Experimental porosity data for banana versus normalized moisture content (● HTST/AD, □ ADP)

Figure 26.3 shows the porosity average values for bananas during the drying process. It can be seen that the increase in this parameter was more intense during the final part of HTST pulse (0.5 to 0.3 X/Xo), from 10% to 50%. This increase in porosity continued, due to a very low shrinkage, during the cooling and AD stage, and porosity rose from 50% to 70% at the end of the process. During ADP treatment, this property progressively increased, attaining a value of 40% at the end of process. Observing HTST/AD curves from Fig. 26.2 and 26.3, it can be seen that there was a continuous increase in porosity until after the HTST pulse, due to very low shrinkage (1 to 0.82 Vb/V_{b0}), with an important increment of porosity as drying proceeded.

In general, porosity increases as moisture is removed at high drying rates, leading to a more porous structure; however, lower drying rates result in a more compact and denser product (Aguilera, 2003). Moreover, in the early stages of drying, the cellular tissues are elastic enough to shrink into the space left by the evaporated moisture. As the drying process proceeds, structural changes in the cellular tissue result in a more rigid skeleton, thus favoring the development of porosity (Mayor and Sereno, 2004; Krokida et al., 1997). In this work, during the HTST/AD treatment, volume decreased initially because of the loss of water and the collapse of the material. As the drying proceeded, the puffing effect started to occur and volume started to increase, partially compensating for the initial shrinkage. The puffing effect ended in the cooling period; there was no volume increase, and the development of a crust began, which retained the shape and volume of the sample. However, this crust cannot totally avoid the shrinkage in the AD stage, since a slight decrease in the volume was observed until the end of the drying. This can be verified in Figs. 26.4 and 26.5: the HTST pulse developed a crust that retained the shape and volume of the sample and formation of big pores can be

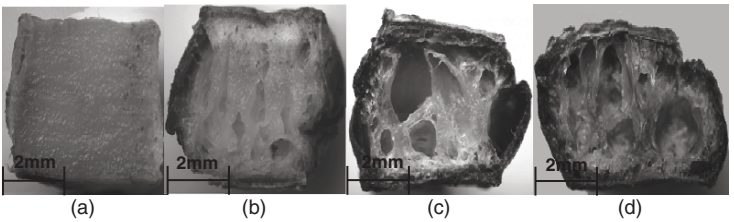

FIG. 26.4. changes of banana pieces during HTST/AD treatment. a) after 3 min at HTST pulse; b) after 12 min at HTST pulse; c) after 25 min at the cooling period; d) after 4 hours at AD stage (70 °C)

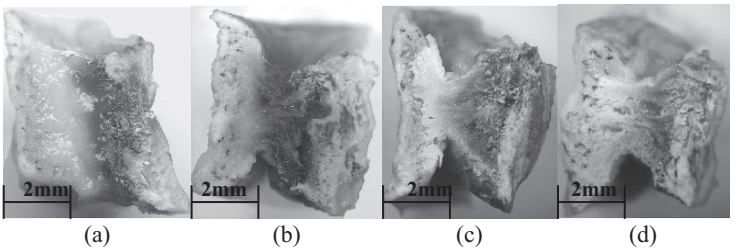

FIG. 26.5. Microstructural changes of banana pieces during ADP treatment at 70 °C a) after 1 h; b) after 3 h; c) after 6 h; d) after 8 h.

observed (Fig. 26.4); for ADP there is no crust formation and medium size pores can be observed (Fig. 26.5).

26.4. Conclusion

The combined HTST/AD treatment of bananas showed non-linear shrinkage behavior in the HTST pulse. Bananas shrank up to around 60% of their original volume, and porosity reached 70%.

In the ADP treatment, the volume decreased linearly with moisture content during drying to around 32% of their initial volume, and porosity progressively increased, reaching a value near 40% at the end of process.

The HTST/AD treatment resulted in the saving of at least 30% in total drying time and in higher porosity and less shrinkage when compared with the ADP dried product. However, energy and economic studies were not done in this work to compare both processes. These tasks will be completed in future work.

Acknowledgements The author, Kelly Hofsetz, is grateful to Capes-Grices (proc. BEX 1466/04-6) for their financial support during the sandwich scholarship at University of Porto (UP), Portugal, to CNPq financial support scholarship in Brazil (proc.141294/2003-5), FAPESP and Requimte/Dept. of Chemical Engineering at UP.

References

Aguilera J.M., 2003, Drying and Dried Products Under the Microscope, *Food Sci. Tech. Int*. **9**(3):137–143.

AOAC., 1984, *Official Methods of Analysis*, 14th ed., Association of Official Analytical Chemists, Washington.

Hofsetz, K., and Lopes C.C., 2005, Crispy Banana Obtained by the Combination of a High Temperature and Short Time Drying Stage and a Drying Process, *Braz. J. Chem Eng*. **22**(2):285–292.

Jayaraman, K.S., and Das Gupta D.K., 1992, Dehydration of Fruits and Vegetables—Recent Developments in Principles and Techniques, *Drying Technol*. **10**(1):1–50.

Katekawa, M.E., and Silva M.A., 2004, *Study of Porosity Behavior in Convective Drying of Bananas*, CD-ROM Proceedings, 14th International Drying Symposium, São Paulo, August 22-25, 2004, B:1427–1434.

Katz, E.E., and Labuza T.P., 1981, Effect of Water Activity on the Sensory Crispness and Mechanical Deformation of Snack Food Products, *J. Food Sci*. **46**:403–409.

Kim, M.H., and Toledo R.T., 1987, Effect of Osmotic Dehydration and High Temperature Fluidized Bed Drying on Properties of Dehydrated Rabbiteye Blueberries, *J. Food Sci*. **52**(4):980-984, 989.

Krokida, M.K., Zogzas, N.P., and Maroulis Z.B., 1997, Modeling Shrinkage and Porosity During Vacuum Dehydration, *Int. J. Food Sci. Technol*. **32**:445–458.

Lozano, J.E., Rotstein, E., and Urbicain M.J., 1980, Total Porosity and Open-Pore Porosity in The Drying of Fruits, *J. Food Sci*. **45**:1403–1407.

Lozano, J.E., and Saca S.A., 1992, Explosion Puffing of Bananas, *Int. J. Food Sci. Technol*. **27**:419–426.

Mayor, L., and Sereno A.M., 2004, Modeling Shrinkage During Convective Drying of Food Materials: A Review, *J. Food Eng*. **61**:373–386.

Mayor, L., Silva, M.A., and Sereno A.M., 2005, Microstructural Changes During Drying of Apple Slices. *Drying Technol*. **23**(9-11):2261–2276.

Payne, F.A., Taraba, J.L., and Saputra D., 1989, A Review of Puffing Processes for Expansion of Biological Products, *J. Food Eng*. **10**:183–197.

Ratti C., 2001, Hot Air and Freeze-Drying of High-Value Foods: A Review, *J. Food Eng*. **49**:311–319.

Sereno, A.M., Silva, M.A., and Mayor, L., 2007, Determination of the particle density and porosity in foods and porous materials with high moisture content, *Int. J. Food Properties*, **10**(3):455–469.

Toledo R.T., 1991, Dehydration, in: *Fundamentals of Food Process Engineering*, 2nd ed., Chapman and Hall, New York, pp. 456–506.

Varnalis, A.I., Brennan, J.G., and MacDougall D.B., 2001, A Proposed Mechanism of High Temperature Puffing of Potato. Part I. The Influence of Blanching and Drying Conditions on the Volume of Puffed Cubes, *J. Food Eng*. **48**:361–367.

27
Isolation, Purification and Partial Characterization of Laccase from *Ustilago maydis*

R.M. Desentis-Mendoza, H. Hernández-Sánchez, and M.E. Jaramillo-Flores

27.1. Introduction

Huitlacoche is a fungus that has been consumed in Mexico since prehispanic times. This Aztec name is given to the galls or tumors that form in corn cobs by the fungus scientifically known as *Ustilago maydis*. When infection takes place, a great mass of mycelium is formed in different zones in the corn plant. In the end, a great mass of black spores replaces the mycelium, and it is at this stage that the product is consumed as food (Valverde et al., 1995). Laccase (*p*-diphenol oxygen oxidoreductase, E. C. 1.10.3.2) catalyzes the oxidation of *p*-hydroxyphenols. Its activity depends on copper, oxidizes *o*- and *p*-dihydroxyphenols and compounds such as *p*-phenylendiamine and syringaldazine to color final products. Laccases differ from *p*-diphenol oxidases in their ability to hydroxylate monophenols (Walker, 1995; Palmieri et al., 1997). The objective of this work was to isolate, purify and partially characterize (biochemically and physico-chemically) the laccase from *U. maydis*.

27.2. Methodology

Corn cobs infected with *Ustilago maydis* were bought at a local market in Mexico City. A raw extract was obtained by fractional precipitation (Valero et al., 1988) and the purification was done by molecular exclusion (Pharmacia Biothech, 1995) and affinity (Ganem and Martín, 2000) (concanavalin A) chromatography. Protein was quantified by the Lowry method (Lowry et al., 1951), and the enzyme activity was measured with different substrates (diammonium 2,2 -azinobis (3-ethyl-benzothiazoline-6-sulfonate) or ABTS, hydroquinone, *p*-phenylendiamine, and syringaldazine) (Kimberly and Lee, 1980). The maximal activity pH (Kimberly and Lee, 1980), the molecular weight evaluated by SDS-PAGE Bio-Rad Laboratories, 1998, the isoelectric point (Righetti, 1983) and denaturation temperature (Floury et al., 2002) were also determined.

27.3. Results and Discussion

Table 27.1 shows the degree of purification attained in each of the stages. It can be observed that the highest enzyme activity (2.380 U/ml) is reached in the Sephadex G-150 stage, which has 1.42 mg of protein/ml. However, in the case of the Con A (2) stage, the specific activity rose to 9.82 U/mg with a very small amount of protein (0.081 mg/ml).

The above mention indicates that the protein is molecularly homogeneous, since a small amount of protein has a very high enzyme activity. It can also be observed that the specific activity increased ten times during the purification process. This same trend in purification has also been observed in other studies (Palmieri et al., 2000; Edens et al., 1999).

The SDS-PAGE indicated that the enzyme has a 99 kDa molecular weight and the measured isoelectric point and denaturation temperature were 5.5 and 99.31 °C, respectively.

Laccase activity was measured with the above mentioned substrates (see also Fig. 27.1) at a 2 mM concentration and at different pH values (3, 4, 5, 6, 7, 8 and 9). The results are shown in Figs. 27.2 and 27.3.

It can be observed in Fig. 27.2A that the enzyme activity with ABTS as substrate is higher in the pH range from 3 to 4, whereas in the range from 6 to 9 the activity is very low. In the case of hydroquinone (Fig. 27.2B), the range of higher activity is also from 3 to 4 with the peak in 3. No activity could be detected in the pH range from 8 to 9. It can be seen that *p*-phenylendiamine (Fig. 27.2C) is a substrate that can be used by the enzyme at almost any pH but with a better activity from 7 to 8.

For every substrate, the feasibility of the reaction depends on the pH due to changes in the charge or in the structure of the enzyme and/or the substrate. It is well known that this enzyme has a positive charge at pH values below 5.5 (the isoelectric point) and has a negative charge at higher values.

Similar changes at different pH values also occur for the substrates. In the case of the syringaldazine (Fig. 27.2D) the peak of activity occurs at pH 3; however, this activity is 60% lower than the one presented with the other substrates.

Figure 27.3A shows that at pH 3 there are peaks of activity for ABTS and hydroquinone, less activity for syringaldazine and almost nil for *p*-phenylendiamine.

Table 27.1. Stages in the purification of the *Ustilago maydis* laccase

Work stage	Total activity (u/ml)	Protein (µg/ml)	Specific activity (u/mg)	Fold purification (times)
Corn smut	0.112	4.7	0.023	-
$(NH_4)_2SO_4$ (95% saturation)	2.380	1.42	1.67	1
SEPHADEX G-150	3.041	0.53	5.66	3.38
CON A	1.250	0.20	6.25	3.74
CON A (2)	0.796	0.081	9.82	5.88

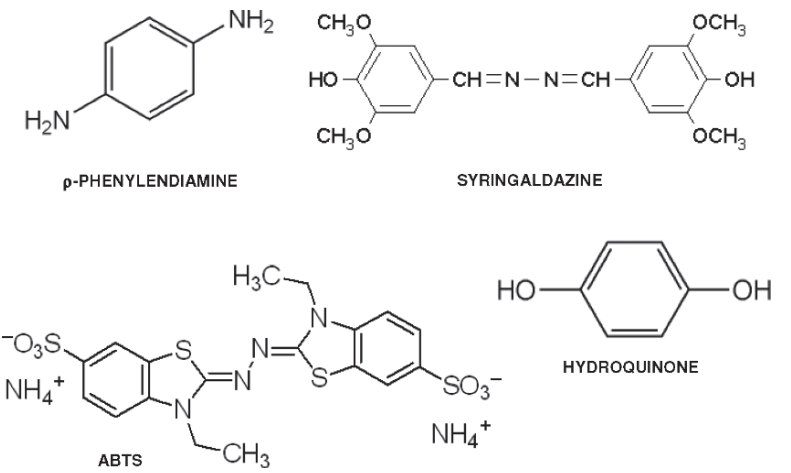

FIG. 27.1. Chemical structures for *p*-phenylendiamine, syringaldazine, ABTS and hydroquinone

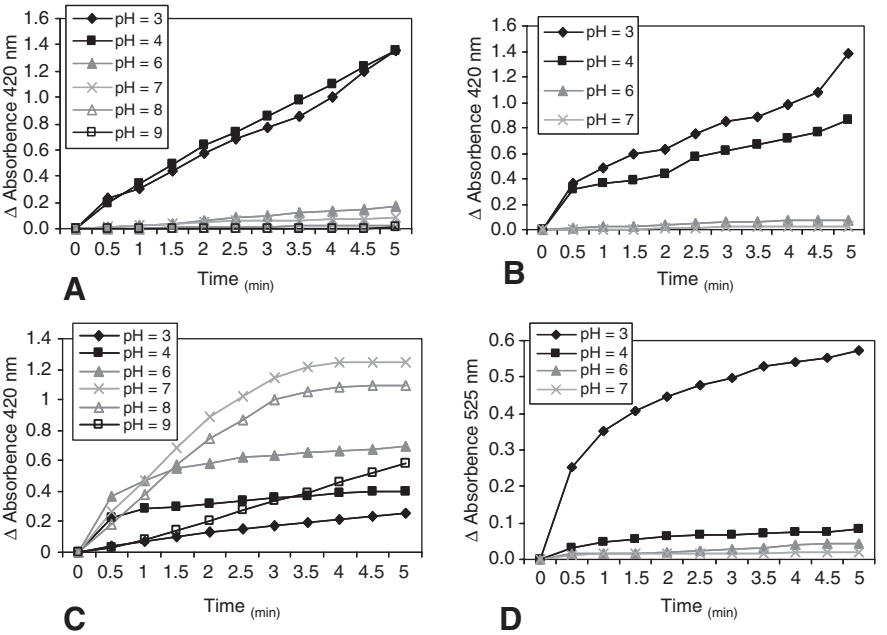

FIG. 27.2. Effect of pH on the activity of laccase with different substrates. (A) ABTS, (B) hydroquinone, (C) *p*-phenylendiamine and (D) syringaldazine

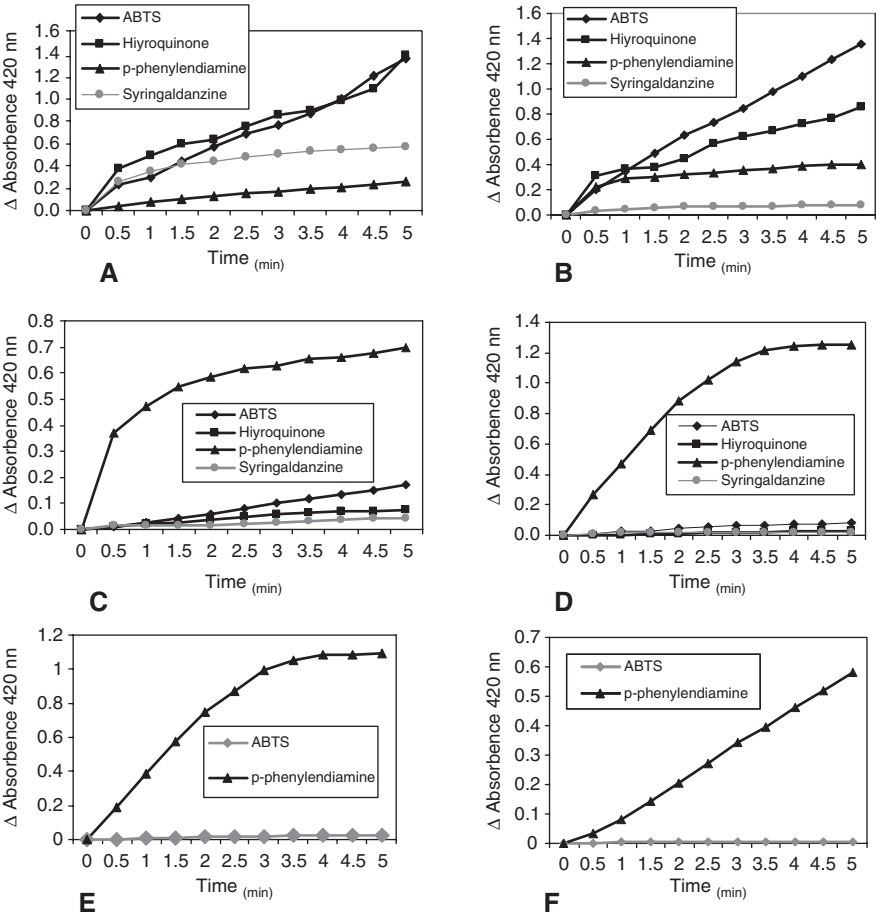

FIG. 27.3. Laccase activity with different substrates at pH values of 3 (A), 4 (B), 6 (C), 7 (D), 8 (E) and 9 (F)

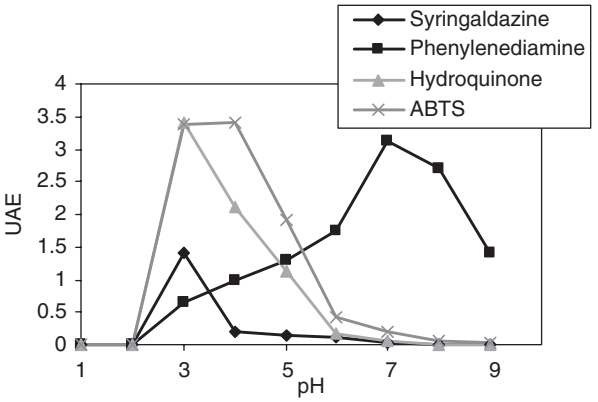

FIG. 27.4. Laccase activity peaks for different substrates

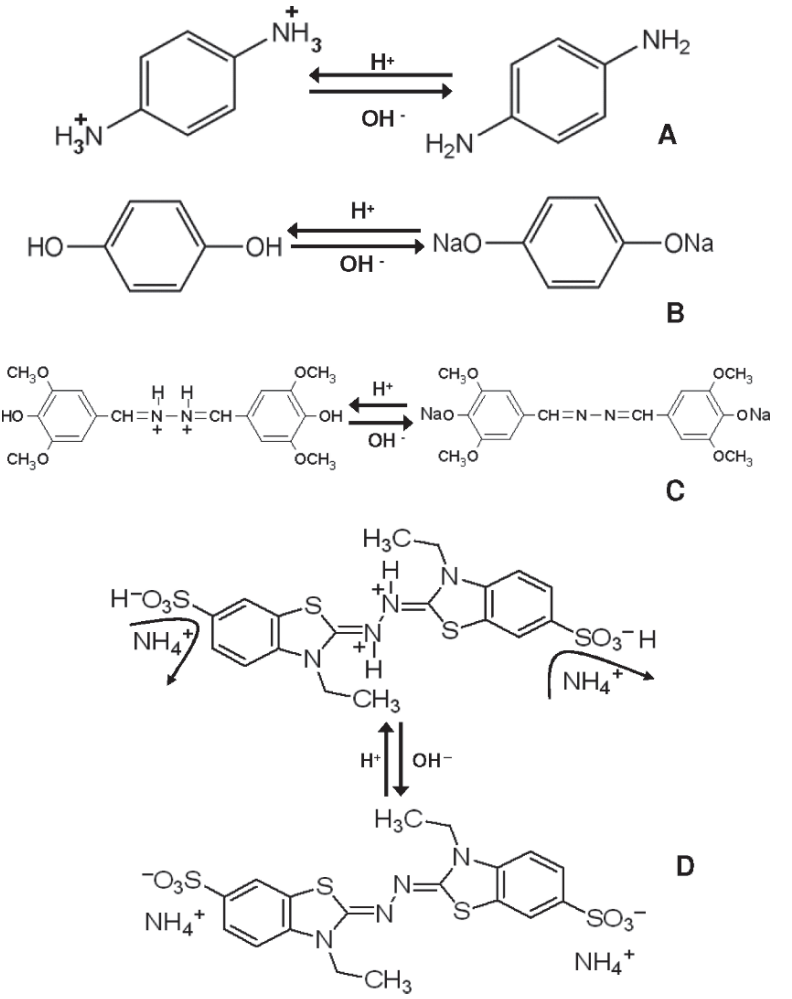

FIG. 27.5. pH-related changes in structure of the molecules of *p*-phenylendiamine (A), hydroquinone (B), syringaldazine (C) and ABTS (D)

At pH 4 (Fig. 27.3B) the behavior is similar; however, in this case, the activity is higher in *p*-phenylendiamine than in syringaldazine. At the pH values of 6 (Figure 27.3C), 7 (Fig. 27.3D), 8 (Fig. 27.3E) and 9 (Fig. 27.3F) *p*-phenylendiamine is the only substrate with significant activity, having a peak at pH 7. It was also observed that this enzyme has very little activity toward ABTS and almost no activity toward hydroquinone and syringaldazine at pH values of 7, 8, and 9.

The highest laccase activity was registered for the ABTS at pH 3, followed by hydroquinone at pH values of 3 and 4, *p*-phenylendiamine at pH 7 and syringaldazine at pH 3. These activity peaks can be observed more clearly in Fig. 27.4.

Figure 27.5A shows that at a low pH the *p*-phenylendiamine molecule is completely protonated and therefore unavailable for the laccase. However, at higher pH values the structure becomes adequate for the enzyme activity. This could explain the higher activity of laccase toward this substrate in the pH range of 6 to 9 with a peak at 7 (Fig. 27.4).

In the cases of hydroquinone (Fig. 27.5B) and syringaldazine (Fig. 27.5C), at lower values of pH, there are two free hydroxyl groups which form an adequate structure for the action of laccase. At higher pH values the hydroxyl groups are in their ionized form and cannot be used by the enzyme. This fact can explain the higher activity of laccase towards these molecules at pH 3.

27.4. Conclusion

A 99 kDa laccase with an isoelectric point of 5.5 and a denaturation temperature of 99.31 °C was purified from *Ustilago maydis*. Maximal activity was registered at pH 3 in the cases of ABTS, hydroquinone and syringaldazine and at pH 7 for *p*-phenylendiamine. The best substrate for the laccase was ABTS at pH 3.

Acknowledgements The authors thank COFFA and CGPI of the Instituto Politécnico Nacional and to Universidad Panamericana (México) for their support of this research.

References

Bio-Rad Laboratories, 1998, *Mini Protean II. Electrophoresis Cell. Instruction Manual*. Bio-Rad Laboratories, USA. 1–25.

Edens, W., Goins, T., Dooley, D., and Henson J., 1999, Purification and Characterization of a Secreted Laccase of Gaeumannomyces graminis var. Tritici, *Appl. Environ. Microbiol*. **65**(7):3071–3074.

Floury, J., Desrumaux, A., and Legrand J., 2002, Effect of Ultra-high-pressure Homogenization of Structure and Rheological Properties of Soy Protein-stabilized Emulsions, *J. Food Sci*. **67**(9):3388–3395.

Ganem, B.F., and Martín O.G., 2000, Lectina Concanavalina A: Obtención y Purificación, *Universo Di-agnóstico* **1**(1):1–41.

Kimberly, W.W., and Lee C.Y., 1980, Purification of Grape Polyphenoloxidase with Hydrophobic Chromatography, *J. Chromat*. **192**:232–235.

Lowry, O.H., Rosebrough, N.J., Farr, A.L., and Randall R.J., 1951, Protein Measurement with the Folin Phenol Reagent, *J. Biolo. Chem*. **193**:265–275.

Palmieri, G., Giardina, P., Bianco, C., Fontanella, B., and Sannia G., 2000, Copper Induction of Laccase Isoenzymes in the Ligninolytic Fungus Pleurotus ostreatus, *Appl. Environ. Microbiol*. **66**(3):920–924.

Palmieri, G., Giardina, P., Bianco, C., Scaloni, A., Capasso, A., and Sannia G., 1997, A Novel White Laccase from Pleurotus ostreatus, *J. Biological Chem*. **272**(50):12, 31301–31307.

Pharmacia Biotech, 1995, *Gel Filtration Calibration Kit Instruction Manual for Protein Molecular Weight Determinations by Gel Filtration*, Pharmaia Biotech, Sweden, pp. 1–17.

Righetti P.G., 1983, *Isoelectric Focusing: Theory, Methodology and Applications*, Elsevier Biomedical Press, Amsterdam.

Valero, E.M. Varón, R., and García-Carmona 1988, Characterization of Polyphenol oxidase from Airen Grapes, *J. Food Sci*. **53**(5):1482–1485.

Valverde, M.E., Paredes-Lopez, O., Pataky, J. K., and Guevara-Lara F., 1995, Huitlacoche (*Ustilago maydis*) as a Food Source—Biology, Composition, and Production, *Crit. Rev. Food Sci. Nutr*. **35**(3):191–229.

Walker J.R.L., 1995, *Enzymatic Browning in Fruits: Its Biochemistry and Control. Enzymatic Browning and its Prevention*. C.Y. Lee and J.R. Whitaker (eds.), American Chemical Society Symposium Series 600: Washington, pp. 8–22.

28
Phase Behavior of Phospholipid-Cholesterol Liposomes Stabilized With Trehalose

S. Ohtake, C. Schebor, and J.J. de Pablo

28.1. Introduction

Achieving long-term stability in biological systems has been a long-standing goal of the food, pharmaceutical, and biomedical industries. Avoiding the need for refrigeration would reduce production and storage costs drastically. The desiccation of phospholipidic vesicles has been studied in an effort to understand biological membranes under low water content conditions (Crowe and Crowe, 1988; Ohtake et al., 2004).

Trehalose is effective in protecting biological membranes upon freeze-drying, and it has been widely used to preserve the integrity of phospholipid liposomes (Crowe and Crowe, 1988; Ohtake, et al., 2004; Crowe et al., 1986). Despite the abundance of cholesterol in mammalian plasma membranes (Rouser, et al., 1968), studies examining the effects of dehydration on cholesterol-containing model membranes are scarce (Van Winden and Crommelin, 1999; Harrigan, et al., 1990). Furthermore, the ability of well known lyoprotectants, such as trehalose, to stabilize cholesterol-containing liposomes has not been examined in detail. The aim of this work is to understand how cholesterol containing liposomes behave upon lyophilization.

28.2. Methodology

Liposomes were obtained by extruding (through 100 nm membrane filters) mixtures consisting of 1,2-Dipalmitoyl-*sn*-Glycero-3-Phosphocholine (DPPC), 1,2-Dipalmitoyl-*sn*-Glycero-3-Phosphoethanolamine (DPPE) and cholesterol (Ch) at a temperature above the phase transition temperature, T_m, of the respective mixtures. Cholesterol molar ratios ranged from 0% to 41%. Samples were freeze-dried for 48 h in a Virtis Genesis 12EL (New York, USA) freeze-dryer at a pressure of 30 mtorr and a condenser temperature of −80 °C. The samples under vacuum were transferred to a glove box (Vac, Nexus One, Hawthorne, CA) and then loaded into pre-weighed DSC pans and sealed for calorimetric analysis.

Fully hydrated samples were also analyzed by DSC, for which the DSC pans were loaded immediately following extrusion.

DSC was used to determine the T_m of the phospholipids. T_m represents the peak temperature of the endotherm for the lipid gel-to-fluid phase transition recorded during the heating scan. The instrument used was a TA Q100 DSC (New Castle, DE). All measurements were made at 10 °C/min, using sealed aluminum pans (crimped pans, TA), and an empty pan was used as a reference. The average value of at least three replicate samples was reported. Data was analyzed using Universal Analysis.

Residual water contents for the dehydrated samples were analyzed using a Karl Fisher Coulometer Metrohm, Model 737 (Herisau, Switzerland).

28.3. Results and Discussion

The thermotropic phase behavior of liposomes composed of DPPC, DPPE and their mixtures with cholesterol was studied using differential scanning calorimetry (DSC). Thermograms of fully hydrated DPPC-cholesterol liposomes containing cholesterol at molar ratios ranging from 0% to 41% (molar) are shown in Fig. 28.1. The phase transition temperature (T_m) of DPPC in the fully hydrated state is 42 °C, which is in agreement with previous reports (McMullen et al., 1993; Ohtake et al., 2005). The addition of cholesterol to DPPC liposomes did not change the T_m significantly. The enthalpy of the transition, however, decreased considerably, until it became negligible at 41% cholesterol, consistent with literature data (McMullen et al., 1993; Vist and Davis, 1990). Addition of trehalose did not significantly alter the melting behavior of cholesterol-containing liposomes in the fully hydrated state (data not reported). The addition of cholesterol to DPPE and DPPE-DPPC mixtures exhibited behavior similar to

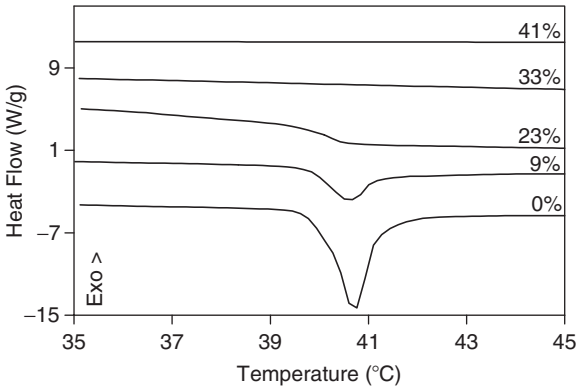

FIG. 28.1. Thermograms of fully hydrated DPPC-cholesterol mixtures at the indicated cholesterol molar ratios

that observed for DPPC, namely a decrease in the enthalpy of transition. The transition temperature decreased for DPPE (data not reported), as was also reported previously (Blume, 1980).

Figure 28.2 shows the thermograms of freeze-dried DPPC-cholesterol liposomes with (solid lines) and without (dotted lines) trehalose. The T_m of DPPC increased from 42 °C to 105 °C upon dehydration, in accordance with previous studies (Crowe and Crowe, 1988; Ohtake et al., 2004). The increase in phase transition temperature was caused by the decrease in the spacing between the headgroups, which allowed for increased van der Waals interactions between the lipid hydrocarbon chains (Crowe et al., 1998). The transition peak observed at 105 °C for dehydrated DPPC decreased dramatically, both in magnitude and in temperature, as the proportion of cholesterol in the liposomes increased (Fig. 28.2, dotted lines). The intercalation of cholesterol between the phospholipids destabilized their packing in the gel phase, leading to a depression in the T_m of the dehydrated samples. A second broad endothermic transition, having a main peak at 70 °C, became observable at 23% cholesterol (Fig. 28.2, dotted line). The peak corresponding to this transition increased as the cholesterol proportion increased, and at 41% cholesterol the two transitions merged. The presence of the two endothermic peaks can be explained by the existence of Ch-rich and Ch-poor domains, as described for these same systems in the fully hydrated state (McMullen et al., 1993; Vist and Davis, 1990). In the presence of trehalose, the phase transition temperature of dehydrated DPPC dropped by 80 °C, to 25 °C (Fig. 28.2, solid line), as was reported previously (Crowe and Crowe, 1988; Ohtake et al., 2004). This T_m depression has been ascribed to hydrogen bond formation between the sugar molecules and the phospholipid headgroups, allowing the phospholipids to maintain an intermolecular spacing similar to that present in the hydrated state (Crowe

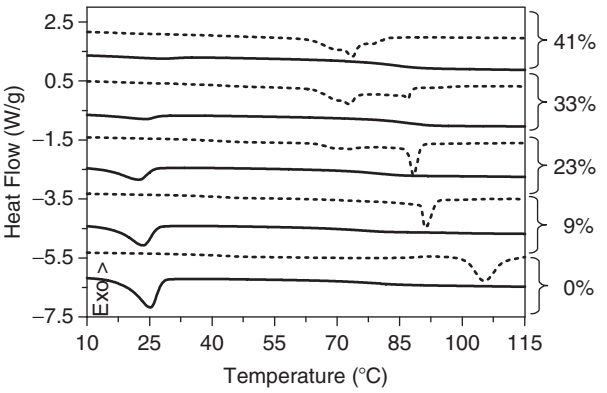

FIG. 28.2. Thermograms of lyophilized DPPC-cholesterol mixtures in the presence (solid lines) and absence (dotted lines) of trehalose. The cholesterol molar ratios (%) in the liposomes are indicated in the figure. The samples contain less than 1.5 % (wt) water

and Crowe, 1988; Ohtake et al., 2004; Tsvetkova et al., 1998). In the presence of trehalose, cholesterol addition did not have a significant effect on the T_m, although the enthalpy of the transition decreased monotonically as the proportion of cholesterol increased (Fig. 28.2, solid lines), as was observed in the fully hydrated state (Fig. 28.1).

Figure 28.3 shows the thermograms of freeze-dried DPPE–Ch mixtures with (solid lines) and without (dotted lines) trehalose. Two transitions at 52 °C (corresponding to the gel-to-liquid crystalline phase transition) and 94 °C (corresponding to the crystal-to-liquid crystalline phase transition) are observed for dehydrated DPPE (Fig. 28.3, bottom dotted line), which are in accordance with previously reported data (Handa et al., 1985). All of the DPPE–Ch mixtures exhibit multiple transitions: (i) the phase transition at approximately 94 °C was always present, irrespective of the proportion of cholesterol; (ii) the transition at 52 °C decreased both in magnitude and in temperature with increasing cholesterol content; and (iii) a new transition at approximately 72 °C appeared upon the addition of cholesterol, and was present at all of the cholesterol concentrations examined in this work. The consistency of the peak observed at 94 °C suggests that the crystalline phase of DPPE does not incorporate cholesterol. The gel phase, however, is more prone to interact with cholesterol, as the enthalpy of the peak at 52 °C diminished considerably with increasing cholesterol proportion. We speculate that the transition at 72 °C represents an intermediate DPPE phase (between gel and crystal) enriched in cholesterol. In the presence of trehalose, only one transition can be observed, and the T_m reduced from 52 °C to 39 °C for pure DPPE (Fig. 28.3, bottom solid line). The T_m further reduced upon the addition of cholesterol to approximately 21 °C (Fig. 28.3, solid lines). T_m corresponds to the melting of neighboring phospholipid molecules. As previously described,

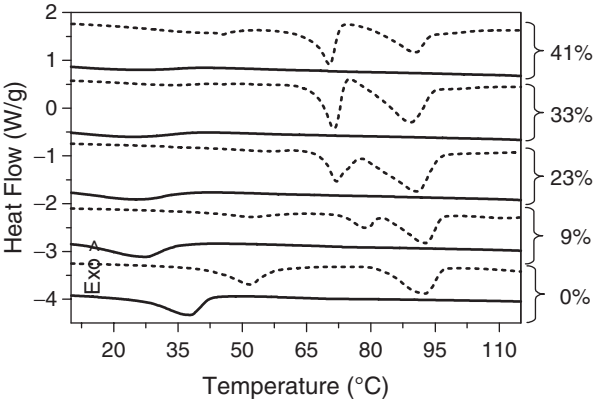

FIG. 28.3. Thermograms of lyophilized DPPE-cholesterol mixtures in the presence (solid lines) and absence (dotted lines) of trehalose. The cholesterol molar ratios (%) in the liposomes are indicated in the figure. The samples contained less than 1.5 % (wt) water

cholesterol addition can affect its surrounding environment, which in turn can affect the T_m. The decrease in T_m observed for DPPE-Ch mixtures suggests that trehalose is better able to interact with the PE molecules upon the intercalation of cholesterol between phospholipid molecules, which most likely results from the perturbation of the PE–PE hydrogen bonding network by cholesterol. This is in contrast to DPPC–Ch mixtures, in which the PC–PC headgroup interactions are not significantly modified with cholesterol incorporation. Trehalose interaction with DPPC molecules, hence, is not affected by the presence of cholesterol (Fig. 28.2, solid lines).

A freeze-dried DPPE–DPPC mixture (1:1 molar ratio) exhibited a single transition at 83 °C (Fig. 28.4, bottom dotted line). In the hydrated state, the DPPE–DPPC mixtures were miscible, exhibiting a single transition peak (54 °C) (Blume, 1980; Blume and Ackerman, 1974). This suggests that the two phospholipids remain miscible upon dehydration. Upon the addition of cholesterol, the T_m at 83 °C decreased both in temperature and in magnitude. A new transition at 60 °C appeared above 9 mol% Ch and grew in magnitude with increasing cholesterol content (Fig. 28.4, dotted lines). As was previously described for DPPC–Ch systems (Fig. 28.2), the two peaks can be ascribed to Ch-rich and Ch-poor regions. It has been reported that cholesterol does not interact preferentially with either PE or PC in the DPPE–DPPC–Ch mixtures in excess water (Blume and Ackerman, 1974). As we did not observe phase separation of DPPC from DPPE upon dehydration, we expect the two peaks in the DPPE–DPPC–Ch mixtures to contain a constant DPPE/DPPC ratio (although containing different amounts of cholesterol). In the presence of trehalose, a decrease in T_m can be observed, from 83 °C to 21 °C (Fig. 28.4, bottom solid line). Note that DPPE–DPPC–Ch mixtures show a more pronounced depression of T_m by the addition

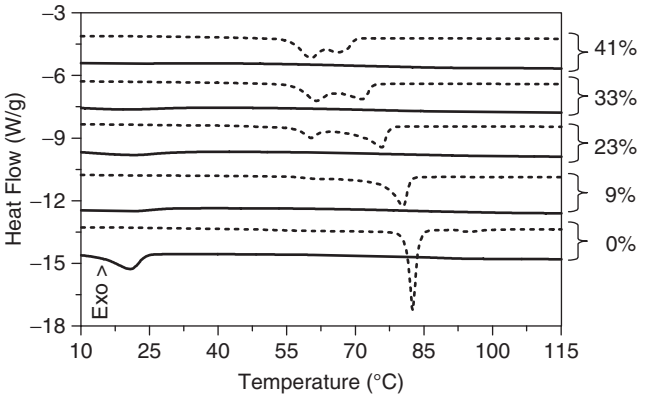

FIG. 28.4. Thermograms of lyophilized DPPE-DPPC-cholesterol mixtures in the presence (solid lines) and absence (dotted lines) of trehalose. The cholesterol molar ratios (%) in the liposomes are indicated in the figure. The samples contained less than 1.5 % (wt) water

of cholesterol (Fig. 28.4, solid lines) than that observed for DPPC (Fig. 28.2, solid lines), but less than that observed for DPPE (Fig. 28.3, solid lines). This suggests that DPPC is able to disrupt the strong PE–PE interaction, thereby facilitating the interaction with trehalose.

28.4. Conclusion

The phase behavior of various freeze-dried mixtures of DPPE, DPPC, and cholesterol has been analyzed. As the cholesterol proportion is increased, the phase behavior becomes more complex owing to the inhomogeneous mixing of cholesterol with the phospholipids. The effects of trehalose addition have also been examined. The main focus of the use of trehalose has been to reduce the T_m of phospholipids upon dehydration. This is an important aspect, since liposomes undergoing phase transition during rehydration can lead to leakage of encapsulated components. In this study we show that for dehydrated systems containing cholesterol, trehalose is also necessary to limit phase separation. Despite the abundance of reports examining the Ch-containing liposomes in the fully hydrated state, there is a shortage of studies on these systems in the dried state. Examination of cholesterol-containing model membranes may offer a more realistic view of how mammalian cells behave upon dehydration, and may aid in evaluating the effectiveness of lyoprotectants in conferring stability.

Acknowledgements The authors are thankful for financial support from the National Science Foundation and the MRSEC program. Carolina Schebor thanks CONICET (PIP5977) and UBACYT X226.

References

Blume A., 1980, Thermotropic Behavior of Phosphatidylethanolamine-Cholesterol and Phosphatidylethanol-Amine-Phosphatidylcholine-Cholesterol Mixtures, *Biochemistry* **19**:4908–4913.

Blume, A., and Ackermann T., 1974, Calorimetric Study of Lipid Phase-Transitions in Aqueous Dispersions of Phosphorylcholine-Phosphorylethanolamine Mixtures, *FEBS Lett*. **43**:1–74.

Crowe, J., Carpenter, J., and Crowe L., 1998, The Role of Vitrification in Anhydrobiosis, *Annu. Rev. Physiol*. **6**:73–103.

Crowe, L., and Crowe J., 1988, Trehalose and Dry Dipalmitoylphosphatidylcholine Revisited, *Biochim. Biophys. Acta* **946**:193–201.

Crowe, L., Womersley, C., Crowe, J., Reid, D., Appel, L., and Rudolph A., 1986, Prevention of Fusion and Leakage in Freeze-Dried Liposomes by Carbohydrates, *Biochim. Biophys. Acta* **861**:131–140.

Handa, T. Ichihashi, C., and Nakagaki M., 1985, Polymorphic Phase Transition and Monomolecular Spreading of Synthetic Phospholipids, *Prog. Colloid Polym. Sci*. **71**:26–31.

Harrigan, P., Madden, T., and Cullis P., 1990, Protection of Liposomes During Dehydration or Freezing, *Chem. Phys. Lipids* **52**:139–149.

McMullen, T., Lewis, T., and McElhaney R., 1993, Differential Scanning Calorimetric Study of The Effect of Cholesterol on the Thermotropic Phase Behavior of a Homologous Series of Linear Saturated Phosphatidyl-Cholines, *Biochemistry* **32**:16–522.

Ohtake, S., Schebor, C., Palecek, S., and de Pablo J.J., 2004, Effect of Sugar-Phosphate Mixtures on the Stability of DPPC Membranes in Dehydrated Systems, *Cryobiology* **48**:81–89.

Ohtake, S., Schebor, C., Palecek, S., and de Pablo J.J., 2005, Phase Behavior of Freeze-Dried Phospholipids-Cholesterol Mixtures Stabilized with Trehalose, *Biochim. Biophys. Acta* **1713**:57–64.

Rouser, G., Nelson, G., Fleischer, S., and Simon G., 1968, *Biological Membranes Physical Fact and Function*, D. Chapman-Academic Press, London, pp. 5–69.

Tsvetkova, N., Philips, B., Crowe, L., Crowe, J., and Risbud S., 1998, Effect of Sugar on Headgroup Mobility in Freeze-Dried Dipalmitoylphosphatidylcholine Bilayers: Solid-State 31P NMR and FTIR Studies, *Biophys. J*. **75**:2947–2955.

Van Winden, E., and Crommelin D., 1999, Short Term Stability of Freeze-Dried, Lyoprotected Liposomes, *J. Controlled Release* **58**:69–86.

Vist, M., and Davis J., 1990, Phase Equilibria of Cholesterol/Dipalmitoylphosphatidylcho line Mixtures: 2H Nuclear Magnetic Resonance and Differential Scanning Calorimetry, *Biochemistry* **29**:451–464.

29
Zeta-Potential as a Way to Determine Optimal Conditions During Fruit Juice Clarification

M.V. Fillipi, D.B. Genovese, and J.E. Lozano

29.1. Introduction

Cloudy fruit juice is caused by colloidal suspension where the continuous medium is a solution of pectin, sugars and organic acids, and the dispersed matter is mainly formed by cellular tissue comminuted during fruit processing. To obtain a clear juice, these suspended particles have to be removed. This process is known as clarification or fining, one of the most important unit operations in apple juice processing. The procedure helps also to remove active haze precursors, and thus decreases the potential for haze formation during storage, while providing a more limpid juice (Hsu et al., 1987; 1989; 1990). Therefore, the fining step is an important procedure that must be carefully controlled during the processing of clarified apple juice.

Genovese et al. (1997) determined that cloudy apple juice particles measure 450 nm diameter on average. If particles in a cloudy juice adhere together and form aggregates of increasing size (*flocculation*), they may settle due to gravity. If flocks change to a much denser form, it is said to undergo *coagulation*, which is an irreversible process. It may seem simple merely to filter them out, but unfortunately some soluble pectin remains in the juice, making it too viscous to filter quickly. A dose of commercial enzyme is the accepted way of removing unwanted pectin. Enzyme depectinization has two effects: It degrades the viscous soluble pectin, and it also causes the aggregation of cloud particles.

In an acidic environment such as that of apple juice (pH = 3.5- 3.7), the nucleus of apple particles is a protein that carries a positive charge, coated by pectin and other carbohydrates that carry negative charges. The dispersed phase is so small (~1-1000 nm) that gravitational forces are negligible and short-range forces, such as Van der Waals attraction and surface charges, dominate interactions. The inertia of the dispersed phase is also small enough to exhibit random Brownian motion, driven by momentum imparted by collisions with molecules of the suspending medium. Conventional enzyme clarification appears to be a critical processing step which, if excluded, may result in the

formation of larger quantities of haze (Tajchakavit et al., 2001). Enzymatic treatment also allows efficient use of clarifying agents to assist with cloud removal. Addition of fining or clarifying agents is intended to modify clarity, color, flavor and/or stability of juices. They are grouped according to their general nature in (i) Minerals (bentonite, kaolin); (ii) Proteins (gelatin, isinglass, casein, albumen); (iii) Polysaccharides (agars); (iv) Carbons; (v) Synthetic polymers (PVPP, nylon); (vi) Silicon dioxide (kieselsols); and (vii) Others, including metal chelators, enzymes, etc. (Zoecklein, 1988).

Clarification or fining of apple juice with gelatin and bentonite is a common industrial practice (Peterson and Johnson, 1978; Stocké, 1998). These fining agents work either by sticking to the particles or by using charged ions to cause particles to stick to each other, in any case making them heavy enough to sink to the bottom by the action of gravity. What is left is a transparent though not clear juice. Subsequent filtration operations are needed to obtain a crystal-clear product. Differences in the nature of ionic charges of protein, polyphenols and the fining agents induce flocculation and sedimentation, resulting in the removal of these potential haze precursors from the solution.

Determination of appropriate doses of clarifying apple juice agents (bentonite, gelatin) is usually made in the industry by trial and error; in a matrix of test tubes filled with enzymatically treated juice, increasing quantities of bentonite and gelatin are added in rows and columns, respectively. The dose that in a shorter time gives the most compact flocks and transparent supernatant is selected for the bulk treatment of juice.

It is known that electrically charged particles in aqueous media are surrounded by ions of opposite charge (counterions) and electrolyte ions, namely, the electrical double layer (Fig. 29.1).

The quantity U_E represents the energy of repulsion due to the interaction of the electrical double layers. The expression for U_E depends on the ratio between the particle radius and the thickness of the electrical double layer, κ^{-1}, called the Debye length. For $\kappa.a > 5$ (Quemada and Berli, 2002):

$$U_E = 2\pi\varepsilon_0\varepsilon_r\psi_0^2 a \ln[1+\exp(-\kappa H)] \tag{29.1}$$

where ε_0 is the permittivity in vacuum, ε_r is the relative permittivity (=dielectric constant) of the medium, ψ_0 is the surface potential of particles. The value of ψ_0 is often unknown; however, the potential to be used in calculating the repulsion is the potential in the Stern plane (plane of closest approach of counterions to the surface), ψ_δ, rather than ψ_0. In most cases, the nearest practical approximation to ψ is the zeta-potential (ζ), and this presupposes that the Stern plane and the slipping plane are nearly identical.

As previously mentioned, when two particles come so close that their double layers overlap, they repel each other. The strength of this electrostatic force depends on the zeta potential. If the zeta potential is too small (typically less than about 25 mV in magnitude), the repulsive force will not be strong enough to overcome the Van der Waals attraction between the particles, and they will begin to

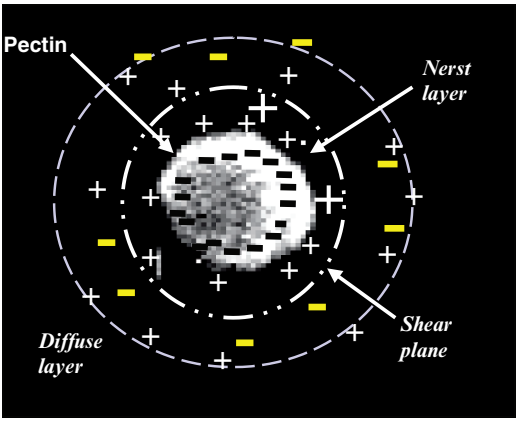

FIG. 29.1. Electrical double layer representation in an apple juice cloud particle

agglomerate. The suspension is said to be unstable when this happens, and other repulsive forces, such as hydration, are insignificant. A high zeta potential will prevent particle-particle agglomeration and keep the dispersion uniform and free flowing. The adding of clarifying agents such as gelatin is supposed to reduce the net surface charge and the thickness of the double layer, reducing the electrostatic repulsion and favoring flocculation.

Therefore, it is interesting both from a technological and scientific point of view to study the effect of pectolytic enzymes on apple juice flocculation and precipitation, and to explain on a more systematic basis (essentially through the determination of zeta-potential and particle size) the empirical test used to determine gelatin and bentonite doses during conventional clarification.

29.2. Clarification Studies

Juice was manufactured from the *Granny Smith* apple variety. Fresh pressed (NJ) and pasteurized-enzymatically treated juice (PJ) was left to flocculate in a thermally isolated glass settling column. The enzymatic treatment (Rohapect 1,5 mg/L; 2 h; 50 °C) was done following the hot technique. Commercial sodium bentonite type I (La Helcha) and gelatin (Cristagel Stauffer, Type A, 175 bloom; 180 mg/L) were used as clarifying agents. Conventional method for bentonite and gelatin dosage was made with an array of 12 × 8 50 mL apple juice assay tubes with increasing gelatin and bentonite content addition. Turbidity was determined with a PC Compact Turbidimeter (Aqualitic, Germany) as (NTU). Particle size distribution (PSD) and Zeta-potential (ξ) were determined by photon correlation spectroscopy in a Malvern Zetasizer 3000 (Malvern Instruments Inc., London). All results reported are means of replicate measurements.

29.2.1. *Behavior Of Enzymatically Treated Apple Juice In The Settling Column*

Settling column assays of NJ indicated that during the first 20 min, a distribution of particles by size occurred along the column, from particles about 1500 nm on top, to particles with diameter near 2000 nm at the bottom. The only exception was less dense particles floating on the surface, which had an intermediate size (1700 nm). On the other hand, Zeta-potential (ξ) remained practically constant at −9 mV (± 3,2 MV). Turbidity, as NTU, also showed a rapid decrease for the period of sedimentation of NJ during the first 45 min. However, natural juice did not sediment by itself, remaining turbid all the time along the column. When an appropriate dose of pectolytic enzyme was added to a pasteurized cloudy juice, Zeta-potential (ξ) remained practically constant at −9 mV, as in the previous assay with natural juice. Particles increased their size (P_s) during the first 10 min, starting from a lower value as compared with the natural juice, and then reaching a maximum, a phenomenon attributed to the effect of pectinase on particle structure. It was speculated that enzyme depectinization had three effects on cloudy juice:

- Destruction of the weak soluble pectin net, reducing juice viscosity (This favored Brownian and convection movement inside the column);
- Aggregation of cloud particles, at least during the first 10 min in this assay (Pectinase degrades pectin and partially exposes the positively-charged protein beneath, reducing electrostatic repulsion between cloud particles);
- Finally, it seems that after most of the native pectin is destroyed, aggregation structures collapsed, increasing the number of small particles and resulting in the decrease in size and increase in turbidity observed.

These facts, associated with a negligible variation in ξ, explain the need for other clarifying agents, like bentonite and gelatin, to reach flocculation condition.

29.2.2. *Fining Reactions*

A *type A* gelatin is a protein (collagen) usually derived from acid-pretreated pigskin, and has isolectric point (pI) between 6 and 9. The significance of pI is that the higher the pI, the greater the cationic charge on the molecule at the juice pH. At the apple juice pH (~ 3.6), all gelatins would be positively charged (Cole, 1986).

The primary reaction occurring with gelatin is a complex formation between polyphenols in the juice and the protein of gelatin to give the desired precipitate. The second reaction, less well understood, but equally important, is the complex formation between the natural proteins of the juice and the added protein, gelatin finally. A third reaction occurs after addition of bentonite (which should be added after the gelatin) which absorbs or complexes with any residual dissolved protein, either gelatin or any other natural protein in the juice (Cole, 1986). Bentonite is an industrial mineral, rich in montmorillonite. Montmorillonite is a clay consisting of aluminum silicate anions ($Al_2O_3.SiO_2$)(H_2O)n neutralized by cations such as sodium, calcium, potassium and magnesium. High-swellable sodium bentonite is more difficult to handle. Sodium bentonite offers high adsorption of proteins and

good clarification capacity, although it may produce a high volume of sediments. Alternatively, a sodium calcium bentonite with average properties is also commercialized (Herbslöh, 2005). The microscopic structure of bentonite consists of many plates that position in such a way as to swell considerably when absorbing water. The mechanisms of protein removal are absorptive interactions between positively charged proteins and negatively charged plate surfaces. Some bentonite absorption of uncharged molecules also occurs. Bentonite may indirectly adsorb some phenolic compounds via binding with proteins that have complexed with phenolics. Bentonite is known to affect juice color directly by binding with positively charged anthocyanins (Zoecklein, 1988). However, the amount of phenols and anthocyanins removed is usually not great. The interaction of bentonite with proteins occurs within minutes. Bentonite is used to counterfine residual gelatin haze and creates high quantities of light sediment. However, excessive dosage can impart an earthy taste to juice.

It was observed that the particle size (Ps) of a depectinized cloudy apple juice was drastically reduced after the addition of at least 0.02% gelatin. This phenomenon was attributable to the effect of gelatin on the flocculation of particles sized 1.6 μm and higher. This fact was also visually observed as the formation of compact sediments. Particles smaller than 1.6 μm remained in suspension. On the other hand, ξ reduced its absolute value from the original –9 mV to the isolectric point ($\xi = 0$) corresponding to a gelatin concentration of 0.02%. This value should correspond with the minimum electrostatic repulsion force among particles, facilitating flocculation.

From the results obtained through turbidity determinations as NTU (Fig. 29.2), two regions of optimal clarifying dose of bentonite-gelatin were found in the

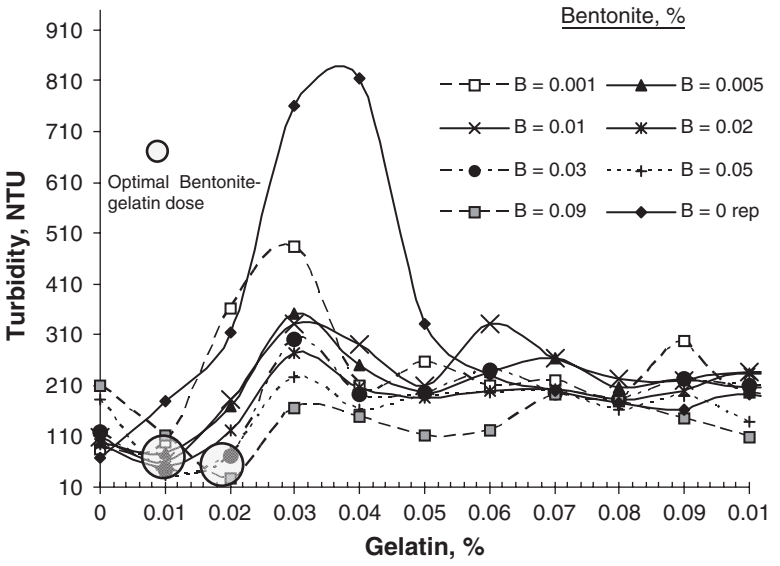

FIG. 29.2. Effect of gelatin and bentonite on the turbidity as NTU, of an enzymatically treated apple juice (Rohapect 1,5 mg/L; 2 h; 50 °C). Shaded circles indicate gelatin-bentonite doses for optimal clarification

range of ξ −0.5 to 0.0 mV: (i) a dose of 0.01% gelatin- 0.02% bentonite, obtaining a supernatant juice of 60 NTU; and for (ii) a dose of 0.02% gelatin–0.09% bentonite, obtaining a supernatant juice averaging 55 NTU. These are very good clarification values, considering that after finishing (filtering through diatomaceous earth and/or cellulose filters) an acceptably transparent apple juice counts up to 5 NTU units (TREETOP, 1999).

It must be noted, however, that ξ was practically at the isolectric point among 0.01 and 0.02% gelatin, when low doses of bentonite were used (< 0,05%). Moreover, excessive fining may result in haze precursors in the juice, and lower doses of clarifying agents are recommended.

29.3. Conclusions

Experiments were conducted to study the colloidal behavior of turbid apple juice, and to evaluate the efficacy of using Zeta-potential (ξ) as a test for determining optimal doses of gelatin and bentonite as clarification agents. When fresh pressed apple juice (NJ) was allowed to settle in a sedimentation column, partial clarification occurred, determined as a reduction in turbidity from 1900 to 100 NTU. Average particle size also reduced from approximately 1.9 µm to 1.3 µm. After juice was pasteurized and subjected to enzymatic treatment (pectinase) in the sedimentation column, a maximum particle size was observed. This phenomenon was attributed to the partial degradation of the negative charged pectin. Adding 0.02% gelatin to the juice reduced its ξ absolute value from the original −9 mV to almost the isolectric point (ξ = 0). When 0.03% bentonite was added, the ξ = 0 point was reached with 0.01% gelatin. Higher doses of bentonite required a higher dose of gelatin. Turbidity determinations as NTU indicated that at least two regions of optimal clarifying doses of bentonite-gelatin occur.

Acknowledgements This research was supported by a grant (BID 1201/OC-AR) from the *Agencia Nacional de Promoción Científica y Tecnológica* of Argentina.

References

Cole C.G.B., 1986, The Use of Gelatin in Wine Fining, in: *the Proceedings of the 1st SAAFoST Technical Symposium, Emulsifiers, Stabilizers and Thickeners in the Food Industry 1*, Natal Technikon Printers, Durban.

Genovese, D.P., Elustondo, M.P., and Lozano J.E., 1997, Color and Cloud Stabilization by Steam Heating During Crushing in Cloudy Apple Juice, *J. Food Sci*. **62**:1171–1174.

Herbslöh. 2005, The Clay Bentonite. A Fascinating Natural Substance and Its Application in Beverage Treatment. Australia (October 8, 2002); http://www.swiftco.com.au/swift/pdf/Bentonite.pdf

Hsu, J.C., Heatherbell, D.A., and Yorgey B.M., 1987, Heat-Unstable Proteins in Wine. I. Characterization and Removal by Bentonite Fining and Heat Treatment, *Am. J. Enol. Viticult*. **38**:11-15.

Hsu, J.C., Heatherbell, D.A., and Yorgey B.M., 1989, Effects of Fruit Storage and Processing on Clarity, Proteins and Stability of Granny Smith Apple Juice, *J. Food Sci*. **54**:660-662.

Hsu, J.C., Heatherbell, D.A., and Yorgey B.M., 1990, Effects of Variety, Maturity and Processing on Pear Juice Quality and Protein Stability, *J. Food Sci*. **55**:1610-1613.

Peterson, E.M., and Johnson A., 1978, *Encyclopedia of Food Science*, AVI, Westport.

Quemada, D., and Berli C., 2002, Energy of Interaction in Colloids and Its Implications in Rheological Modeling, *Adv. Colloid Int. Sci*. **98**:51.

Stocké R., 1998, The 3-Component Stabilization with Bentonite, Gelatin and Silica Sol, *Fruit Process*. **1**:6–10.

Tajchakavit, S., Boye, J.I., and Couture R., 2001, Effect of Processing on Post-Bottling Haze Formation in Apple Juice, *Food Res. Int*. **34**:415-424.

TREETOP, 1999, Apple Juice Concentrate—TYPE I, TYPE II, TYPE III. Ingredient Division. Product Data Sheet TDS-116. Selah WA: (1999); http://www.treetop.com/ingredient/ Products/ products/ concentrates/ ingpds Apple Concentrate.pdf. pp. 1-3.

Zoecklein B., 1988, *Bentonite Fining of Juice and Wine*, Publication 463-014. Department of Horticulture. Virginia Polytechnic Institute & State University. Virginia.

30
Engineered Food/Protein Structure And Bioactive Proteins And Peptides From Whey

I. Recio, M. Ramos, and A.M.R. Pilosof

30.1. Introduction

Traditionally, whey was considered a by-product in the manufacturing of cheeses with little or no commercial value. This view is changing as novel technical and nutritional applications are being discovered for whey or whey components. The composition of whey depends on the method of cheese manufacture, but the major components are proteins, lactose and minerals. Some whey constituents have unusual properties that make them valuable commercially as sources of flavor enhancers, fat substitutes, food binders, and recently, as functional ingredients with biological activities. This contribution summarizes some of the biological activities attributed to whey proteins and peptides derived thereof and advances in the use of whey proteins in biopolymer mixtures for engineered food structure development.

30.2. Biological Functions of Whey Proteins

The primary functions of dietary proteins, and hence of whey proteins, is to supply the body adequately with indispensable amino acids and organic nitrogen; some of these proteins also have a specific biological activity.

The bovine whey protein fraction consists of α-lactalbumin, β-lactoglobulin, bovine serum albumin, immunoglobulin, lactoferrin, transferrin and the proteose-peptone fraction. In addition, cheese whey contains caseinmacropeptide (CMP), which is the product of milk κ-casein hydrolysis with chymosin. The concentrations of these proteins in milk, together with their attributed biological functions, are shown in Table 30.1. In addition to these biological functions, which will be briefly reviewed, whey proteins are of high nutritional value because they contain all of the essential amino acids, and in higher concentrations compared to various vegetable protein sources such as soy, corn, and wheat gluten (Walzem et al., 2002).

TABLE 30.1. Concentration and biological functions of major milk proteins (adapted from Séverin and Wenshui, 2005)

	Concentration (g/l)		
Protein	Bovine	Human	Function
Total caseins	26.0	2.7	Mineral carrier, precursor of bioactive peptides
Total whey proteins	6.3	67.3	
β-Lactoglobulin	3.2		Retinol carrier, binding fatty acids, antioxidant
α-Lactalbumin	1.2	1.9	Lactose-synthesis in mammary gland, Ca carrier, immunomodulation, anticarcinogenic
Immunoglobulins (A, M and G)	0.7	1.3	Immune protection
Serum albumin	0.4	0.4	
Lactoferrin	0.1	1.5	Antimicrobial, antioxidative, immunomodulation, iron absorption, anticarcinogenic
Lactoperoxidase	0.03		Antimicrobial
Lysozyme	0.0004	0.1	Antimicrobial
Proteose-peptone	1.2		
Caseinmacropeptide	1.2		Antiviral, bifidogenic
Others	0.8		

Lactoferrin plays an important role in iron uptake in the intestine (Hutchens et al., 1994; Viljoen, 1995) and is thought to play a role in innate defense. Its broad antimicrobial spectrum (including Gram-positive and Gram-negative bacteria, yeasts and fungi), and the recently discovered antiviral activity (including cytomegalovirus, herpes, influenza, HIV, rotavirus, hepatitis C) support this envisaged role (Floris et al., 2003; Berkhout et al., 2004). Lactoferrin has proven to exert other biological activities such as antioxidant, immunomodulatory, modulation of cell growth, and binding and inhibition of several bioactive compounds (lipopolysaccharide and glycosaminoglycan) (Baveye et al., 1999; Chierici, 2001). The pepsin-hydrolysate of lactoferrin has more potent antimicrobial activity than the native protein, and a peptide, called lactoferricin, which also exhibits various biological activities, has been purified. Recently, it has been recognized that oral administration of lactoferrin exerts various beneficial health effects such as anti-infective activities, not only in infants, but also in adult animals and humans (for a recent review see Wakabayashi et al., 2006). Current commercial applications of bovine lactoferrin include infant formulas, nutritional iron supplements and drinks, fermented milks, chewing gums, immune-enhancing nutraceuticals, cosmetic formulas, and feed and pet care supplements (Jan, 2001).

The enzyme lactoperoxidase is a glycoprotein member of the mammalian peroxidase family. The lactoperoxidase system consists of three primary components: the lactoperoxidase enzyme, thiocyonate and hydrogen peroxyde. The lactoperoxidase system has been demonstrated to be very effective in inhibiting the growth of Gram-positive foodborne organisms, including *Staphylococcus aureus*. Gram-negative, catalase-positive organisms such as pseudomonas, coliforms, salmonellae and shigellae are not only inhibited by the lactoperoxidase system, but, depending on the medium conditions, lactoperoxidase may also show

bactericidal activity. Lactoperoxidase may be a useful additive for infant formulae because human milk contains very little or no lactoperoxidase (Fox, 2001).

Lysozyme is known to be a powerful antibacterial protein widely distributed in various biological fluids and tissues, hen egg white and human milk and colostrum being especially rich sources. The enzyme hydrolyses bacterial cell walls, resulting in cell lysis. Milk lysozyme is active against a number of Gram-positive bacteria and some Gram-negative bacteria that are completely resistant to egg-white lysozyme (Floris et al., 2003). There seems to be a synergistic action of lysozyme and lactoferrin against *Escherichia coli*, as the latter damages the outer membrane of Gram-negative bacteria and the organism becomes susceptible to lysozyme.

The antibacterial activity of lysozyme was first exclusively attributed to its catalytic function. In the last two decades, the literature abounds with evidence implicating a non-enzymatic mechanism of action (Ibrahim et al., 2002; Ibrahim, 2003; Masschalck and Michiels, 2003). Aside from its antibacterial activity, it has been demonstrated that lysozyme may exert other functions including inactivation of certain viruses, enhancement of antibiotic effects, anti-inflammatory and antihistaminic action, activation of immune cells and antitumor activity.

Recent progress in the fractionation technologies has enabled large-scale isolation of immunoglobulins from bovine colostrum and milk for commercial purposes. Subsequently, immunoglobulin concentrates derived from colostrum, cheese whey or blood serum have been developed and launched on the market for neonatal calf, lamb or piglet feeding. Such immune milk preparations have been found to be effective in the prevention or treatment of various enteric diseases in animals and humans (Pihlanto and Korhonen, 2003).

The biological activity of bovine caseinmacropeptide has received much attention in recent years. It corresponds to the C-terminal hydrophilic peptide released by the action of chymosin on κ-casein. Physiological functions attributed to CMP include binding of cholera and *Escherichia coli* enterotoxins, inhibition of bacterial and viral adhesion, suppression of gastric secretions, promotion of bifidobacterial growth and modulation of immune system responses (Manso and López-Fandiño, 2004; Brody, 2000).

The physicochemical and functional characteristics of β-lactoglobulin (β-Lg) are well known, but its biological function is not yet clear. It is the major whey protein in ruminants, and its ability to bind a variety of small hydrophobic molecules, such as retinol, lipids and fatty acids, is well documented. Intestinal receptors specific for β-Lg and the protein's resistance to proteolytic activity in the stomach might indicate that it is involved in retinol transport from mother to neonate. In addition, β-Lg has been shown to exhibit different mitogenic activities *in vitro* and immunomodulatory properties (Pihlanto and Korhonen, 2003).

α-Lactalbumin (α-La) is a subunit of lactose synthase, and is a calcium-binding metalloprotein of major importance from a nutritional point of view. In addition, it has been suggested that it possesses immunomodulatory and anticarcinogenic properties (Parodi, 1998). Interestingly, Håkansson et al. (2000) have

found an α-La folding variant from human milk with bactericidal activity against antibiotic-resistant and susceptible strains of *Streptococcus pneumoniae*, but this variant had little or no activity against other bacteria. The active form contained α-La in a partially unfolded molten globule-like state. Tumor cells and immature cells were also sensitive to this fraction and were shown to undergo apoptosis, but this α-La variant leaves normal differentiated cells unaffected (Håkansson et al., 1995; Svensson et al., 1999). This molecular complex of human α-La and oleic acid with antitumor activity has been designated HAMLET (human α-La made lethal to tumor cells), and has received much attention due to its potential use as a new therapeutic agent against tumour cells (Gustafsson et al., 2005).

30.3. Bioactive Peptides

During the last two decades, besides the high functional value of various milk proteins, such as lactoferrin or immunoglobulins, the presence of other components with biological activity, such as peptides, has been demonstrated. These peptides are hidden in a latent state within the precursor protein sequence but can be released by enzymatic proteolysis during gastrointestinal digestion *in vivo*, or during the manufacture of milk products. Enzymatic hydrolysis of milk proteins can release fragments able to exert specific biological activities, such as antihypertensive, antimicrobial, opioid, antioxidant, immunomodulant, or mineral binding. Due to the increasing production of whey as a byproduct of cheesemaking, the development of processes to isolate or concentrate added-value molecules with biological activity, which can be used as ingredients in functional foods, has acquired a special relevance. The biological properties of peptides derived from whey proteins, focusing special attention on studies carried out on antihypertensive, and antioxidant peptide, are discussed below.

30.3.1. ACE-Inhibitory Peptides

Hypertension, which is estimated to affect one third of the Western population, is a risk factor for cardiovascular disease. The renin-angiotensin-aldosterone system is a key factor in the maintenance of arterial blood pressure. One of the main components of this system is angiotensin-converting enzyme (ACE) [EC 3.4.15.1], which catalyzes the conversion of angiotensin I, an inactive decapeptide, into angiotensin II, an octapeptide with a potent vasoconstrictor action (Ondetti et al., 1977). Moreover, ACE catalyzes the inactivation of bradykinin, which has an important vasodilator activity. Therefore, inhibition of this enzyme results in a lowering of blood pressure. Several proteins from different foods, such as, eggs, tuna, and soy sauce, have been identified as precursors of ACE-inhibitory peptides but, to date, milk proteins are the main source of this kind of bioactive peptides. These fragments have been generated from the precursor proteins by enzymatic hydrolysis, fermentation, combined processes and/or chemical synthesis based on combinatorial library designs of peptides.

The ACE-inhibitory peptides derived from milk caseins are known as casokinins, while the peptides derived from whey proteins are generally called lactokinins. Due to the relevance of this group of peptides, extensive research has been aimed at identifying novel peptide sequences and elucidating the structure-activity relationships, production methods, etc. These results have been recently reviewed (Korhonen and Pihlanto., 2006; Gobetti et al., 2004; Silva and Malcata, 2005). Even more recently, aspects related to the bioavailability of ACE inhibitory peptides and other aspects related to the physiological, chemical and technological properties of peptides have been reviewed by other authors (Fitzgerald et al., 2004; Vermeirssen et al., 2004; Meissel., 2005; López-Fandiño et al., 2006).

Concerning the whey proteins, hydrolysis with a combination of digestive enzymes or with highly proteolytic and less specific enzymes, such as thermolysin or proteinase K, resulted in digests containing a number of potent ACE-inhibitory peptides (Mullally et al.,1997; Abubakar et al., 1998; Pihlanto-Lepälä et al., 2000; Fitzgerald and Meissel, 1999; Nurminen et al., 2000; Hernández-Ledesma et al., 2002). However, peptides with an ACE-inhibitory activity *in vitro* do not necessarily exert an antihypertensive effect after oral ingestion. To exert an antihypertensive effect, they must be able to survive gastrointestinal digestion, be absorbed, and reach the cardiovascular system in an active form. For instance, studies made on the stability *in vitro* of a tryptic fragment of β-lactoglobulin (β-Lg f (142-148) with sequence ALPMHIR with potent ACE-inhibitory activity demonstrated that this peptide is probably not sufficiently stable to gastrointestinal and serum proteinases to act as a hypotensive agent in humans following oral ingestion (Walsh et al., 2004). On the contrary, the action of gastrointestinal enzymes can release the active form of peptide. Interestingly, a shorter fragment corresponding to the same region of β-Lg (β-Lg f(142-145), ALPM) has demonstrated antihypertensive effects in spontaneously hypertensive rats (SHR), although the IC_{50} value of this β-Lg fragment was not high. Therefore, the active form of this peptide can be produced by the action of gastrointestinal enzymes, or other mechanisms can be involved in the antihypertensive activity of ALPM (Murakami et al., 2004).

Other multifunctional peptides have been reported from whey proteins: α-lactorphin, α-La f(50-53), and β-lactorphin, β-Lg f(102-105), which showed opioid-like activity (Yoshikawa et al., 1986) and ACE-inhibitory activity with IC_{50} (concentration needed to inhibit 50% of the ACE activity) values of 733 and 172 μM, respectively (Mullally et al., 1996). These opioid peptides improved vascular relaxation in SHR, and α-lactorphin improved vascular relaxation in SHR (Sipola et al., 2001; Nurminen et al., 2000).

Hernández-Ledesma et al. (2002) have carried out studies on the ACE-inhibitory activity of hydrolysates of β-Lg from ovine and caprine milk with enzymes of digestive and microbial origin. The results suggested a more efficient cleavage of milk proteins by microbial enzymes for the formation of ACE-inhibitory peptides. Four new caprine β-Lg derived peptides with ACE-inhibitory activity were purified and identified from the hydrolysate prepared with thermolysin (Table 30.2). These peptides corresponded to β-Lg fragments f(46-53), f(58-61), f(103-105), and f(122-125), and their IC_{50} values ranged from 34.7 to 2470 μM. Of special

TABLE 30.2. ACE-inhibitory and/or antioxidant activity of peptides derived from whey proteins

Peptide Fragment	Sequence[a]	IC_{50} μM[b]	Orac-Value	Origin	Reference
α-La f(50-53)	YGLF	733	-	Hydrolysis with gastric and pancreatic enzymes	Nurminen et al., 2000
β-Lg f(78-80)	IPA	141	-	Hydrolysis with proteinase K	Abukakar et al., 1998
β-Lg f(142-145)	ALPM	928	-	Commercial whey product	Murakami et al., 2004
β-Lg f(103-105)	LLF	79.8	-	Hydrolysis with Thermolysin	Hernández-Ledesma et al.,2002
β-Lg f(58-61)	LQKW	34.7	-	Hydrolysis with Thermolysin	Hernández-Ledesma et al.,2002
β-Lg f(142-148)	ALPMHIR	42.6	-	Hydrolysis with Trypsin	Mullally et al., 1997
β-Lg f(145-149)	MHIRL	-	0.306	Hydrolysis with Corolase PP	Hernández-Ledesma et al., 2005
β-Lg f(42-46)	YVEEL	-	0.799	Hydrolysis with Corolase PP	Hernández-Ledesma et al., 2005
β-Lg f(19-29)	WYSLAMAASDI	-	2.61	Hydrolysis with Corolase PP	Hernández-Ledesma et al., 2005
β_2-m[c] f(18-20)	GKP	352	-	Hydrolysis with proteinase K	Abukakar et al., 1998
BSA f(221-222)	FP	315	-	Hydrolysis with proteinase K	Abukakar et al., 1998

[a] One letter amino acid sequence

[b] Peptide concentration needed to inhibit 50% of the original ACE activity

[c] β_2-microglobulin

interest is peptide LLF, included within the sequence of the opioid peptide β-lactorphin (YLLF), which is considered a "strategic zone" partially protected from digestive breakdown.

The most potent caprine β-Lg fragment found in this study corresponded to LQKW, β-Lg (58-61) with IC_{50} values of 34.7 μM. LLF and LQKW peptides also showed an antihypertensive activity in spontaneously hypertensive rats (Hernández-Ledesma et al., 2007a). More recently, Hernández-Ledesma et al. (2006) have evaluated the effect of heat denatured treatments on the release of new and potentially ACE-inhibitory peptides from bovine β-Lg during the hydrolysis with thermolysin. For this purpose, the peptides released from this whey protein at different incubation temperatures and times are identified by HPLC-MS/MS, and their potential biological activity is discussed in relation to their structure. In this work, a more rapid release of some peptides of interest at increasing temperatures was found. Moreover, novel cleavage sites for

thermolysin localized inside the most buried zones of the β-Lg monomer have been found. In general, heating of β-Lg during enzyme treatments enhanced the formation of peptides with ACE-inhibitory activity. Concretely, one of the peptides released under heat-denaturing conditions was LQKW, which had previously been described as a potent ACE inhibitor.

Manso and López-Fandiño (2003) evaluated the ACE-inhibitory activities of bovine, caprine and ovine kappa-caseinmacropeptides and their tryptic hydrolysates. The results indicated that kappa-caseinmacropeptides exhibit moderate ACE-inhibitory activity that increased considerably after digestion under simulated gastrointestinal conditions.

The active peptides could be produced from CMPs via proteolysis with trypsin. Peptides MAIPPK and MAIPPKK, corresponding to κ-CN fragments f (106-111) and f(106-112), respectively, were identified, and the latter significantly reduced blood pressure of model animals (Miguel et al., 2007). These peptides showed a moderate activity, but their digestion under simulated gastrointestinal conditions allowed the release of potent ACE-inhibitory peptide IPP (IC_{50} value of 5 μM). These findings might help to promote further exploitation of kappa-casein-macropeptides as multifunctional active ingredients, broadening the potential uses of rennet whey from various sources.

30.3.2. Antioxidant Peptides

Reactive oxygen species (ROS) are produced as part of normal cell metabolism. However, an abnormal increase in their production can be caused by some external agents. A high level of ROS can perturb the redox balance and promote "oxidative stress" in cells. This situation is implicated in the etiology of age-associated chronic diseases, such as cardiovascular diseases, cancer, diabetes, cataracts, neurodegenerative disorders, and aging (Ames et al., 1993). In addition to the endogenous defense systems, the organism can also defeat ROS by exogenous antioxidants provided by the diet. Although antioxidants of vegetable origin have attracted the interest of researchers and consumers, antioxidants from animal sources are also consumed in the diet. Recent studies have focused on searching for antioxidant peptides derived from casein and whey proteins (Peña-Ramos and Xiong, 2001).

Few studies about the antioxidant properties of peptides derived from whey proteins have been performed (Table 30.2). Oxygen radical antioxidant capacity (ORAC) was shown by several peptides identified in a β-Lg A hydrolysate with Corolase PP (Hernández-Ledesma et al., 2005). In addition, some of these peptides exhibit a synergistic effect with other well-known antioxidants, such as ascorbic acid (Hernández-Ledesma et al., 2007b). The presence in their sequence of certain amino acids such as Trp, Tyr and Met has been found to be the most important structural characteristic for their antioxidant activity. The ORAC value of the most active peptide was 2.62 μmol Trolox equivs/μmol peptide, and its sequence was WYSLAMAASDI. The antioxidant activity of this peptide was slightly higher than that of butylated hydroxyanisole (BHA) currently used in the

food industry as a synthetic antioxidant (2.43 μmol Trolox/μmol BHA) (Dávalos et al., 2004).

30.4. Whey Proteins in Biopolymer Mixtures for Food Structure Development

In recent years, considerable interest has been devoted to study the gelation of whey proteins in presence of polysaccharides (Galazka et al., 1999; Capron et al., 1999a; Eleya and Turgeon, 2000; Beaulieu et al., 2001; Baeza et al., 2002; Baeza et al., 2003; Tavares and Lopes da Silva, 2003). The results obtained from these studies are important contributions to the adequate manipulation of the rheological properties of biopolymer mixtures, and they support the attractive concept of engineered food structure development since mixed gels can be viewed as self-assembling systems, and the control of morphologies would allow designing of their properties (Turgeon et al., 2003).

The presence of unfavorable repulsive interactions between segments of chemically different polymers (i.e., proteins and polysaccharides) in solution leads to a high probability of the mutual exclusion of each polymeric solute component from the local vicinity of the other. At a sufficiently high polymer concentration, the net repulsion between the two species at the molecular level causes the system to separate spontaneously into two distinct phases. This phenomenon, known as thermodynamic incompatibility, is commonly exhibited by semi-dilute or concentrated mixed solutions of protein + polysaccharide and is the main cause of synergistic effects. Incompatibility mainly occurs at pH higher than the protein isoelectric point and/or at high ionic strengths (Grinberg and Tolstoguzov, 1997). The protein and polysaccharide structures (molecular weight, size and conformation) have a strong influence on the intensity of the interactions.

Phase separation of protein-polysaccharides occurs above a critical concentration. At lower concentrations, they co-exist in a single phase, containing the biopolymers in domains in which they mutually exclude one another, which increases the thermodynamic activity of a protein and results in specific changes in functional properties (Carp et al., 2001; Sánchez et al., 1995; Tolstoguzov, 1997). Polysaccharides under conditions of limited thermodynamic compatibility (below minimal total concentration for phase separation) can be viewed as modifiers of the kinetics of whey protein aggregation, of the size of aggregates and of the degree of association of particles in the gel network mechanical properties of protein. A consequence of polymer incompatibility is the lowering of the critical concentration for gelation of the components and the acceleration of the aggregation (Capron et al., 1999b; Ould Elaya and Turgeon, 2000; Baeza et al., 2002; Baeza et al., 2003; Renard et al., 2006).

Several microstructures, ranging from a fine to a coarse particulate, may be induced in mixed β-Lg/non-gelling gum gels by varying the type of gum, the proportion of the components and pH (Baeza and Pilosof, 2001; Monteiro et al.,

2005; Tavares et al., 2005). Photomicrographs of mixed β-Lg/gum gels (Baeza and Pilosof, 2001) revealed particulate microstructures, except for β-Lg/ propyleneglycol alginate (PGA) gel at pH 7, that showed a smooth and continuous microstructure (Fig. 30.1a). At pH 7 the β-Lg aggregated in the presence of λ-carrageenan into large, almost smooth spherical particles of approximately 8 μm in diameter packed with few junctions between them (Fig. 30.1b). β-Lg/xanthan gel at pH 7 showed a dense microstructure formed of smooth clusters of irregular shape of about 2 μm in diameter consisting of fused particles (Fig. 30.1c). More regular gel networks were formed at pH 6 in presence of λ-carrageenan and xanthan. The particles forming β-Lg/PGA gels at pH 6 showed a flat irregular flake-like shape, fused together in a dense structure.

Large deformation tests have proved to be more correlated to microstructure of particulate gels than small deformation tests. Hardness and cohesiveness of β-Lg/ polysaccharide gels increased in the order λ-carrageenan < xanthan < PGA (Baeza and Pilosof, 2001). It appears that the size of particles forming the gel structure and the size of voids between them are related to texture parameters. In fact, β-Lg/ λ-carrageenan gels consisting of large, loosely packed particles, with large voids between them (Fig. 30.1b) showed the lowest texture properties. Contrarily, β-Lg/PGA gels consisting of a continuous and dense structure without apparent pores (Fig. 30.1a) showed the highest values for texture parameters.

It appears that a delicate balance between β-Lg and polysaccharide concentration is needed to obtain gels with good mechanical and water holding properties. This implies that polysaccharides should promote a limited aggregation of the protein. In this sense, PGA showed an outstanding performance as induced gels with a fine dense structure and very good properties.

The role of propyleneglycol alginate on the dynamics of gelation and properties of β-Lg gels under conditions where the protein alone does not gel (6% wt) has been analyzed by Baeza et al. (2003). To this end, the kinetics of gelation, aggregation and denaturation of β-Lg in the mixed systems (pH 7) were studied at

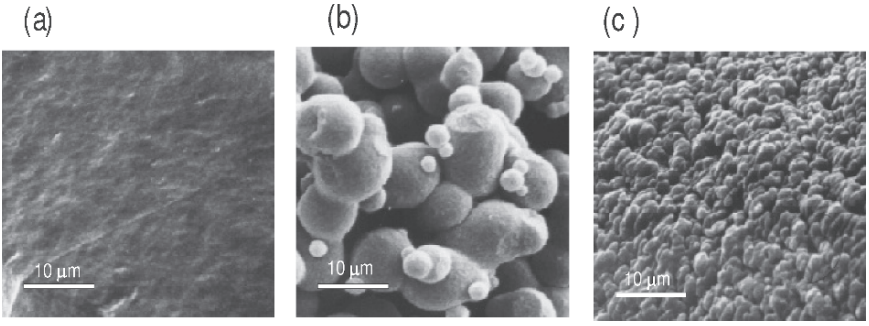

FIG. 30.1. SEM micrographs of 6% β-Lg + 0.5% gum gels at pH 7: (a) β-lg/PGA; (b) β-Lg/λ-carrageenan;(c) β-Lg/xanthan

different temperatures (64–88.8 °C). It was found that the extent of polysaccharide induced protein aggregation and the type of interactions involved prior to denaturation are very important in determining the gel structure and its properties.

The role of propyleneglycol alginate on the dynamics of gelation and properties of β-Lg gels under conditions where the protein alone does not gel (6% wt) has been analyzed by Baeza et al. (2003). To this end, the kinetics of gelation, aggregation and denaturation of β-Lg in the mixed systems (pH 7) were studied at different temperatures (64 – 88.8 °C). It was found that the extent of polysaccharide induced protein aggregation and the type of interactions involved prior to denaturation are very important in determining the gel structure and its properties.

Dynamic light scattering has been used for studying the heat-induced aggregation of β-Lg over a wide range of medium conditions (Hoffmann et al., 1996; Verheul et al., 1998). This technique gives quantitative and qualitative information about the aggregates formed during heating, as well as on the rate of particle formation.

The effect of PGA concentration on the size and scattered intensity of β-lg aggregates is shown in Fig. 30.2, where the mean hydrodynamic diameter (d_h) and the scattered intensity (Is) of aggregates formed during heating at 72 °C are

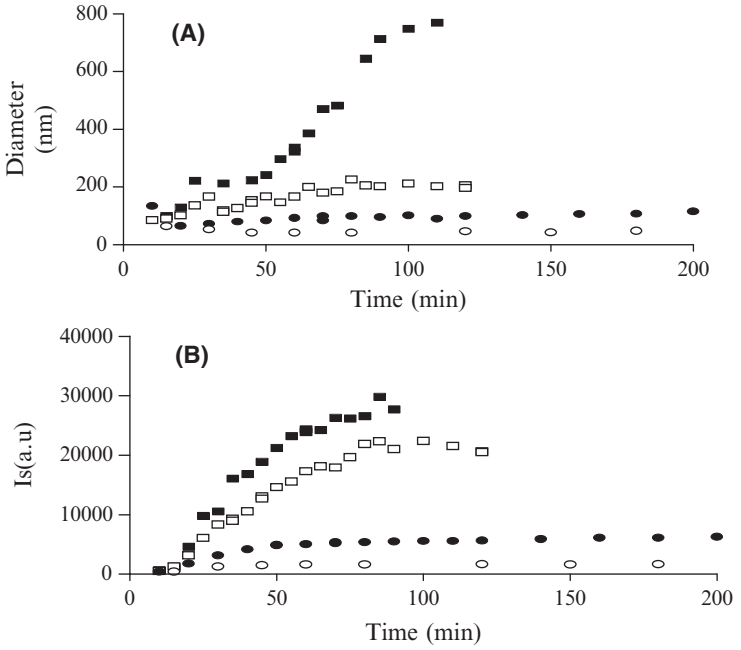

FIG. 30.2. Effect of PGA concentration on the aggregation of β-Lg (6%)/PGA solutions at neutral pH. Aggregation was carried out at 72 °C. (A) apparent mean diameter, d_h (nm) and (B) scattered intensity, I_s (a. u.) versus time. PGA concentration: (○) 0%, (●) 0.25%, (●) 0.75%, (■) 1%

plotted as a function of heating time. The presence of PGA promoted the formation of large β-Lg aggregates that, upon heating, continued to grow over time. In the pure β-Lg solution (6% wt) the aggregates formed were small (40-60 nm), and after a short time reached a constant value. Both d_h and Is increased with PGA concentration, indicating that higher amounts of PGA enhanced the formation of larger particles and accelerated the aggregation process. The initial increase of the scattered intensity $(dIs/dt)_0$, taken from the initial slope of the curves, describes the rate of protein aggregation during the formation of the primary gel structure. Hoffman et al. (1996) obtained similar results by increasing β-Lg concentration in pure β-Lg solutions. The results obtained in the presence of the polysaccharide might be explained by a more pronounced thermodynamic incompatibility between both biopolymers with higher PGA concentrations.

The diameters of protein aggregates increased with heating temperature, but a change in temperature dependence of the particles' size was observed at around 80.8 °C, which is close to the onset temperature of protein denaturation (77.9 °C). In the presence of 0.5 % wt PGA, the mean diameter of these aggregates increased up to 600 nm for heating temperatures up to 85 °C (Baeza et al., 2003).

A similar behavior has been reported for β-Lg in the presence of other polysaccharides. Xanthan increased diameters of β-Lg aggregates (Baeza and Pilosof, 2001), k-carrageenan accelerated the aggregation of small β-Lg particles to larger fractal constituents (Capron et al., 1999), λ-carrageenan (0.5%) promoted the formation of very large particles (8 mm) in β-Lg gels (6%) (Baeza and Pilosof, 2001), and amylopectin accelerated the particle aggregation of β-Lg because of phase separation between the protein and the polysaccharide rich phases (Olsson et al., 2002).

Different gel structures can be obtained by using hydroxypropylmethylcellulose (HPMC) in combination with whey proteins (Perez et al., 2006). HPMC is used in the food industry, printing technology, and has pharmaceutical applications because it is nontoxic and possesses good mechanical properties.

In the pharmaceutical industry, HPMC has acquired special interest for controlled drug-release matrices (McCrystal, et al., 1997; Ford, 1999). The usefulness of HPMC is essentially based upon four key attributes: efficient thickening, surface activity, film forming ability, and the capacity to form gels on heating that melt upon cooling.

The phase diagram for WPC/HPMC mixtures, recently reported by Perez et al. (2006), show that the binodal curve is very close to axis, which means the compatibility zone is relatively small and phase separation takes place in a broad range of biopolymer concentrations. Mixtures of whey proteins and HPMC at neutral pH and 25 °C rapidly separate in an upper HPMC rich phase and a lower WPC rich phase (Fig. 30.3) above a minimal total concentration of 5%. Upon heating mixtures of WPC and HPMC at neutral pH, several complex events can take place, some of them simultaneously: a) HPMC chains dehydration, hydrophobic groups exposition and their interaction; b) aggregation/gelation of dehydrated HPMC; c) denaturation of WPC; d) aggregation/gelation of WPC; e) phase separation. The dynamics of gelation and gel macrostructure upon heating

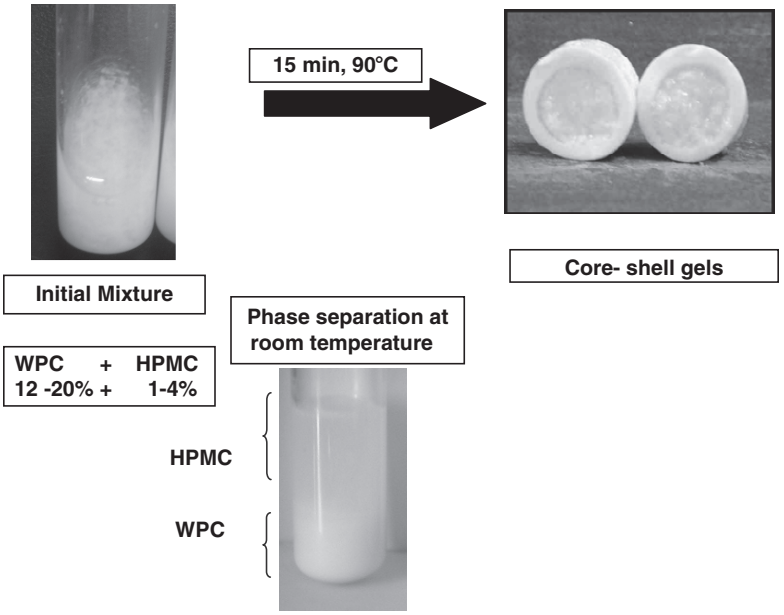

FIG. 30.3. Phase separation and gelation of whey protein/HPMC mixtures

and cooling point out that there are two competitive phenomena: phase separation and gelation of both biopolymers.

By heating WPC/HPMC mixtures at 90 °C, non-self supporting gels are obtained at 8% wt WPC, and self-supporting gels are obtained when WPC concentration is ≥ 12% wt. The self-supporting gels showed a *core-shell* structure that consisted of an external shell of gelled protein and a core of gelled HPMC that did not melt upon cooling (Fig. 30.3). The rigidity and the thickness of the protein shell, as well as the solid character of the HPMC core, increased with WPC and HPMC concentration in the mixture.

Core-shell macrostructure of gels should be related to the competition between gelation and phase separation that results in a very interesting macrostructure at WPC concentrations equal or above 12% and variable HPMC concentration (1-4 %). This structure could find potential applications in the design of microcapsules or controlled delivery systems, in which an active component could be partitioned between the separated phases, or to develop new structures and food products.

In conclusion, the practical consequence of using whey proteins in admixture with polysaccharides in conditions of thermodynamic incompatibility is the design of new gel structures with a lower amount of protein, whose properties may be manipulated by selecting the appropriate polysaccharide at adequate concentrations. The time/ temperature as well as the heating rate of the gelation process also appear as important variables to be controlled in order to meet the desired final structure.

Acknowledgements This work was supported by projects CYTED 1.105PI0274, ANPCYT-PICT 13723, UBACYT X128, CM-S0505-AGR-0153 and AGL-2005-03381.

References

Abubakar, A., Saito, T., Kitazawa, H., Kawai, Y., and Itoh T., 1998, Structural Analysis of New Antihypertensive Peptides Derived from Cheese Whey Protein by Proteinase K Digestion, *J. Dairy Sci*. **81**:3131–3138.

Ames, B.N., Shigenaga, M.K., and Hagen T.M., 1993, Oxidants, Antioxidants, and Degenerative Diseases of Aging, *Proc. Natl. Acad. Sci*. **90**:7915–7922.

Baeza, R.I., and Pilosof A.M.R., 2001, Mixed Biopolymer Gel Systems of B-Lactoglobulin and Non-Gelling Gums, in: *Food Colloids, Fundamentals of Formulation*, E. Dickinson and R. Miller (eds.), The Royal Society of Chemistry, Cambridge, pp. 392–403.

Baeza, R.I., Carp, D.J., Pérez, O.E., and Pilosof A.M.R., 2002, K-Carrageenan-Protein Interactions: Effect of Proteins on Polysaccharide Gelling and Textural Properties, *Lebensm.-Wiss.U.-Technol*. **35**:741–747.

Baeza, R.I., Gugliotta, L.M., and Pilosof A.M.R., 2003, Gelation of B -Lactoglobulin in the Presence of Propylene Glycolalginate: Kinetics and Gel Properties, *Colloids Surf. B: Biointerfaces* **31**:8192–93.

Baveye, S., Elass, E., Mazurier, J., Spik, G., and Legrand D., 1999, Lactoferrin: A Multifunctional Glycoprotein Involved in the Modulation of the Inflammatory Process, *Clin. Chem. Lab. Med*. **37**:281–286.

Beaulieu, C.M., Turgeon, S.L., and Doublier J.L., 2001, Rheology, Texture and Microstructure of Whey Proteins/Low Methoxyl Pectins Mixed Gels with Added Calcium, *Int. Dairy J*. **11**:961–967.

Berkhout, B., Floris, R., Recio, I., and Visser S., 2004, The Antiviral Activity of the Milk Protein Lactoferrin Against the Human Immunodeficiency Virus Type 1, *BioMetals* **17**: 291–294.

Brody E.P., 2000, Biological Activities of Bovine Glycomacropeptide, *Br. J. Nutr*. **84**: S39–S46.

Capron, I., Nicolai, T. and Durand D., 1999a, Heat Induced Aggregation of B-Lactoglobulin in the Presence of K-Carrageenan, *Food Hydrocolloid*. **13:**1–5.

Capron, I., Nicolai, T., and Smith C., 1999b, Effect of Addition of K-Carrageenan on the Mechanical and Structural Properties of B -Lactoglobulin Gels, *Carbohydr. Polym*. **40**:233–238.

Carp, D.J., Bartholomai, G.B., Relkin, P., and Pilosof A.M.R., 2001, Electrophoretic Studies for Determining Soy Proteins–Xanthan Gum Interactions in Foams, *Colloids Surf. B* **21**:163–171.

Chierici R., 2001, Antimicrobial Actions of Lactoferrin, *Adv. Nutr. Res*. **10**:247–269.

Dávalos, A., Gómez-Cordovés, C., and Bartolomé B., 2004, Extending Applicability of the Oxygen Radical Absorbance Capacity (ORAC-Fluoresceine) Assay, *J. Agric. Food Chem*. **52**:48–54.

Eleya, M.M.O., and Turgeon S.L., 2000, Rheology of K-Carrageenan And β-Lactoglobulin Mixed Gels, *Food Hydrocolloid*. **14**:29–40.

Fitzgerald, R.J., and Meisel H., 1999, Lactokinins: Whey Protein-Derived ACE-Inhibitory Peptides, *Nahrung* **43**:165–167.

Fitzgerald, R.J., Murray, B.A., and Walsh D.J., 2004, Hypotensive Peptides from Milk Proteins, *J. Nutr*. **134**: 980S–988S.

Floris, R., Recio, I., Berkhout, B., and Visser S., 2003, Antibacterial and Antiviral Effects of Milk Proteins and Derivatives Thereof, *Curr. Pharm. Design* **9**:1257–1275.

Ford J.L., 1999, Thermal Analysis of Hydroxypropylmethycellulose and Methylcellulose: Powders, Gels and Matrix Tables. *Int. J. Pharmaceutics* **179**:209–228.

Fox P.F., 2001, Milk Proteins as Food Ingredients, *Int. J. Dairy Technol*. **54**:41–55.

Galazka, V.B., Smith, D., Ledward, D.A., and Dickinson E., 1999, Interactions of Bovine Serum Albumin with Sulphated Polysacchaides: Effects of Ph Ionic Strength and High Pressure Treatment, *Food Chem*. **64**:303–310.

Gobbetti, M., Minervini, F., and Rizello C.G., 2004, Angiotensin I-Converting- Enzyme-Inhibitory and Antimicrobial Bioactive Peptides, *Int. J. Dairy Technol*. **57**:173–188.

Grinberg, V.Y.A., and Tolstoguzov V.B., 1997, Thermodynamic Incompatibility of Proteins and Polysaccharides in Solutions, *Food Hydrocolloid*. **11**:145–158.

Gustafsson, L., Hallgren, O., Mossberg, A.K., Pettersson, J., Fischer, W., Aronsson, A., and Svanbourg C., 2005, HAMLET Kills Tumour Cells by Apoptosis: Structure, Cellular Mechanisms and Therapy, *J. Nutr*. **135**:1299–1303.

Håkansson, A., Malin, S., Mossberg, A.K., Sabharwal, H., Linse, S., Lazou, I., Lönnerdal, B., and Svanborg C., 2000, A Folding Variant of α–Lactalbumin with Bactericidal Activity Against *Streptococcus pneumoniae, Mol. Microbiol*. **35**:589–600.

Håkansson, A., Zhivotovski, B., Orrenius, S., Sabharwal, H., and Svanborg C., 1995, Apoptosis Induced by a Human Milk Protein, *Proc. Nat. Acad. Sci. USA*, **92**:8064–8068.

Hernández-Ledesma, B., Miguel, M., Aleixandre, M.A., Recio, I., 2007a, Effect of Simulated Gastrointestinal Digestion on Antihypertensive Properties of Beta-lactoglobulin-derived peptides, *J. Dairy Res.* **74**:336–339.

Hernández-Ledesma, B., Amigo, L., Recio, I., 2007b, ACE-Inhibitory and Radical Scavenging Activity of Peptides Derived from Beta-Lactoglobulin f(19–25). Synergism with Ascorbic Acid, *J. Agric. Food Chem*. **55**:3392–3397.

Hernández-Ledesma, B., Dávalos, A., Bartolomé, B., and Amigo, L., 2005, Preparation of Antioxidant Enzymatic Hydrolysates from Alpha-Lactoalbumin and Beta-Lactoglobulin. Identification of Active Peptides by HPLC-MS/MS, *J. Agric. Food Chem*. **53**:588–593.

Hernández-Ledesma, B., Recio, I., Ramos, M., and Amigo L., 2002, Preparation of Ovine and Caprine β- Lactoglobulin Hydrolysates with ACE-Inhibitory Activity. Identification of Active Peptides from Caprine β-Lactoglobulin Hydrolysed with Thermolysin, *Int. Dairy J*., **12**:805–812.

Hernández-Ledesma, B., Amigo, L., Ramos, M., Recio, I., 2006, Effect of (β-Lactoglobulin Hydrolysis with Thermolysin Under Denaturing Temperatures on the Release of Bioactive Peptides, *J. Chromatography A*. **1116**:31–37.

Hoffmann, M.A., Roefs, S.P., Verheul, M., Van Mil, P., and De Kruif C.G., 1996, Aggregation of B-Lactoglobulin Studied by *in Situ* Light Scattering, *J. Dairy Res*. **63**:423–440.

Hutchens, T.W., Rumball, S.V., and Lönnerdal B., 1994, Lactoferrin: Structure and Function. Advances in Experimental Medical and Biological, Plenum Press, New York, pp.1–298.

Ibrahim H.R., 2003, Hen Egg White Lysozyme and Ovotransferrin: Mystery, Structural Role and Antimicrobial Fuction. *Proceedings of the Xth European Symposium on the Quality of Eggs and Egg Products*. Saint-Brieuc, pp, 1113–1128.

Ibrahim, H.R., Aoki, T., and Pellegrini A., 2002, Strategies for New Antimicrobial Proteins and Peptides: Lysozyme and Aprotinin as Model Molecules, *Curr. Pharm. Design* **8**:671–693.

Jan M.S., 2001, Milk Ingredients as Nutraceuticals, *Int. J. Dairy Technol*. **54**:81–88.

Korhonen, H.J.T., and Pihlanto A., 2006, Bioactive Peptides: Production and Functionality, *Int. Dairy J*. **16**(9): 945–960.

López-Fandiño, R., Otte, J., and van Camp J., 2006, Physiological, Chemical and Technological Aspects of Milk Protein Derived Peptides with Antihypertensive and ACE-Inhibitory Activity, *Int. Dairy J*. (In press).

Manso, M.A., and López-Fandiño R., 2003, Angiotensin I Converting Enzyme-Inhibitory Activity of Bovine, Ovine and Caprine Kapa Caseinmacropeptides and Their Tryptic Hydrolysates, *J. Food Prot*. **66**:1686–1692.

Manso, M.A., and López-Fandiño R., 2004, κ-Caseinmacropeptides from Cheese Whey: Physicochemical, Biological, Nutritional and Technological Features for Possible Uses, *Food Rev. Int*. **20**:329–355.

Masschalck, B., and Michiels C.W., 2003, Antimicrobial Properties of Lysozyme in Relation to Foodborne Vegetative Bacteria, *Crit. Rev. Microbiol*. **29**:191–214.

McCristal, C.B., Ford, J.L., and Rajabi-Siahboomi A.R., 1997, A Study on the Interaction of Water and Cellulose Ethers Using Differential Scanning Calorimetry, *Thermochimica acta* **294**:91–98.

Meisel H., 2005, Biochemical Properties of Peptides Encrypted in Bovine Milk Proteins, *Curr. Med. Chem*. **12**:1905–1919.

Miguel, M., Manso, M.A., López-Fandiño, R., Alonso, M.J., and Salaices, M., 2007, Vascular Effects and Antihypertensive Properties of Kappa-casein Macropeptide, *Int. Dairy J*. **17**:143–147.

Monteiro, S.R., Tavares, C., Evtuguin, D.V., Moreno, N., and Lopes da Silva J.A., 2005, Influence of Galactomannans with Different Molecular Weights on the Gelation of Whey Proteins at Neutral pH, *Biomacromolecules* **6:**3291–3299.

Mullally, M.M., Meisel, H., and FitzGerald R.J., 1996, Synthetic Peptides Corresponding to A-Lactalbumin and B-Lactoglobulin Sequences with Angiotensin-I-Converting Enzyme Inhibitory Activity, *Biol. Chem. Hoppe-Seyler* **377**:259–260.

Mullally, M.M., Meisel, H., and Fitzgerald R.J., 1997, Identification of a Novel Angiotensin I-Converting-Enzyme-Inhibitory Peptide Corresponding to a Tryptic Fragment of Bovine β-Lactoglobulin, *FEBS Lett*. **402**:99–101.

Murakami, M., Tonouchi, H., Takahashi, R., Kitazawa, H., Kawai, Y., Negishi, H., and Saito T., 2004, Structural Analysis of a New Anti-Hypertensive Peptide (β-Lactosin B) Isolated from a Commercial Whey Product, *J Dairy Sci*. **87**:1967–1974.

Nurminen, M.L., Sipola, M., Kaarto, H., Pihlanto-Leppälä, A., Piilola, K., Korpela, R., Tossavainen, O., Korhonen, H., and Vapaatalo H., 2000, α-Lactorphin Lowers Blood Pressure Measured by Radiotelementry in Normotensive and Spontaneously Hypertensive Rats, *Life Sci*. **66**:1535–1543.

Olsson, C., Langton, M., and Hermansson A.M., 2002, Microstructures of B -Lactoglobulin/ Amylopectin Gels on Different Length Scales and Their Significance for Rheological Properties, *Food Hydrocolloid*. **16**:111–126.

Ondetti, M.A., Rubin, B., and Cushman D.W., 1977, Design of Specific Inhibitors of Angiotensin Converting Enzyme: New Classes of Orally Active Antihypertensive Agents, *Science* **196**:441–444.

Ould Eleya, M.M., and Turgeon S.L., 2000, Rheology of κ-Carrageenan And β-Lactoglobulin Mixed Gels, *Food Hydrocolloid*., **14**:29–40.

Parodi P.W., 1998, A Role for Milk Proteins in Cancer Prevention, *Aust J Dairy Technol*. **53**:37–47.

Peña-Ramos, E.A., and Xiong Y.L., 2001, Antioxidative Activity of Whey and Soy Protein Hydrolyzates in a Liposomal System, *J. Dairy Sci*. **84**:2577–2583.

Pérez, O.E., Wargon, V., and Pilosof A.M.R., 2006, Gelation and Structural Characteristics of Incompatible Whey Proteins/Hydroxypropylmethylcellulose Mixtures, *Food Hydrocolloid*. **20**:966–974.

Pihlanto, A., and Korhonen H., 2003, Bioactive Peptides And Proteins, *Adv Food Nutr. Res*. **47**:175–276.

Pihlanto-Leppälä, A., Koskinen, P., Piilola, K., Tupasela, T., and Korhonen H., 2000, Angiotensin I- Converting-Enzyme-Inhibitory Properties of Whey Proteins Digests: Concentration and Characterization of Active Peptides, *J. Dairy Res*. **67**:53–64.

Renard, D., van de Velde, F., and Visschers R.W., 2006, The Gap Between Food Gel Structure, Texture and Perception, *Food Hydrocolloid*. **20**:423–431.

Sánchez, V.E., Pilosof, A.M.R., and Bartholomai G.B., 1995, Rheological Properties of Food Gums as Related to Their Water Binding Capacity and to Soy Protein Interaction, *Lebensm.Wiss u-Technol*. **28**:380–385.

Séverin, S., and Wenshui X., 2005, Milk Biologically Active Components as Nutraceuticals: Review, *Crit. Rev. Food Sci. Nutr*. **45**:645–656.

Silva, S.V., and Malcata F.X., 2005, Caseins as Source of Bioactive Peptides, *Int. Dairy J*., **15**:1–15.

Sipola, M., Finckenberg, P., Santisteban, J., Korpela, R., Vapaatalo, H., and Nurminen M.L., 2001, Long-Term Intake of Milk Peptides Attenuates Development of Hypertension in Spontaneously Hypertensive Rats, *J. Physiol. Pharmacol*. **52**:745–754.

Svensson, M., Sabharwal, H., Håkansson, A., Mossberg, A.C., Lipniunas, P., Leffler, H., Svanborg, C., and Linse S., 1999, Molecular Characterization of Folding Variants of α–Lactalbumin That Induces Apoptosis in Human Cells, *J. Biol. Chem*. **274**:6388–6396.

Tavares, C., and Lopes da Silva J.A., 2003, Rheology of Galactomannan-Whey Protein Mixed Systems, *Int. Dairy J*. **13**:699–706.

Tavares, C., Monteiro, S.R., Moreno, N., and Lopes da Silva J.A., 2005, Does the Branching Degree of Galactomannans Influence Their Effect on Whey Protein Gelation? *Colloids and Surfaces A: Physicochem. Eng. Aspects* **270**-**271**:213–219.

Tolstoguzov V., 1997, Multicomponent Biopolymer Gels, *Food Hydrocolloid*. **11**:159–170.

Turgeon, S.L., Beaulieu, M., Schmitt, C., and Sánchez C., 2003, Protein-Polysaccharide Interactions: Phase-Ordering Kinetics, Thermodynamic and Structural Aspects, *Curr. Opin. Colloid Interface Sci*. **8**:401–414.

Verheul, M., Roefs, S., and De Kruif K., 1998, Kinetics of Heat-Induced Aggregation of β-lactoglobulin. *J. Agr. Food Chem*. **46**:896–903.

Vermeirssen, V., van Camp, J., and Verstraete W., 2004, Bioavailability of Angiotensin I-Converting-Enzyme-Inhibitory Peptides, *Br. J. Nutr*. **92**:357–366.

Viljoen M., 1995, Lactoferrin: A General Review, *Haematologica*, **80**:252–267.

Wakabayashi, H., Yamauchi, K., and Takase M., 2006, Lactoferrin Research, Technology and Applications. *Int Dairy J*. **16**:1241–1251.

Walsh, D.J., Bernard, H., Murray, B.A., MacDonald, J., Pentzien, A.K., Wright, G.A., Wal, J.M., Struthers, A.D. Meisel, H., and FitzGerald R.J., 2004, In Vitro Generation and Stability of the Lactokinin Beta-Lactoglobulin Fragment (142-148), J. *Dairy Sci*. **87**: 3845–3857.

Walzem, R.L., Dillard, C.J., and German J.B., 2002, Whey Components: Millennia of Evolution Create Functionalities for Mammalian Nutrition: What We Know and What We May be Overlooking, *Crit. Rev. Food* **42**:353–375.

Yoshikawa, M., Tani, F., Yoshimura, T., and Chiba H., 1986, Opioid Peptides from Milk Proteins, *Agric. Biol. Chem*. **50**:2419–2421.

31
Whey Proteins: Bioengineering and Health

M. García-Garibay, J. Jiménez-Guzmán,
and H. Hernández-Sánchez

31.1. Introduction

Whey, obtained mainly from cheese production, has been considered for a long time as a low added value byproduct. It is a highly polluting material with a biological oxygen demand (BOD) of 30,000 to 50,000 mg l^{-1}, and it has been used as a low cost raw material for the production of several commodities (Marwaha and Kennedy, 1988; Garcia-Garibay et al., 1993). Whey production worldwide has for years represented a challenge to find interesting ways for its utilization. During the last 10 or 20 years, it has been difficult to economically dispose of whey, even in developed countries, due to the increase in cheese production and the installation of larger cheese factories. Although whey utilization has been the subject of much research, very few processes have led to economically attractive ways for its utilization. The most successful processes for its utilization are those that have led to the elaboration of products with a high added value. For instance, whey proteins have high nutritional value and very good functional properties, leading to the interest in developing ultrafiltration techniques in order to recover such proteins without losing their functional properties (Trejo-Vázquez et al., 1995).

Proteins that are found in whey are too diluted (in a concentration less than 10 g l^{-1}); on the other hand, they have high nutritional value, unique functional properties and nutraceutical or bioactive characteristics that are worth their recovery from this byproduct. From the beginning of the 1980s, the development of ultrafiltration and other membrane processes has allowed the efficient recovery of whey proteins; the further advance of this technology improved the concentration process and reduced the cost of the equipment, opening new alternatives for the utilization of these proteins. Whey proteins recovered by ultrafiltration with different degrees of concentration are known as whey protein concentrates (WPC), and they are currently used in many applications in the food industry (Morr, 1989; Mulvihill and Ennis, 2003).

The technology for whey proteins recovery has been developed beyond the conventional membrane processes, allowing the separation or concentration of specific fractions such as α-lactalbumin, β-lactoglobulin, lactoferrin,

TABLE 31.1. Composition and biochemical characteristics of major whey proteins (Data from Fox, 2003)

Protein	Amino acids	Molecular mass kDa	Concentration in milk g/L	Total protein in milk (%)
β-Lactoglobulin (β-lg)	162	18	2-4	12
α-Lactalbumin (α-la)	123	14	1-1.5	3.5
Bovine serum albumin (BSA)	582	66	0.1-0.4	1
Proteose peptone (PP)	—	—	0.6-1.8	2
Immunoglobulins (Ig; specific Ig: IgG, IgA, IgM)	—	1000-1430	0.6-1	2
Lactoferrin (LF)	689	80	0.1	—
Lactoperoxidase (LP)	612	78	0.01-0.03	—
Glycomacropeptide (GMP)	64	7	—	—

lactoperoxidase and glycomacropeptide for particular uses or nutraceutical applications (Mulvihill and Ennis, 2003). This implies the development of selective transfer membranes and great scale emerging technologies such as ionic exchange chromatography and gel permeation (Morr, 1989; Pearce, 1992; Foegeding and Luck, 2003). Research investigating more selective techniques at great or small scales is currently being conducted, such as affinity chromatography (Mulvihill and Ennis, 2003), affinity/selective membranes (Chiu and Etzel, 1997; Mulvihill and Ennis, 2003), molecular imprinting (Mendez-Palacios et al., 2006) and colloidal gas aphrons (Fuda et al., 2004; 2005).

The utilization of whey proteins as food ingredients in many products due to their unique nutritional and functional properties and, even more, due to their bioactive characteristics, has been the driving force for research on the development of new techniques for their concentration, recovery and fractionation.

In the present chapter, a review of the most important characteristics of whey proteins, together with the techniques for their separation, is presented. Table 31.1 shows some important biochemical characteristics of major or important whey proteins.

31.2. Functional Properties

Whey proteins have been used since long ago as food ingredients in several applications. Of all food proteins, they are of the proteins with the highest nutritional value (Renner, 1989; Hambræus and Lönnerdal, 2003), but in the past, this was not enough to attract the interest of food technologists in order to use them extensively as food ingredients. However, today we know that whey proteins have excellent functional properties, such as high solubility (even at low pH), foaming capability, water binding capacity, emulsifying properties, gel formation ability, etc.; these characteristics are highly appreciated when they are used in food formulations (Mulvihill and Fox, 1989), and they have made possible a wide variety of uses for whey proteins in different degrees of concentration and purity (WPC, WPI, WPF).

In order to keep their functional properties, whey proteins must retain their native conformation. Heat coagulation processes allow the recovery of whey proteins with practically unaffected nutritional value with respect to native proteins; however, their functional properties are lost with thermal treatment due to configuration changes. This is why the possibility of recovering native proteins by means of membrane or other non-denaturing processes has greatly expanded the use of whey proteins as food ingredients. No other proteins are equal in terms of functional properties; therefore, their utilization in food technology and food products development is certainly the most important in terms of food proteins utilization. For instance, native whey proteins are soluble under acid, neutral and alkaline conditions, which is unusual in proteins, allowing them to be used in many liquid foods and beverages (Mangino, 1992).

The characteristics known as functional properties are related to physicochemical parameters of proteins when they are found in aqueous solution, and are particularly useful to predict the utility of proteins when they are used as food ingredients (de Wit, 1989). The functional properties arise from the interaction of proteins with water and other food components, and rather than precise physicochemical characteristics, are just practical parameters that allow researchers, under limited conditions, to obtain some information about the performance of the proteins in food formulations. For instance, the interaction of whey proteins with water is responsible for many of their functional properties; this property, generally referred to as hydration, is related to solubility, dispersibility, swelling, water absorption, viscosity, etc. (Mulvihill and Fox, 1989). Additionally, proteins contain hydrophobic and hydrophilic dominions; this amphipathic nature is important in properties such as emulsifying and foaming capacities, coagulation, and their utilization as cosolvents of hydrophobic compounds, such as β-lg as a carrier of liposoluble vitamins (Mulvihill and Fox, 1989; Mangino 1992). Table 31.2 shows some applications of whey proteins in relationship to their functional properties.

31.3. Effect of High Pressure Processing on Whey Proteins

Currently, there are many processes, such as drying, freezing, irradiation, pasteurization and sterilization, for increasing the shelf life of foods. Traditional thermal processing has the inconvenience of slow rates of heating and cooling, which can adversely affect the products. An alternative to these processes has been recently applied for the preservation of a whole range of foods. High hydrostatic pressure (HHP) processing has been used commercially to pasteurize guacamole, ham, fruit juices and oysters, and experimentally to homogenize and pasteurize milk. At nearly room temperature, the application of 400–600 MPa has been effective in inactivating microbial vegetative cells and spores, as well as enzymes (Matser et al., 2004). HHP results in shorter processing times and lower maximal temperatures in the product. In the case of milk (2% fat), an average temperature change of 3 °C

TABLE 31.2. Main applications of whey proteins related to their functional properties

Function	Characteristics/mode of action	Applications
Emulsification	Amphipathic dominions/ surface activity. Creates and stabilizes fat emulsions. Dispersion of milkfat.	Meat products, ice cream, saladdressings, coffee whitener, mayonnaise, cakes, baked products, soups
Foaming/ whipping	Amphipathic dominions/surface activity. Forms stable films to entrap gas. Improves whip volume	Baked products, cakes, whipped toppings, icings, meringues, ice cream/frozen desserts
Gelling	Protein matrix formation and entrapment of water	Meat and seafood products, cheese foods, yogurt, dairy desserts, baked goods
Solubility	High hydration capability leading to protein solvation	Soft drinks, nutritional beverages, nutritional/sport powder products, soups
Water absorption and binding	High hydration capability. Swelling	Sausages, meat and seafood products, cakes, baked goods, dairy products
Viscosity development	High hydration capability. Swelling	Soups, gravies, salad dressings, beverages, coffee whitener

per 100 MPa due to adiabatic compression has been recorded (Ting et al., 2002). Important parameters in HHP processing include initial temperatures of the product, container and pressurization liquid, work pressure, amount of pressure cycles and the increase in temperature during the treatment.

There are several HHP processes that have been reported in the case of milk, and good results have been obtained when two-pulse HHP treatments were used. In these cases, initial temperatures of 60 °C or 90 °C and pressures of 1700 and 700 MPa, respectively, were used. Each pulse lasted 1 min, and the time between pulses was 30 s. However, pressures from 100 MPa to 600 MPa are also commonly used. In HHP-treated milk, changes in the proteins, such as disruption of the structure of casein micelles and denaturation of the whey proteins, have been reported. HHP also induces shifts in the mineral balance and crystallization of milk fat. However, some enzymes in the milk (alkaline phosphatase and plasmin) seem to be resistant to these treatments (Huppertz et al., 2002). López-Fandiño et al. (1996) studied the effects of HHP on cheese-making properties of milk and found that after a 300 MPa / 30 min treatment, the coagulation time was reduced by 19% and the firmness increased by 58%.

HHP treatments (600 MPa, 50 °C, 0 to 30 min) of whey protein concentrate (WPC80) solutions (0.2 or 1%) induced conformational changes and aggregation, affecting the hydrophobicity and binding properties, thus changing the functional properties of the product (Liu et al., 2005).

In the case of β-lg, Aouzelleg et al. (2004) studied pressures up to 294 MPa, temperatures up to 62 °C and processing times up to 30 min. These HHP treatments resulted in important effects on the secondary and tertiary structures, suggesting a transition to the molten globule state. This study suggested the possibility of process optimization to obtain the best structure for different applications.

Temperature is a very important parameter in these kinds of processes, and care must be taken to control it. It has been observed that when β-lg is heated between 70 °C and 75 °C, the native dimers begin to dissociate into monomers, and further heating leads to the formation of aggregates via sulfhydryl–disulfide interchange reactions and hydrophobic interactions (Sava et al., 2005). Anema et al. (2005) studied the effect of pressures from 100 MPa to 600 MPa and temperatures from 10 °C to 40 °C on β-lg in skim milk. They found that at 100 MPa no denaturation was observed at any temperature or holding time. At higher pressures, denaturation increased with increasing temperatures and holding times. The authors suggested that a transition is possible from an aggregation-limited reaction to an unfolding-limited reaction as the pressure was increased. A synergistic effect of pressure and temperature on the denaturation of β-lg has been observed. Almost total denaturation has been reached when raw milk was treated at 300 MPa/50–60 °C or 400 MPa/40–60 °C (López-Fandiño and Olano, 1998). Differential scanning calorimetry (DSC) showed that the addition of dextran sulfate sensitized the β-lg structure to pressure. The species created by this process could be in the molten globule state and possessed improved functional properties (Aouzelleg and Bull, 2004).

Compared to β-lg, α-la is much more barostable. López-Fandiño and Olano (1998) concluded that α-la in raw milk is resistant to denaturation at pressures up to 500 MPa. These differences in stability could be due to the presence of four disulfide bridges and the absence of free thiol groups in the α-la, which results in a more rigid structure (Farrell et al., 2004). Some studies have found that the unfolding of α-la at high pressures (1000 MPa) is reversible even in alkaline media and at protein concentrations as large as 10%. The addition of low molecular weight thiol reagents (cysteine, 2-mercaptoethanol) significantly increased the aggregation rate (Jegouic et al., 1996). The HHP-induced oligomerization of mixtures of α-la and β-lg at 1000 MPa has also been studied. High-molecular weight oligomers are formed during the HHP treatments, and the free thiol group of the β-lg triggers the thiol–disulfide exchange reaction responsible for the oligomerization (Jegouic et al., 1997).

Very little information is available for BSA. It has been reported that this protein, in raw milk, is resistant to pressures up to 400 MPa (López-Fandiño et al., 1996).

Further research is necessary to evaluate the full potential of HHP treatments to modify the functional properties of whey proteins. Few studies are available on concentrates (WPC) or isolates (WPI) and optimization research is lacking in this field.

31.4. Bioactivity of Whey Proteins

Bioactive substances of food origin are defined as food components that may have some regulatory functions in the human organism beyond basic nutrition. Many of these substances, which have little or no nutritional value, may be helpful in the

maintenance of human health (Meisel, 2002) and hence are the subject of many studies dealing with their origin and production, as well as the mechanism of their activity and their introduction as parts of functional foods.

Milk is a complete food for the newborn mammal. Its composition may vary depending on the species that produces it; cows' milk for example, contains approximately 5% lactose, 3.2% proteins, 4% lipids and 0.7% minerals. Its high nutritive value is due to its complete composition, providing all the essential components in the necessary amounts required by the young animal. Milk is the only food for the new-born during a period of its life in which growth is most accelerated and its organism is still immature; therefore, it is not surprising to find that milk contains molecules with different physiological functionalities such as immunoglobulins, or other compounds that help prevent infections and favor the growth of the new-born.

Nowadays, it is widely recognized that milk provides a lot more than simple nutrition and passive immunity to the offspring; it contains a wide variety of bioactivities that range from the modulation and improvement of gastrointestinal functions, essential for nutrient adsorption, to hemodynamic regulation or several hormone-like growth factors that influence the development of the gut; immunoregulation or active defense against infections including bactericidal or bacteriostatic effects, as well as a prebiotic one, have also been reported (Schanbacher et al., 1997; Shah, 2000; Meisel, 2002; Philanto-Leppälä, 2003).

Since the 1990s, several studies have established the important role of the protein system in milk's biological activity. It has been demonstrated that some whey proteins such as α-la, β-lg or LF are physiologically active (Bos et al., 2000; van Belzen, 2002; Walzem et al., 2002). LF and β-lg, for example, have shown antimicrobial and antiviral activities capable of inhibiting pathogens in the gut; they have also shown an enhancement of the immune response of the human organism (Meisel and Schlimme, 1990; Meisel, 1997; Schanbacher et al., 1997).

On the other hand, other bioactivities are latent within the peptide structure of the protein and become active as the peptide is released through the hydrolysis of the protein (mainly caseins) due to the action of either gastric enzymes or the proteolytic system of fermenting microorganisms (Meisel, 1997; Clare and Swaisgood, 2000; Shah, 2000; Philanto-Leppälä, 2001; Léonil and Maubois, 2002; Meisel, 2002; van Belzen, 2002; Sava and Malcata, 2005). In this chapter, the biological effects of some native whey proteins will be reviewed.

The physicochemical characteristics of whey proteins are very different from those of casein. From the digestive point of view, they remain soluble at the acid pH of the stomach, unlike caseins, which easily coagulate under those conditions. This accelerates their transit through the stomach, allowing them to get to the gut practically intact; hence, their absorption in the intestine is very slow, facilitating a great variety of functions, for example, interactions with the gastrointestinal flora, having an inhibiting or selective effect on it; or with the minerals in the bollus, improving their absorption.

On the other hand, the amino acid composition of whey proteins gives them a very special physiological functionality: firstly, whey proteins contain a high

amount of sulfured amino acids, which contributes to their great nutritional quality (whey protein PER is 3.2, with respect to 2.0 for casein). Furthermore, sulfured amino acids seem to enhance the immune function of the organism, probably due to the regulation of glutation, a sulfured tripeptide which interacts with the cell membranes of microorganisms killing them.

Whey proteins, mainly α-la, are particularly rich in the branched amino acids isoleucine (CH_3-CH_2-$CH(CH_3)$-$CH(NH_2)$-COOH), leucine ($(CH_3)_2$-CH-CH_2-$CH(NH_2)$-COOH) and valine ($(CH_3)_2$-CH-$CH(NH_2)$-COOH). These are necessary in the muscle cells to promote protein synthesis. Even more, these amino acids are metabolized to generate energy in the muscle rather than in the liver, hence increasing the bioavailability of carbohydrates as an energy source and preventing muscle degradation under extreme conditions such as prolonged exercise. (Walzem et al., 2002). Diets supplemented with these kinds of proteins and light energetic restrictions have been tested in athletes, showing a selective diminution of adipose tissue while maintaining a high exercise yield in the athletes.

For some time now, various functions have been reported for whey proteins, from intestinal motility to immune responses; in the last decade different bioactivities have been reported such as antihipercolesterolemic and antiaging effects, as well as inhibition of cancerous cells (Shah, 2000; Walzem et al., 2002; van Belzen, 2002; Korhonen and Marnila, 2003). Some of these are reported in Table 31.3.

Milk contains different hormone-like stimulating growth factors (LF included) such as the epidermal growth factor (EGF), transformed growth factor (TGF) and insulin growth factor (IGF). The growth stimulation properties of these factors have been extensively studied, and several mechanisms have been proposed for their activity: 1) They help improve nutrient absorption such as calcium and other minerals; 2) They stimulate the controlled transport of essential amino acids to specific tissues; 3) They direct growth stimulation via receptor activation; and 4) They inhibit cytokines, avoiding cell destruction and indirectly diminishing growth. Nevertheless, given the importance of milk as a "growth stimulating

TABLE 31.3. Biological functions of whey proteins (From Walzem et al., 2002)

Target	Mechanism	Example	Implications
Growth	Stimulation of intestinal cells. Cell cycle.	Insulin Growth Factor (IGF-1)	Promote tissue repair
Maturation	Bind to, and activate natural receptors in intestinal cells	Transformed Growth Factor β (TGFβ)	Intestinal integrity
Protection	Disrupt pathogenic bacterial membrane	Lactoferricin and LF	Pathogen inhibition
Prevention	Stimulate beneficial bacteria	LG	Prebiotic effects
Elimination	Endotoxin binding	Ig	Toxina excretion

food," it is very likely that there may be other stimulating mechanisms that have not been reported (Shah, 2000).

Milk's growth factors have demonstrated a great importance as part of some adult therapies by helping calcium adsorption and bioavailability in patients with osteoporosis, increasing the rate of recovery of bone tissue, as well as helping the rege-neration of damaged tissues and in the treatment of some gastrointestinal disorders.

Another function associated with whey proteins is an increase in the recognition of contaminating bacteria in the organism. This interaction with the immune system is of special importance in adults, in whom the immune response is stimulated. Furthermore, some whey proteins participate in more active defense systems by affecting the growth of contaminant bacteria, either by binding minerals essential for their development (for example, LF binds iron which is essential for bacteria like *E.coli*, *Staphylococcus aureus*, *S. albus*, and *Vibrio cholerae*), or by affecting the bacterial cell wall, facilitating the activity of the natural defense systems such as lisozyme or LP that kill microorganisms. Besides favoring the immune response of the organism, some whey proteins like LF, acting as a prebiotic, favor the growth of beneficial bacteria in the gut; this gives whey value as a prebiotic. (Bos et al., 2000; van Bel-zen, 2002).

The most important bioactive proteins in whey are β-lg, α-la and LF; hence, they will be reviewed in more detail.

31.4.1. β-Lactoglobulin

This is the most abundant protein in the whey of most mammals, even though it is completely absent from human milk; one of the bioactivities that has been reported for this protein is mineral binding. The molecular structure of β-lg has a very charged locus with amino acids such as cysteine, lysine or methionine. This allows it to bind minerals and carry them through the intestinal wall. Besides its capacity for mineral binding, β-lg also has a slightly hydrophobic dominium, which helps bind and absorb liposoluble substances such as vitamins like retinol. Due to its high content of sulphured amino acids, β-lg participates in the active immune system favoring the action of glutation.

31.4.2. α-Lactalbumin

This protein also has some highly charged dominions, which facilitates calcium adsorption. It also has a high affinity for metal ions like zinc, manganese, cadmium, copper and aluminum, all of which are essential for the human organism. Even more, due to its high content of long-chained amino acids, α-la has been used for diminishing muscle tissue damage caused by exercise or anoxia. Some studies also suggest that this protein could be of help in cancer treatments, since it may induce cell-apoptosis, a function which is lost in tumor cells.

31.4.3. Lactoferrin (LF)

LF has very special characteristics; among the most studied ones are its antibacterial and antioxidant properties. LF binds iron, thus helping to dissolve it in the blood serum, diminishing its availability for bacterial growth and at the same time making it available for intestinal adsorption. It has also been demonstrated that LF favors the immune response in the human organism by promoting: a) the proliferation of beneficial bacteria (acting as a prebiotic), b) lymphocyte proliferation and c) cell differentiation, thus helping the repair of damaged tissues (Walzem et al., 2002).

One of the most promising bioactivities of LF is based on its utility for cancer prevention. Several studies have demonstrated that it may be helpful in the treatment of this disease, and several mechanisms have been proposed for this bioactivity (Tsuda et al., 2002; van Belzen, 2002).

Some of the simplest mechanisms through which this protein might prevent cancer could be based on its antioxidant capacity, since this protein may turn off tumor promoting-free-radicals. Its bactericidal effect could also help prevent stomach cancer by acting against *Helycobacter pylori* bacteria, which have been associated with this disease. On a more general level, some studies have proposed that by stimulating the immune system, LF could promote the recognition of tumor cells by cytokines, thus preventing the growth of the tumor.

Preliminary studies demonstrate that LF could inhibit vascular growth factors, which play an important role during tumor development. Studies performed with rats fed with LF solutions have demonstrated that it diminishes the formation of capillary networks in the tumor, thus diminishing its growth rate (van Belzen, 2002).

It has been demonstrated that milk components, particularly proteins, have physiological functions beyond basic nutrition. There are several studies that prove the physiological activity of milk proteins, which has raised great expectations in terms of their health and technological applications, such as their commercial exploitation as bioactive substances, and their application as part of functional foods. More research is needed related to the physiological as well as the technological and functional aspects, in order to completely know the bioactive properties of milk and milk products, as well as their effects on consumers, and the effects of milk processing on their functionality as nutraceuticals.

31.5. Whey Proteins Separation

Thermocoagulation is an old way to recover whey proteins, which product is known as lactalbumin or just albumin. It consists of the acidification of whey, boiling it for several minutes, leading to denaturation and the precipitation of major whey proteins, and finally the separation of the precipitated proteins and drying (Pearce, 1992). This technique is suitable for the production of widely

accepted dairy products such as Italian ricotta cheese or the Mexican requeson, but the functional properties of the proteins resulting from this operation lead to a poor quality, low added value product (Garcia-Garibay et al., 1993). However, some functional properties, mainly solubility, of denatured proteins could be recovered or improved by hydrolysis with several proteases (Pearce, 1992). Additionally, enzymatic hydrolysis of milk proteins may eliminate the sequential epitopes, resulting in a much less antigenic protein (Vázquez-Lara et al., 2003). The most allergenic fraction is β-lg, followed by caseins, α-la and BSA (Bahna, 1993). This approach is also valid for native proteins obtained by membrane processes.

The most successful processes for the recovery of whey proteins have been the membrane techniques, particularly ultrafiltration. These techniques are pressure-driven filtration processes in which tiny-diameter porous membranes are used as filtration media in order to separate small solid components from a liquid phase. Table 31.4 describes the membrane processes that are currently applied to milk and whey.

These processes have been used for whey treatment since the late 1970s and early 1980s, using cellulose acetate membranes in the early stages of development, which were later replaced by more resistant and durable membranes made of polysulphones or polyetersulphones.

By means of ultrafiltration, one of the most successful efforts for the utilization of whey has been possible. This technique has allowed the use of whey protein concentrates (WPC) as food ingredients in many applications. The utilization of WPC is certainly the most successful example of the application of food proteins as ingredients in food technology, thanks mainly to their functional properties, which allow their utilization in many foodstuffs with several purposes.

In order to obtain WPC, good quality whey must be used as raw material, which also implies the use of milk of the highest possible quality. This means whey with low microbiological counts, particularly low psychrotrophic bacteria, because they produce proteases that can hydrolyze caseins, increasing the content of PP in whey and also hydrolyzing whey proteins, diminishing their functional properties (Fajardo-Lira and Nielsen, 1998).

Table 31.4. Characteristics and applications of membrane processes

Technique	Nominal pore diameter (μm)	Molecular mass cutoff (kDa)	Retentated particles/ molecules	Application
Microfiltration	0.2-10.0	40-1000	Fat globules, suspended solids	Skimming and casein particles separation
Ultrafiltration	0.001-0.1	1-200	Proteins	Protein concentration: WPC, MPC
Nanofiltration	0.0001-0.001	0.1-1	Multivalent ions	Demineralization
Reverse Osmosis	< 0.0001	< 0.1	Lactose	Lactose recovery

Commercial WPC can contain different concentrations of proteins, such as 35%, 50%, 60%, 65%, 75% or 80%, but the most commercial ones are those which have 35% (WPC34) and 80% (WPC80) protein (Morr, 1989; Foegeding and Luck, 2003). Products with more than 85% protein (usually 92%) are known as whey protein isolates (WPI) (Foegeding and Luck, 2003). Obviously, the higher the protein content, the higher the cost of the product. The first step for WPC production is the removal of residual fine particles of casein or curd and fat. This can be done by centrifugal clarifier, rotary screen filter or microfiltration. The whey is then preheated at 50–65 °C to stabilize calcium phosphate to avoid or reduce fouling on the membranes, and then pasteurized at 72 °C for 15 s. The ultrafiltration itself is done at 50 °C. Several equipment designs are available, including tubular, plate and frame, spiral wound, and hollow fiber. WPC containing more than 65% protein is processed by diafitration rather than by ultrafiltration, which is used only in WPC34, WPC50 and WPC60. Once the desired level of concentration is reached, the retentate may need to be cooled at 4 °C during storage; the concentrated products to obtain WPC with high protein content such as WPC80 may require further pasteurization to reduce bacterial counts that are concentrated during the ultrafiltration. Finally, the retentate is concentrated before drying by means of a high-vacuum falling-film evaporator, which minimizes to 50 °C the boiling temperature; then the product is spray dried (Hobman, 1992).

Commercial WPIs contain between 88% and 95% protein. For the production of these, whey has to be skimmed by microfiltration and demineralized by ionic exchange, electrodialysis or nanofiltration. The concentration of the proteins is done by diafiltration. Finally the retentate is concentrated and spray dried. Alternatively, WPI can be obtained by a combination of ion exchange chromatography (IEC) and ultrafiltration (Morr, 1989; Neville et al., 2001). WPIs obtained by the first technique contain the GMP, while those obtained by IEC do not (Neville et al., 2001).

WPIs are considerably more expensive than WPCs, but their uses are specific for high-added-value foods.

Table 31.5 shows the composition of commercial WPC and WPI of different protein concentrations.

Table 31.5. Composition of commercial WPC and WPI (Data from Mangino 1992; Foegeding and Luck 2003)

	WPC34	WPC65	WPC80	WPI
	Composition (%)			
Moisture	3-5	3-5	3-5	3-5
Protein	34-36	65-68	80-82	90-95
Lactose	47-53	18-23	4-8	1
Fat	3-4	5-7	4-8	1
Ash	6-8	4-6	3-4	2-3

Specific whey protein fractions (WPF) are also available at the commercial level. These are protein concentrates that are rich in some specific proteins, and are obtained by different techniques. The most important technique is separation by IEC. In this way, cationic resins (negatively charged) are used to retain the positively charged proteins at the pH of whey (LF and LP); at the same pH, the other major proteins, β-lg, α-la, and BSA, are negatively charged; thus, they are not retained by the resin, obtaining a fraction rich in these proteins. LF and LP are later released by elution with alkaline solutions. The fractions are finally washed and spray dried (Pearce 1992; Chiu and Etzel, 1997).

More selective ultrafiltration membranes, made with hydrophilic cellulose or other materials, have been developed in recent years (Cheang and Zydney, 2003). These membranes have wider pore size than conventional membranes, allowing the separation of smaller whey proteins (β-lg and α-la) from those of higher molecular mass (BSA, Ig and LF). This, similar to the fractions obtained by IEC, allows the separation of WPF with different proteins.

Techniques for the separation of β-lg from α-la have been developed based on the reversible thermocoagulation of the latter. The heat treatment of whey or a mixture of these two proteins at moderate temperatures (less than 55 °C) for several minutes at low pH, produces the reversible aggregation of α-la, which then can be separated from the mixture by microfiltration; the permeate, rich in β-lg, can be treated separately by ultrafiltration/diafiltration to concentrate the protein, while the α-la in the retentate can be redissolved at neutral pH and then concentrated by ultrafiltration (Bramaud et al., 1997; Gésan-Guizion et al., 1999).

High purity fractions of whey proteins can be obtained by these techniques or a combination of them. Additionally, as in the case of the GMP, the techniques can be combined by precipitation by alcohol.

Experimentally, several techniques are currently been explored; Two interesting cases in point are the following.

Colloidal gas aphrons (CGAs) have been explored as an alternative for whey protein fractionation. These are microbubbles created by intense stirring of surfactant solutions. Their large interfacial area per volume, short separation time from the bulk phase, and low viscosity make them particularly attractive for protein separation. Fuda et al. (2004; 2005) investigated the fractionation of whey proteins using CGAs generated with either the anionic surfactant sodium bis-2-ethylhexyl sulphosuccinate (Fuda et al., 2004) or cetyl trimethyl ammonium bromide (Fuda et al., 2005), and proved that CGAs can be analogous to ion exchangers when applied to whey; the selectivity of the process can be manipulated by changing the type of surfactant, pH and ionic strength. These authors demonstrated that the recovery and separation of LF and LP (Fuda et al., 2004) or β-lg (Fuda et al., 2005) from whey can be done using CGAs.

Molecular imprinting is a method for preparing synthetic materials able to mimic the molecular recognition phenomena present in living systems. It consists of the selection of a template molecule (the target molecule specified for recovery by the polymer), which is later associated with some functional

monomers through non-covalent binds; then, a polymerization around the template-monomer complex is conducted, resulting in a molecularly imprinted polymer (MIP) that has a cavity that recognizes the template molecule, allowing its capture, specifically separating it from a complex mixture. This method was used to recover LF (Mendez-Palacios et al., 2006). Using vinylpiridin as a functional monomer and etylenglycol dimetacrilate as a crosslinker, it was possible to create a specific cavity for LF. The polymers obtained, tested against a protein mixture containing LF, had an efficiency of 27%, while the control polymer retained only 1.6%, demonstrating that the retention of the protein is not due to an unspecific adsorption in the polymer, but rather to a selective retention in the cavity formed by the template.

31.6. Conclusions

The recovery and separation of whey proteins without losing their functional characteristics has allowed the successful utilization of whey, considerably increasing its added value. That is due to the possible use of whey proteins in many aspects of food formulation, food technology and nutraceuticals. However, more specific applications with special purposes in food formulations and functional foods sometimes require more purity and the possibility of recovering specific proteins. Current processes do not allow a high degree of purification, which is why researchers are actively seeking new separation techniques, as well searching for new applications of whey proteins, particularly with improved functional characteristics, and in the field of health.

References

Anema, S.G., Stockmann, R., and Lowe E.K., 2005, Denaturation of B-Lactoglobulin in Pressure-Treated Skim Milk, *J. Agric. Food Chem*. **53**:7783–7791.

Aouzelleg, A., and Bull L., 2004, Differential Scanning Calorimetry Study of Pressure/Temperature Processed β-Lactoglobulin: The Effect of Dextran Sulphate, *Food Res. Int*. **37**:933–940.

Aouzelleg, A., Bull, L., Price, N.C., and Kelly S.M., 2004, Molecular Studies of Pressure/Temperature-Induced Structural Changes in Bovine B-Lactoglobulin, *J. Sci. Food Agric*. **84**:398–404.

Bahna S.L., 1993, Food Intolerance. Milk Allergy, in: *Encyclopedia of Food Science Food Technology and Nutrition*, vol. 3, R. Macrae, R.K. Robinson and M.J. Sadler (eds.), Academic Press, London, pp. 2001–2004.

Bos, C., Gaudichon, C., and Tomé D., 2000, Nutritional and Physiological Criteria in the Assessment of Milk Protein Quality for Humans, *J. Am. College Nutr*. **19**:191–205.

Bramaud, C., Aimar, P., and Daufin G., 1997, Precipitation of α-Lactalbumin Under Gentle Heat Treatment, *Biotechnol. Bioeng*. **56**:391–397.

Cheang, B., and Zydney A.L., 2003, Separation of α-Lactalbumin and β-Lactoglobulin Using Membrane Ultrafiltration, *Biotechnol. Bioeng*. **83**:201–209.

Chiu, C.K., and Etzel M.R., 1997, Fractionation of Lactoperoxidase and Lactoferrin from Bovine Whey Using a Cation Exchange Membrane, *J. Food Sci*. **62**:996–1000.

Clare, D.A., and Swaisgood H.E., 2000, Bioactive Milk Peptides: A Prospectus, *J. Dairy Sci*. **83**:1187–1195.

de Wit J.N., 1989, Functional Properties of Whey Proteins, in: *Developments in Dairy Chemistry—4*, P.F. Fox, Elsevier Applied Science, London, pp. 285–321.

Fajardo-Lira, C.E., and Nielsen S.S., 1998, Effect of Psychrotrophic Microorganisms on the Plasmin System in Milk, *J. Dairy Sci*. **81**:901–908.

Farrel, H.M., Jiménez-Flores, R., Bleck, G.T., Brown, E.M., Butler, J.E., Creamer, L.K., Hicks, C.L., Hollar, C.M., Ng, K.F., and Swaisgood H.E., 2004, Nomenclature of The Proteins of Cow's Milk—Sixth Revision, *J. Dairy Sci*. **87**:1641–1674.

Foegeding, E.A., and Luck P.J., 2003, Whey Protein Products, in: *Encyclopedia of Dairy Science*, vol. 3. H. Roginski, J.E. Fuquay and P.F. Fox (eds.), Academic Press, Amsterdam, pp. 1957–1967.

Fox P.F., 2003, Milk Proteins: General and Historic Aspects, in: *Advanced Dairy Chemistry, Vol.1. Proteins*. P.F. Fox and P.L.H. McSweeney (eds.), Kluwer Academic, New York, pp. 1–48.

Fuda, E., Bhatia, D., Pyle, D.L., and Jáuregui P., 2005, Selective Separation of B-Lactoglobulin from Sweet Whey Using Cgas Generated from Cationic Surfactant CTAB, *Biotechnol. Bioeng*. **90**:532–542.

Fuda, E., Juaregui, P., and Pyle D.L. 2004, Recovery of Lactoferrin and Lactoperoxidase from Sweet Whey Using Colloidal Gas Aphrons (Cgas) Generated from an Anionic Surfactant, AOT, *Biotechnol. Prog*. **20**:514–525.

Garcia-Garibay, M., Revah, S., and Gómez-Ruiz L., 1993, Productos Lácteos, in: *Biotecnología Alimentaria*, M. García Garibay, R. Quintero, and A. López-Munguía (eds.), Editorial Limusa, S.A., México D.F., pp. 153–223.

Gésan-Guizion, G., Daufin, G., Timmer, M., Allersma, D., and van der Horst C., 1999, Process Steps for the Preparation of Purified Fractions of α-Lactalbumin and β-Lactoglobulin from Whey Protein Concentrates, *J. Dairy Res*. **66**:225–236.

Hambræus, L., and Lönnerdal B., 2003, Nutritional Aspects of Milk Proteins, in: *Advanced Dairy Chemistry*, vol. 1. *Proteins*. P.F. Fox and P.L.H. McSweeney (eds.), Kluwer Academic, New York, pp. 605–645.

Hobman P.G., 1992, Ultrafiltration and Manufacture of Whey Protein Concentrates, in: *Whey and Lactose Processing*. J.G. Zadow (ed.), Elsevier Science Pub., London, pp. 195–230.

Huppertz, T., Kelly, A.L., and Fox P.F., 2002, Effect of High Pressure on Constituents and Properties of Milk, *Int. Dairy J*. **12**:561–572.

Jegouic, M., Grinberg, V., Guingant, A. and Haertlé T., 1996, Thio-Induced Oligomerization of α-Lactalbumin at High Pressure, *J. Protein Chem*. **15**:501–509.

Jegouic, M., Grinberg, V., Guingant, A., and Haertlé T., 1997, Baric Oligomerization of α-Lactalbumin/B-Lactoglobulin Mixtures, *J. Agric. Food Chem*. **45**:19–22.

Korhonen, H., and Marnila P., 2003, Lactoferrin. Milk Proteins, in: *Encyclopedia of Dairy Science*, vol. 3. H. Roginski, J.E. Fuquay and P.F. Fox (eds.), Academic Press, Amsterdam, pp. 1946–1950.

Léonil, J., and Maubois J.L. 2002, Milk-Derived Bioactive Peptides and Proteins: Future Perspectives, *Proceedings of the 26th International Dairy Congress*. IDF, Paris.

Liu, X., Powers, J.R., Swanson, B.G., Hill, H.H., and Clark S., 2005, Modification of Whey Protein Concentrate Hydrophobicity by High Hydrostatic Pressure, *Innovative Food Sci. Emerging Technol*. **6**:310–317.

López-Fandiño, R., Carrascosa, A.V., and Olano A., 1996, The Effects of High Pressure on Whey Protein Denaturation and Cheese-Making Properties of Raw Milk, *J. Dairy Sci*. **79**:929–936.

López-Fandiño, R., and Olano A., 1998, Effects of High Pressures Combined with Moderate Temperatures on the Rennet Coagulation Properties of Milk, *Int. Dairy J*. **8**:623–627.

Mangino M.E., 1992, Properties of Whey Protein Concentrates, in: *Whey and Lactose Processing*. J.G. Zadow (ed.), Elsevier Science Pub., London, pp. 231–270.

Marwaha, S., and Kennedy J., 1988, Review: Whey Pollution Problem and Potential Utilization, *Int. J. Food Sci. Technol*. **23**:323–336.

Matser, A.M., Krebbers, B., van den Berg, R.W., and Bartels P.V., 2004, Advantages of High Pressure Sterilisation on Quality of Food Products, *Trends Food Sci. Technol*. **15**:79–85.

Meisel H., 1997, Biochemical Properties of Bioactive Peptides Derived from Milk Proteins: Potential Nutraceuticals for Food and Pharmaceutical Applications, *Livesock Prod. Sci*. **50**:125–138.

Meisel H., 2002, Milk Protein-Derived Peptides as Potentially Bioactive Components of Cheese, *Proceedings of the 26th International Dairy Congress*, IDF, Paris.

Meisel, H., and Schlimme E., 1990, Milk Proteins: Precursors oOf Bioactive Peptides, *Trends Food Sci. Technol*. **1**:41–43.

Mendez-Palacios, I., López-Luna, A., Bárzana, E., Jiménez-Guzmán, J., and García-Garibay M., 2006, Development of a Molecularly Imprinted Polymer (MIP) for the Recovery of Lactoferrin, *Proceedings of the 13th World Congress of Food Science and Technology*, IUFOST, Nantes, France.

Morr C.V., 1989, Whey Proteins: Manufacture, in: *Developments in Dairy Chemistry—4*. P.F. Fox, (ed.), Elsevier Applied Science, London, pp. 245–284.

Mulvihill, D.M., and Ennis M. P., 2003, Functional Milk Proteins: Production and Utilization, in: *Advanced Dairy Chemistry, Vol. 1. Proteins*. P.F. Fox and P.L.H. McSweeney (eds.), Kluwer Academic, New York, pp. 1175–1228.

Mulvihill, D.M. and Fox P.F., 1989, Physico-Chemical and Functional Properties of Milk Proteins, in: *Developments in Dairy Chemistry—4*. P.F. Fox (ed.), Elsevier Applied Science, London, pp. 131–172.

Neville, J.R., Armstrong, K.J. and Price J., 2001, Ultra Whey 99: A Whey Protein Isolate Case Study, *Int. J. Dairy Technol*. **54**:127–129.

Pearce R.J., 1992, Whey Protein Recovery and Whey Protein Fractionation, in: *Whey and Lactose Processing*, J. G. Zadow (ed.), Elsevier Science Pub., London, pp. 271–316.

Philanto-Leppälä, A., 2001, Bioactive Peptides Derived from Bovine Whey Proteins: Opioid and Ace-Inhibitory Peptides, *Trends Food Sci. Technol*. **11**:347–356.

Philanto-Leppälä, A., 2003, Bioactive Peptides. Milk Proteins, in: *Encyclopedia of Dairy Science Vol. 3*, H. Roginski, J.E. Fuquay and P.F. Fox (eds.), Academic Press, Amsterdam, pp. 1960–1967.

Renner E., 1989, Nutritional Aspects, in: *Whey and Lactose Processing* J.G. Zadow (ed.), Elsevier Science Pub., London, pp. 449–471.

Sava, N., van der Plancken, I., Claeys, W., and Hendrickx M., 2005, The Kinetics of Heat-Induced Structural Changes of β-Lactoglobulin, *J. Dairy Sci*. **88**:1646–1653.

Schanbacher, F.L, Talhouk, R.S., and Murray F.A., 1997, Biology and Origin of Bioactive Peptides in Milk, *Livestock Prod. Sci*. **50**:105–123.

Shah N., 2000, Effects of Milk Derived Bioactives: an Overview, *Brit. J. Nutr*. **84** suppl. 1:3–10.

Ting, E., Balasubramaniam, V.M., and Raghubeer E., 2002, Determining Thermal Effects in High Pressure Technology, *Food Technol*. **56**:31–35.

Trejo-Vázquez, R., Revah-Moiseev, S., Jiménez-Gutiérrez, A., and Ramírez-García F.P., 1995, Solving the Whey Pollution Problem by Ultrafiltration: An Economic Assessment, *Rev. Int. Contam. Amb*. **11**:47–57.

Tsuda, H., Sekine, K., Fujita, K., and Ligo M., 2002, Cancer Prevention by Bovine Lactoferin and Underlying Mechanisms—A Review of Experimental and Clinical Studies, *Biochem. Cell Biol*. **80**:131–136.

van Belzen N., 2002, The Role of Lactoferrin in Cancer Prevention, *Proceedings of the 26th International Dairy Congress*, IDF, Paris, France.

Vázquez-Lara, L., Tello-Solís, S., Gómez-Ruiz, L., García-Garibay, M., and Rodríguez-Serrano G.M., 2003, Degradation of α-Lactalbumin and B-Lactoglobulin by Actinidin, *Food Biotechnol*. **17**:117–128.

Walzem, R.L, Dillard, C.J., and German J.B., 2002, Whey Components: Millenia of Evolution Create Functionalities for Mammalian Nutrition: What We Know and What We May be Overlooking, *Crit. Rev. Food Sci. Nutr*. **42**:353–375.

32
Innovations in Starch-Based Film Technology

M. García, A.M. Rojas, J.B. Laurindo, C.A. Romero-Bastida, M.V.E. Grossmann, M.N. Martino, S. Flores, P.B. Zamudio-Flores, S. Mali, N.E. Zaritzky, P. Sobral, L. Famá, L.A. Bello-Pérez, F. Yamashita, and A. del P. Beleia

32.1. Introduction

Edible and biodegradable films can offer great potential to enhance food quality, safety and stability. The unique advantages of edible films and coatings may lead to new product developments, such as individual packaging of particulate foods, carriers for different additives, and nutrient supplements (Vermeiren et al., 1999). Composite films can be formulated to combine the advantages of each component. Proteins and polysaccharides provide the supporting matrix and are good barriers to gases, while lipids provide a good barrier to water vapor (Krochta and De Mulder Johnston, 1997). Over the last few years, there has been a renewed interest in biodegradable films and films made from renewable and natural polymers such as starch (Lawton, 1996; Vicentini et al., 2005). Several studies have been done to analyze the properties of starch-based films (Lawton and Fanta, 1994; Lourdin et al., 1995; Arvanitoyannis et al., 1998; Garcia et al., 1998a, 1998b, 2000a, 2000b, 2001; Mali et al., 2002; Vicentini et al., 2005). The use of a biopolymer such as starch can be an interesting solution because this polymer is quite cheap, abundant, biodegradable and edible. Amylose is responsible for the film-forming capacity of the starches.

Starches are polymers that naturally occur in a variety of botanical sources such as wheat, corn, potatoes and tapioca or cassava. It is a renewable resource widely available and can be obtained from different by-products of harvesting and raw material industrialization.

Grown in tropical areas (Latin America, Asia and Southern Africa) of the world, tapioca (cassava) is used in Latin America as a meal, as animal fodder, or cooked and eaten as a vegetable. The Food and Agriculture Organization (FAO) recently highlighted that tapioca is a good commercial cash crop and a major source of food security, and that it needs a competitive edge to thrive in the global starch market. Due to the shortage or high price of traditional starch sources, such as wheat and soybeans, tapioca starch is viewed as an alternative source by food companies for use as an ingredient (FAO, 2004).

Yam tubers (*Dioscorea alata*) are another potential starch source that could be used as a food ingredient, but that has not been explored commercially (Mali et al.,

2002). Yam starch, although not commercially available, has some interesting functional properties, as a function of its relatively high amylose content (approximately 30%) and amylopectin chain structure (Mali et al., 2004). This high amylose content motivated the initial studies about yam starch films (Mali et al., 2002, 2004).

Banana is an edible fruit cultivated in the tropical and subtropical regions and is an important food crop. Banana fruits are included in the genus *Musa* of the family *musaceae* (Bello-Pérez et al., 2000). Starch is the principal component of green bananas, and this polysaccharide undergoes important changes during ripening. Lii et al. (1982) investigated changes in physical and chemical properties of banana starch, as well as banana components, during ripening. Morphological studies showed that banana starch has an irregular and elongated oval with ridged shapes (Zhang et al., 2005). Gonzalez-Soto et al. (2006) reported 34.9% amylose content in starch isolated from Mexican plantain.

In film technology, starches can be used in their native form or modified. For example, the use of cassava starch acetate (CSA) to impregnate Kraft paper is a good alternative to improve the water vapor permeability (K_w) of this material. This barrier property depends on the water vapor diffusion coefficient (D_{eff}) and on the material adsorptivity property (β). Kraft paper is used as a material for the manufacture of low cost packaging, which needs good mechanical properties. It is used as industrial packaging for products of great volume, due to its low cost and high mechanical resistance to tearing and to tension forces. On the other hand, the hygroscopic properties and the water vapor barrier of Kraft paper are not suitable for foodstuff storage in environments with high relative humidity, since this material is hygroscopic and porous (Sobral and Ocuno, 2000). To minimize this problem, several techniques have been used with the aim of reducing the hygroscopicity and improving the water vapor barrier of papers, with a focus on the impregnation of papers with non-hygroscopic and biodegradable materials like starch acetate (Narayan et al., 1999; Larotonda et al., 2005).

In the absence of additives, films made from these polysaccharides are brittle. Plasticizers are necessary to enhance flexibility and to improve mechanical properties. Hydrophilic compounds such as polyols are commonly used as plasticizers in hydrophilic film formulations. At the same time, the use of hydrophobic substances is also proposed as a form to overcome the problem of instability of films when submitted to different ambient conditions (Petersson and Stading, 2005).

The objective of this work was to present and discuss some results obtained with coatings or films based on different starches.

32.2. Film Production and Characterization

32.2.1. Tapioca Films

Mixtures of tapioca starch, glycerol, potassium sorbate and water (5.0:2.5:×:92.2, in weight) with X taking values of 0.3 or 0.2, were used for filmmaking. Films were prepared according to different methods:

a) Method 1: heating at an initial rate of 1.6°C/min for ≅ 25 min. Afterwards, heating was maintained at a lower rate ≅ 0.3°C/min) for an additional period of 40 min. After gelatinization, films were cast over glass plates and dried at 50°C (2 h). Drying was completed in a controlled temperature chamber at 25°C (1 week).
b) Method 2: heating at a constant rate of 1.8°C/min for ≅ 30 min. The rest of the procedure was described above.
c) Method 3: heating at a constant rate of 1.8°C/min for ≅ 30 min. After gelatinization, films were cast over glass plates and dried at 50°C (2 h). Drying was completed over $CaCl_2$ at 25°C (2 d).

Once constituted, films were conditioned at 25°C, over a saturated solution of NaBr (water activity, $a_W \cong 0.575$).

Potassium sorbate content for films containing the preservative was determined through the oxidation technique, which involves distillation and a colorimetric reaction using thiobarbituric acid, as proposed by the AOAC (1990). A Philips X-ray diffracto-meter with vertical goniometer was used for effective percent crystallinity of films determination.

The viscoelastic properties of the studied material were carried out in a DMTA IV Rheometric Scientific equipment (Rheometric Scientific Inc., New Jersey). The samples were studied in the Rectangular Tension mode. Specimens for the tests were cut according to ASTM D4092 (1996), strain rate was fixed in a value of 5.10^{-3} sec^{-1} and stress (σ) - strain (ε) curves were recorded. Water vapor permeability (WVP) of films was determined gravimetrically at 25°C using a modified ASTM E96-00 (2000) procedure.

32.2.1.1. Effect of Filmmaking Technique on Film Properties

For this part of the research, X took a value of 0.3. Method 3 showed the highest sorbate concentration two weeks after gelatinization (5.98 g/100 g film, dry basis vs. 4.00 and 4.51 for methods 1 and 2, respectively), a fact that can be attributed to the shorter gelatinization and drying process applied for its development.

Films showed a B-V crystalline pattern (Manzocco et al., 2003) and a crystallinity of 9.4, 8.4 and 6.4% for methods 1, 2 and 3, respectively. Slow drying could promote ordering of chains, causing a similar and higher crystallinity level for methods 1 and 2 compared to method 3.

Method 1 and method 2 produced films with significantly higher tensile stress than did method 3 for the formulation assayed (Fig. 32.1). Slow drying provided a longer time for the occurrence of network formation, further thickening and rigidity development, contributing to a more elastic film and higher tensile stresses than when methods 1 or 2 were applied. It is important to remark that the films studied did not show a discernible maximum (rupture) in the force-displacement curve until 80% strain, which is the maximum strain attainable in the equipment for the geometry of the samples used.

Films made through method 3 resulted in the highest WVP value (16.1×10^{-10} g/s m Pa) as the result of a less ordered starch network, practically doubling

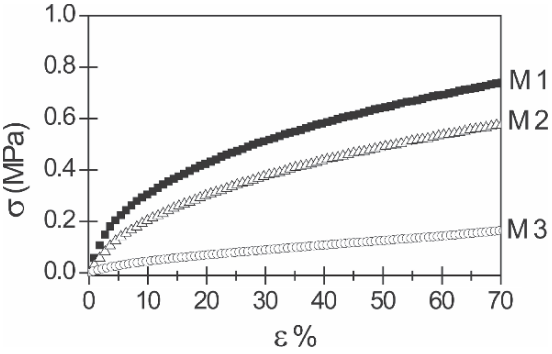

FIG. 32.1. Effect of gelatinization/drying technique on stress-strain relationship of tapioca starch edible films. ■ Method 1 (M1), Δ Method 2 (M2), ○ Method 3 (M3)

the WVP value attained with method 1. It is well known that edible films tend to be poor moisture barriers due to abundant hydrophilic groups in the biopolymer matrix; however, the technique applied to prepare films can help to improve moisture barrier properties.

32.2.1.1. Effect of Storage on Film Properties

For this part of the research, X took values of 0.2, and method 2 was used to make the films. Storage was performed at 25°C and $a_W \cong 0.575$.

Crystalline degree increased from 22.2% after 2 weeks to 30.3% after 8 weeks. Tensile stress increased during storage, changing from 1.23 MPa for 2 weeks to 2.8 MPa for 8 weeks of storage. These results are in accordance with the increase in crystalline degree with time and with the decrease in moisture content from 36.0 to 24.8 g/100 g, dry basis, for times of storage of 2 weeks and 8 weeks, respectively.

In conclusion, it can be considered that different processing methods applied to obtain tapioca starch-glycerol edible films as well as storage affected physical properties. It was observed that to preclude antimicrobial destruction, it was better to apply short gelatinization and drying times; however, this technique produced films with poorer mechanical characteristics that may affect film performance. The goal of film application will determine the method of obtention. The storage time produced a decrease in moisture and an increase in crystalline degree, increasing the stiffness of films.

32.2.2. Corn Starch And Amylomaize Based Films And Coatings

Commercial corn starch (Molinos Río de la Plata, Argentina) with 250 g/kg amylose and amylomaize (Amaizo, USA) with 650 g/kg amylose were used for film and coating formulations. Starch suspensions (2 g/L) were prepared as described

in a previous work (García et al., 1998a,b, 2000a,b). Either 20 g/L glycerol or sorbitol (Merk, USA) were added as plasticizers. Then, 2 g/L sunflower oil (AGD, Argentina) was added to the formulation. In all cases, to obtain films, 40 g of solutions were poured on rectangular acrylic plates (10 × 20 cm). The solutions were dried at 60°C in a ventilated oven to constant weight. Films were stored under controlled temperature and relative humidity conditions (20°C and 65% RH).

A tensiometer CSC-DUNOUY 70535 (USA) was used to determine the surface tension of the formulations. Suspensions were analyzed at 20°C using a rotational viscometer Haake Rotovisko RV2 (Germany) with a sensor system MVIP of concentric cylinder. Shear stress was measured as a function of shear rate from 0 to 692s^{-1}. Power law model was applied to determine consistency index (k) and flow behavior index (n). Apparent viscosity was calculated at 692s^{-1}.

Equilibrium moisture content: Water content of the films was determined measu-ring weight loss of films upon drying in an oven at 110°C until constant weight (dry sample weight). Thickness of the films was determined using a digital coating thickness gauge Elcometer A 300 FNP 23 (England) for non-conductive materials on non-ferrous substrates. Film solubility in water was determined using film pieces of 2 × 3 cm; samples were weighed to the nearest 0.0001 g and placed into test beakers with 80 ml deionizated water. The samples were maintained under constant agitation at 200 rpm for 1 h at room temperature (approximately 25°C). After soaking, the remaining pieces of film were collected by filtration and dried again in an oven at 60°C to constant weight. The percentage of total soluble matter (% solubility) was calculated.

For film microstructure analysis, scanning electron microscopy (SEM) analysis was performed with a JEOL JSPM 100 electron microscope (Japan). Film pieces were mounted on bronze stubs using a double-sided tape and then coated with a layer of gold (40–50 nm), allowing surface and cross-section visualization. All samples were examined using an accelerating voltage of 5 kV.

Film samples were analyzed between 2θ= 4° to 2θ= 60° with a step size 2θ = 0.02° in an X-ray diffractometer X'Pert Pro PANalytical Model PW3040/60 (Almelo, The Netherlands) using a Cu Kα radiation, 40 kV and 40 mA. The diffractometer was equipped with 1 ° divergence slit and a 0.3 mm receiving slit.

Differential scanning calorimetry (DSC): Film samples were tested in a Polymer Laboratories DSC (Rheometric Scientific, Surrey, UK) working under a PL-V5.41 software. Indium was used to calibrate temperature and heat flux. Samples of 1.5–2 mg were weighted in aluminum pans and were hermetically sealed; an empty pan was used as a reference. Samples were run between 0 and 130°C with 10°C/min heating rate; then, pans were punctured and dried until constant weight at 100°C to get sample dried weight. Enthalpies ΔH (mJ/mg), onset and peak transition temperatures were obtained from the thermograms.

Water vapor permeability tests were conducted using a modified ASTM (1996) method E96 as described in a previous work (García et al., 2004) using an especially designed permeation cell that was maintained at 20°C. After steady state

conditions were reached (about 2 h), eight weight measurements were made over 24 h. A driving force of 1753.55 Pa, expressed as water vapor partial pressure, was used.

CO_2 and O_2 permeabilities of the films were assessed by the accumulation method in a specially designed stainless steel cell (García et al., 2000b). The quasiisostatic method used was based on the measurement of the amount of gas diffusing through a film, which was quantified by a gas chromatograph (Varian Start 3400, USA). Gas permeability assays were performed in a room under controlled conditions (20°C and 65% RH) and expressed as $cm^3\ m^{-1}\ sec^{-1}\ Pa^{-1}$.

Tensile tests were performed in a texturometer TA.XT2i—Stable Micro Systems (England) as described in a previous work (García et al., 2004) using a tension grip system A/TG and probes of 6 cm in length and 0.7 cm width. Puncture tests were performed using a cylindrical probe 2 mm in diameter at a constant rate of 1 mm/s. Tests were carried out with samples of 3 × 3 cm from each film formulation. Curves of force (N) as a function of deformation (mm) were automatically recorded by the Texture Expert Exceed software. Maximum breaking force (N), tensile strength (MPa), deformation at break (mm), percent of elongation at break (%) and elastic modulus (N/mm) were calculated according to the ASTM D882-91 method (1996).

32.2.2.1. Characterization of Corn and Amylomaize Starch-Based Films and Coatings

Suspensions can be used to obtain either coatings or films. In the case of coatings, surface tension becomes an important factor. Plasticizer and lipid addition decreased surface tension (Table 32.1), facilitating coating adhesion to foodstuffs. Power law model satisfactory fitted experimental data ($r^2 > 0.96$).

All suspensions showed pseudoplastic behavior ($n < 1$). Plasticizer and lipid addition to corn and amylomaize suspensions decreased flow behavior index and increased consistency index (Table 32.1). ANOVA showed that apparent viscosity of amylomaize suspensions were significantly ($P < 0.05$) higher than corn starch suspensions; this was attributed to the higher amylose content of amylomaize. Apparent viscosity of corn starch suspensions with different compositions are shown in Table 32.1.

TABLE 32.1. Characterization of corn starch-based suspensions

Additives	Surface tension(dyn/cm)	Consistency index k ($Pa.s^n$)	Flow behavior index n (dimensionless)	Apparent viscosity η_{ap} at 692,48 s^{-1} (mPa.s)
WA	60.68 ± 0.120	0.09 ± 0.032	0.69 ± 0.064	12.85 ± 0.063
Glycerol	59.6 ± 0.764	0.12 ± 0.014	0.63 ± 0.024	11.95 ± 0.182
Glycerol + SO	59.08 ± 0.679	0.14 ± 0.026	0.60 ± 0.028	11.31 ± 0.092
Sorbitol	51.44 ± 0.082	0.13 ± 0.029	0.64 ± 0.037	12.59 ± 0.176
Sorbitol + SO	54.02 ± 0.266	0.21 ± 0.017	0.52 ± 0.011	9.64 ± 0.182

WA= Corn starch based suspension without additives
SO= Sunflower oil

Film integrity is a critical factor, since pore presence could modify mechanical and barrier properties. Microscopic and SEM observations allow evaluation of film integrity. Films without plasticizer showed pores and cracks in the surface, while cross-sections evidenced a multilayer structure. Plasticized films with lipid showed smooth surfaces and a compact structure. These results indicated that lipids were homogeneously dispersed in the film matrix (Fig. 32.2).

X-ray diffraction analysis indicated that films exhibited an amorphous-crystalline structure. Crystallinity degree of the films increased during storage, resulting in extremely brittle and rigid films. The addition of plasticizer increased the proportion of amorphous phase and facilitated the formation of a thermodynamically more stable crystalline structure at short times. The diffraction pattern of plasticized films did not change with storage time; peaks only increased in intensity, maintaining the initial positions (Fig. 32.3). Lipid addition did not affect the crystalline structure developed in the films.

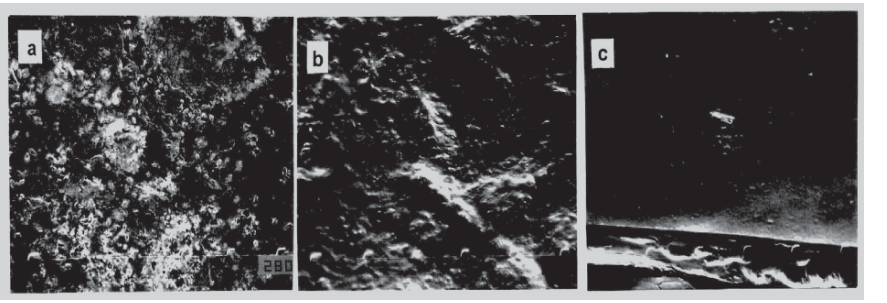

FIG. 32.2. SEM micrograph of the surface of corn starch-based films a) without plasticizer, b) with 20 g/L glycerol and c) with 20 g/L sorbitol and 2 g/L sunflower oil. Magnification: 100 µm between marks

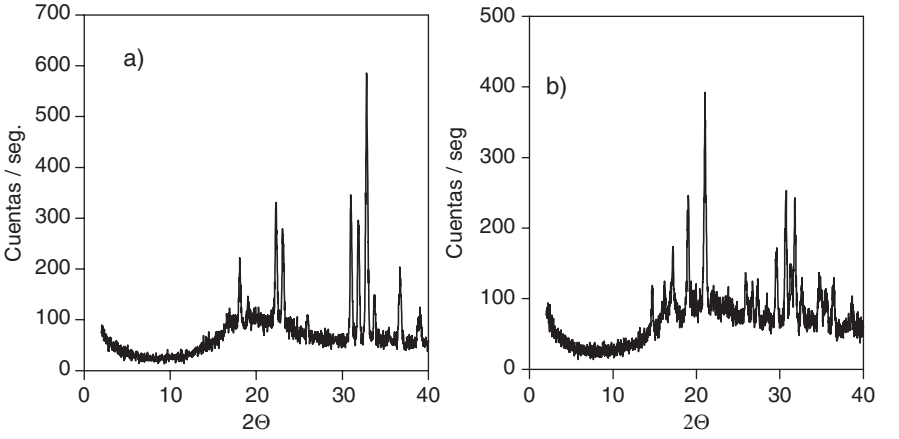

FIG. 32.3. Diffractograms of amylomaize films plasticized with glycerol and with the addition of sunflower oil a) initial and b) stored during 60 days at 20 °C and 65% RH

At initial storage time, corn starch and amylomaize films did not show any peak on DSC thermograms, indicating that starch gelatinization was complete. However, stored films showed an endothermic transition with a peak temperature between 50°C and 54°C. This thermal transition could be associated with crystal growth and recrystallization processes that take place during storage. Amylomaize-formulated films, due to a higher amylose content, showed higher ΔH values compared to those of corn starch films along storage time. During storage this structure is perfected, since the peak is narrower, increasing its temperature and enthalpy. These results correlated well with those of X-ray diffraction.

Plasticizers limit crystal growth and recrystallization because they interact with the polymeric chains, hindering their alignment and, thus, crystal formation. Thus, crystallization is produced in a lower degree (lower ΔH) and with lower peak temperatures than unplasticized films. Experimental results were modeled using the Avrami's model, which is applied to crystallization polymers kinetics (Fig. 32.4).

Coating water vapor permeability was determined by application of the coating on a model system with defined geometry (carrot slices). The WVP values obtained with coatings and those obtained with films did not differ significantly ($P>0.05$). Plasticizer type and the presence of lipid significantly decreased ($P<0.05$) the WVP of films (Table 32.2). McHugh and Krochta (1994), using similar plasticizer concentrations, found similar results working with alginate and pectin films. The more effective films were those of high amylose content, since they presented a more compact matrix. Starch-based films showed WVP values an order lower than those reported for some protein films. With regard to synthetic polymers, the obtained WVP values were similar to those of cellophane and higher than those reported for low density polyethylene, a commonly used packaging material (Table 32.2).

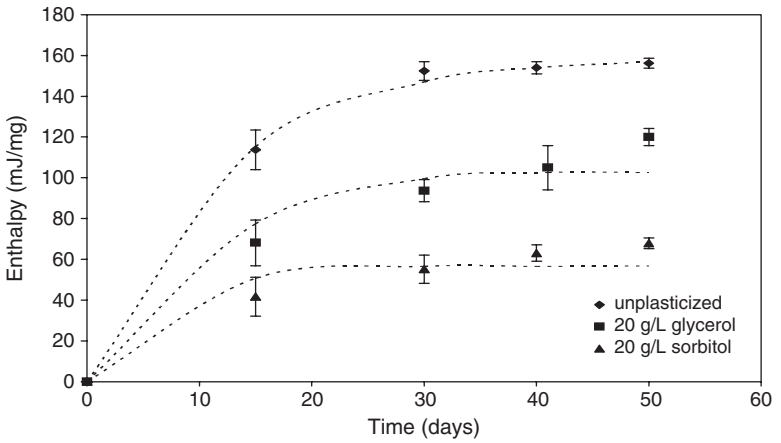

FIG. 32.4. Enthalpy evolution of the thermal transition observed as a function of storage time of corn starch-based films

TABLE 32.2. Barrier properties of edible starch based films and synthetic films

Film type	Formulation	Water vapor permeability × 10^{10} ($gm^{-1}s^{-1}Pa^{-1}$)	CO_2 Permeability × 10^{10} ($cm^3m^{-1}s^{-1}Pa^{-1}$)	O_2 Permeability ×10^{10} ($cm^3m^{-1}s^{-1}Pa^{-1}$)	Selectivity factor (PCO_2/PO_2)
Edible	S	2.62	280.5	26.45	10.59
	S + G	2.14	38.5	3.21	11.99
	S + G + L	1.76	43.9	2.36	18.60
	S + Sorb	1.21	29.6	2.28	12.98
	S + Sorb +L	0.97	34.3	2.18	15.73
Synthetic	LDPE	0.00914	0.945	0.216	4.37
	PVC	0.000308	0.000554	0.000128	4.33

S: amylomaize starch, G: glycerol, Sorb: sorbitol, L: lipid, LDPE: low density polyethylene, PVC: polyvinylchloride

Starch-based films have much lower O_2 permeabilities than those for CO_2, indicating a selective action of these films on gas permeabilities (Table 32.2). These effects can be attributed to a higher solubility of CO_2 in the starch films (Arvanitoyannis et al., 1994). Films with sorbitol exhibited statistically lower ($P<0.05$) oxygen permeability values than films with glycerol. The type of both plasticizer and starch used in film formulations were significant factors ($P<0.05$) on gaseous permeabilities. Sorbitol combined with the amylomaize film matrix gave the best results. Arvanitoyannis et al. (1994) found a similar trend for rice- and potato starch-based films. Lipid presence did not significantly modify ($P>0.05$) CO_2 permeability of plasticized films. Synthetic materials show lower gas permeabilities for CO_2, but have low selectivity between CO_2 and O_2 (Table 32.2).

The development of edible films and coatings with selective gas permeability could be very promising for controlling respiratory exchange and improving the conservation of fresh or minimally processed vegetables (Cuq et al., 1998; García et. al, 1998 a and b). According to Donhowe and Fennema (1993 a and b), permeability increases with the decrease of crystalline/amorphous ratio. Thus, the increase in film crystallinity evidenced by X-ray diffraction and DSC analysis explains the observed decrease of CO_2 permeability during storage (Fig. 32.5).

With regard to mechanical properties, films without additives showed rigid and brittle characteristics, evidenced by high elastic modulus and small elongation at break. The higher values of elastic modulus of amylomaize films were attributed to their higher amylose content (Fig. 32.6). Higher elongation and break and lower elastic modulus were obtained in films with plasticizer, enhancing film flexibility and tenacity. Mechanical properties of composite films highly depend on additive-matrix interaction. Plasticizer-matrix interaction showed a similar trend for both corn starch and amylomaize films, although plasticized corn starch films were more flexible (lower elastic modulus) than amylomaize films. Lipid addition increased film flexibility and reduced the effect of starch type. Similar results were reported by Cunningham et al. (2000) with soy protein films. Synthetic polymers like LDPE and HDPE exhibited high elongation values but similar tensile strength, while cellophane showed similar elongation values but higher tensile strength than those obtained with natural polymers.

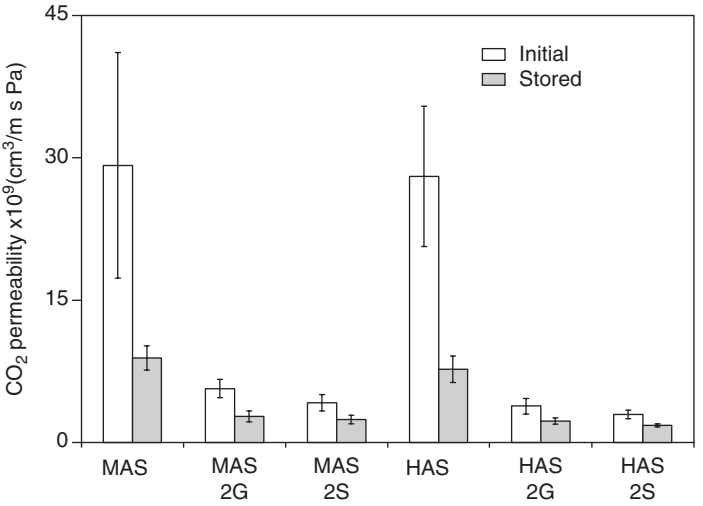

FIG. 32.5. Effect of storage time (20 days at 20 °C and 65% RH) in the CO_2 permeability of starch-based films. MAS: medium amylose content starch, HAS: high amylose content starch, G: 20 g/L glycerol and S: 20 g/L sorbitol

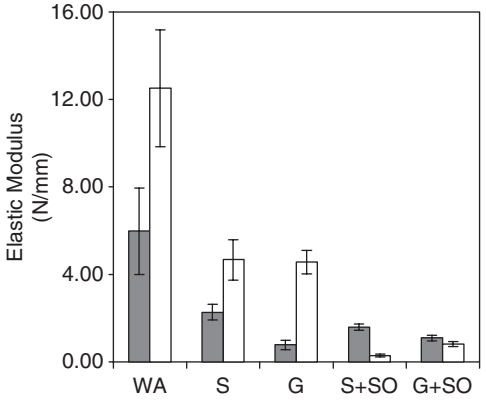

FIG. 32.6. Tensile properties: elastic modulus of corn (■) and amylomaize (□) films. WA= without additives; S= with sorbitol; G= with glycerol; S + SO= with sorbitol and sunflower oil and G + SO= with glycerol and sunflower oil

The starch formulations tested as films were also applied as coatings on refrigerated strawberries. Spoilage is the main factor that determines shelf-life of food products. The addition of potassium sorbate to film formulation increases the effectiveness of starch-based coatings as a barrier to microorganisms; moreover, the addition of citric acid enhances the action of the antimicrobial agent. Thus, when these coatings were applied on strawberries (*Fragaria* × *ananassa*) cv. Selva, fruit shelf-life, defined as the time needed to reach 10^6 CFU/g, was 21 days

for formulations with plasticizer and 14 days for the control fruits. Formulations with potassium sorbate extended the shelf life to 28 days, demonstrating the effectiveness of the coatings.

Water vapor barrier properties determine the capacity of coatings to control weight loss and texture of food products, since these parameters limit their shelf-life, particularly that of vegetable products. The addition of lipid phase significantly reduced ($P < 0.05$) weight loss of coated strawberries (García et al., 2001), leading to a reduction of 63.2% compared to the control fruits stored for one month at 0°C. Besides, edible films and coatings with selective gas permeability allow modification of the internal atmosphere of packaged products. In the case of coated strawberries, this was evidenced by a reduction in the respiration rate and in the kinetics of physiological parameters development, such as reductor sugars, anthocyanin content and titratable acidity, during the refrigerated storage (García et al., 1998 a, b, 2001).

In conclusion, it can be considered that polysaccharides form a supporting matrix of films and coatings, giving selective barrier properties to gases. Native or modified starches are a natural mixture of compatible polysaccharides; amylose proportions determine the properties of films. These characteristics, in addition to their low cost and high availability, increase their potential applications.

Plasticizer and lipid addition allows the optimization of barrier and mechanical properties of starch-based films and coatings. In the formulation and application of an active film or coating, deteriorative mechanisms that limit the shelf-life of the substrate must be considered. On the other hand, film performance can be evaluated by microstructural analysis, transfer and mechanical properties, and their relation with film composition.

32.2.3. Acetate Starch Coating

Commercial Kraft paper with 75 g/m^2 was impregnated with cassava starch acetate (CSA) with acetylation degree of about 1.4 (Larotonda et al., 2005). Paper samples were dried in an oven at 50°C for 24 h. The solution used in the Kraft paper impregnations was prepared from the solubilization of starch acetate in chloroform at the ratio of 1:5. This solution was placed in a desiccator, where the samples of Kraft paper were immersed and kept for 10 min. Depending on the case, a vacuum of 600 mmHg was used. After impregnation, samples were dried at 50°C for 24 h. Before mechanical tests, samples were conditioned for seven days at 25°C and RH of 75%. The samples were codified in accordance with the following: Kraft paper (KP), impregnated Kraft paper (IKP) and vacuum impregnated Kraft paper (VIKP). The specific area and pore volume distribution were determined by N_2 adsorption using equipment from Quantachrome Instruments, model Autosorb®-1-C. Specific area was determined by BET method, while pore volume as a function of pores diameter was determined by BJH method (Barrett et al., 1951). The specific gravity was determined by the relation $\rho = m/(S \times \delta)$, where m is the dried sample weight, and S and δ are the sample area and average thickness, respectively. Water sorption isotherms were

TABLE 32.3. Experimental conditions of essays performed to determine water vapor permeabilities of KP, IKP and VIKP (38 °C)

Water activity (a_w)	Interior of diffusion cell	Exterior of diffusion cell (chamber)
0.02 – 0.33	Calcium chloride ($CaCl_2$)	Magnesium chloride ($MgCl_2$)
0.33 – 0.62	Magnesium chloride ($MgCl_2$)	Sodium nitrite ($NaNO_2$)
0.62 – 0.90	Sodium nitrite ($NaNO_2$)	Barium chloride ($BaCl_2$)

determined by saline solutions method. The water vapor permeabilities (K^w) were determined gravimetrically, based on ASTM standard method E96 (ASTM, 1996). Pre-conditioned discs of paper (90 mm diameter) were placed in permeation cells with saturated saline solutions (lower a_w) and hermetically stamped on the edges. These permeation cells were placed in a glass chamber of dimensions $400 \times 400 \times 250\,mm^3$, with another saturated saline solution (higher a_w). A small fan was installed inside the chamber to promote circulation of internal air. The experimental conditions used to determine the water vapor permeabilities of each sample are presented in Table 32.3.

The water permeability K^W of the film, usually represented as [g water × mm /m^2 × Pa ×h] Eq. (32.1).

$$K^w = \rho^s \beta D_{eff} \tag{32.1}$$

On the other hand, the material sorption isotherm can be represented by the extensively used GAB model (Guggenheim, Anderson, de Boer), given in Eq. (2).

$$X = \frac{CkX_0 a_w}{[(1-ka_w)(1-ka_w+CKa_w)]} \tag{32.2}$$

where C, X_o and k are constants, with X_o representing the monolayer moisture content, on a dry basis. Differentiating equation 2 in relation to a_w and dividing the result by p_s, the water adsorptivity in the film, β [kg water/kg dry solid × Pa], can be given by Eq. (3) (Larotonda et al., 2005). The modification of the hygroscopic and water permeability properties of Kraft paper following its impregnation with starch acetate was studied. The influences of the properties β and D_{eff} on the Kraft paper permeability, before and after the impregnation, were evaluated.

$$\beta = \frac{CkX_0}{p_s}\left[\frac{1}{(1-ka_W)(1-ka_W+Cka_W)} - \frac{a_W}{[(1-ka_W)(1-ka_W+Cka_W)]^2} - [-k(1-ka_W+Cka_W)+(1-ka_W)(-k+Ck)]\right] \tag{32.3}$$

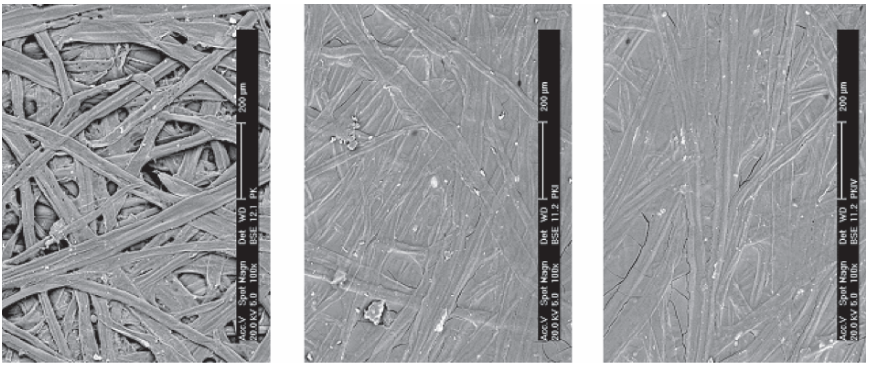

FIG. 32.7. Micrographs (100×) of Kraft paper samples: (left) non-impregnated, (middle) impregnated at atmospheric pressure and (right) impregnated under vacuum conditions

Micrographs of samples KP, IKP and VIKP, obtained with a magnification of 100×, are presented in Fig. 32.7. The starch acetate coating the surface of the Kraft paper can be clearly observed.

The specific gravity values of KP, IKP and VIKP were 0.637 ± 0.032, 0.870 ± 0.037 and 0.919 ± 0.030 g/cm^3, respectively. The specific superficial areas of samples, obtained by the BET method, were 2.999, 0.952 and 1.084 m^2/g, for KP, IKP and VIKP, respectively. Starch acetate impregnation promoted an increase of around 40% in the paper specific gravity, while the specific superficial area of impregnated samples decreased to a third of the value of the original Kraft paper, due to the reduction of its internal and superficial porosity. These results are in agreement with the pictures obtained by SEM, indicating the filling of a considerable fraction of the Kraft paper pores.

The cassava starch isotherm presented the sigmoidal form (type II isotherm), while the isotherm of starch acetate presented a form characteristic of a type III isotherm, related to hydrophobic materials. This behavior also appears in the samples of impregnated Kraft papers IKP and VIKP, which were less hygroscopic than the original Kraft paper, although more hygroscopic than the starch acetate. There was a synergic effect between starch acetate and the porous matrix of KP that caused a great decrease of the paper moisture content at equilibrium. For example, at a_w=0.95 the equilibrium moisture content of starch acetate, KP, IKP and VIKP were estimated by GAB equation as 0.3137, 0.007385, 0.1769 and 0.1644 g water/g dry solid, respectively. On the other hand, the equilibrium moistures contents of IKP and VIKP calculated by means of a simple mixture law were 0.3278 and 0.3190 g water/g dry solid, respectively. The decrease of the superficial area of impregnated samples for a third of KP superficial area value can partially explain this behavior, given that starch acetate solution penetrated

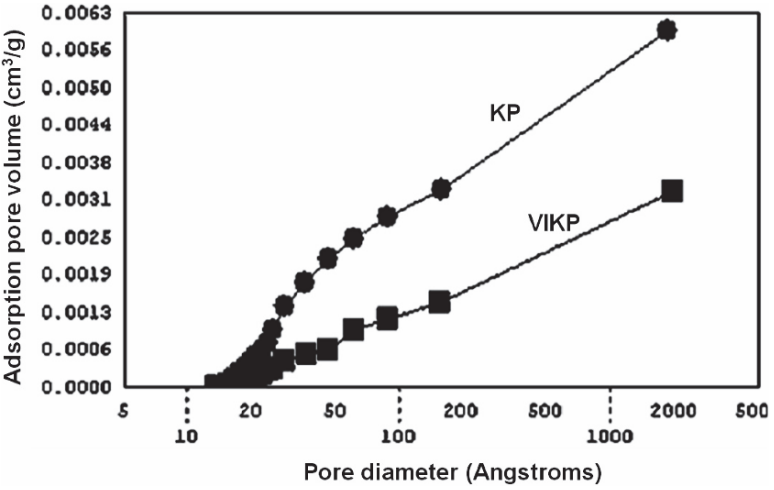

FIG. 32.8. KP and VIKP adsorption cumulative pore volumes before and after impregnation, determined by BJH method.

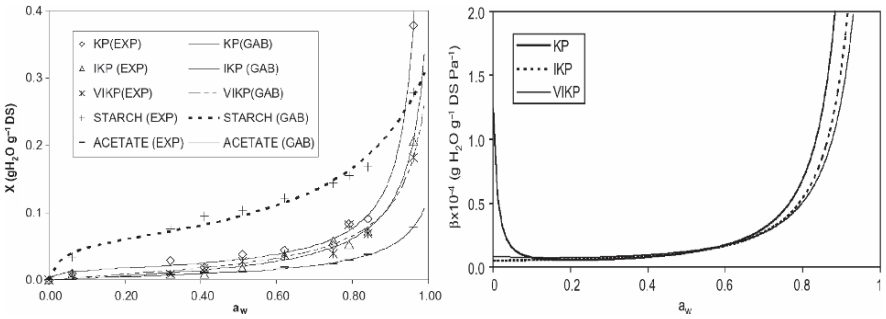

FIG. 32.9. a) Adsorptivity (β) values of KP, IKP and VIKP; b) Comparison of average water vapor permeabilities of KP, IKP and VIKP, determined at different a_w ranges

and filled a great number of the paper pores. KP and VIKP adsorption cumulative pore volumes, before and after impregnation, are presented in Fig. 32.8.

These results showed that KP pores in the whole range of KP and VIKP pore diameters were filled by starch acetate, which decreased the total pore volume from 5.035×10^{-3} to 2.980×10^{-3} cm^3/g. These results corroborate that Kraft paper impregnation with cassava starch acetate is a good alternative for obtaining a waterproof paper, as has been previously reported (Larotonda et al., 2003). The moisture sorption isotherms and the behavior of the β parameter for the Kraft paper, in relation to the water activity, is presented in Fig. 32.9 a and b, respectively.

For original Kraft paper, a β value close to 1×10^{-4} [g water/g dry solid×Pa] was calculated for water activity values tending toward zero. With the formation of the adsorbed molecular monolayer, typical of type II isotherms, the adsorptivity β falls to values close to 5×10^{-6} [g water/g dry solid×Pa], coinciding with the isotherms of IKP and VIKP, until a_w values close to 0.63. From this point, the KP isotherm differentiates from the isotherms of IKP and VIKP, evidencing its greater adsorptivity. These behaviors will be useful in identifying the relative influences of β and D_{eff} on the water vapor permeability of the KP.

The values for the water vapor permeability of the samples are presented in Table 32.4. KP permeability was always larger than IKP and VIKP permeability, increasing by around 17% when a_w increased from 0.02-0.33 to 0.33-0.62 and about 20% when a_w increased from 0.33-0.62 to 0.62-0.90. The overall increase in K^w, when a_w increased from 0.02-0.33 to 0.62-0.90 was around 40%. The water vapor permeability for IKP and VIKP also increased with the increase in water activity, but they did not significantly differ from each other. It can be observed that the KP permeability was about 4.2 and 3.7 times greater than the IKP and VIKP permeability, respectively, for the experiment using a_w values of 0.02 and 0.33. This difference decreased with increasing a_w values in the other experiments. For the experiments carried out with a_w values of 0.33 and 0.62, the KP permeability was around 1.75 and 1.96 times greater than the IKP and VIKP permeability, respectively. For the essays with a_w values of 0.62 and 0.90, KP permeability was about 1.20 and 1.24 times greater than the IKP and VIKP permeability, respectively. The effective mass diffusivities values calculated from the adsorptivity values and permeability data are presented in Table 32.4.

The D_{eff} value for KP was around 1.8 times the D_{eff} for IKP and VIKP. The calculation of D_{eff} was performed with the average value of the adsorptivity β. Therefore, the numeric value of D_{eff} needs to be analyzed carefully, in order to understand the mechanisms that control Kraft paper permeability variation with moisture content and with the starch acetate impregnation. For the values of a_w used in the diffusion cell (0.02-0.33), the reduction in Kraft paper permeability after impregnation was due to the great decrease in its adsorptivity and also to a

TABLE 32.4. Permeabilities, adsorptivity values and effective diffusion coefficient values for KP, IKP and VIKP

Water activity (a_w)	Sample	K^W (10^{-7} g w mm h^{-1} cm^{-2} Pa^{-1})	β(10^{-5} g w g^{-1} dm Pa^{-1})	D_{eff} (10^{-11} m^2 s^{-1})
0.02 – 0.33	KP	2.901	2.201	5.791
	IKP	0.694	0.643	3.475
	VIKP	0.795	0.838	2.890
0.33 – 0.62	KP	3.398	1.296	11.521
	IKP	1.935	1.300	4.806
	VIKP	1.732	1.366	3.864
0.62 – 0.90	KP	4.073	14.556	1.229
	IKP	3.385	8.750	1.245
	VIKP	3.295	7.500	1.339

D_{eff} decrease, which was due to the Kraft paper's impregnation with starch acetate (see Fig. 32.8). When a_w values of 0.33 and 0.62 were used for the diffusion cells, the KP, IKP and VIKP β values were very close to each other (Table 32.4). However, the D_{eff} value for IKP and VIKP was around 42% lower than that for KP. Therefore, for these a_w values, the Kraft paper permeability reduction was due to the filling of the paper's internal pores with starch acetate, reducing the area available for water diffusion and consequently reducing D_{eff}. When KP, IKP and VIKP samples were submitted to the a_w of 0.62 and 0.90 in the permeation cells, the results clearly indicated that the adsorptivity reduction promoted by impregnation controlled the paper's permeability to water vapor. As shown in Table 32.4, there were no significant differences between the D_{eff} values for KP, IKP and VIKP, while the average adsorptivity β decreased by around 80%, due to impregnation.

In conclusion, the results obtained in this work showed that significant reductions in water adsorptivity and water vapor permeability of Kraft paper might well be achieved through starch acetate impregnation, mainly in low relative humidity conditions. This is associated with two factors: a) the partial filling of the Kraft paper's superficial and internal pores by the starch acetate impregnated, reducing the water vapor permeability; b) as starch acetate is much less hygroscopic than paper, its adsorptivity is reduced significantly by impregnation.

The K^W values obtained varied greatly with a variation in a_w, showing the importance of carrying out permeability essays with the diffusion cells simulating the atmospheric conditions close to the real case. Otherwise, large errors may be made. Therefore, the starch acetate impregnation of Kraft paper demonstrated here offers an interesting alternative for the improvement of the hygroscopic properties and water vapor permeability of Kraft paper. Moreover, the use of starch acetate in the impregnation of hygroscopic materials reveals an interesting alternative for the use of starch, adding value to this raw material.

32.2.4. Yam Starch Films

As a way to overcome the problem of instability of films when submitted to different ambient conditions, the substitution of traditional plasticizers by monoglyceride (glycerol-monoestearate) was studied in yam starch films (Ferreira, 2005).

Starch was extracted from fresh tubers of yam (*Dioscorea alata*) according to Alves et al. (1999) and presented the following composition on a dry basis: ash (0.21 ± 0.01%), protein (0.50 ± 0.01%), lipids (0.07 ± 0.02%) and amylose (33.7%). Glycerol-monoestearate was supplied by Ceralit S/A (Campinas, Brazil).

Yam starch and monoglyceride (100:2 w/w) were complexed before film preparation. The two substances were mixed (15 min) in an electric mixer and moisture content was adjusted at 18% with distilled water. A single screw extruder (Cerealtec CT-L15, Campinas, Brazil) was used to produce the complex. The extruder worked with a barrel 420 mm in length and 19.4 mm in diameter, 1:2 compression ratio screw and 5 mm die diameter. The extruder temperature was

maintained at 70-80°C for the feeding section, and 145°C for the mixing and metering sections. Screw speed was fixed at 120 rpm. Samples were collected and dried at 55°C in a forced-air convection oven (Tecnal TE 394-3, Brazil) for 12 h and finely ground in a Quimis Mill (Q-298 A21, Brazil). The complex formation was confirmed by DSC analysis performed in a Shimadzu DSC, model 50 (Shimadzu Corporation, Japan).

The films were prepared by mixing the starch-monoglyceride complex (4 g/100 g solution) with distilled water to make batches with a total weight of 500 g. The film-forming solutions were transferred to a Brabender Viscograph Pt 100 (OHG, Duisburg, Germany), and heated from 30°C to 95°C and maintained at 95°C for 10 min, with regular shaking (75 rpm) and constant (3°C/min) heating rate (this treatment did not disrupt the starch-monoglyceride complex, as proved by DSC tests).

The films were prepared by casting on rectangular acrylic plates (10 × 20 cm), where the starch suspensions were dried at 45°C in a ventilated oven model TE-394-3 (Tecnal, Piracicaba, Brazil) to constant weight (about 20 h). The result was translucent films, which could be easily removed from the plate. Starch films without monoglyceride (4 g starch/100 g filmogenic solution) and glycerol-starch films (4 g yam starch and 1.3 g glycerol/100 g filmogenic solution) were produced at the same conditions for comparative purposes. Glycerol and starch concentrations were established in a previous study (Mali et al., 2002). All films were stored for 7 days before analysis; they were placed at 25 ± 2°C over saturated salt solutions in separated desiccators having different relative humidity (11, 33, 54, 75 and 81% RH) conditions (Rockland, 1960).

Water vapor permeability (WVP) tests were conducted using ASTM (1996) method E96. Each film sample was sealed over a circular opening of 0.00181 m2 in a permeation cell that was stored at 25°C in a desiccator. To maintain a 100% RH gradient across the film, anhydrous calcium chloride (0% RH) was placed inside the cell and distilled water (100% RH) was used in the desiccators. The water vapor transport was determined from the weight gain of the permeation cell. After steady state conditions were reached (about 2 h), eight weight measurements were made over 24 h. Changes in the weight of the cell were recorded to the nearest 0.0001 g and plotted as a function of time. The slope of each line was calculated by linear regression ($r^2 > 0.99$), and the water vapor transmission rate (WVTR) was calculated from the slope of the straight line (g/s) divided by the cell area (m^2). After the permeation tests, film thickness was measured and WVP (g Pa^{-1} s^{-1} m^{-1}) was calculated as WVP = [WVTR = S (R_1 - R_2)] d; where S is the saturation vapor pressure of water (Pa) at the test temperature (25°C), R_1, the RH in the desiccators, R_2, the RH in the permeation cell and d is the film thickness (m).

Samples were analyzed between 2θ = 2° and 2θ = 60° with a step size 2θ = 0.02° in an X-ray diffractometer Philips PW 1710 (The Netherlands) using a Cu Ka radiation (λ =1.543), and 40 kV and 30 mA. Relative crystallinity was calculated for B and V_H crystals by dividing the area of the diffraction peaks at 2θ = 17° and 22° (for B-type) and 2θ = 19.8° (for V_H-type) by the total area of the diffractogram (Hullemann et al., 1999).

The tensile properties of starch films were determined using a TA.TX2i Stable Micro Systems texture analyzer (Surrey, England) in accordance with ASTM D-882-91 method (1996). The samples were clamped between pneumatic grips, and force (N) and deformation (mm) were recorded during extension at 50 mm.min^{-1} and with an initial distance between the grips of 50 mm. The parameters determined were stress at break (MPa) and strain at break (%). Five film specimens (100 mm × 25 mm) of each formulation were used in the analysis.

Statistical software (Oklahoma, USA, 1996) version 5.0 was used for all statistical analysis. Analysis of variance (ANOVA), Tukey test for means comparison and regression analysis were applied. The significance level used was 0.05.

32.2.4.1. Characteristics of Yam Starch-Based Films

The use of extrusion to prepare starch-monoglyceride complex before film preparation by casting was effective to practically inhibit phase separation that other researchers (Petersson and Stading, 2005) reported in films associated with the increase of monoglyceride concentration. The addition of the hydrophobic compound reduced water vapor permeability of the films (0.999×10^{-10} gPa^{-1}s^{-1}m^{-1}) when compared with the films containing starch-glycerol (1.685×10^{-10} gPa^{-1}s^{-1}m^{-1}) or only starch (1.150×10^{-10} gPa^{-1}s^{-1}m^{-1}). According to Petersson and Stading (2005), the effectiveness of monoglycerides to improve barrier properties in starch films is affected by phase separation. In films with phase separation, the WVP increase instead decreases because the film structures have areas without the hydrophobic compound. Starch films and glycerol plasticized films showed large variations in stress and strain at break under different relative humidity (RH); a decrease in stress and an increase in strain were evidenced when RH increased (Fig. 32.10a, b). The decrease of stress and the increase of strain in starch films were related with the variation of water content in these hydrophilic materials and have been reported previously (Monterrey and Sobral, 1999; Mali et al., 2004). Although monoglyceride starch films presented poor mechanical properties when compared to starch and glycerol-starch films (Fig. 32.10a, b), they presented a desirable stable behavior. The low stress at break could be related to the weakening effect of the monoglyceride on the starch network (Petersson and Stading, 2005); probably, the monoglyceride groups sterically interfered with the intermolecular alignment of starch chains, decreasing its tendency to form hydrogen bonds (Wurzburg, 1986). The lower flexibility presented by these films agreed with isotherms (data not presented), which show that monoglyceride starch films had a lower water binding capacity, and this probably contributed to a lower flexibility.

The crystallinity pattern of films could be assigned to a B-type characteristic of biofilms containing starch (van Soest and Vliegenthart, 1997; Mali et al., 2002). X-ray diffractograms (data not shown) were used for the purpose of calculating the relative crystallinity of starch films at specific angles that corresponded at particular crystal types. In Fig. 32.11a, b the relative crystallinities for B and V_H crystals were plotted against the different relative humidities tested for film

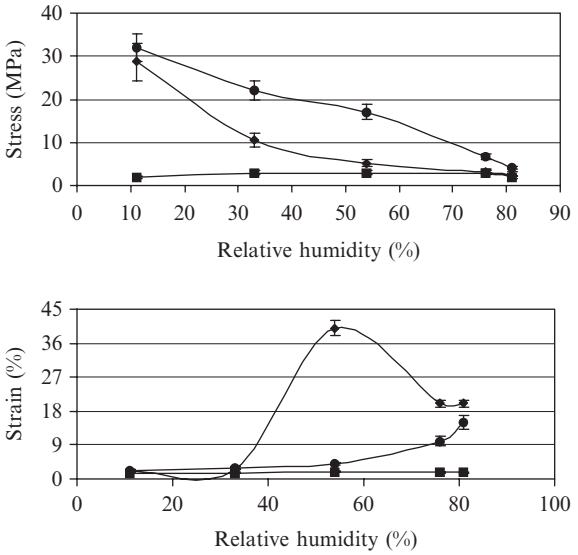

FIG. 32.10 – Stress at break (a) and strain at break (b) for: ● = starch films, ◆ = starch-glycerol films and ■ = starch-monoglyceride films

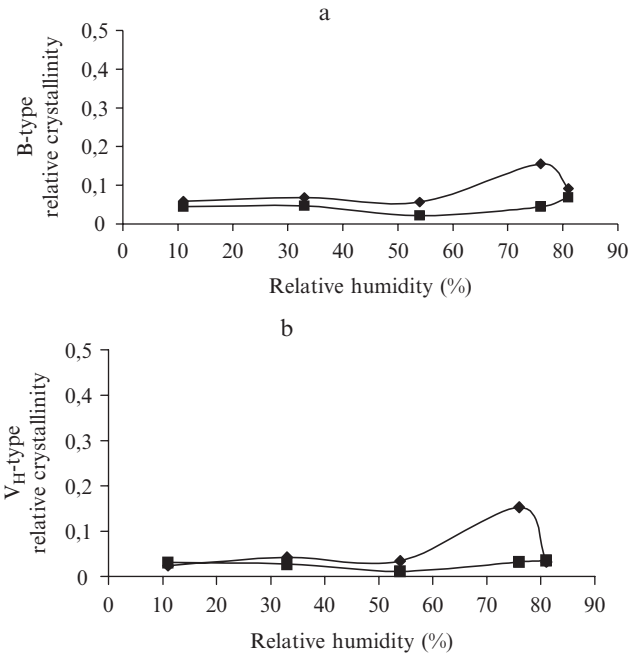

FIG. 32.11 - Type-B (a) and Type VH (b) relative crystallinity of ◆ = starch- glycerol films and ■ = starch-monoglyceride films

storage. In both cases, glycerol films presented higher crystallinity degree, with a slight increase at higher RH values, while monoglyceride starch films showed constant crystallinity degree. Rindlav-Westling et al. (1998) demonstrated that increasing levels of relative humidities increased the relative crystallinity of glycerol plasticized amylopectin films.

Theorically, the V_H structure that is found in extruded starches (van Soest et al., 1996) and in this work should appear more significantly in the monoglyceride starch films, but probably the short storage time and the low water content did not favor the starch crystallization in these films.

It is possible to conclude that the use of extrusion to complex yam starch and monoglyceride was effective and permitted production of starch-monoglyceride films with only a slight phase separation. The stability of mechanical properties of these films when submitted to different RH conditions was their most desirable characteristic, and at the same time, these films showed lower hydrophilicity and water vapor permeability than starch and glycerol-starch films. Although starch-monoglyceride films presented poor mechanical properties when compared with glycerol films, certainly it will be found application for them.

32.2.5. Banana Starch Films

32.2.5.1. Native Starch

Films were prepared using banana starch with and without plasticizer using two gelatinization methods. The thickness of the films elaborated with these two methods was different, since thermal gelatinization produced films with higher value (113.05 μm) than those obtained with cold gelatinization (83.26 μm). The extensive degradation during cold gelatinization produced thinner films. Interactions between plasticizer and starch chains might slightly increase this characteristic. Due to the hydrophilic character of starch, one of the major problems of the starch-based films is high permeability. Difference between the two methods for film preparation was observed in the water vapor permeability (WVP), since the film made by cold gelatinization showed lower permeability than those made by thermal gelatinization (Table 32.5).

TABLE 32.5. Water vapor permeability of banana starch films[a]

Film	Permeability × 10^{11}g/msPa	Relative humidity (%) (in/out)	Gelatinization method
Starch + water + glycerol[1,b]	27.01 ± 0.26	92.5/75	Thermal
Starch + water + glycerol[2,c]	24.85 ± 1.22	0/75	Thermal
Starch + water + glycerol[2,c]	13.59 ± 1.90	0/75	Cold

[a] Values are the mean of three replicates ± standard error. [b] Glycerol concentration was 2 % (w/v) of filmogenic solution. [c] Glycerol concentration was 1.5 % (w/v) of filmogenic solution. [1] Zamudio-Flores et al., 2006; [2] Ro-mero-Bastida et el., 2005)

Differences in permeability value can be attributed to alterations in film structure. Similar permeability value was obtained in films prepared with gelatin, soluble starch and glycerol (Arvanitoyanis et al., 1997). Slight difference was found in films prepared with thermal gelatinization but with different starch and glycerol concentrations. The tensile strength (TS) value of film elaborated with thermal gelatinization method was higher than that obtained with cold gelatinization (Table 32.6). Lower TS was obtained in banana film added with glycerol (4.7 MPa) and prepared by thermal gelatinization than film prepared with a similar procedure (24.3 MPa). This difference can be attributed to the starch and glycerol concentration in the composite, and to the experimental conditions.

32.2.5.2. Oxidized Starch

Thickness of the films did not change with the oxidation level of banana starch, and those values were similar to that obtained in a film elaborated with native banana starch and glycerol (119 μm). This parameter can be influenced by the preparation method of the filmogenic solution (Romero-Bastida et al., 2005).

Films prepared with banana starch at different active chlorine concentrations stored for 90 days (Table 32.7) increased the WVP when the chlorine level in the starch also increased. Interactions among carboxyl groups of adjacent side-chains can produce a structure with a larger cavity and higher WVP in the films (Zamudio-Flores et al., 2006).

The tensile strength (TS) value of film elaborated with modified banana starch increased with the degree of starch modification (Table 32.8). Since carbonyl and carboxyl groups are formed during the oxidation of starch molecules, they might produce hydrogen bridges with the OH groups of both starch components (amylose and amylopectin), where those linkages gave more structural integrity in the

TABLE 32.6. Mechanical properties of banana starch films[a]

Film	Tensile strength (MPa)	Elongation (%)	E.C.[b]
Starch + water + glycerol[1,c]	4.70 ± 0.17	37.38 ± 0.76	6/1.0 ; 24
Starch + water + glycerol[2,d]	24.31 ± 3.42	39.85 ± 6.23	8/0.7 ; 10
Starch + water + glycerol[2,d,e]	16.76 ± 2.88	19.320 ± 4.58	8/0.7 ; 10

[a] Values are the mean of three replicates ± standard error. [b] Essay conditions sample size (large/wide, cm) and velocity (mm/min)]. [c] Glycerol concentration was 2 % (w/v) of filmogenic solution. [d] Glycerol concentration was 1.5 % (w/v) of filmogenic solution. [e] Elaborated by cold gelatinization method. [1] Zamudio-Flores et al., 2006. [2] Romero-Bastida et al., 2005

TABLE 32.7. Water vapor permeability (WVP) of oxidized banana starch[a]

Film	WVP × 10^{11} g/msPa	RH[b]	Thickness (μm)
Oxidized starch (0.5% a.c[b].) + water + glycerol	36.24 ± 0.36	92.5/75	120 ± 1.20
Oxidized starch (1.0% a.c[b].) + water + glycerol	45.65 ± 0.30	92.5/75	121 ± 0.80
Oxidized starch (1.5% a.c[b].) + water + glycerol	55.01 ± 1.03	92.5/75	121 ± 2.30

[a] Values are the mean of three replicates ± standard error. [b] Relative humidity conditions (in/out)

Table 32.8. Mechanical properties of oxidized banana starch films[a]

Film	Tensile strength (MPa)	Elong ation (%)	EC[c]
Oxidized starch (0.5% a.c[b].) + water + glycerol[1]	5.55 ± 0.19	30.32 ± 0.63	6/1.0; 24
Oxidized starch (1.0% a.c[b].) + water + glycerol[1]	6.86 ± 0.23	28.24 ± 0.69	6/1.0; 24
Oxidized starch (1.5% a.c[b].) + water + glycerol[1]	7.64 ± 0.27	25.56 ± 0.33	6/1.0; 24

[a] Values are the mean of three replicates ± standard error. [b] Active chlorine. [c] Essay conditions [sample size (large/wide, cm) and velocity (mm/min)]. [1] Zamudio-Flores et al., 2006

polymeric matrix that increased the TS. The addition of higher active chlorine concentration in the starch decreased the elongation of the films. These results suggest that films with a higher amount of carboxyl and carbonyl groups produce higher interactions among polymer chains that affect the crystallinity and the flexibility of the films.

Acknowledgements To CYTED (Project XI.20). The authors acknowledge the financial support from Agencia Nacional de Promoción Científica y Tecnológica (ANPCyT), Universidad de Buenos Aires (UBA), Universidad Nacional de La Plata (UNLP), Consejo Nacional de Investigaciones Científicas y Técnicas (CONICET) and Fundación Antorchas, from Argentina; to CNPq, FAPESP and Fundo Paraná, from Brazil; to SEPI-IPN and COFAA-IPN, EDI-IPN, PIFI-IPN from México. They also thank Elsevier for permission to use some data published in Food Research International (Flores, Famá, Rojas, Goyanes, and Gerschenson, 2006, Physical Properties of Tapioca-Starch Edible Films: Influence of Filmmaking and Potassium Sorbate, In Press).

References

Alves, R.M.L., Grossmann, M.V.E., and Silva R.S.S.F., 1999, Pregelatinized Starches of *Dioscorea alata* - Functional Properties, *Food Chem*. **67**:23–127.

AOAC, 1990, Official Methods of Analysis, 13th ed., Association of Official Analytical Chemists, Washington, DC.

Arvanitoyannis, I., Billiaderis, C.G., Ogawa, H., and Kawasaki N., 1998, Biodegradable Films Made from Low-Density Polyethylene (LDPE), Rice Starch and Potato Starch for Food Packaging Applications: Part 1. *Carbohydr. Polym*. **36**:89–104.

Arvanitoyannis, I., Kalichevsky, M., Blanshard, J., and Psomiadou E., 1994, Study of Diffusion and Permeation of Gases in Undrawn and Uniaxially Drawn Films Made from Potato and Rice Starch Conditioned at Different Relative Humidities, *Carbohydr. Polym*. **24**:1–15.

Arvanitoyannis, I., Psomiadou, E., Nakayama, A., Aiba, S., and Yamamoto N., 1997, Edible Films Made From Gelatin, Soluble Starch And Polyols, Part 3, *Food Chem*. **60**:593.

ASTM, 1996, Standard Test Methods for Water Vapor Transmission of Material, E96–95, in: *Annual Book of ASTM*.: American Society for Testing and Materials, Philadelphia.

ASTM D4092, 1996, *Standard Terminology: Plastics: Dynamic Mechanical Properties*, American Society for Testing and Materials, Philadelphia.

ASTM E96–00, 2000, *Standard Test Method for Water Vapor Transmission of Materials*, American Society for Testing and Materials, Philadelphia.

Barrett, E.P., Joyner, L.G., and Hallena P.P., 1951, The Determination of Pore Volume and Area Distribution in Porous Substances, Computation from Nitrogen Isotherms, *J. Am. Chem. Soc*. **73**:373–380.

Bello-Pérez, L.A., Agama-Acevedo, E., Sáyago, S.G., and Figueroa J.D.C., 2000. Some Structural, Physcochemical and Functional Studies of Banana Starches Isolated from Two Varieties Growing in Guerrero, México, *Starch/Stärke*. **52**:68.

Cunningham, P., Ogale, A., Dawson, P., and Acton J., 2000, Tensile Properties of Soy Protein Isolate Films Produced by a Thermal Compaction Technique, *J. Food Sci*. **65**(4):668–671.

Cuq, B., Gontard, N., and Guilbert S., 1998, Proteins as Agricultural Polymers for Packaging Production. *Cereal Chem*. **75**:1, 1–9.

Donhowe, I.G., and Fennema O., 1993a, The Effects of Plasticizers on Crystallinity, Permeability and Mechanical Properties of Methylcellulose Films, *J. Food Process. Preserv*. **17**:247–258.

Donhowe, I.G., and Fennema O., 1993b, The Effects of Solution Composition and Drying Temperature on Crystallinity, Permeability and Mechanical Properties of Methylcellulose Films, *J. Food Process. Preserv*. **17**:231–246.

FAO, 2004, Proceedings of the Validation Forum on the Global Cassava Development Strategy, Volume 6, Global Cassava Market Study Business Opportunities for the Use of Cassava, International Fund for Agricultural Development, Rome

Ferreira F.A.B., 2005, Estabilidade de Filmes de Amido de Inhame Plastificados com Monoglicerídio e com Glicerol em Diferentes Condições Ambientais, Dissertação de Mestrado, Universidade Estadual de Londrina, Londrina.

García, M.A., Martino, M.N., and Zaritzky N.E., 1998a, Plasticizer Effect on Starch-based Coatings Applied to Strawberries (*Fragaria* × *Ananassa*), *J. Agric. Food Chem*. **46**:3758–3767.

García, M.A., Martino, M.N., and Zaritzky N.E., 1998b, Starch-based Coatings: Effect on Refrigerated Strawberry (*Fragaria* × *Ananassa*) Quality, *J. Sci. Food Agric*. **76**:411–420.

García, M.A., Martino, M.N., and Zaritzky N.E., 2000a, Lipid Addition to Improve Barrier Properties of Edible Starch-based Films and Coatings, *J. Food Sci*. **65**(6):941–947.

García, M.A., Martino, M.N., and Zaritzky N. E., 2000b, Microstructural Characterization of Plasticized Starch-Based Films, *Starch/Stärke* **52**(4):118–124.

García, M.A., Martino, M.N., and Zaritzky N. E., 2001, Composite Starch-Based Coatings Applied to Strawberries (*Fragaria* × *ananassa*), *Nahrung/Food* **45**(4):267–272.

García, M.A., Pinotti, A., Martino, M., and Zaritzky N., 2004, Characterization of Composite Hydrocolloid Films, *Carbohydr. Polym*. **56**(3):339–345.

González-Soto, R.A., Sánchez-Hernández, L., Solorza-Feria, J., Nuñez-Santiago, C., Flores-Huicochea, E., and Bello-Pérez L. A., 2006, Resistant Starch Production from Non-Conventional Starch Sources by Extrusion, *Food Sci. Technol. Int*. **12**(1):5.

Hullemann, S.H.D., Kalisvaart, M. G, Janssen, F.H.P., Feil, H., and Vliegenthart J.F.G., 1999, Origins of B-Type Crystallinity in Glycerol-Plasticised, Compression Moulded Potato Starches, *Carbohydr. Polym*. **39**:351–360.

Krochta, J.M., and De Mulder-Johnston C., 1997, Edible and Biodegradable Polymer Films: Challenges and Opportunities, *Food Technol*. **51**(2):61–77.

Larotonda, F.D.S., Matsui, K.N., Sobral, P.J.A., and Laurindo J.B., 2005, Hygroscopicity and Water Vapor Permeability oof Kraft Paper Impregnated with Starch Acetate, *J. Food Eng*. **71**:394–402.

Larotonda, F.D.S., Matsui, K.S., Paes, S.S., and Laurindo J.B., 2003, Impregnation of Kraft Paper with Cassava-Starch Acetate-Analysis of the Tensile Strength, Water Absorption and Water Vapor Permeability, *Starch/Starke* **55**:504–510.

Lawton J.W., 1996, Effect of Starch Type on the Properties of Starch Containing Films. Carbohydrate Polymers, **29**: 203–208.

Lawton, J.W., and Fanta G.F., 1994, Glycerol—Plasticized Films Prepared from Starch Poly(Vinyl Alcohol) Mixtures: Effect of Poly (Ethylene—Co-Acrylic Acid), *Carbohydr. Polym*. **23**:261–270.

Lii, C.Y., Chang, S.M., and Young Y.L., 1982, Investigation of the Physical and Chemical Properties of Banana Starches, *J. Food Sci*., **47**:1493.

Lourdin, D., Della Valle, G., and Colonna P., 1995, Influence of Amylose Content on Starch-Films and Foams. Carbohydrate Polymers, **27**:275–280.

Mali, S., Grossmann, M.V., García, M.A., Martino, M.N., and Zaritzky N.E., 2002, Microstructural Characterization of Yam Starch Films, *Carbohydr. Polym*. **50**(4):379–386.

Mali, S., Karam, L.B., Ramos, L.P., and Grossmann M.V.E., 2004, Relationships Among the Composition and Physicochemical Properties of Starches with the Characteristics of Their Films, *J. Agric. Food Chem*. **52**(25):7720–7725.

Manzocco, L., Nicoli, M.C., and Labuza T., 2003, Study oof Bread Staling by X-Ray Diffraction Analysis, *Italian Food Technol*. **XII**(31):17.

McHugh, T.H., and Krochta J.M., 1994, Milk-Protein-Based Edible Films and Coatings, *Food Technol*. **48**(1):97–103.

Monterrey-Quintero, E.S., and Sobral P.J., 1999, Caracterização de Propriedades Mecânicas e Óticas de Biofilmes a Base de Proteínas, *Ciência e Tecnologia de Alimentos*, **19**(2):294–301.

Narayan, R., Bloembergen, S., and Lathia A., 1999, *Method of Preparing Biodegradable Modified-Starch Moldable Products and films*, US Patent 5,869,647.

Petersson, M., and Stading M., 2005, Water Vapor Permeability and Mechanical Properties of Mixed Starch-Monoglyceride Films and Effect of Film Forming Conditions, *Food Hydrocolloid*. **19**:123–132.

Rindlav-Westling, A., Stading, M., Hermansson, A.M., and Gatenholm P., 1998, Structure, Mechanical and Barrier Properties of Amylose and Amylopectin Films, *Carbohydr. Polym*. **36**:217–224.

Rockland L.B., 1960, Satured Salt Solutions for Static Control of Relative Humidity, *Anal. Chem*. **32**:1375–1376.

Romero-Bastida, C.A., Bello-Pérez, L.A., García, M.A., Martino, M.N., Solorza-Feria, J., and Zaritzky N.E., 2005, Physicochemical and Microstructural Characterization of Films Prepared by Thermal and Cold Gelatinization from Non-Conventional Sources of Starches, *Carbohydr. Polym*. **60**(22):235.

Sobral, P.J.A., and Ocuno D., 2000, Permeabilidade ao Vapor de Água de Biofilmes a` Base de Proteínas MiofiBrilares de Carne, *Brazilian J. Food Technol*. **3**:11–16.

van Soest, J.J.G., Hulleman, S.H.D., de Wit, D., and Vliegenthart J.F.G., 1996, Crystallinity in Starch Bioplastics, *Ind. Crop. Prod*. **5**:11–22.

van Soest, J.J.G., and Vliegenthart J.F.G., 1997, Crystallinity in Starch Plastics: Consequences for Material Properties, *Trends Biotechnol*. **15**(6):208–213.

Vermeiren, L., Devlieghere, F., van Beest, M., de Kruijf, N., and Debevere J., 1999, Developments in the Active Packaging of Foods, *Trends Food Sci. Technol*. **10**:77–86.

Vicentini, N.M., Dupuy, N., Leitzelman, M., Cereda, M.P., and Sobral P.J.A., 2005, Prediction of Cassava Starch Edible Film Properties by Chemometric Analysis of Infrared Spectra, *Spectroscopy Lett*. **38**(6):749–767,.

Wurzburg O.B., 1986, Cross-Linking Starches, in: *Modified Starches: Properties and uses*, O.B. Wurzburg (ed.), CRC Press, Boca Raton, p. 41–53.

Zamudio-Flores, P.B., Vargas-Torres, A., Pérez-Gónzalez, J., Bozquez-Molina, E., and Bello-Pérez L.A., 2006, Films Prepared with Oxidized Banana Starch: Mechanical and Barrier Properties, (In press.).

Zhang, P., Whistler, R.L., BeMiller, J.N., and Hamaker B.R., 2005, Banana Starch: Production, Physicochemical Properties, and Digestibility—A Review. *Carbohyd. Polym*. **59**:443–458.

33
Programme Alβan: European Union Programme of High Level Scholarships for Latin America

A.M. Sereno

33.1. Introduction

In 2002 the European Commission adopted Programme Alßan, a high level scholarship program specifically addressed to Latin America. It is expected that around 3,900 Latin American students and professionals will benefit from these scholarships, in the European Union, until 2010. Programme Alßan will enable Latin American students and professionals, future academics and decision-makers in their own countries, to benefit from the excellence of the Higher Education Area in the European Union.

The first scholarship holders of Programme Alßan started their postgraduate education (master or doctorate degrees) or higher level professional training/ upgrading in the academic year 2003/2004.

The periods of education and training may range from 6 months to 3 years, depending on the type of project and the level envisaged.

The financial contribution of the European Commission to Alßan scholarships amounts to € 75 Million.

33.2. Objectives

Programme Alβan aims at the reinforcement of the European Union-Latin America cooperation in the area of higher education and covers studies for post-graduates as well as higher-level training for Latin American professionals/future decision-makers in institutions or centers in the European Union.

In addition to opening the European Higher Education Area to Latin Americans, Alβan scholarships will contribute to better employability skills and career opportunities for Latin American postgraduates and professionals in their own countries.

Education and training in the European Union will take place in the context of mobility projects counting on the support of hhigher education institutions or their networks and other relevant organizations, among which enterprises will play a role, with a view to training or upgrading their staff.

To consolidate the experiences and benefits that Latin Americans will receive from education and training in the European Union, an Alumni Network will be set up to create a network of grant recipients. This Alumni Network will also be open to previous grant-holders of the ALFA Programme, as well as other Latin American students or professionals who may have benefited from cooperation programmes between the two regions.

33.3. A Quick Tour of Alβan

33.3.1. What Are Alβan Scholarships?

Alßan scholarships are a means to support postgraduate studies and professional training or upgrading of Latin American students in the European Union. It is open to Latin American citizens living in one of the following 18 Latin American countries: Argentina, Bolivia, Brazil, Chile, Colombia, Costa Rica, Cuba, Ecuador, El Salvador, Guatemala, Honduras, Mexico, Nicaragua, Panama, Paraguay, Peru, Uruguay and Venezuela.

33.3.2. Minimum Requirements to Apply for an Alβan Scholarship

The minimum requirements to apply for an Alßan scholarship are:

- To be a citizen of one of the 18 eligible countries from Latin America, with residence in one of those countries (Argentina, Bolivia, Brazil, Chile, Colombia, Costa Rica, Cuba, Ecuador, El Salvador, Guatemala, Honduras, Mexico, Nicaragua, Panama, Paraguay, Peru, Uruguay and Venezuela);
- To have completed the minimum university qualifications required for acceptance for post-graduate studies (at master or doctorate level) in a Higher Education Institution (HEI) of the European Union and be supported for such a program by a Higher Education Institution eligible to Alßan; alternatively, to be a professional working at a recognized organisation in one of the eligible Latin American countries, wishing to obtain a higher level of professional training or upgrading in the European Union, counting on the support of such organization;
- To be accepted by one higher education institution or higher level training center in the European Union (Austria, Belgium, Cyprus, the Czech Republic, Estonia, Germany, Denmark, Hungary, Finland, France, Greece, Ireland, Italy, Latvia, Lithuania, Luxembourg, Malta, The Netherlands, Poland, Portugal, Slovakia, Slovenia, Spain, Sweden, United Kingdom) for the proposed education/training project;
- To describe how he/she will be reintegrated as an active member in any organization of his/her home country, once the education/training period in the European Union is over.

33.3.3. How to Apply for an Alβan Scholarship?

Preferably, the application should be made on-line by completing and submitting a specific application form through the Internet. It is also possible to submit paper applications.

33.3.4. What Are the Deadlines for the Submission of Applications?

Annual calls for the submission of applications state deadlines and other requirements or priorities, where and if relevant.

The first call for applications was published on 20 December 2002, with a view to education/training projects starting in the academic year 2003/2004. The second call launched on 17 October 2003, aimed at projects starting in the academic year 2004/20005 in the European Union. The third call opened in September 2004, closed on 22 December 2004, and is intended for projects starting in the academic year 2005/2006.

33.3.5. How Are Applications Evaluated?

Applications for Alßan scholarships will initially undergo an eligibility assessment. The technical and scientific quality of eligible applications will then be evaluated by a minimum of two international independent academic experts.

The group of Alßan experts is composed of recognized academics and scientists from all eligible countries, both in Latin America and the European Union.

33.3.6. Where to Obtain Information About the Preparation of the Application?

Alßan program websites constitute the main information source about the program:

- http://www.programalban.org
- http://europa.eu.int/comm/europeaid/projects/alban

The Alßan Office will provide all required information concerning the application, ensuring equal and impartial treatment to all candidates.

33.4. Results Achieved

The following overall results observed in Fig. 33.1 were obtained after the first two/three calls for applications that constitute the first phase of Programme Alβan.

In Fig. 33.2, the results of Country of Origin of the applications selected during the first two calls for application are listed:

The applications selected during the first two calls went to the following EU member states:

	2003/04	2004/05	2005/06
RECEIVED	6525	3901	*2821*
EVALUATED	4010	2829	*2173*
SELECTED	251	779	*553*
STARTED	214	612	
ACTIVE	103	546	

FIG. 33.1. Applications received and selected in the first three calls

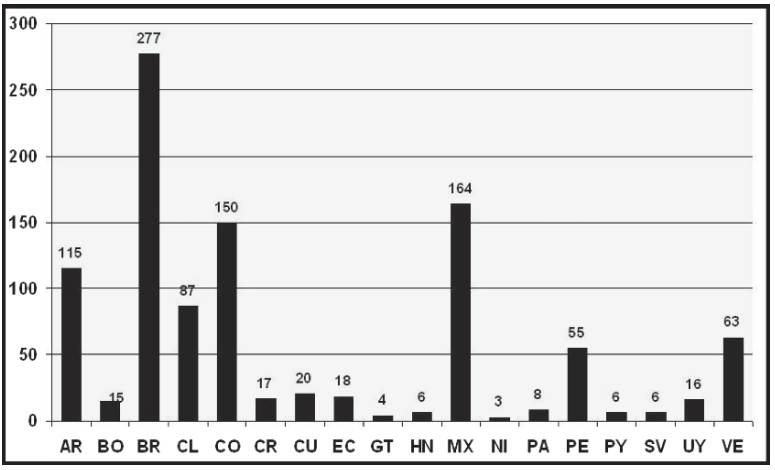

FIG. 33.2. Country of origin of the applicants selected in the first two calls

Three types of scholarships are awarded; scholarship distribution during the first two calls by type and sex is as follows:

Programme Alβan awards scholarships in all subject areas except language learning. This is the distribution for the first two calls:

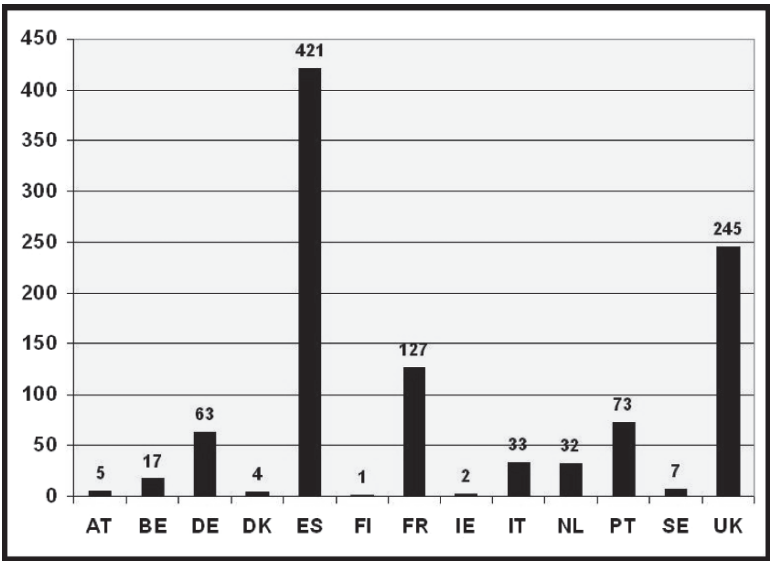

FIG. 33.3. Country of destination of the applicants selected in the first two calls

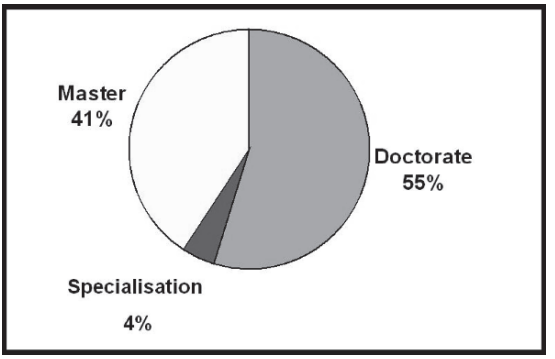

FIG. 33.4. Types of scholarships

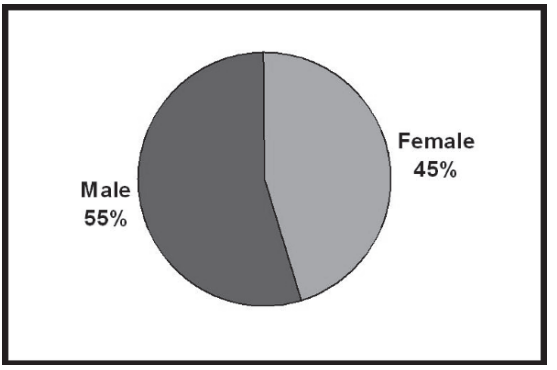

FIG. 33.5. Gender distribution

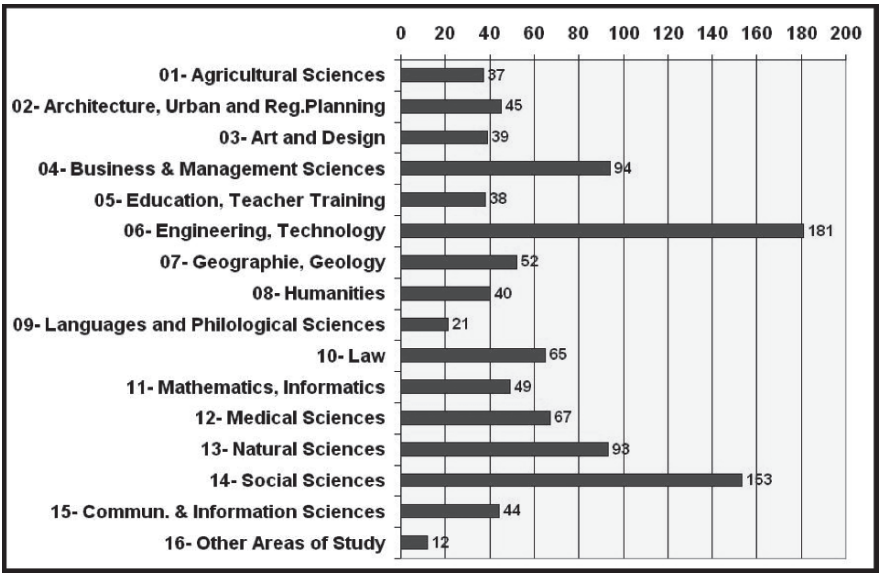

FIG. 33.6. Subject areas of study

33.5. Conclusions

Programme Alβan is achieving its main objectives, and it will go into the 2nd Phase of its implementation up to 2010, as expected. The next Call for Scholarship Applications is planned to open next September and to remain open up to late December 2005. Grupo Santander de Universidades will continue to lead the consortium responsible for its implementation through the Alβan Office, located at University of Porto in Portugal.

The Alβan Office has the following responsibilities:

- Prepare documentation and open new Calls for Applications;
- Receive applications, check eligibility and promote technical evaluation by experts;
- Prepare a ranked list of applications and submit to the EC a proposal of applications to be selected;
- Help the selected grantees to travel to the EU;
- Follow up the work and pay the scholarships;
- Promote Alβan in LA and EU and coordinate the network of Focal Points in LA.

All required information is available at www.programalban.org.

Acknowledgements The Alβan Office/AGS acknowledges the opportunity offered by CIBIA V to inform all participants of this important meeting about the main results achieved and opportunities offered by Programme Alβan.

34
ISEKI-Food: Integrating Safety and Environmental Knowledge into Food Studies Towards European Sustainable Development

C.L.M. Silva

34.1. Introduction

European curricula in food science and engineering (taking into account the following degrees: bachelor, higher diploma, master, Ph.D., post-graduate and continuing education) are very diverse. There are, for example, backgrounds with a stronger component in science, others in engineering, and a three year BSc duration followed by two years of master or higher diploma courses, etc. Although this diversity has a positive value in terms of the variety of the backgrounds and types of teaching materials available, it also causes a problem in terms of the recognition of the degrees, which is not the same in all countries.

The analysis of the curricula in Europe was studied by the Socrates Thematic Network—FOODNET—Food Studies in Europe (Project n°. 55792-CP-3-00-FR-ERASMUS-ETN), in which a database was prepared, available on the web site *http://www2.esb.ucp.pt/foodnet/*. Although a large diversity of backgrounds is offered, there is a big lack in terms of the knowledge of safety aspects, particularly consumer public health and environment; backgrounds on renewal resources are almost unavailable in the majority of the institutions offering diplomas in food science and engineering.

The main objectives of the ISEKI-Food project (104934-CP-1-2002-1-PT-ERASMUS-TN, 104934-CP-2-2003-1-PT-ERASMUS-TN, 104934-CP-3-2004-1-PT-ERASMUS–TN) were to contribute to the studies in food science and engineering in Europe, and to develop and adapt the curricula to include safety and environmental topics.

The main activities underway and conclusions can be obtained at the web sites *http://www.esb.ucp.pt/iseki* and *http://www.esb.ucp.pt/isekipast*. More specific objectives are to:

- Increase the interchange between partners (universities, industry and students) in a teaching point of view: topics studied, materials and methods (including ICT and ODL);
- Contribute to a higher knowledge of the transformation processes for food products;

- Develop new and improved teaching methods, with the main purpose of developing the personal skills of the students;
- Contribute to continuing education, by carrying out workshops and ODL courses;
- Contribute to the higher information of the public in general (particularly students in preparatory and secondary levels) about topics of food science and engineering, and more specifically about safety topics (from the public health point of view), environmental impact and protection;
- Sustainability of the network by establishing an association.

This network included 67 university institutions that offer degrees in food and environmental science and engineering, microbiology and biotechnology, and 25 industrial and research partners from 29 different European countries. It does not include three of the eligible countries under the Socrates Program, which are Luxemburg, Lichtenstein and Cyprus.

This thematic network worked actively to achieve the goals of the nine action lines established in the Bologna Declaration: "Establishment by 2010 of a coherent, compatible and competitive European Higher Education Area, attractive for European students and for students and scholars from other continents."

34.2. Management Structure

Five working groups have been established to achieve the above-mentioned objectives. The activities were divided as follows:

- Promote the studies in Food Science and Engineering, with emphasis on safety and environmental topics;
- Collection and development of teaching materials and methods;
- Dissemination of food science and engineering topics to the general public, with special attention to safety and environmental topics;
- Relationship between university and enterprises, with particular relevance to mobility and industrial placement of students and teachers;
- Practical and laboratory teaching at pilot plant scale.

Each working group is led and coordinated by one of the partners of the network, in collaboration with a second partner.

An extra activity on the network's sustainability was also developed during the third and final year of the project.

The project had a steering committee that assessed and supervised all activities and disseminated results under the ISEKI-Food TN. This committee consisted of the coordinator, coordinators of the working groups and five non-university partners, experts on safety and environmental topics and food science and engineering.

In every year of the project, two overall meetings were organized with all partners. Steering committee meetings took place between the six overall meetings.

34.3. Results and Discussion

A critical analysis of food science and engineering curricula, with emphasis on environmental and safety topics, and a collection of materials and syllabi of environmental and safety disciplines were the main outputs of this TN. The results of the five working groups were:

Working Group 1

- Implementation of a curricula database in food science and engineering in Europe, available in the web site: http://www.esb.ucp.pt/iseki/isekiapp
- Publication of the following documents: "*Critical analysis on European Curricula in Food Studies—Work Towards the Proposal for European Tuned Curricula*"; "*Generic and Subject-Specific Competences in Food Studies*"; "*Minimum Requirements for Curricula in Food Science and Engineering with Emphasis on Environmental and Safety Topics*"
- Publication of a document about the generic and subject specific competences of food science and engineering degrees identified, and its importance defined for academics, graduates, professional bodies and employers

Working Group 2

- A web catalogue of materials and teaching methods, available in the web site: http://iseki.anet.at/
- Preparations of articles for food technology and dissemination for partners
- Workshops for dissemination and continuing education of teachers: "*Using E-Learning in the Fields of Food Safety and Environment"; "ISEKI e-learning course: 'Train the Trainer"; "Progress Workshop on ISEKI E-Learning Course: 'Train the Trainer"; "ISEKI Forum on Integrating Research into Teaching*"
- E- learning courses, glossary and a guide for E-learning
- Development of criteria for evaluation e-learning products; ODL courses on safety and environmental topics; publication of four books on safety and environmental topics: *"Food Safety, a Practical and Case Study Approach", "Air Pollution Control: Odours Treatment in the Food Industry"; "Utilization of By-Products and Treatment of Waste in the Food Industry"* and *"Predictive Modelling and Risk Assessment"*

Working Group 3

- Preparation of a multilingual web page with FAQ on food science and engineering, available at the web site http://food-info.net
- Publication of a report on "*Food Science and Engineering and the General Public*"

Working Group 4

- Preparation of a report concerning the relationship of university/enterprise; publications of the documents:*"Professional Placements During Studies in Food*

Science and Technology: Industry–University Relationship"; "Relationship University–Industry: How to Organize Training Periods, Modes of Assessment, Diploma Supplement"; "Methods for Assessment of Industry Placements"
- Report on *"Existing Relationship/Structures Between Universities and Enterprises in Teaching, and in Research & Development"*

Working Group 5

- A web catalogue about practical/laboratory teaching at pilot plant scale (equipment, movies, protocols and teaching methods), available on the web site http://www.ualg.pt/est/adea/iseki.php
- Publication of the documents: *"Ways of Sharing Pilot Plant Laboratory Resources," - Importance of ODL, Mobility and Industry*
- Publication of two books: *"Protocols of Laboratory Pilot Plant Experiments on Food Science and Engineering, with Emphasis on Safety and Environment; Case Studies on Food Safety and Environment"*; *"Case studies on Food Safety and Environment"*
- Foundation of the ISEKI-Food Association, available at the site www.iseki-food.net, accepted by Austrian authorities; Creation of a data base on food experts, available on the web site www.esb.ucp.pt/foodexperts

During the first year, a Webpage of the ISEKI-Food TN project was created. Leaflets and a poster were published, and six newsletters were prepared and put on the webpage. The main activities underway and conclusions can be obtained at the web sites *http://www.esb.ucp.pt/iseki* and *http://www.esb.ucp.pt/isekipast/*.

The quality of the project was evaluated in terms of the materials prepared, number of people requesting permission to access the partner's zone of the ISEKI-Food web page: *www.esb.ucp.pt/isekipast*, number and curricula of people attending workshops and following the ODL courses, degree of implementation of suggestions and recommendations of the network on curricula, syllabi and teaching methods, and others. Furthermore, the quality of the workshops and ODL courses was evaluated by the participants and by using appropriate questionnaires. The project was also evaluated by checking if the planned activities and corresponding outputs and deadlines were achieved.

34.4. Further Work

The European Commission, recognizing the work being developed by this network, approved a second edition of the project: ISEKI-Food 2—Integrating Safety and Environment Knowledge in Food Towards European Sustainable Development (226032-CP- 1-2005-1-PT-ERASMUS-TN; *start date*: October 2005; *end date*: September 2008).

The main objective of the Socrates Thematic Network (226032-CP-1-2005-1-PT-ERASMUS-TN), coordinated by Escola Superior de Biotecnologia–Universidade Católica Portuguesa, is to contribute to the realization of the European Higher Education Area in the field of food studies.

More specific objectives are to work for the development of:

- Quality assurance of European Food Studies, with the recognition of degrees at the European level
- The curricula in food studies, taking into consideration safety and environmental aspects, participating in the implementation of the "Bologna Process"
- Teaching materials and methods in the field of food studies
- Synergies between research in food science and engineering with education/teaching and industry
- Communication with the general public and consumers to enhance knowledge of food products and the food industry
- An offer of a virtual community of experts in the field of food
- Sustainability of the ISEKI-Food network by creating the ISEKI-FOOD Association, available on the web site *http://www.iseki-food.net*.

This network includes a total of 113 institutions (74 universities, two EU student associations, and 37 industrial and research partners), 93 coming from EU and 20 from non-EU countries.

Acknowledgements The present work was supported by ERASMUS THEMATIC NETWORKS (104934 -CP-1-2002-1-PT-ERASMUS-TN, 104934-CP-2-2003-1-PT-ERASMUS-TN, 104934- CP- 3-2004-1-PT-ERASMUS–TN and 226032-CP-1-2005-1-PT-ERASMUS-TN).

Index